# Plasma Assisted Combustion:


## Yiguang Ju

## Princeton University


**2017. 6. 13**

**Princeton Combustion Summer School**


Copyright ©2017 by Yiguang Ju. This material is not to be sold, reproduced or distributed without prior written permission of the owner, Yijuang Ju

# Acknowledgement

Sang Hee Won
Associate professor,
Univ. South Carolina

Timothy Ombrello,
Senior research
engineer
AFRL

Wenting Sun
Assistant professor,
Georgia Tech

Joseph Lefkowitz
Research fellow
AFRL

Aric Rousso
Graduate student

Timothy Chen
Graduate student

Prof. Haibao Mu
XiAn Jiaotong Univ.

Prof.Qi Chen
Beijing Jiaotong Univ.

Xingqian Mao
Visiting student

Prof. Walter R. Lempert

Prof. Min Suk Cha
KAUST

Prof. Anne Bourdon
Ecole Centrale Paris

Prof. Rechard Yetter
Penn-state Univ.

Prof. Haixin Wang
Beihang Univ.

Prof. Richard B Miles
Princeton

Dr. Andrey Starikovskiy
Princeton

Prof. Christophe Laux
Ecole Centrale Paris

Prof. Igor V. Adamovich
Ohio State University

Prof. Svetlana Starikovskaya
Ecole Polytechnique

# Lecture contents and review articles

1. **Introduction and plasma discharge**
2. **Plasma Assisted Combustion and Applications in Engines**
3. **Effects of plasma on ignition, flame propagation, and minimum ignition energy**
4. **Effects of electric field on combustion: Joule heating and ionic wind**
5. **Physics and kinetic studies of plasma assisted combustion**
6. **Modeling of plasma assisted combustion**
7. **Perspectives of future research in plasma assisted combustion**

**Review papers of plasma assisted combustion**


1. Ju, Y. and Sun, W., 2015. Plasma assisted combustion: dynamics and chemistry. *Progress in Energy and Combustion Science*, *48*, pp.21-83.
2. Starik AM, Loukhovitski BI, Sharipov AS, Titova NS. 2015 Physics and chemistry of the influence of excited molecules on combustion enhancement. *Phil. Trans. R. Soc.* A 373: 20140341.
3. Igor V Adamovich and Walter R Lempert, 2015, Challenges in understanding and predictive model development of plasma-assisted combustion, *Plasma Physics and Controlled Fusion*, Volume 57, Number 1.
4. Starikovskiy A, Aleksandrov N. Plasma assisted ignition and combustion. *Prog. Energy Combust. Sci*. 2013;39:61–110.
5. Starikovskaia SM. Plasma assisted ignition and combustion. 2006*; J. Phys. D: Appl. Phys*. 39:R265–R299.
6. CO Laux, TG Spence, CH Kruger, RN Zare, Optical diagnostics of atmospheric pressure air plasmas, *Plasma Sources Science and Technology* 12 (2), 125
7. A Fridman, S Nester, LA Kennedy, A Saveliev, O Mutaf-Yardimci, Gliding arc gas discharge, *Prog. Energy Combust. Sci*. 25 (2), 211-231

# 1. Introduction: Plasma assisted combustion

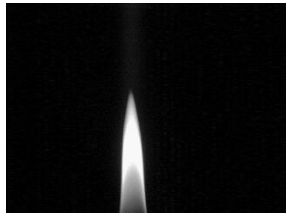

**1814 – W.T. Brande. Phil.Trans.Roy.Soc, 104, 51. (Electric field-flame interaction)**

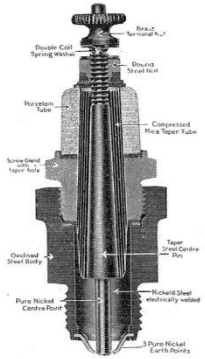

**1860 Étienne Lenoir used an electric spark plug in his gas engine, the first internal combustion piston engine. (Spark ignitor for engines)**

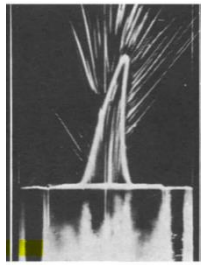

**1948, Calcote, 3rd Symposium on Combustion and Flame, and Explosion Phenomena (Vol. 3, No. 1, pp. 245-253) (Ionic wind)**

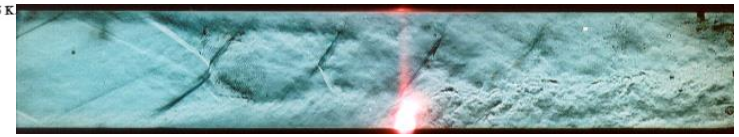

**1981: Kimura, L, et al., Combustion and Flame, Vol. 42, No. 3, pp. 297- 305 (Plasma jet in supersonic combustion)**

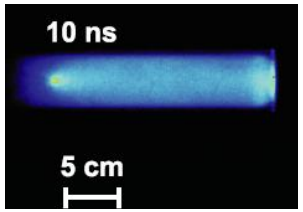


**1998: Starikovskaia, S.M., Starikovskii, A.Y. and Zatsepin, D.V., Journal of Physics D: Applied Physics, 31(9), p.1118. ]Anikin N B and Marchenko N 2005 (Nanosecond discharge).**

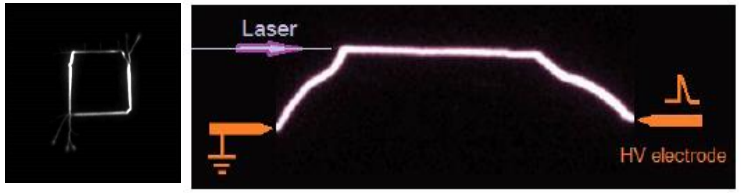


**2013: Leonov, S.B., Firsov, A.A., Shurupov, M.A., Michael, J.B., Shneider, M.N., Miles, R.B. and Popov, N.A., 2012. Physics of Plasmas, 19(12), p.123502. (laser guiding plasma discharge)**

**2015: Won, S.H., Jiang, B., Diévart, P., Sohn, C.H. and Ju, Y., Proc Combust Inst, 35(1), pp.881-888. (Plasma assisted cool flames)**

**(200 years)**

# Plasma Assisted Combustion: a multi-disciplinary and multi-physics problem

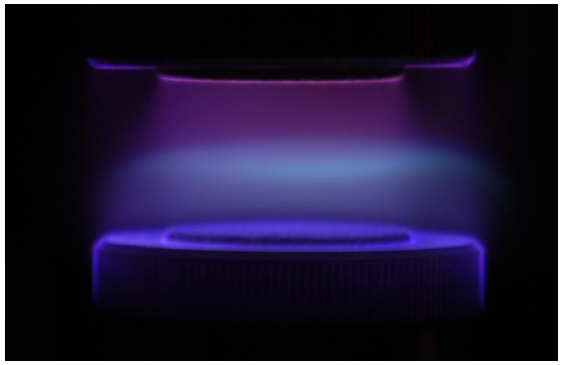

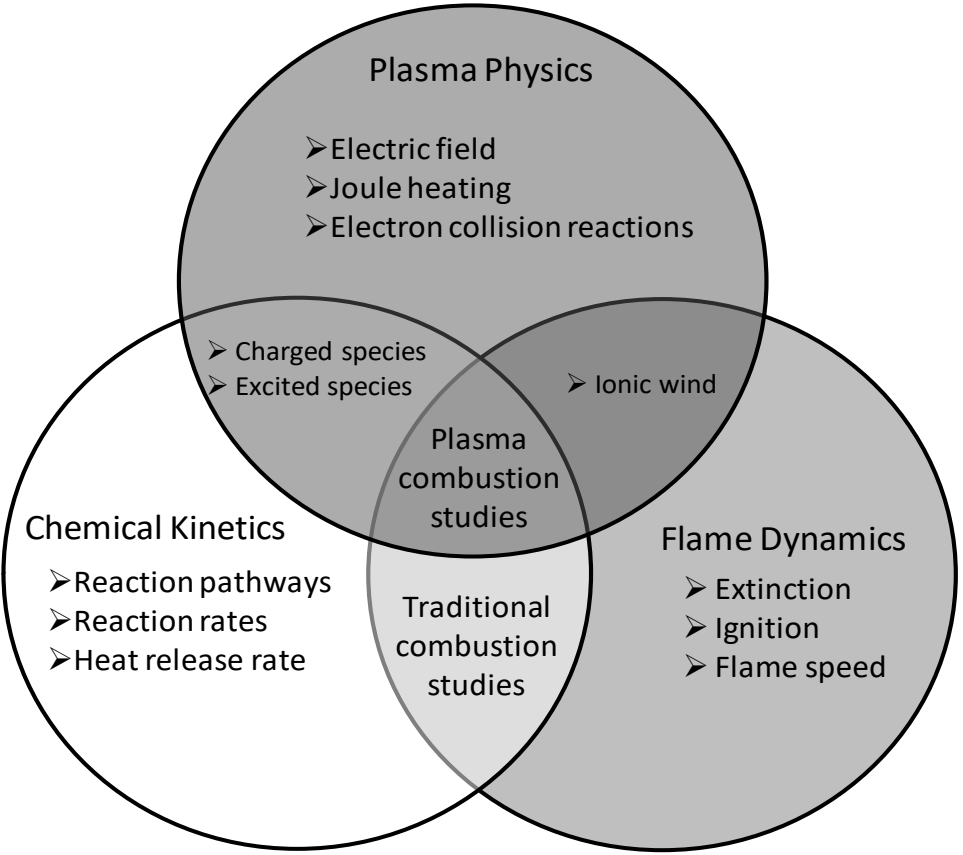


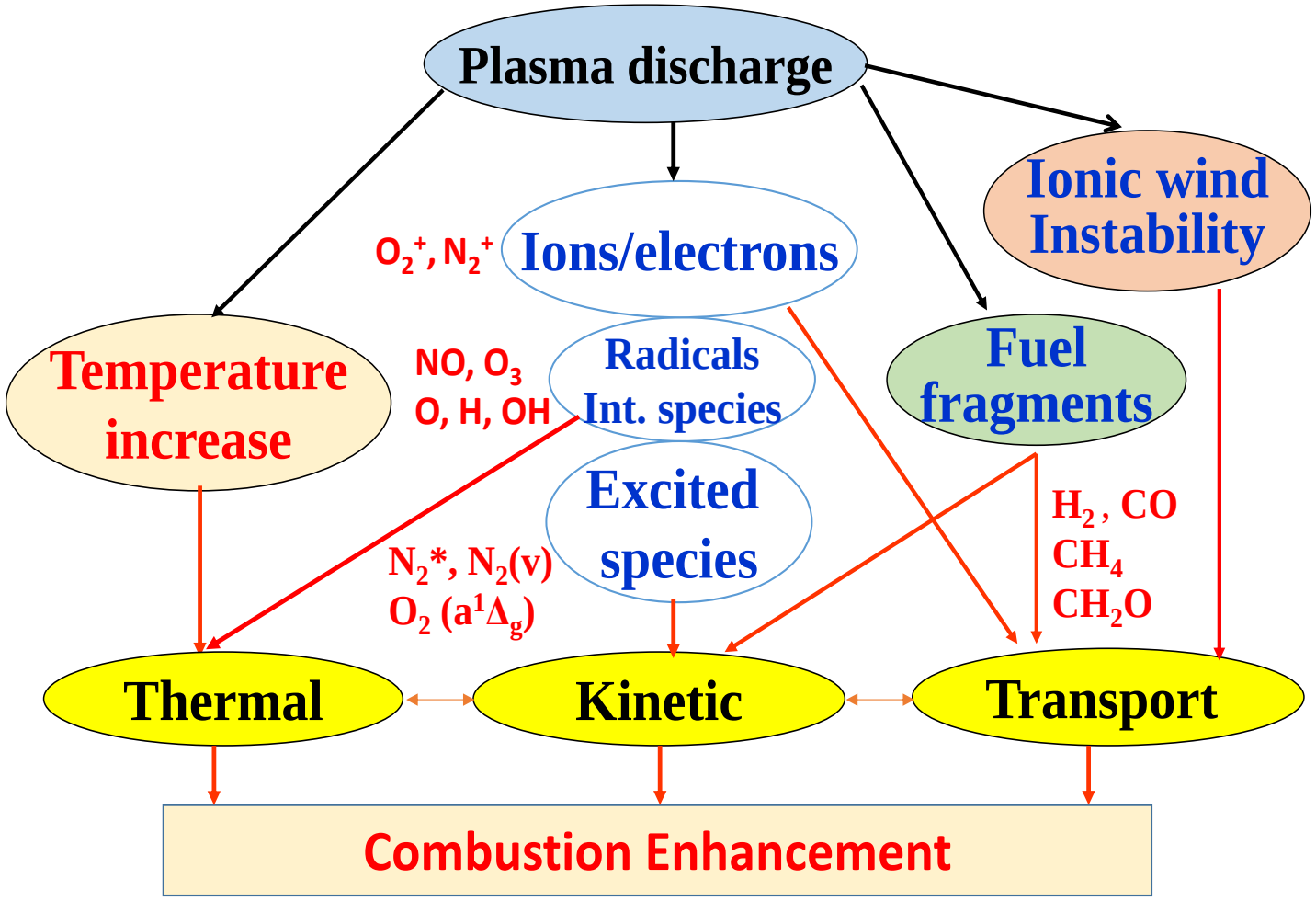


Ju and Sun: Plasma assisted combustion, Progress of Energy & Combustion Science, 2015

# Applications of plasma assisted combustion

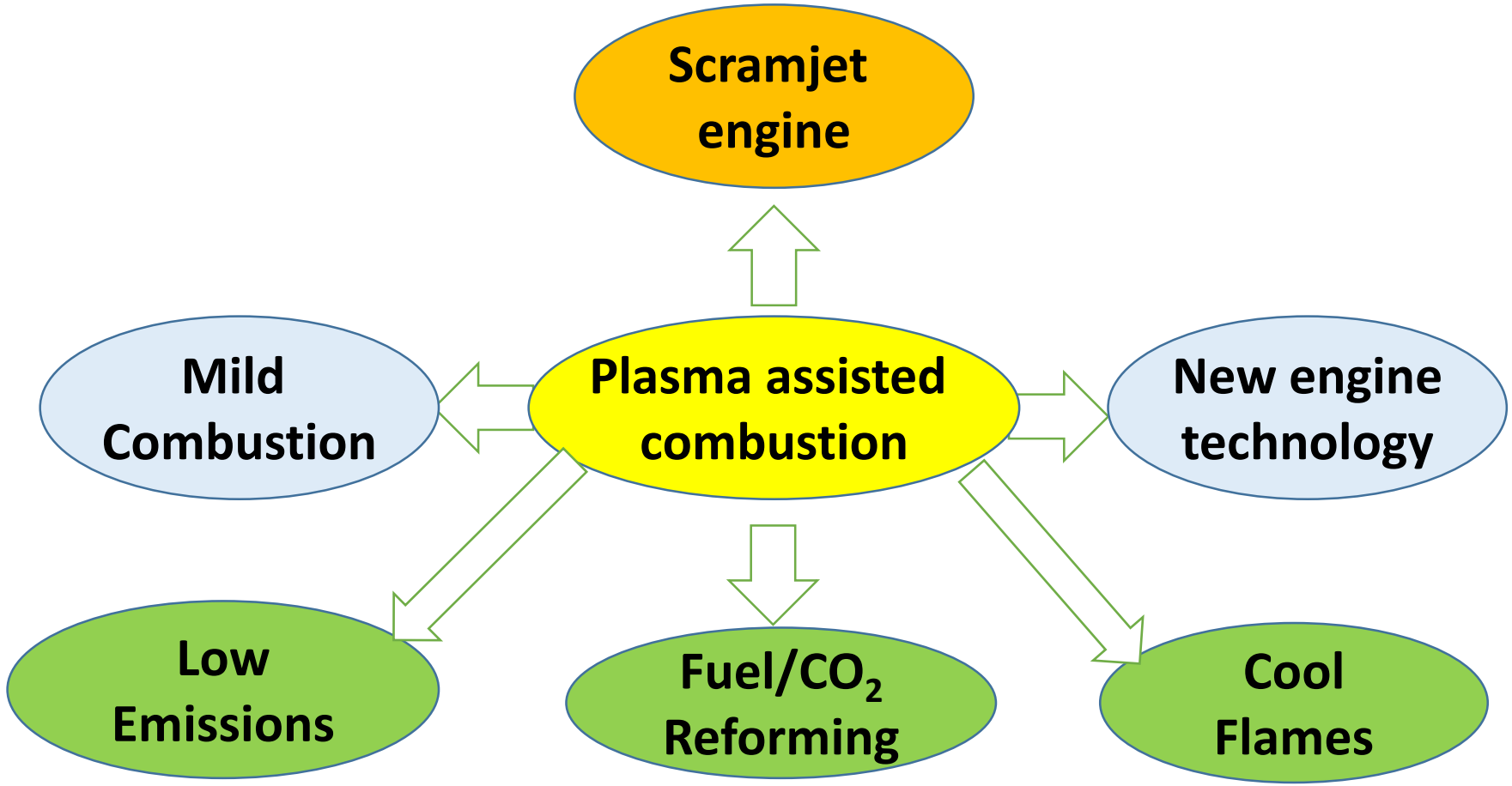

# 2. Plasma Discharges

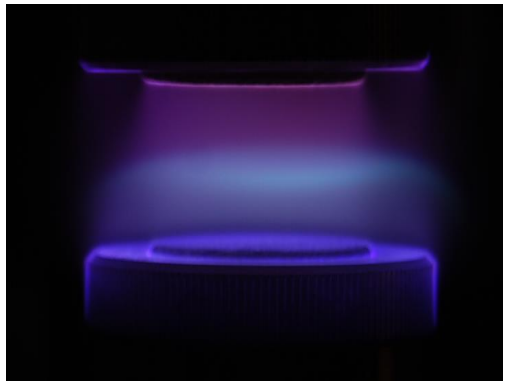

**Plasma:** A partially ionized, quasi-neutral charged mixture in which electrons and ions are separately free.

**Frequency:** DC, AC, RF, MW, Pulsed…

**Temperature:**

- Non-thermal (Non-Equilibrium plasma) $T_{gas}$ ~ 300K-2000K
  Cold plasma: $T_{trans} = T_{rot} < T_{vib} < T_e$

  Low pressure – DC, RF glow discharges

  Atmospheric pressure – DBD, Microwave, Corona & Micro-plasmas

- Thermal plasma (Equilibrium) $T_{gas}$ ~ 2000K-20000K
  Hot plasma: $T_{trans} = T_{rot} = T_{vib} = T_e$

**Discharge processes:** Electric field, Corona, glow, arc

**Discharge types:** Electron-beam, Corona, Dielectric barrier discharge (DBD), gliding arc, arc, micro discharge, surface discharge…

# Plasma frequency

## Perturbation of a neutral plasma

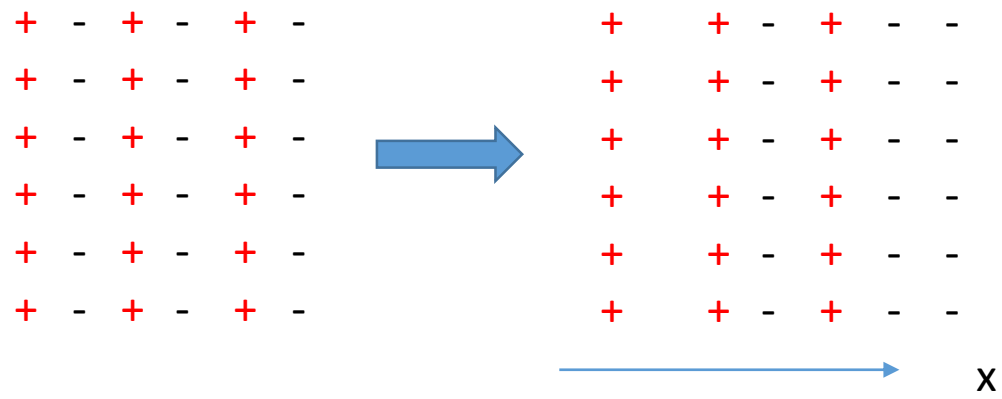


Total charge number: $Q = eVne$

Electric field (between two slabs): $E=\frac{Q}{\varepsilon A}=\frac{eVn_e}{\varepsilon A}=\frac{en_e}{\varepsilon}x$

Coulomb force on an electron: F=-eE

ε: permittivity

Equation of electron motion: $\mathbf{F}=m_e\mathbf{a}$ ⇒ $m_e\frac{d^2x}{dt^2}=-\frac{e^2n_e}{\varepsilon}x$

The frequency of electron plasma oscillation is: $\omega_p=\sqrt{\frac{e^2n_e}{m_e\varepsilon}}=9000\sqrt{n_e}$ (Hz)

If the electron density is $10^9$ $cm^{-3}$ , the frequency is about 300 MHz. Therefore, plasma is very fast to restore charge neutral properties.

The electron plasma frequency is critical to the propagation of electromagnetic wave in plasma. If the electromagnetic wave frequency (ω) is less than $\omega_p$, electrons in the plasma will response and extracts energy from the electric field and reflect the incident wave. If $\omega>\omega_p$, electrons in plasma can not response and the electric field will transmit through the plasma without reflection. Therefore, for a given ω, there is a critical plasma electron number density ($cm^{-3}$):

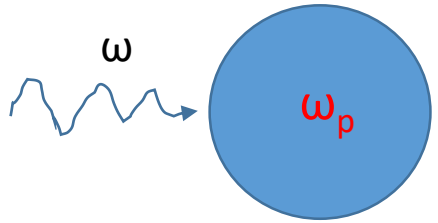


$$n_{e,c}=\frac{\omega_p^{\,2}m_e\varepsilon}{e^2}$$

At microwave frequency of 2.45 GHz, if the electron density is $7.5\times10^{10}$ $cm^{-3}$ , $\omega_p > 2.45$Gz, microwave will not penetrate to the interior of the plasma, but the plasma surface with reflection.

# Mean free path and collisional frequency

## Mean free path:

u: mean velocity
v: relative mean velocity
d: neutral particle diameter

$$\bar{u} = \int_0^\infty v f(u) du = \sqrt{\frac{8k_B T}{\pi m}}, \quad v = \sqrt{2}\bar{u}$$

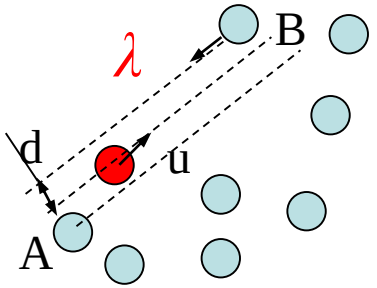


Mean free path

Cross section area : $\pi d^2$

The collision number per unit time : $\pi d^2 v n$

***the mean free path***

$$\lambda = \frac{\text{traveling distance per unit time}}{\text{number of collisions per unit time}} = \frac{u}{\pi d^2 v n} = \frac{1}{\sqrt{2}\pi d^2 n}$$

T=300K, p=1 atm, Molecule diameter: d=3.5A$^0$, the molecule number density:

$$n = p/(k_B T) = \frac{1.013\times10^5}{1.38\times10^{-23}\times300} = 2.5\times10^{25}/m^3 = 2.45\times10^{19}/cm^3$$

$$\lambda = \frac{1}{\sqrt{2}\pi(3.5\times10^{-10})^2\times2.5\times10^{25}} = 0.075\ \mu m$$

$$\nu_c = u/\lambda = 500/0.075\times10^{-6} = 6.7\times10^9/\sec$$

**For electron neutral molecule collisions in weakly ionized gas,**

$$\lambda_{e,n} = \frac{u_e}{n\ (\pi d^2/4)u_e} = \frac{4}{\pi d^2 n}$$

**Collision frequency**

$$\nu_{e,n} = u_e/\lambda_{e,n} = \frac{\pi d^2 n}{4}\sqrt{\frac{8k_B T_e}{\pi m_e}}$$

# Debye Shielding and plasma sheath

- Shielding effect: the free charges move towards a perturbing objective and neutralize the perturbing electric field effect in a characteristic distance of $\lambda_D$. $\lambda_D$ is the Debye length.

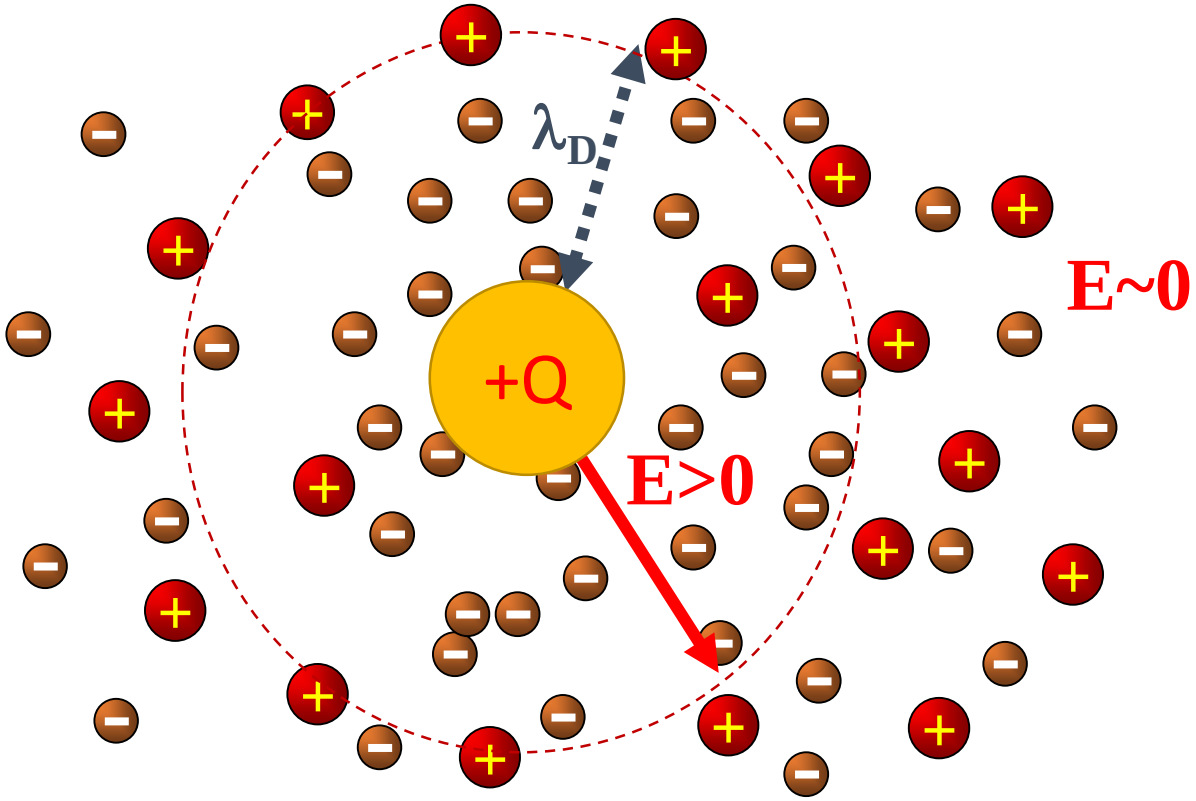


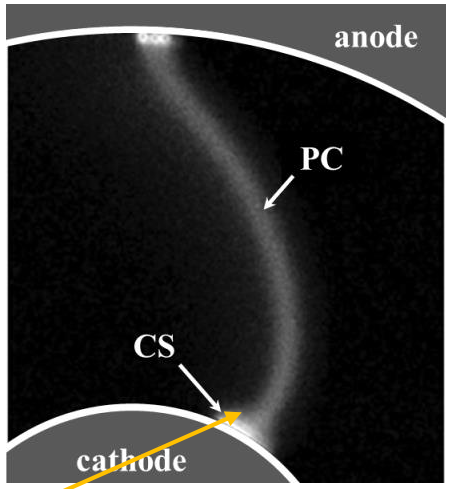


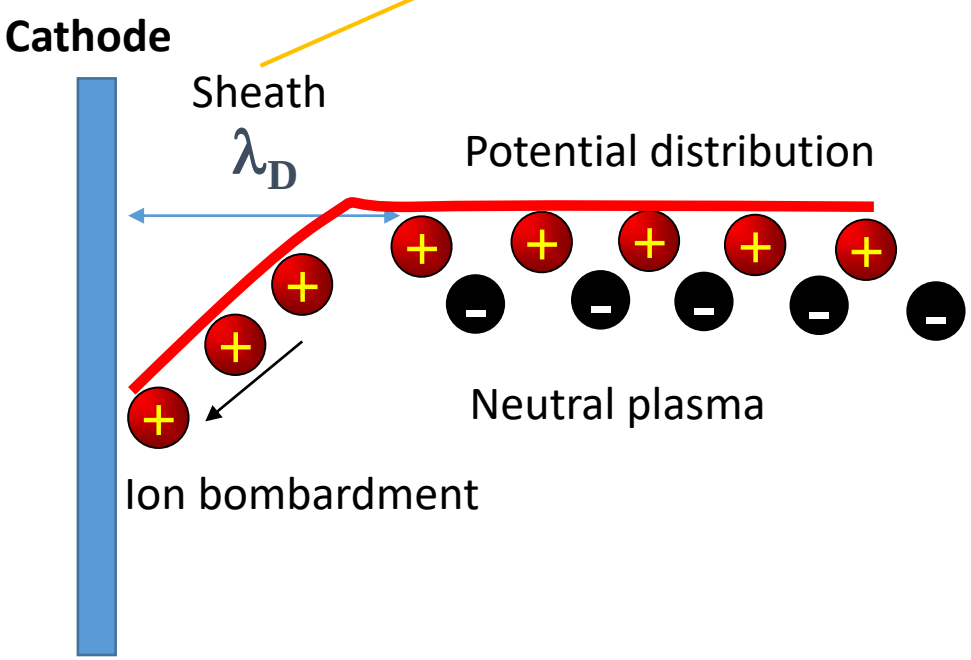


**How large is Debye length?**

## Maxwell equation

$$\nabla \bullet \mathbf{E} = \frac{e}{\varepsilon}(n_i - n_e)$$

$$\nabla \bullet \mathbf{B} = 0$$

$$\nabla \times \mathbf{E} = -\frac{\partial \mathbf{B}}{\partial t}$$

$$\nabla \times \mathbf{B} = \mu_B \mathbf{j} + \frac{1}{c^2}\frac{\partial \mathbf{E}}{\partial t}$$

**E:** electric field,
**B**: magnetic field
**j:** current
*ε:* permittivity
$\mu_{B:}$ permeability

$$\mathbf{j} = e(n_i v_i - n_e v_e) = e(n_i - n_e)\bar{v} + e(n_i V_i - n_e V_e)$$

$$v_i = \bar{v} + V_i$$

Mean + relative velocity

**Diffusion with an external electric field:** diffusion velocity and drifting velocity

$$n_i V_i = -D_i \nabla \cdot n_i + \mu_i n_i \mathbf{E}$$

$$n_e V_e = -D_e \nabla \cdot n_e - \mu_e n_e \mathbf{E}$$

$D_i$ Charge diffusivities,
$\mu_i$ *electron and ion mobilities*

**For weakly ionized plasma: $n_i << n$; $n_e << n$**

## Einstein relation

$$\frac{\mu_i}{D_i} = \frac{e}{k_B T}$$

$$\frac{\mu_e}{D_e} = \frac{e}{k_B T_e}$$

# Debye length

**In the Maxwell's equation:** $\nabla \cdot \boldsymbol{E} = \frac{e}{\varepsilon}(n_i - n_e)$ ε: the permittivity of the plasma

For a steady state problem: $\boldsymbol{E} = -\nabla\varphi \Rightarrow \nabla^2\boldsymbol{\varphi} = -\frac{e}{\varepsilon}(n_i - n_e)$

**Debye length**

$$\nabla^2\left(\frac{e\varphi}{k_B T_e}\right) = -\frac{1}{\lambda_D^2}\left(\frac{n_i}{n_0} - \frac{n_e}{n_0}\right)$$

$$\lambda_D = \sqrt{\frac{k_B T_e \varepsilon}{n_0 e^2}}$$

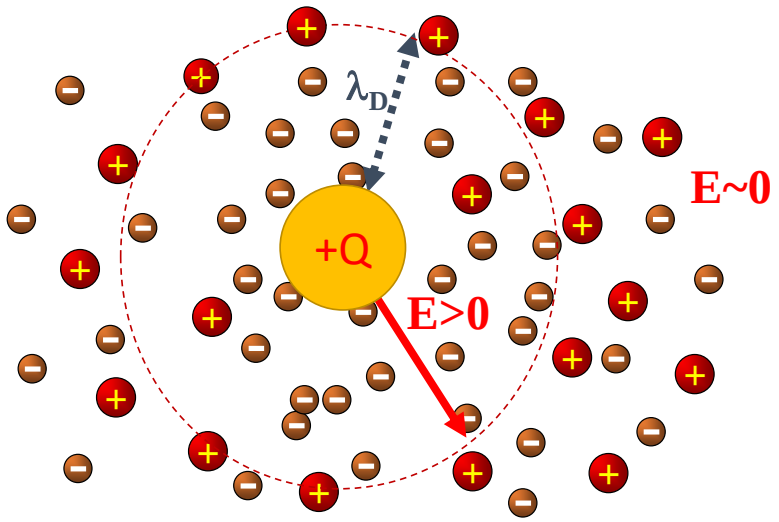


In air, if $T_e$ = 1000K and $n_0 = 10^{13}cm^{-3}$, we have $\lambda_D = 6.9 \times 10^{-5}$cm.

Therefore, plasma is almost quasi-neutral everywhere.

The equation means that the net charge potential will decrease exponentially in a length scale of $\lambda_D$

# Ambipolar diffusion (steady state neutral plasma)

**In one-dimensional plasma (zero flow velocity):** The ion and electrons fluxes are,

$$\Gamma_i = n_i V_i = -D_i \nabla \cdot n_i + \mu_i n_i \mathbf{E}$$
$$\Gamma_e = n_e V_e = -D_e \nabla \cdot n_e - \mu_e n_e \mathbf{E}$$

In steady state and quasi-neutral plasma:

$$\Gamma_i = \Gamma_e \qquad \mathbf{E} = -\frac{(D_e - D_i)\nabla n_e}{n_e(\mu_i + \mu_e)} : \text{ambipolar electric field}$$

Therefore: $\Gamma_i = \Gamma_e = -D_i \nabla n_i + \mu_i n_i \mathbf{E}$

$$= -D_i \nabla n_i - \mu_i n_i \frac{(D_e - D_i)\nabla n_i}{n_i(\mu_i + \mu_e)}$$
$$= -D_{ambi} \nabla n_i$$

In non-equilibrium plasma, Te is much greater than Ti, the ambipolar diffusivity is much higher than ion diffusivity.

$$D_{ambi} = \frac{(\mu_i D_e + \mu_e D_i)}{(\mu_i + \mu_e)} \approx D_i + \frac{\mu_i}{\mu_e} D_e = D_i(1 + \frac{T_e}{T_i}) \qquad (\mu_i << \mu_e)$$

# Energy transfer in Plasmas

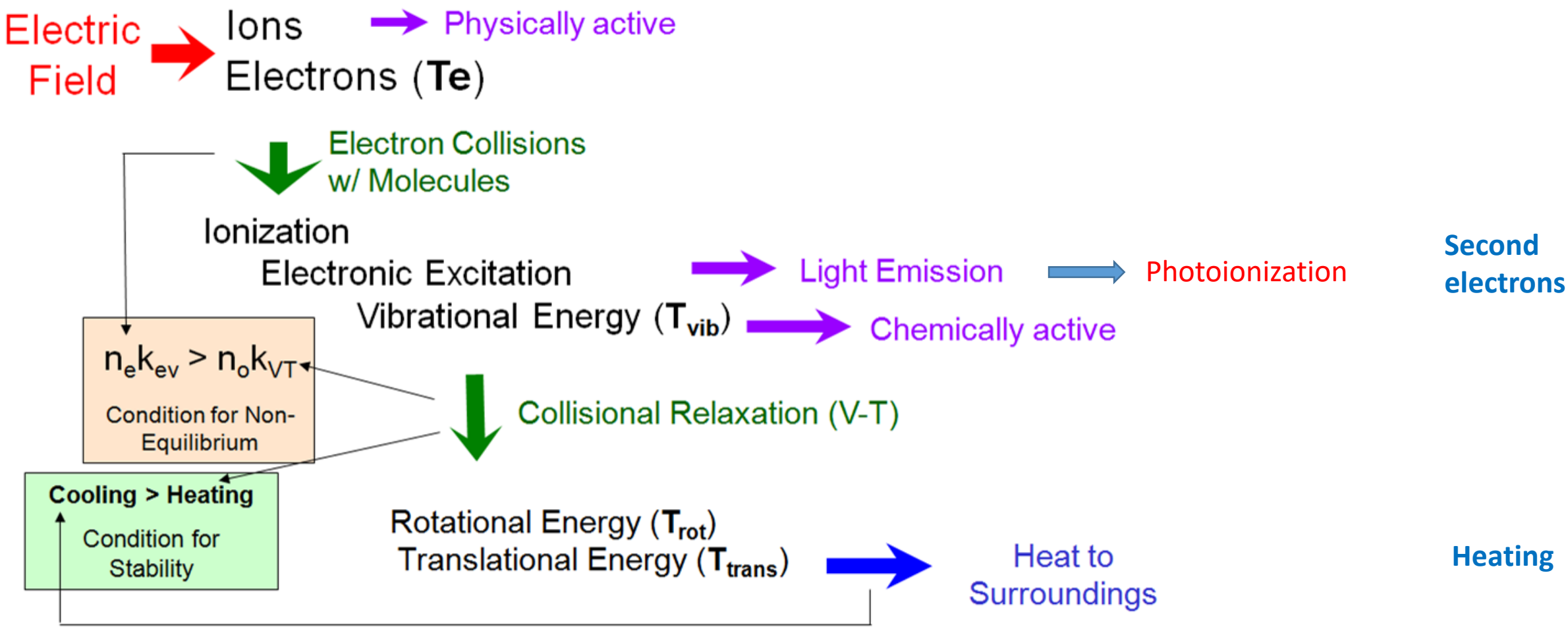

# Energy transfer in Plasmas: fast heating and vibrational energy relaxation

time-resolved and spatially-resolved measurements of $N_2$ vibrational temperature

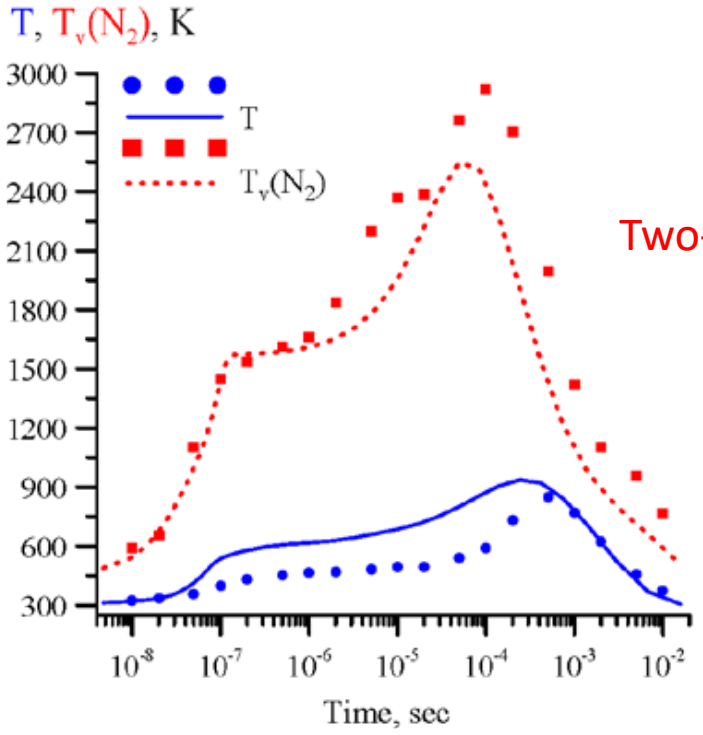


Two-step thermalization

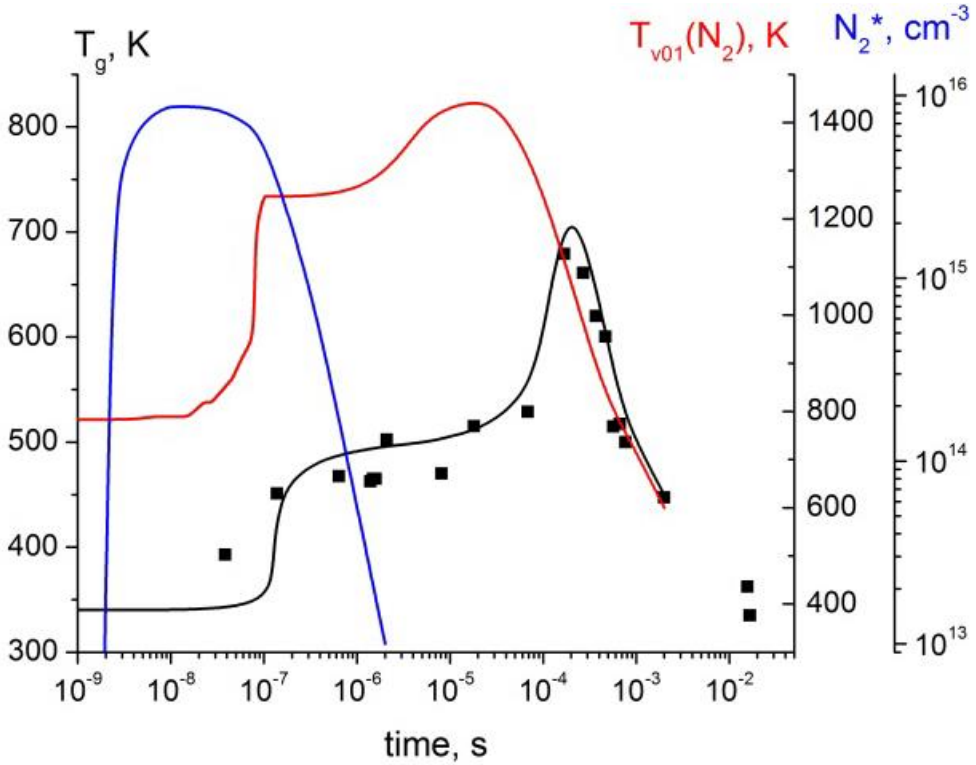


Figure 1. Experimental and predicted temperature and $N_2$ vibrational temperature during and after a ns pulse discharge in air between two spherical electrodes 1 cm apart at 100 Torr.

Figure 2. Experimental and predicted temperature during and after a ns discharge pulse in an $H_2$-air mixture ($\phi$=0.14) between two spherical electrodes 0.9 cm apart at 40 Torr, plotted together with predicted number density of electronically excited $N_2$ molecules and $T_v(N_2)$.

*Igor V Adamovich and Walter R Lempert, 2015, Challenges in understanding and predictive model development of plasma-assisted combustion, Plasma Physics and Controlled Fusion, Volume 57, Number 1.*

# Plasma and Plasma Properties

**Ionization processes**: Thermal ionization, electron impact ionization, photo-ionization for second electrons

$h\nu + O_2 = O_2^+ + e$

$e + O_2 = 2e + O_2^+$

$M + O_2 = M + O_2^+ + e$

**Electron quenching processes:** recombination and attachment

$e + O_2 = O_2^-$

$e + O_2^+ = O(^3P) + O(^1D)$

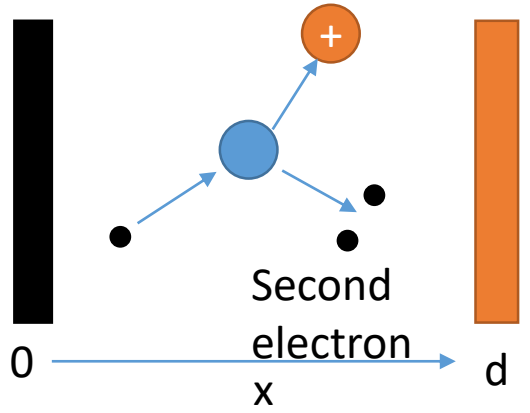


**Plasma temperature:** Electron temperature, vibrational and rotational temperature

**Electron temperature**: 1 eV = 11600 K = $1.6 \times 10^{-19}$ Joules.

**Equilibrium and non-equilibrium plasma:**

**Equilibrium:** Distribution function: Boltzmann

$$Q(1,E,V) = \sum_i g_i \exp(-\varepsilon_i / k_B T)$$

**Temperature: $T_e \approx T_v \approx T_n$**

**Non-equilibrium:** Distribution function: non-Boltzmann

$$\frac{\partial f}{\partial t} + \boldsymbol{v} \cdot \nabla f - \frac{e}{m}\boldsymbol{E} \cdot \nabla_v f = C[f]$$

**Temperature: $T_e >> T_v >> T_n$**

# A few examples

$T_e \approx T_v \approx T_n$

Near Equilibrium plasma

Electron temperature

arc

$T_n$~n*10,000 K

$T_e > T_v > T_n$

Electron number density

Gliding arc

$T_n$~n*1000 K

Non-Equilibrium plasma

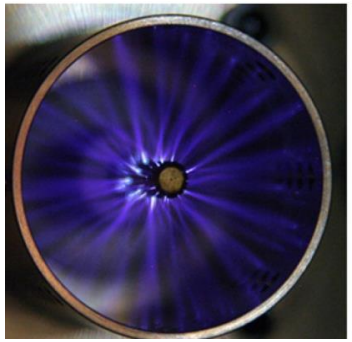

$T_e >> T_v >> T_n$

Corona

$T_n$~n*100 K

**Electron impact avalanche**

$$\frac{dn_e}{dx} = \alpha n_e$$

$$\alpha = Ape xp\left(-\frac{Bp}{E}\right) n_e$$

$$n_e = e^{\alpha x}$$

A,B: constants
E: electric field
p: pressure
$n_e$: electron number density

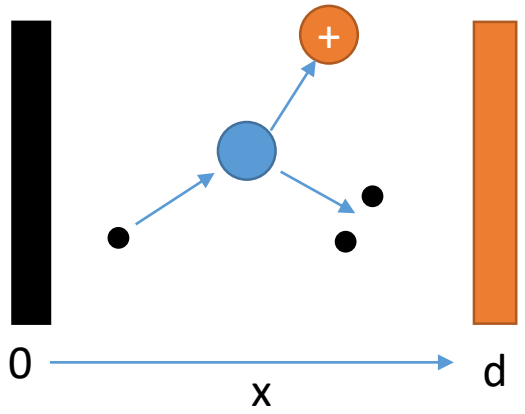


α: The 1st Townsend coefficient, inverse of net ionization length scale. It is determined exponentially by E/p or E/N

If $\alpha > 0$, electron avalanche phenomenon.

**Breakdown voltage:**

The minimum voltage between two electrodes that causes an arc. At the breakdown voltage, the rates of ionization and dissociative attachment becomes equal.

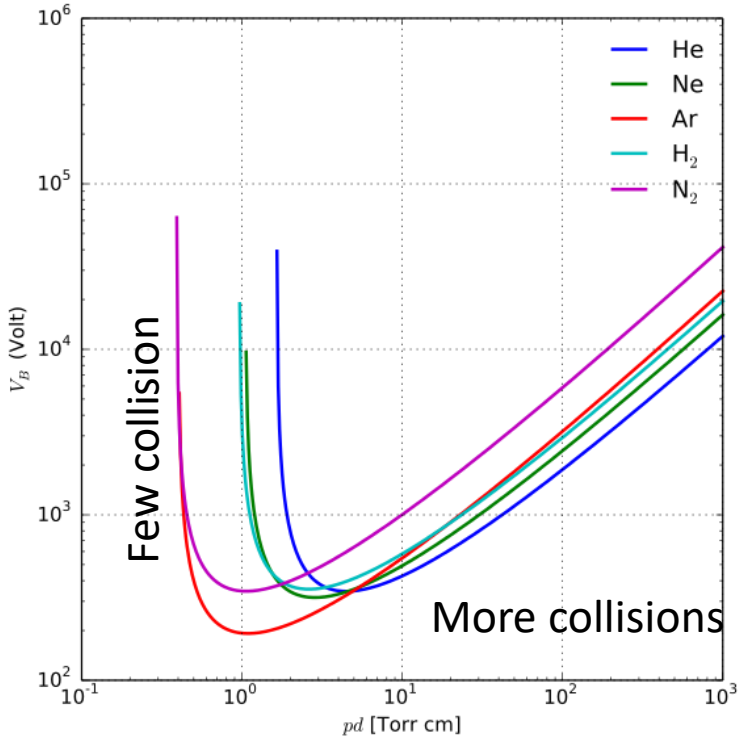


Lieberman, Michael A.; Lichtenberg, Allan J. (2005)

**Paschen's law:** The nonlinear dependence of breakdown voltage is to due to electron impact avalanche via collisioinal energy transfer

The breakdown field for atmospheric air~28.7 kV $cm^{-1}$

**Mean free path** (1 atm, air): Molecules: 0.1 μm, Electron-molecule: 5.5 μm

$pd_{min}$=1 torr cm at 760 Torr, $d_{min}$=13.2 μm, twice of the mean free path.

**How to produce uniform plasma at high pressure?**

# Plasma Discharges

**Streamer discharge**: a non-thermal narrow filamentary discharge channels formed at the initial stage of a spark breakdown by a high voltage pulse (1-100 ns). A streamer has a **streamer head** (space charge) with a high reduced electric field (~100 Td, 5-10 kV cm$^{-1}$ for air at atmospheric pressure) followed by a **streamer channel** with lower electric field and higher conductivity (charge number density). Formation of a streamer discharge occurs when the electric field in the streamer head is at the same magnitude or greater than a critical external electric field (4.4 kV cm$^{-1}$ in air at atmospheric pressure for a positive streamer, 8–12.5 kV cm$^{-1}$ for negative streamer). Streamers are fundamental components in many kinds of discharges such as the dielectric-barrier discharges, corona discharge, and spark. It is widely used in industrial ozone production, biomedical treatment, plasma assisted combustion, pollution control. Note: a microwave streamer is a hot plasma not a streamer.

**Streamer** Positive streamer

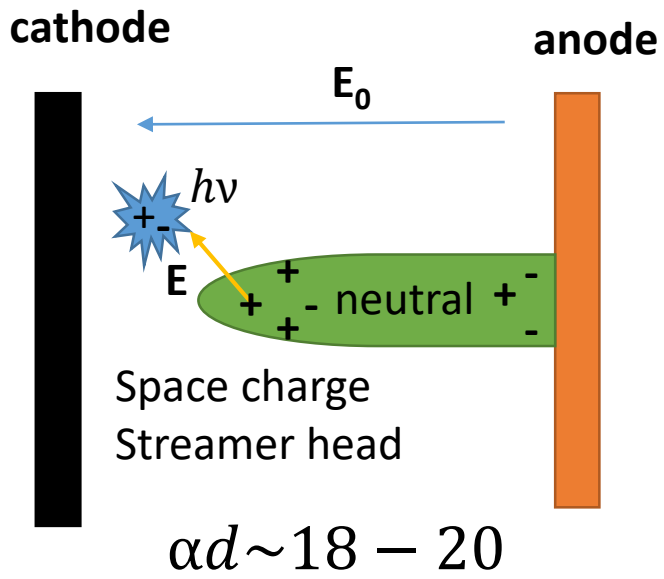


**Meek and Loeb criterion**: Streamer is formed once the total number of electrons in the electron avalanche is so large that their space charge field becomes comparable to $E_0$, the avalanche-to-streamer transition occurs. $\alpha d \sim 18 - 20$ and $n_e = 10^{13}$ cm$^{-1}$

**Stream propagation**: A space charge wave, which can penetrate into neutral gas with a velocity much higher than the electron drift velocity, up to a fraction of the speed of light.

**Energy balance:**

Power input by external field: $N_0 q_e E_0 V_s$

Power consumed in ionization: $\frac{dn_0}{dt} Q_e$

**Positive and negative streamers:**
Propagation of negative streamer requires a much stronger space charge field.

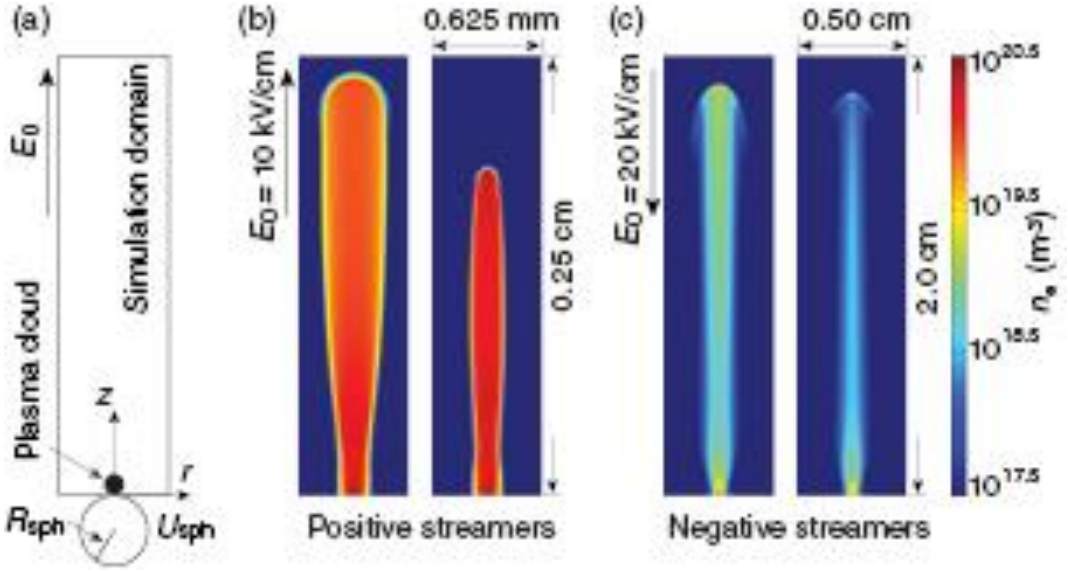


Fig. (a) Geometry of the simulation domain. (b) Propagation of growing and decaying positive streamers in an external field of 10 kV cm−1. Both positive streamers are initiated from a Gaussian distributed plasma cloud with a peak density of $10^{20}$ $m^{-3}$ and a characteristic size σ0 of 0.05 mm. The radius of the spherical electrode Rsph is 0.5 mm. The only difference is that in the left panel the spherical electrode has a potential Usph = 3.5 kV, whereas in the right panel Usph = 3.2 kV. (c) Propagation of negative streamers in an external field of 20 kV cm−1. For both negative streamers, the initial plasma cloud has a peak density of 1018 m−3 and a characteristic size of 0.10 mm. The electrode radius Rsph = 1.0 mm, and in the left panel Usph = 4.0 kV, whereas in the right panel Usph = 3.4 kV

Qin et al., J. Phys. D: Appl. Phys. 47 (2014) 435202 (9pp)

## Streamer propagation vs. Flame propagation

**Flame front**: auto-ignition and diffusive heat transfer, self-supported propagation
**Streamer**: ionization and space charge transfer, external field supported propagation

# Corona Discharge

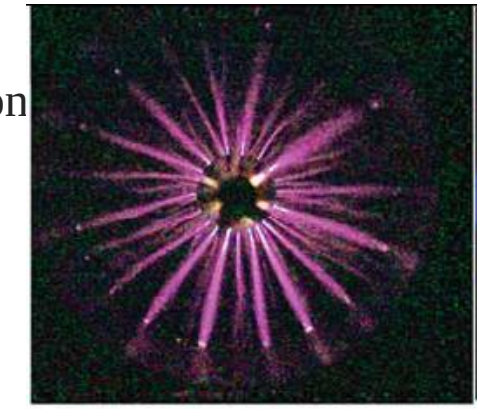

An discharge around a highly curved conducting electrode induced by a high electric field, but the external electric field is not high enough to cause a breakdown or arc. Widely used in ozone generation

**Positive corona**: electrons are attracted to curved positive electrode and have enough energy to cause electron avalanche. Electron energy is high, density is low.

**Negative corona**: ions are attracted to curved negative electrode. The photon emissions via ion-bombardment on electrode surface cause electron avalanche. Electrons have lower energy but higher density.

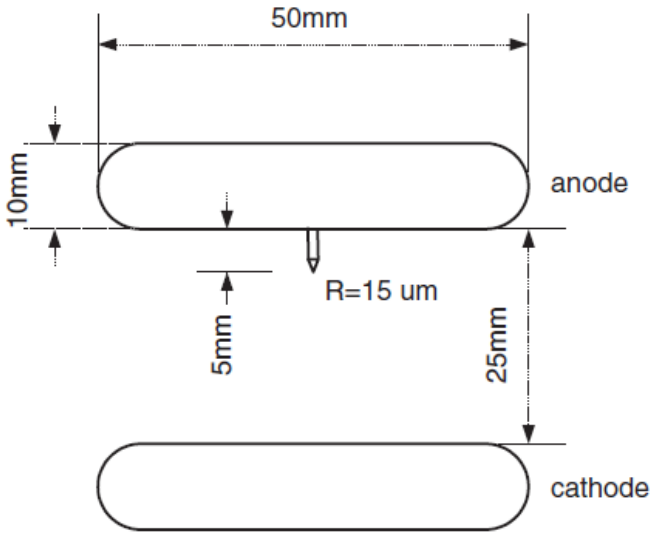


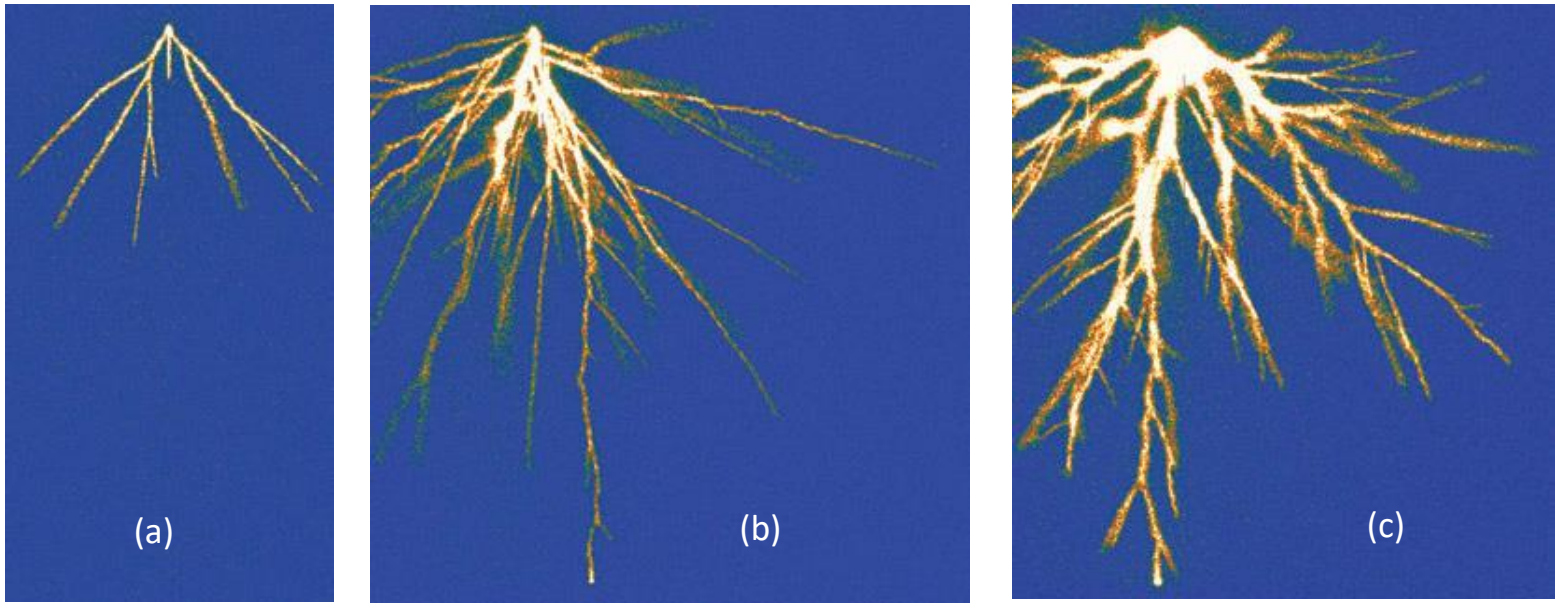


**Fig**. Pulsed corona discharge and positive streamer development**:** CCD photos of the point-wire discharge in air using 5$\mu$s optical gate. Applied voltages: (*a*) at 7.5 kV, (*b*) and (*c*) at 12.5 kV. For (*a*) and (*b*) the semiconductor switch is used, for (*c*) the spark gap. The electron temperature is about 5-10 eV. By E M van Veldhuizen and W R Rutgers**,** J. Phys. D: Appl. Phys. **35** (2002) 2169–2179 PII: S0022

# Dielectric barrier discharge (DBD) and NS DBD

A discharge that occurs between electrodes with at least one electrode is covered by dielectric materials. It is a corona discharge with a dielectric electrode. The existence of dielectric barrier limits the current and restricts transition of DBD discharge to arcing. DBD discharge often has filamentary micro discharge structures and is physically behaving like an incomplete streamer breakdown. DBD discharge has low electron number density and high electron energy and been widely used in ozone generators.

Rectangular quartz channel 22 mm x 10 mm in cross-section and 280 mm in length. Rectangular copper electrodes, 15 x 60 mm. High-voltage pulses 20 kV on the high voltage electrode, 25 ns duration at the half-amplitude, up to 20 KHz.

**Andrey Starikovskiy et al., 2014, AIAA-paper**

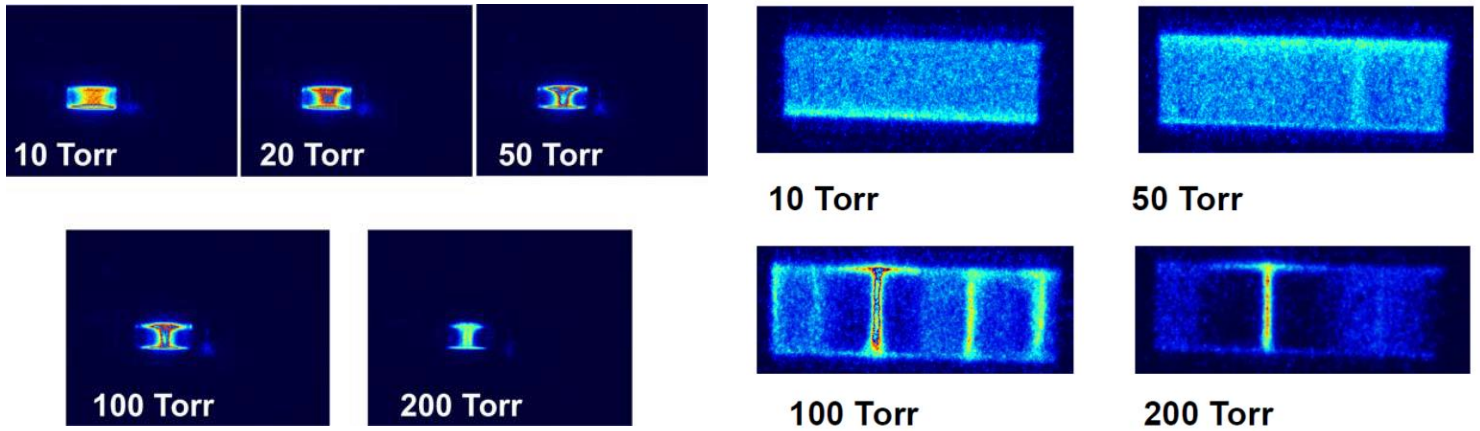


Nanosecond DBD discharge in air: 20 kV, 10 kHz, pulse N10. Left: Front view; Right: side view

**Conclusion:** NS discharge in DBD geometry in air is non-uniform. Initial electrical field's distribution and thermal ionization instability development form the non-uniform energy distribution in the discharge. This non-uniformity can play a key role in kinetic experiments in this type of the discharge.

# DC Glow Discharge (high special uniformity and volumetric)

A self sustained weakly ionized volumetric (non-filamentary) discharge supported by the secondary electron emission from the cathode. It has three distinctive structures: Negative glow, Faraday dark space, and positive column.

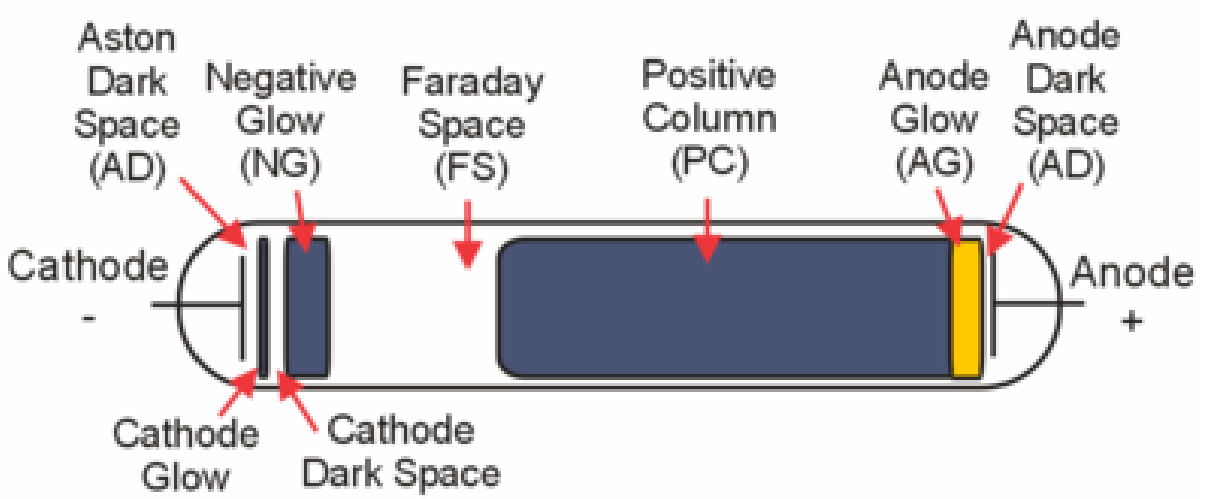


http://en.wikipedia.org/wiki/File:Electric_glow_discharge_schematic.png

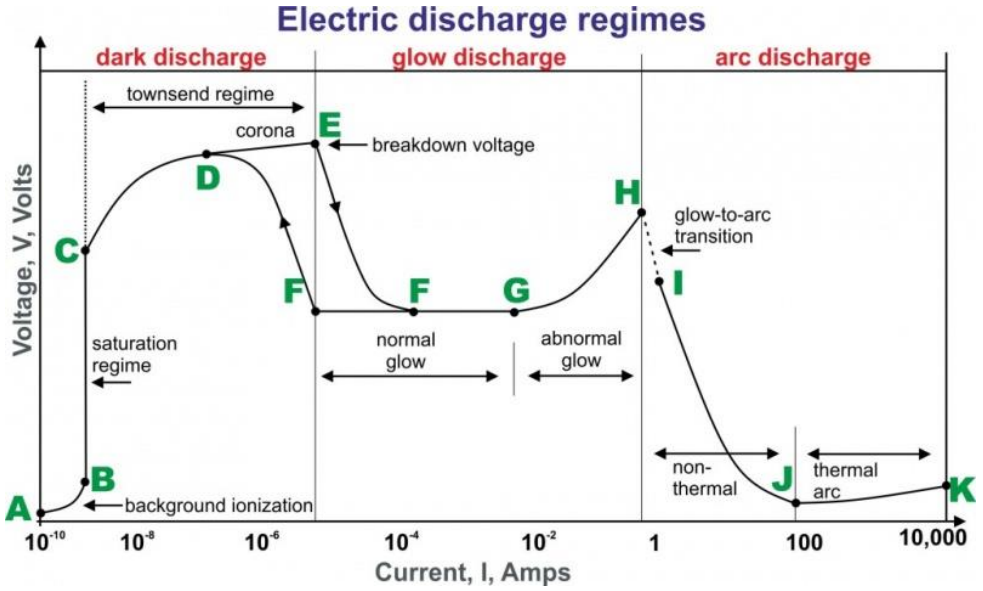


Princeton Plasma Physics Laboratory

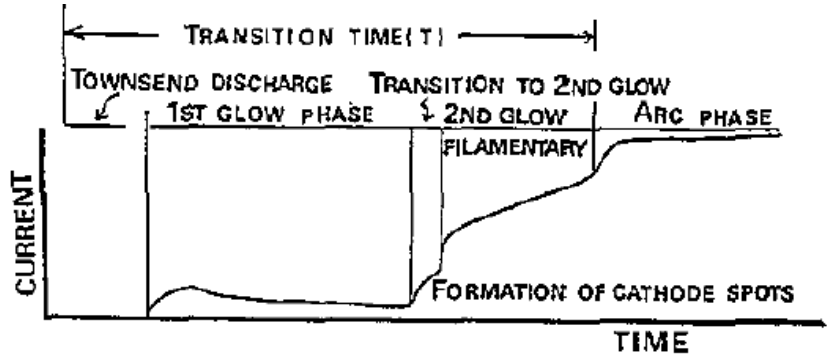


Figure 1. Transition from a glow discharge to an arc discharge (Kekez *et al* 1970).

The glow discharge is stable in a low pressure, but it is possible to stabilize such a plasma at atmospheric pressure if three requirements are met: (i) use of a source frequency of over 1 kHz, (U) insertion of a dielectric plate (or plates) between the two metal electrodes, (iii) use of a helium dilution gas.

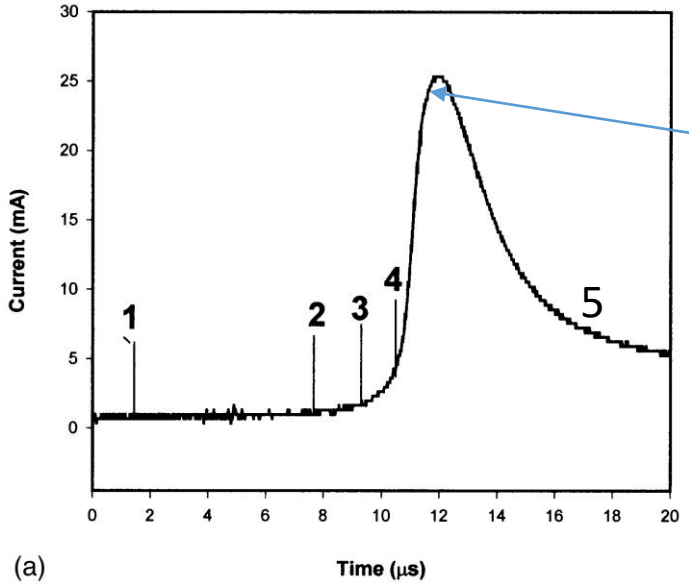


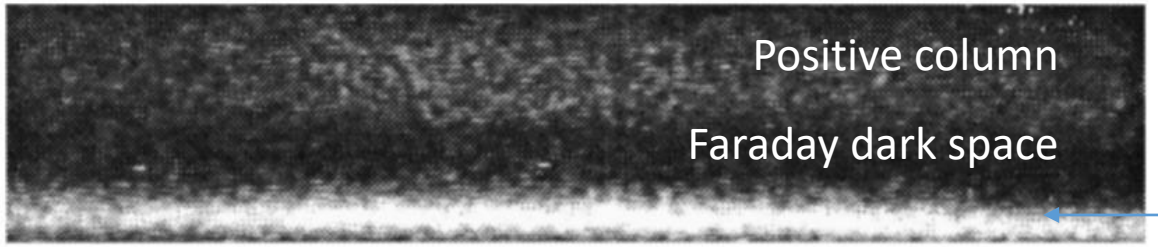


FIG. 2. 10 ns exposure time photograph of the gap taken when the discharge current is maximum. The gap length is 5 mm and the cathode is located at the bottom.

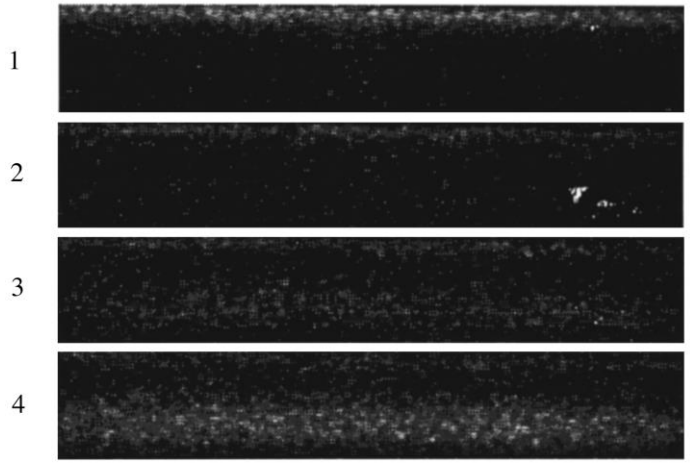


Cathode is at the bottom

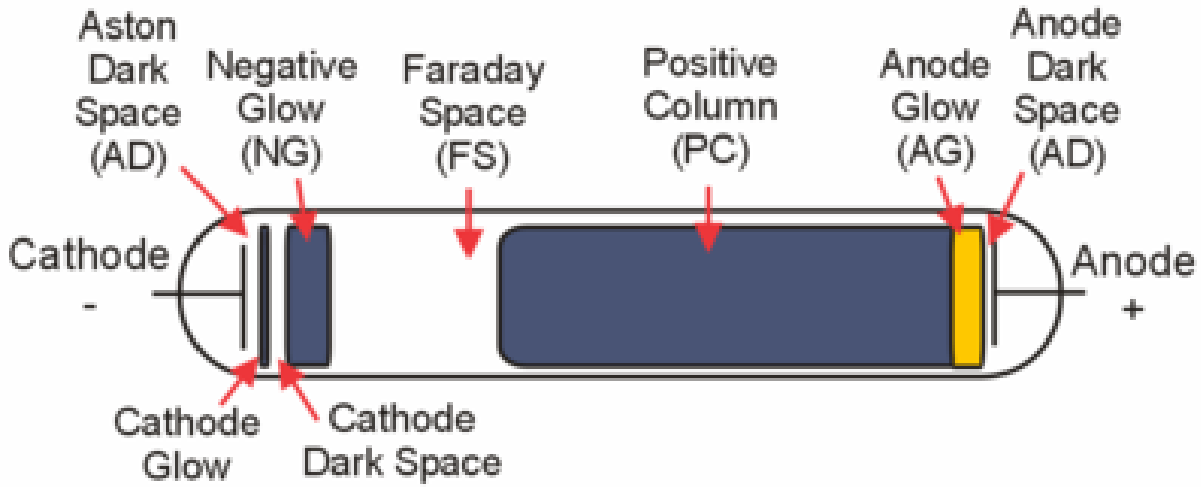


FIG. 1 100 ns exposure time photographs of the gap taken during the discharge initiation, the discharge current being periodic. The number on the current wave form a) corresponds to the number on the left side of the picture b) and indicates the time when the picture was taken. The gap length is 5 mm. In each picture, the cathode is located at the bottom. Francoise Massines et al., J. Appl. Phys., Vol. 83, No. 6, 15 March 1998

# Atmospheric pressure DC glow discharge

David Staack, Bakhtier Farouk, Alexander Gutsol and Alexander Fridman, Plasma Sources Sci. Technol. 14 (2005) 700–711

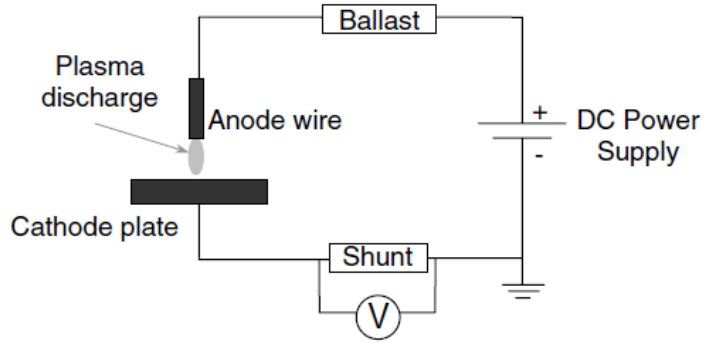


**Figure 1.** Electrical circuit used to generate and analyse the glow discharge.

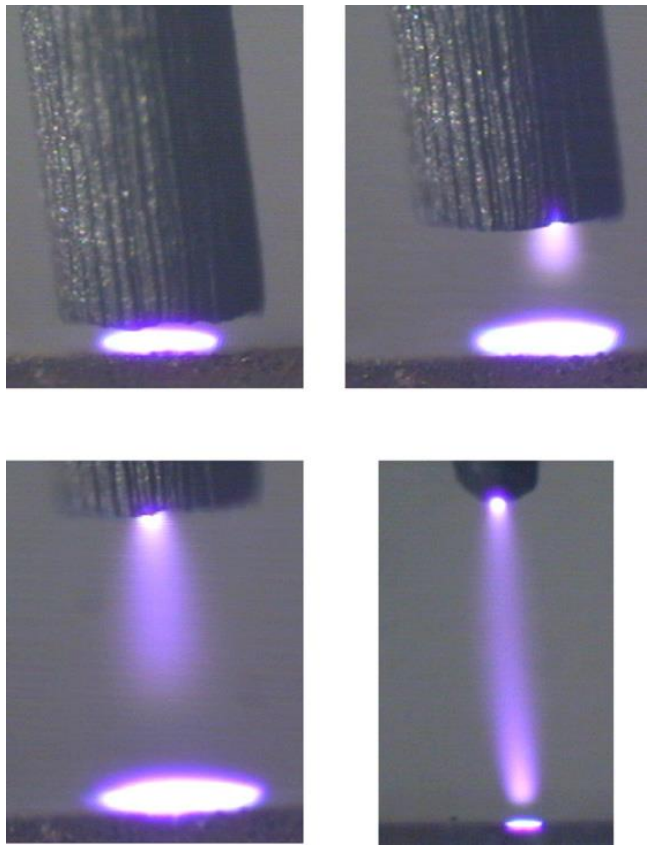

**Figure 2.** Images of glow discharge in atmospheric pressure air at (*a*) 0.1 mm, (*b*) 0.5 mm, (*c*) 1mm and (*d*) 3mm electrode spacing

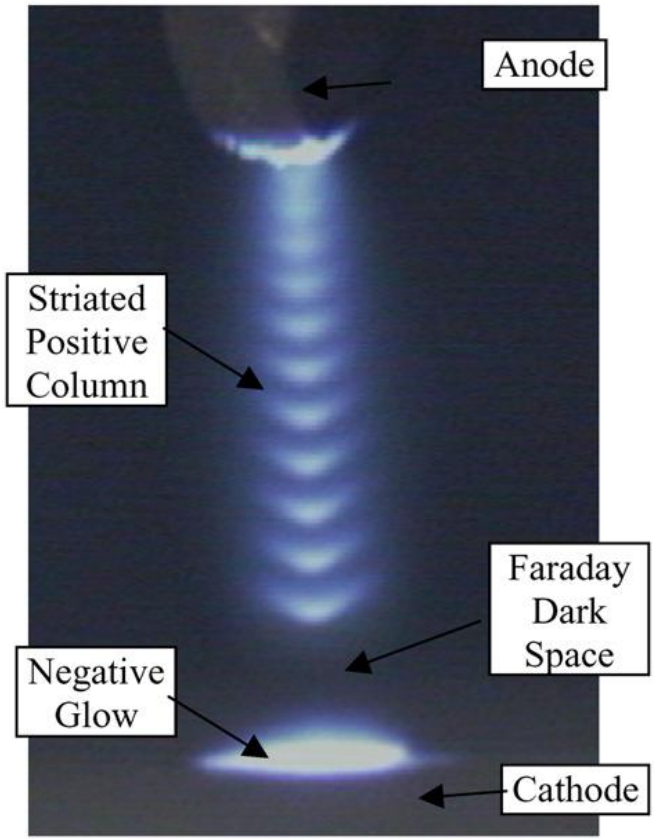


**Figure 3.** Image of the glow discharge in atmospheric pressure hydrogen. Positive column and negative glow are visible. In addition standing striations are visible in the positive column.

# Transition from micro glow discharge to equilibrium arc discharge

- Rotational temperature ($T_{rot}$) increases with vibrational temperature ($T_{vib}$) decreases with increase in pressure.
- Above 100 psi, they are measured to be within 500K of each other which is equal to the uncertainty in $T_{vib}$ fitting.

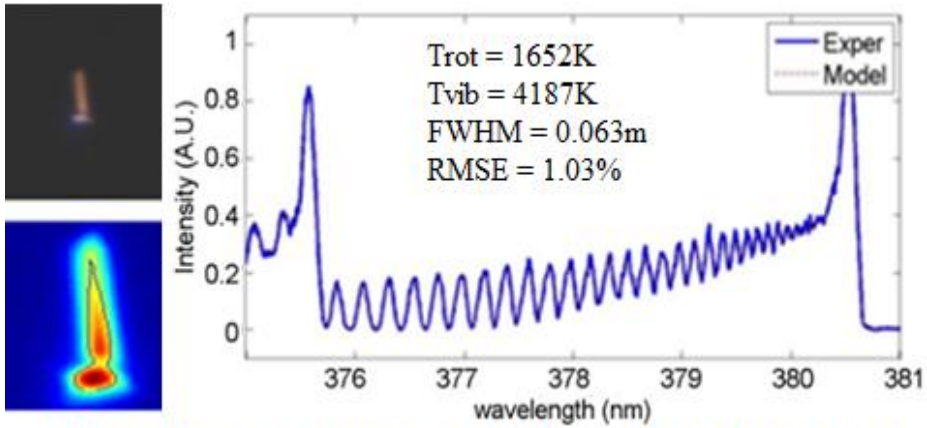


0.5 mA, 50 psi, 33.4 μm, Trot =1652K, Tvib = 4187K, RMSE =1.03%

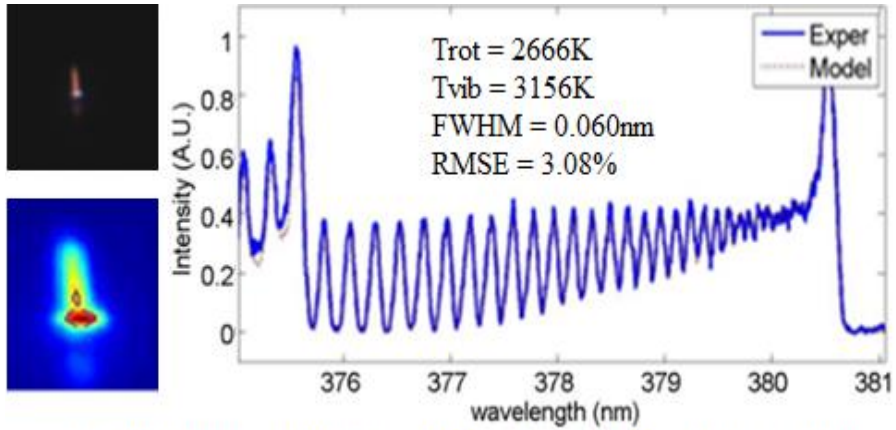


0.5 mA, 120 psi, 13 μm, Trot =2666K, Tvib = 3156K, RMSE =3.08%

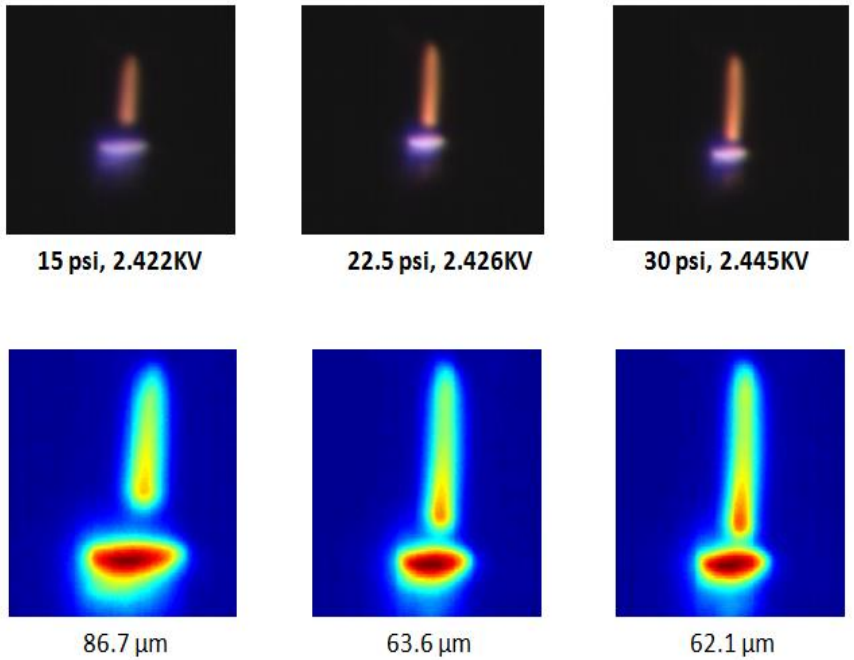


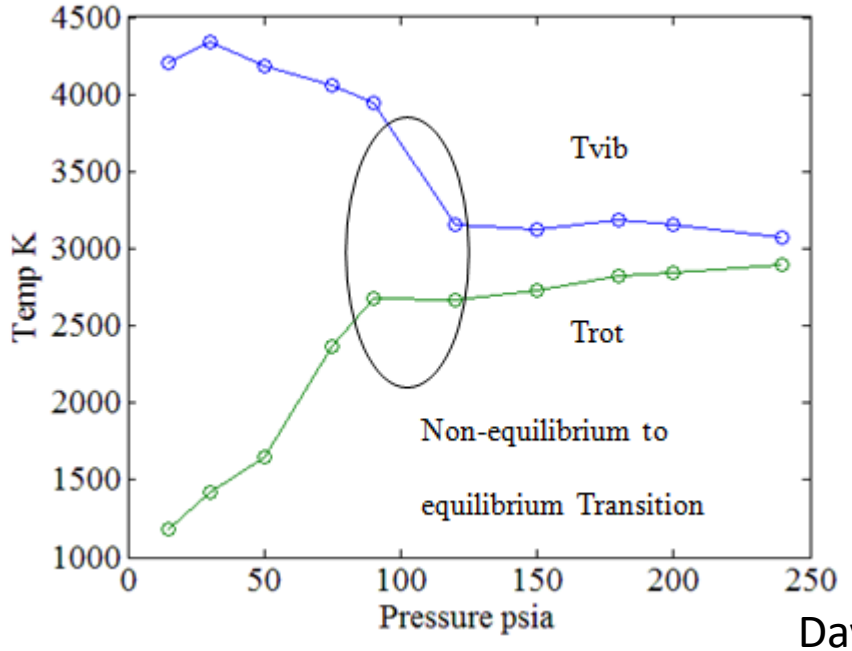

# Spark Discharge

A small volume, high temperature, and high current equilibrium arc initiated by a high voltage breakdown discharge (~10 ns). It has high current (1-1000 A), low voltage (10-100 V), and low electron temperature (~1 eV). Spark discharge is widely used in gasoline engines. The role of spark discharge is to create high temperature environment for ignition. Laser ignition is also to create a spark.

# Plasma torch

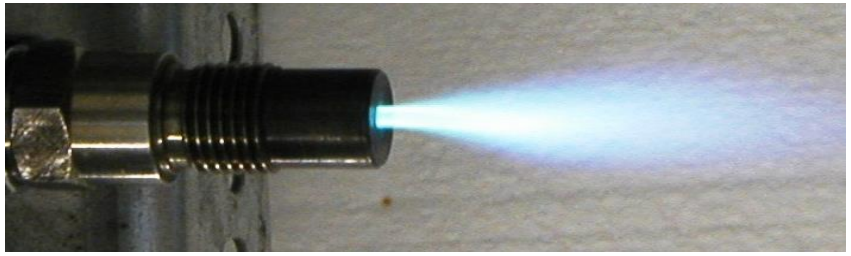

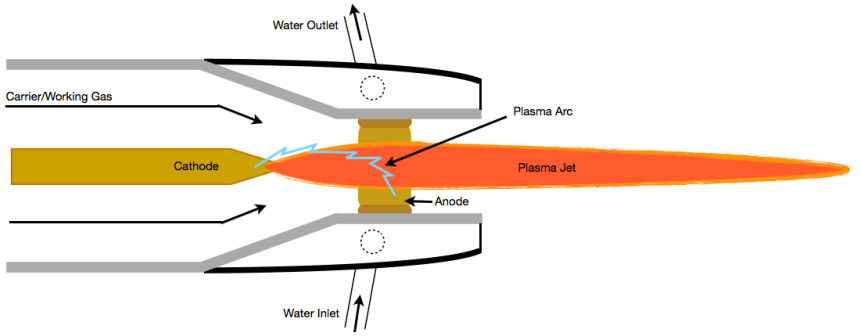


Plasma torch is also a continuous electric arc. It is high temperature near equilibrium plasma. It is widely used in ignition and materials processing. The temperature, power, and electron number density is very high. It mostly places a thermal effect in dissociating reactants and accelerating chemical reactions.

Meghnad Saha derived an equation for the relative number of atoms in each ionization state in an equilibrium plasma:

$$\frac{n_{i+1}}{n_i} = \frac{2g_{i+1}}{n_e g_i}\left(\frac{2\pi m_e k_B T}{h^2}\right)^{3/2} e^{-\frac{E_{i+1}-E_i}{k_B T}}$$

It depends on the number density of electrons, $n_e$. This is because as the number density of electrons increase, the electric field decreases and thus lower the ionization state.

# Gliding arc

a gliding non-equilibrium electric discharges invented by Lesueur et al. [1]. The main distinctive aspect of the gliding arc is a high level of non-equilibrium with both high electron temperature (1-2 eV) and high electron density as well as high gas temperature (~2000 K). It can be inexpensively generated under near-to-atmospheric pressures.

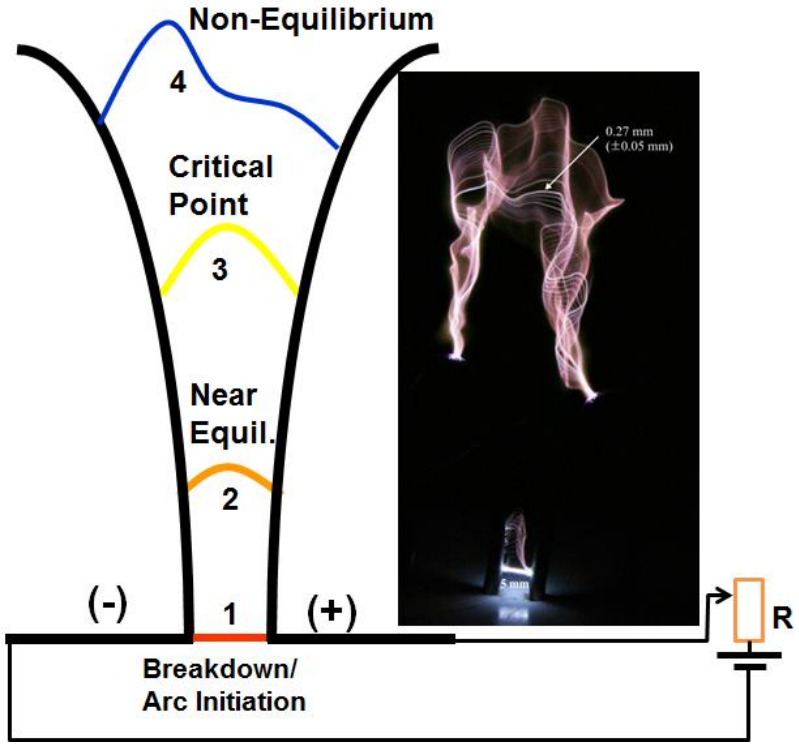


Fig. 1 Left: Schematic of a traditional gliding arc plasma discharge with the numbers corresponding to the sequence in time evolution of the arc as it moves along the electrodes (Ombrello and Ju). Right: direct image of a gliding arc time trajectory [Courtesy from Dr. Z.S. Li at Lund University].

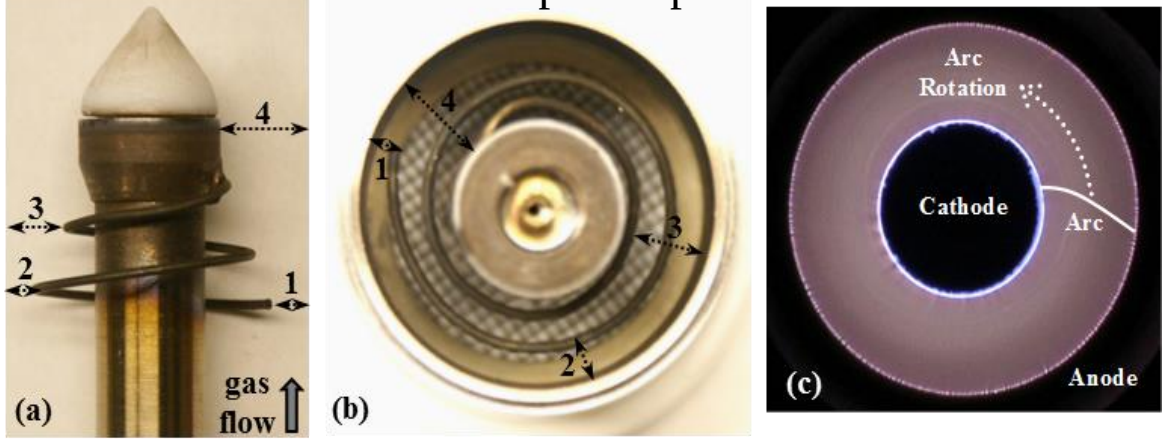


Fig. 2 Pictures of the gliding arc plasma system with the (a) side view of central electrode, (b) top view of system, and (c) time integrated top view photograph of the magnetic gliding arc creating a plasma disk to quasi-uniformly activate the flow. The numbers in (a) and (b) indicate the path of the gliding arc from initiation, point 1, to arc rotation/elongation, points 2 and 3, and final arc stabilization, point 4.

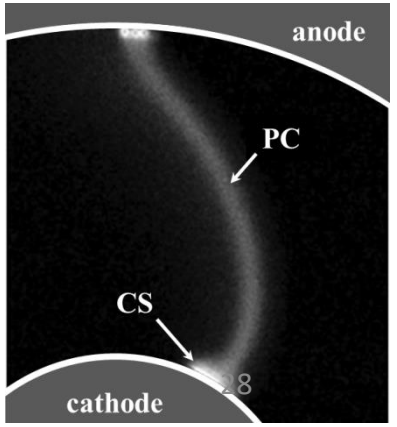


Fig. 3 Short exposure grayscale photograph of the magnetic gliding arc discharge once stabilized at the largest gap, with the cathode spot (CS) and positive column (PC) shown.


[1]. H. Lesueur, A. Czemichowski and J. Chapelle, *Frenchpatent* 2 639 172.

[2] A Fridman, S Nester, LA Kennedy, A Saveliev, O Mutaf-Yardimci, Gliding arc gas discharge, *Prog. Energy Combust. Sci*. 25 (2), 211-231

[3] Ombrello et al., AIAA Journal 2006.

**Energy conservation equation** $$\frac{1}{r}\frac{\partial}{\partial r}\left(r\lambda(T)\frac{\partial T}{\partial r}\right)=\sigma(T)E^2$$

Electrical conductivity. $\sigma^2(T)/\sigma_0{}^2=\exp(-E_0/k_BT)$

Temperature: $T$

Effective electric field strength: $E_0$

**Conductive arc heat loss per unit length from the solution**

$$W=2\pi r\lambda(T)\frac{\partial T}{\partial r}=16\pi\lambda(T_0)k_BT_0{}^2/E_0$$

From Ohm's law: $V_0=RI+Wl/I$

, We have: $I=(V_0\pm\sqrt{V_0^2-4WlR})/2R$

Corresponding to steady and unsteady gliding arc.

**Electric field:** $E=\frac{W}{I}=2WR/(V_0\pm\sqrt{V_0^2-4WlR})$

**Critical condition:** $V_0^2-4WlR=0$

$$l_{crit}=V_0^2/(4WR),\qquad I_{crit}=V_0/(2R),$$

$$V_{crit}=V_0/2,\qquad W_{crit}=V_0{}^2/(4R),$$

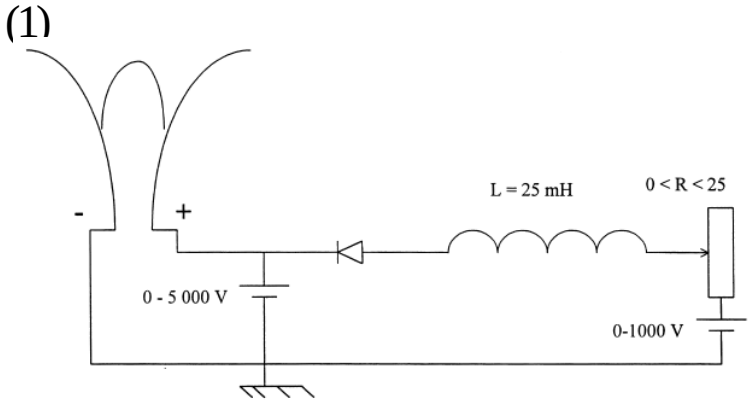

Fig. 1. Typical gliding arc discharge electrical scheme.

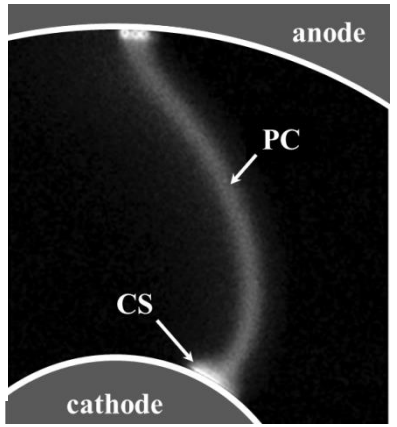


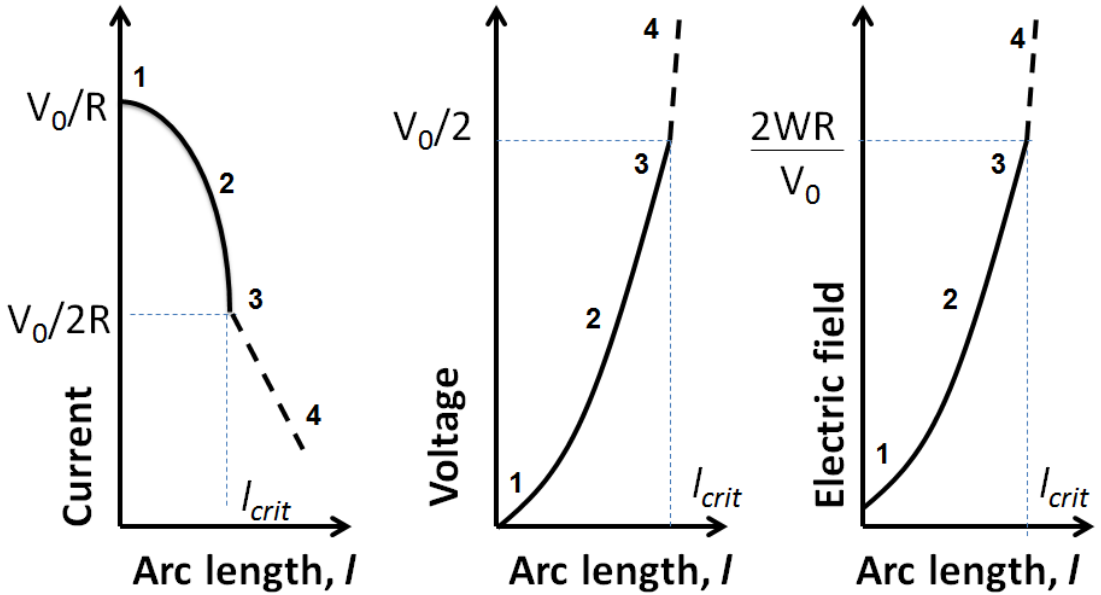

# Gliding arc voltage

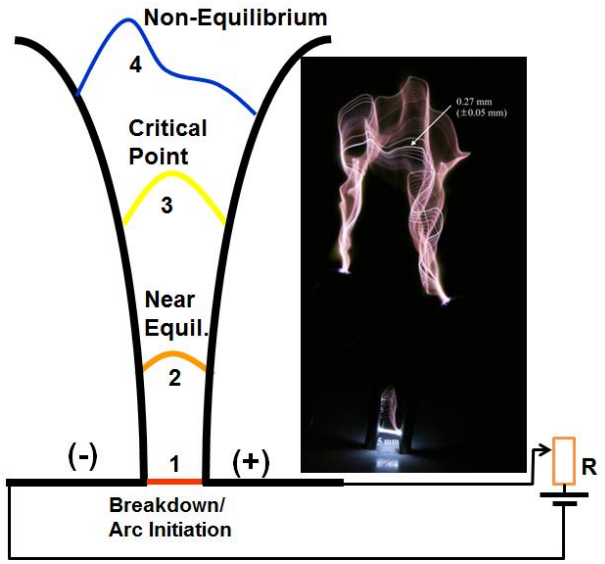


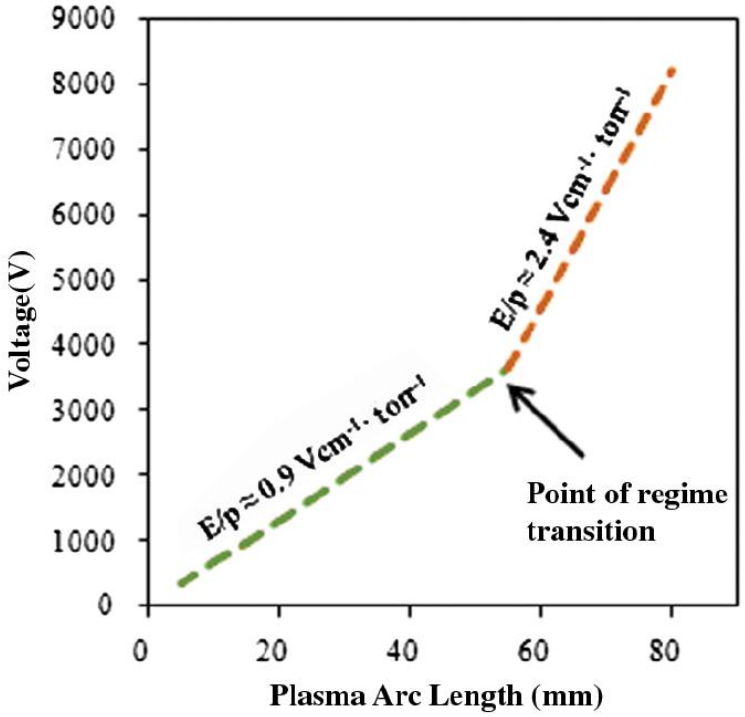


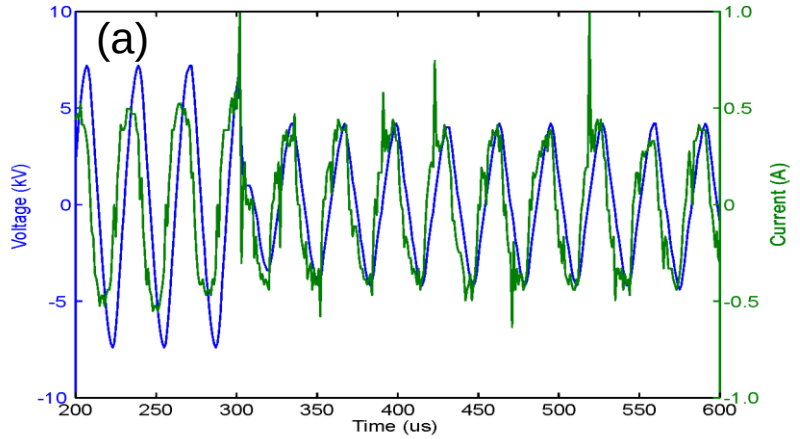


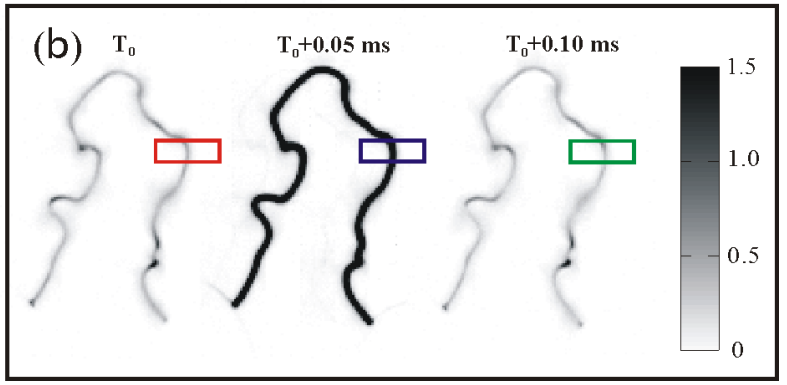


Fig. 2 Left: Plot of the increase in electric field in plasma after the transition point in a gliding arc discharge [8]. Right: three sequential frames of gliding arc images recorded by a high-frame-rate camera, showing the conversion from a glow-type discharge to a much brighter spark-type discharge [7]. (Courtesy from Dr. Z.S. Li at Lund University)

# Gliding arc dynamics and radial production

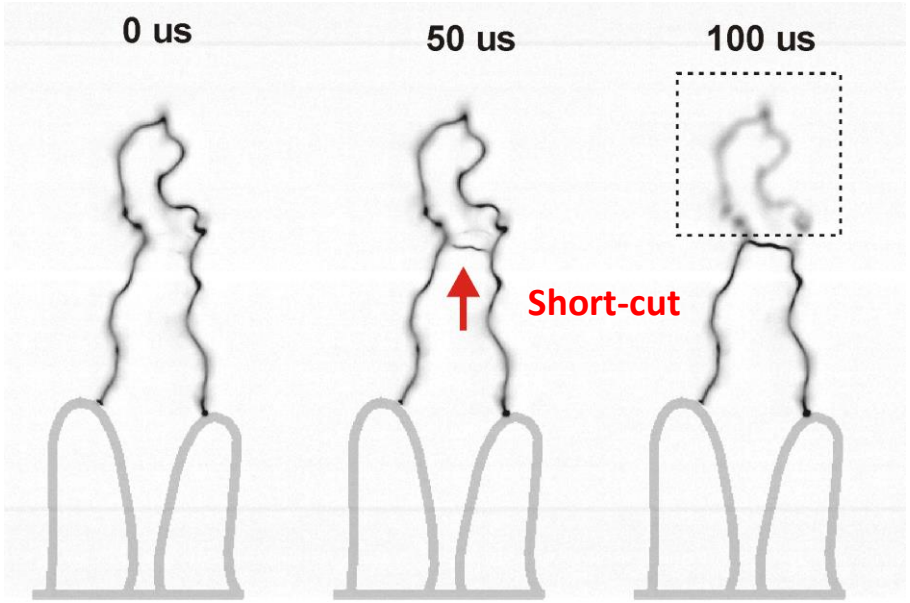


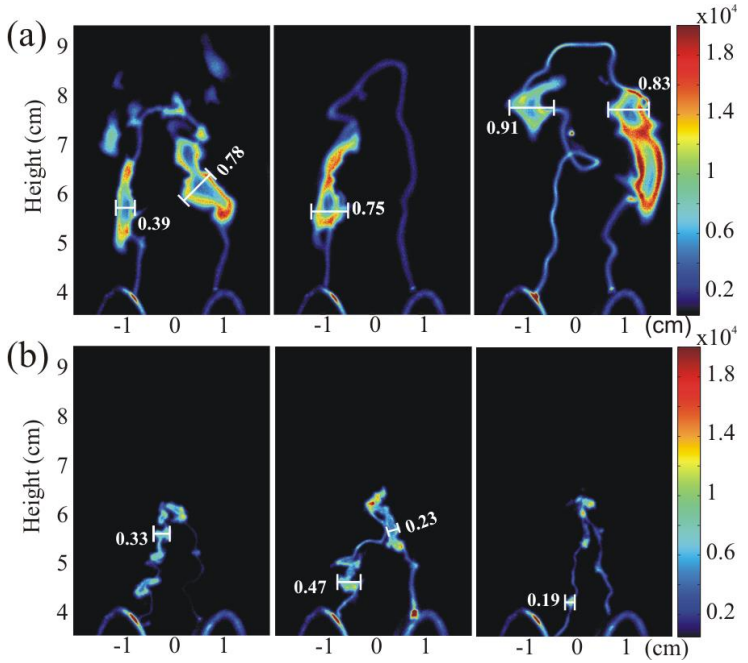


**Fig. 3 Left: A short-cut event recorded at 20 kHz framing rate using an exposure time of 13.9 μs. The short-cut current path is indicated by the arrow in the frame of t = 50 μs. Right: Three typical single-shot OH PLIF images of a gliding arc using an exposure time of 2 μs, at two flow rates (a) 17.5 SLM, (b) 42 SLM. The typical thickness of the OH distribution is labelled in the images with unit of centimeters [6, 7] (Courtesy from Dr. Z.S. Li at Lund University)**

# Magnetic gliding arcs

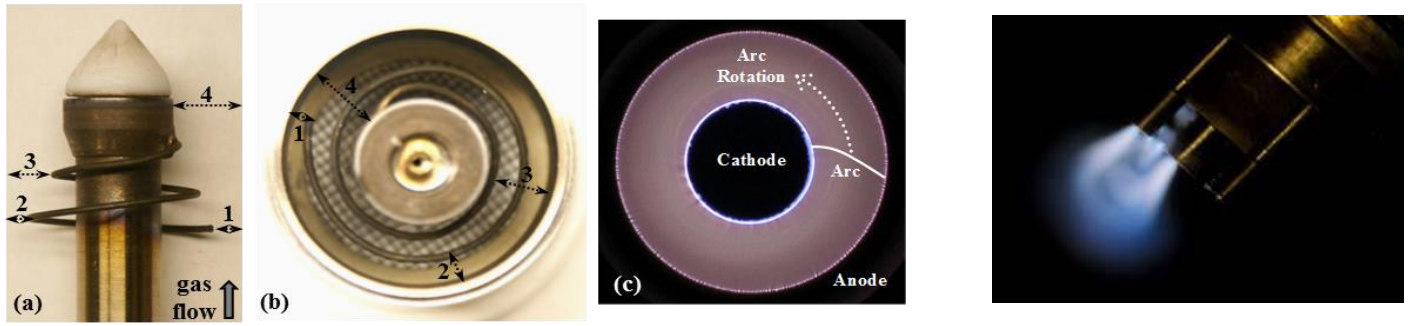

# RF and Microwave discharges

In DC and AC discharges, electrical power is delivered to plasma by moving electrons/ions to the electrodes across the cathode and anode sheaths. When the electrical frequency is very high like RF and MW, the time required for charge particles to move across the sheath becomes comparable or longer than the wave period of electrical field . Therefore, the interaction between electrical field and plasma is exclusively by charge displacement current, not by a directed current to electrodes. Therefore, it can be delivered without requirement of an electrode in contact with plasma by a sheath.

## RF & MW plasma coupling

- Inductive coupling: via oscillating magnetic field
- Capacitive coupling: via oscillating electric field

### RF discharge (10k-100M Hz)

$\omega > \omega_p$ Particle interaction

Low pressure-1 atm
Field wavelength: meters
Lower electron energy (1-2 eV)
Some sheath

### Microwave discharge (1G-300G Hz)

$\omega(n_e > 7\times10^{10} cm^{-1}) > \omega_p$ Collective interaction

Low pressure-high pressure
Field wave length: 12.24 cm at 2.45 GHz
Higher electron energy (5-15eV)
No high voltage sheath

# Breakdown condition of microwave discharge

**Electron production, attachment, and diffusion:**

$$\frac{dn_e}{dt} = n_e(\nu_i - \nu_a) + D\nabla^2 n_e$$

**$\nu_i$: ionization rate, $\nu_a$: attachment rate**

**Diffusivity of electrons (no Ambipolar diffusion):**

$$D = \frac{1}{3} l\bar{v} = \frac{\bar{v}^2}{3\nu_c} = \frac{8eT_e}{3\pi\nu_c m_e}$$

**Introducing a diffusion length scale:**

$\Lambda$ : characteristic diffusion length of electrons

**Electron production, attachment, and diffusion:**

$$\frac{dn_e}{dt} = n_e(\nu_i - \nu_a) - \frac{D}{\Lambda_2} n_e$$

$$n_e = n_{e0} e^{(\nu_i - \nu_a - \frac{D}{\Lambda_2})t}$$

**Breakdown condition:**

$$\nu_i(E/N) - \nu_a(E/N) = \frac{D}{\Lambda_2}$$

# Microwave discharge for ignition and flames

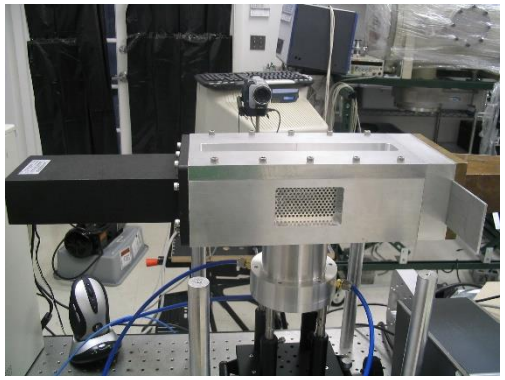

Miles et al., Princeton

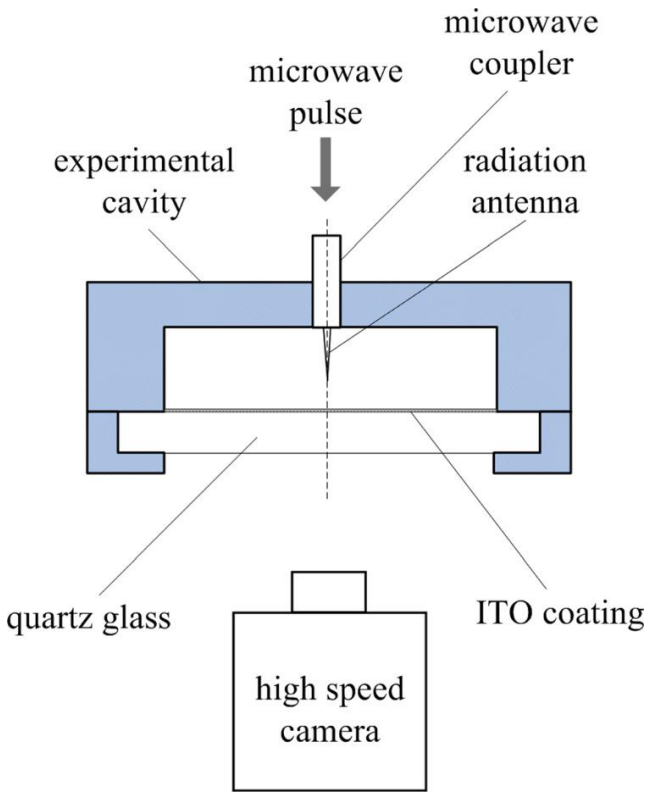


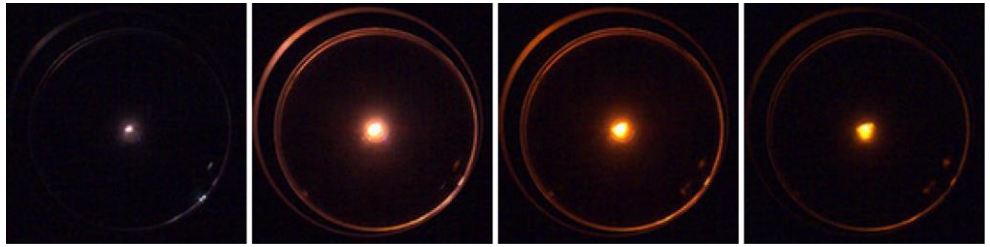

microwave resonator

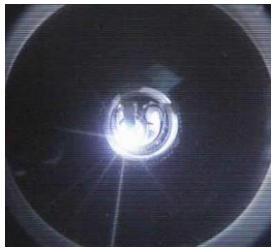

Ikeda et al., Imagineering Inc.

Qiang Wang et al, APPLIED PHYSICS LETTERS 104, 074107 (2014)

# Micro-discharge 1

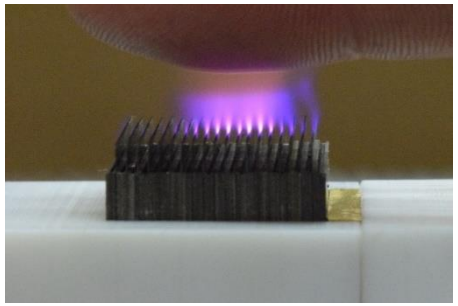

Microscale Discharge micro tips

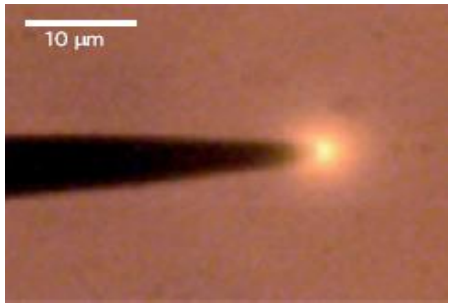


Microscale Discharges in Liquids

Courtesy by David Staack

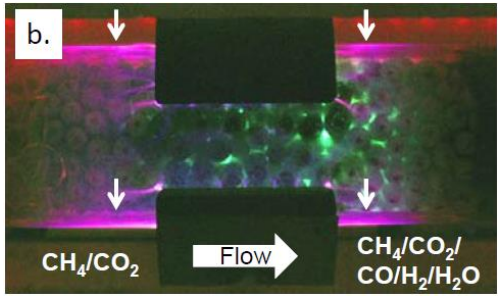


Microdischarge between ceramic spheres (Tomohiro Nozaki, 2015)

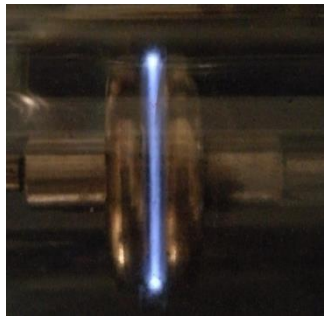

Micro-discharge in CH4/He 250 torr (Princeton, 2017)

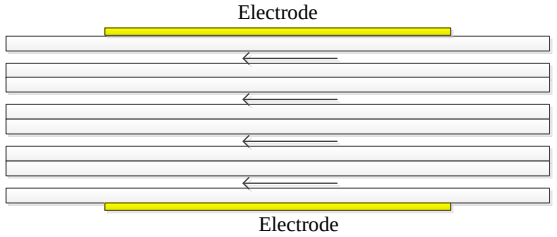


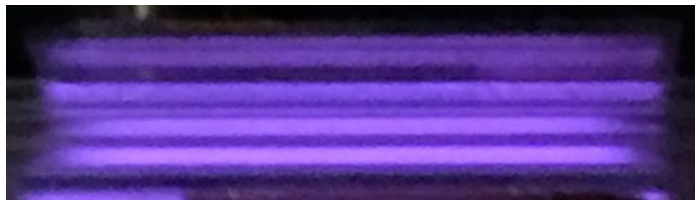

Preliminary tests of single (top) and four channels (bottom) micro-discharge using single a RF power supply. The channel is 76mm X 26 mm with a gap distance about 0.5 mm, (Princeton, 2017)

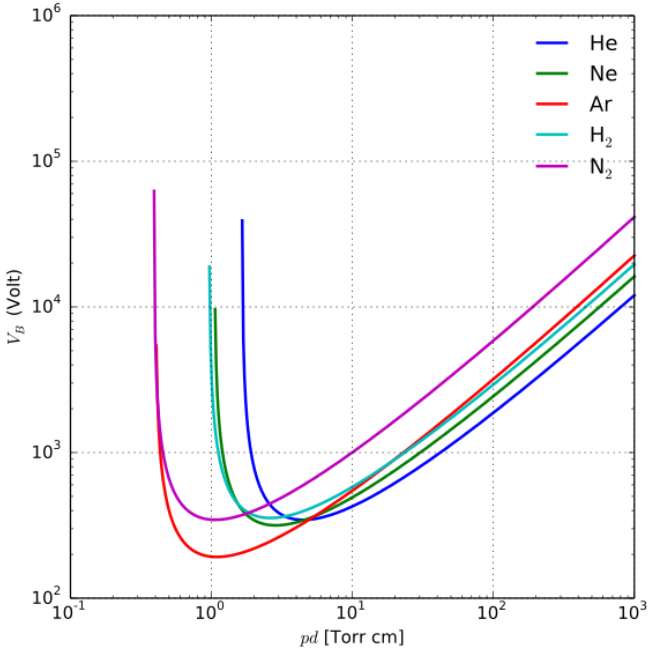


## Applications

- Largescale surface ignition
- Crude Oil Fuel Reforming
- Medical Treatments
- Plasma catalysts
- Aerodynamic Control
- High pressure materials processing

# Nanostructured discharge

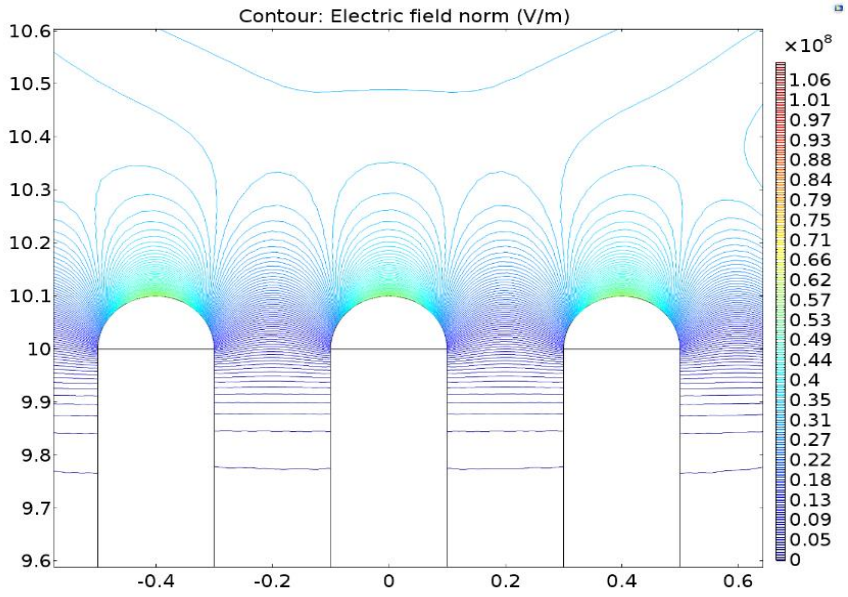


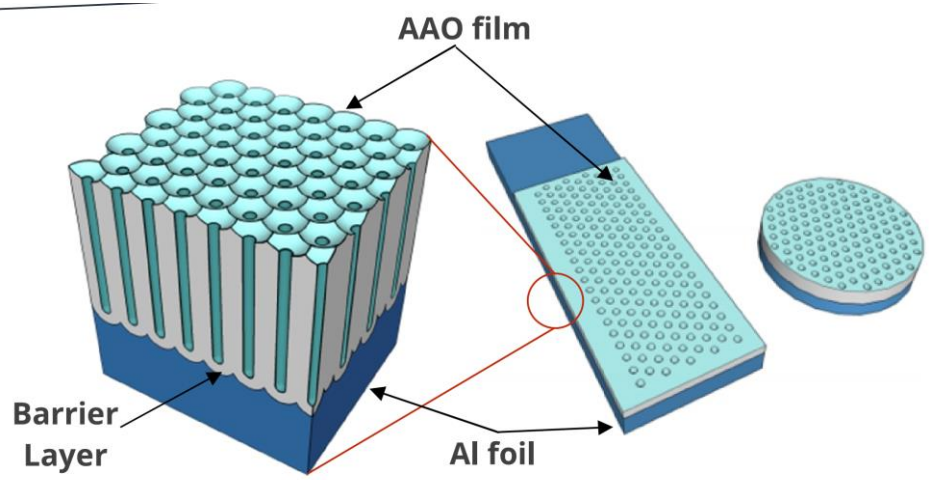


- Parallel Plate electrodes
- Dielectrics(Al2O3 of 0.6 mm with AAO
- AAO film of 50 μm, holes of 200nm
- p= 60Torr
- d= 1 inches
- rf power =1~100W

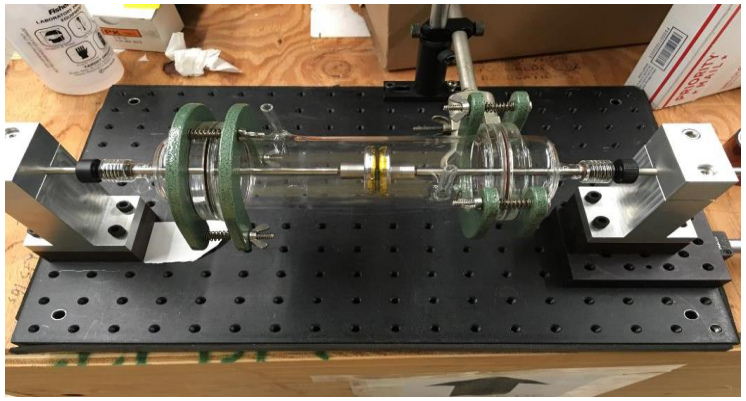

## Findings

- α to ϒ discharge mode transition is observed
- Under α discharge mode, dielectric materials has small effect on the discharge
- Under ϒ discharge mode, the discharge on AAO area is difficult to transit from α to ϒ mode than $Al_2O_3$
- Possibility of plasma control using nanostructures

Haibo Mu and Yiguang Ju, 2017, unpublished work

# Equilibrium & Non-equilibrium Various Plasmas

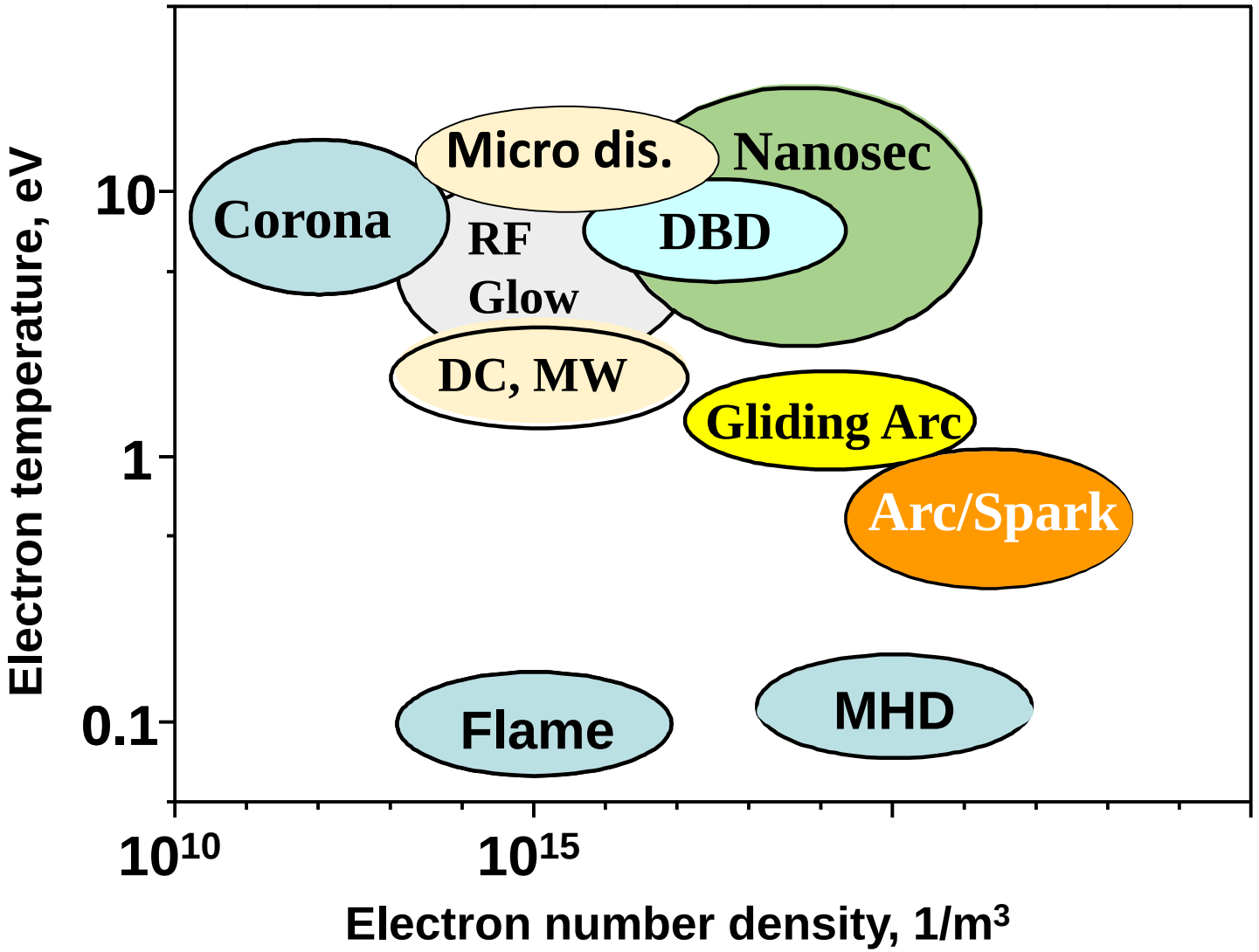


Ju and Sun: Plasma assisted combustion, Progress of Energy & Combustion Science, 2015

# 2. Plasma Assisted Combustion and Applications in Engines

**Yiguang Ju**

1. PAC in scramjet engines and pulse detonation engines
2. PAC in spark ignition engines
3. PAC in flame stabilizations for gas turbine engines
4. PAC in ignition, combustion, and emission control

Princeton University

# Motivation

## Development of High Speed/Low Emission Power Systems & Synfuels

- Enhanced combustion efficiency and flame stability
- Predictive new engine design with alternative fuels for low emissions

Advanced Gas Turbines

(Low NOx, after burner, renewable fuels)

⇨ Ignition and Flame Stabilization

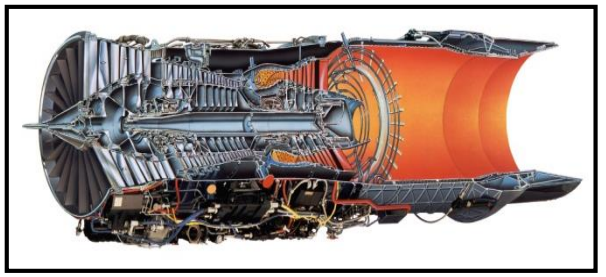

Pulse Detonation Engines

⇨ Ignition and DDT

Internal combustion engines:

⇨ Ignition timing control

Conventional discharge?

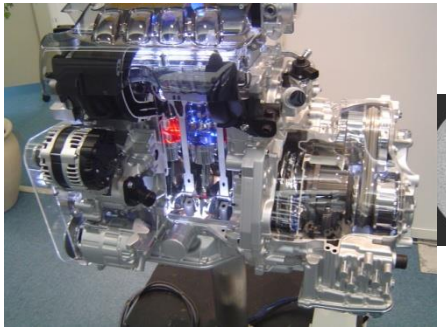

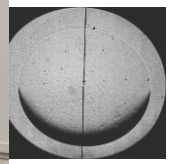

Princeton University

*Combustion lab.*

# 1. PAC for Ramjets and Scramjets

X43: Hydrogen
Silane: ignition enhancer

Mach 10

X-51 (AFOSR)
- Mach 4-8
- Hydrocarbon fuels (JP-8, JP-7)

- *Flow time scale <1 ms*

$$\frac{\text{Flow Residence Time}}{\text{Chemical Reaction Time}} << 1$$

Difficulty in ignition, flame stabilization, and combustion completion

Princeton University

*Combustion lab.*

Princeton University

## Solutions:

***Increase residence time or reduce combustion time***

- Cavity

- Oblique shocks

  Niioka et al.1998

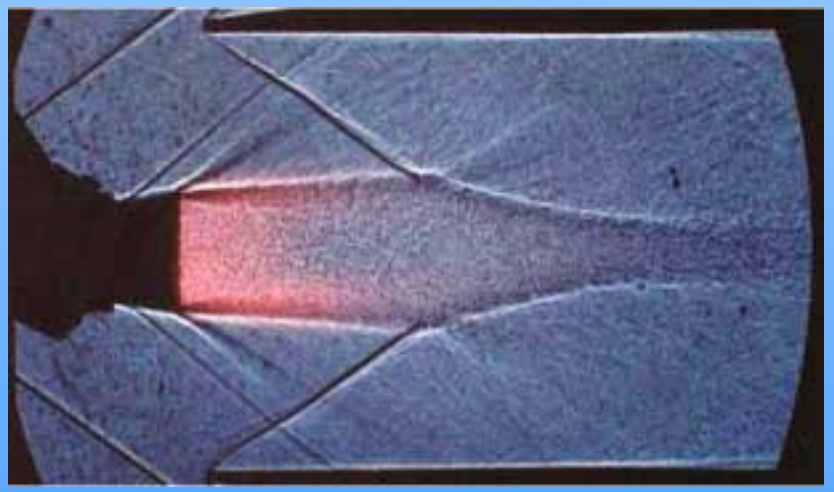

- Plasma

  Takita et al.

  Kimura et al. 1981

  Masuya et al. 1993

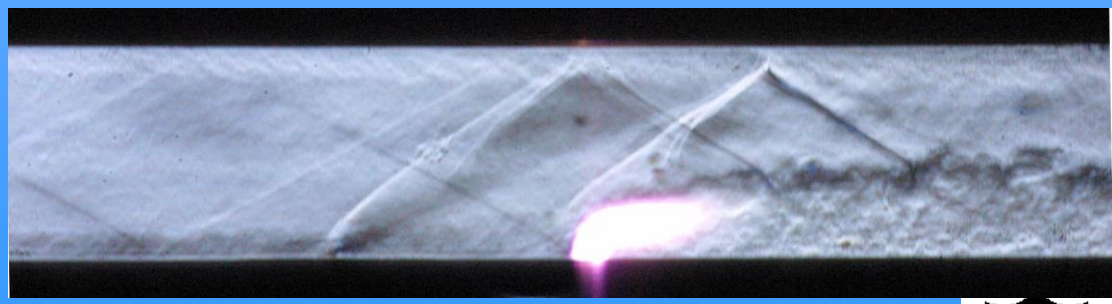

*Combustion lab.*

# Plasma-Assisted Combustion

**Ignition & Flame speed ~(a, $D_{fuel,}$ , $\Phi$, $R_c$, e $^{-E_a}/_{T_f}$ , …)**

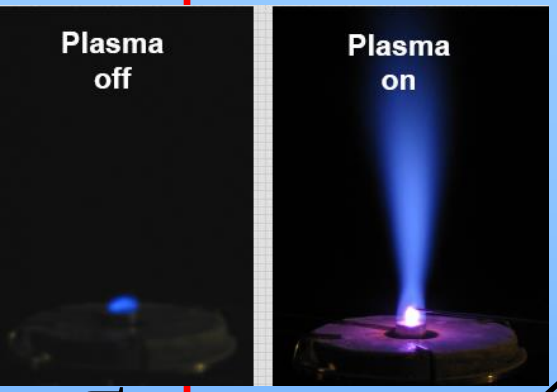


Princeton Un

**Plasma discharge**

Mixing, flow

Ionic wind

Ions/electrons

$O_2^+$

**Temperature increase**

O, NO

Radicals

Fuel fragments

Excited species

$H_2$, $CH_4$
$C_2H_4$

$N_2$ *(A)
$O_2$ ($a^1\Delta_g$)

**Thermal Enhancement**

**Kinetic enhancement**

**Transport enhancement**

*Combustion lab.*

# O Radical Production by Plasma on ignition and flame extinction

Princeton University

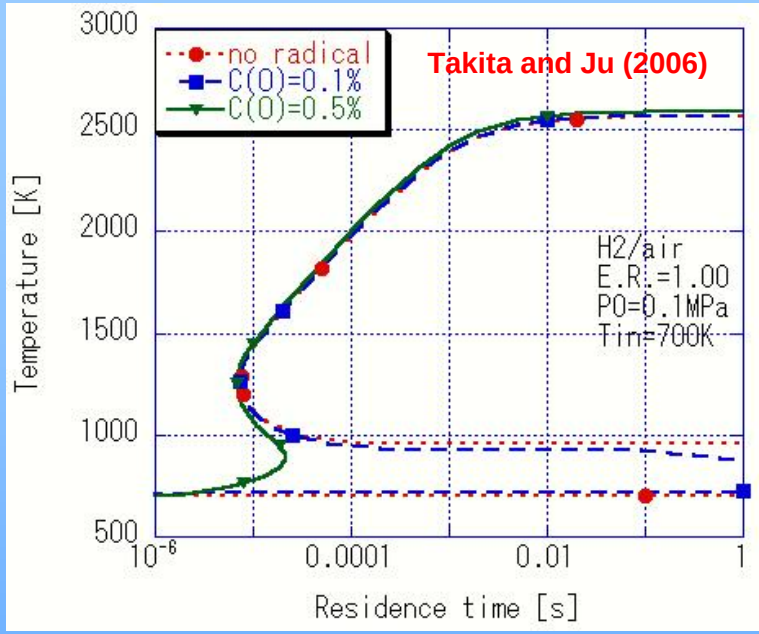


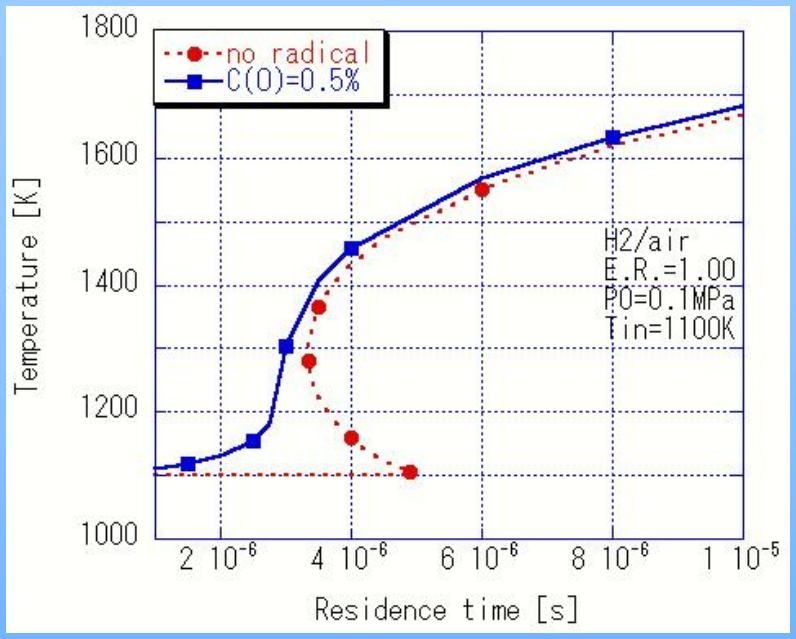


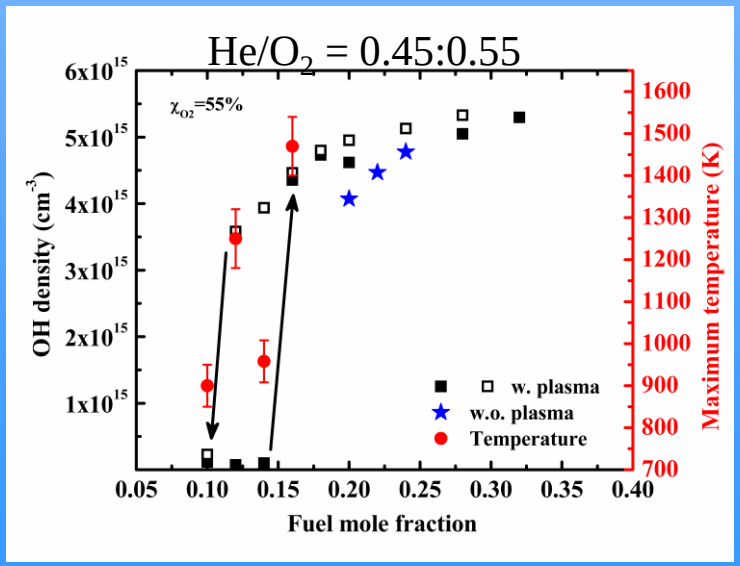


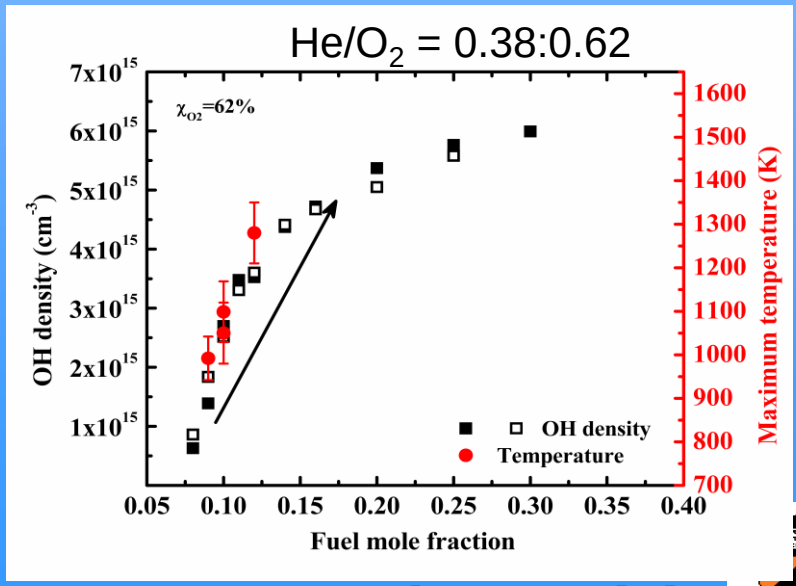


Effect of PAC on methane flame ignition and extinction, Sun W. et al. 2010, 2011

*Combustion lab.*

Princeton University

# Plasma jet ignition enhancement

**Electron-impact reactions ($CH_4$, $O_2$, $N_2$, $H_2$)**

$e + CH_4 = CH_4^+ + 2e$

$e + CH_4 = CH_3 + H + e$

$e + O_2 = 2O + e$

$e + N_2 = 2N + e$

$N + O_2 = NO + N$

$NO + HO_2 = NO_2 + OH$

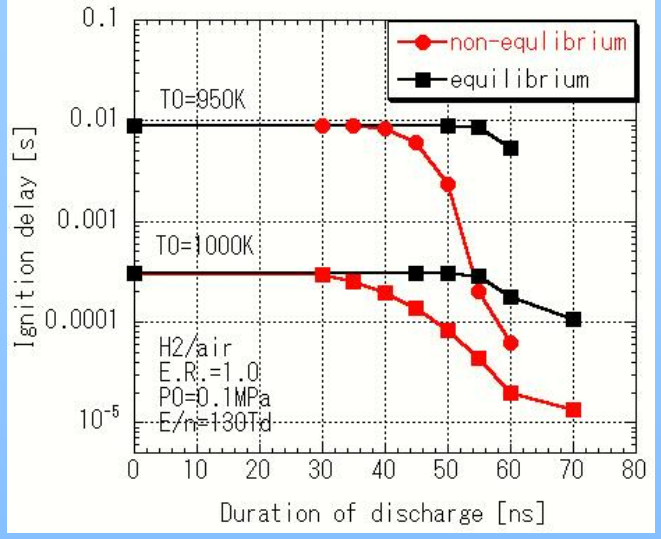


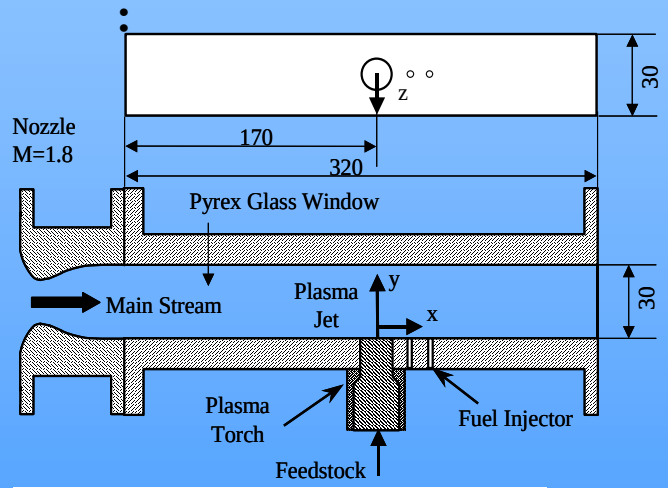


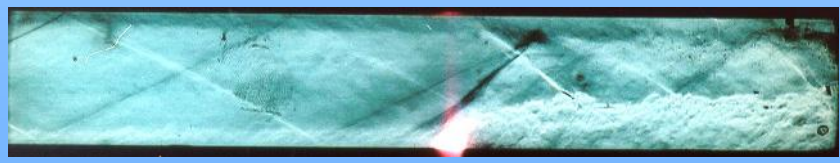

**(a) $X_{H2,PJ}$ = 0.3, $P_{IN}$ = 3.0 kW, $P_{IN\ total}$ = 4.3 kW**

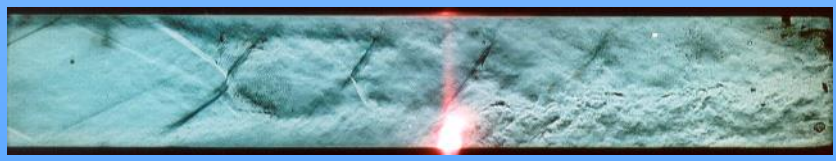

**(b) $X_{H2,PJ}$ = 0.5, $P_{IN}$ = 6.0 kW, $P_{IN\ total}$ = 8.2 kW**

Fig. 2.1 $H_2$ ignition by plasma torch in a $M$=2.3 flow and the effect of total heat addition on pre-combustion shock wave, $X_{H2}$ is hydrogen mole fraction in $H_2/N_2$ plasma torch; $P_{in}$: plasma torch electric power, $P_{in\ total}$: total heat addition ($P_{in}$+$H_2$ enthalpy flux) [192]

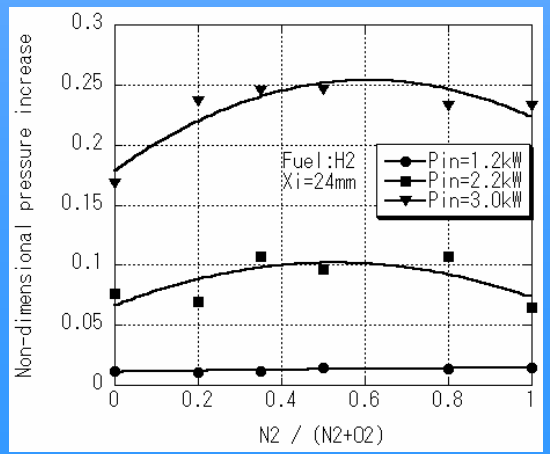


Effect of mixing ratio of $N_2/O_2$ feedstock on wall pressure increase due to combustion of fuel injected at $X_i$ = 24 mm in experiment, $H_2$/air mixture, Takita, Abe, Masuya, and Ju, 2006,

# DBD/plasma jet ignition

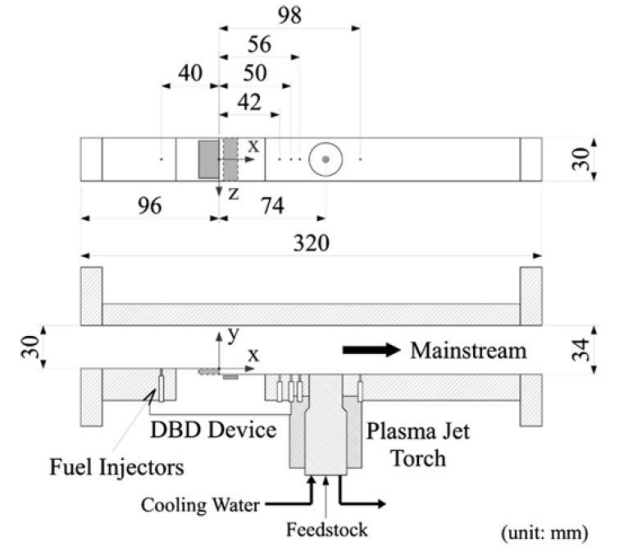


Fig. 2.2a Schematic of the test section with DBD and plasma torch [181]

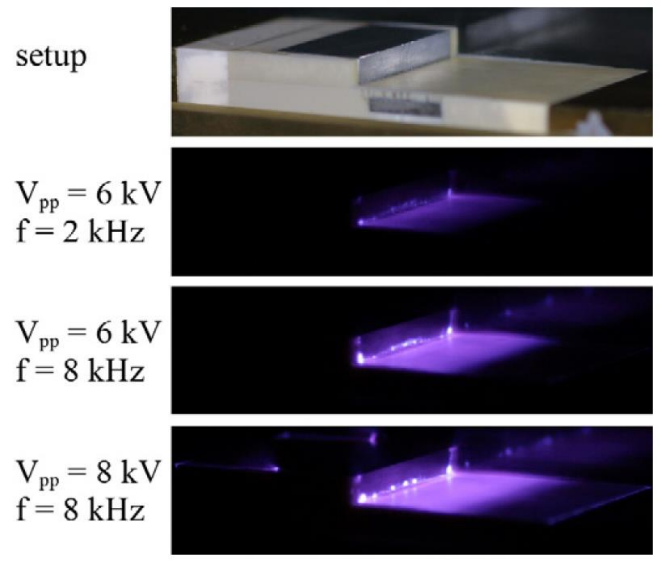


Fig. 2.2b Direct photographs of DBD plasma in $M$=2.0 supersonic flow [181]

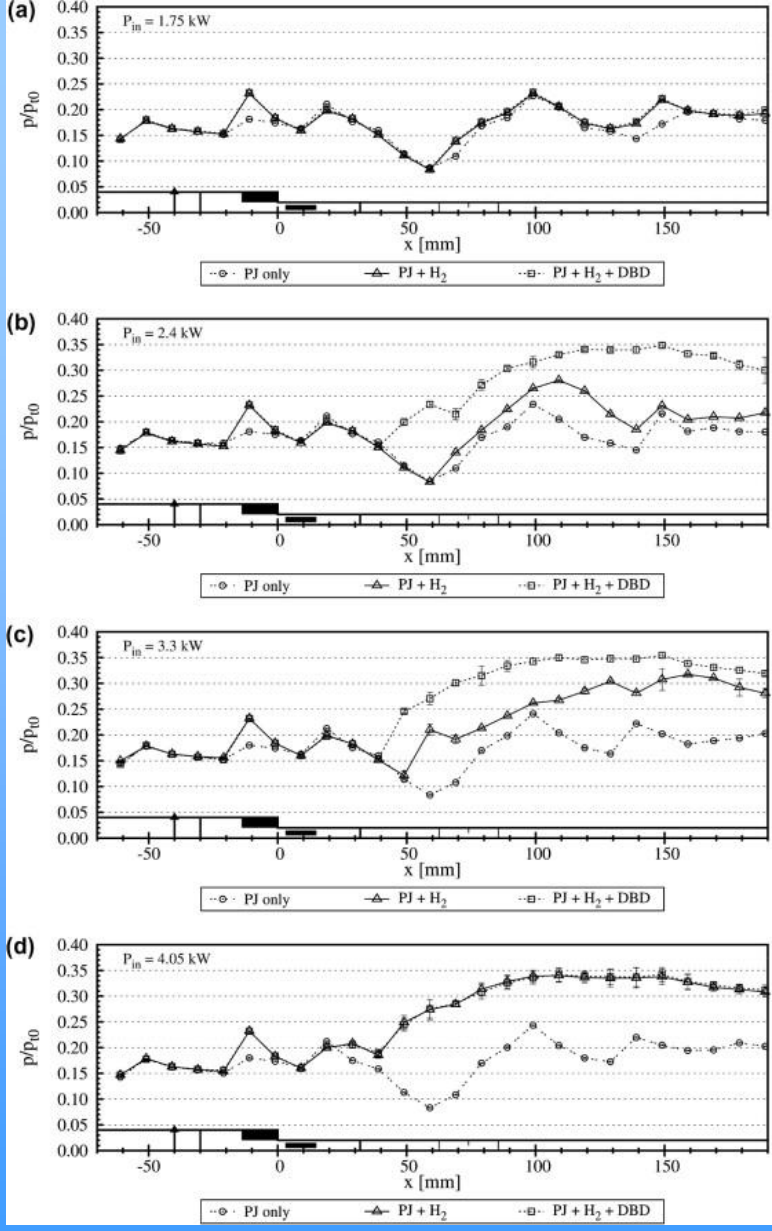


Wall pressure distributions when $H_2$ fuel was injected from $x_i$ = −40 mm under simultaneous operations of DBD device and PJ torch. (a) $P_{in}$ = 1.75 kW. (b) $P_{in}$ = 2.4 kW. (c) $P_{in}$ = 3.3 kW. (d) $P_{in}$ = 4.05 kW.

Princeton University

# A nanosecond pulsed plasma discharge, arc jet vitiated ignition

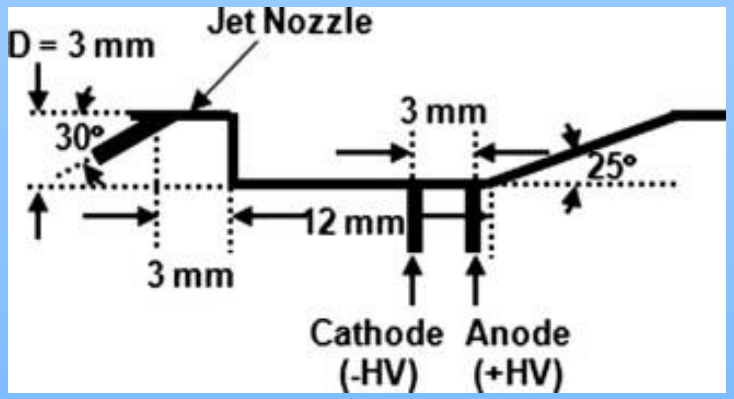


Fig. 2.4 Schematic of the cavity model [182]

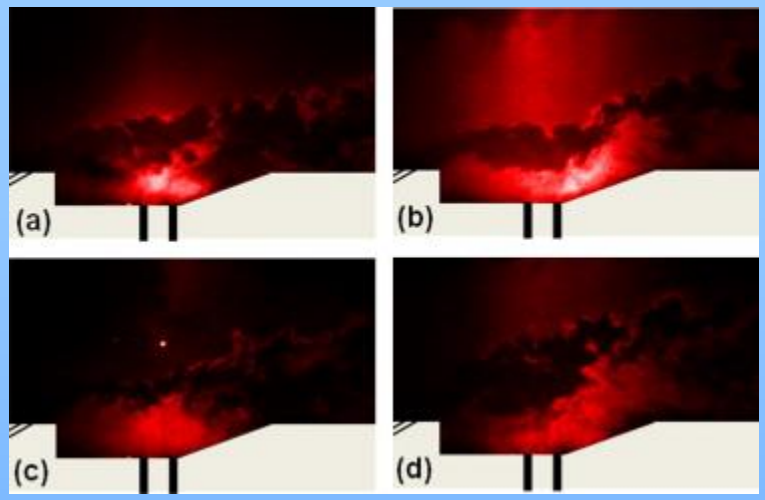


Fig. 2.5 OH PLIF images of a cavity flame in supersonic flows of two different enthalpies: (a) without the plasma and (b) with plasma at $M$=2.9, $J_n$~4 of $H_2$ jet, and (c) without plasma and (d) with plasma at $M$=2.6 $J_n$~3.5 of $H_2$ jet [182]

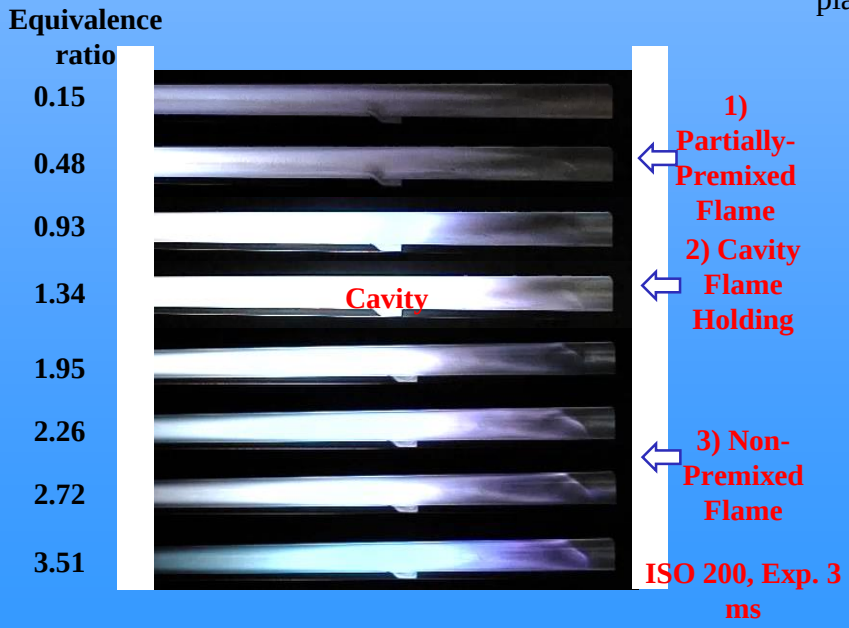


**$N_2$ arc jet heated air free stream: $T_0$ = 2,500 K, $P_0$ = 1**

Arc jet vitiated ignition, Do et al. 2013

Princeton University

# Gliding arc flame stabilization

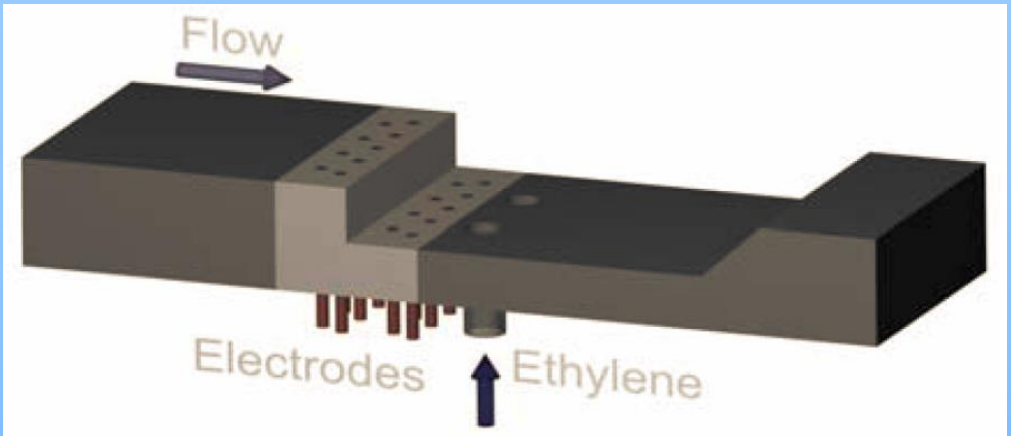


Fig. 2.6 Schematic of experimental setup and electrodes arrangement [184]

Fig. 2.7 Left: discharge without fuel injection.
Right: discharge interaction with $H_2$ injection [184]

large volume and forced ignition

# Subcritical streamer microwave discharge

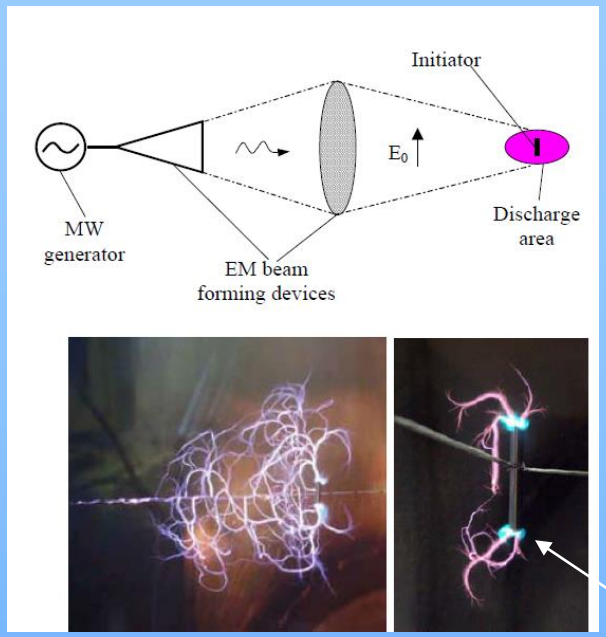


The discharge in the undercritical field can be initiated, for example, at the location of a cylindrical MW vibrator in the EM beam. Conditions of local electrical breakdown ***E*** ≥ ***Ec***r in this case are realized at the ends of the vibrator.

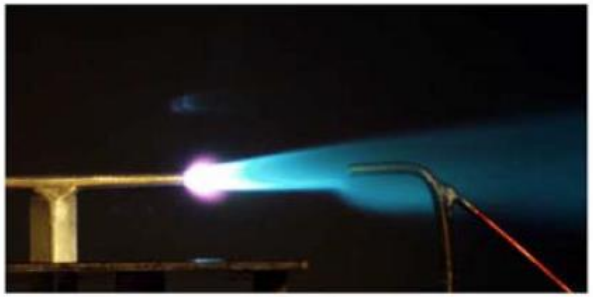

**Figure 4. Propane – air flammable mix ignition by deeply undercritical MW discharge in a high-speed flow**

I. Esakov et al., IEEE TRANSACTIONS ON PLASMA SCIENCE, VOL. 37, NO. 12, DECEMBER 2009

Esakov et al. AIAA-paper-2005

Princeton University

*Combustion lab.*

Princeton University

# Microwave flame stabilization in a high speed flow (200 m/s) as a preburner

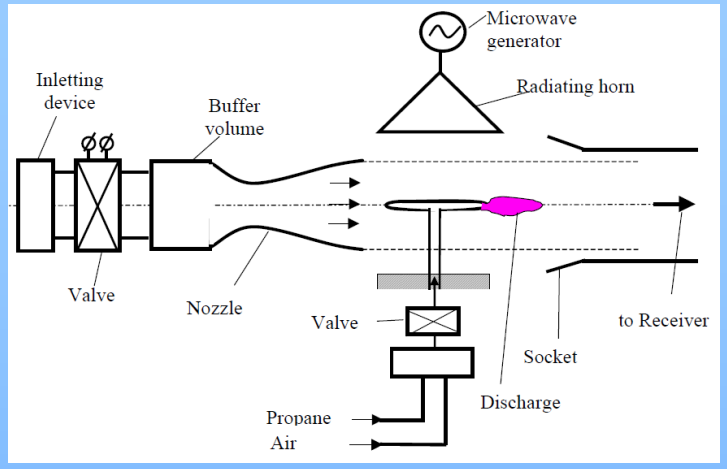


cylindrical MW vibrator

Van Wie et al., AIAA 2006-1212

Fig. 2.9 Schematic of experimental setup [186]

**Figure 8. MW discharge initiated by optimal vibrator in SS stream, exposure time was $\tau_{ex} = 1$ s (in the left) and $\tau_{ex} = 10^{-3}$ s.**

Precombustor

*Combustion lab.*

# Nanosecond plasma ignition in PDE

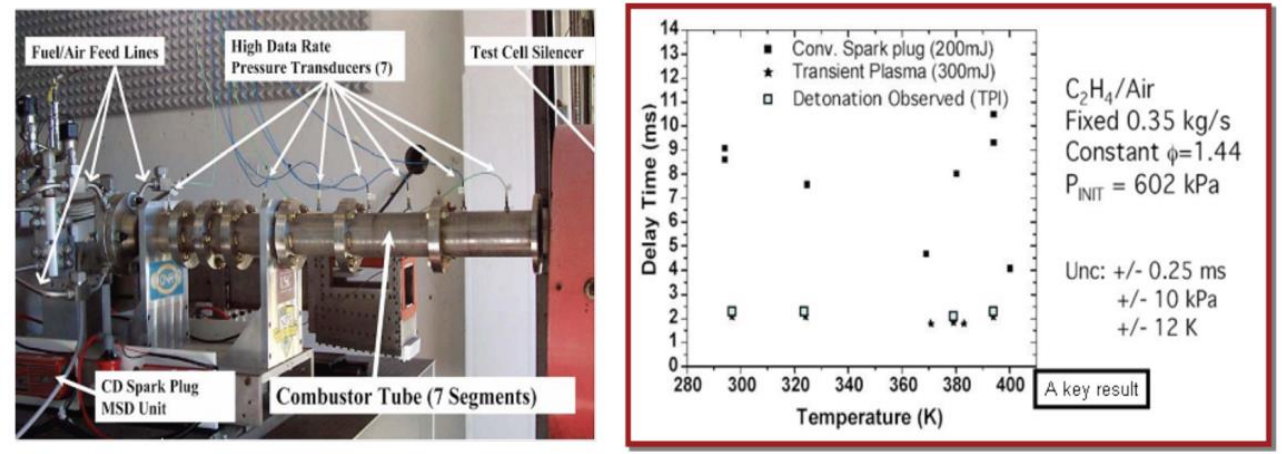


Fig. 2.22 Left: A valve less PDE setup at the Naval Postgraduate School. This type of architecture requires a booster and its anticipated applications are missiles or rockets. Right: Comparison of ignition delays for $C_2H_4$/air mixture using spark plug and transient plasma igniter [178]

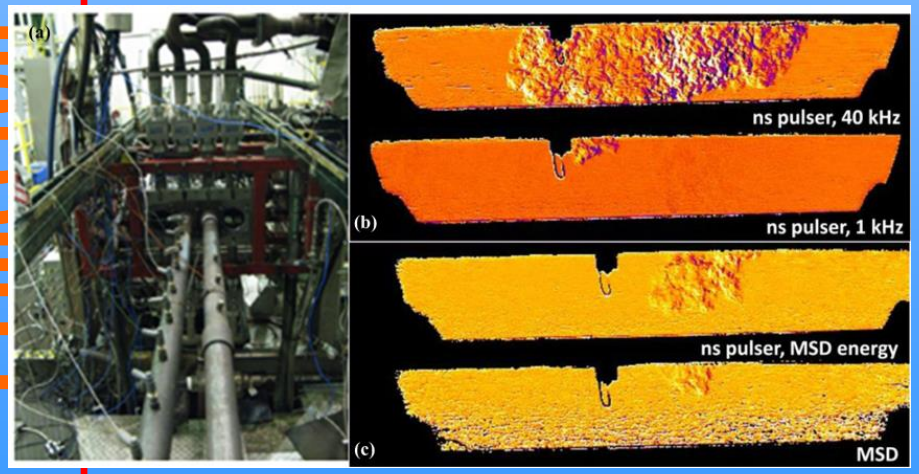


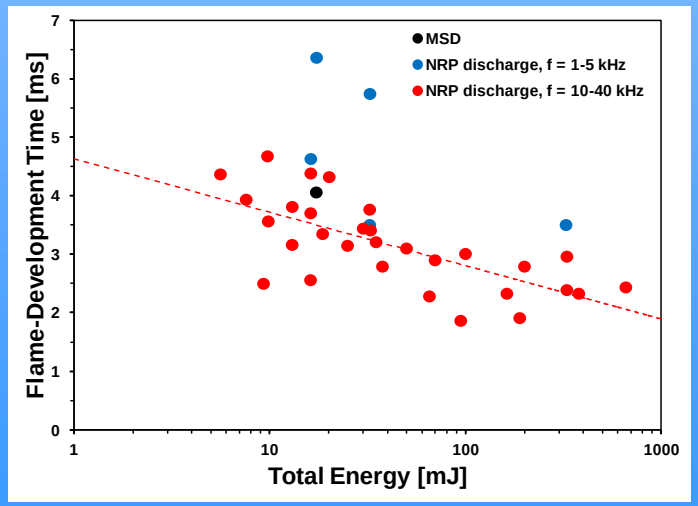


Fig. 2.23 (a) PDE engine facility at the Air Force Research Lab at Wright-Patterson Air Force Base, (b) Schlieren imaging of nanosecond pulsed discharge igniter in $CH_4$/air mixture, Φ=1, (c) Schlieren imaging of nanosecond pulsed discharge igniter in $CH_4$/air mixture, Φ=0.8 [62]

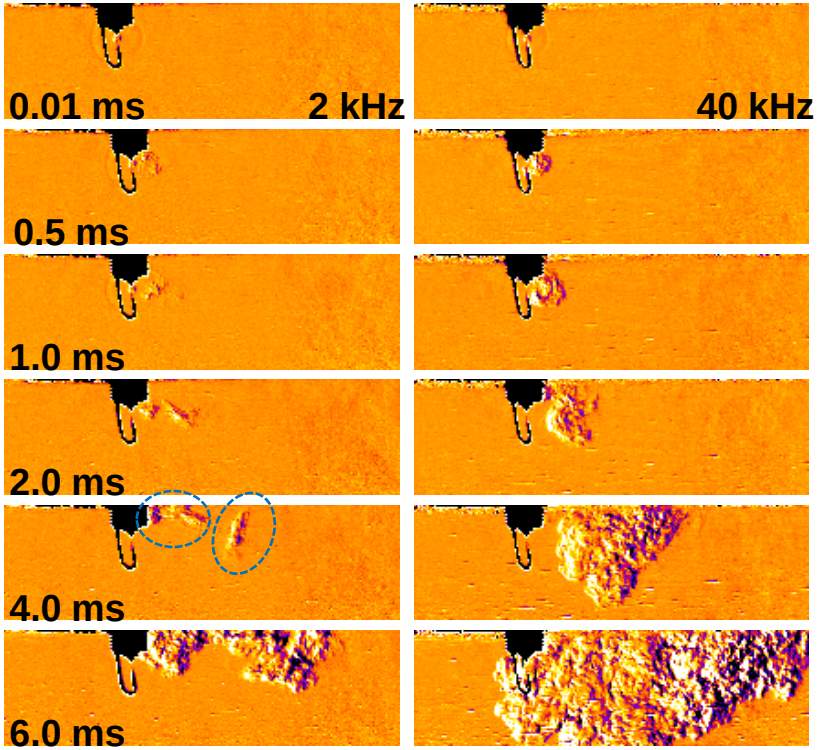


Figure 3: Ignition kernel development for 5 pulses of 3.2 mJ per pulse. Left images: pulse repetition frequency of 2 kHz. Right images: pulse repetition frequency of 40 kHz.

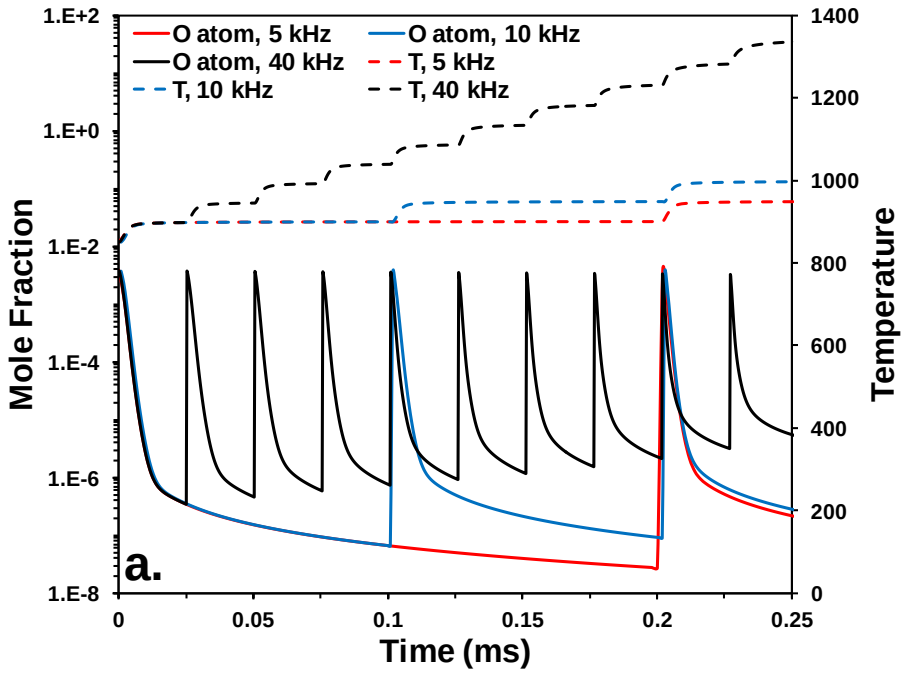


Figure 6. a) Computed atomic oxygen concentration and temperature as a function of time with 1% oxygen dissociation repeated at 5 kHz, 10 kHz, and 40 kHz frequencies for stoichiometric methane-air mixtures at 850 K. b) . Computed atomic oxygen concentration and temperature as a function of time with 0.1%, 0.5%, and 1% oxygen dissociation repeated at 40 kHz frequency for stoichiometric methane-air mixtures at 850 K.

- **Increase of ignition kernel volume**
- **Reactivate chemical radicals before quenching**

Lefkowitz, J.K., Guo, P., Ombrello, T., Won, S.H., Stevens, C.A., Hoke, J.L., Schauer, F. and Ju, Y., 2015. *Combustion and Flame*, *162*(6), pp.2496-2507.

Princeton University

# 2. PAC for IC engines

**Fig. 1 2HP FUJI-IMVAC 34 is used current for both US and Foreign UAVs.**

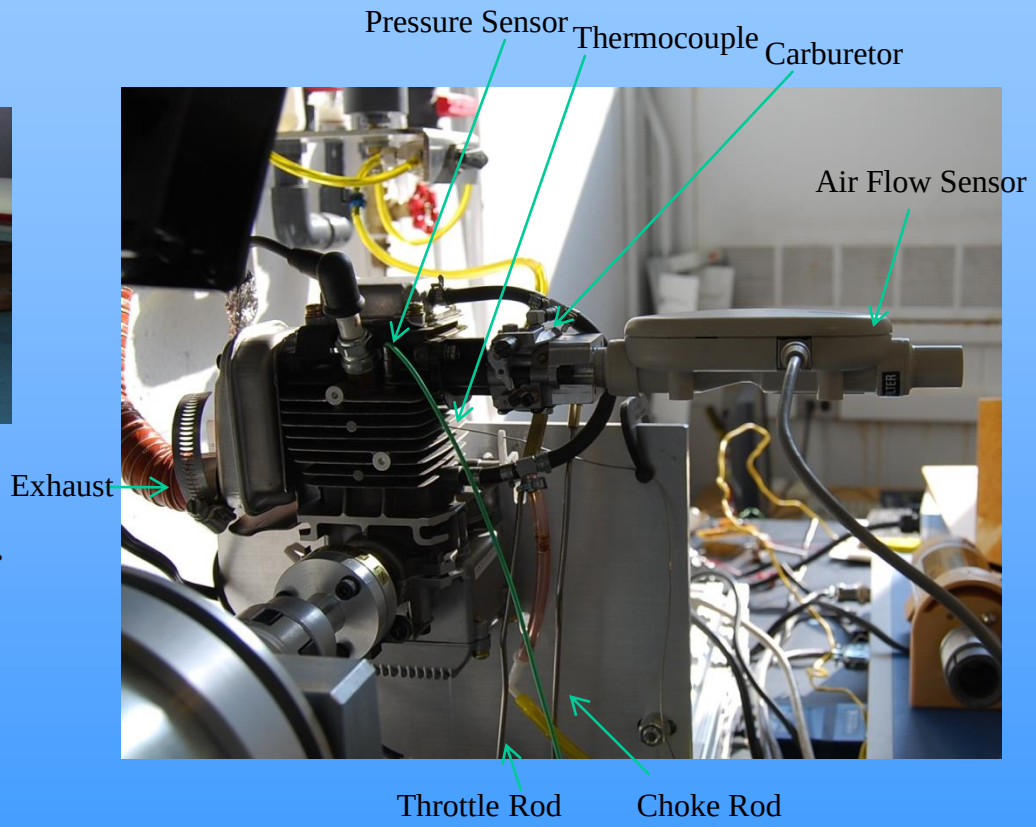

**PU-Imagineering Inc.**

Princeton University

# Transient corona discharge

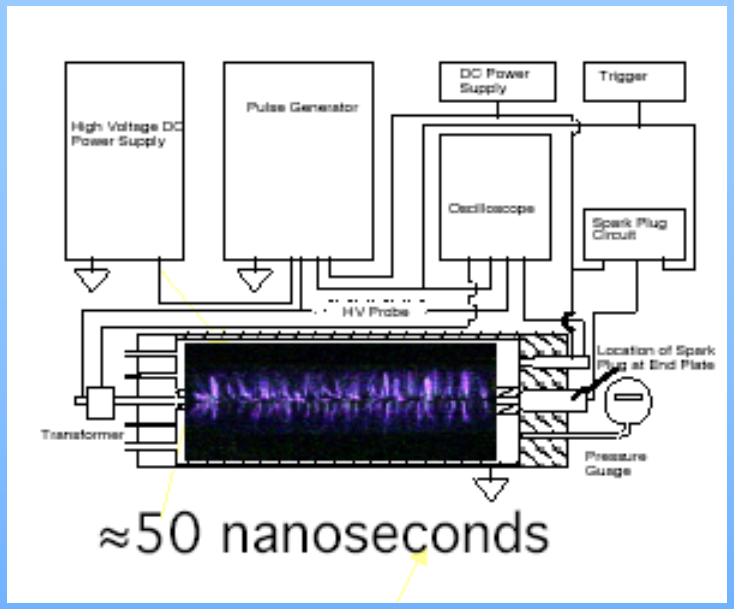


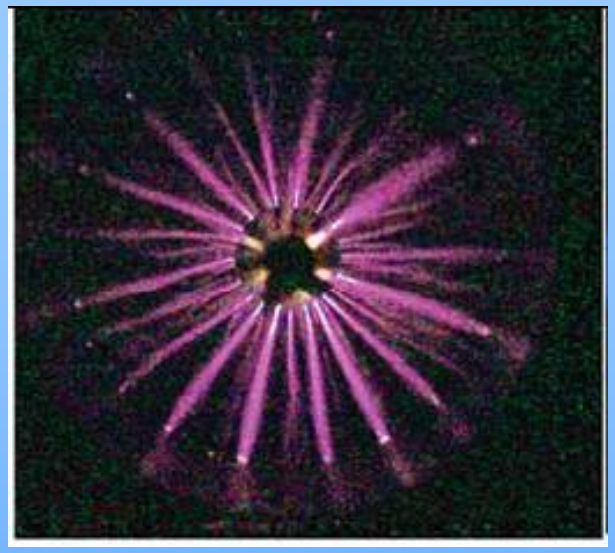

**Disk electrode & streamers**

Corona enhanced ignition

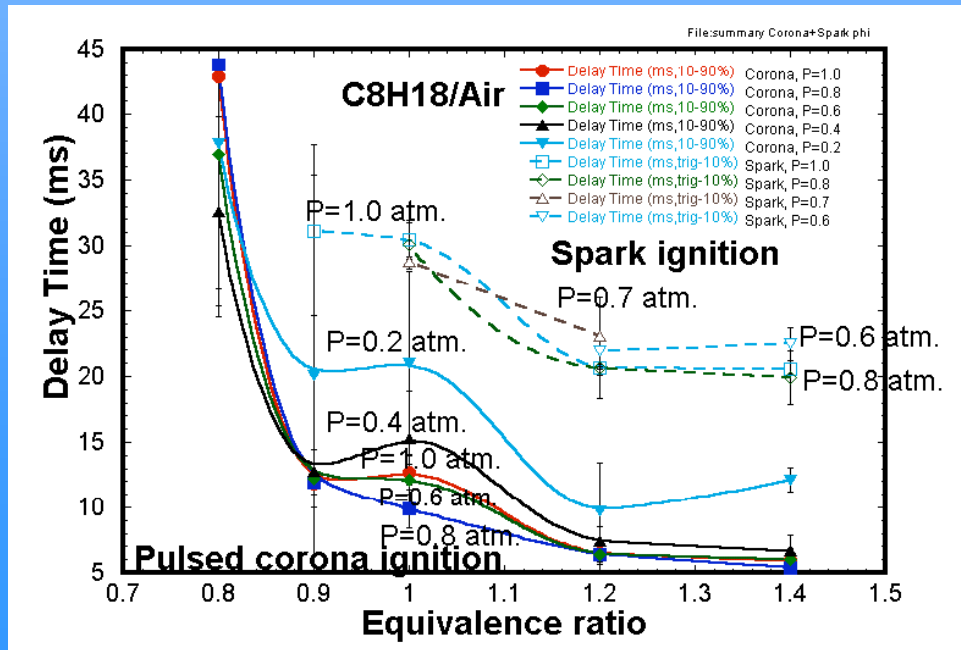


**Gundersen et al., 2003**

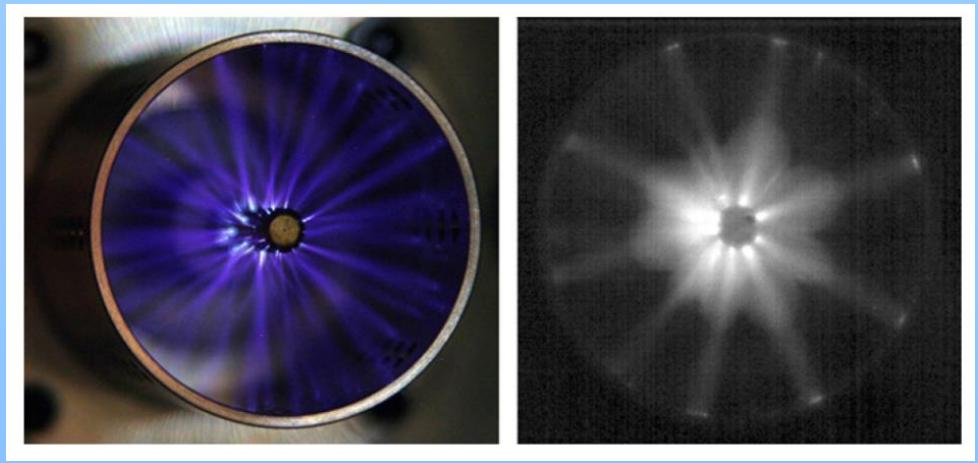

Fig. 2.19 Left: streamers generated by a single 370 mJ, 56 kV, 54 ns pulse (maximum E/N~400 Td) in air (10 s gate time); Right: flame propagation from multiple ignition sites at the base of the streamers after a single pulse in Φ=1.1 $C_2H_4$/air mixture (1 ms gate time) [81]

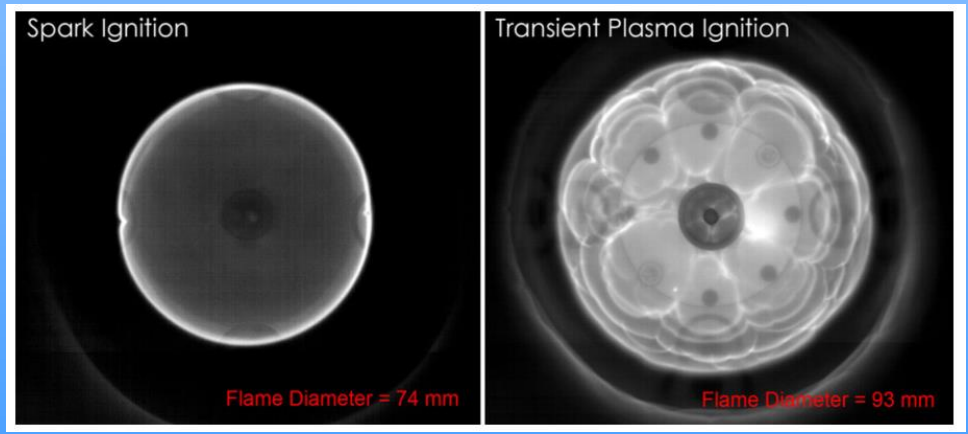


Fig. 2.20 Images of flame development in Φ=1.1 $C_2H_4$/air mixture, 6 ms after ignition. A 300 μs gate time was used with equal sensitivity for both images and 996×990 resolution. Left: spark ignition using a standard 105 mJ, 10 μs, 15 kV spark ignition system and a spark plug with a 1 mm gap. Right: transient plasma ignition using a 70 mJ, 12 ns, 54 kV pulse with a 6 mm gap [81]

1. Shiraishi T, Urushihara T, Gundersen MA. A trial of ignition innovation of gasoline engine by nanosecond pulsed low temperature plasma ignition. J. Phys. D: Appl. Phys. 2009;42:135208.

Princeton University

# Microwave and nanosecond plasma assisted ignition

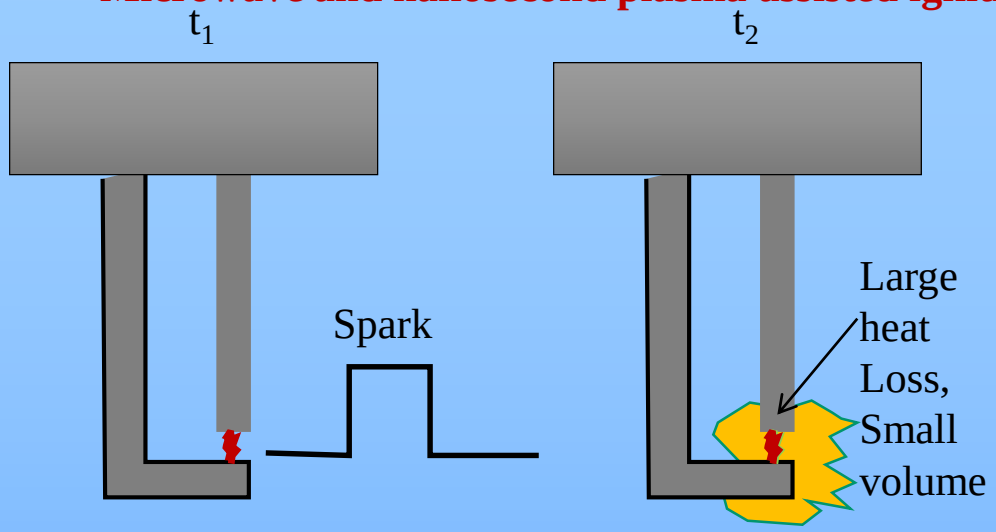


**Fig.1 Current spark ignition plug: large heat loss, small volume**

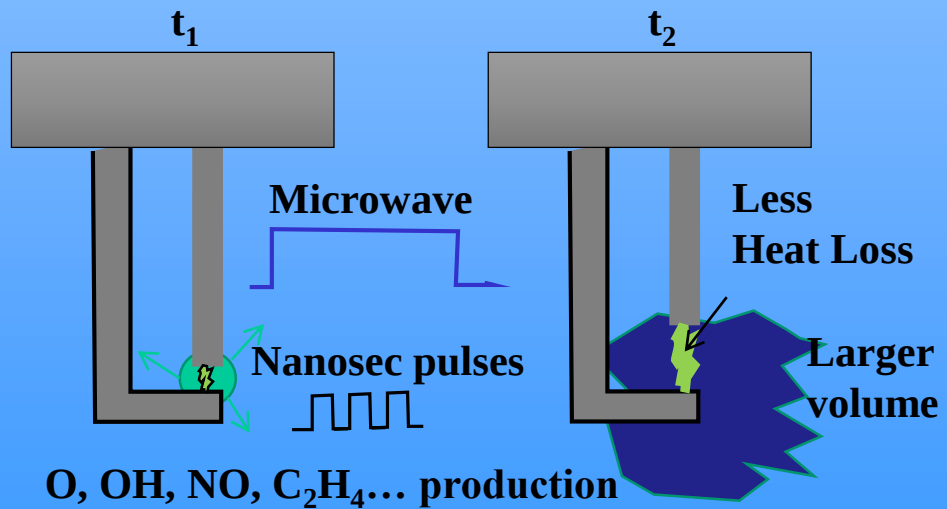


**microwave repetitive nanosecond ignition with radical production, Increased volume, less heat loss**

*Combustion lab.*

Spark, Microwave, Gliding arc

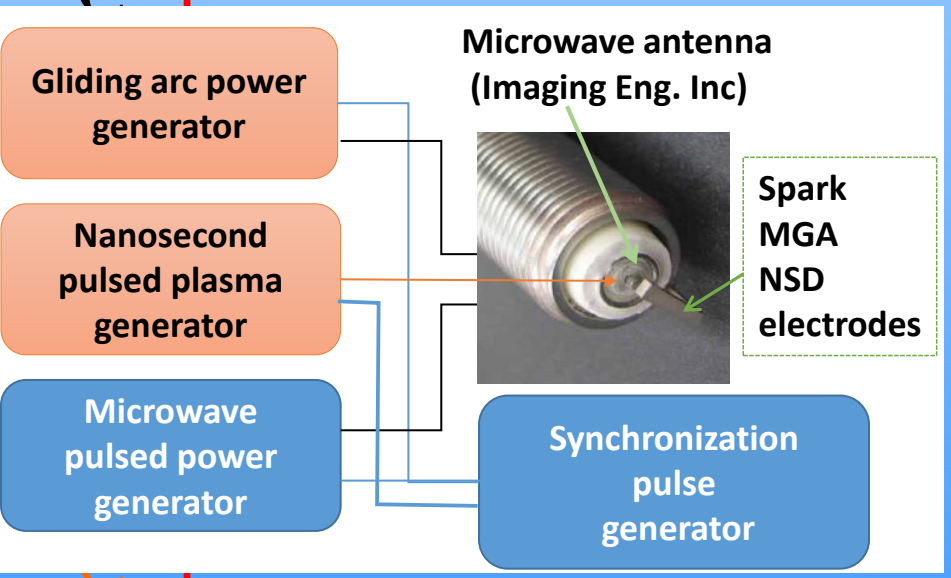


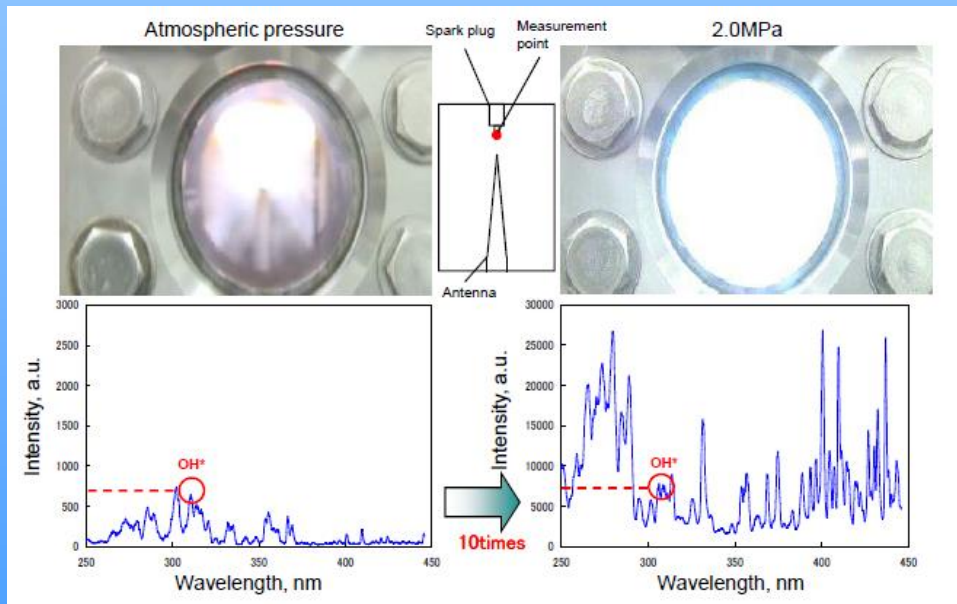


OH* Comparison between Spark and MW ignition. Imagineering Inc.

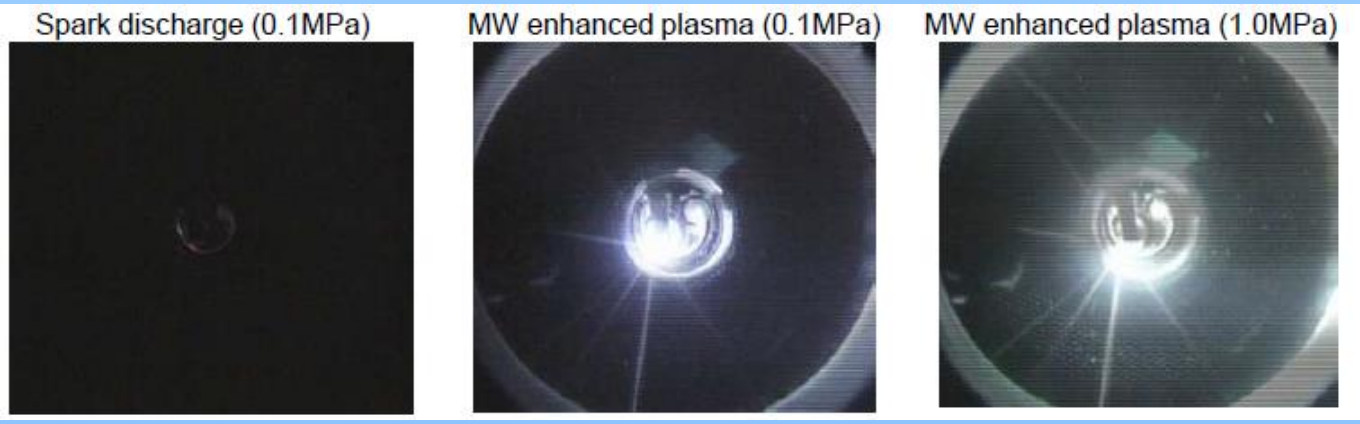


Ikeda et al., Imagineering Inc.

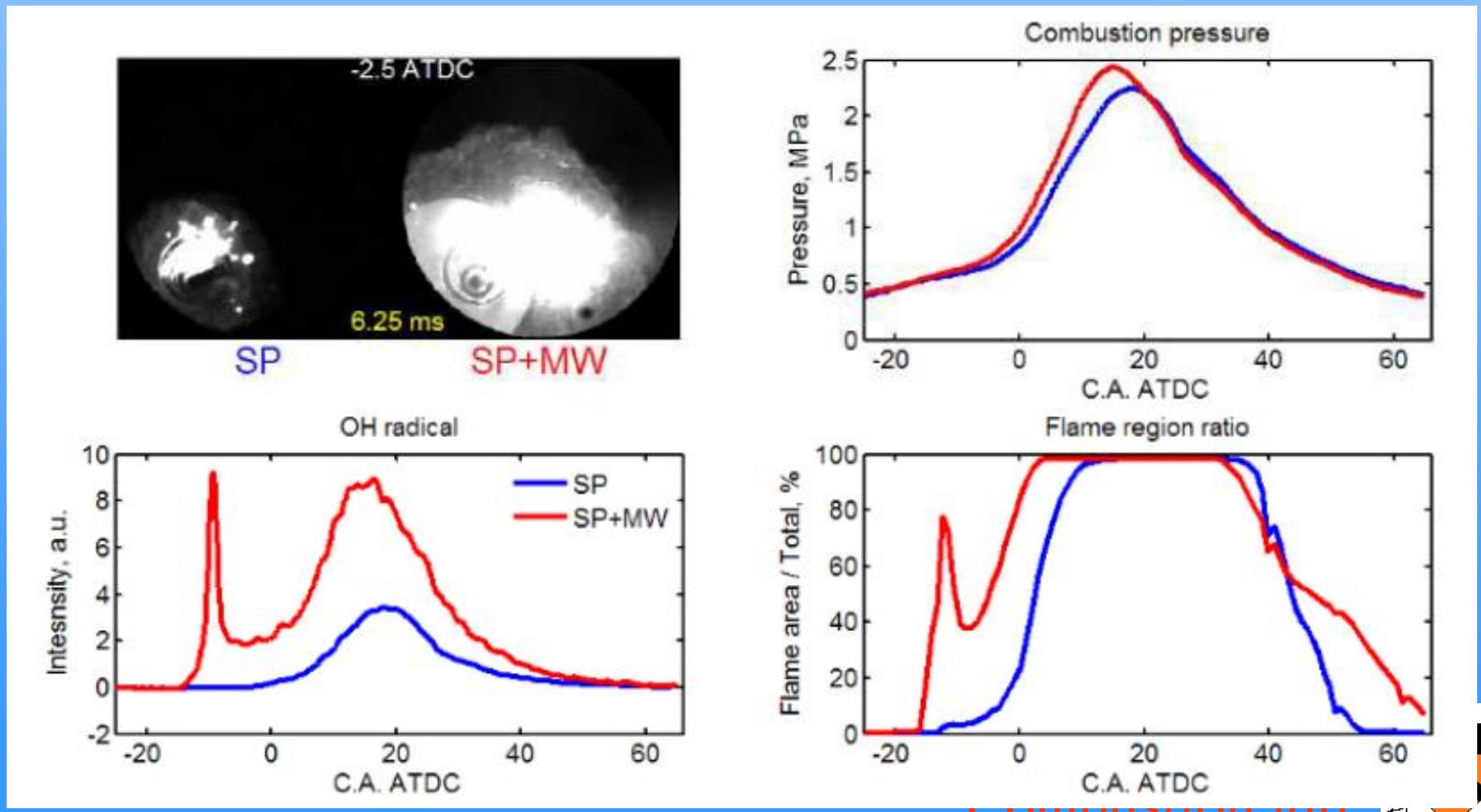


Princeton University

Combustion lab.

Princeton University

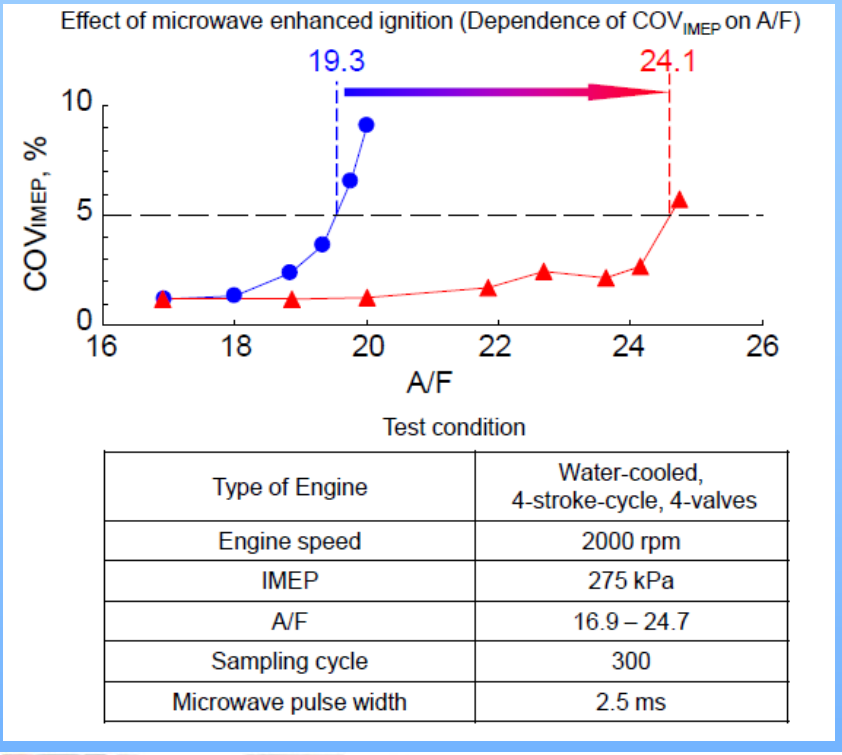


Test condition

| | |
|---|---|
| Type of Engine | Water-cooled, 4-stroke-cycle, 4-valves |
| Engine speed | 2000 rpm |
| IMEP | 275 kPa |
| A/F | 16.9 – 24.7 |
| Sampling cycle | 300 |
| Microwave pulse width | 2.5 ms |

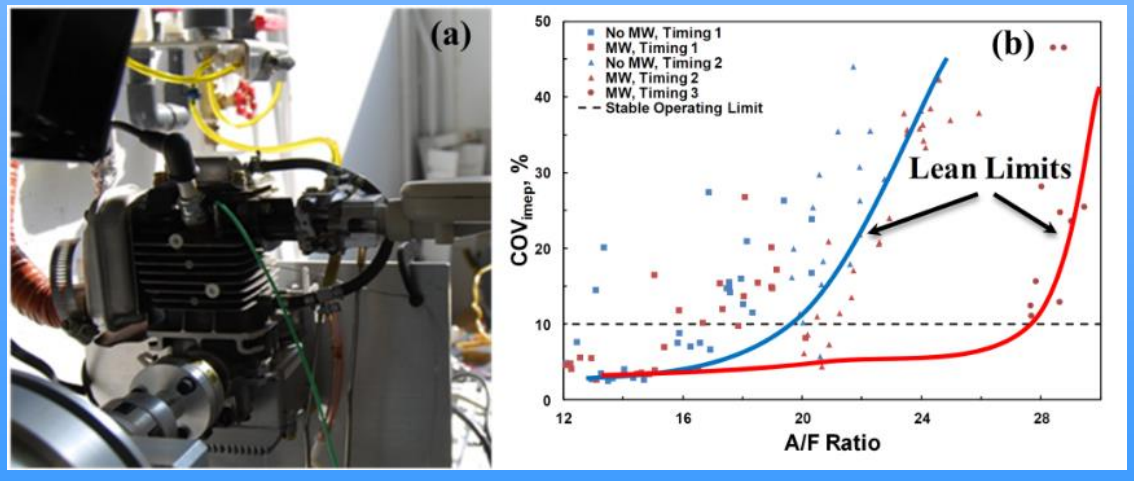


Fig. 2.16(a) direct photograph of plasma assisted 34 cc Fuji engine test setup and (b) the comparison of limits of stable engine operating conditions with and without microwave (MW) discharge at 2000 rpm [69] . Lefkowitz, J.K., Ju, Y., Tsuruoka, R. and Ikeda, Y., 2012. A study of plasma-assisted ignition in a small internal combustion engine. *AIAA paper-2012-1133*.

# Microwave/spark ignition

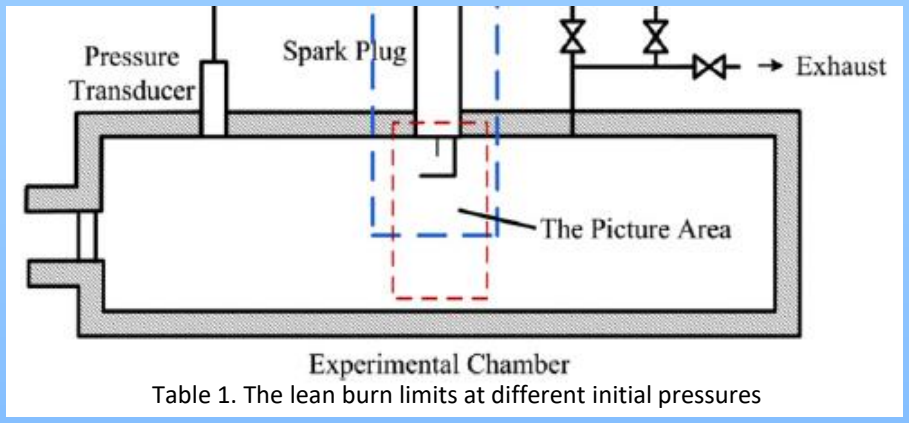


| | Spark plug ignition (Φ) | Microwave ignition |
|---|---|---|
| 1 bar | >2 | 1.6 |
| 2 bar | 1.8 | 1.0 |
| 4 bar | 0.9 | 0.7 |
| 6 bar | 0.9 | 0.7 |
| 8 bar | 0.9 | 0.7 |

Table 1. The lean burn limits at different initial pressures

The pressure curve of MW ignition at 8 bar

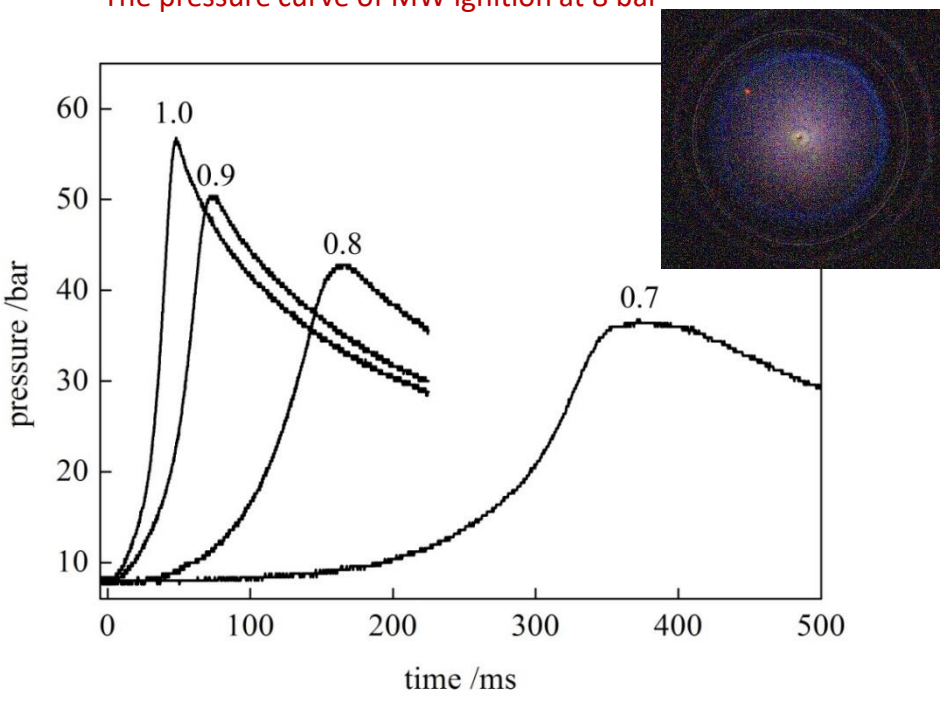


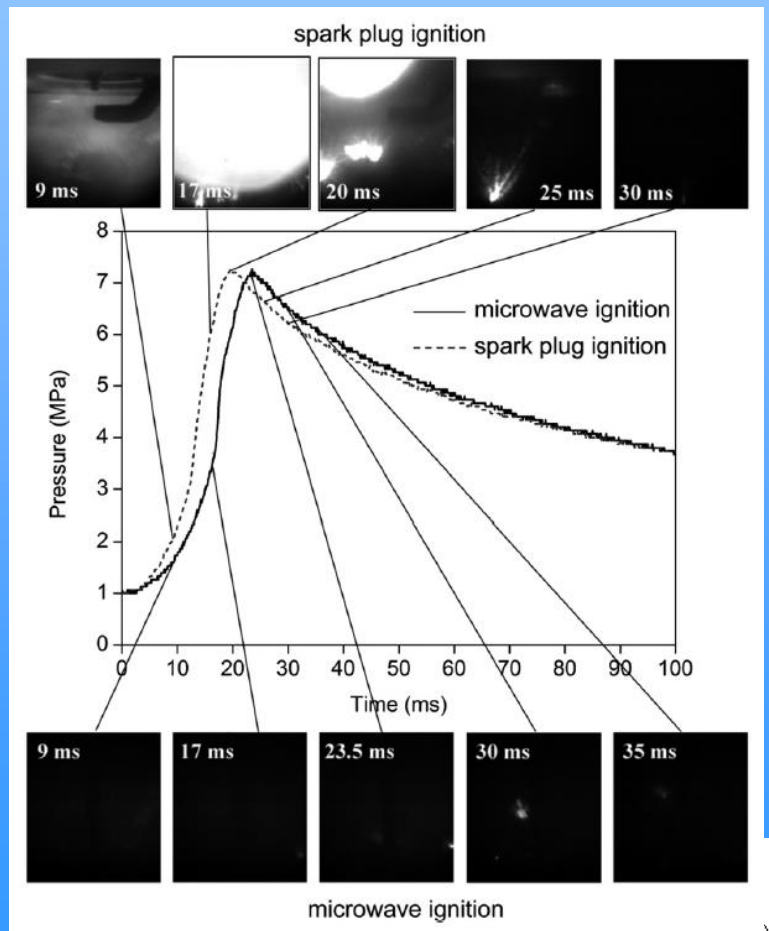


FIG. 6. The pressure curves of microwave ignition and spark plug ignition.

Q Wang et al., Applied Physics Letters **103**, 204104 (2013); doi: 10.1063/1.4830272

Drinceton University

# Microwave/spark ignition in engine

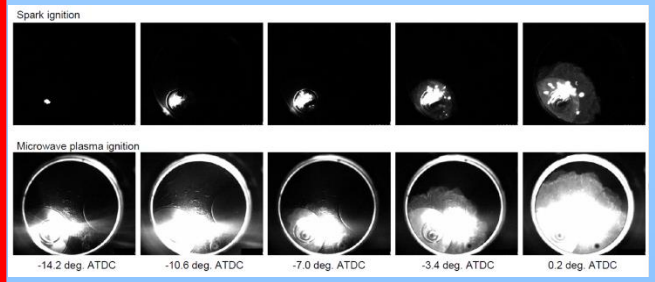


Fig. 2.12 Comparison of $C_3H_8$ flame images in a compression-expansion engine using conventional spark plug and microwave enhanced spark plug, Φ=1, initial pressure 600 kPa, initial engine speed 600 rpm [172]

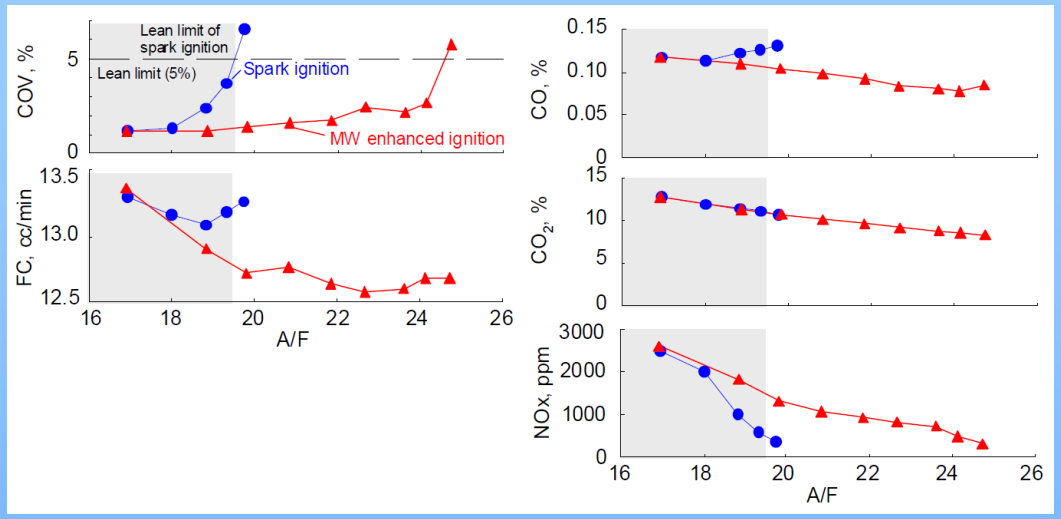


Fig. 2.13 The effect of spark ignition and microwave enhanced spark ignition on $COV_{IMEP}$, fuel consumption and exhaust emission [172]

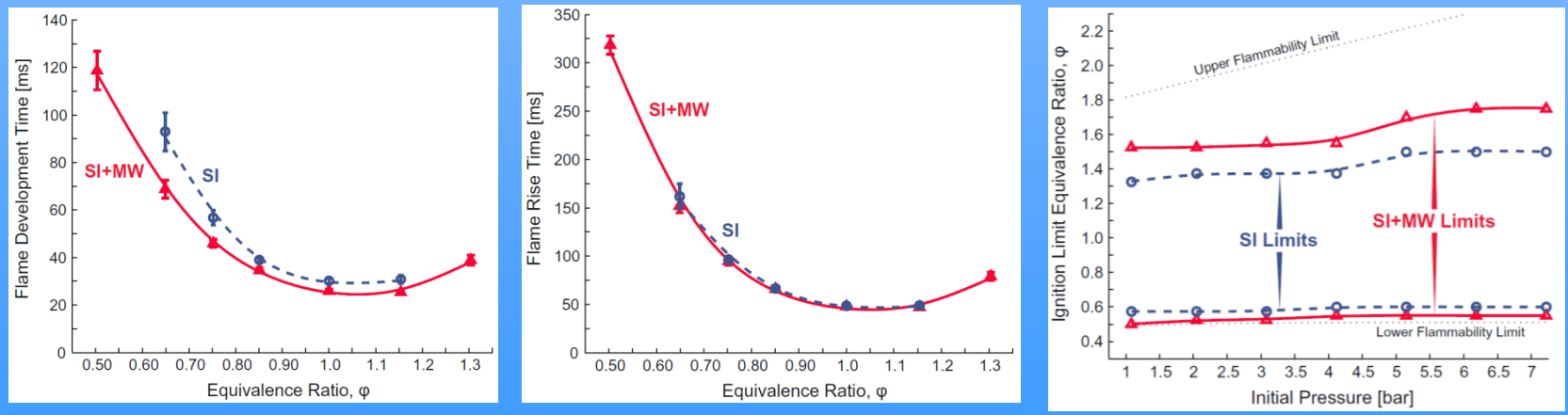


Fig. 2.14 the SI and SI+MW modes as a function of equivalence ratio at an initial pressure of 1.08 bar and 300 K (a) for FDT, (b) for FRT [70]

Princeton University

Combustion lab.

# Why do we see a significant extension of lean burn in engines with microwave?

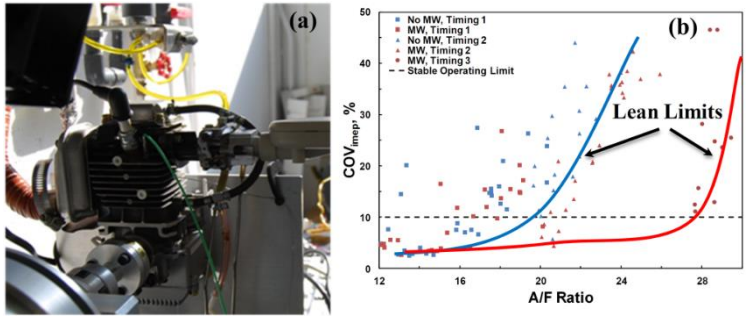

Fig. 2.11 Comparison of ignition using spark plug (left), microwave (middle), gliding arc (right) (Photos were provided by Knite Inc. and Imagineering Inc.) [197]

## Ignition to flame transition (critical radius, $R_c$)

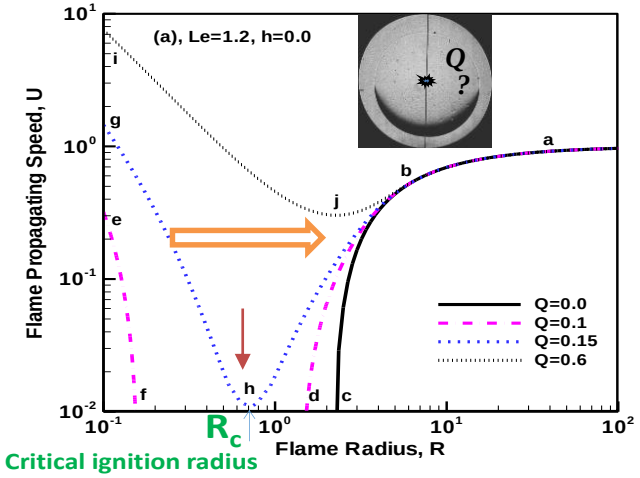


**Role of plasma:**

- **Mainly increase the initial ignition volume, Rc; not increase flame speed!**
- **The thermal effect is not very large.**

# Ignition by nanosecond surface dielectric barrier discharge (SDBD)

S M Starikovskaia

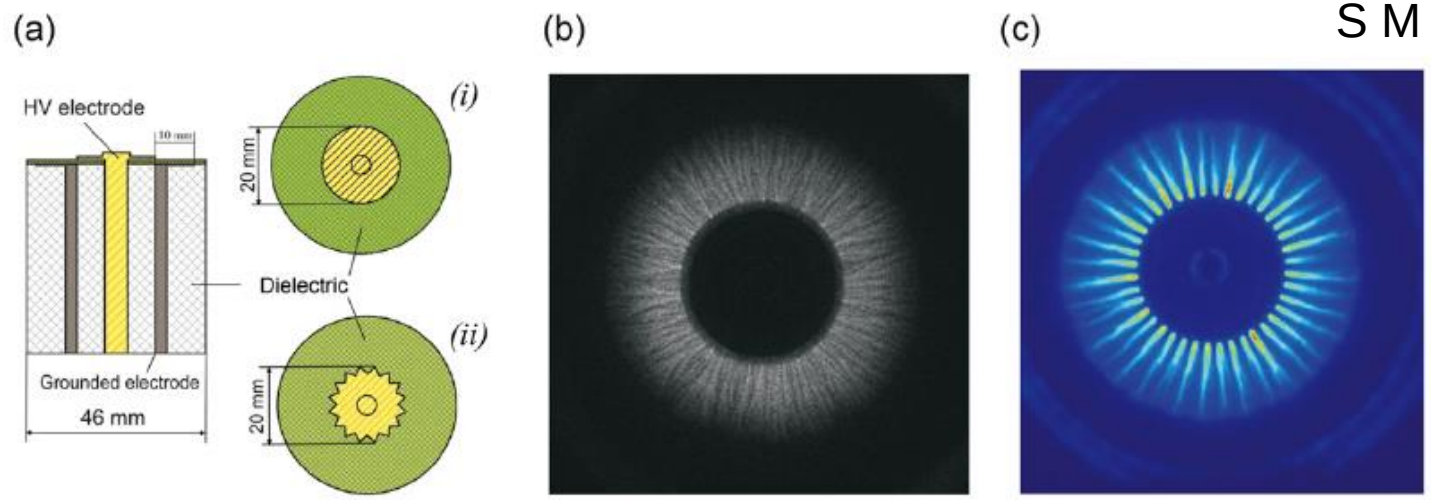


**Figure 21.** Images of nanosecond SDBD discharge in air: (*a*) coaxial system of electrodes for SDBD ignition suggested in (i) [155] and (ii) [159]; (*b*) typical ICCD image of the discharge with a smooth edge electrode taken with a 2 ns camera gate for $P = 1$ bar and $U = +24$ kV [158]; (*c*) snapshot of the discharge with gear-like electrode for $P = 1$ bar and $U = +24$ kV. Reproduced from [159], courtesy of N Aleksandrov.

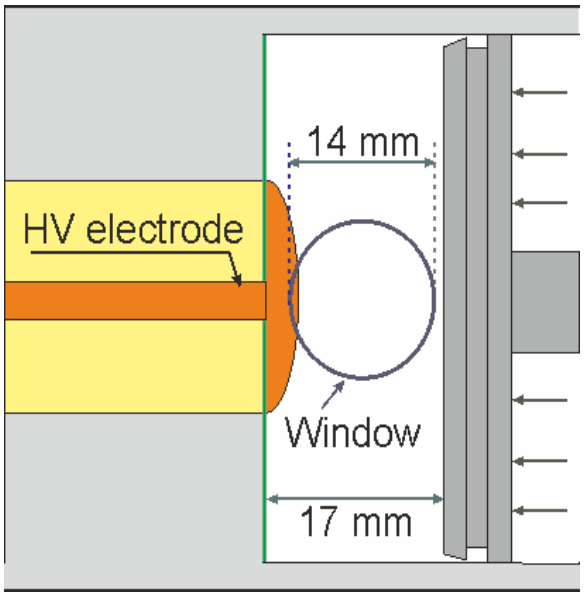


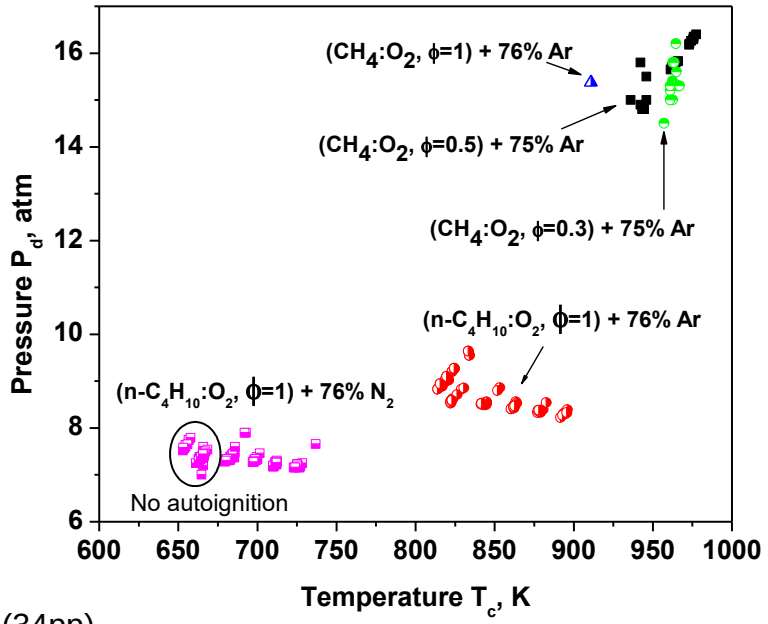


S M Starikovskaia, J. Phys. D: Appl. Phys. 47 (2014) 353001 (34pp)

S.A. Stepanyan, M.A. Boumehdi, G. Vanhove, P. Desgroux, N.A. Popov, S.M. Starikovskaia, Comb. & Flame, 162 (2015) 1336-1349

# Dissociation and fast gas heating *via* electronic excitation of molecular nitrogen

N. Popov, 2011, J. Phys. D: Appl. Phys. 44, 285201 (16pp)

$N_2 + e \rightarrow N_2(C^3\Pi_u) + e$

$N_2(C^3\Pi_u) + O_2 \rightarrow N_2 + O + O(^1D)$

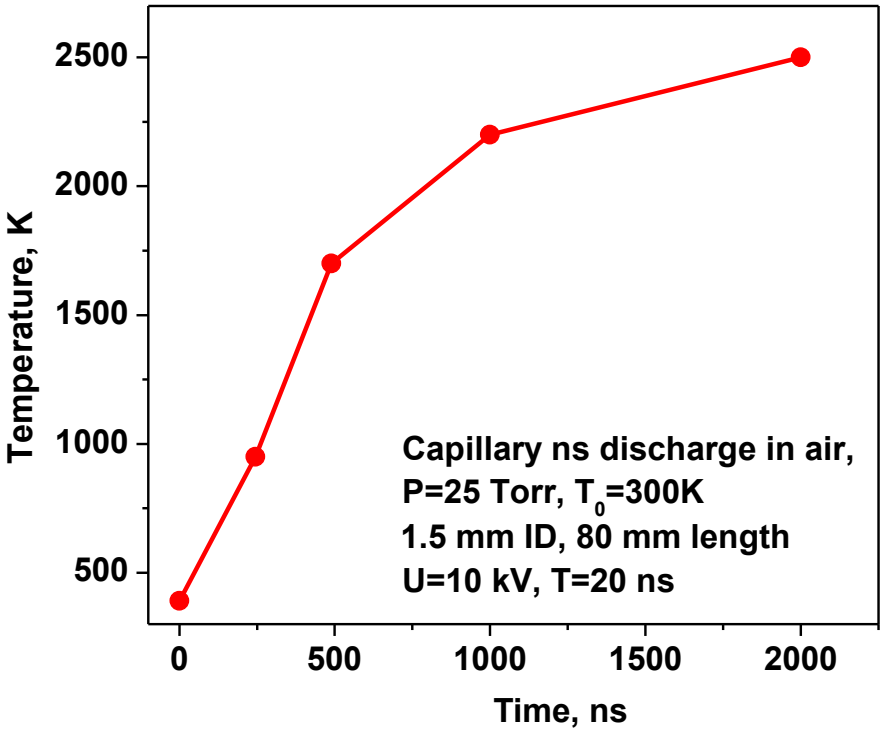


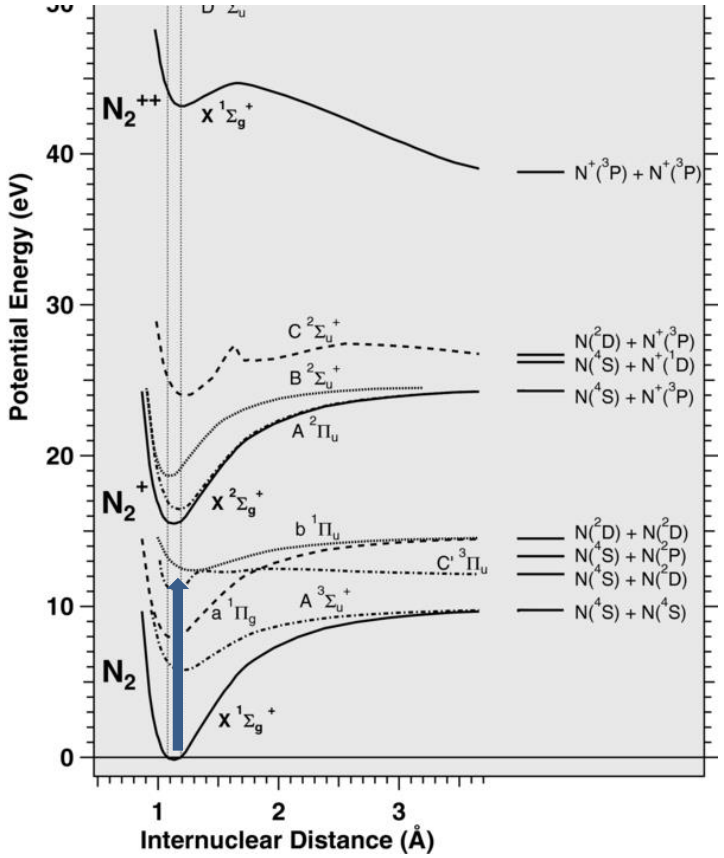


O. Dutuit, N. Carrasco, R. Thissen et al. 2012 The Astrophysical J. Suppl. Series, 204/2

# Autoignition *vs* plasma ignition in RCM at $P_{TDC}$=15 bar and $T_C$=970 K, ($CH_4$:$O_2$)+76%Ar

**E=0.1-5 mJ, 100 "kernels"**

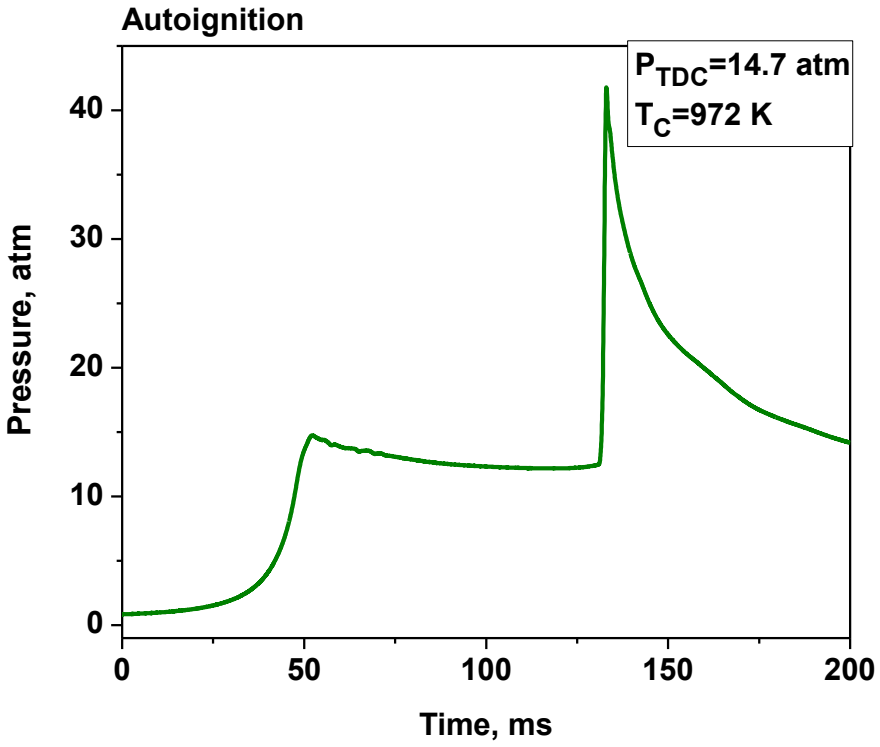


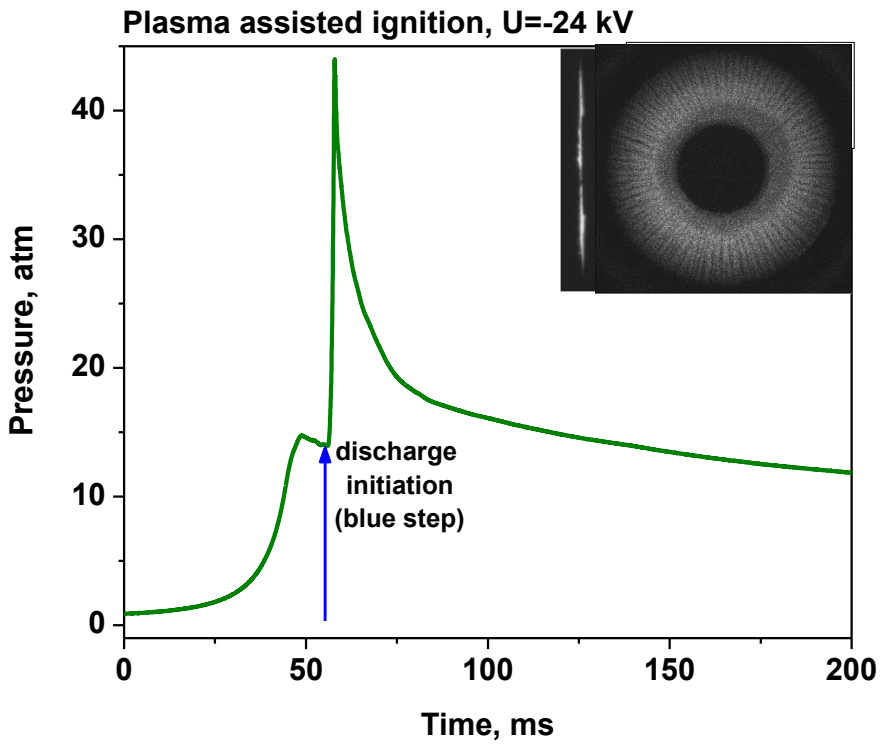


S.A. Stepanyan, M.A. Boumehdi, G. Vanhove, P. Desgroux, N.A. Popov, S.M. Starikovskaia, Comb. & Flame, 162 (2015) 1336-1349

# Pressure trace and corresponding fast imaging of flame propagation

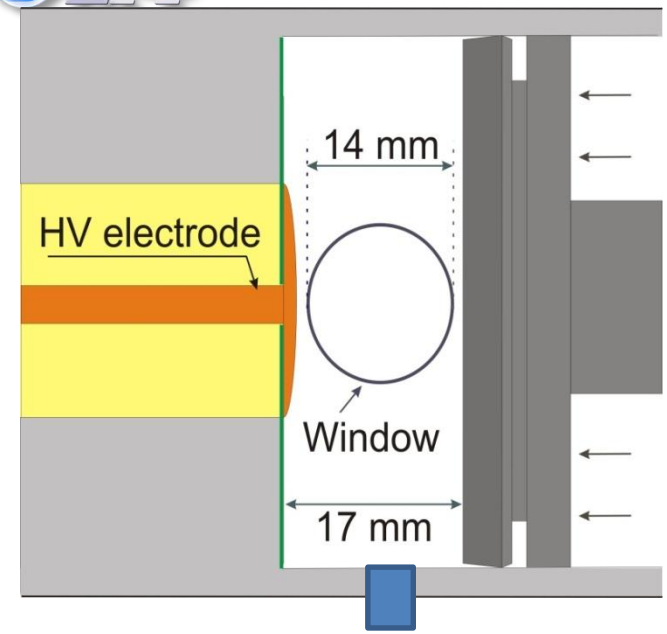


**Pressure detector**

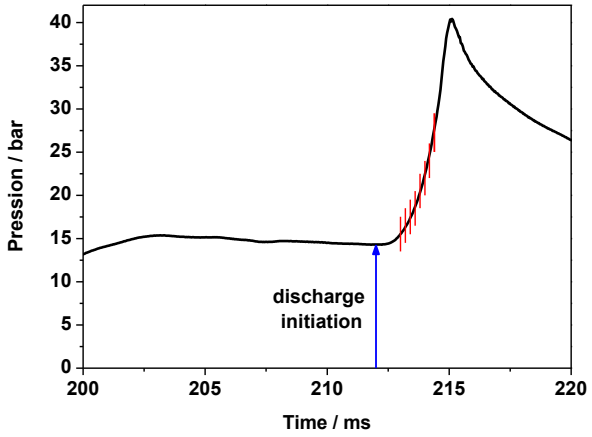


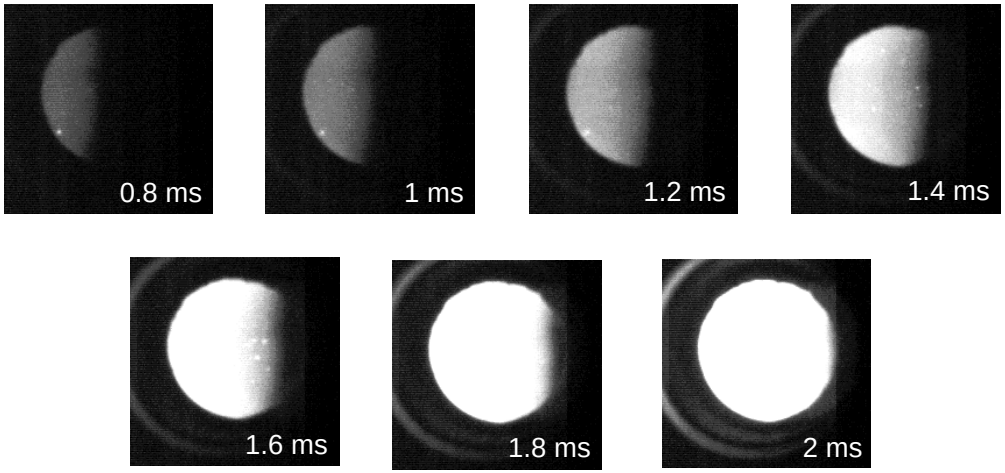


**$CH_4$:$O_2$, ER=1 + 70% Ar,**
**$T_C$=947 K, $P_{TDC}$=15.4 bar**

S.A. Stepanyan, M.A. Boumehdi, G. Vanhove, P. Desgroux, N.A. Popov, S.M. Starikovskaia, Comb. & Flame, 162 (2015) 1336-1349

# Experiments in n–$C_7H_{16}$:$O_2$:$N_2$ Autoignition (black) and plasma ignition (red)

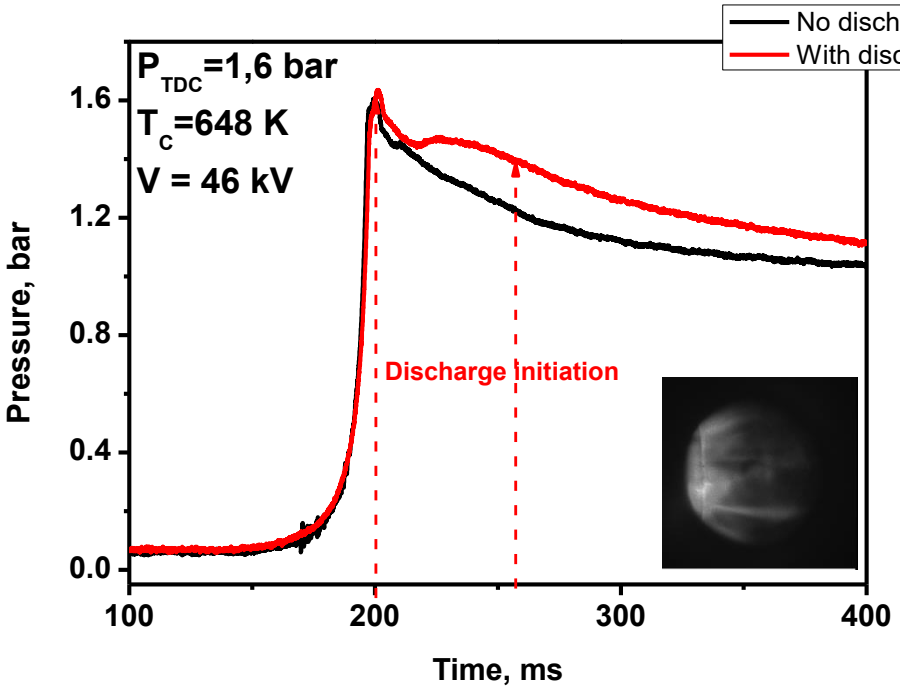


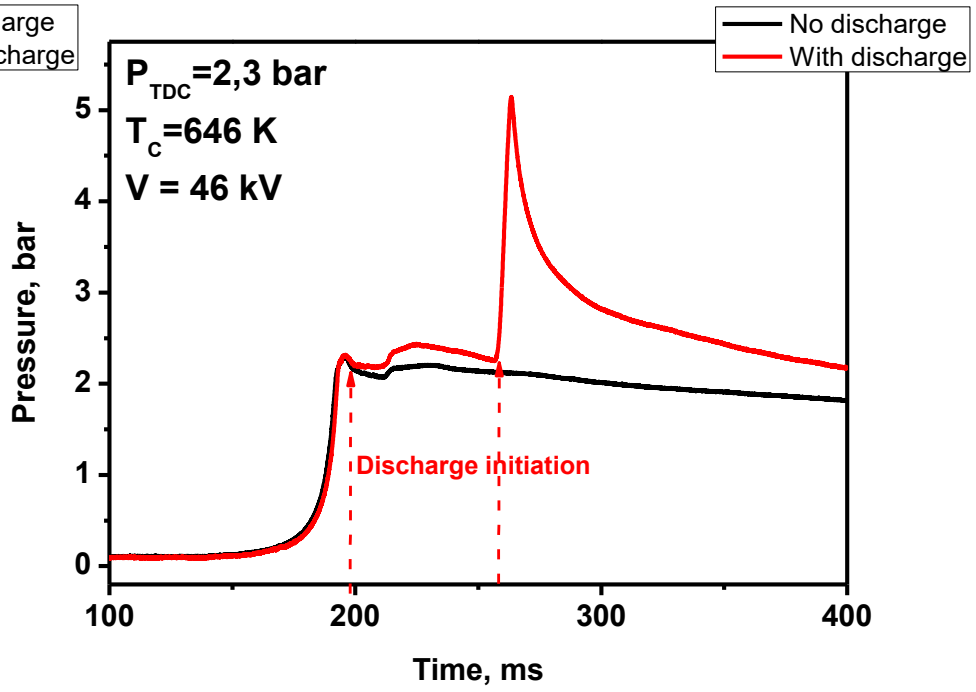


The discharge is able to modify gradually a cool flame (U increase or P increase) and to initiate a 2-stage flame

# Flame Initiation in $H_2$/Air ER=0.5, P=6 bar

Second regime of ignition:
**Ignition along the perimeter of HV electrode**

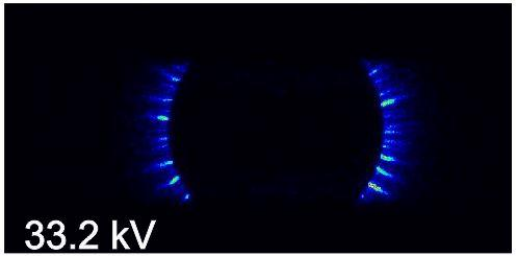


**Polarity: U>0**

**Energy deposition**
**W= 4.8 mJ**

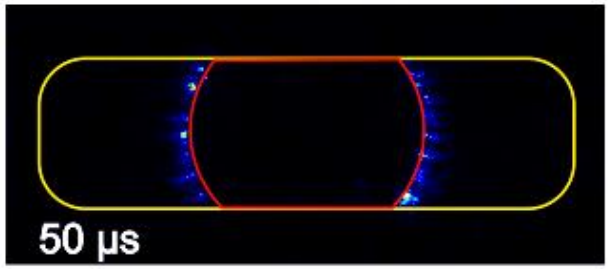


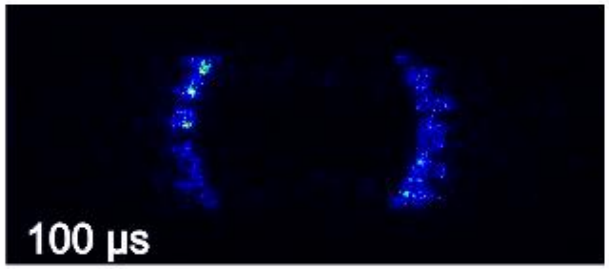


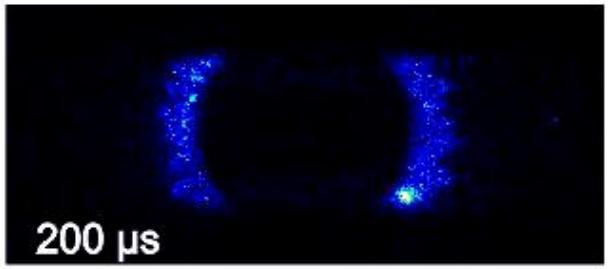


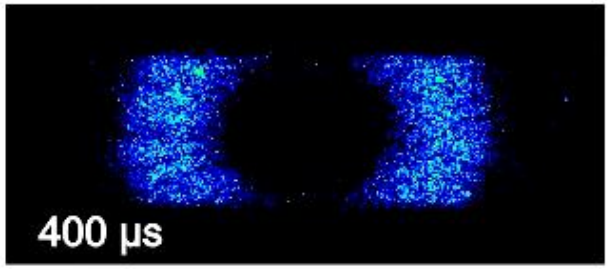


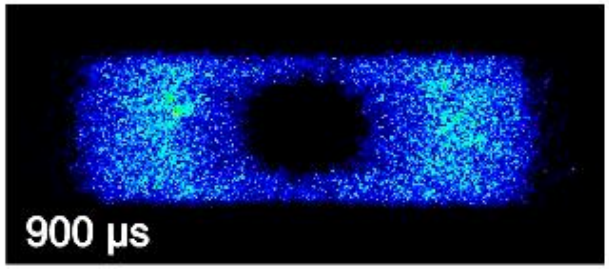


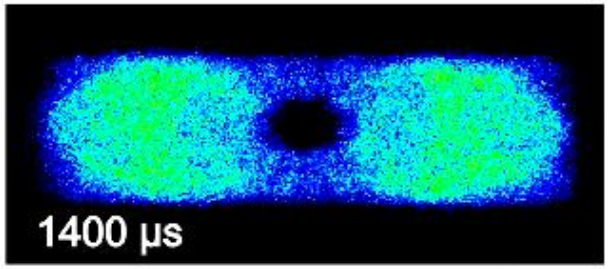


**Quasiuniform ignition around HV electrode. Streamer discharge.**
**Pressure 6 bar, Temperature 300 K.**

S.A. Shcherbanev, N.A. Popov, S.M. Starikovskaia, Comb. & Flame, 176 (2017) 272-284

# Flame Initiation in $H_2$/Air ER=0.5, P=6 bar

Third regime of ignition:
**Ignition along the discharge channels**

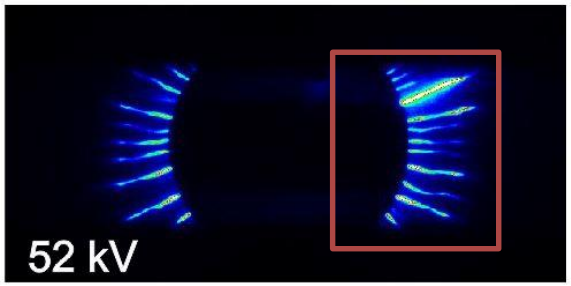


**Polarity: U>0**

**Energy deposition**
**W= 12 mJ**

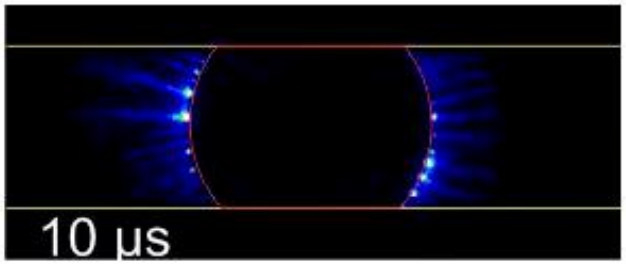


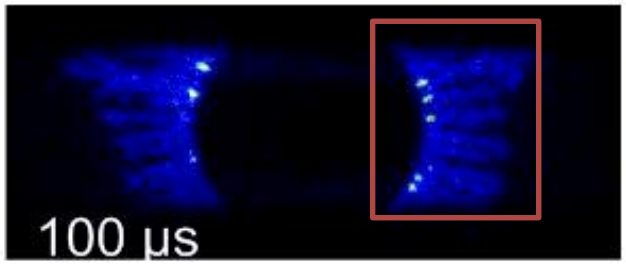


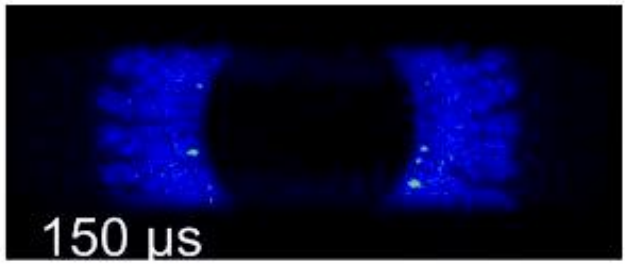


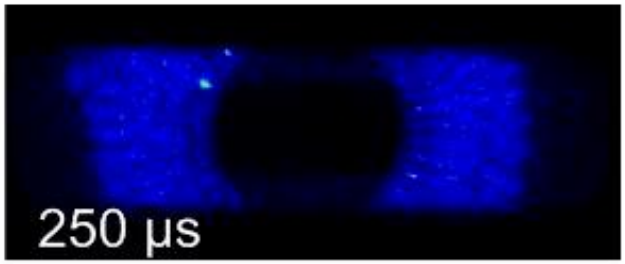


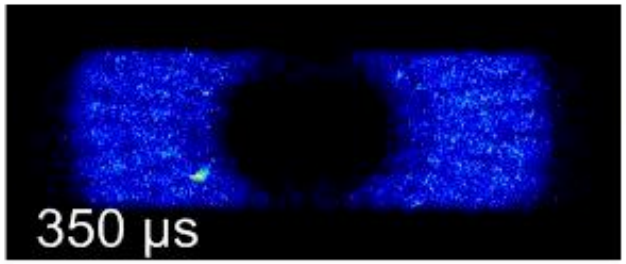


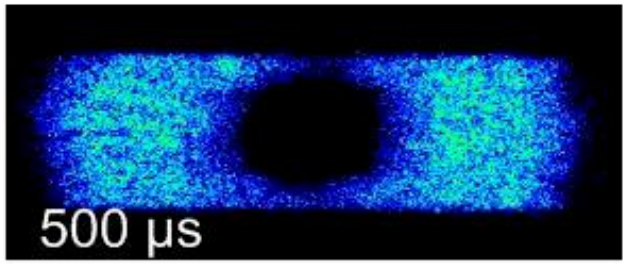


**Ignition along the channels. Filamentary discharge.**
**Pressure 6 bar, Temperature 300 K.**

S.A. Shcherbanev, N.A. Popov, S.M. Starikovskaia, Comb. & Flame, 176 (2017) 272-284

# Controlled plasma discharge for volumetric ignition

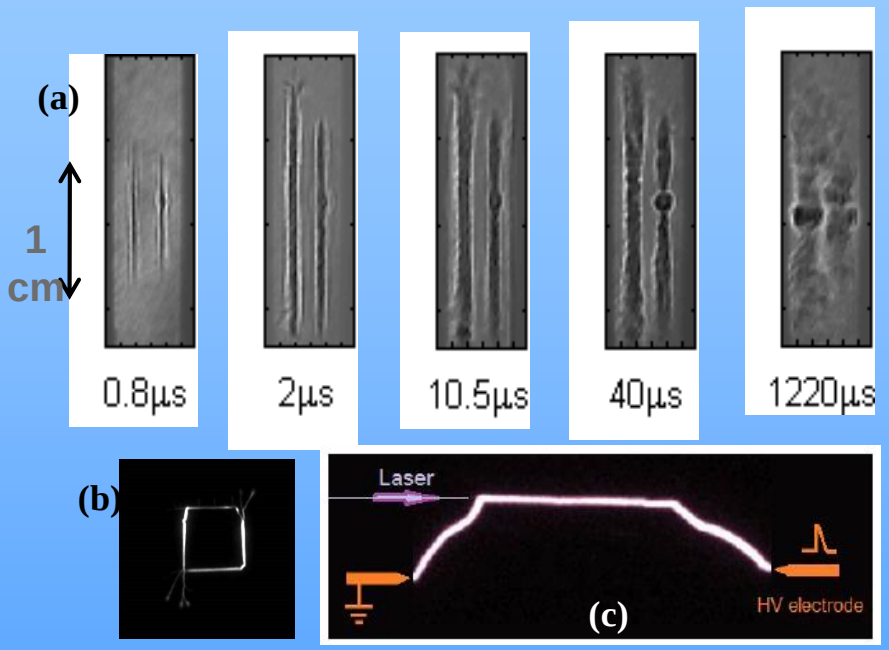


Laser ignition and laser guided discharge control, Miles et al. 2013

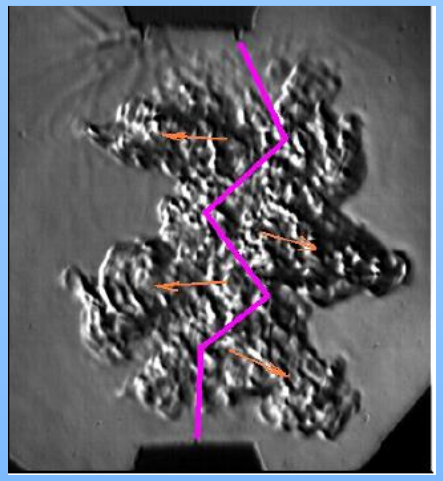

Fig. 3.16 Arc produced flow instability and jets [238]

Fig. 2.21 Direct photograph of a prototype laser igniter showing breakdown in air at multiple points [200]

# Lean flame stabilization demonstrations

- MINI-PAC Bluff-body stabilized flame (propane or methane, 1 bar, 11 kW)

  - LEL: reduced by 10%
  - Plasma power = 75 W

- TWO-STAGE SWIRLED INJECTOR (Propane air, 1 bar, 52 kW)

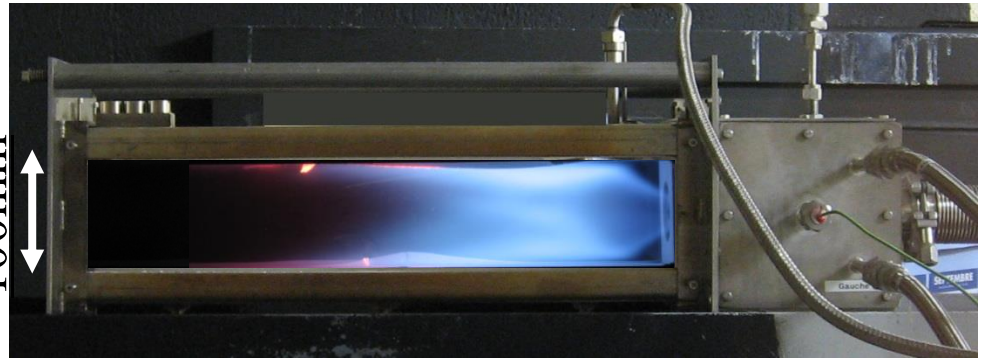


  - LEL: reduced from 0.4 to 0.11
  - Plasma power = 300 W

- AERODYNAMIC INJECTOR (MERCATO, Kerosene/air, 3 bar, 200 kW)

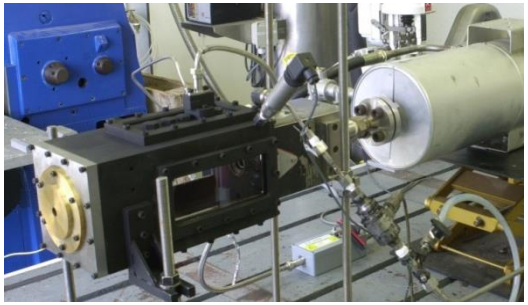

  - LEL: reduced from 0.44 to 0.21
  - Plasma power = 1 kW

# Nanosecond discharge on fuel lean flame stabilization

Princeton University

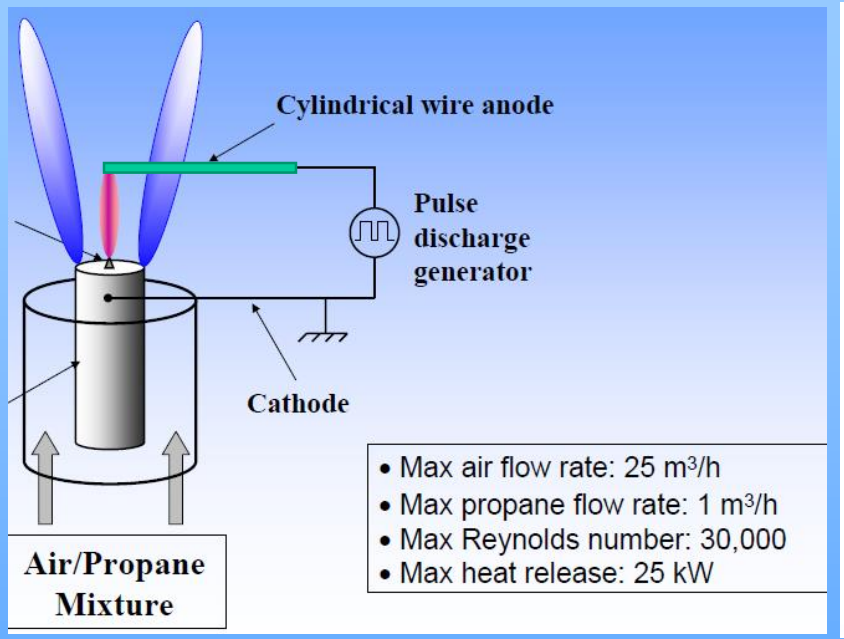
Cylindrical wire anode
Pulse discharge generator
Cathode
Air/Propane Mixture
• Max air flow rate: 25 m³/h
• Max propane flow rate: 1 m³/h
• Max Reynolds number: 30,000
• Max heat release: 25 kW

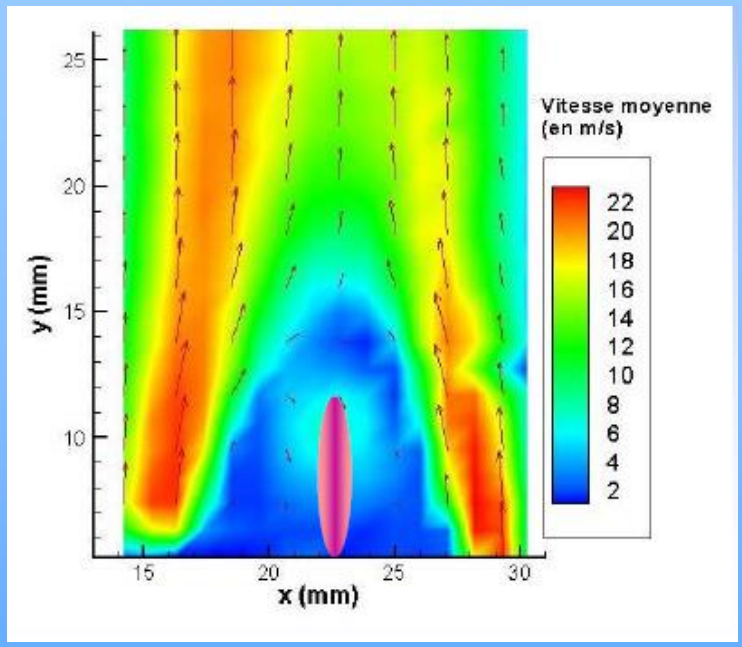


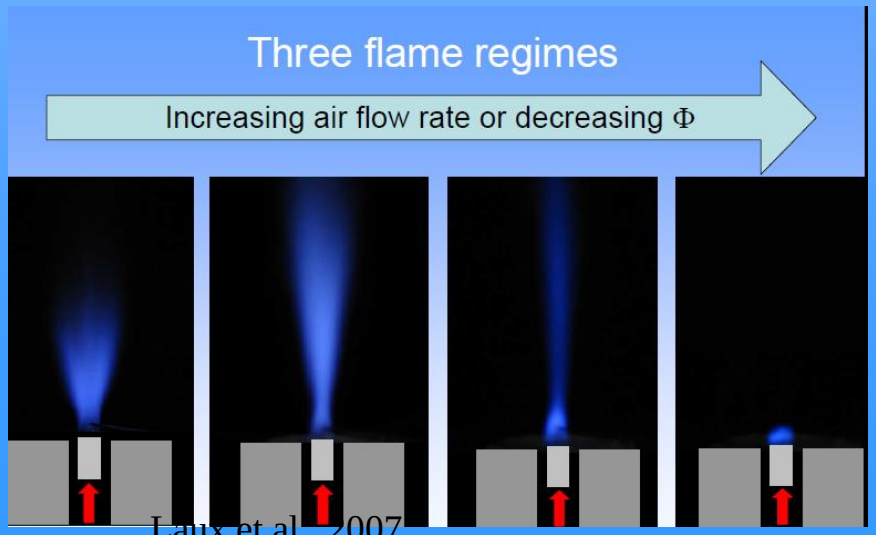


Laux et al., 2007

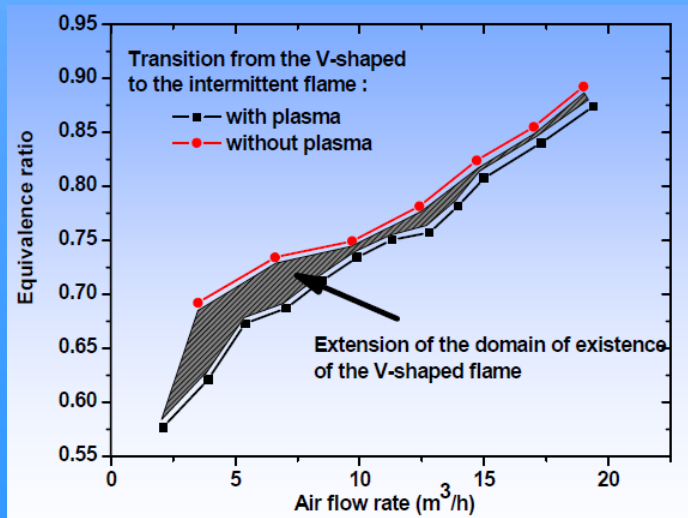
Transition from the V-shaped to the intermittent flame :
with plasma
without plasma
Extension of the domain of existence of the V-shaped flame
Equivalence ratio
Air flow rate (m³/h)

# Plasma assisted fuel reforming

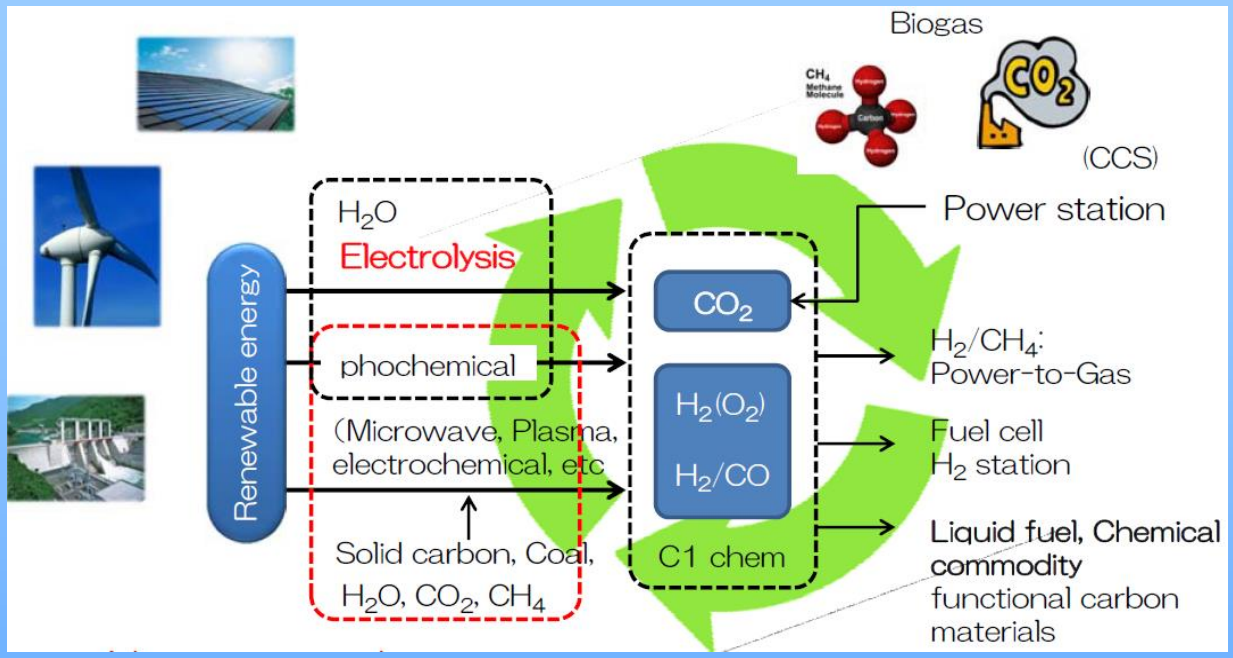


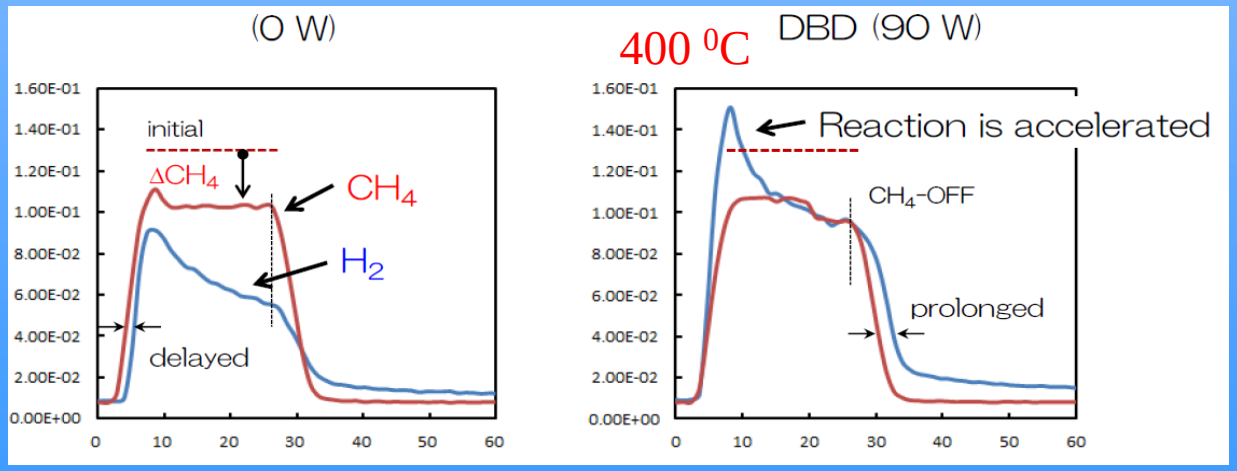


Experimental conditions

| Duty ratio | $CH_4$:$CO_2$ | GHSV (STP) | Plasma | Pressure |
|---|---|---|---|---|
| 25 % | 600/400 ccm | 10300 $h^{-1}$ | 70 W (1 eV/molec) | 5 kPa |

Ozaki, 22nd ISPC, 2015

Princeton University

Princeton University

# Technical questions:

1. Plasma can do a lot of “magics” in combustion enhancement. Does it really have any “kinetic merits” on combustion enhancement?

2. How does plasma kinetically enhance ignition, flame speed, and minimum ignition energy?

3. What are the reaction pathways of plasma assisted combustion?

# Lecture 3 Effects of plasma on ignition, flame propagation, burning limits, and the minimum ignition energy

Yiguang Ju

- The impact of plasma on Ignition and ignition limits
- Flame propagation and the effects of heat loss and stretch
- Extinction, quenching distance, and flammability limits
- The Minimum ignition energy and the critical flame initiation radius
- The effect of electric field on flame propagation speed

# 3.1.1 Ignition and ignition limits

**Auto-ignition** Considering an auto-ignition problem at constant pressure, p, at initial temperature of $T_0$, and fuel mass fraction of $Y_{F0}$.

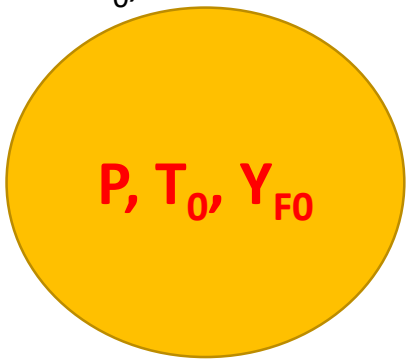


ρ:density
T: temperature
Y: mass fraction
Q: heat release per unit mass of fuel
E: activation energy

Conservation equation

$$\rho C_p \frac{dT}{dt} = BQ\rho Y_F e^{-E/RT}$$

$$\rho \frac{dY_F}{dt} = -B\rho Y_F e^{-E/RT}$$

$$T(0) = T_0, \qquad Y_F(0) = Y_{F0}$$

Adding the mass and energy equations:

$$\rho \frac{d}{dt}(C_p T/Q + Y_F) = 0$$

$$C_p T/Q + Y_F = C_p T_0/Q + Y_{F0} = C_p T_{ad}/Q + 0$$

Normalization:

$$\theta \equiv T/T_0$$

$$q = QY_{F0}/C_p T_0$$

$$\beta = E/RT_0$$

$$\tau = t/\tau_0$$

$$\tau_0 = (\beta B e^{-E/RT_0})^{-1}$$

$$T_{ad} \equiv T_0 + QY_{F0}/C_p = T_0(1+q)$$

$$Y_F = Y_{F0} - C_p(T - T_0)/Q = \frac{C_p T_0}{Q}(1+q-\theta)$$

$$e^{-E/RT} = e^{-E/RT_0} e^{E/RT_0 - E/RT} = e^{-E/RT_0} e^{\beta(\theta-1)/\theta}$$

**Normalized equation:**

$$\frac{d\theta}{d\tau} = \frac{1}{\beta}(1+q-\theta)e^{\beta(\theta-1)/\theta}$$

$$\theta(0) = 1$$

Asymptotic theory : in the limit of $\beta \to \infty$,

a small change in temperature will lead to dramatic change in the reaction rate, therefore, in this limiting case, we have

$$\theta - 1 \to O(1/\beta)$$

Define: $\theta - 1 \equiv \vartheta / \beta$

$$\frac{d\vartheta}{d\tau} = qe^{\vartheta}$$

$$\vartheta(0) = 0$$

Solution:

$$\vartheta = -\ln(1-q\tau)$$

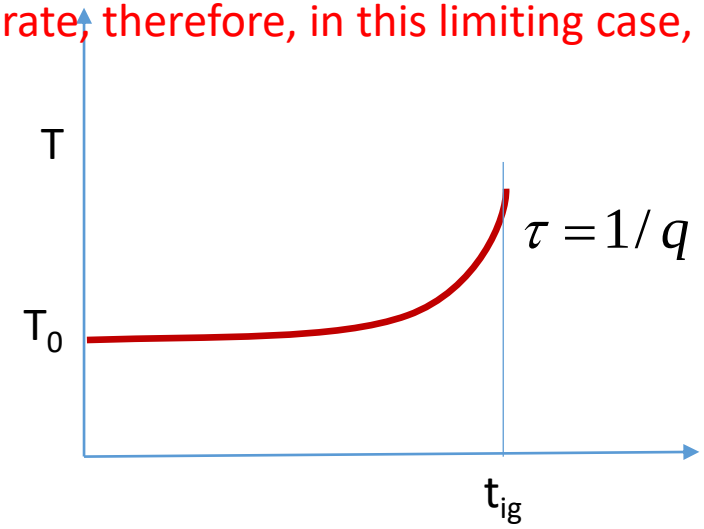


Ignition time : $\tau_{ig} = 1/q$; exponential growth

$$t_{ig} = \tau_{ig}\tau_0 = q^{-1}(\beta B e^{-E/RT_0})^{-1} = \frac{RC_p T_0^{\ 2}}{BQY_{F0}E} e^{E/RT_0}$$

**Plasma effects on homogenous ignition (B, E, T):**

1. Increase reaction rate B; 2. Reduce activation energy E, 3. change temperature (heat loss or addition)

**Auto-ignition with heat loss or heat addition**

Assume: heat addition or loss is a small perturbation O(1/β):

$$\rho C_p \frac{dT}{dt} = BQ\rho Y_F e^{-E/RT} + \frac{4\pi R^2 h(T - T_0)}{4\pi R^3/3}$$

$$\rho \frac{dY_F}{dt} = -B\rho Y_F e^{-E/RT}$$

$$T(0) = T_0, \qquad Y_F(0) = Y_{F0}$$

$$\frac{d\vartheta}{d\tau} = qe^{\vartheta} - H\vartheta$$

$$\vartheta(0) = 0$$

$$H = \frac{3ht_0}{\beta R\rho C_p}$$

Plasma heat addition/loss will shorten/extend the ignition delay time

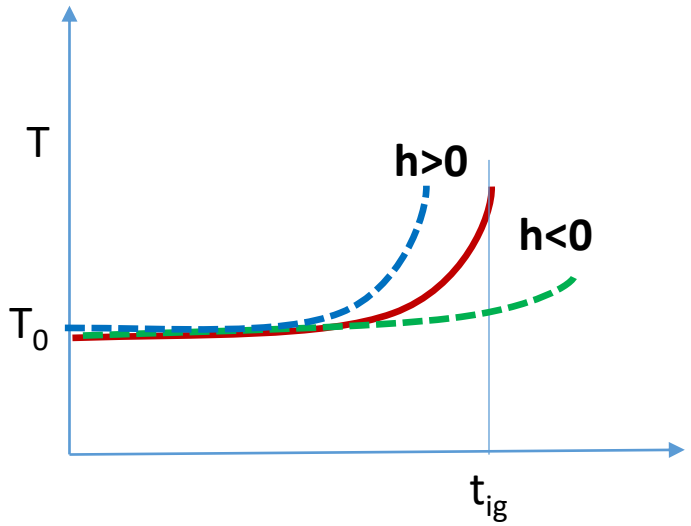

# 3.1.2 Plasma chemistry for radical production and heating

**Electron impact ionization/dissociation/excitation**

| | | | |
|---|---|---|---|
| >10 eV | $e + O_2 = O^+ + O + 2e$ | (R1a) | Radical production |
| ~10 eV | $e + O_2 = O + O(^1D)$ | (R1b) | Excitation |
| ~1 eV | $e + O_2 = O_2(^1\Delta_g) + e$ | (R1c) | |
| 0.2-2 eV | $e + O_2 = O_2(v) + e$ | (R1d) | |

**Electron ion recombination, attachment, charge transfer**

| | | |
|---|---|---|
| $e + O_2^+ = O + O(^1D)$ | (R2a) | Recombination/fast heating |
| $O_2^+ + O_2^- = 2O_2$ | (R2b) | Recombination/fast heating |
| $e + O_2 + M = O_2^- + M$ | (R2c) | Attachment |
| $H_2O + N_2^+ = H_2O^+ + N_2$ | (R2d) | Charge Transfer |

**Dissociation and energy transfer by ions and excited species**

| | | |
|---|---|---|
| $N_2(A,B,C) + O_2 = O + O + N_2$ | (R3a) | |
| $O(^1D) + H_2 = OH + H$ | (R3b) | |
| $H + O_2(^1\Delta_g) = O + OH$ | (R3c) | |
| $N^+ + O_2 = O^+ + NO$ | (R3d) | |
| $CH_3 + HO_2(v) = CH_2O + OH$ | (R3e) | |
| $N_2(v=5) + N_2 = N_2(v=3) + N_2$ | (R3f) | Slow heating |
| $N_2(v) + HO_2 \rightarrow N_2 + HO_2(v)$ | (R3g) | |

# Kinetic ignition enhancement by radiation production

Princeton University

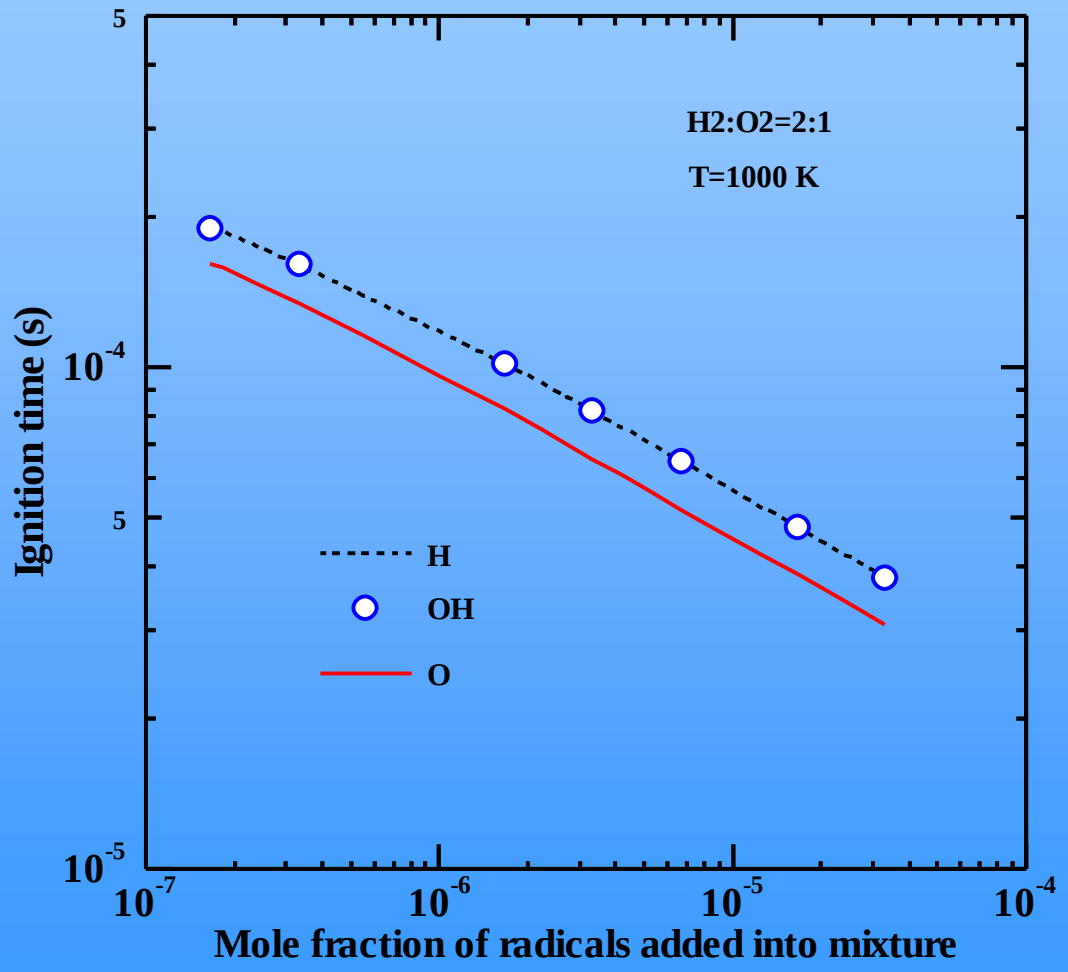


Chain initiation

$H2 + O2 \rightarrow H + HO2$

$H2 + O2 \rightarrow OH + OH$ Slow

Chain branching and propagation

$H + O2 \rightarrow OH + O$

$O + H2 \rightarrow OH + H$

$OH + H2 \rightarrow H2O + H$

Chain-termination

$H + O2 + (M) \rightarrow HO2 + (M)$

$H + OH + (M) \rightarrow H2O + (M)$

*Combustion lab.*

# Kinetic effect by NO production on counterflow ignition

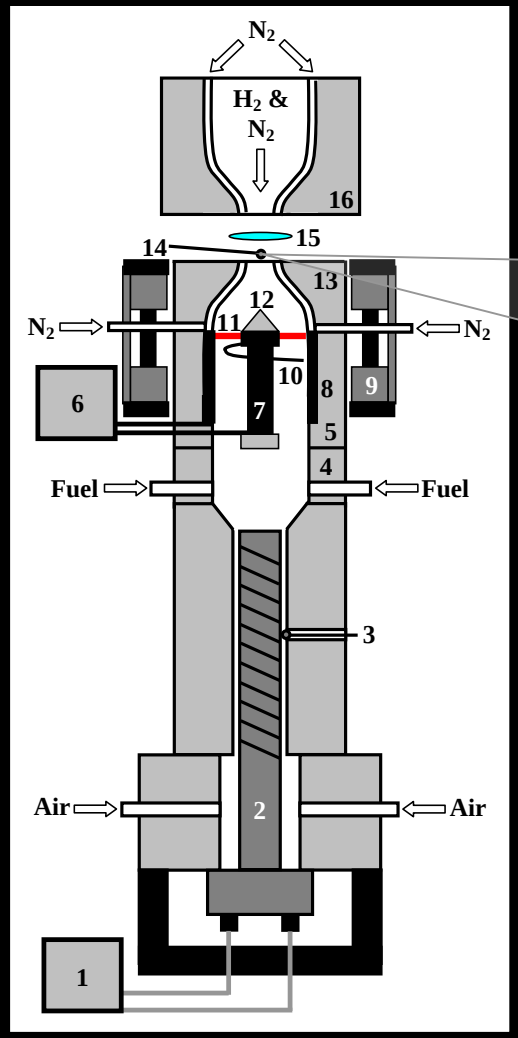


**Temperature & Species Measurements**
- **FTIR, PLIF, Rayleigh**

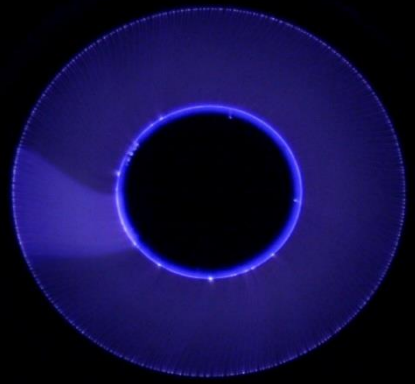

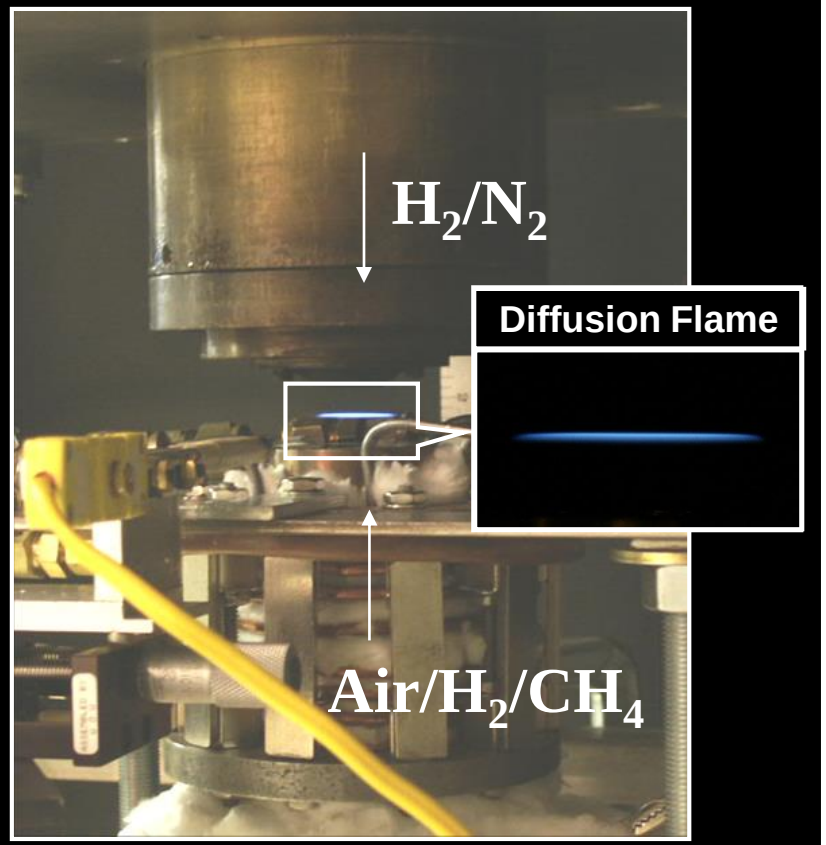


1. Silicon Controlled Rectifier, 2. Silicon carbide heater, 3. R-type thermocouple, 4. Fuel injection spacer 5. MGA plasma power supply, 5. MGA device, 6. MGA power supply, 7. Cathode, 8. Anode, 9. Magnets, 10. Gliding arc initiation wire, 11. MGA, 12. Insulator, 13. Nozzle with $N_2$ co-flow, 14. K-type thermocouple & FT-IR probe, 15. Diffusion flame, 16. Water-cooled nozzle with $N_2$ co-flow.

# Plasma assisted ignition: $H_2$ Ignition by gliding arc

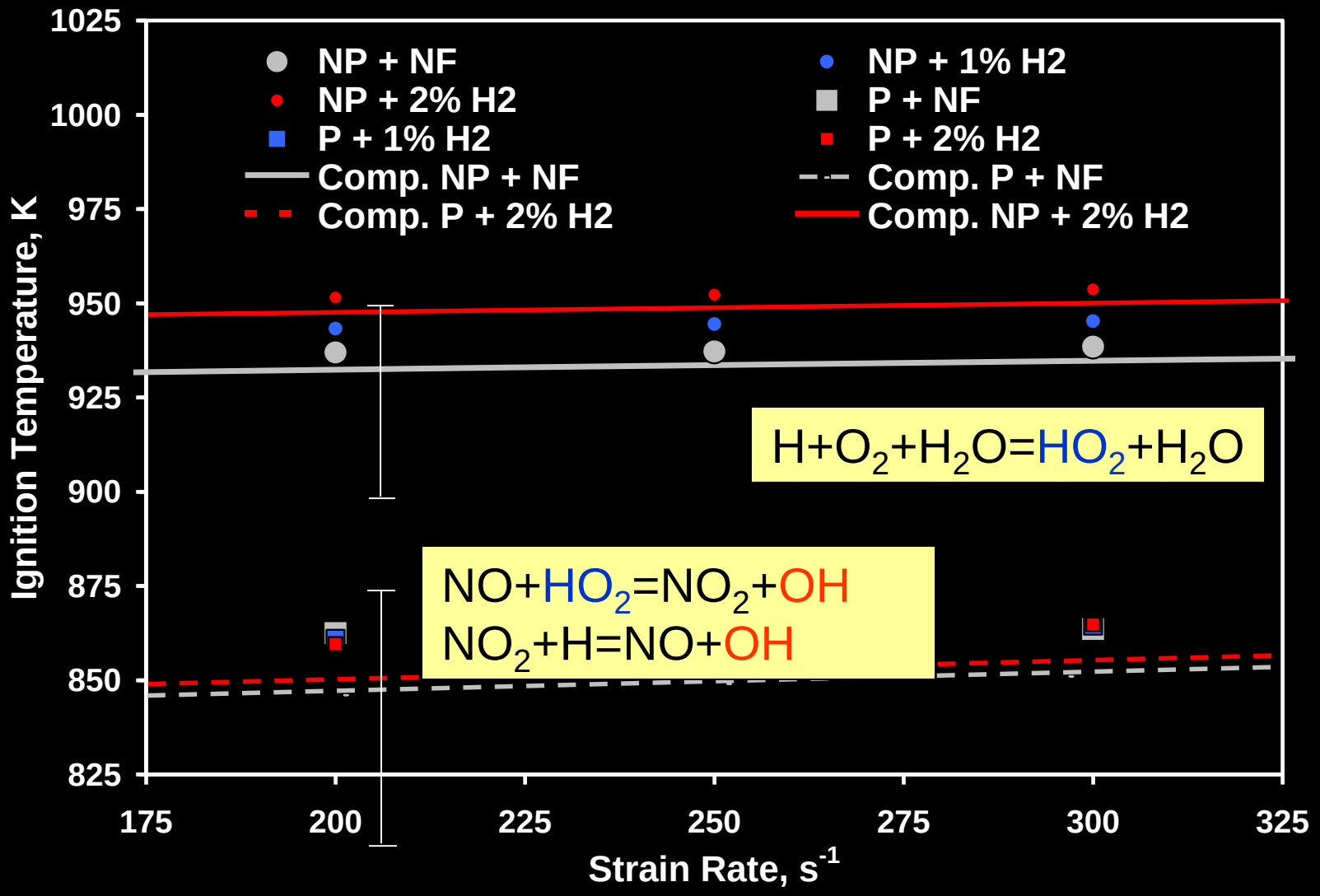


Plasma catalytic effects reduce H2 ignition temperature

(Ombrello, T., Ju, Y. and Fridman, A., 2008. *AIAA journal*, *46*(10), pp.2424-2433.)

# Plasma can break the conventional explosion limit

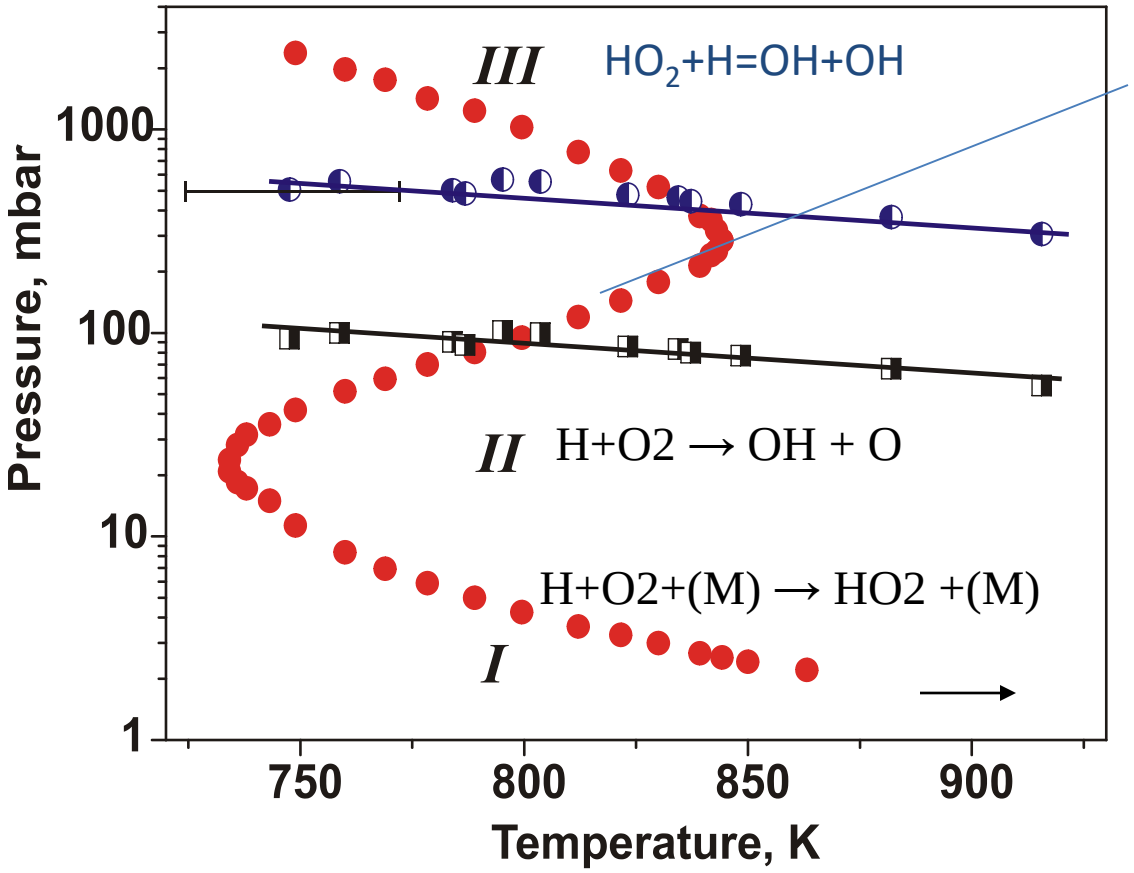


**d[H]/dt→infinity**

$$\frac{2k_1}{k_2[M]} < 1$$ Not explosive

$$> 1 \longrightarrow$$ explosive

$$H+O_2 \begin{cases} \rightarrow OH+O & (R1) \\ +(M) \rightarrow HO_2 & (R2) \end{cases}$$

- Maas, U., Warnatz, J. Combust. Flame, **74**, 1988, 53.
- ◐,◨ Bozhenkov, S.A., Starikovskaia, S.M., and Starikovskii, A.Yu. Combust. Flame, **133**, 2003, 133.

- Radical and heat production by plasma can extend the explosion limit.

Princeton University

# Ignition Chemistry: Elementary chain reactions of $CH_4$-$O_2$ system

Chain initiation:

CH4 +O2 → CH3 +HO2

CH4+(M) → CH3 +H+(M) **Slow**

Chain-branching and propagation

H+O2 → OH + O

**CH3 +O2 → CH3O+O** → **Opportunity of plasma**

**CH3 +O2 → CH2O+OH** **Slow**

**CH3 +HO2 → CH3O+OH**

CH3O + O2 →CH2O+ HO2

CH3O + M →CH2O+ H+M

CH2O +X →HCO+XH (X=H, OH, O, HO2)

HCO+M→CO+H+M

$HCO+O_2 \rightarrow HO_2+CO$

$CO+HO_2 \rightarrow CO_2+OH$

Termination reaction

H+O2+M → HO2 +M

$CO+OH \rightarrow CO_2+H$

*Combustion lab.*

# Kinetics of the ignition: $CH_4$:$O_2$:Ar mixture ($T_5$=1530 K, $n_5$=5x$10^{18}$ $cm^{-3}$)

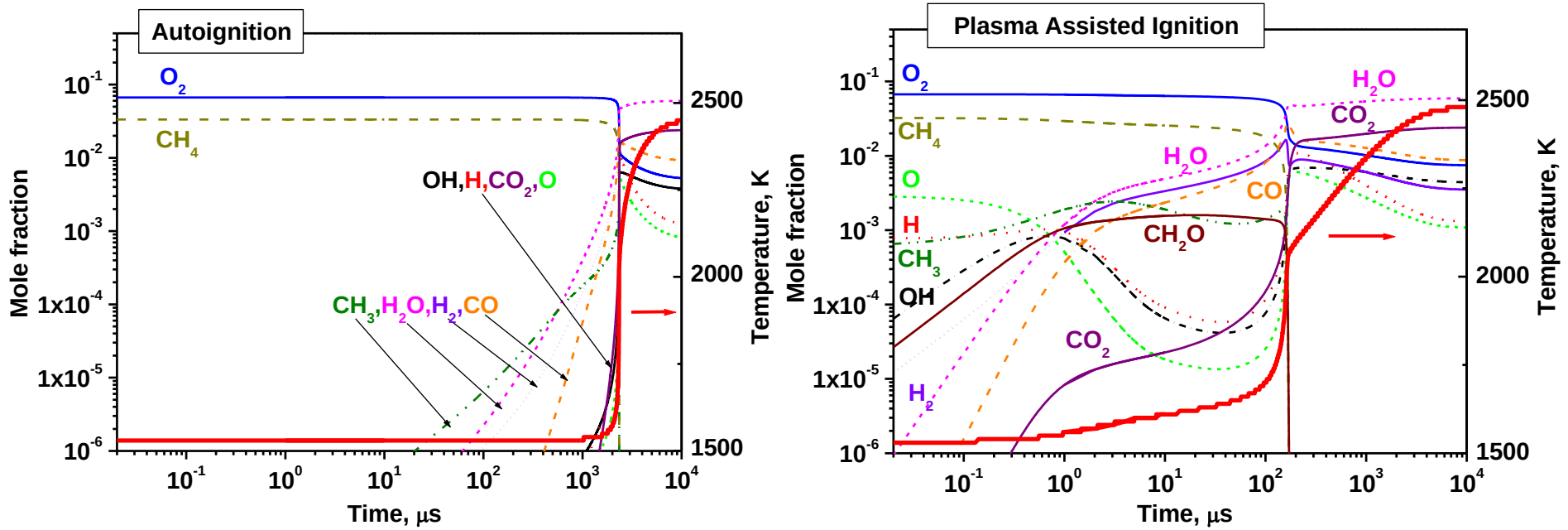


Plasma assisted ignition is characterized by:

– slow increase of gas temperature
– developed kinetics of intermediates
– partial fuel conversion during induction time

I N Kosarev, N L Aleksandrov, S V Kindysheva, S M Starikovskaia, A Yu Starikovskii, Combustion and Flame, 154 (2008) 569-586

# Plasma assisted ignition: experiments and numerical modeling: ($CH_4$-$C_5H_{12}$):$O_2$ + 90% Ar

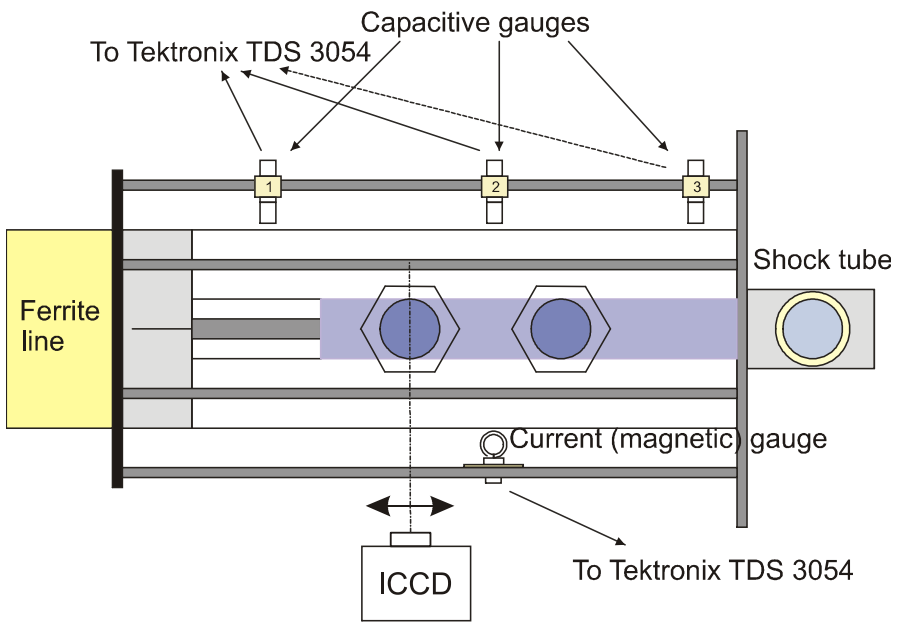


Shock tube/nanosecond dsicharge experiments

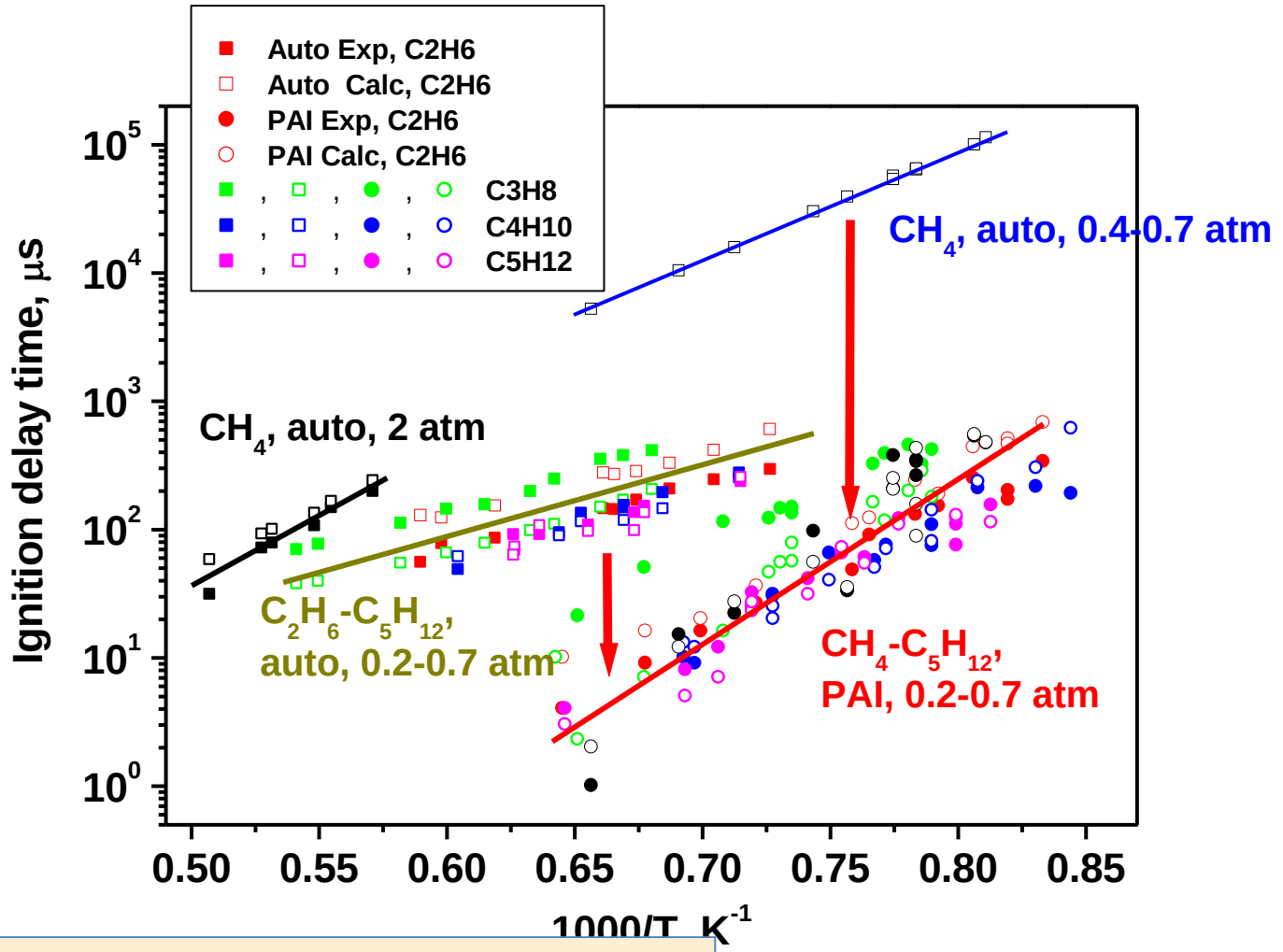


I N Kosarev, N L Aleksandrov, S V Kindysheva, S M Starikovskaia, A Yu Starikovskii, Combustion and Flame, 156 (2009) 221-233

# Plasma kinetic effect on CH4 ignition (gliding arc)

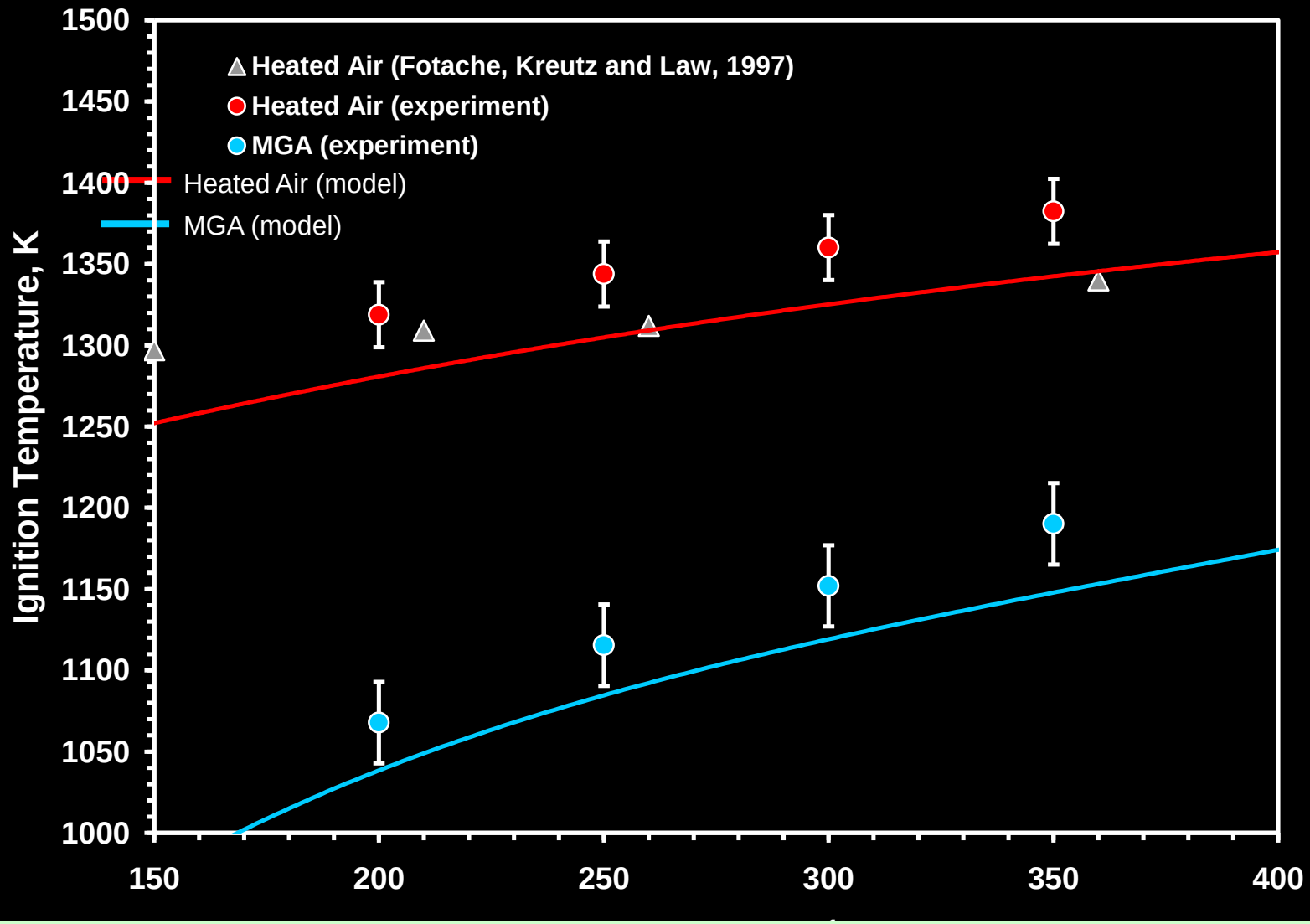


Plasma catalytic effects reduce CH4 ignition temperature

(Ombrello, T., Ju, Y. and Fridman, A., 2008. *AIAA journal*, *46*(10), pp.2424-2433.)

# 3.1.3 Plasma Assisted Combustion: The impact of plasma on the ignition and extinction S-curv

## The effect of kinetic enhancement (μs ~ ms, 800-1200 K)

**New "S-curve" by Plasma assisted combustion for small molecule fuel such as $H_2$, $CH_4$**

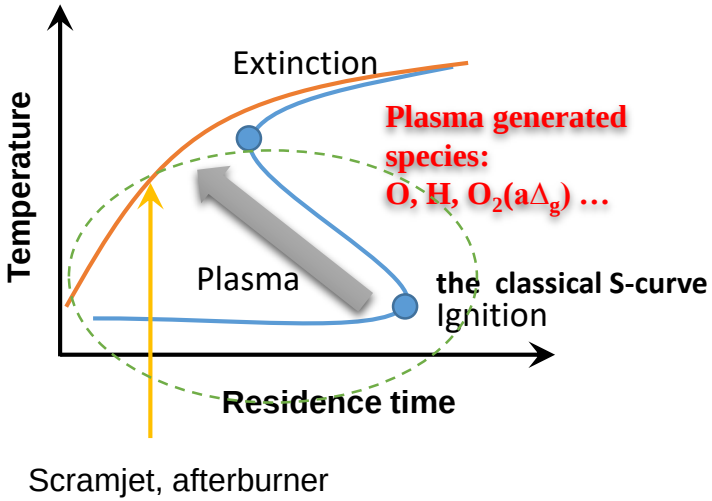


Scramjet, afterburner

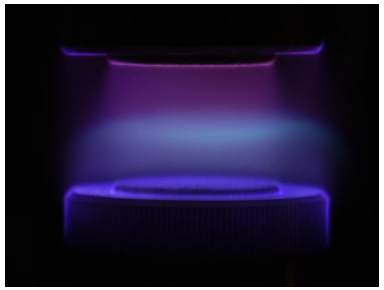

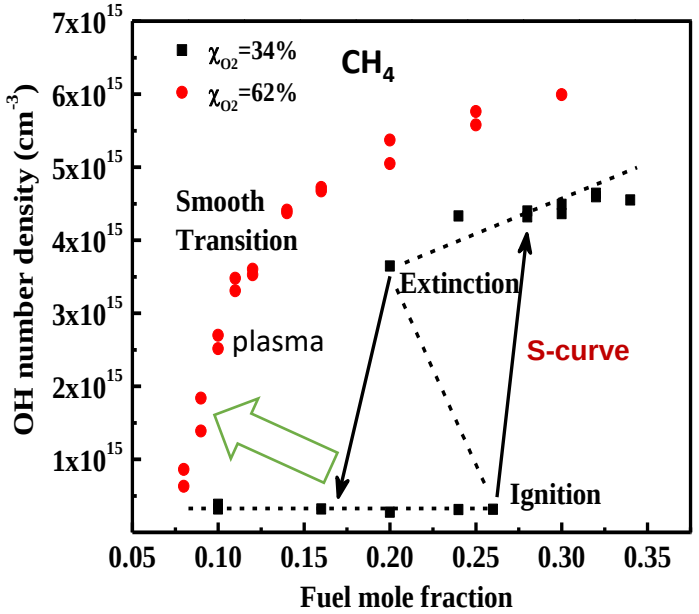


- Strong kinetic enhancement at intermediate temperature
- Less effect at high temperature

**Non-thermal plasma dramatically enhances ignition chemistry, but less impact on flame speed/extinction limit!**

Sun et al. Proc. Comb. Inst. 34, 2010, Combust. Flame 2011, 2012
Ombrello et al. 2008

# Plasma Activated Low Temperature Combustion for large hydrocarbon fuels

**Two-stage ignition**: n-heptane

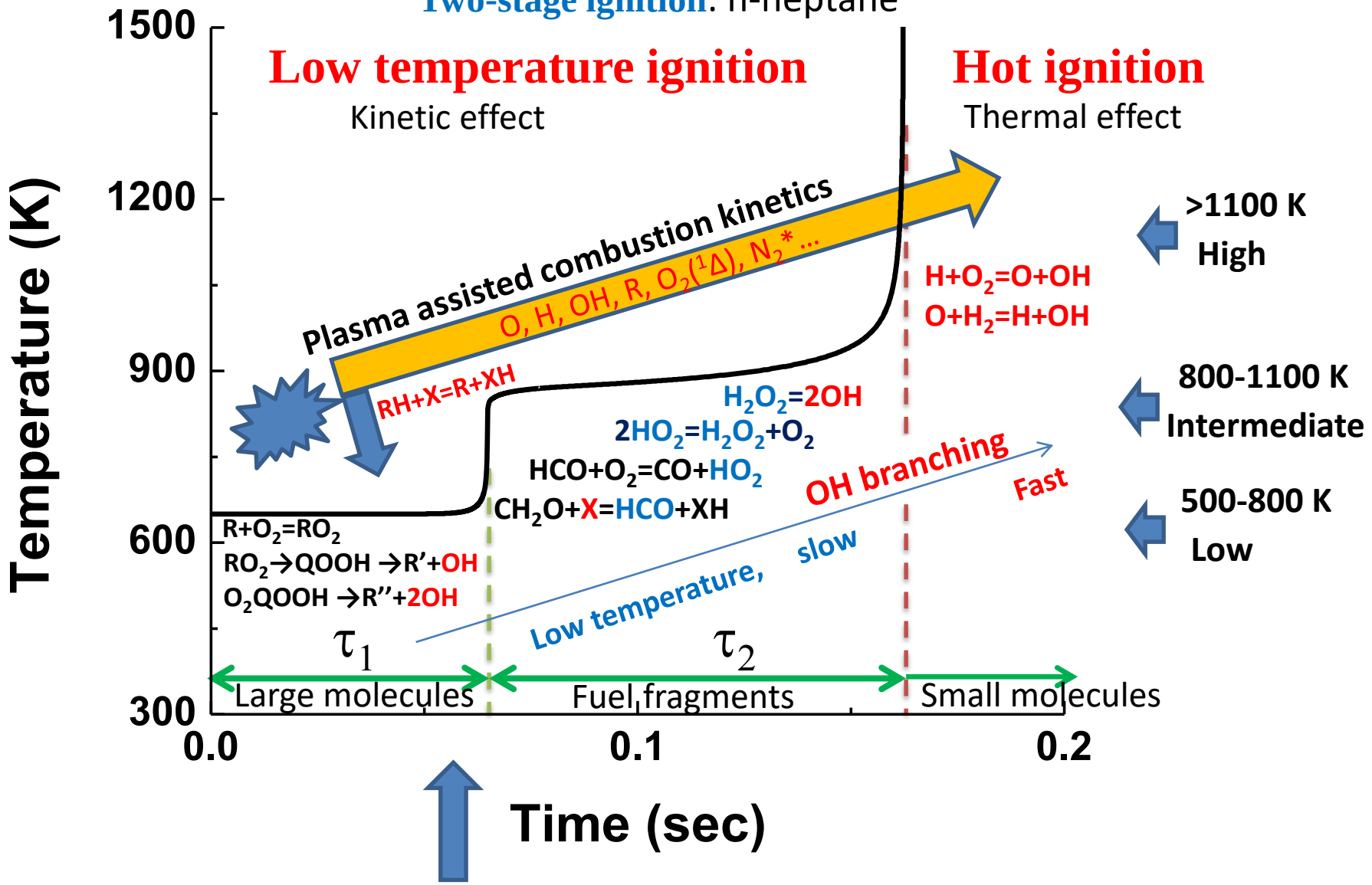


**More kinetics effect of PAC at low temperature combustion?**

# Nanosecond plasma assisted low temperature ignition of dimethyl ether ignition in a diffusion counterflow flame

**P = 72 Torr, a= 250 1/s, *f* = 24 kHz**
**$X_{O_2}$=40%, varying $X_f$**

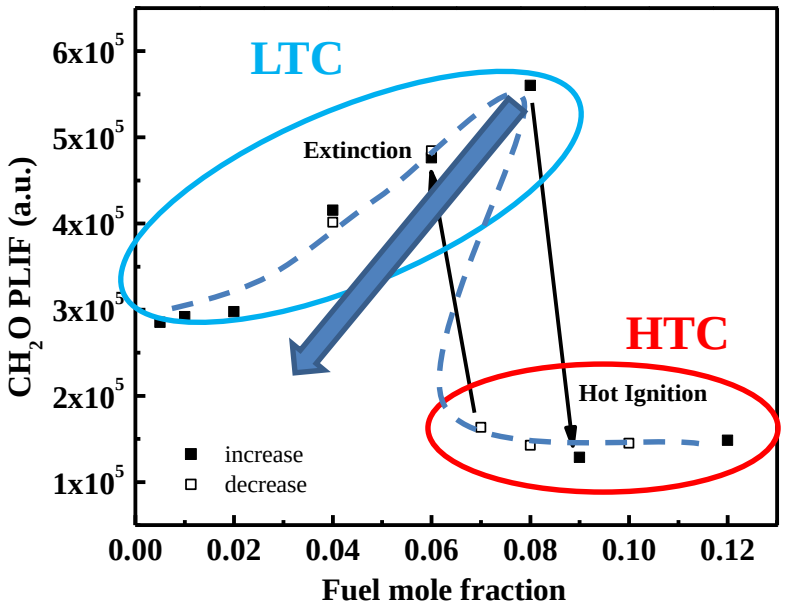


**S-Curve**

**P = 72 Torr, a= 250 1/s, *f* = 34 kHz,**
**$X_{O_2}$=60%, varying $X_f$**

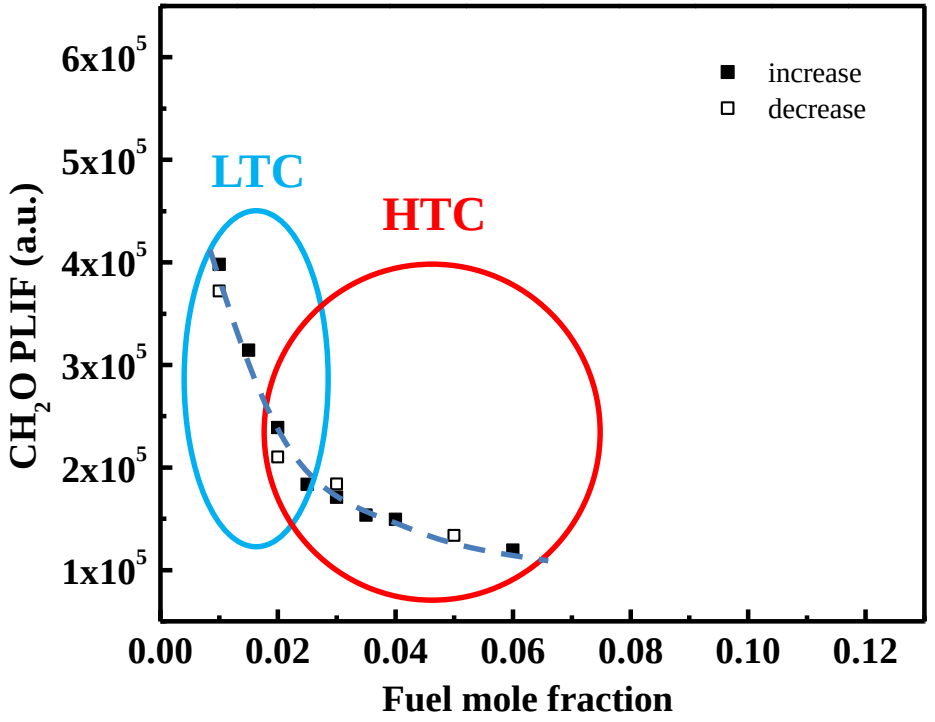


**New ignition/extinction curve without extinction limit**

**Radical production by plasma can activate LTC at much shorter timescale.**

Sun, W., Won, S.H. and Ju, Y., 2014. Combustion and Flame, 161(8), pp.2054-2063.

# Plasma activated low temperature combustion pathway

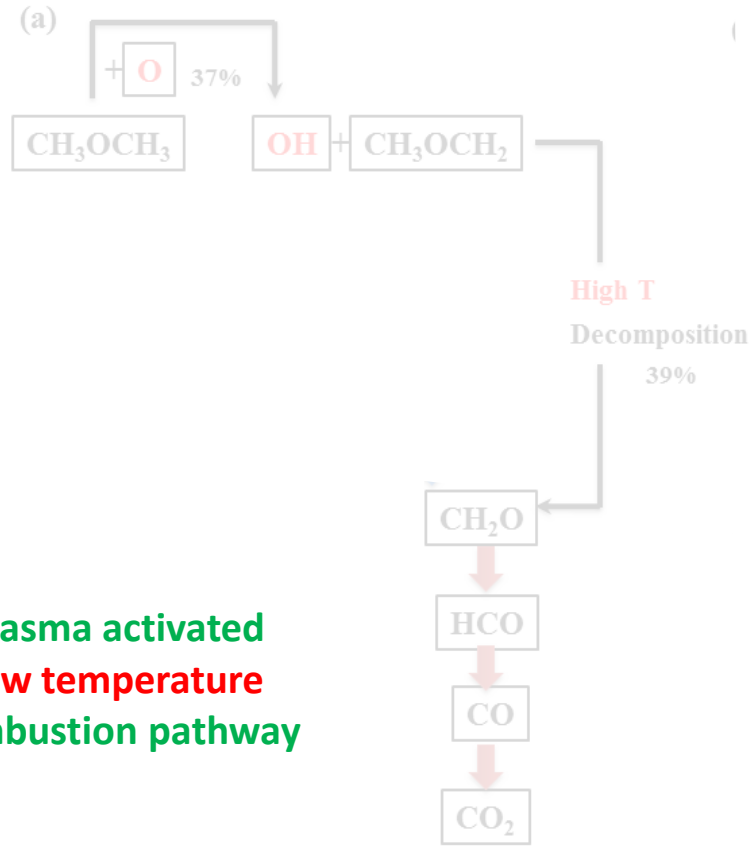


Plasma activated high temperature combustion pathway

Plasma activated low temperature combustion pathway

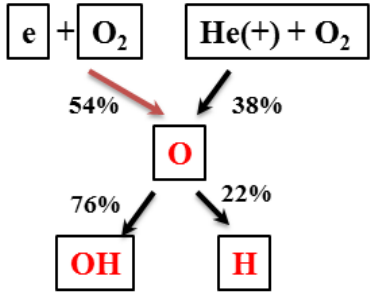


O+RH → R+OH

R → R''+2OH

O+RH → R''+ 3OH

Radical production by plasma

# Flow reactor studies of non-equilibrium plasma-assisted oxidation of *n*-alkanes

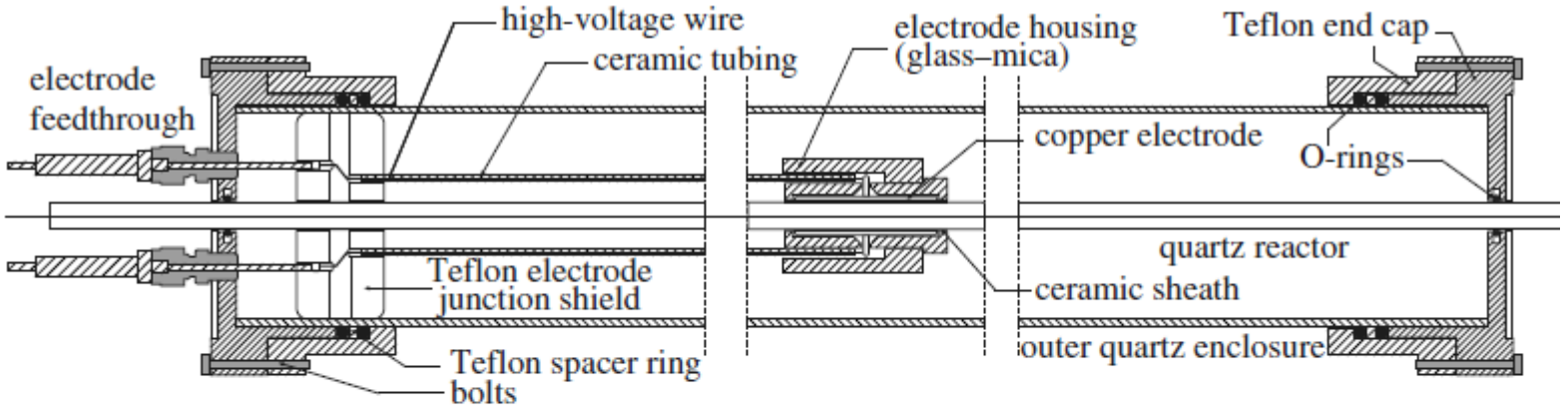


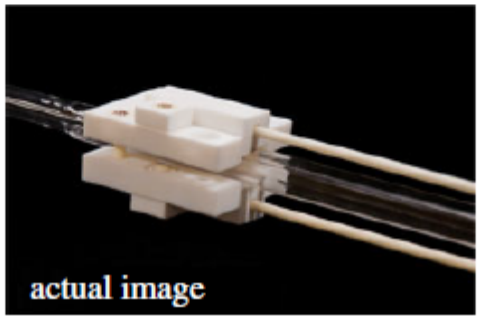


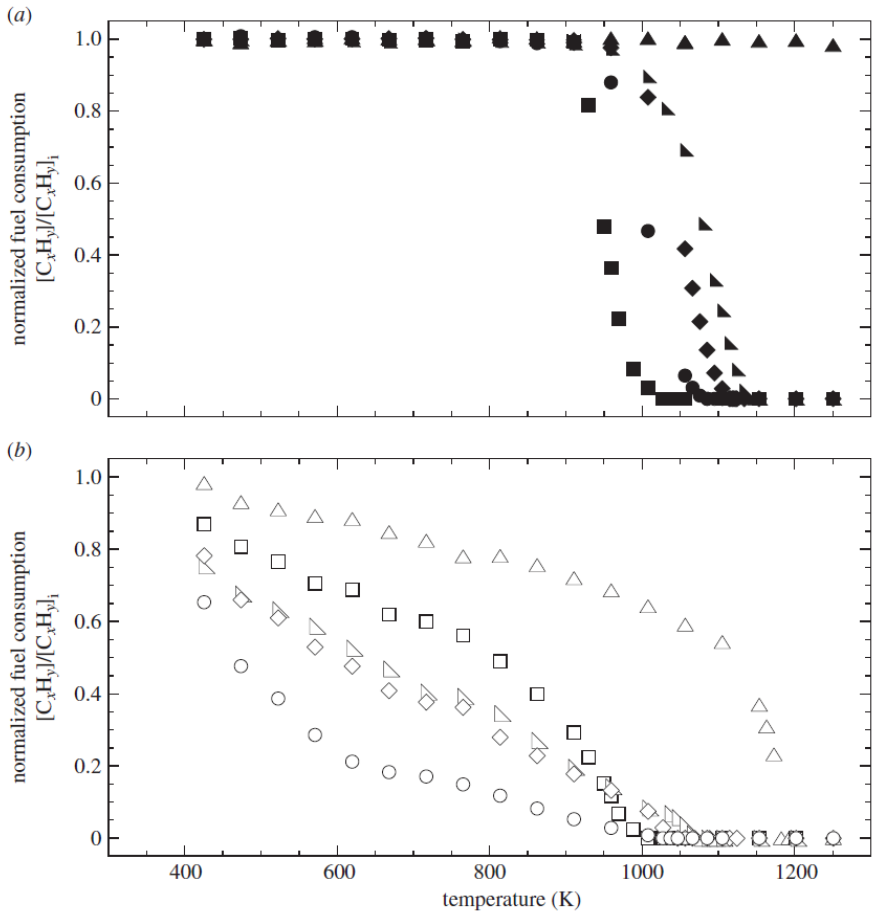


**Figure 3.** Comparison of fuel consumption trends (*a*) without and (*b*) with the plasma. Initial conditions: $X(C_xH_y) = 0.0016/x, X(O_2) = 0.003, X(Ar) = 1 - 0.0016/x - 0.003, P = 1$ atm. Plasma conditions: $V_{discharge} = 10$ kV, $\upsilon = 1$ kHz. Fuel: $CH_4$ (triangle), $C_2H_6$ (square), $C_3H_8$ (right angle triangle), $C_4H_{10}$ (diamond), $C_7H_{16}$ (circle).

Tsolas, N., Lee, J.G. and Yetter, R.A., 2015. *Phil. Trans. R. Soc. A*, *373*(2048), p.20140344.

# Ignition enhancement by transient corona discharge

Princeton University

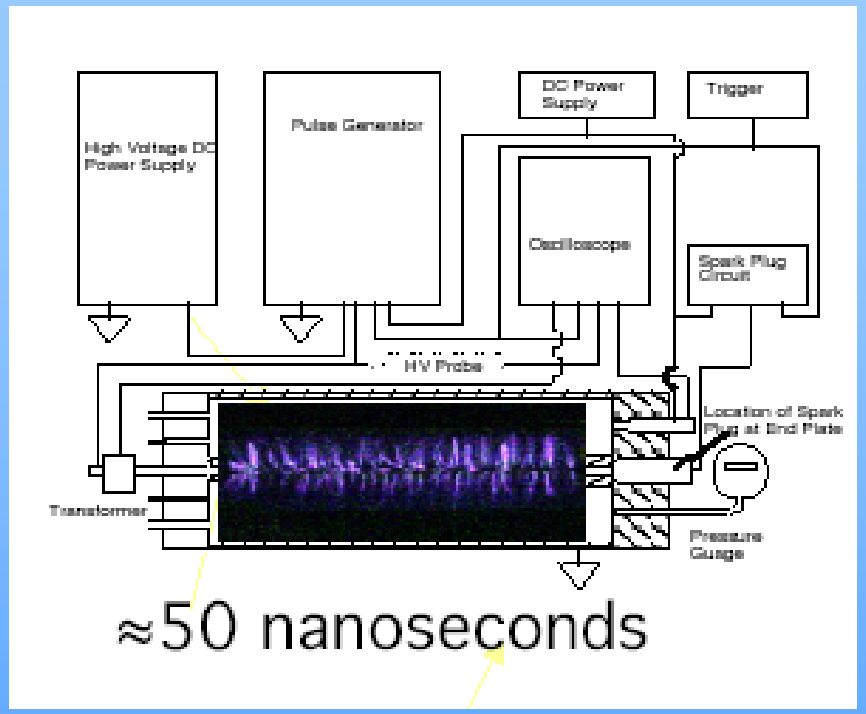


**Gundersen et al.**

- **Increased volume**
- **Transient discharge**

**2-10KV, 20-200ns**

**Disk electrode & streamers**

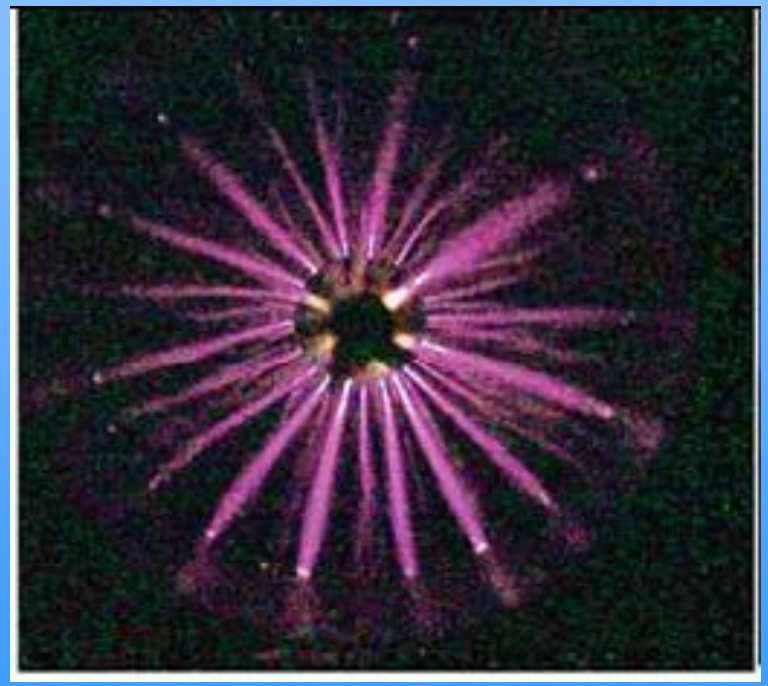

*Combustion lab.*

# Ignition delay time: corona discharge vs. spark

Princeton University

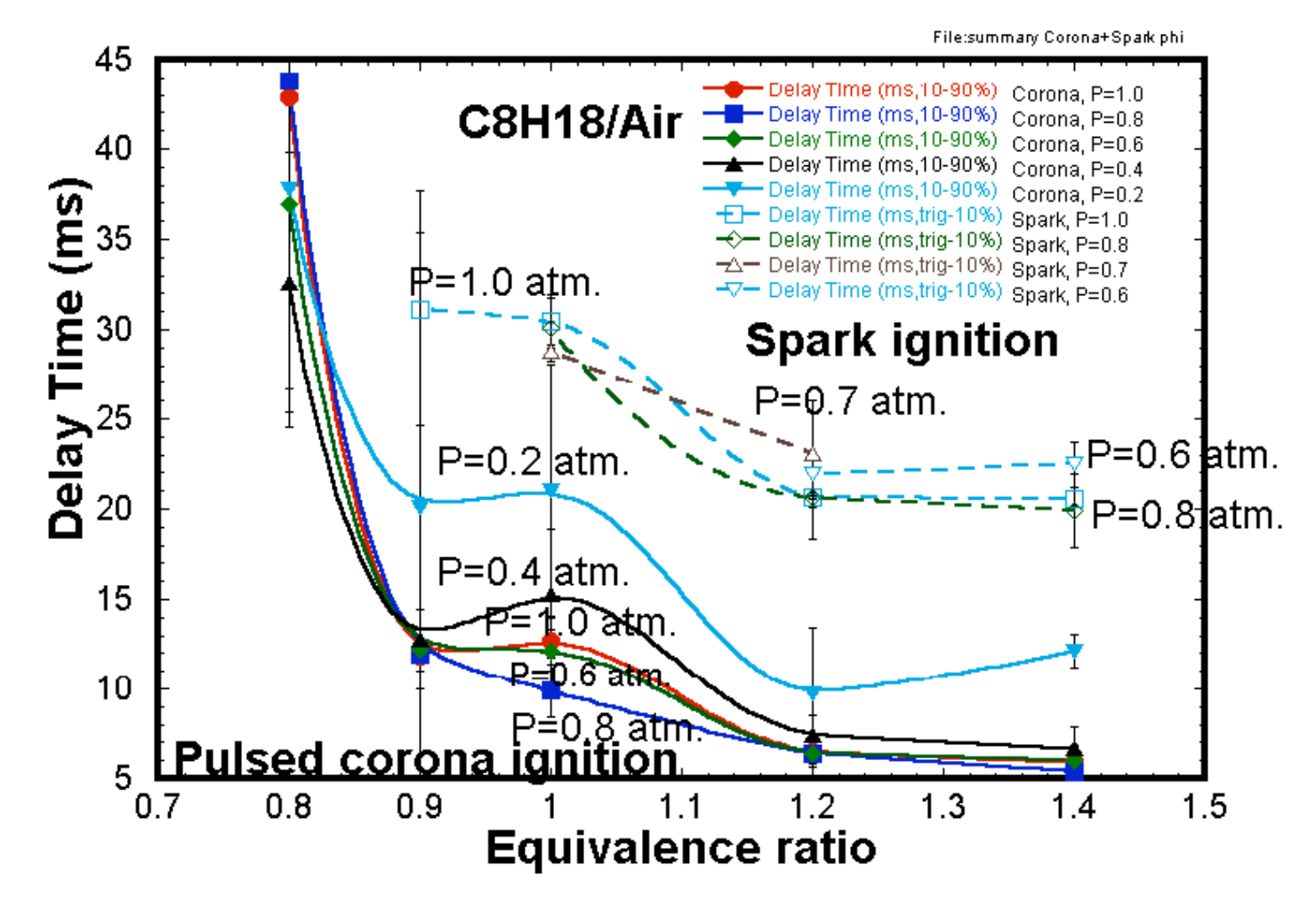


**Radical production**

$C_nH_m+e=C_nH_{m-1}+H^*+e$

$O_2+e=O(^1D)+O(^3P)+e$

**Large ignition volume?**

Liu J, Wang F, Lee L, Ronney P, Gundersen M. In42nd AIAA Aerospace Sciences Meeting and Exhibit 2004 (p. 837).

# 3.2.1 Adiabatic flame propagation

A flame is a self-propagating auto-ignition and thermal diffusion front. The propagation speed of a one-dimensional flame front relative to the far field unburned mixture is the flame speed.

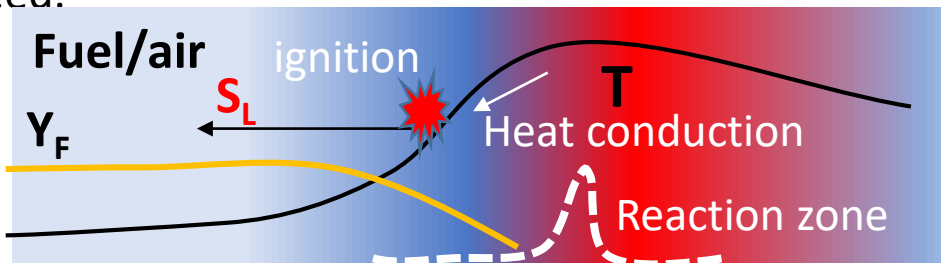


Governing equations

$$\rho u C_p \frac{dT}{dx} = \lambda \frac{d^2T}{dx^2} + q\omega, \qquad (1)$$

$$\rho u \frac{dY_F}{dx} = \rho D \frac{d^2Y_F}{dx^2} - W\omega \qquad (2)$$

$$Y_F = 2P + Q$$

$$\omega = B\rho Y_F e^{-E/RT}$$

1st order reaction

$$T(-\infty) = T_0, \qquad Y_F(-\infty) = Y_{F0}$$
$$T(\infty) = T_{ad}, \qquad Y_F(\infty) = 0$$

Enthalpy conservation outside diffusion zone: $\int_{-\infty}^{\infty} [Eq.(1)/q + Eq.(2)/W]dx$

$$\frac{C_p T_0}{q} + \frac{Y_{F,0}}{W} = \frac{C_p T_{ad}}{q} \quad \Rightarrow \quad T_{ad} = T_0 + \frac{qY_{F,0}}{C_p W}$$

In reaction-diffusion zone:

$$\int_{x}^{x_f+} [Eq.(1)/q + Eq.(2)/W]dx \text{ and neglect convection terms} \quad \Rightarrow \quad \frac{T - T_{ad}}{T_{ad} - T_0} = -\frac{1}{Le}\frac{Y}{Y_{F,0}}$$

Define: $\alpha \equiv \frac{T_{ad} - T_0}{T_{ad}}; \qquad \beta \equiv \frac{T_{ad} - T_0}{T_{ad}} \frac{E}{RT_{ad}}; \qquad \varsigma \equiv \frac{Y_F}{Y_{F,0}} \frac{\beta}{Le}$ $\Rightarrow$ $T = T_{ad}(1 - \alpha\varsigma/\beta)$

In reaction-diffusion zone (neglect convection): $$\frac{d^2Y_F}{dx^2} = -\frac{W}{\rho D}\omega$$

Rewriting: $$d[\frac{dY_F}{dx}]^2 = -2\frac{W}{\rho D}\omega dY_F$$

Integrating from flame front to a location x in the reaction zone:

$$\int_{x_{f-}}^{x} d[\frac{dY_F}{dx}]^2 = -2\frac{W}{\rho D}\int_{Y_{F-}}^{Y_F}\omega dY_F = -2\frac{W}{\rho D}\frac{Y_{F,0}Le}{\beta}\int_{\varsigma_{f-}}^{\varsigma}\omega d\varsigma = -2\frac{W}{\rho D}\frac{Y_{F,0}Le}{\beta}\int_{\varsigma_{f-}}^{\varsigma} B\rho Y_F e^{-E/RT} d\varsigma_F$$

$$= -2\frac{WB\rho_f}{\rho D}(\frac{Y_{F,0}Le}{\beta})^2 e^{-E/RT_{ad}}\int_{\infty}^{0}\varsigma e^{-\varsigma}d\varsigma = -2\frac{WB\rho_f}{\rho D}(\frac{Y_{F,0}Le}{\beta})^2 e^{-E/RT_{ad}}\times 1$$

$$\Rightarrow \boxed{[\frac{dY_F}{dx}]_{x_{f-}}^2 = -2\frac{WB\rho_f}{\rho D}(\frac{Y_{F,0}Le}{\beta})^2 e^{-E/RT_{ad}}} \qquad (1)$$

Integrating from unburned region to flame front to find the fuel concentration gradient at flame front:

$$\int_{-\infty}^{x_{f-}}\rho u\frac{dY_F}{dx} = \int_{-\infty}^{x_{f-}}[\rho D\frac{d^2Y_F}{dx^2} - W\omega]dx \quad \Rightarrow \quad \boxed{\rho u Y_{F,0} = \rho D[\frac{dY_F}{dx}]_{x_{f-}}} \qquad (2)$$

**Mass burning rate:** $$\boxed{m^2 \equiv (\rho u)^2 = 2Le\frac{WB\rho\lambda}{\beta^2 C_p}e^{-E/RT_{ad}}}$$

$$U_{ad} \propto= \rho^{n/2-1}, \qquad n: \text{reaction order}$$

Flame speed is affected by Le, B, E, and T. How does plasma affect flame speed?

# 3.2.2 Flame propagation speed with heat loss and addition:

$$\rho u C_p \frac{dT}{dx} = \lambda \frac{d^2T}{dx^2} + q\omega - 4Kpo(T^4 - T_0^4) \qquad (1)$$

$$\rho u \frac{dY_F}{dx} = \rho D \frac{d^2Y_F}{dx^2} - W\omega \qquad (2)$$

$$T(-\infty) = T_0, \qquad Y_F(-\infty) = Y_{F0}$$

$$\frac{dT(\infty)}{dx} = \frac{dY_F(\infty)}{dx} = 0$$

$$\theta \equiv (T - T_0)/(T_{ad} - T_0)$$

$$y = Y_F / Y_{F0}$$

$$X = x / x_{ref}$$

$$m = \rho u / \rho U_{ad}$$

$$x_{ref} = \frac{\lambda / C_p T_0}{U_{ad}}$$

$$t_{ref} = \frac{x_{ref}}{U_{ad}}$$

$Kp$ : *Planck* mean absorption coefficient

$$m\frac{d\theta}{dX} = \frac{d^2\theta}{dX^2} + W - \frac{H\theta}{\beta}$$

$$m\frac{dy}{dX} = \frac{1}{Le}\frac{d^2y}{dX^2} - W$$

$$W = \frac{\beta^2}{2Le} y \exp\left[\frac{\beta(\theta - 1)}{1 + \alpha(\theta - 1)}\right]$$

$$H = \frac{4\beta Kp\sigma T_{ad}^4}{\rho C_p U_{ad}} \frac{\lambda}{\rho C_p U_{ad}}$$

Outer solution (convection diffusion zone):

$$y_0 = \begin{cases} 1 - \exp(mLeX) & X < 0 \\ 0 & X > 0 \end{cases}$$

$$\theta_0 = \begin{cases} \exp(mX) & X < 0 \\ 1 & X > 0 \end{cases}$$

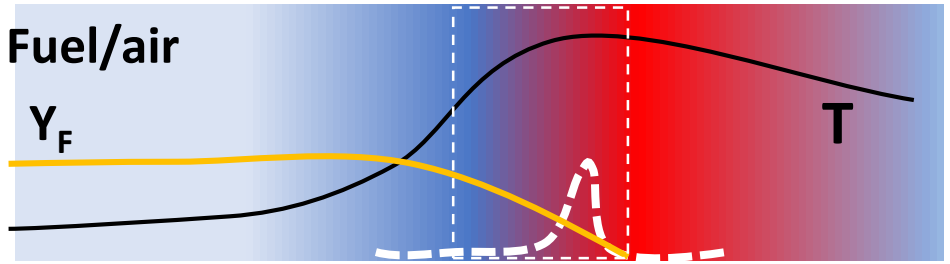

Adding the mass and energy equation and integrate from upstream boundary to flame front:

$$\int_{-\infty}^{0-}(m\frac{dy}{dX}+m\frac{d\theta}{dX})dX=\int_{-\infty}^{0-}(\frac{1}{Le}\frac{d^2y}{dX^2}+\frac{d^2\theta}{dX^2}-\frac{H\theta}{\beta})dX \quad\Rightarrow\quad m(\frac{dy}{dX}+m\frac{d\theta}{dX})_{-\infty}^{0}=(\frac{1}{Le}\frac{dy}{dX}+\frac{d\theta}{dX})_{-\infty}^{0}-\int_{-\infty}^{0-}\frac{H\theta}{\beta})dX$$

Perturbation: assume heat loss or addition only perturb the temperature and mole fraction in O(1/β)

$$y=y_0+y_1,\qquad \theta=\theta_0+\theta_1$$

Rewrite the equation above:

$$m[\theta_1(0^-)-\theta_1(-\infty)]=\left[\frac{1}{Le}\frac{dy}{dX}+\frac{d\theta}{dX}\right]^{0-}-\frac{H}{m}$$

Using the jump condition across the reaction zone:

$$\left[\frac{1}{Le}\frac{dy}{dX}+\frac{d\theta}{dX}\right]_{0+}^{0-}=0,\qquad \frac{d\theta_0}{dX}\Big|^{0-}=\exp\left[\frac{\theta_1(0)}{2}\right]\ \text{or}\ \theta_1(0)=\ln m^2$$

$$m\ln m^2=\left[\frac{1}{Le}\frac{dy}{dX}+\frac{d\theta}{dX}\right]^{0+}-\frac{H}{m}=\left[\frac{d\theta}{dX}\right]^{0+}-\frac{H}{m}=\left[\frac{d\theta_1}{dX}\right]^{0+}-\frac{H}{m}$$

Find the perturbation in the burned gas zone:

$$\left[\frac{d\theta_1}{dX}\right]_{0+}=-\frac{H}{m}$$

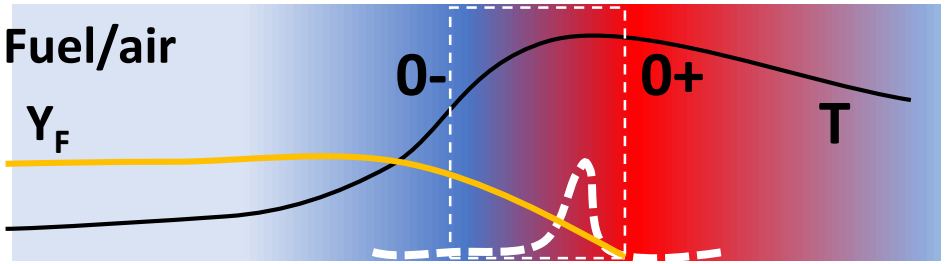


**Flame speed with heat loss/addition:**

$$m^2\ln m^2=-2H$$

How does heat loss/addition affect flame?

# Extinction limit and flammability limit:

$$m^2 \ln m^2 = -2H$$

$$m = \rho u / \rho U_{ad}$$

$$H = \frac{4\beta Kp\sigma T_{ad}^4}{\rho C_p U_{ad}} \frac{\lambda}{\rho C_p U_{ad}}$$

- For a given mixture with a constant adiabatic flame speed, the increase of heat loss will reduce the flame speed and lead to flame extinction at 2H=1/e and the normalized flame speed at extinction limit is $e^{-1/2}$
- For a given heat loss intensity (e.g. Kp), as the mixture fuel concentration decreases, the normalized heat loss H will increases. Therefore, at a critical fuel concentration, 2H becomes 1/e, and no flame is available below this fuel concentration. This defines the lean flammability limit.
- How does plasma can change the flammability limit?

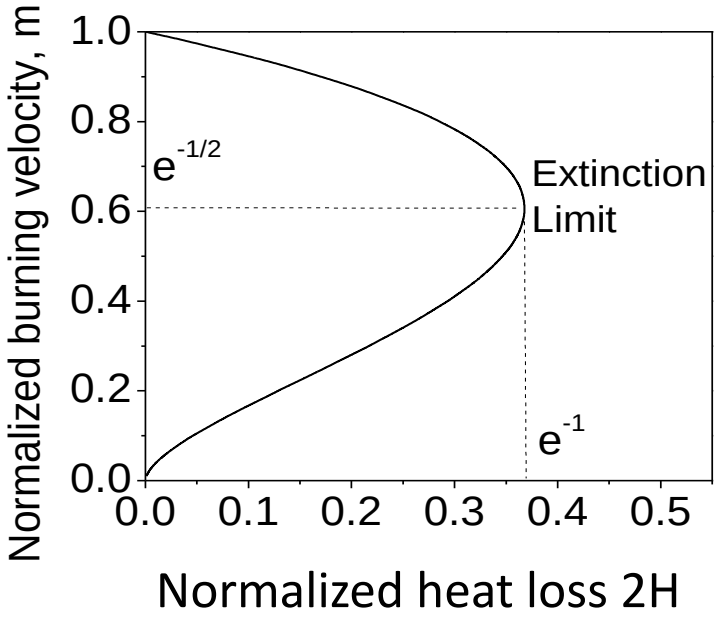


Fig. The dependence of the normalized burning velocity on the normalized radiative heat loss of a one-dimensional planar flame.

# Quenching diameter:

For a flame propagating into a tube, the heat loss from the flame to the wall is governed by the convective heat transfer to the wall

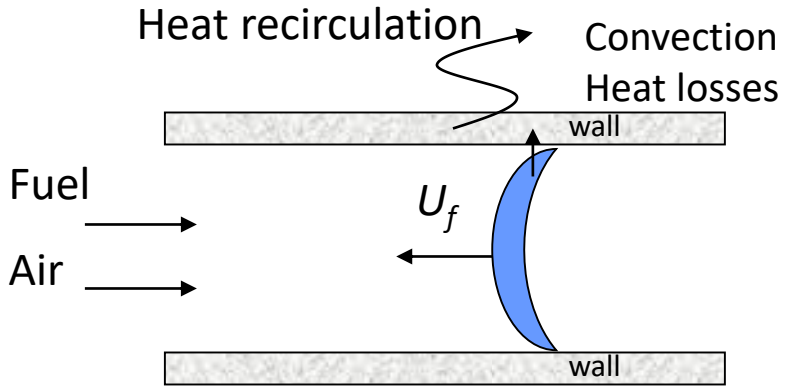


$$2H = \frac{\text{Heat loss to the wall}}{\text{Total chemical heat release}} = \frac{\beta 4\delta_f^2}{d^2} Nu$$

Flame speed:

$$m^2 \ln m^2 = -\beta \frac{4\delta_f^2}{d^2} Nu$$

Quenching diameter:

$$2H = \frac{\beta 4\delta_f^2}{d^2} Nu = \frac{1}{e}$$

$$d_0 = 2\sqrt{e\beta Nu}\,\delta_f$$

$d_0$: the minimum diameter in which a laminar flame can Propagate.

How does plasma discharge affect the quenching diameter?

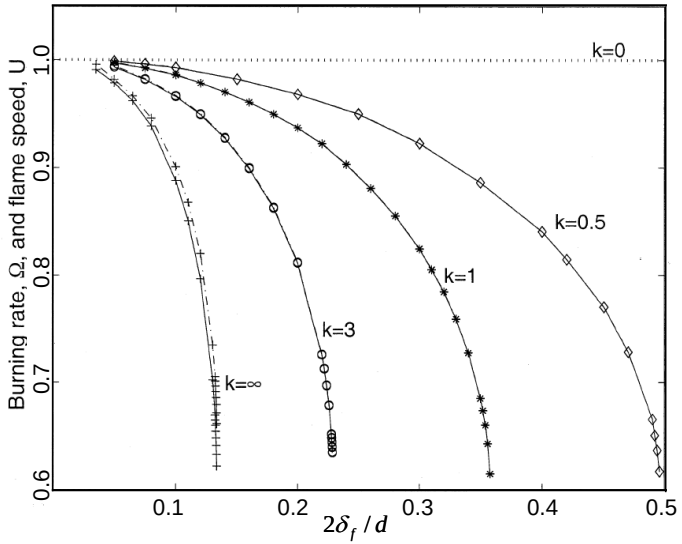


Fig. Burning rate (solid line) and normalized flame propagation speed *U* (U=*m in this figure*) plotted against the ratio of flame thickness to channel width (d) for selected values of reduced heat transfer coefficient (*k*) with in a quiescent, two dimensional channel flow. (Matalon et al. 2003)

# Effect of chemistry and transport on diffusion flame extinction:
## Radical Index and Transport-Weighted Enthalpy

- Extinction of diffusion flames are governed by
  - Fuel loading: fuel concentration (mole/cm$^3$)
  - Energy content: heat of combustion (cal/mole)
  - Transport (diffusivity): molecular weight of fuel and diluent
  - Chemical kinetics: **Radical index**
- **Transport-weighted Enthalpy (TWE)**
  - Normalize the energy content and transport effects
  - **TWE = [fuel] $\times \Delta H_c \times (MW_f/MW_{n2})^{-0.5}$**
  - Universal correlation of extinction limits has been derived with **Radical index.** [Won et al, CNF 2012]

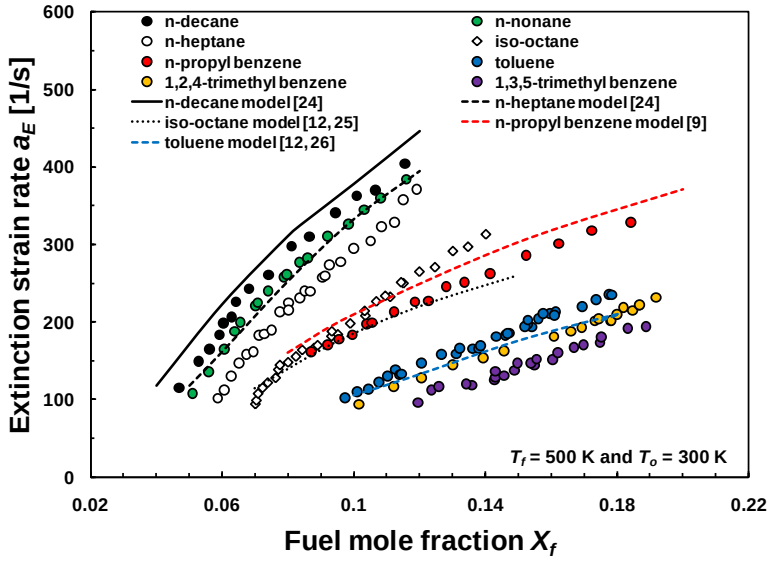


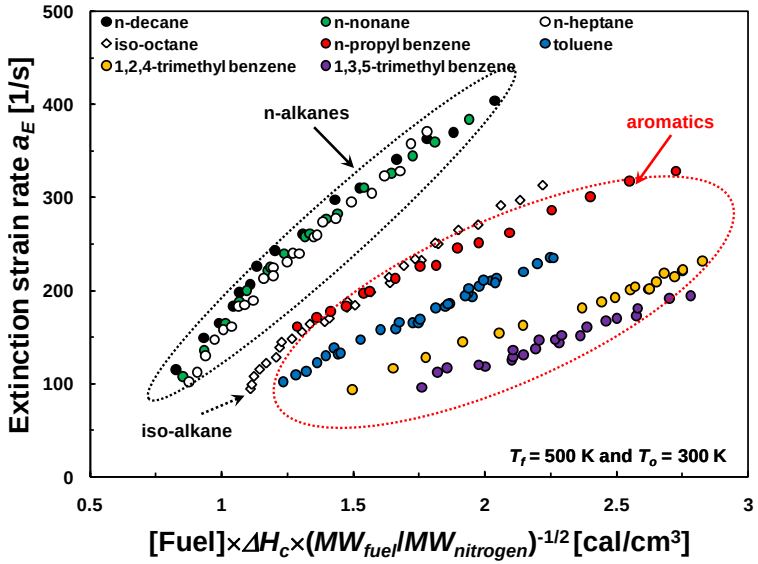


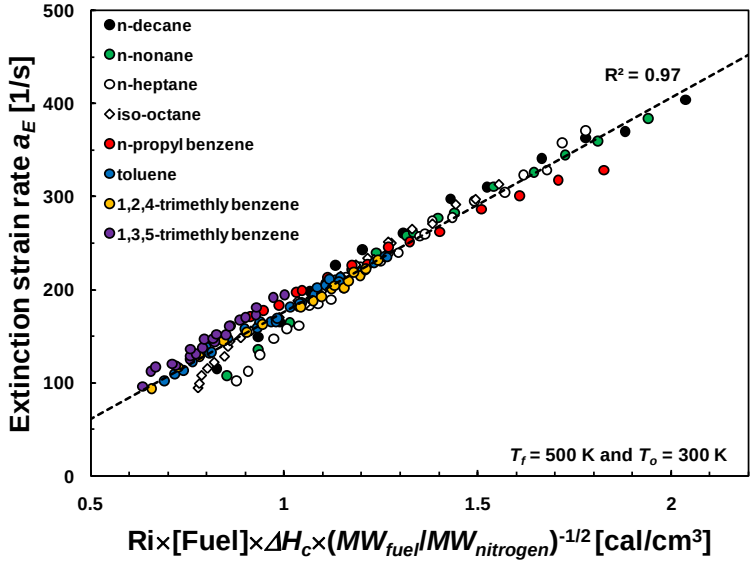


Plasma can change the chemistry and transport

# Does plasma really kinetically enhance flame speed?

## Gliding arc on flame extinction experiment

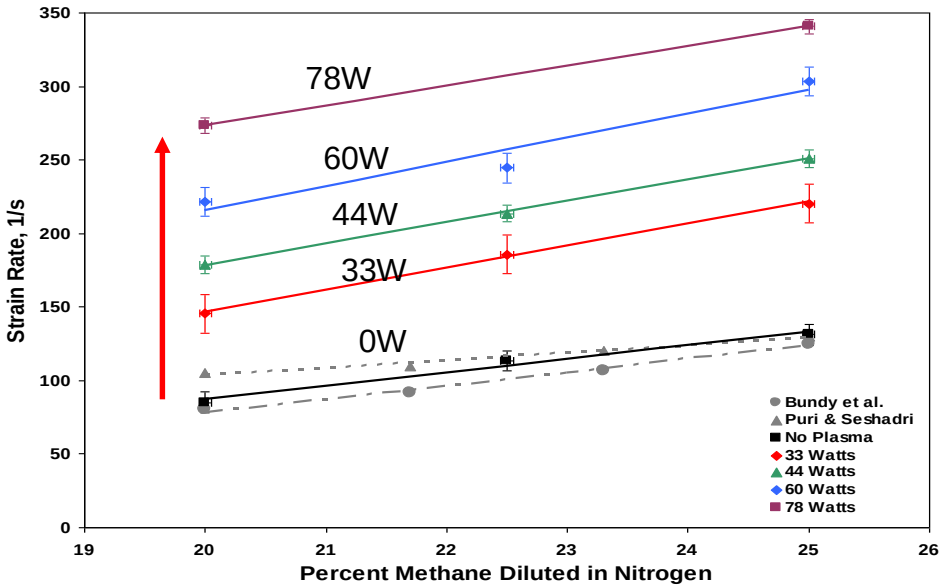


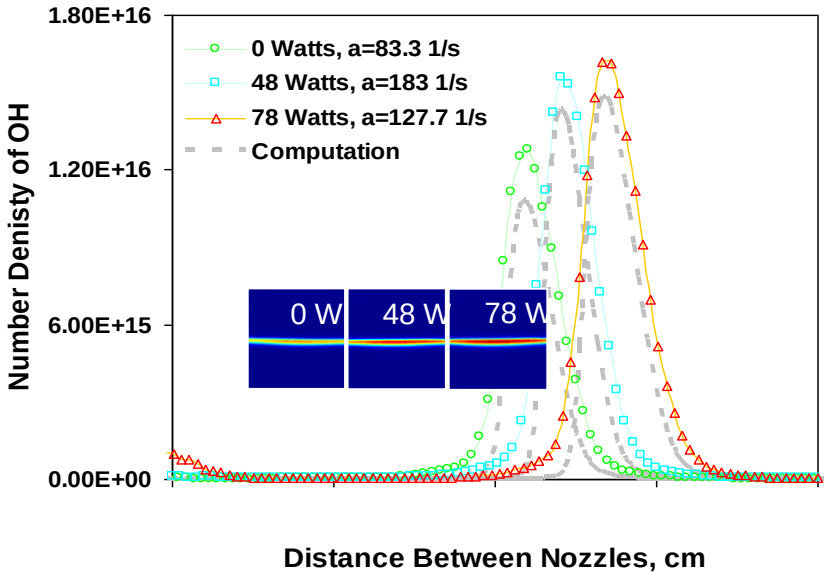


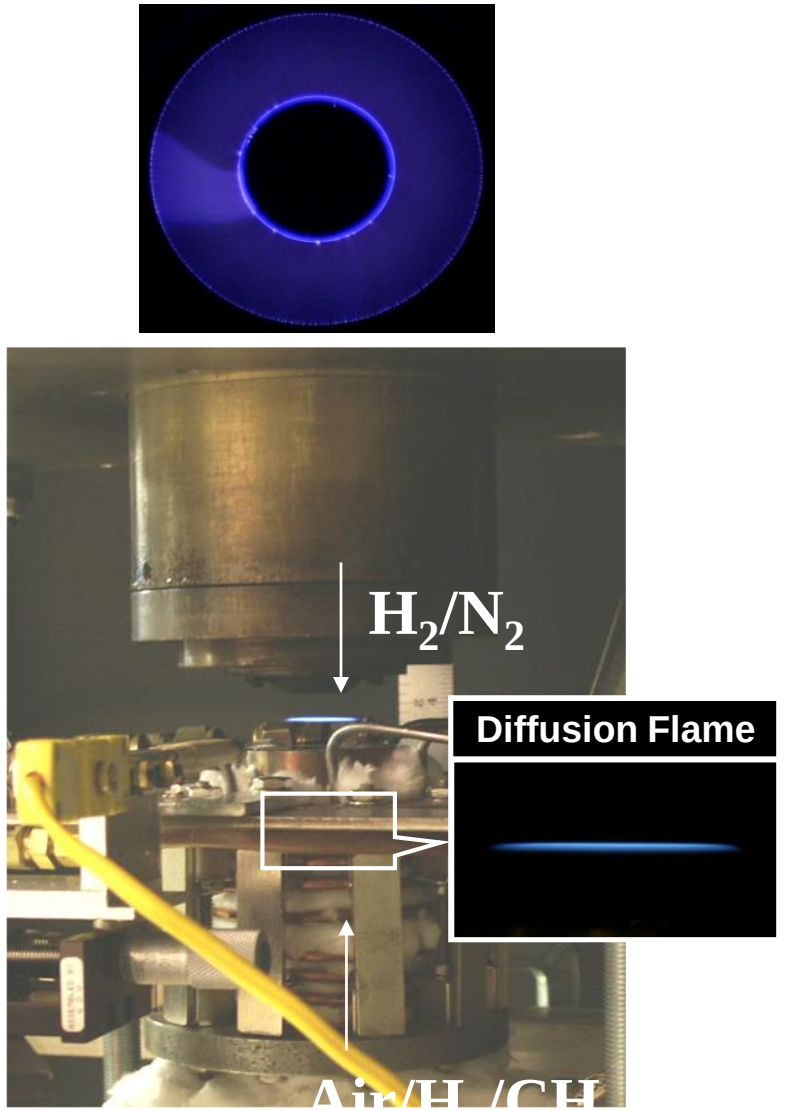


**Role of plasma: mainly thermal effect**

Ombrello, T., Qin, X., Ju, Y., Gutsol, A., Fridman, A. and Carter, C., 2006. *AIAA journal*, *44*(1), pp.142-150.

# Plasma Generated Active Species Lifetime vs. Pressure

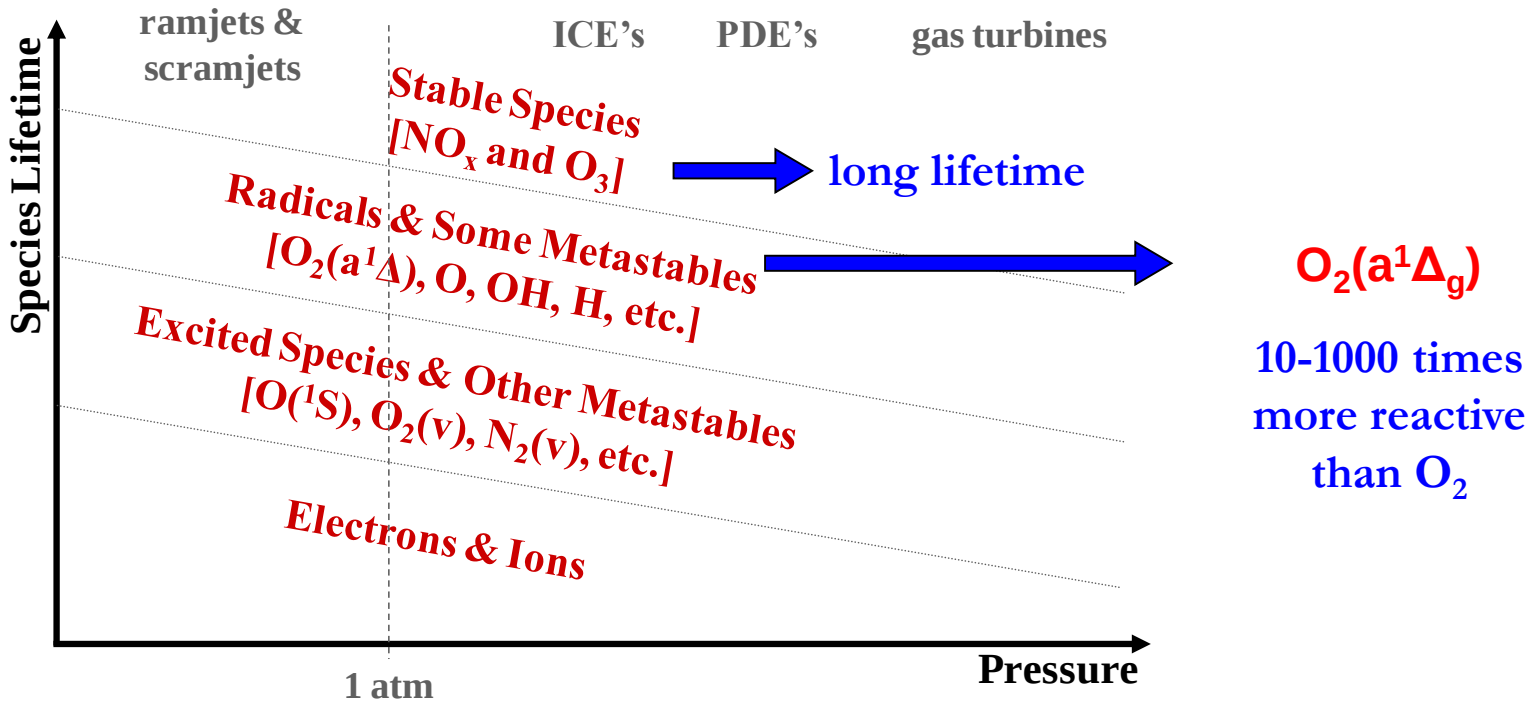


**What are the effects of $O_3$, $O_2(a^1\Delta_g)$, O, … on flame propagation?**

# Enhancement of flame Speed by plasma generated $O_3$

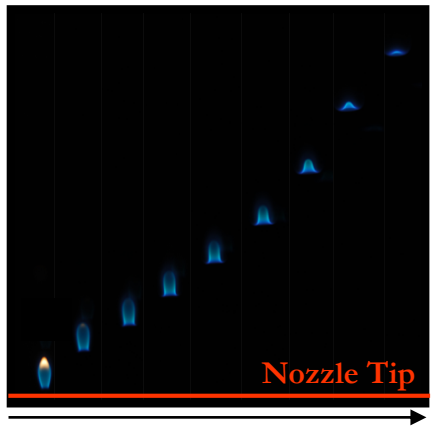


Lifted C3H8/O2/N2 flames

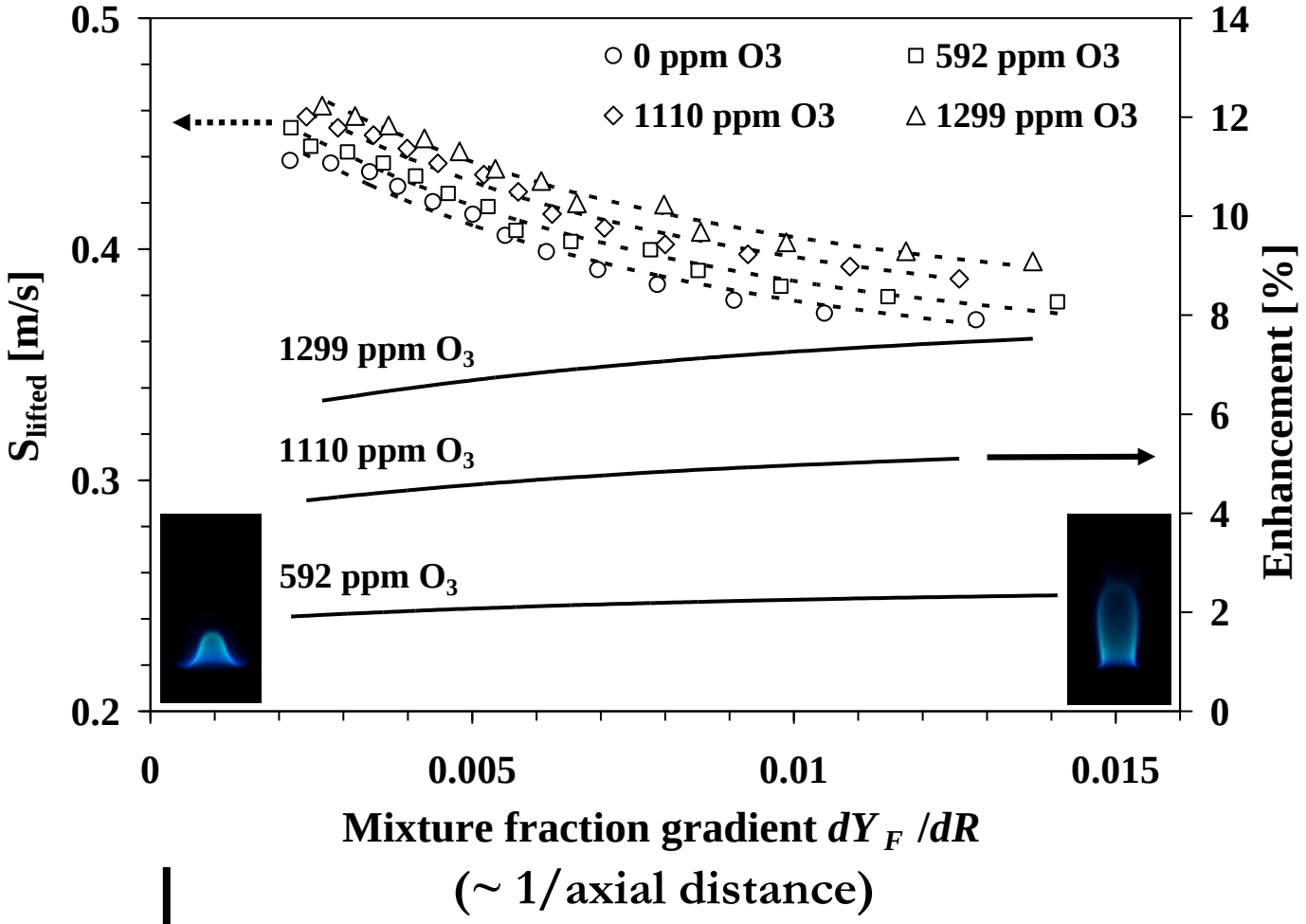


**Flame speed extraction**

$$S_L \approx S_{lifted} \sqrt{\frac{\rho_b}{\rho_u}}$$

Ombrello, T., Won, S.H., Ju, Y. and Williams, S., 2010. Part I: Effects of O 3. *Combustion and flame*, *157*(10), pp.1906-1915.

# Kinetic *Thermal* Enhancement Mechanism by $O_3$

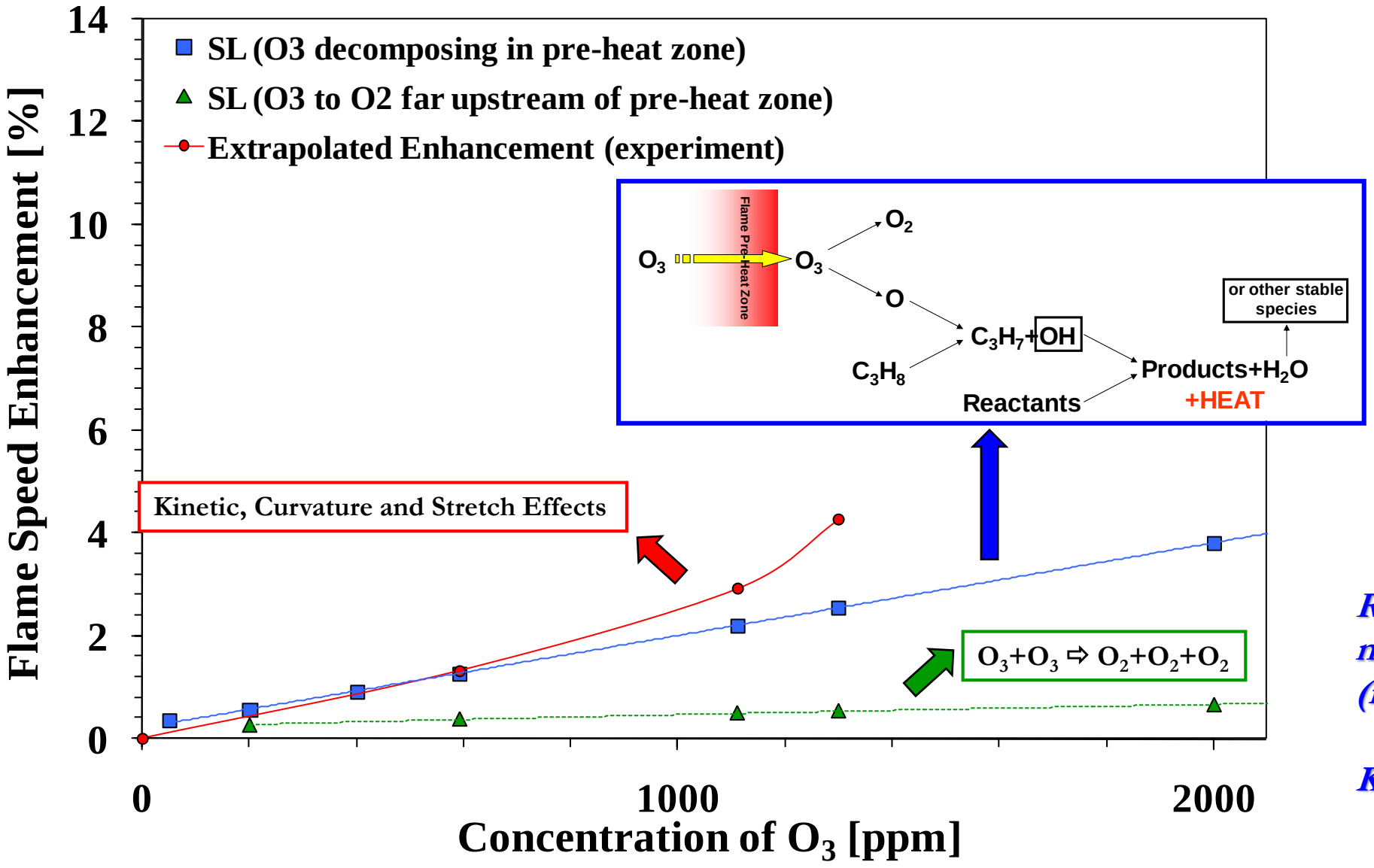


***Radical production by plasma mainly accelerates heat release (not change branching).***

***Kinetic-thermal effect!***

# Kinetic Effect by $O_2(a^1\Delta_g)$ on flame propagation

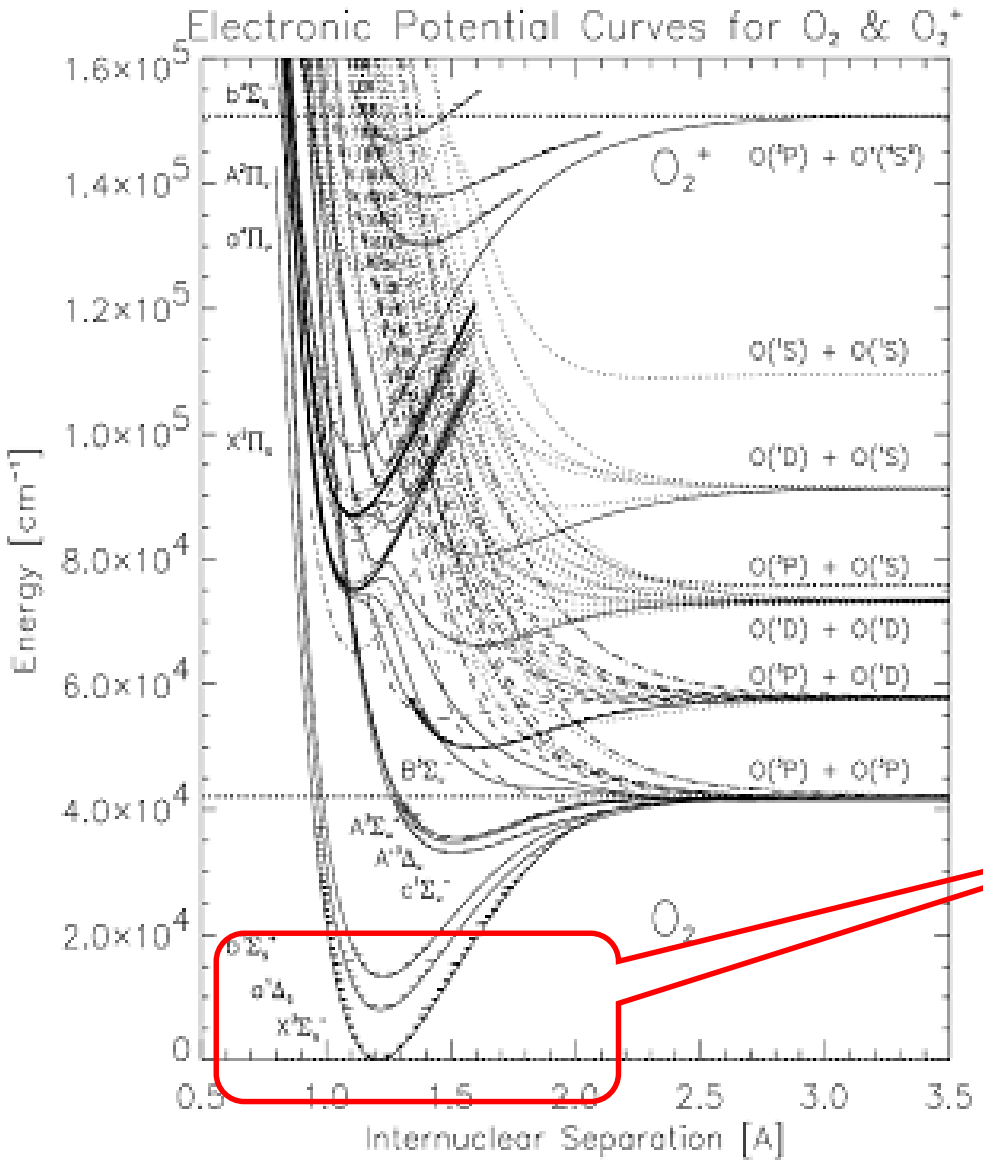


J.S. Morrill et al www.nist.gov

$O_2(a^1\Delta_g) + H = OH + O$ fast

$O_2 + H = OH + O$ slow

$O_2(a^1\Delta_g)$ at 0.98 eV

$O_2(b^1\Sigma_g^+)$ at 1.6 eV

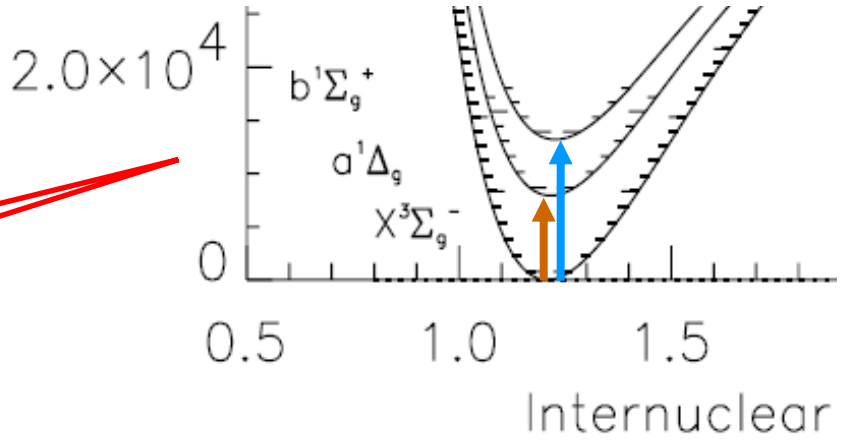

# Lifted flame experimental system

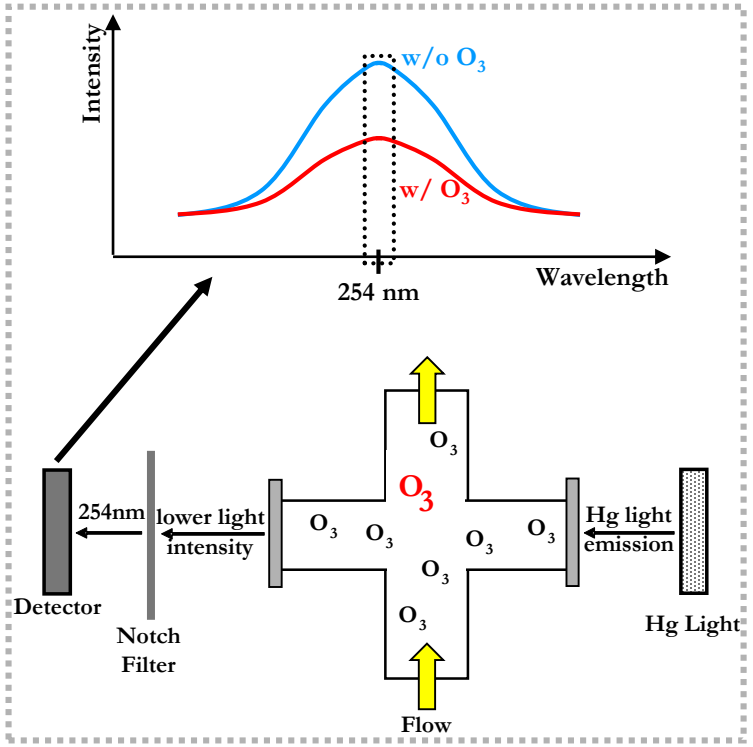


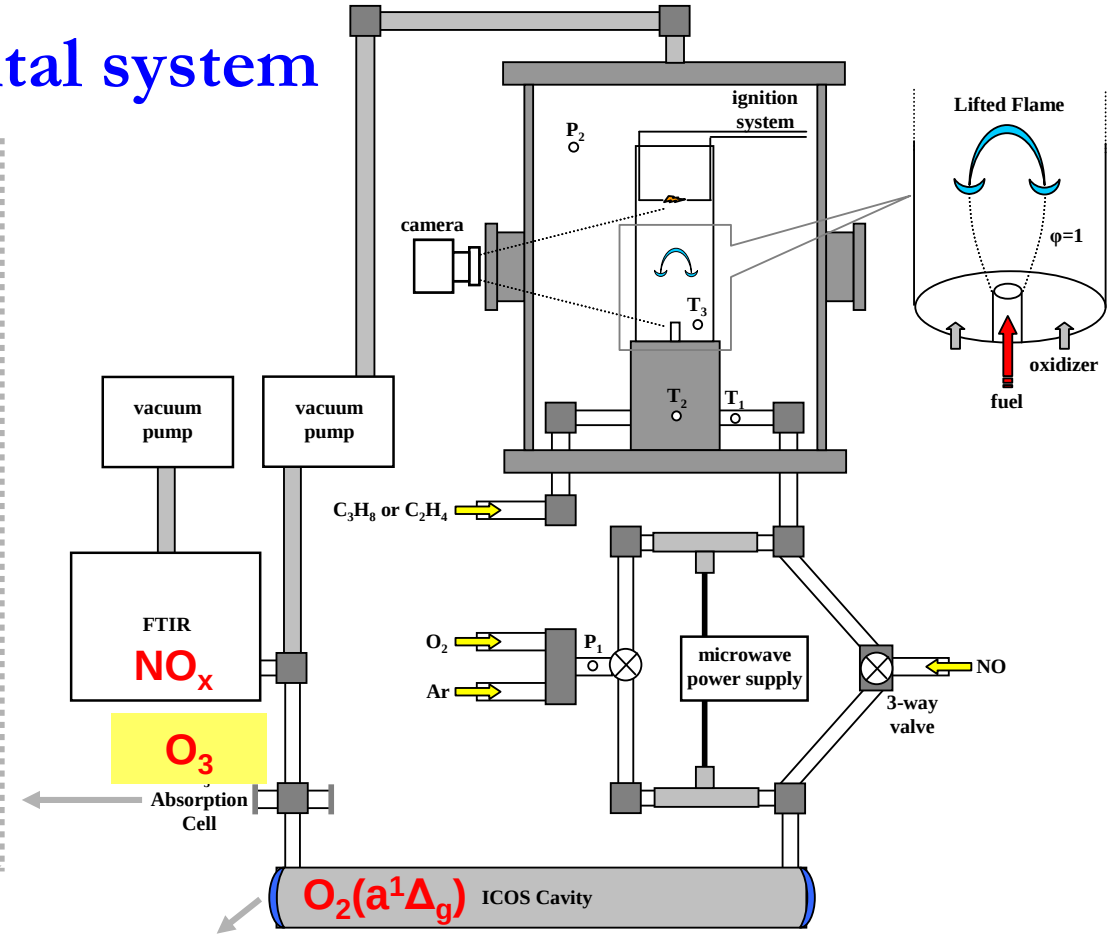


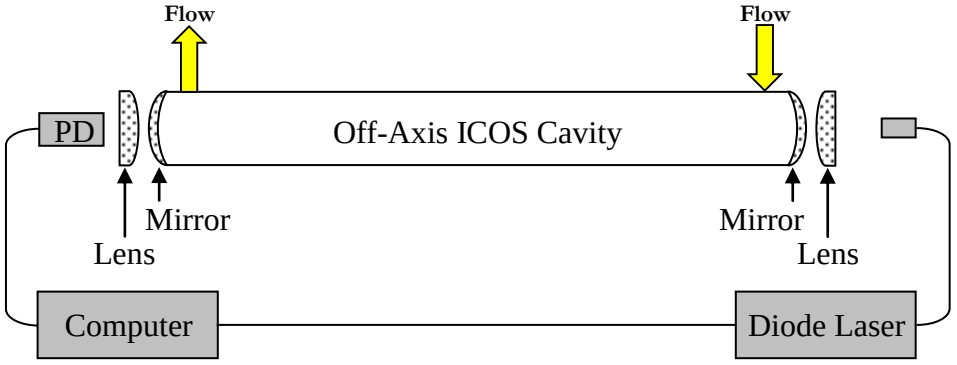


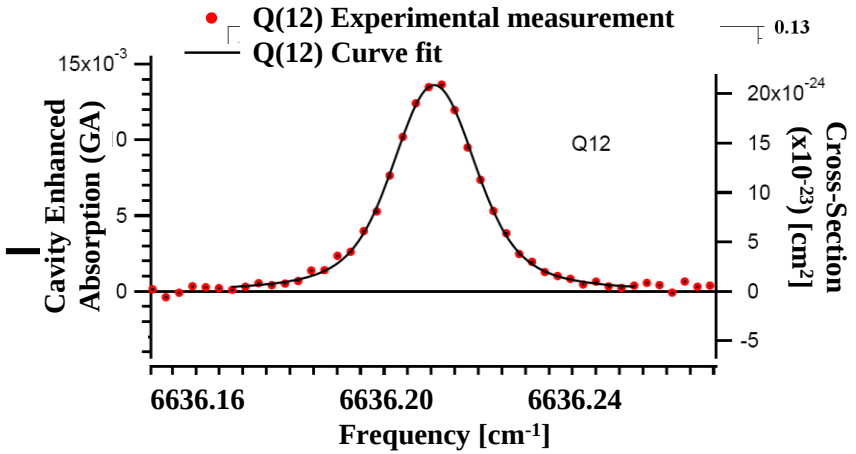

# $O_2(a^1\Delta_g)$ Enhancement of $C_2H_4$ Flame Speed

| $[O_2(a^1\Delta_g)]$, ppm | $\Delta H_L$, mm |
|---|---|
| 3137 | 4.76 |
| 4470 | 6.82 |
| 4627 | 6.83 |
| 5098 | 7.31 |

Far less than

$O_2(a^1\Delta_g) + H = OH + O$ fast

$O_2 + H = OH + O$ slow

**Hydrocarbon quenching?**

→ ≈ 5000 ppm $O_2(a^1\Delta_g)$ → 2-3 % Lifted Flame Speed Enhancement

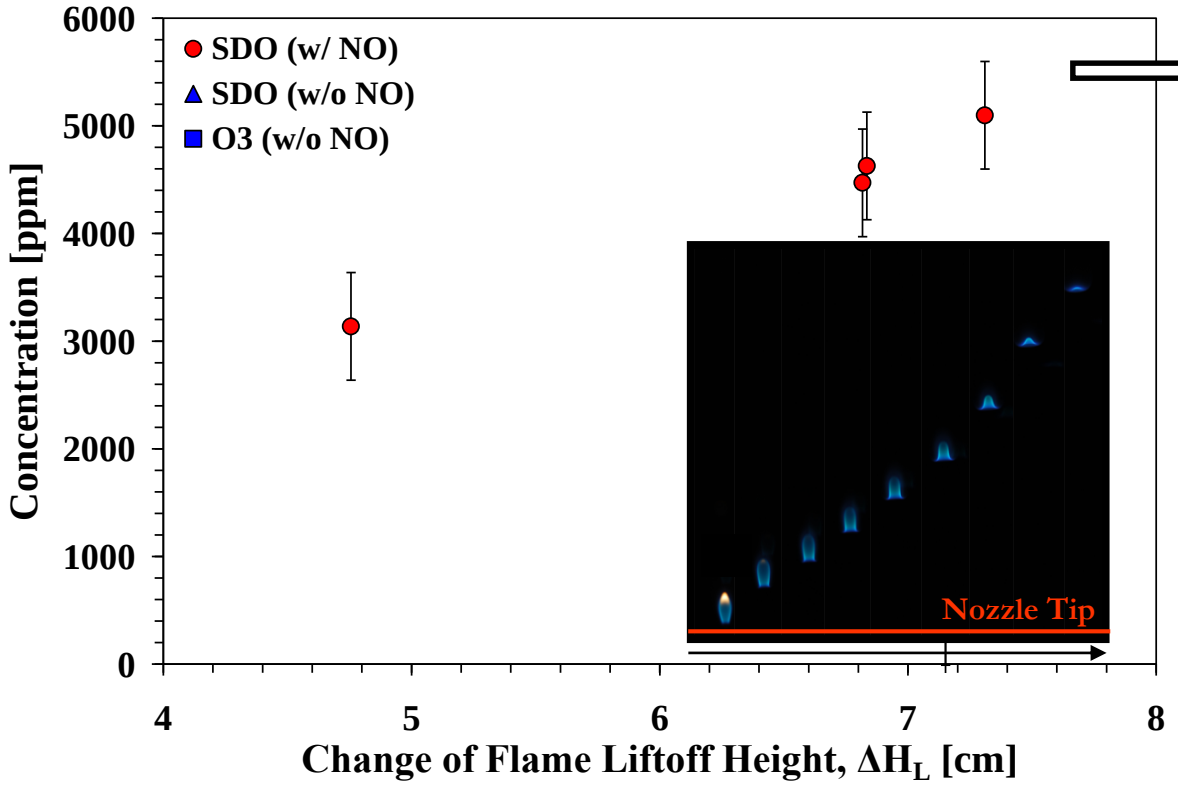


→ Microwave Power = 80 Watts

Energy Coupling Into Flow

≈ 1 eV to produce $O_2(a^1\Delta_g)$

**The kinetic effect of $O_3$ and $O_2(a^1\Delta_g)$ on flame speeds is small.**


Ombrello, T., Won, S.H., Ju, Y. and Williams, S., 2010. Part II: Effects of O 2 (a 1 Δ g). *Combustion and Flame*, *157*(10), pp.1916-1928.

# Effect of O production in nanosec plasma on flame extinction

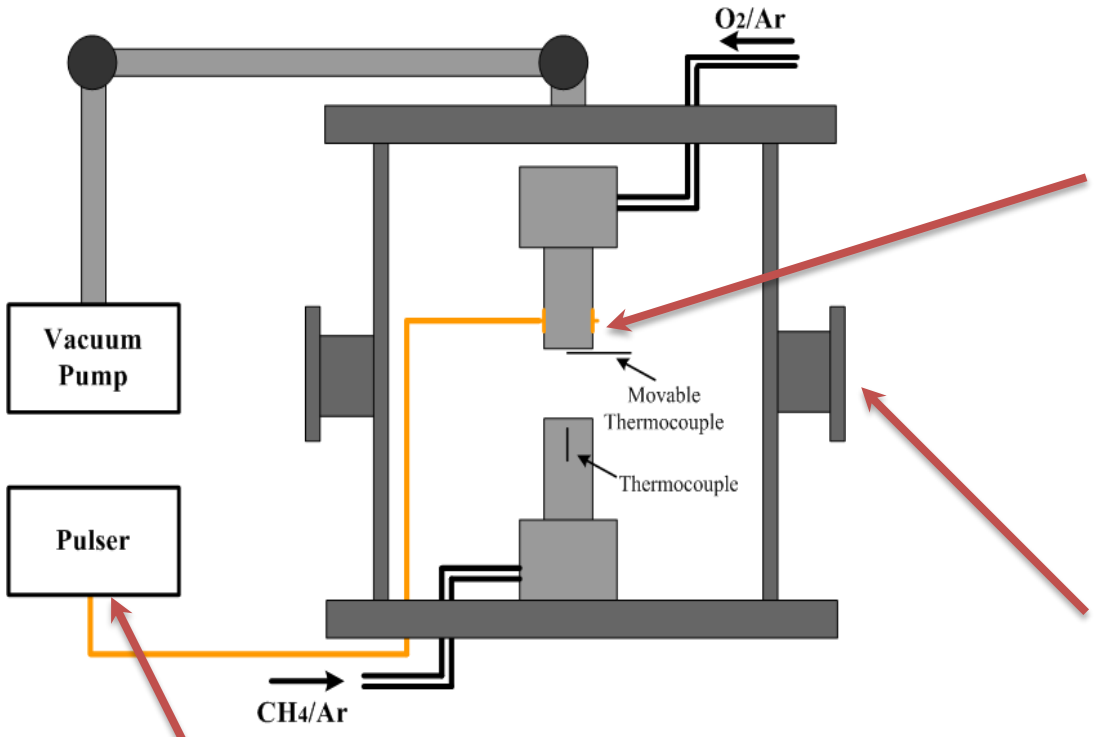


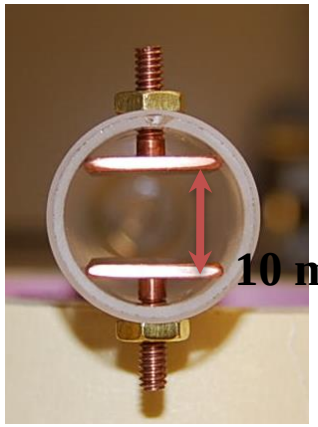

15.24 mm × 22 mm

10 mm

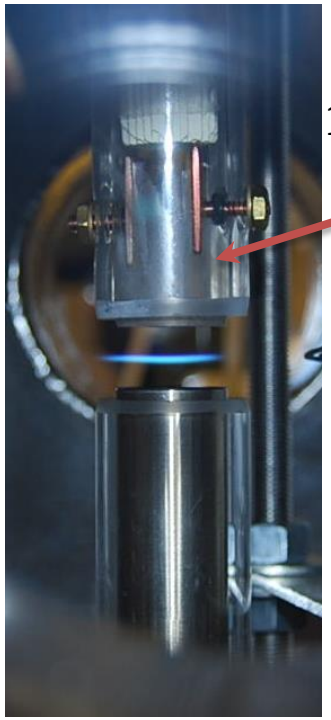

10 mm away from exit

20 & 28 mm ID

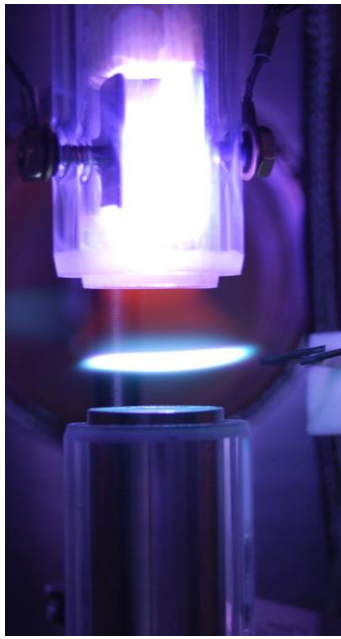

*f*=40 kHz

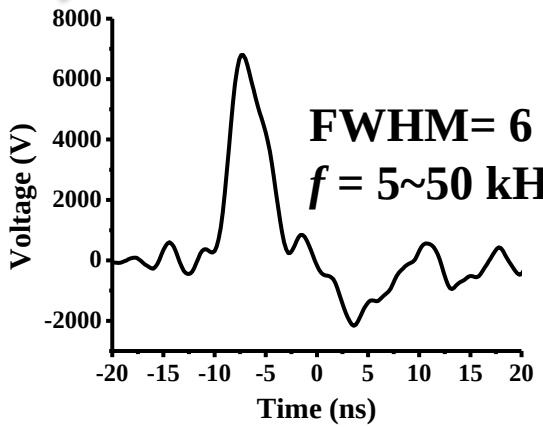


FWHM= 6 ns

*f* = 5~50 kHz

E/N~$10^{-15}$ $Vcm^2$

Power~0.7 mJ

# Atomic O measurement (TALIF) and effect of extinction limit

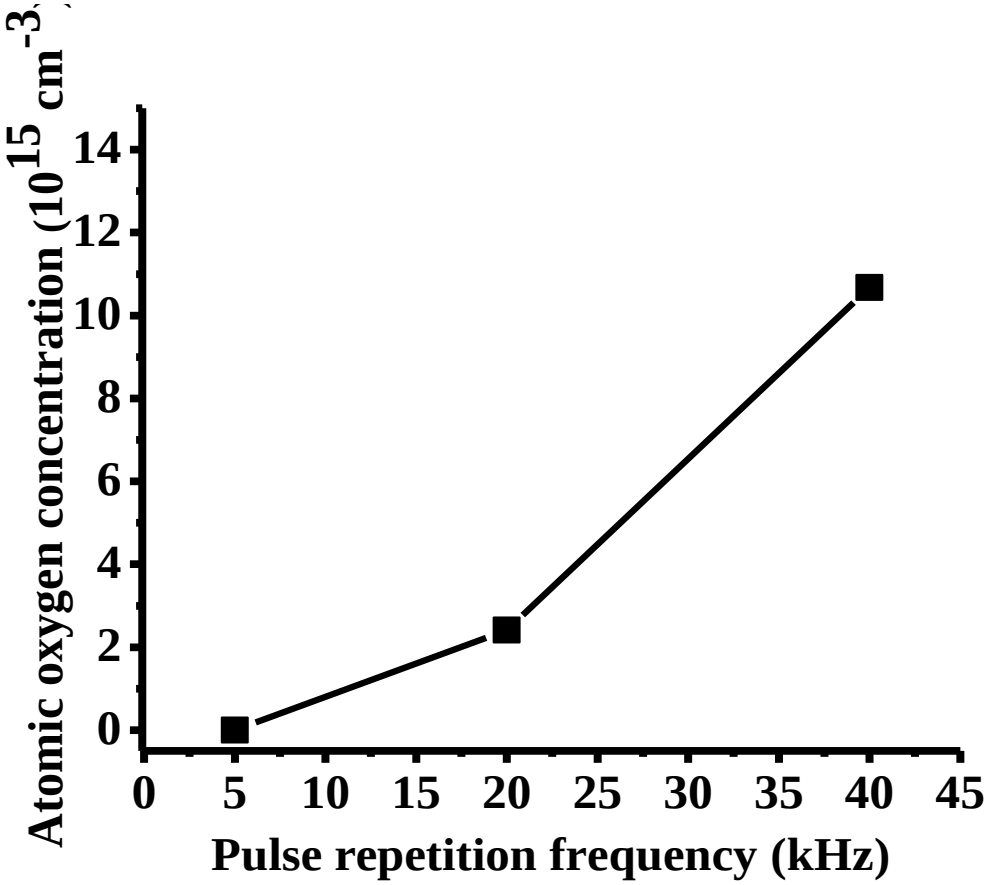


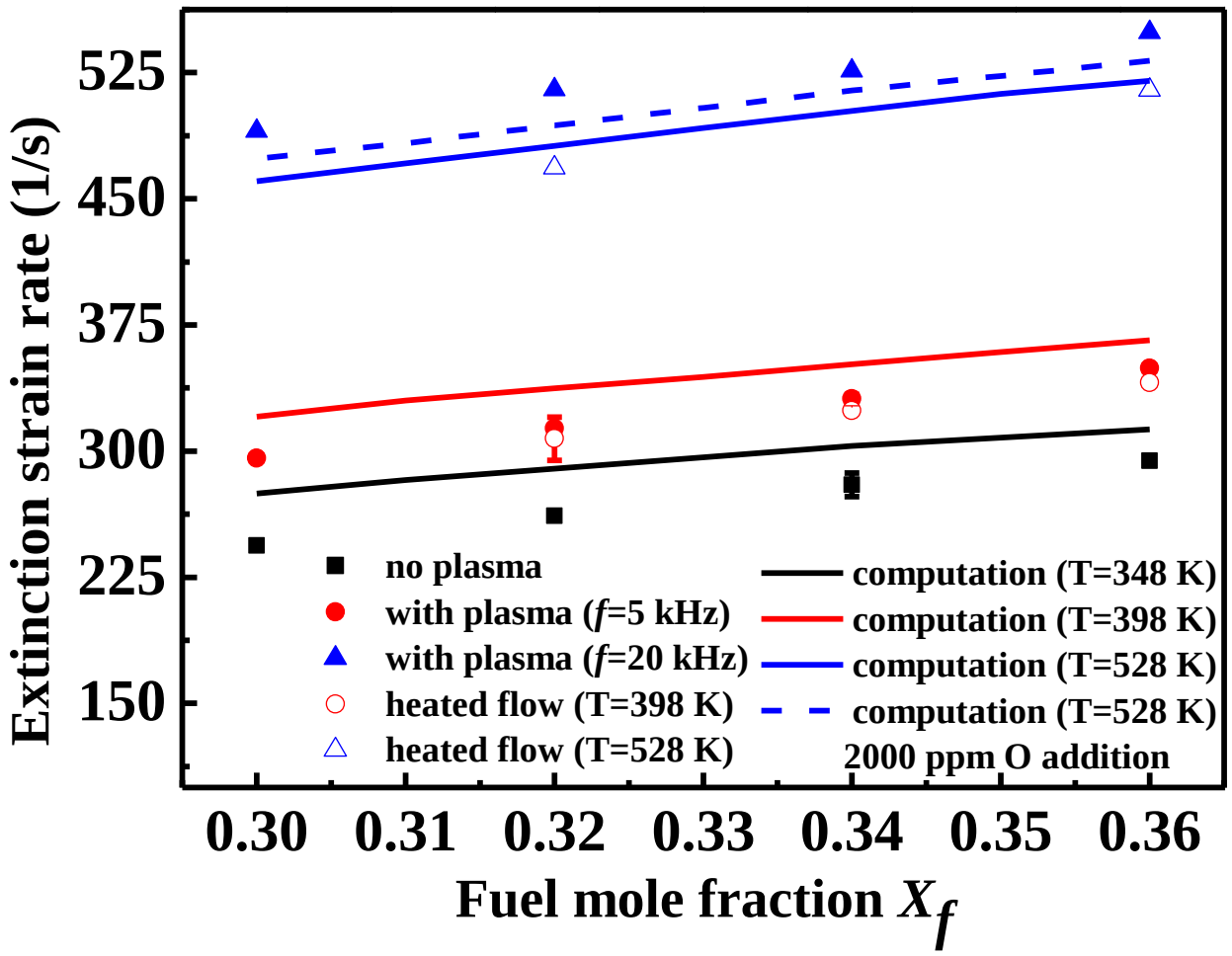


Ar diluted $CH_4/O_2$ diffusion flame:
$X_{O_2}$=0.28, Peak voltage= 7 kV, P= 60 Torr

**"O production has minor kinetic effect on flame extinction!"**


Sun, W., Uddi, M., Ombrello, T., Won, S.H., Carter, C. and Ju, Y., 2011. *Proceedings of the Combustion Institute*, *33*(2), pp.3211-3218.

# Plasma enhances flame propagation of cool flames

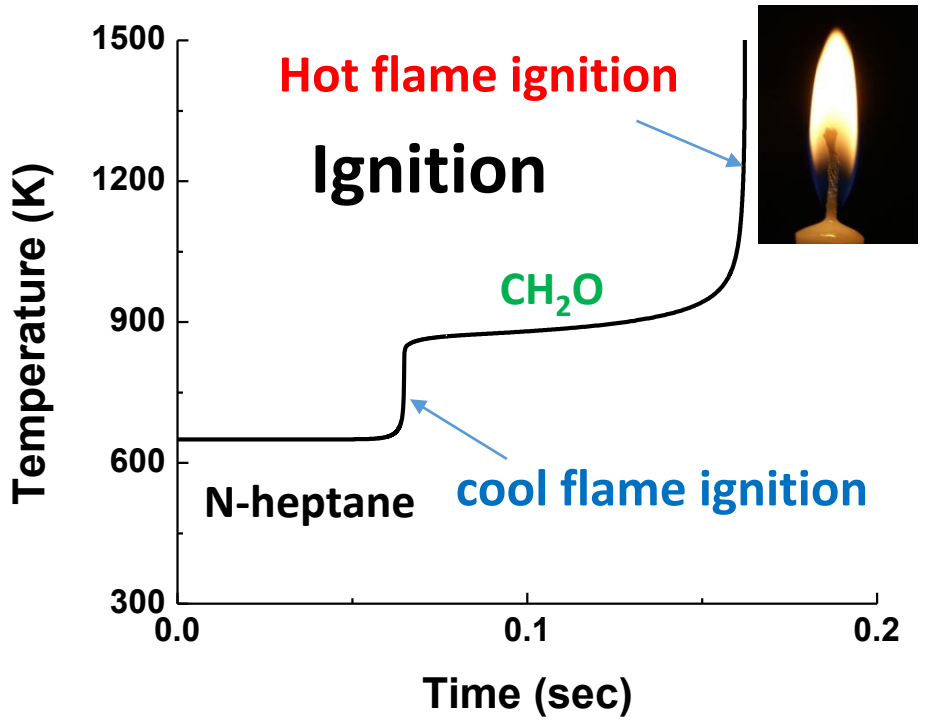


## Flame

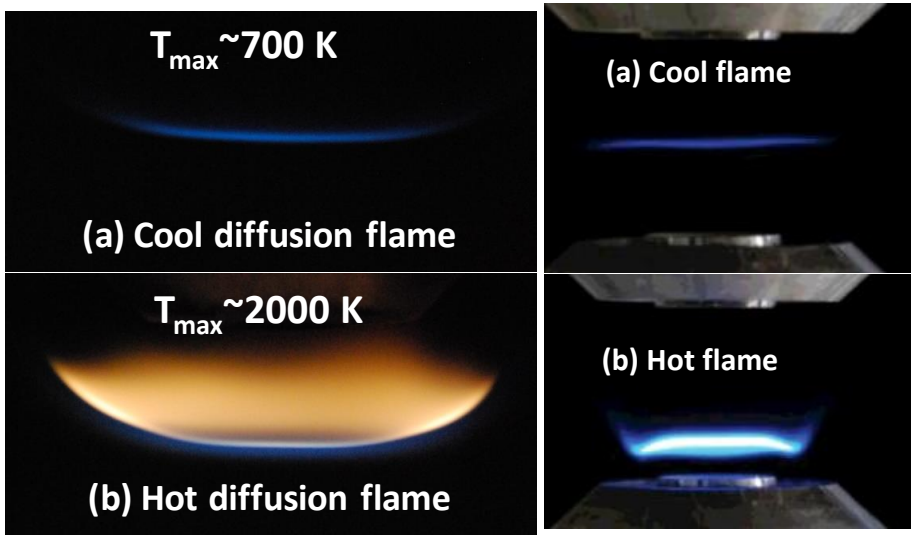


**Diffusion Flames** **Premixed Flames**

The existence of cool flame dramatically change the burning limits on both lean and rich sides.

How will plasma affect cool flames? When the chemistry is slow, plasma has a chance!

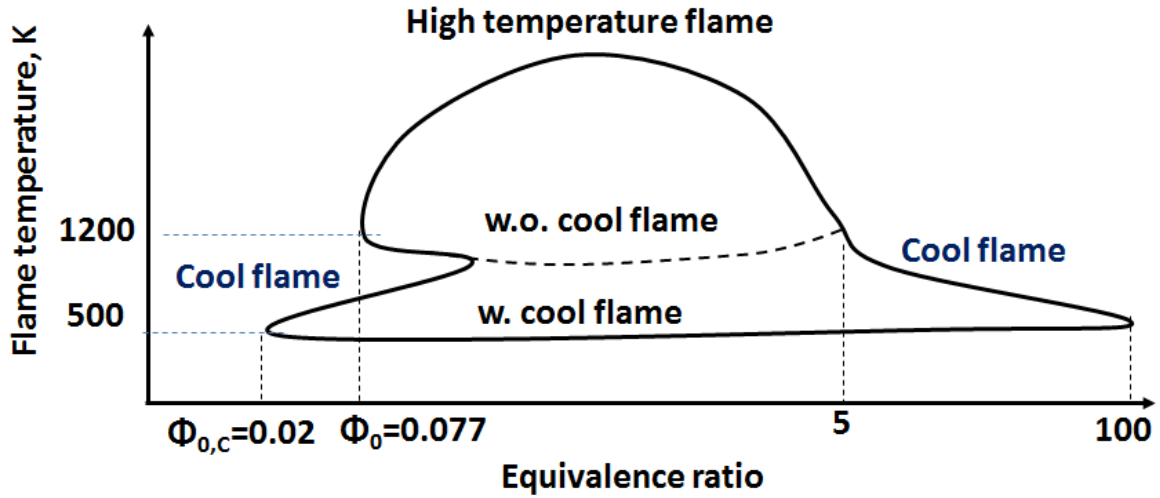



ı & Ju et al., Proc. Combust. Inst. 35, 2015
ter, Won, & Ju, Submitted to 36 symposium, 2016
t al., Combustion and Flame, 2015.

# Plasma Assisted Combustion: a multi-disciplinary and multi-physics problem

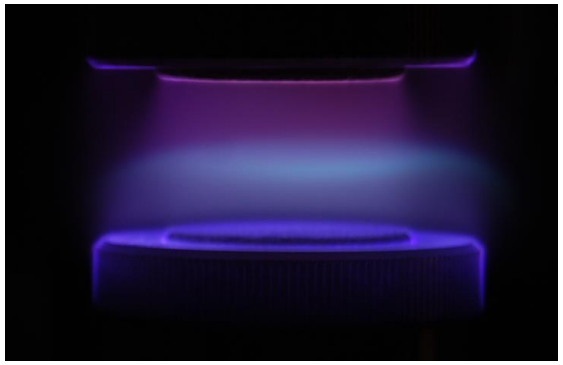

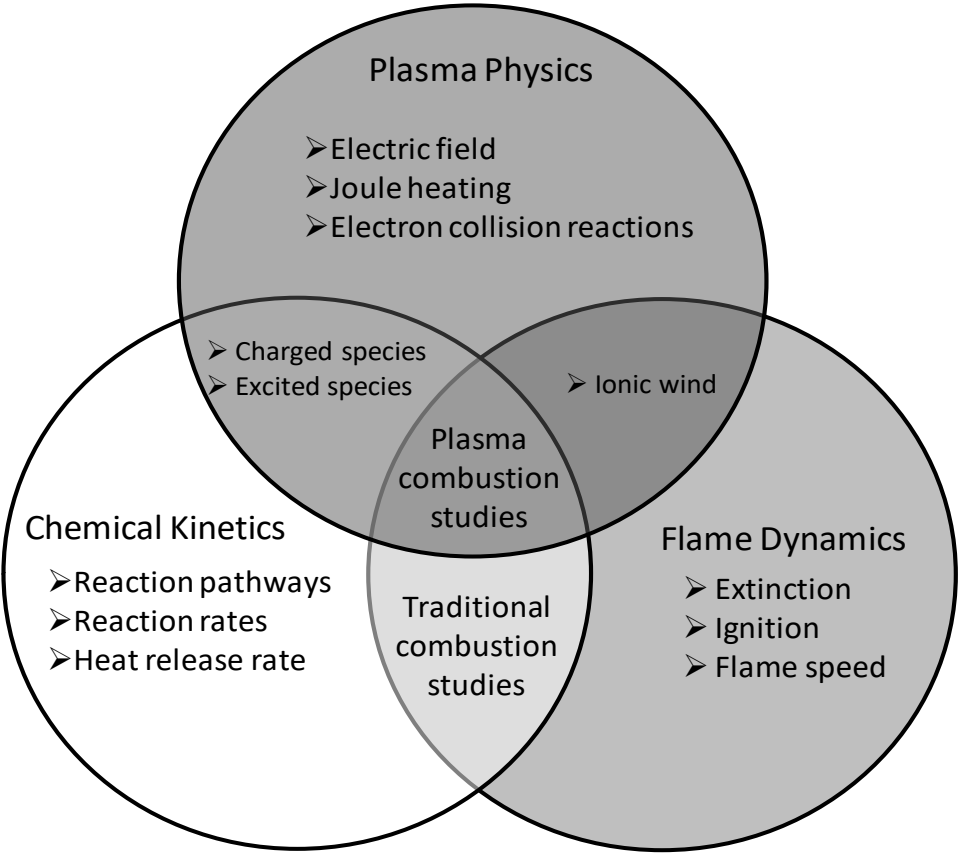


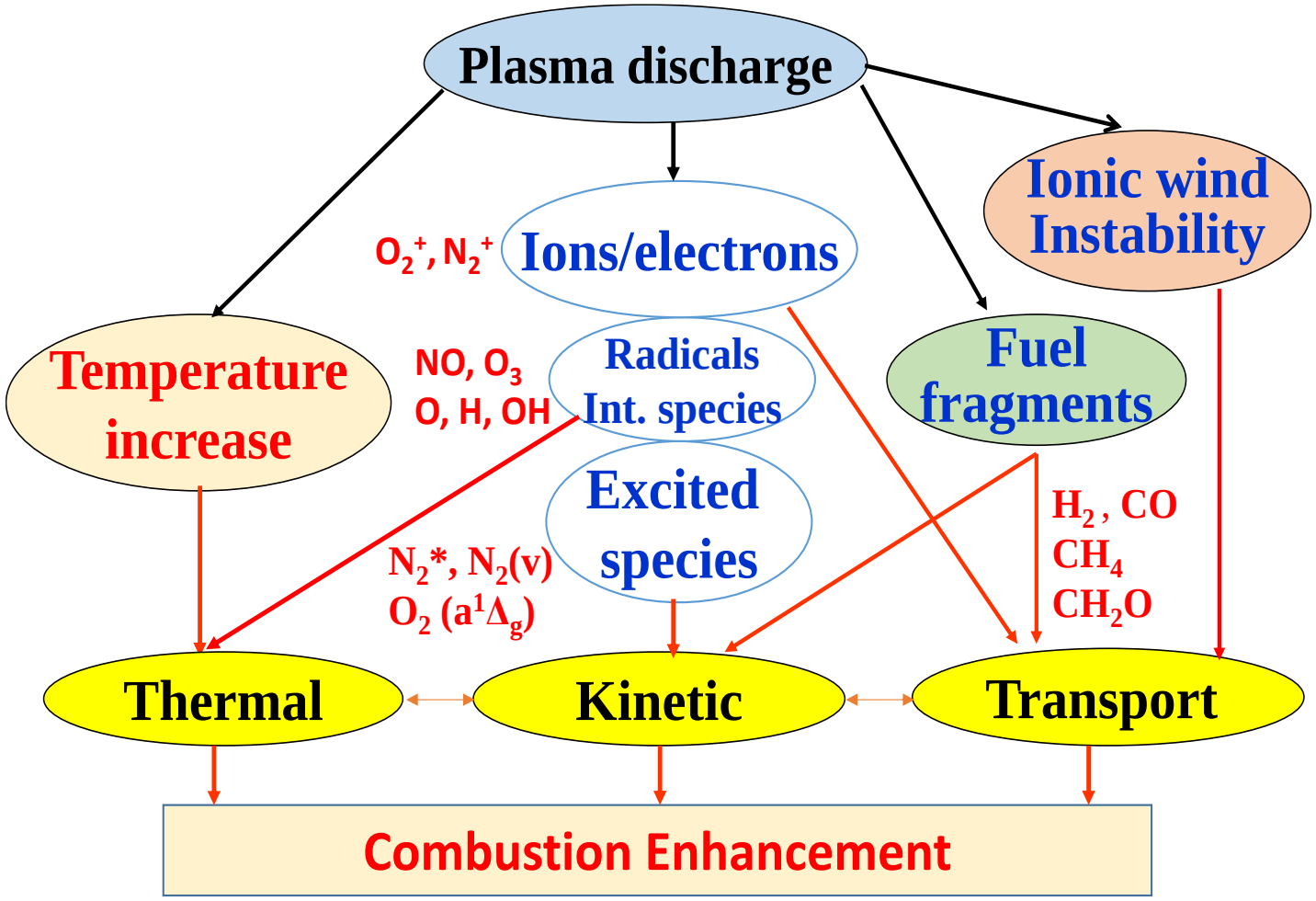




Ju and Sun: Plasma assisted combustion, Progress of Energy & Combustion Science, 2015

# 3.2.2 Flame speed, extinction and flammability limits with by flame stretch (Le)

$$-\rho C_p a x \frac{dT}{dx} = \lambda \frac{d^2T}{dx^2} + QY_{F,0} B e^{-E/2RT_{ad}} \delta(x - x_f) - Q_r (T - T_0)$$

$$-\rho a x \frac{dY_F}{dx} = \rho D \frac{d^2 Y_F}{dx^2} - Y_{F,0} B e^{-E/2RT_{ad}} \delta(x - x_f)$$

$$\frac{dT}{dx}(0) = 0 \qquad \frac{dY_F}{dx}(0) = 0$$

$$T(\infty) = T_0, \qquad Y_F(\infty) = Y_{F,0}$$

$Q_r = 4K_p \sigma (T_{ad}^3 - T_0^3)$

$a = du/dx$

$T_{ad} = T_0 + QY_{F,0}/C_p$

$\rho U_{ad} = B e^{-E/2RT_{ad}}$

$\delta$ : Dirac delta function

$$\beta = \frac{E}{RT_{ad}} \frac{T_{ad} - T_0}{T_{ad}}$$

$$\theta = \frac{T - T_0}{T_{ad} - T_0},$$

$y = Y_F / Y_{F,0}$

$X = x / x_{ref}$,

$T_{ad} = T_0 + QY_{F,0}/C_p$

$\rho U_{ad} = B e^{-E/2RT_{ad}}$

$$x_{ref} = \frac{\lambda / \rho C_p}{U_{ad}}$$

$t_{ref} = x_{ref} / U_{ad}$

$$H = \frac{\beta 4 \sigma K_p T_{ad}^3}{\rho C_p U_{ad}} \frac{\lambda}{\rho C_p U_{ad}}$$

$$Le = \frac{\lambda}{\rho C_p D}$$

$$\eta = \sqrt{\frac{a t_{ref}}{2}} X,$$

In the limit of large β

$$2\eta \frac{d\theta}{d\eta} + \frac{d^2\theta}{d\eta^2} - \frac{2}{a}\frac{H\theta}{\beta} + \sqrt{\frac{2}{a}} e^{\beta(\theta_f - 1)/2} \delta(\eta - \eta_f) = 0$$

$$2\eta \frac{dy_F}{d\eta} + \frac{1}{Le}\frac{d^2 y_F}{d\eta^2} - \sqrt{\frac{2}{a}} e^{\beta(\theta_f - 1)/2} \delta(\eta - \eta_f) = 0$$

**Flame stretch:** $$a = \frac{1}{A_f}\frac{dA_f}{dt}$$

$$u = -ax$$

$$a = du/dx$$

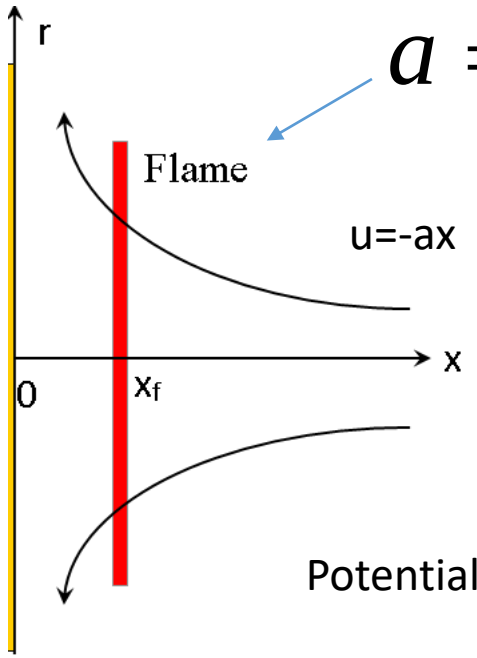


Potential flow (outside)

Here the stretch rate *a* is non-dimensional

**Perturbation**

$$T = T^0 + T^1/\beta + \ldots, \qquad Y_F = Y_F^0 + Y_F^1/\beta + \ldots, \qquad Le = 1 + l/\beta + \ldots \qquad p \equiv T^1 + Y_F{}^1,$$

**Outer solution in convection-diffusion zone**

$$\theta^0 = \int_{\infty}^{\eta} e^{-t^2}\,dt \Big/ \int_{\infty}^{\eta_f} e^{-t^2}\,dt, \qquad y^0 = 1 - \int_{\infty}^{\eta} e^{-t^2}\,dt \Big/ \int_{\infty}^{\eta_f} e^{-t^2}\,dt \qquad \text{at } \eta = (\eta_f, \infty)$$

$$\theta^0 = 1, \qquad y^0 = 0 \qquad \text{at } \eta = (0, \eta_f)$$

**Jump conditions**

(1) Integrating $\dfrac{d^2\theta}{d\eta^2} + \sqrt{\dfrac{2}{a}} e^{\beta(\theta_f - 1)/2}\,\delta(\eta - \eta_f) = 0$ from flame front (-) to end of reaction zone (+)

$$\left[\frac{d\ \theta}{d\eta}\right]_-^+ = \sqrt{\frac{2}{a}} e^{\theta_f^1/2} = 0$$

(2) Integrating the summation of mass and energy equation in reaction-diffusion zone,

$$\left[\frac{dp}{d\eta} - l\frac{dy_F{}^0}{d\eta}\right]_-^+ = 0$$

$$p = 0, \qquad \eta = 0, \text{and} \infty$$

**Governing equation for perturbed variables:**

$$2\eta\frac{dp}{d\eta} + \frac{d^2p}{d\eta^2} - l\frac{d^2y_F{}^0}{d\eta^2} - \frac{2}{a}\frac{H\theta^0}{\beta} = 0$$

**Solution:**

$$\frac{-\sqrt{a}}{\sqrt{2}\eta_f g_1} = e^{p_f/2}, \qquad m = \eta_f \sqrt{2a}$$

Enthalpy change $$p_f = l(-\frac{1}{2} - \eta_f{}^2 - \frac{1}{g_1}) + \frac{2H^+}{a}\eta_f{}^2 g_1 g_2 + \frac{H^-}{a}(-g_3 + I_1 / g_1)$$

$$g_1 = \int_\infty^1 e^{(1-n^2)\eta_f^2} dn$$

$$g_2 = \int_0^1 e^{(n^2-1)\eta_f^2} dn$$

$$g_3 = \int_\infty^1 \frac{1-e^{(1-n^2)\eta_f^2}}{n^2-1} dn$$

$$I_1 = \int_\infty^1 e^{(1-n^2)\eta_f^2} \int_\infty^1 \frac{1-e^{(1-k^2)n^2\eta_f^2}}{k^2-1} dk dn$$

If $\eta_f \to \infty, \quad -2\eta_f{}^2 g_1 = 1,$ ⟹ $m^2 \ln m^2 = -2H$

# Flame propagation speed with stretch and heat loss: sublimit combustion

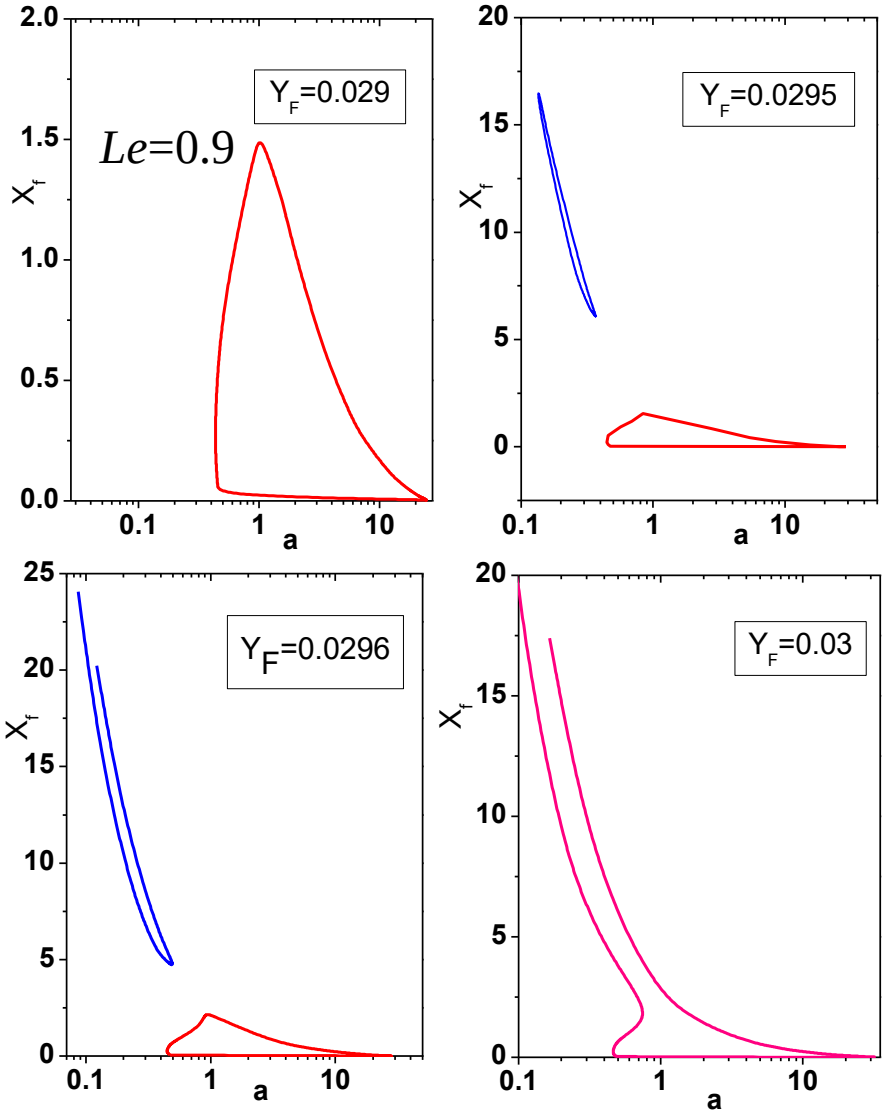


Dependence of flame location on stretch at Le=0.9

- At low fuel concentration ($Y_F$=0.029) below the flammability limit, flame can exist in a narrow range of stretch rate bounded by a radiation extinction limit and a stretched extinction limit.
- As the fuel concentration increase close to the flammability limit, there exist two flame islands, respectively, close and away from the stagnation plane.
- As the fuel concentration further increases to slightly above the flammability limit, there exist both planar flame at zero stretch rate and a near stagnation flame island at Lewis number below unity.
- As the equivalence ratio becomes above flammability limit, the two flame islands merge together and a stretched flame can becomes a planar flame as the stretch rate decreases.

Ju, Y. and Minaev, S., 2002. *Proceedings of the Combustion Institute*, *29*(1), pp.949-956.

## Microgravity experiments

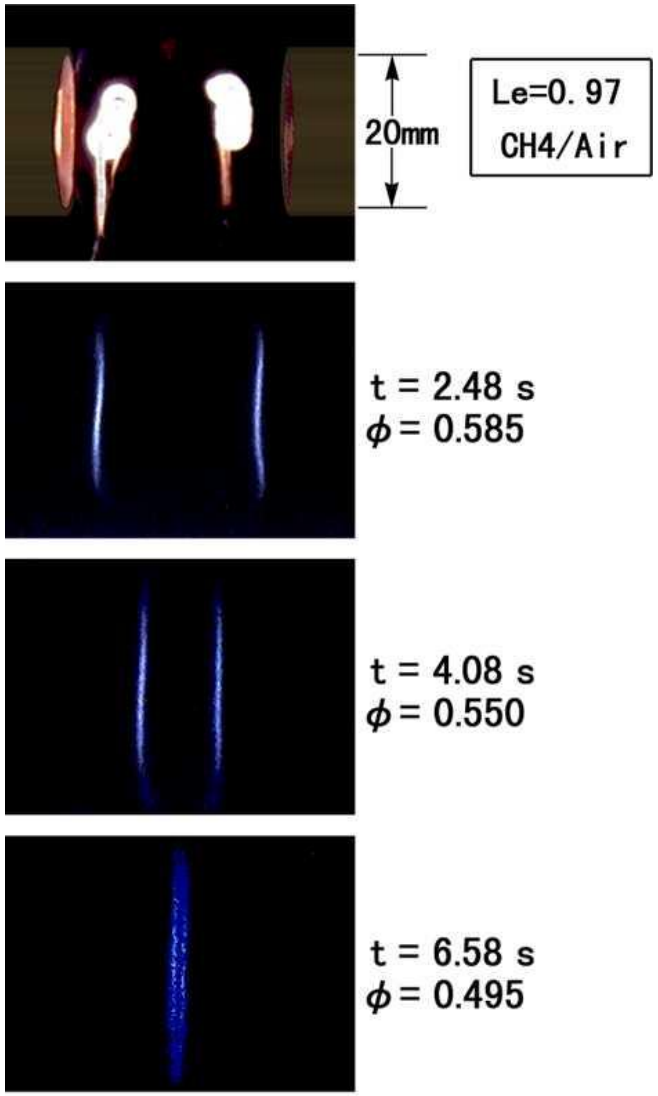


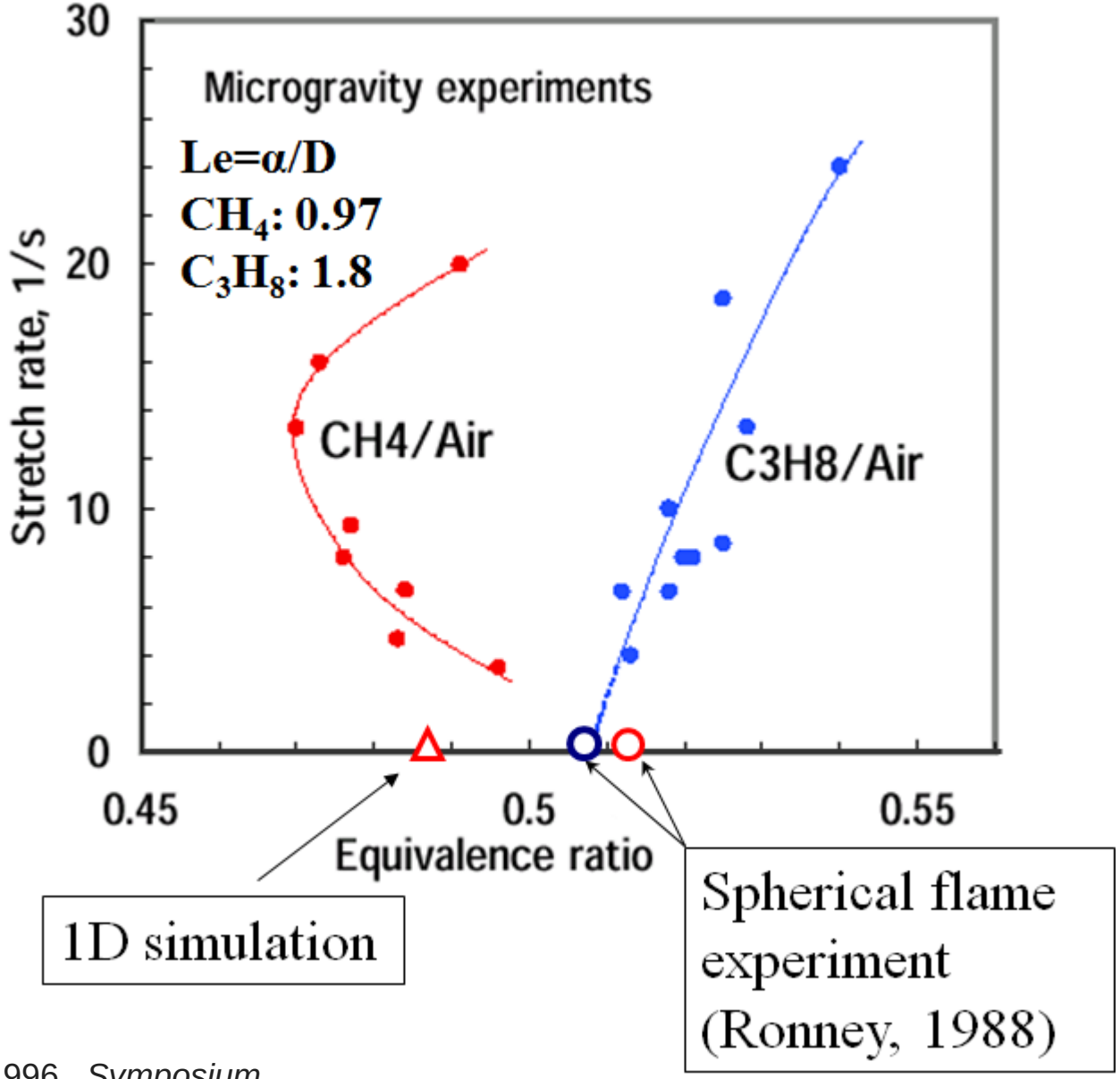


Maruta, K., Yoshida, M., Ju, Y. and Niioka, T., 1996, *Symposium (International) on Combustion* (Vol. 26, No. 1, pp. 1283-1289). Elsevier.

# Numerical simulation: detailed chemistry
# $CH_4$-$O_2$-$N_2$-He

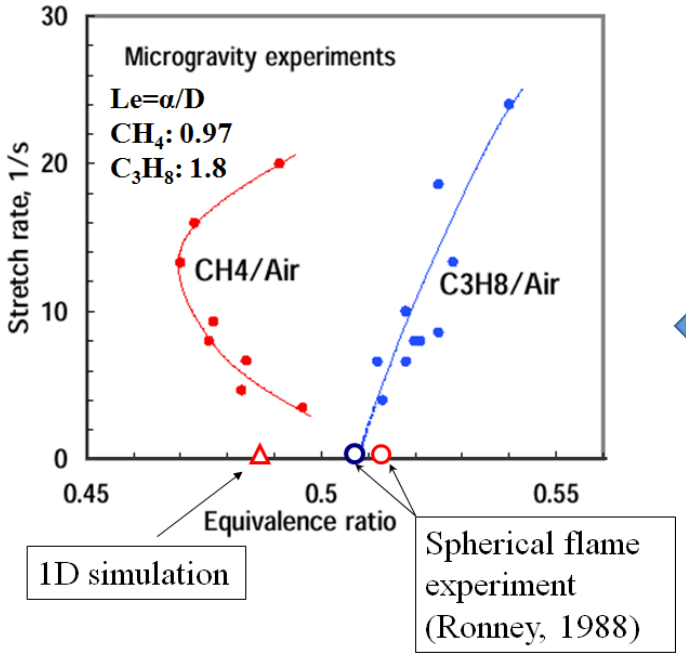


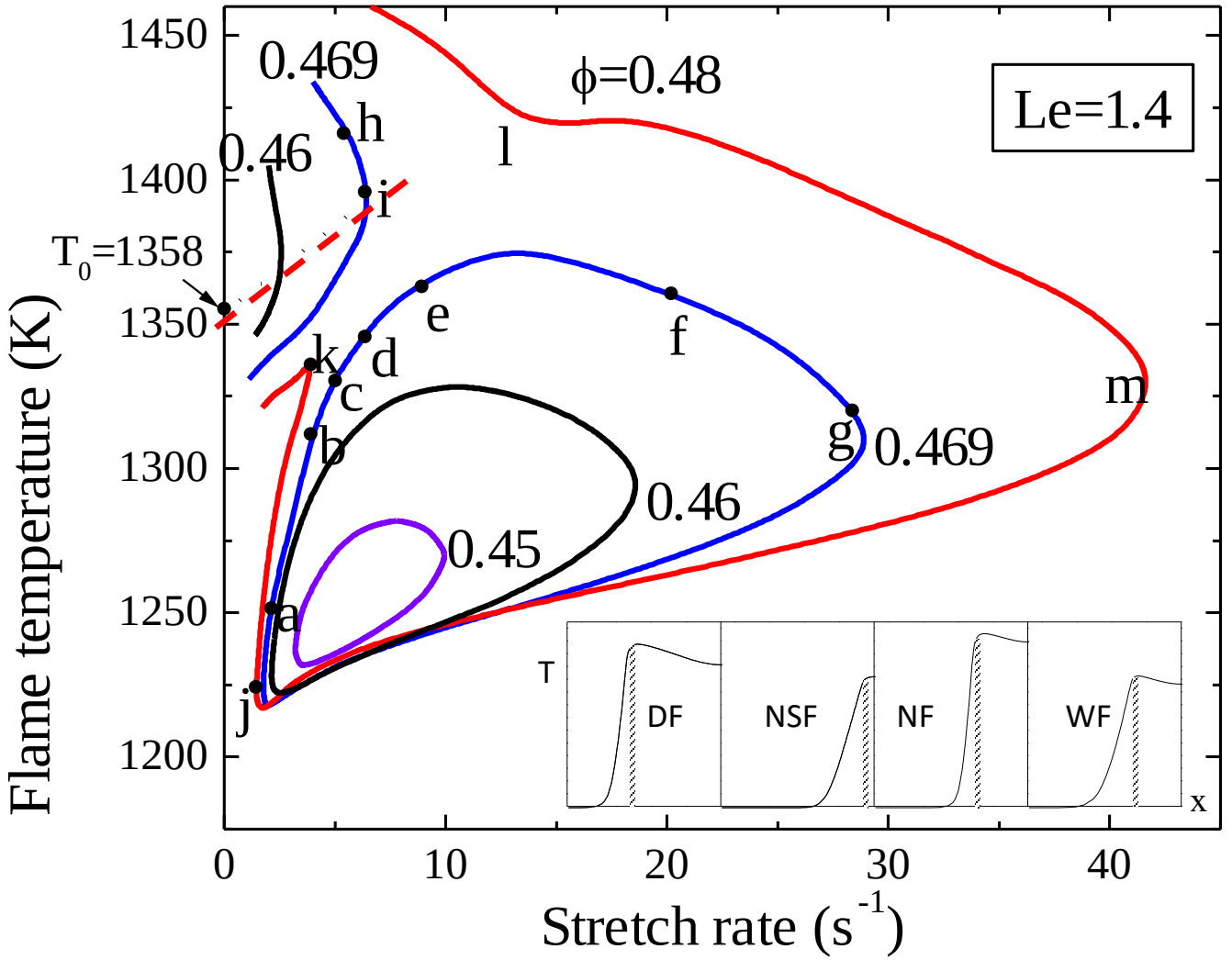

# The G-Curve

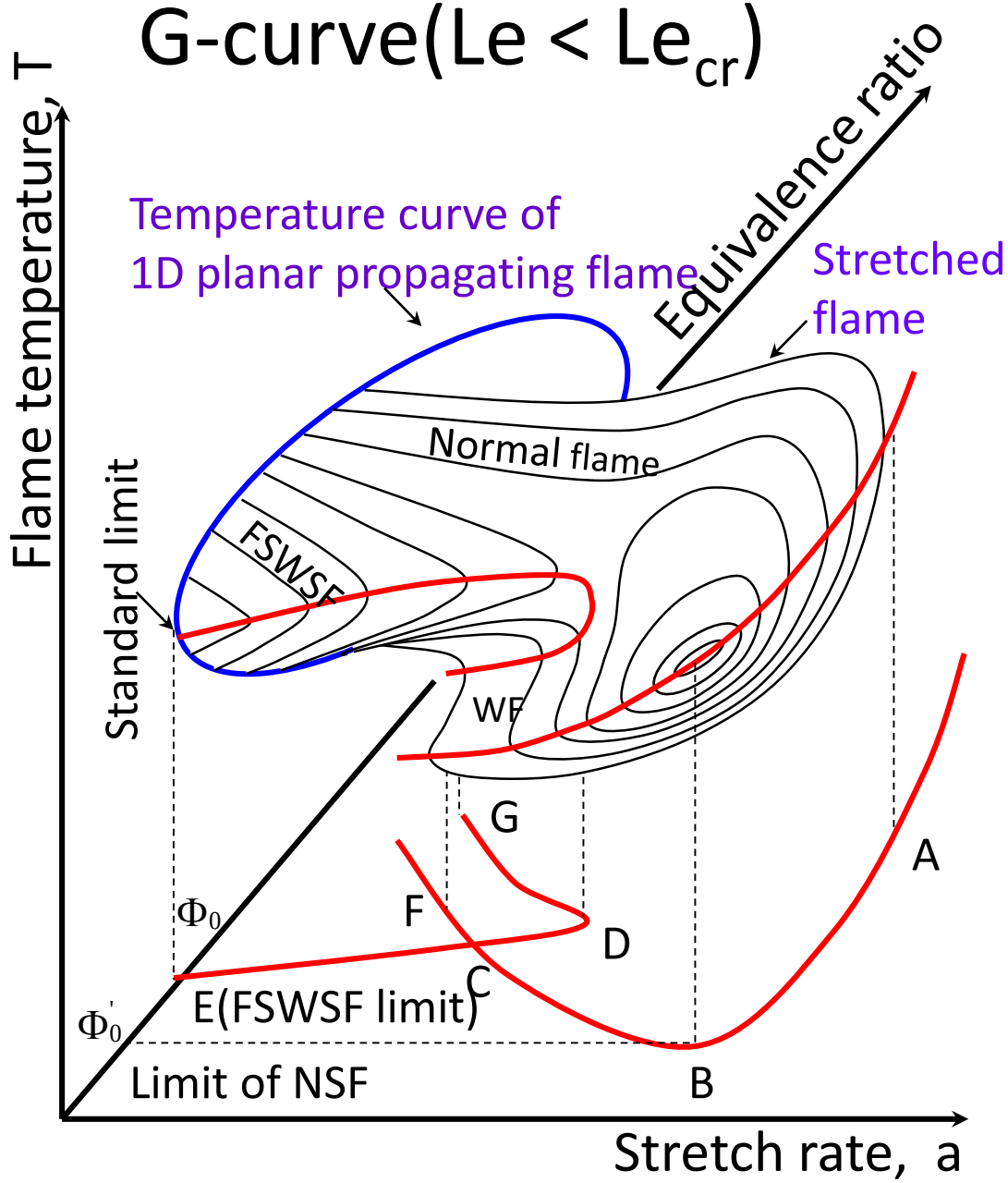
G-curve(Le < Le$_{cr}$)
Flame temperature, T
Equivalence ratio
Temperature curve of
1D planar propagating flame
Stretched
flame
Normal flame
FSWSF
Standard limit
WF
G
A
$\Phi_0$
F
D
C
E(FSWSF limit)
$\Phi_0'$
Limit of NSF
B
Stretch rate, a

# The G-curve (Le < $Le_{cr}$)

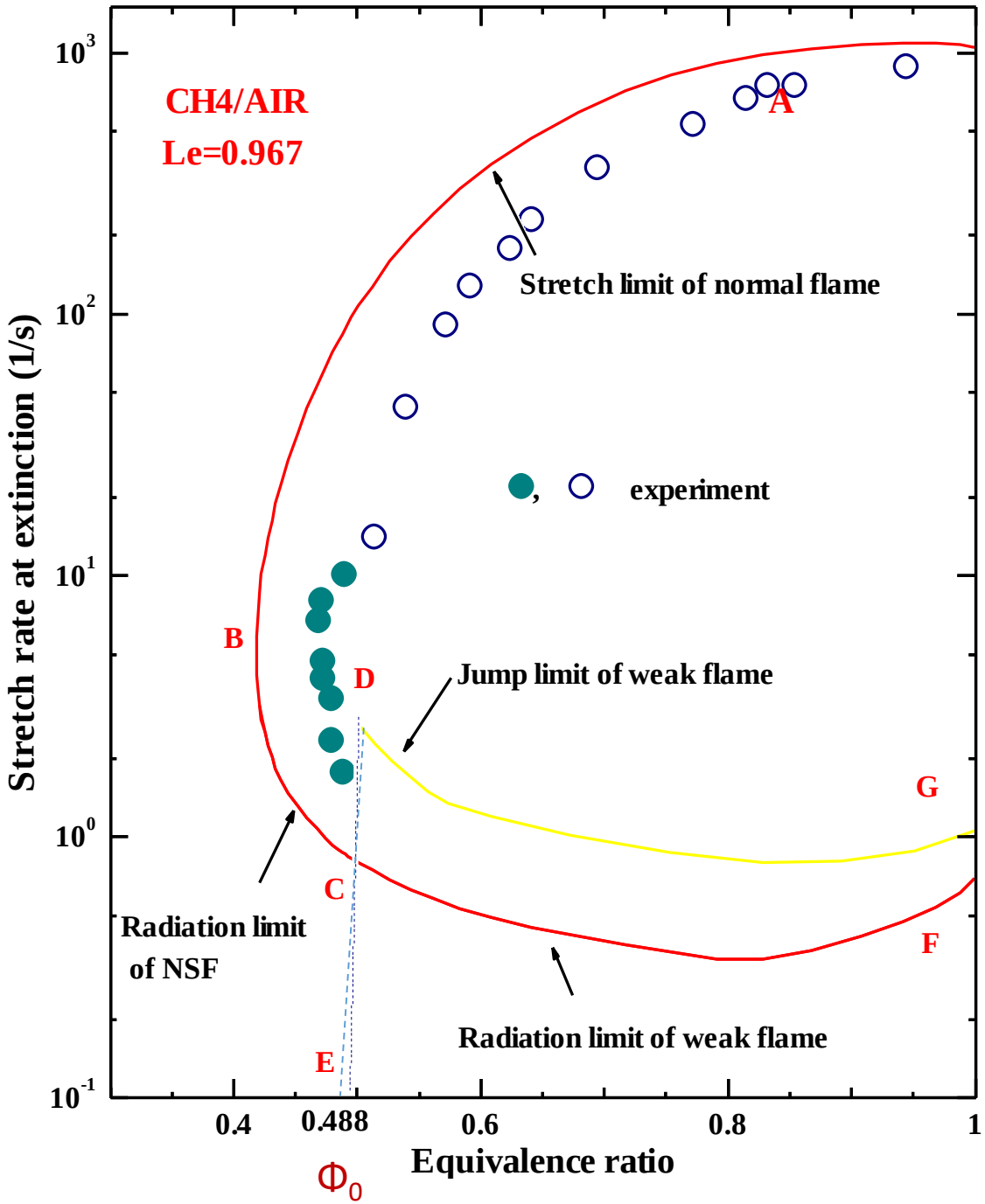


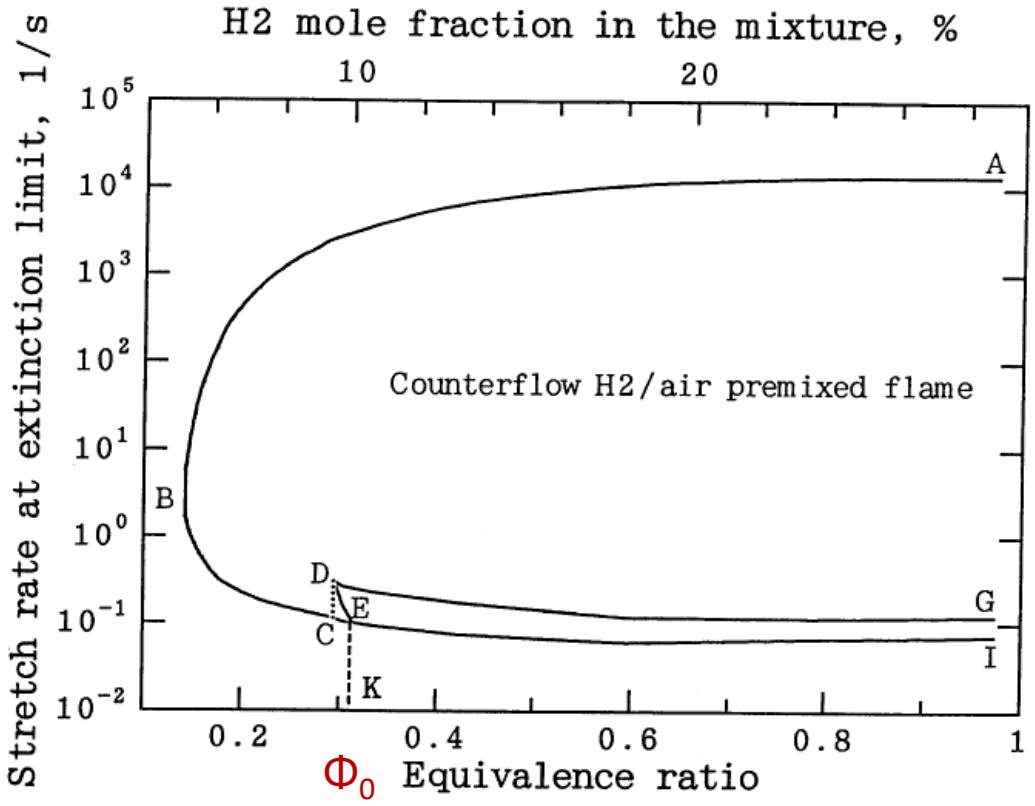


When a mixture has a low Lewis number, the flammability ($\Phi_0$) region can be extended significantly by stretch!


Ju, Y., Guo, H., Maruta, K. and Liu, F., 1997..*JFM*, *342*, pp.315-334.
Guo, H., Ju, Y. and Niioka, T., 2000. *CTM*, *4*(4), pp.459-475.

# The K-curve (Le > $Le_{cr}$ )

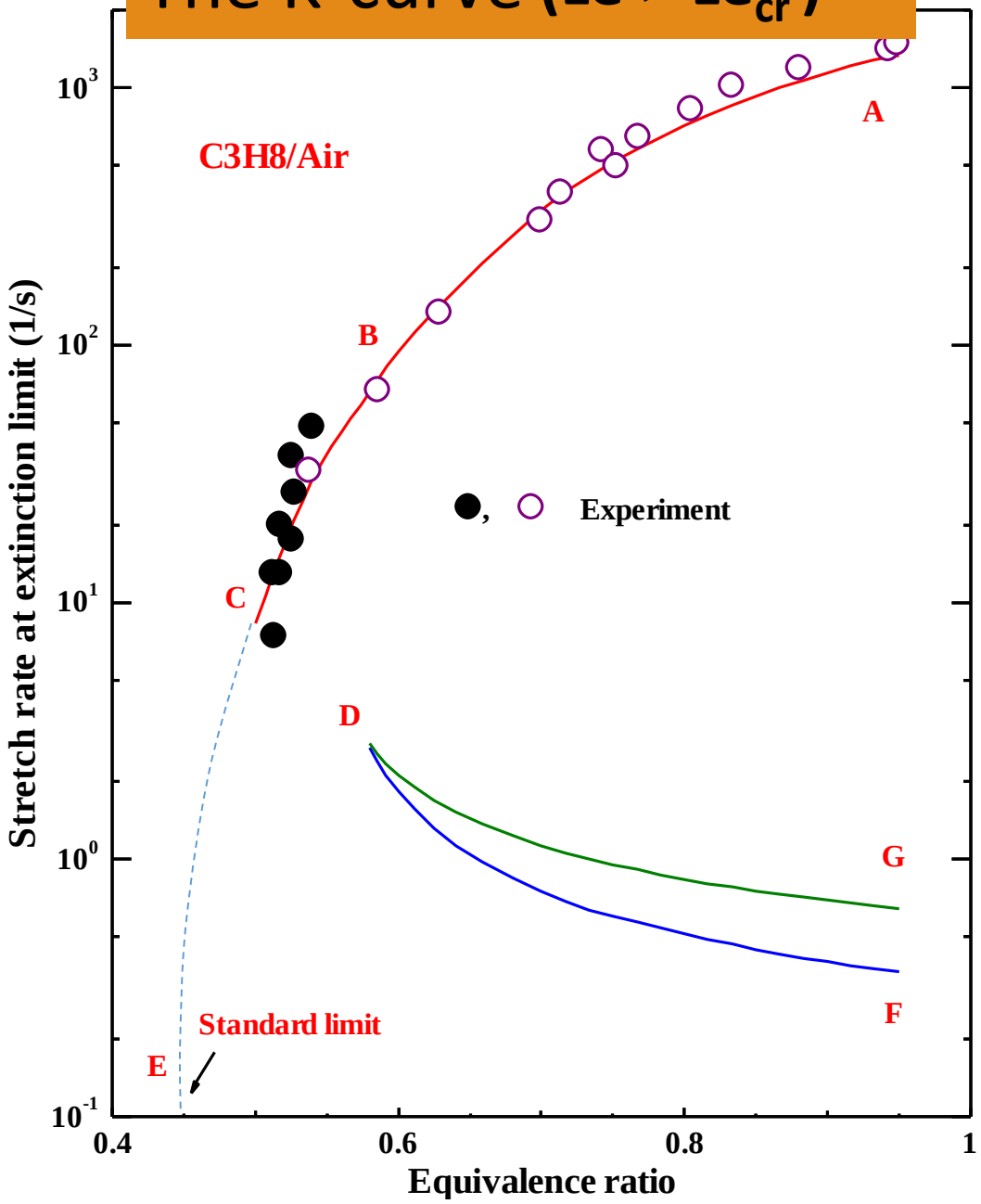


Now we can understand the experimental data on the figure below

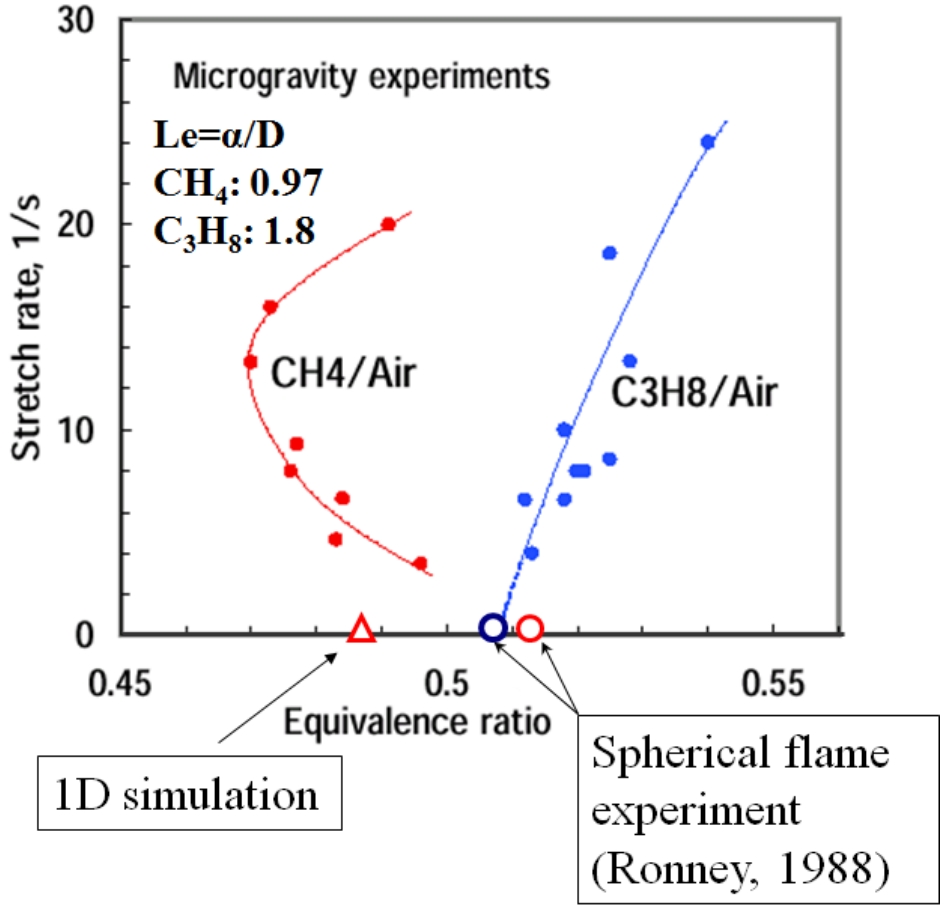


How does plasma change the flammable region of stretched flames?

# 3.3 Plasma effect on the minimum ignition energy and the critical flame initiation radius

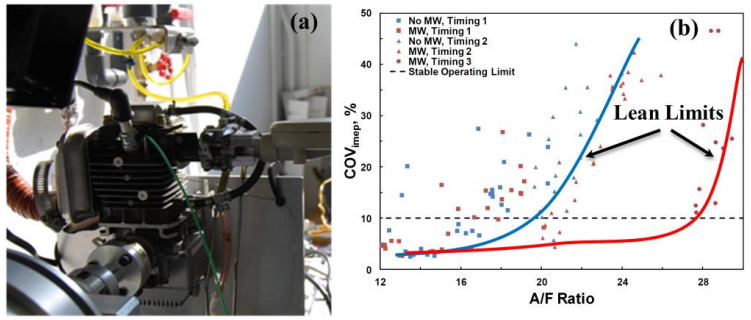


**Flammability limit?**

**Internal combustion engine, microwave**

Lefkowitz et al. 2012, Ikeda et al. 2009

**Spark**

**Microwave**

**gliding arc**

Why does a flammable mixture can not be ignited by a spark for a small engine or at lower pressure?

# Puzzle of high altitude relight:
## an unresolved ignition problem or a flame problem?

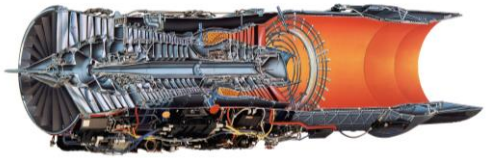

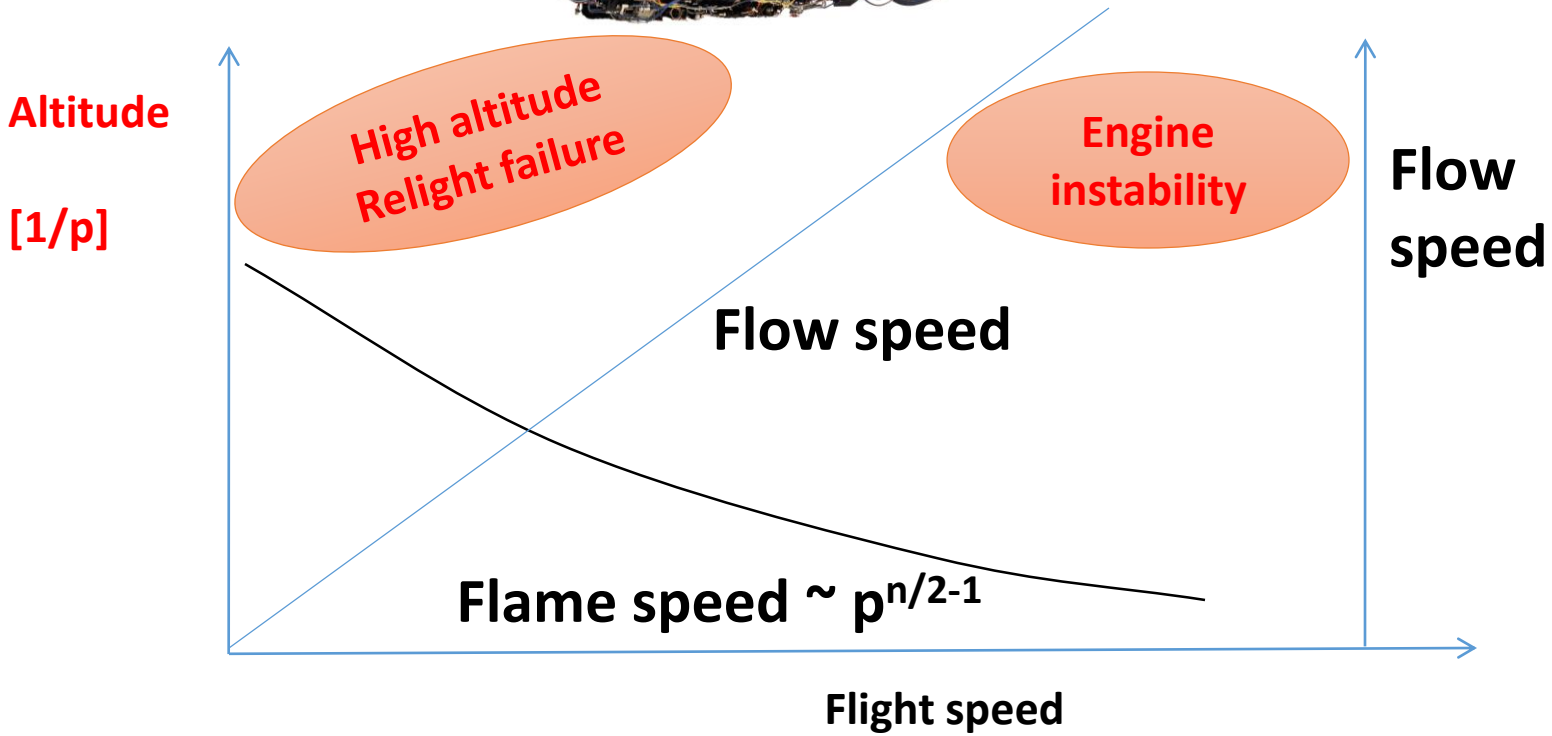


**Is the flame speed really a problem for relight?**

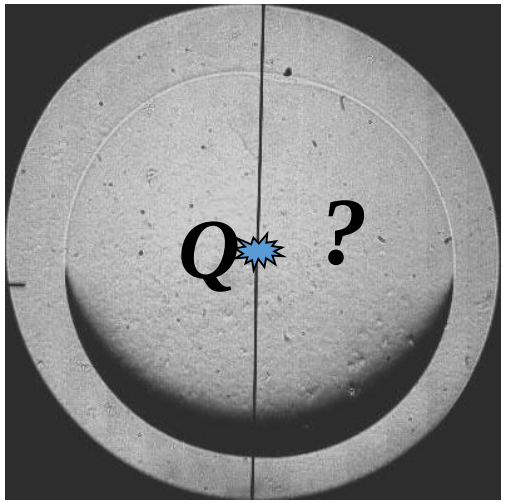


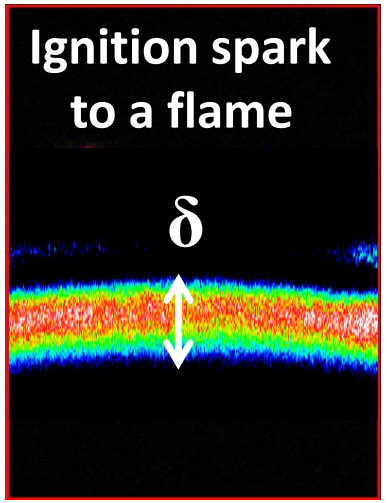


- **What governs the ignition & $E_{ig}$?**
- **What are the chemistry and transport effects?**

$$Le = \frac{\text{Thermal diffusivity}}{\text{Mass diffusivity}} = \frac{oxygen}{Jet\ fuel}$$

**•$E_{ig,min}$: Defined by flame thickness, δ (make a guess)?**

**B. Lewis and Von Elbe (1961), Ronney, 2004, Glassman (2008)**

$$E_{ig} = \frac{4}{3}\pi\delta^3\rho C_p(T_{ad} - T_\infty) \propto \frac{1}{S_u^{\,3}} \propto \frac{1}{Le^{3/2}}$$

volume

heat capacity

**Larger fuel molecules ⇔ smaller $E_{ig}$**

**•$E_{ig,min}$: Defined by stable "flame ball" size?**

**Zeldovich et al. (1985), Champion et al. (1986)**

$$E_{ig} = \frac{4}{3}\pi R_Z^{\,3}\rho C_p(T_{ad} - T_\infty) \sim Le$$

**Larger fuel molecules ⇔ larger $E_{ig}$**

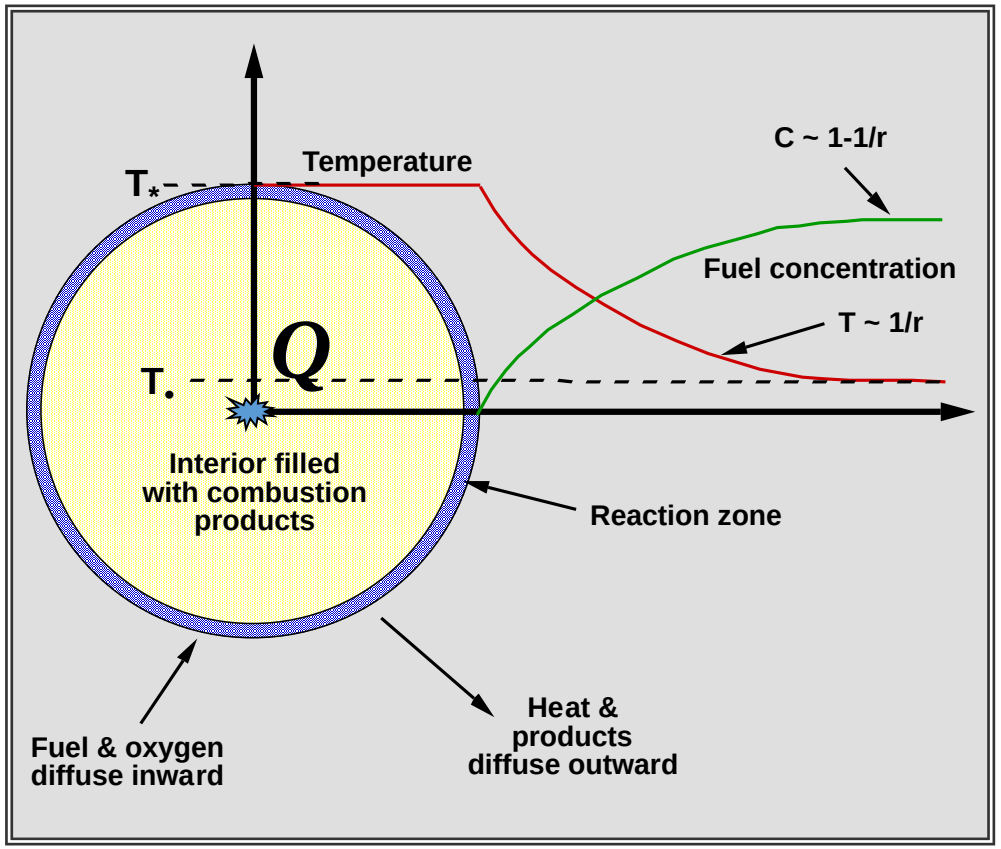


## Assumptions and simplification:

- **1D quasi-steady state, Constant properties**
- **One-step chemistry**
- **Center energy deposition**

$$\frac{\partial T}{\partial t} - U\frac{\partial T}{\partial r} = \frac{1}{r^2}\frac{\partial}{\partial r}(r^2\frac{\partial T}{\partial r}) - H + \omega$$

$$\frac{\partial Y}{\partial t} - U\frac{\partial Y}{\partial r} = \frac{Le^{-1}}{r^2}\frac{\partial}{\partial r}(r^2\frac{\partial Y}{\partial r}) - \omega$$

$$r = 0, \quad r^2\partial T/\partial r = -Q, \quad Y = 0$$

$$r = R, \quad T = T_f, \quad Y = 0$$

$$r = \infty, \quad T = 0, \quad Y = 1$$

$$H = \frac{\tilde{H}\tilde{\delta}_f^0}{\tilde{\rho}\tilde{C}_P\tilde{S}_u^0(\tilde{T}_{ad} - \tilde{T}_\infty)}$$

$$\omega = \exp\left[\frac{Z}{2}\frac{T_f - 1}{\sigma + (1-\sigma)T_f}\right]\cdot\delta(r - R)$$

$$r = \frac{\tilde{r}}{\tilde{\delta}_f^0}, \qquad R = \frac{\tilde{r}_f}{\tilde{\delta}_f^0}$$

## Flame speed: effect of flame radius, heat addition and Lewis number

$$\Omega \cdot T_f + \Omega_Q \cdot Q = \frac{1}{Le}R^{-2}e^{-ULeR} / \int_R^\infty \tau^{-2}e^{-ULe\tau}d\tau = \exp\left[\frac{Z}{2}\frac{T_f - 1}{\sigma + (1-\sigma)T_f}\right]$$

Le: Lewis number
Z: activation energy
σ: density ratio
U: flame speed
Q: ignition energy
Ω: analytic functions

Chen, Z. and Ju, Y., 2007. *Combustion Theory and Modelling*,*11*(3), pp.427-453.

# The Critical Ignition Radius

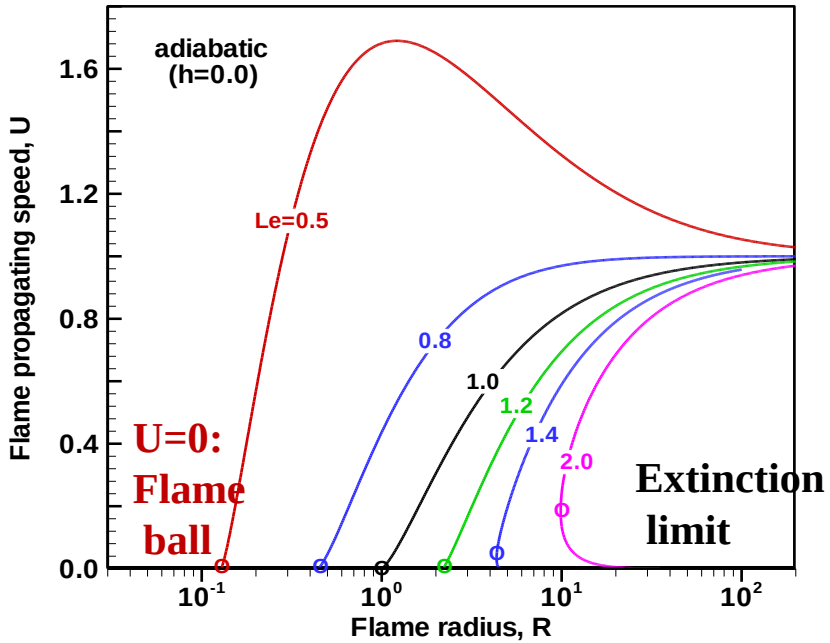


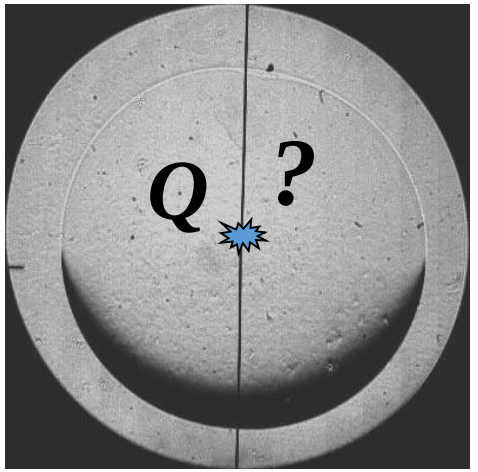


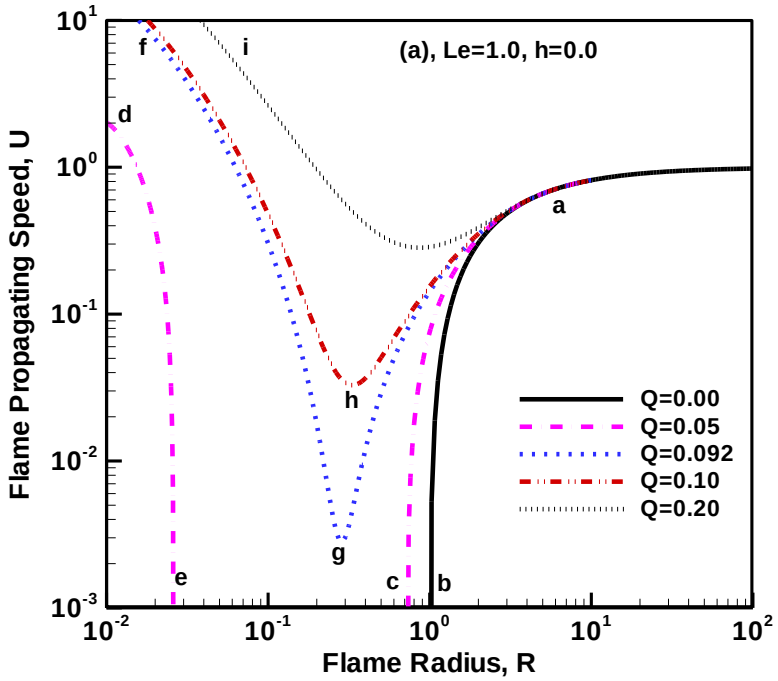


**1. The critical ignition size and energy is governed by two different length scales:**

- **Flame ball size (small Le)**
- **Extinction diameter (large Le)**

**2. With ignition energy, there is a critical flame initiation radius, below which, ignition will fail even the mixture is above the flammability limit.**

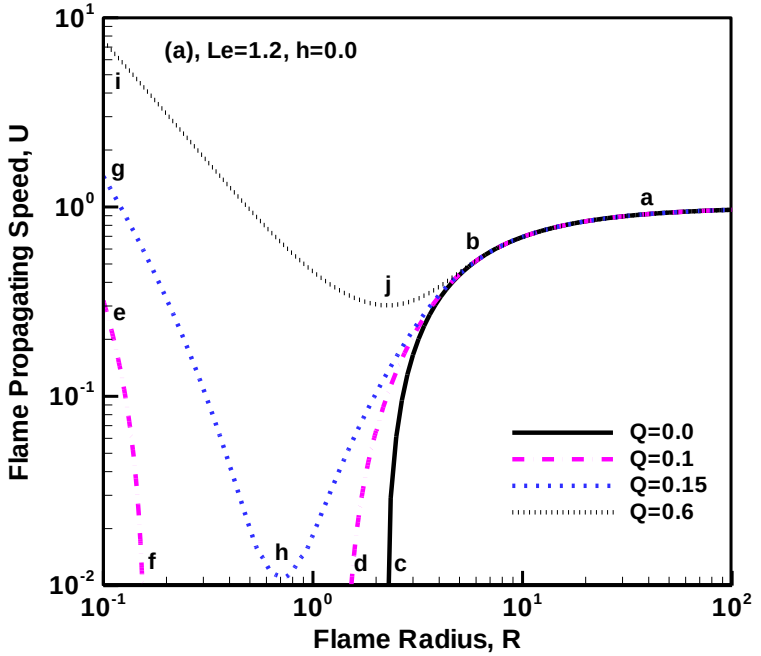


Chen & Ju, Comb. Theo. Modeling, 2007

# Ignition by heat and radical deposition ($q_t$=0.05)

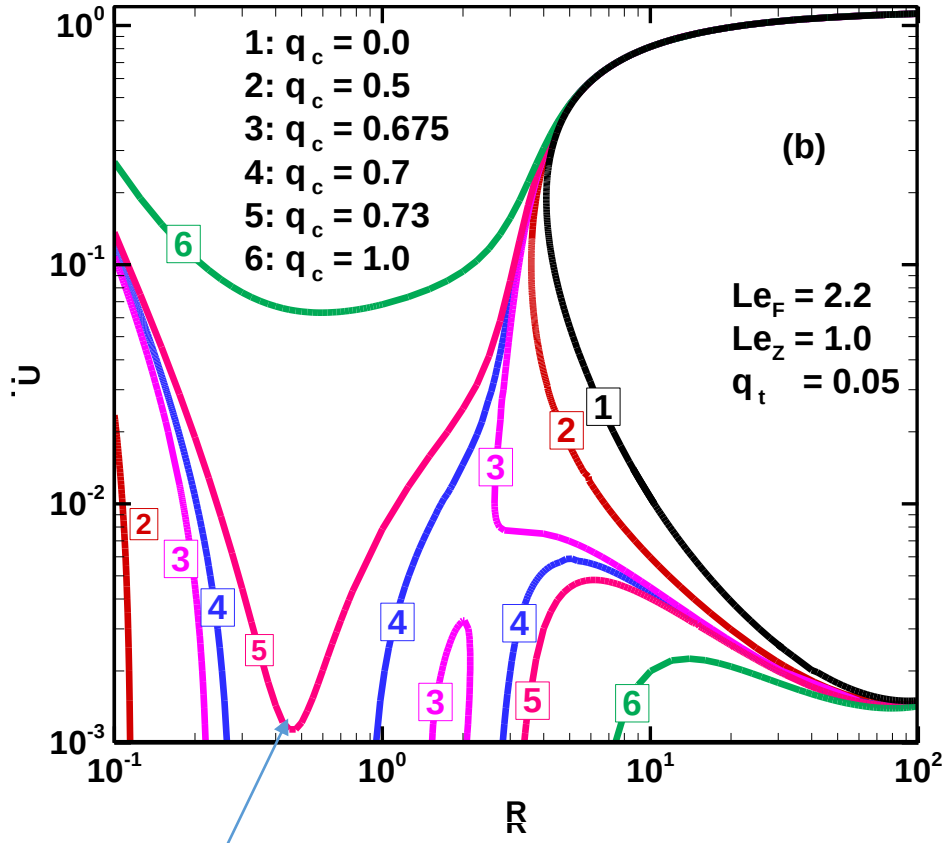


$Le_F$ = 2.2

**Critical flame initiation radius**

Chen et al. 2011

# Minimum Ignition Energy vs. Critical ignition radius: impacts of flame chemistry and transport

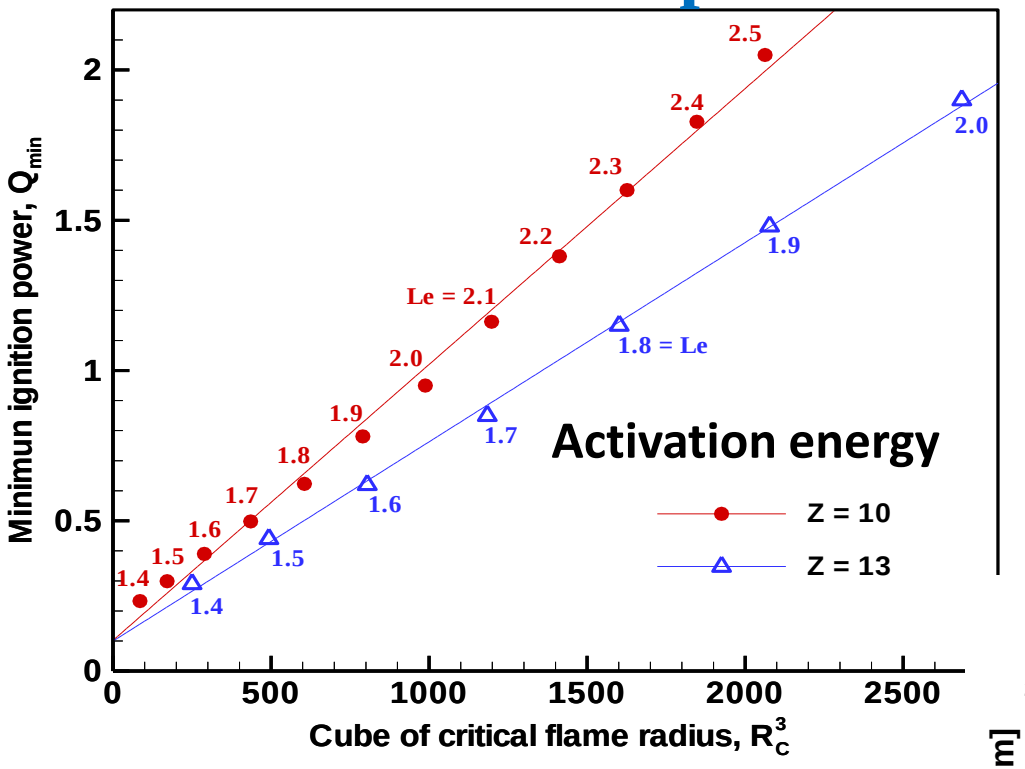


Chen, Burke, Ju, Proc. Comb. Inst. Vol.33, 2010

| Fuel | Mean molecular weight | Radical Index |
|---|---|---|
| JP8 POSF 6169 | 153.9 | 0.80 |
| SHELL SPK POSF 5729 | 136.7 | 0.85 |

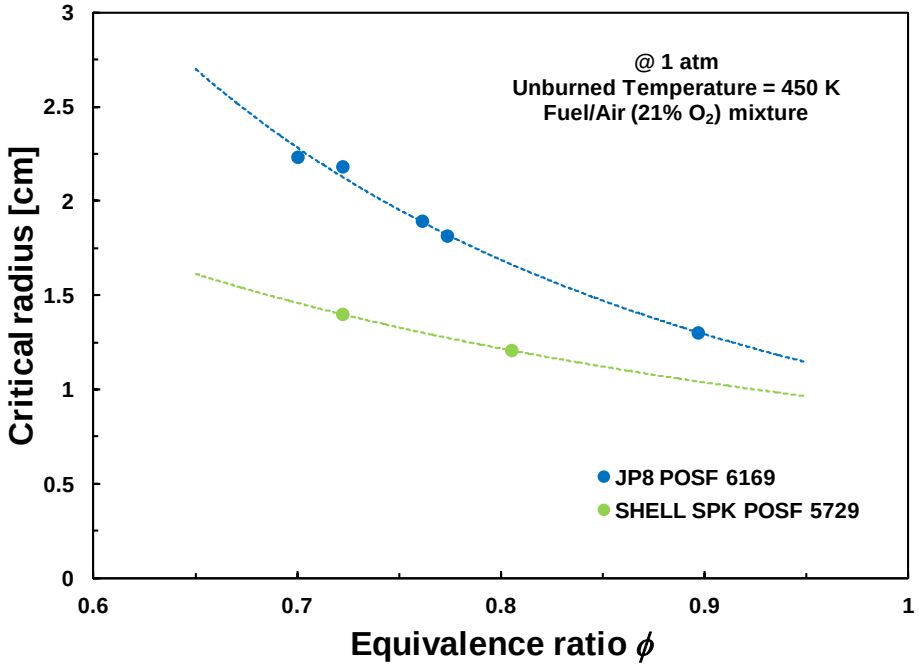


Won, Santer, Dryer, Ju, 2012

# Flame Initiation/Propagation: experimental confirmation

- **Experimental setup**
- Chamber with high speed Schlieren imaging
  - 10 cm radius chamber (2.5 cm flame radius is used)
  - Pressure rise less than 3% when $R_f$ = 2.5cm
  - Unburned gas temperature = 450 K
- Critical flame initiation radius (stretch rate) and steady state flame speed can be measured.
  - Schlieren visualization / High speed camera (15000 fps)

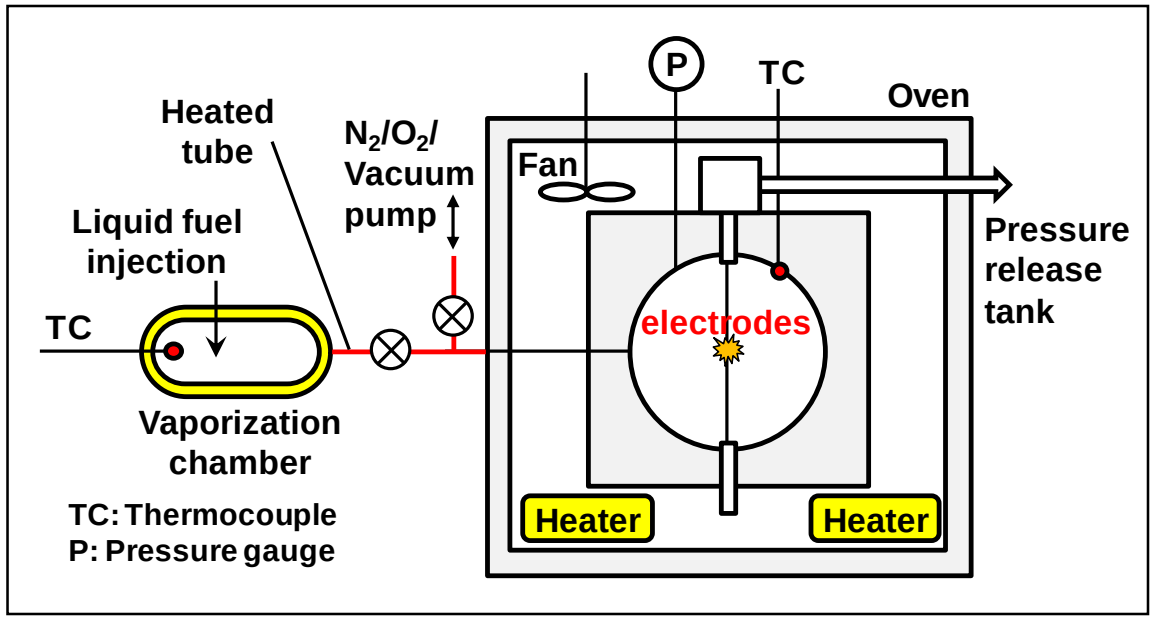

# Outwardly Propagation Flames

- Outwardly propagating flames
  - *n*-Decane/Air at $\phi$ 0.7, 1 atm, 400 K
  - Schlieren imaging 15000 fps

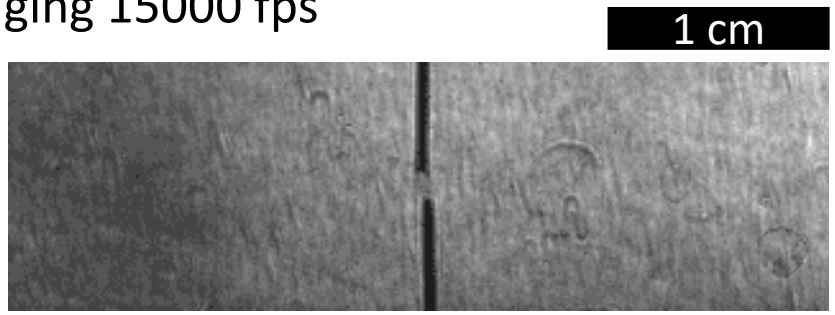


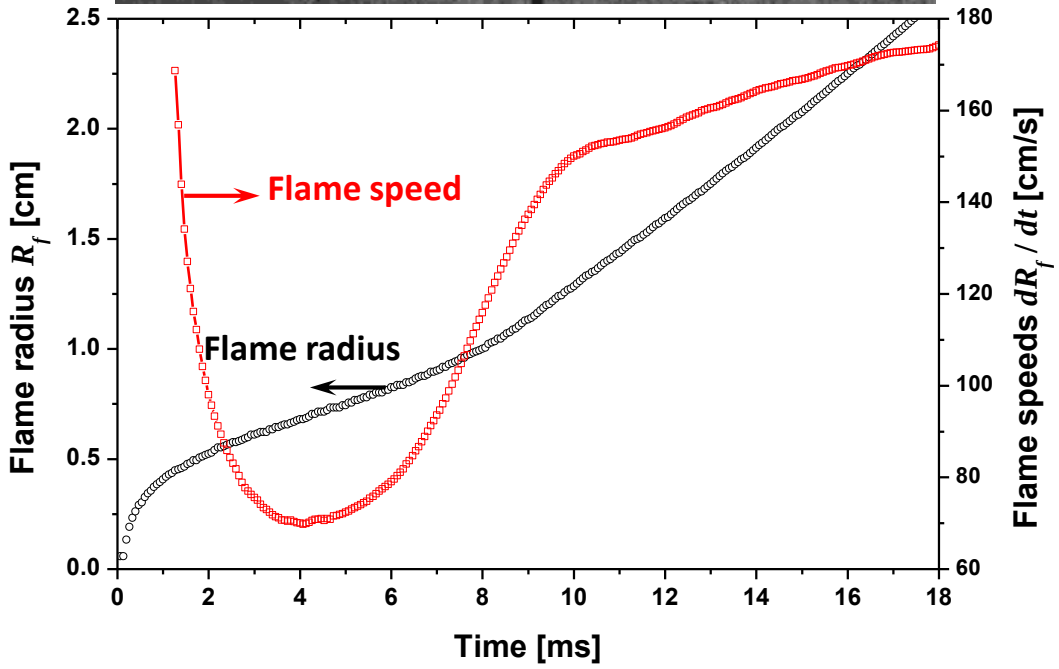


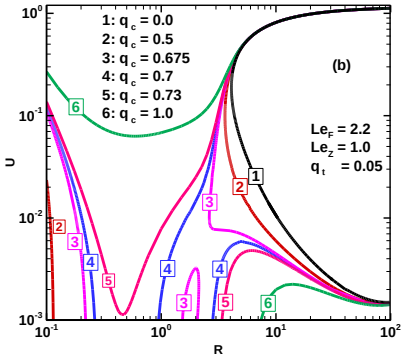

# Flame trajectory / Flame regimes

- Outwardly propagating flame trajectory
  - Flame speed $S_b = dR_f/dt$
  - Stretch rate $K = (2/R_f) \times (dR_f/dt)$[1]
- Three distinct flame regimes
  - **Regime I**
    - Spark assisted ignition kernel
  - **Regime II**
    - Transition from ignition kernel to normal flame
    - **Weak flame regime**
  - **Regime III**
    - Self-sustained stable propagating flame
  - Consistent with previous study[2]
- Laminar flame speed / Critical radius

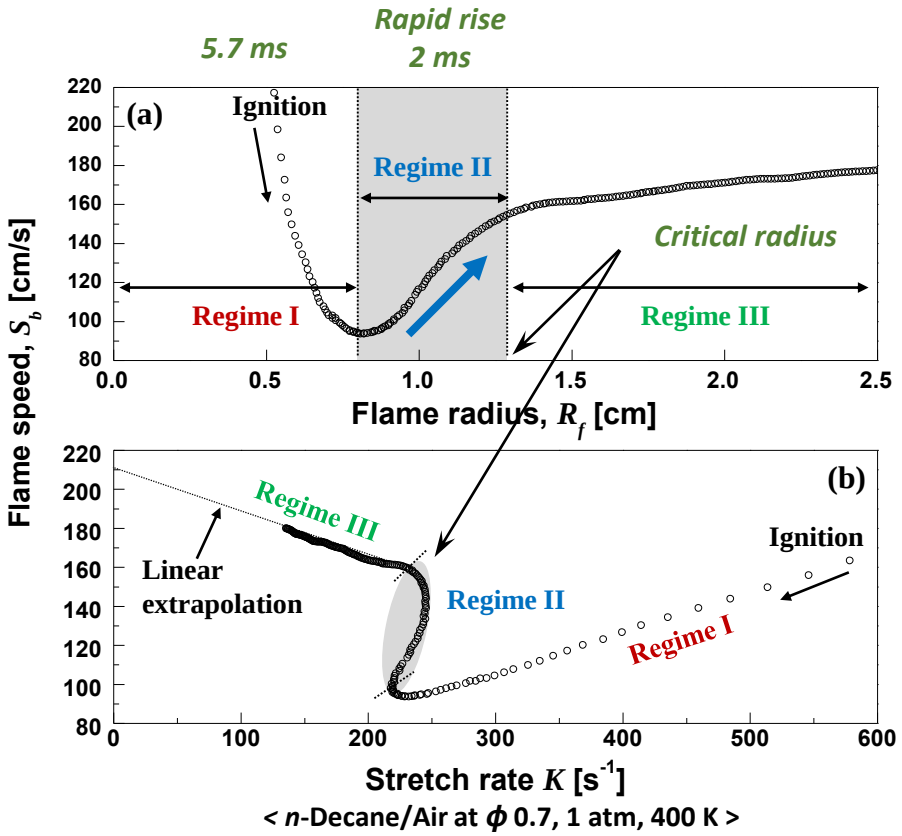


[1]R.A. Strehlow, L.D. Savage, Combust. Flame 31 (1978) 209–211.
[2]D. Bradley, C.G.W. Sheppard, I.M. Suardjaja, R. Woolley, Combust. Flame 138 (2004) 55–77.

# Critical Flame Initiation Radius

- Experiments have been done for JP8, SPK, IPK, and HRJ tallow at lean conditions.
- Reactivity orders from critical radius measurements
  - HRJ tallow ~ SPK ~ JP8 > IPK
- Consistent results to diffusion flame extinction in TWE

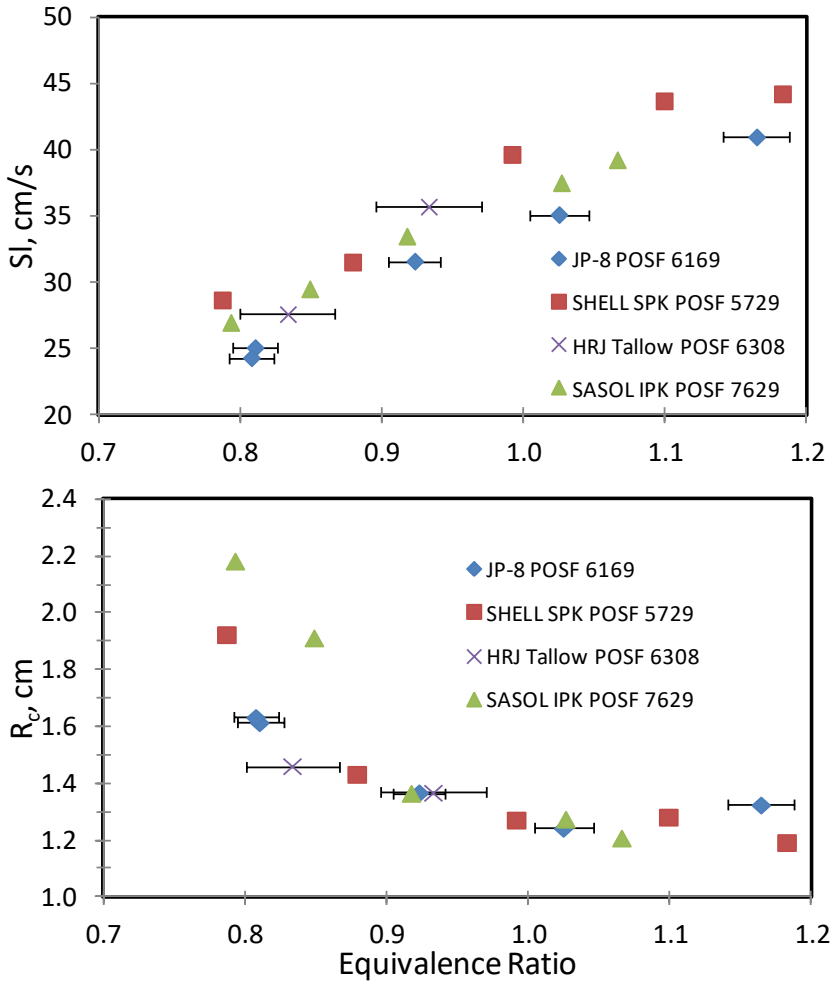


Opportunity: volume ignition by plasma can enhance ignition to flame transition and reduce ignition failure.

Kim, H.H., Won, S.H., Santner, J., Chen, Z. and Ju, Y., 2013. *Proceedings of the Combustion Institute*, *34*(1), pp.929-936.

# Subsonic Ignition Tunnel Utilized to Elucidate Fundamental Interactions

- Subsonic Wind Tunnel
  - Premixed methane/air at room temperature and pressure
  - U = 1 - 10 m/s
  - Re = 6,000 - 24,000
  - Optical access through windows on three sides
- Transient Plasma Systems Pulsed Power Supply
  - 10 ns FWHM
  - Pulse repetition frequency (PRF) up to 330 kHz
  - Peak voltage of 10 kV into 50 Ω resistor
  - Maximum Energy Per Pulse ≈3 mJ

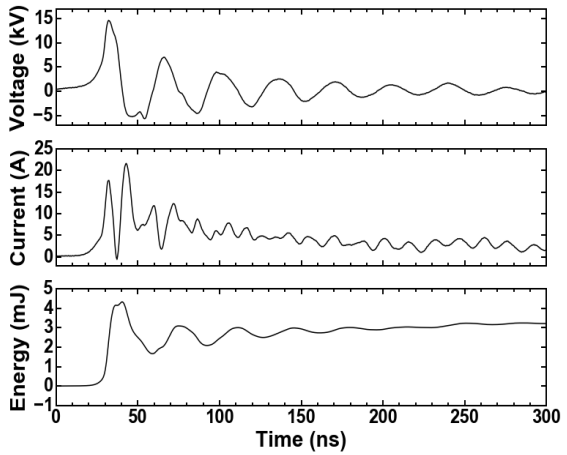


- Electrodes
  - Lanthanated tungsten
  - Pin-to-pin configuration
  - Micrometer controlled inter-electrode gap distance
  - Tip angle of 20°

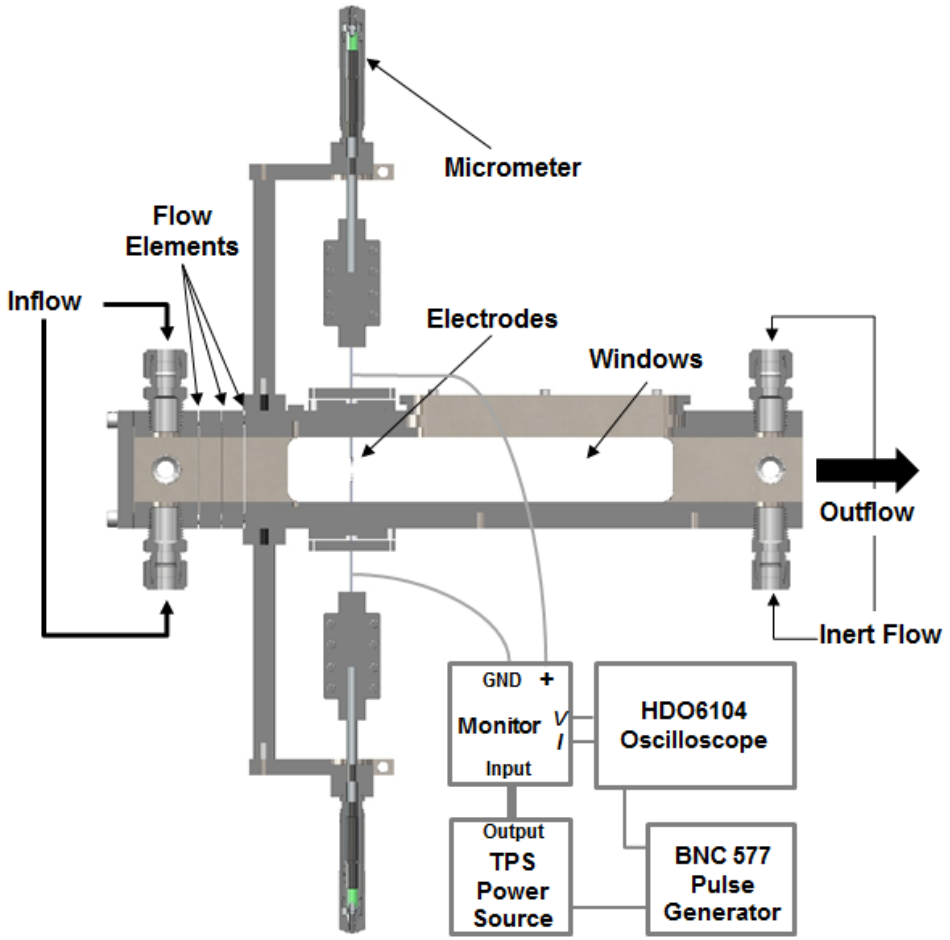


Courtesy of Timothy Ombrello

# Effect of Time Scale of Energy Deposition

## Fixed Total Energy and Varying Pulse Repetition Frequency (PRF)

$CH_4$-Air, $\varphi = 0.6$, U = 10 m/s, D = 2 mm, and N = 20

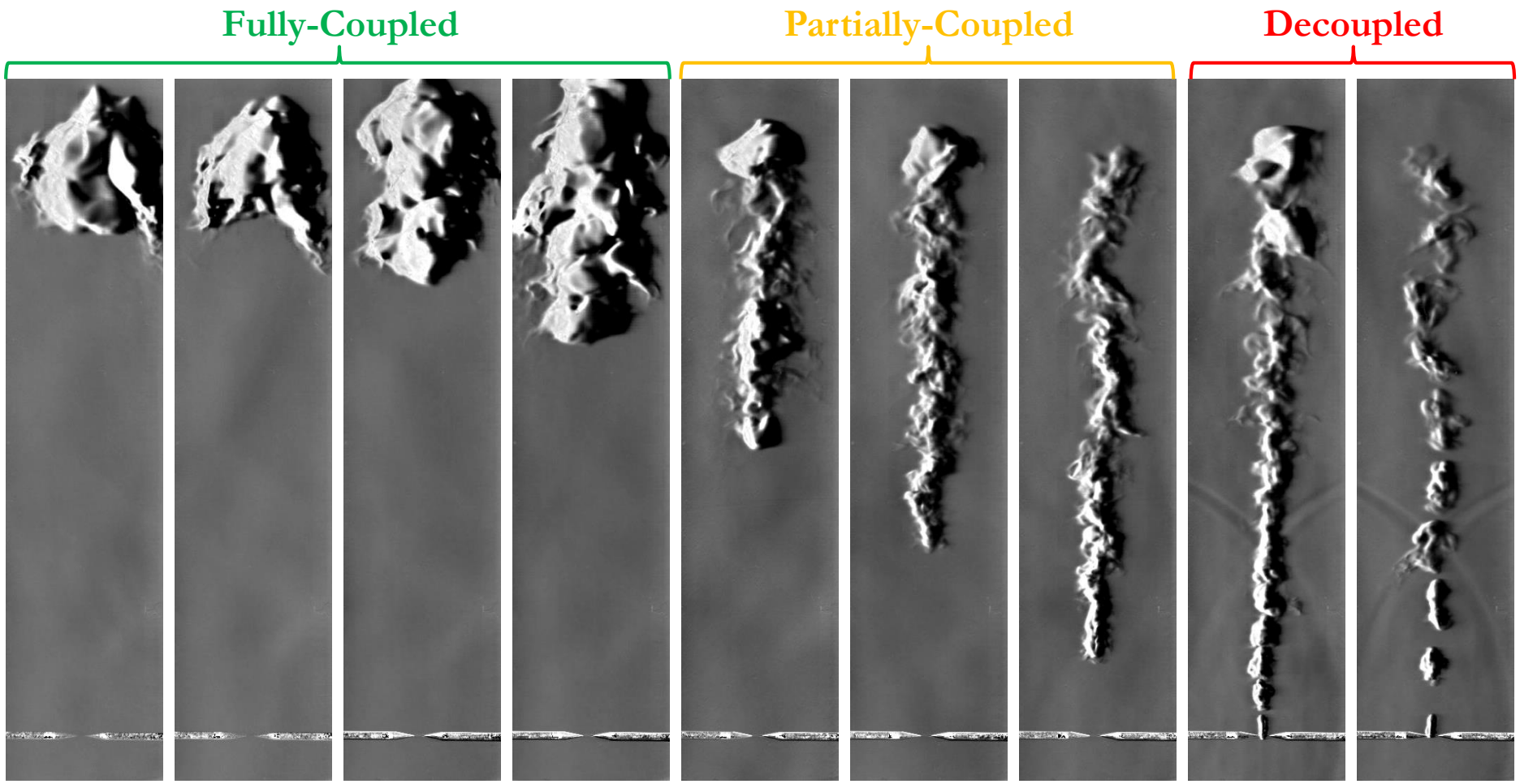


**Three Distinct Regimes Identified**

# Effect of ignition kernel size on ignition probability

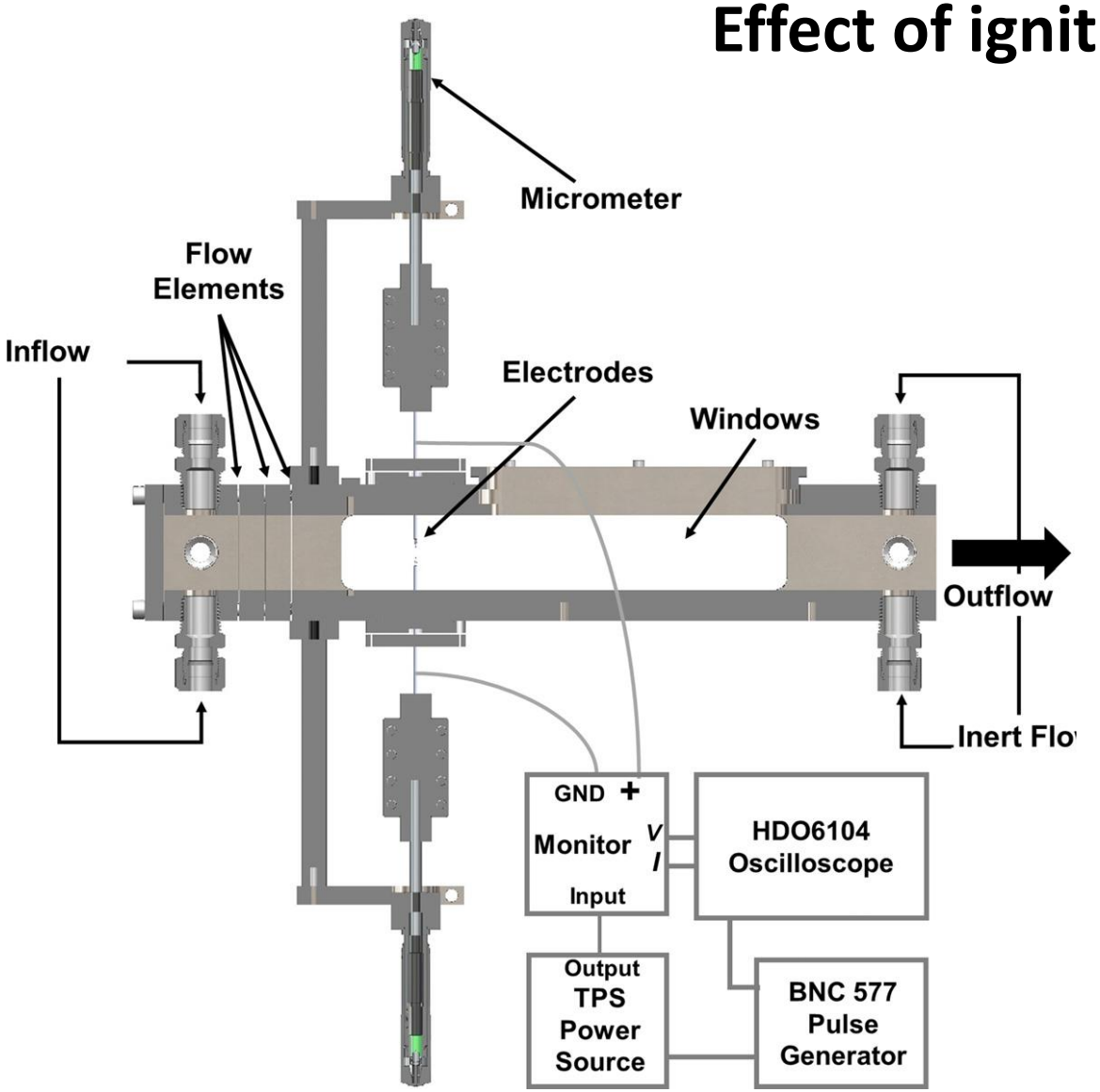


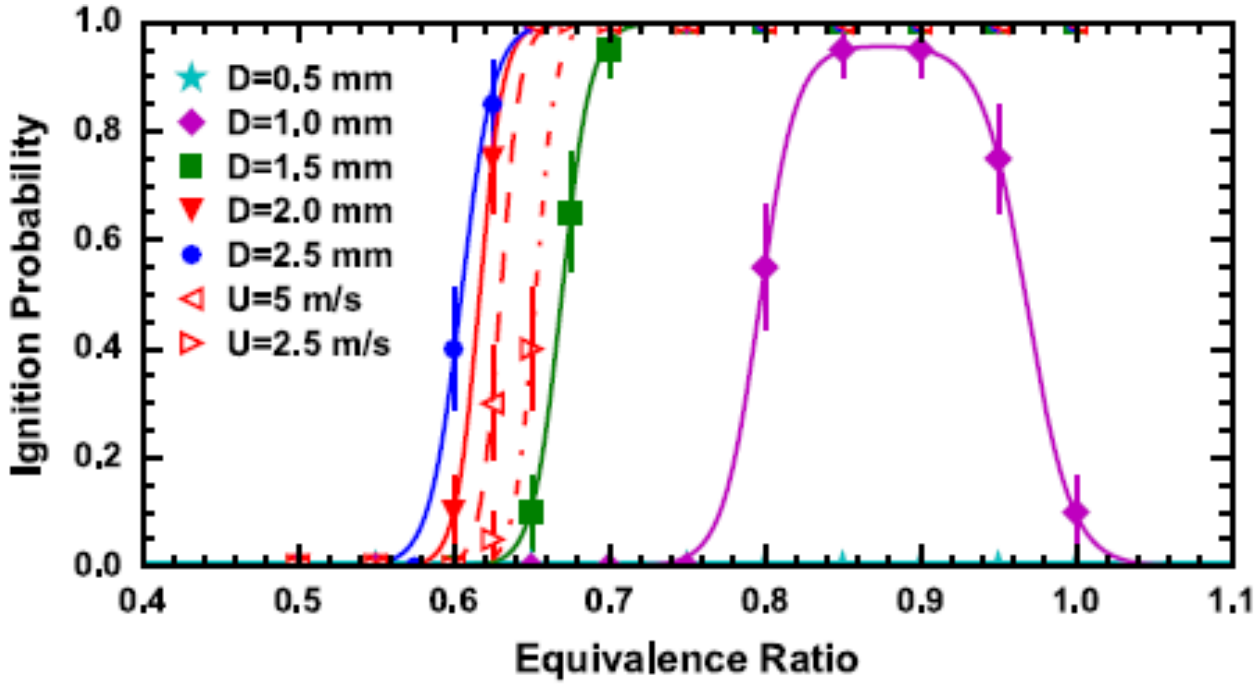


Fig. 4. Probability of a single discharge pulse igniting a flowing methane/air mixture as a function of equivalence ratio, flow velocity, and gap distance. Unless otherwise noted, $U = 10$ m/s and $D = 2.0$ mm.

**Larger ignition size, leaner mixture ignition**

*J.K. Lefkowitz, T. Ombrello / Combustion and Flame 180 (2017) 136–147*

# Effect of Inter-Pulse Time and Number of Pulses

$CH_4$-Air, φ = 0.6, U = 10 m/s, D = 2 mm, and N = 20

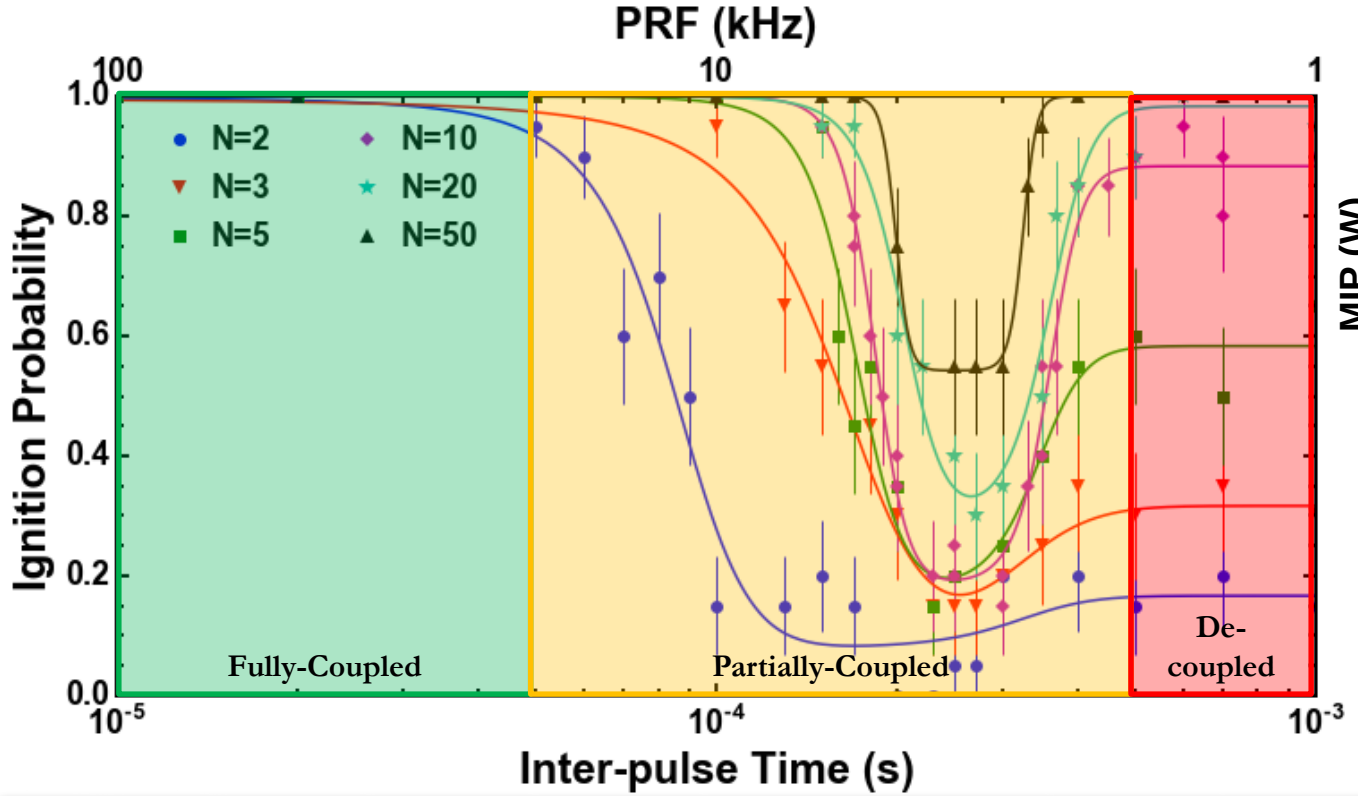


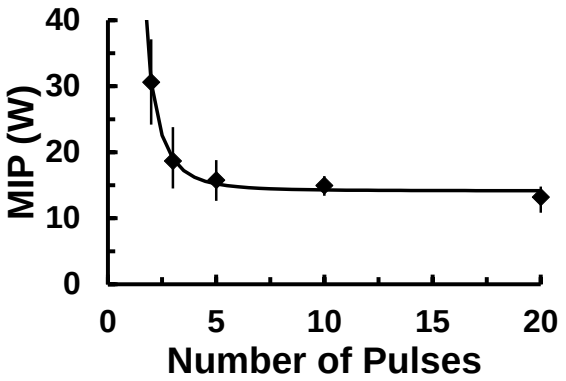


MIP = Minimum Ignition Power
(determined for 50% ignition probability)

**Ignition probability is dependent on PRF (inter-pulse time), not total energy deposition!**

- Increasing power deposition rate (high PRF) is a superior method to ensure ignition
- In partially-coupled regime, more pulses increases ignition probability, but not to 100%
- In decoupled regime, ignition probability is a linear function of number of pulses

# How Does This Translate to a More Realistic Flow

## Implications in a Recirculating Turbulent Reactive Flow: Mach 2 Cavity

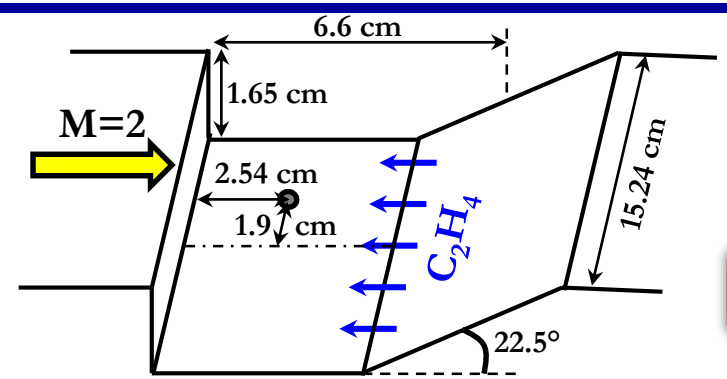


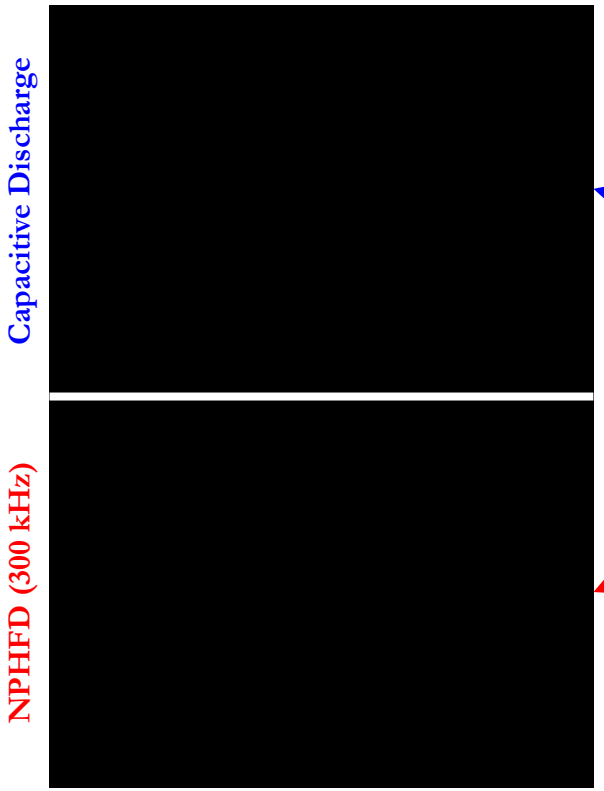


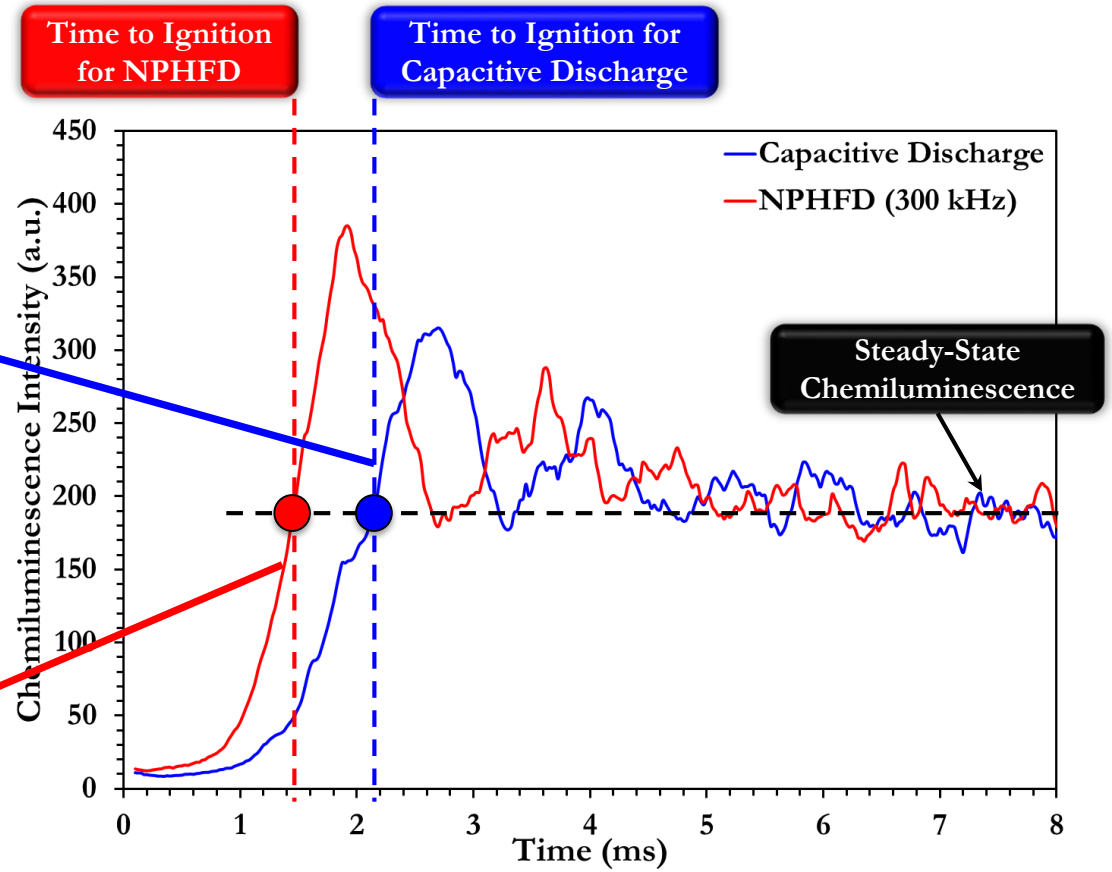

# Time to Ignition for Lean Cavity (~Φ=0.8)

## Energy Deposition of 50-800 mJ

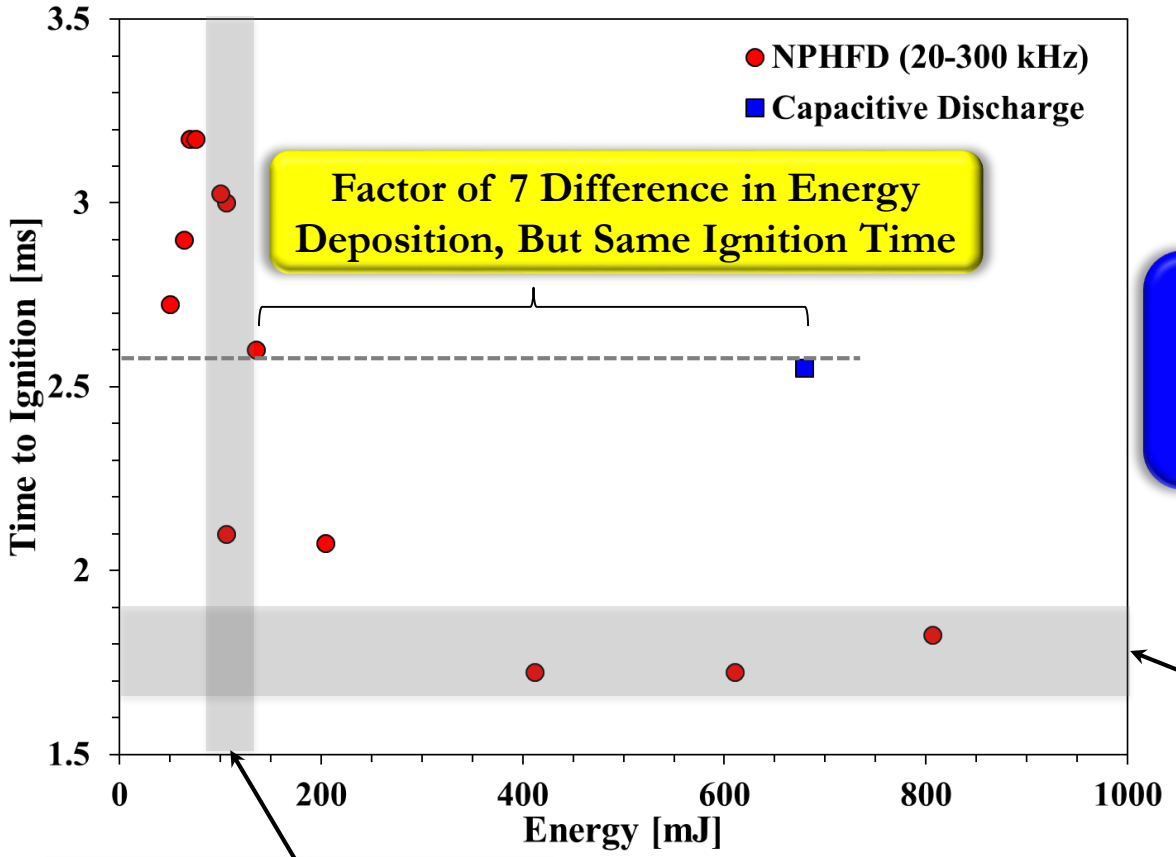


Factor of 7 Difference in Energy Deposition, But Same Ignition Time

Directly Ties to The Subsonic Benchtop Experiments to Highlight Synergy Between Pulses and the Effect on Flame Growth Rates

Approximately 1 Cavity Cycle Time

Drastic Change in Ignition Time Below ~ 100 mJ

# Summary of plasma ignition in a reactive flow

1. **Synergy Between Pulses at High Frequency Changes the Way Ignition is Approached in a Reactive Flow**

2. **Time Scale of Energy Deposition Process is Critical**
   - Can couple into thermal, kinetic, and flow effects

**Power Drives Ignition Process, Not Energy**

3. **Ignition Probability and Flame Growth Rate Can be Enhanced, But There is an Optimization**
   - Depends upon the flow velocity, inter-pulse time, reactivity of mixture

4. **Connections to Realistic Environment Demonstrated**
   - Scramjet cavity ignition

**More Details of What is Contained in These Slides Can Be Found in the Following References**


- J.K. Lefkowitz, T. Ombrello, "An Exploration of Inter-Pulse Coupling in Nanosecond Pulsed High Frequency Discharge Ignition," Combustion and Flame, 180 (2017) 136-147.
- J.K. Lefkowitz, T. Ombrello, "Reduction of Flame Development Time Using Nanosecond-Pulsed High-Frequency Discharges in Flowing Mixtures," 10th U. S. National Combustion Meeting, April 23-26, 2017 College Park, Maryland.
- T. Ombrello, J.K. Lefkowitz, S.D. Hammack, C. Carter, K. Busby, "Scramjet Cavity Ignition Using Nanosecond-Pulsed High-Frequency Discharges," 10th U. S. National Combustion Meeting, April 23-26, 2017 College Park, Maryland.

# Summary: The impact of plasma on fundamental combustion properties:

## How does plasma assist combustion? Ignition, Flame speed/limit, $E_{min}$

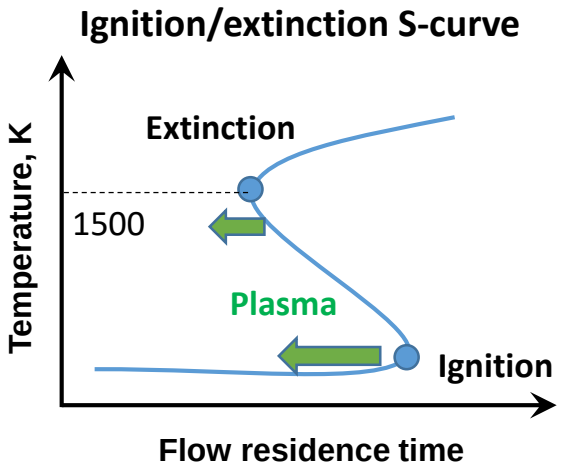


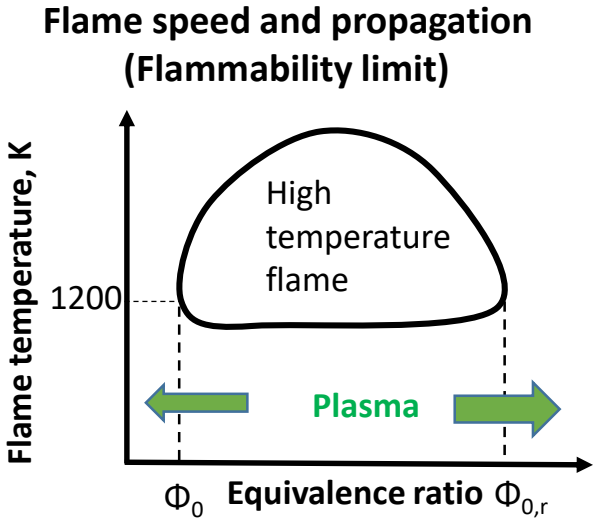


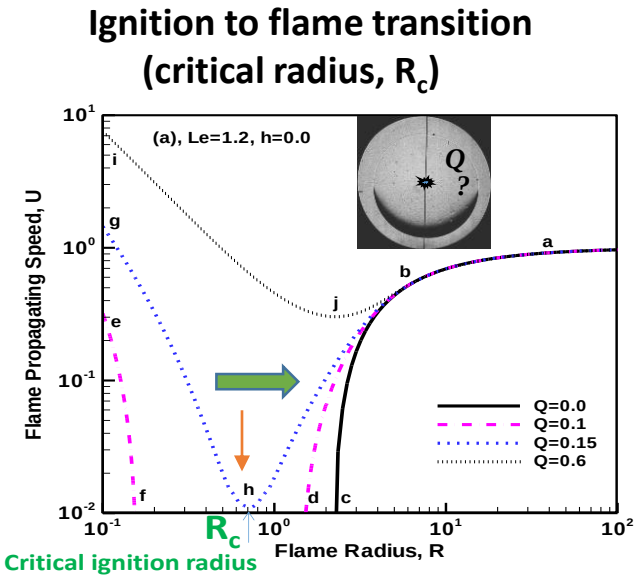


- Shorten ignition time
- Extend extinction limit

$$t_{ig} = \frac{RC_p T_0^{\,2}}{BQY_{F0}E} e^{E/RT_0}$$

Ignition delay

- Increase flame speed
- Extend flammability limit

$$S_L \equiv \sqrt{2Le\frac{WB\lambda}{\rho\beta^2 C_p} e^{-E/RT_{ad}}}$$

Mass burning rate

- Make ignition kernel > Rc
- Accelerate ignition to flame transition

$$E_{\min} \equiv \rho C_p (T_{ad} - T_0) R_c^3$$

Minimum ignition energy

# Summary

1. **Plasma has both kinetic and thermal effects on ignition enhancement.**
2. **Plasma has only minor kinetic effect on flame propagation speed at high temperature. The main effect for the extension of extinction limit is thermal.**
3. **Plasma may have strong kinetic effect on cool flame propagation speed and limits.**
4. **Plasma can cause fuel fragmentation and reduce the fuel Lewis number, thus enhance flame speed via the Lewis number effect (Transport).**
5. **The minimum ignition energy is governed by a Critical Radius. Plasma can create a large volumetric discharge greater than the critical radius to reduce the minimum ignition energy, especially at low pressure and fuel lean conditions.**

# Lecture 4 Electric Field Effect on Flames: Ionic wind and Joule heating

**Yiguang Ju**

**Flame is a weakly ionized plasma. It produces ionic wind, electron heating under an electric field**

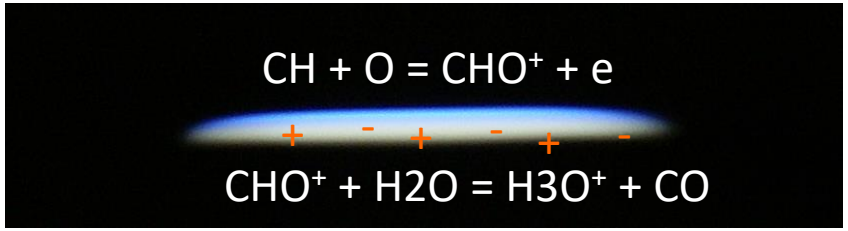


**Flame** **Calcote (1963)**

weak plasma

$n_e, n_i \sim 10^{12}/cm^3$

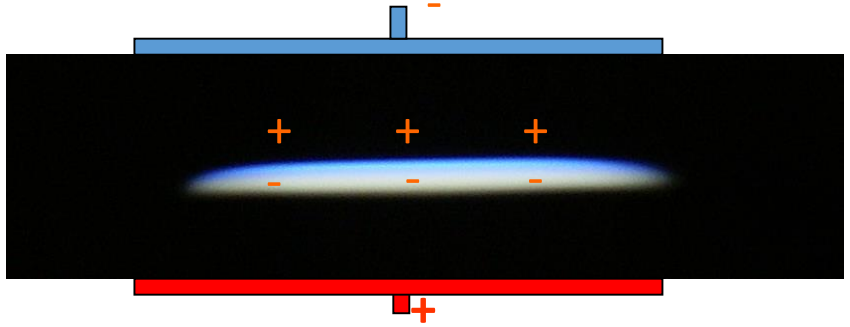

**DC field** **Brande (1814)**

Electron heating: $\sigma E^2$

Ionic wind~10 m/s

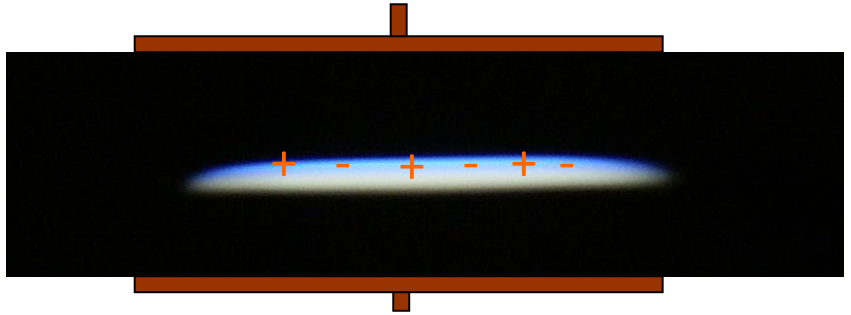

**AC field**

Electron heating

**Timescales**:

$$t_{combustion} >> t_{mw} >> t_{e-n}$$

$$t_{combustion} \sim t_{AC} >> t_{e-n}$$

$$t_{combustion} << t_{DC} >> t_{e-n}$$

$$S_L \propto \exp\left[-\frac{E_a}{2RT_f}\right]$$

# Ionic wind and Joule heating by an electric field

Flow induced by ion collision with neutral molecules in a flame and corona with an electric field. The ionic wind velocity can be 10 m/s which significantly modifies the near electrode flow field.

**Momentum transfer between:** $m_i \nu_{in} (\vec{V}_i - \vec{U})$

$\nu_{in}$ : ion - neutral molecule collision frequency

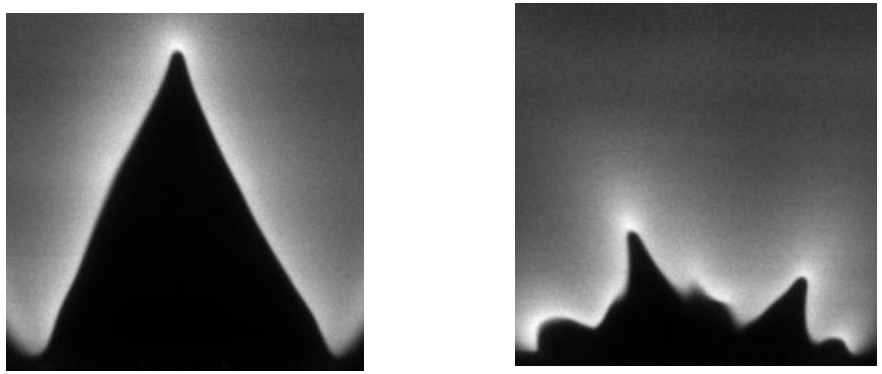

Methane, Φ = 1.0, Air Flow = 30 slm, Fuel Flow = 3.2 slm Flow velocity ≈ 1.0 m/s, Voltage: 0 V vs. t 2000 V, The anode-cathode gap was kept constant at 40mm, Ganguly et al., 2008

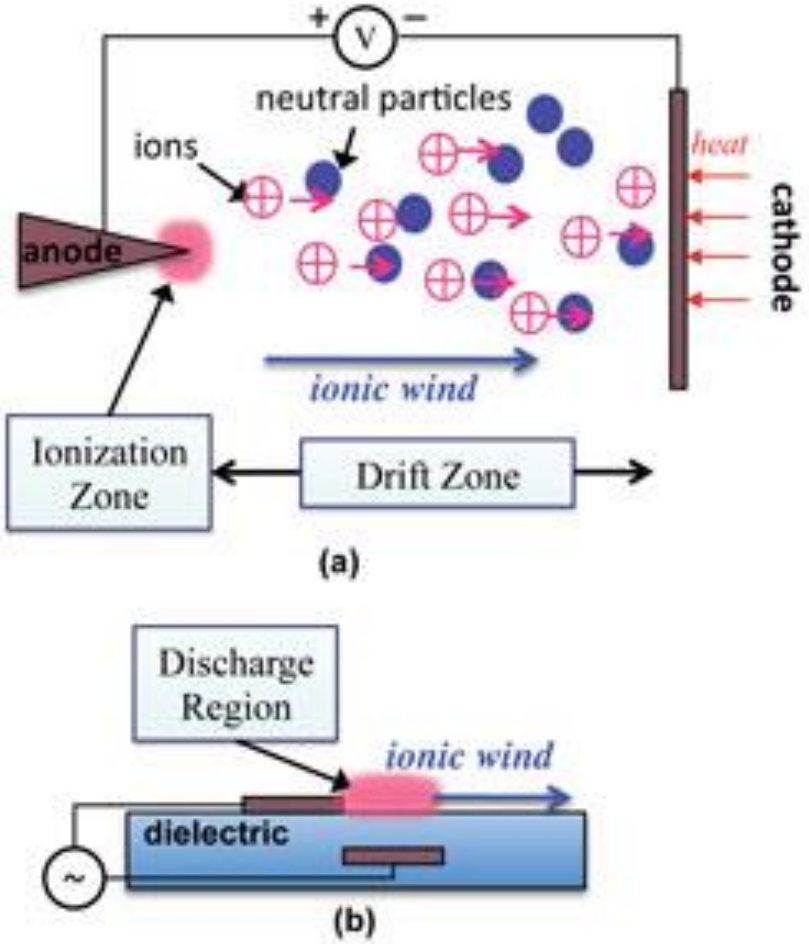


**Electron-molecule collision energy transfer:** $\sigma E^2 = \frac{3}{2} \sum_i k_i \nu_{ei} n_e k_B (T_e - T_g)$

**Joule heating:** $\sigma E^2$

[1] Robinson, M., 1962, "A History of the Ionic Wind," *American Journal of Physics*, Vol. 30, pp. 366-372.

# Ionic wind

Calcote, 3rd Symposium on
Combust. Flame, Explosion Phenomena(1948)

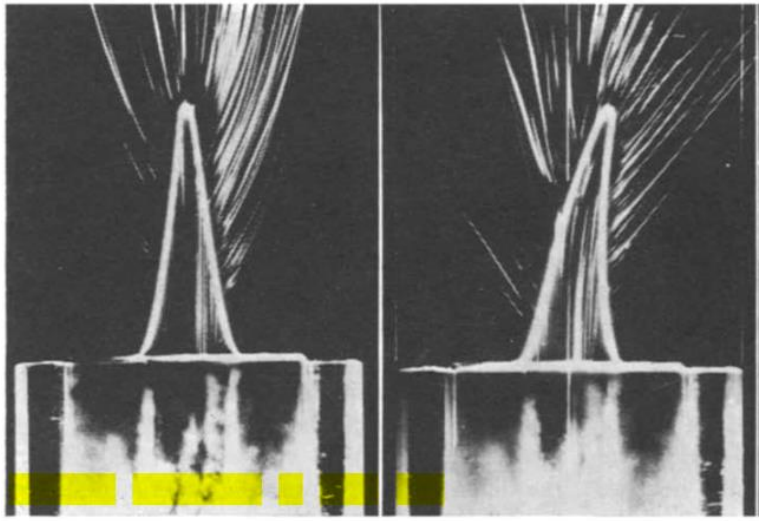


$$F = qE$$

Carleton and Weinberg,
Nature 330 (1987)

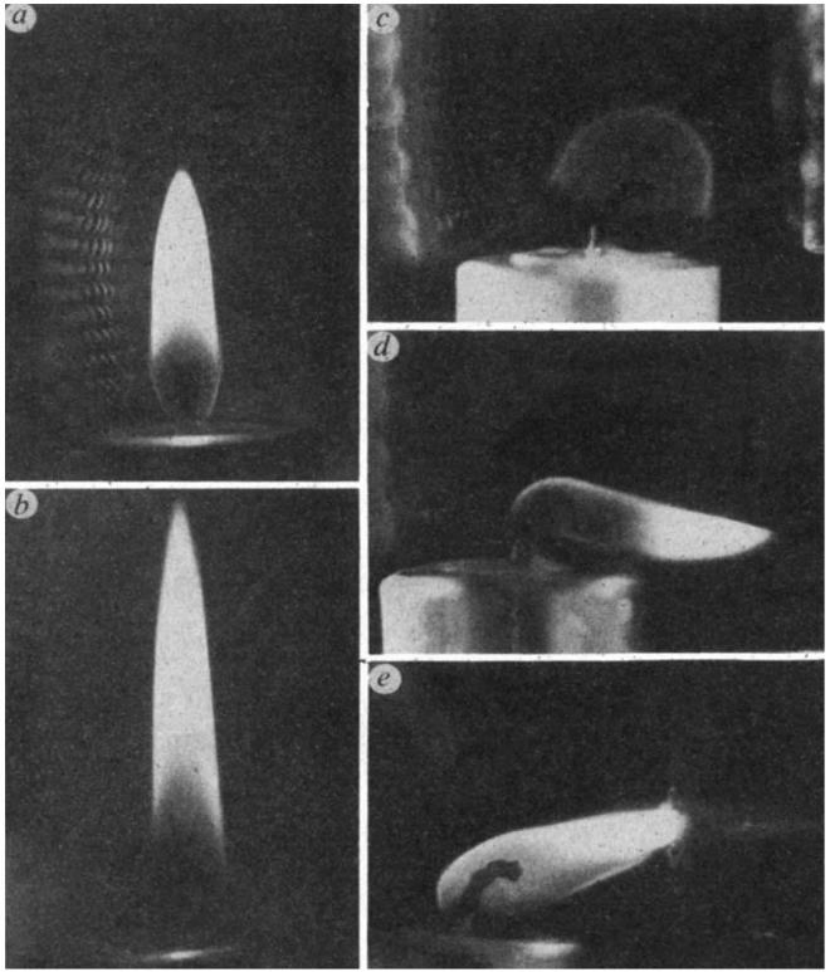


Lawton, Mayo, Weinberg,
Proc. Roy. Soc. A 303 (1968)

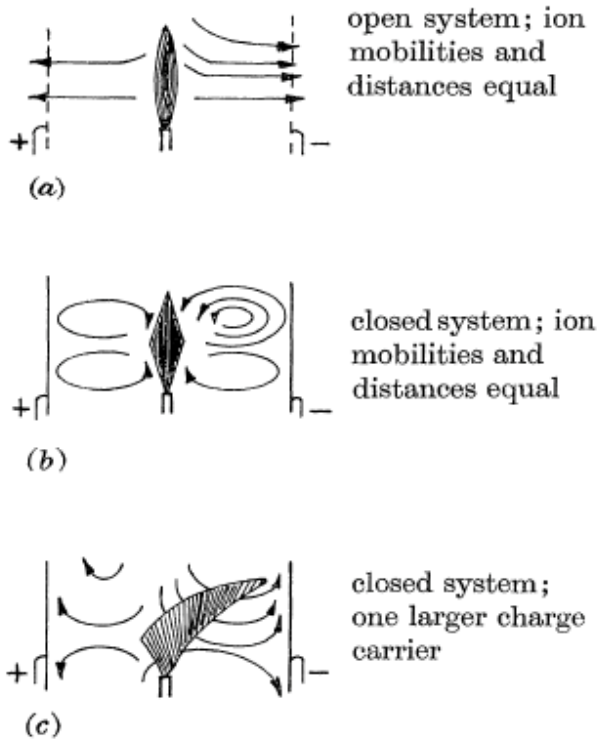


Min Suk Cha

# Ionic wind: Mechanism

$$\left| \xrightarrow{E} \right| \quad \frac{q}{} \quad F=qE$$

$$U_q = \left( \frac{\rho_q V}{\rho} \right)^{1/2}$$

**E** : Electric field

q : Charge

$U_q$ : Characteristic ionic wind velocity (m/s)

V : Voltage change (V)

$\rho$ : gas density ($kg/m^3$)

$\rho_q$ : Charge density ($C/m^3$)

- **In flames, most of ions are positive ions.**
- **Electron mobility is high (smaller mass than ions), its motion is reduced by the motion of positive ions.**
- **Therefore, ionic wind by negative ions and electrons is smaller than that by the positive ions.**

**Comparable positive/negative charge carrier**

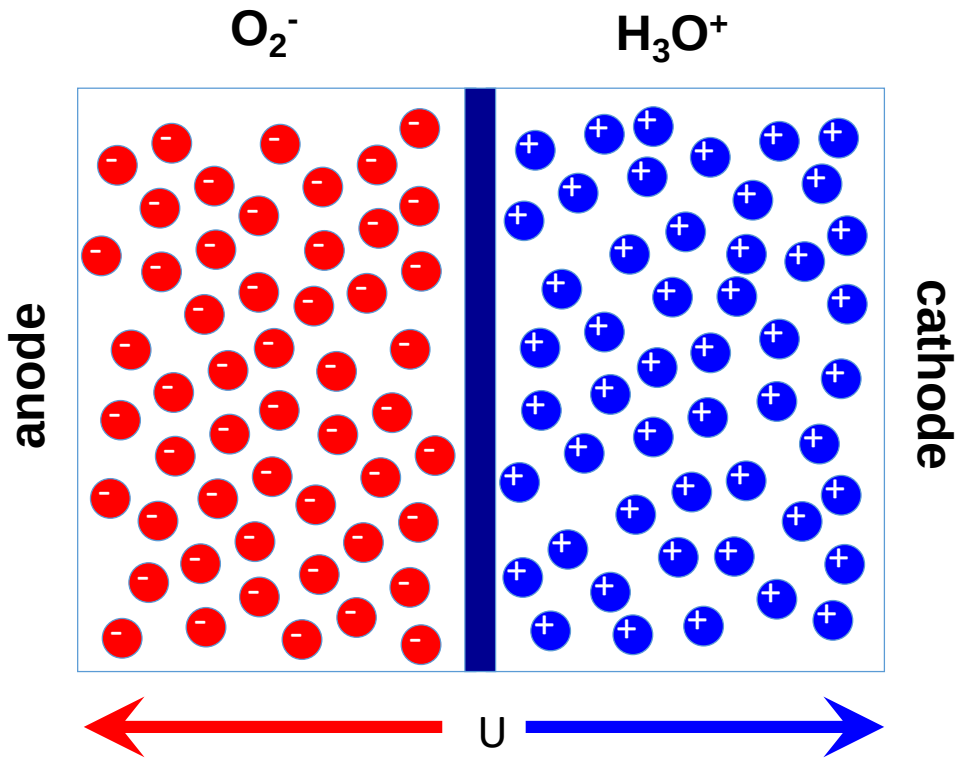


**Heavier positive charge carrier**

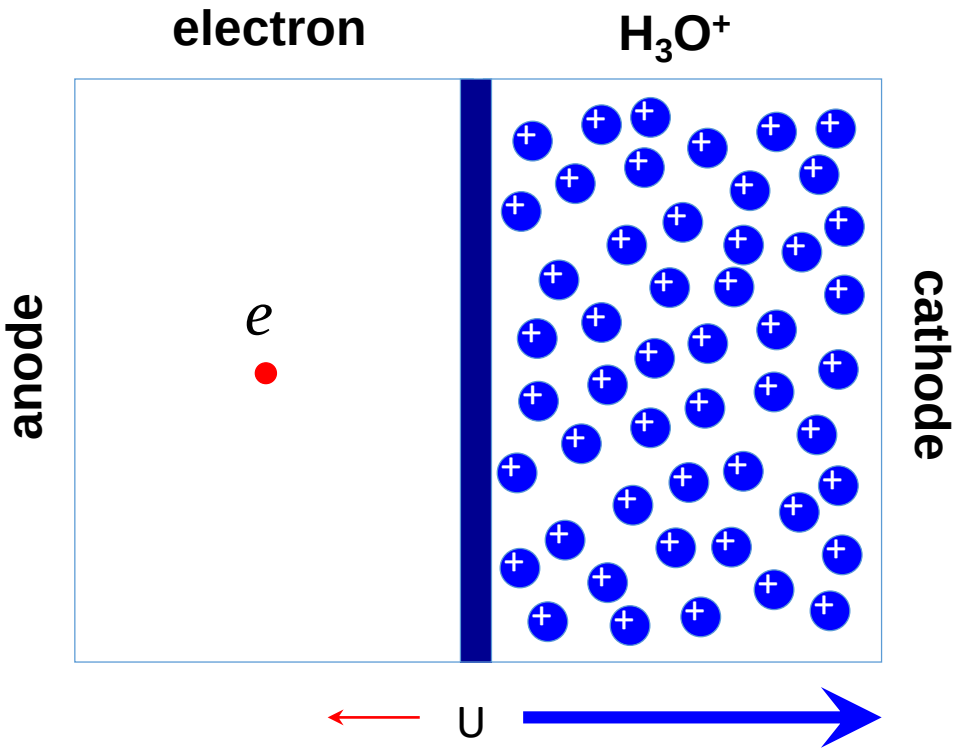

# Axisymmetric jet flames: *transverse DC fields*

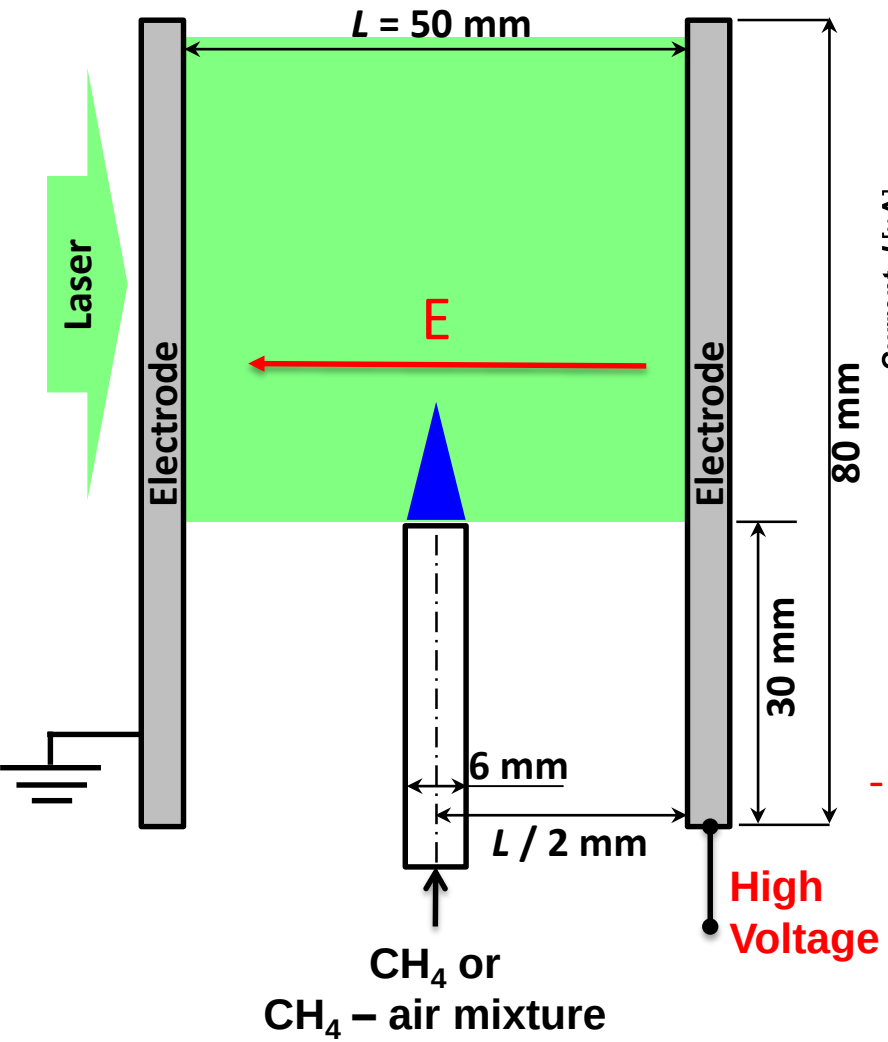


## Premixed

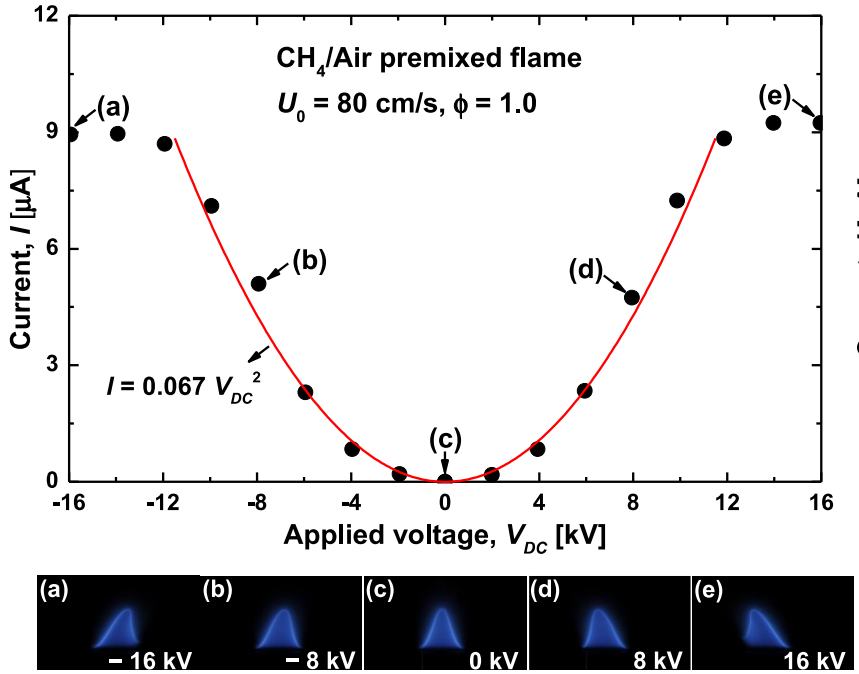





## Non-Premixed

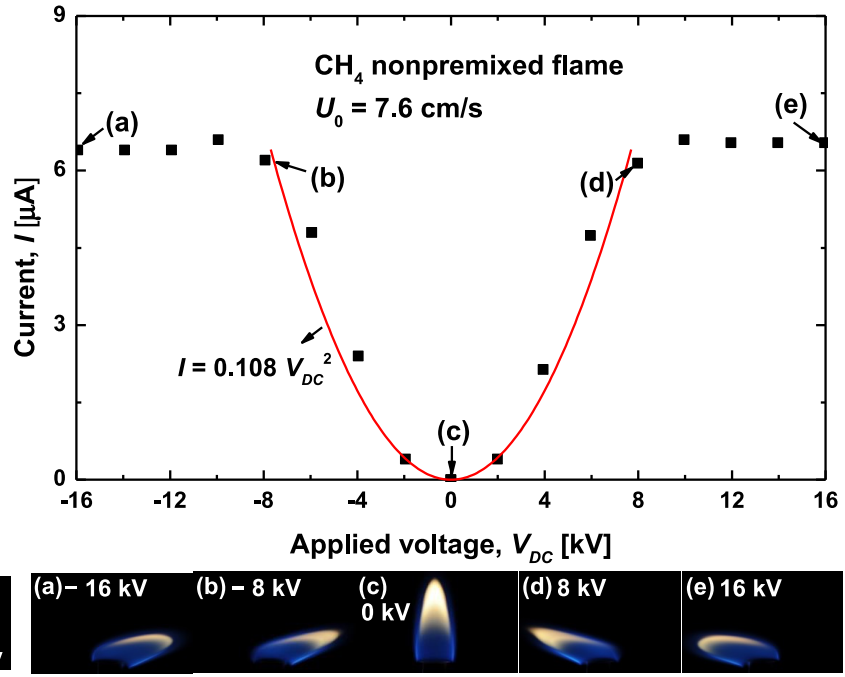





-16kV ⟷ 16kV  -16kV ⟷ 16kV

Most ions are positive.

Park and Cha, Combust. Flame, submitted (2017)

# Axisymmetric jet flames: *transverse DC fields*

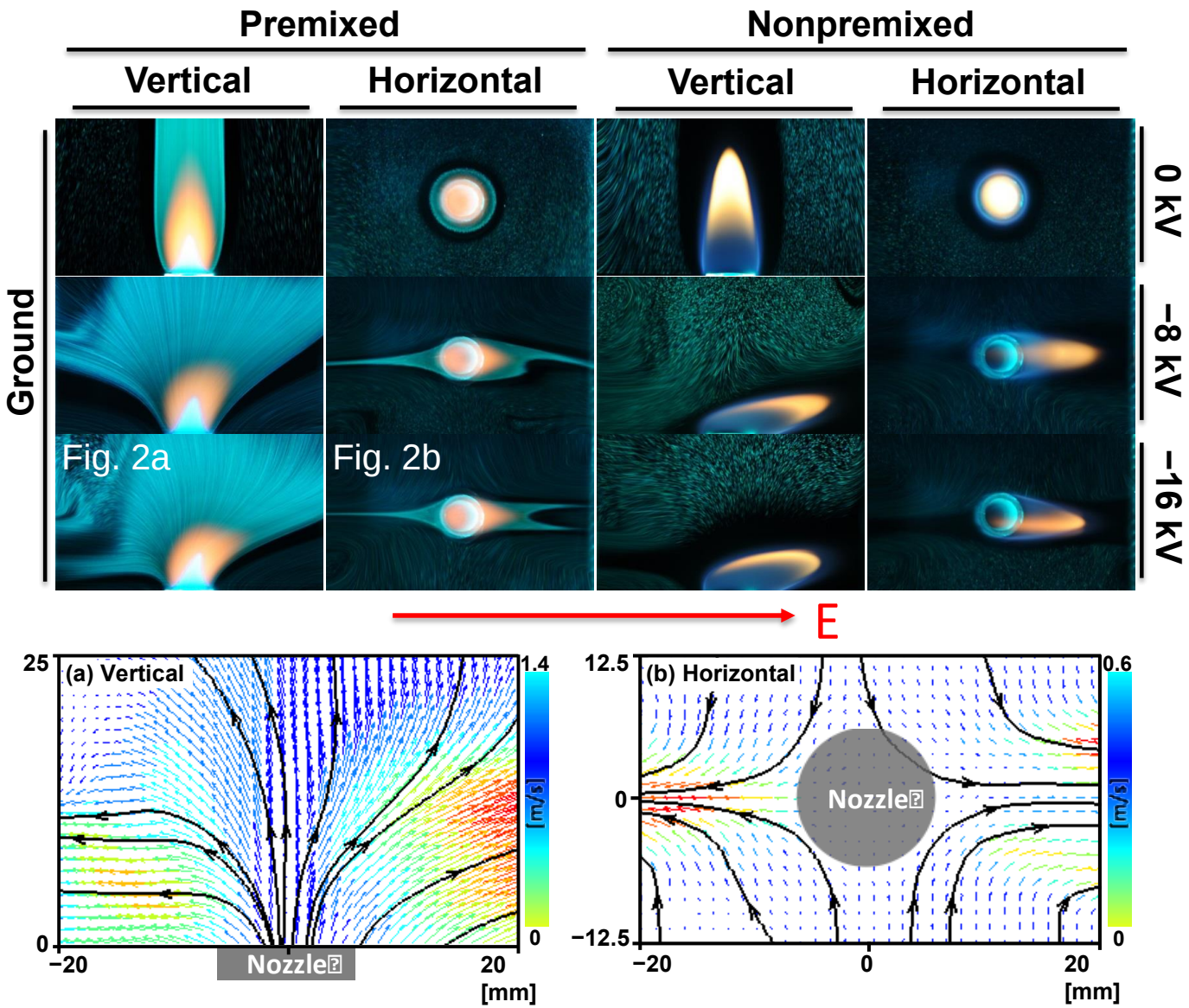


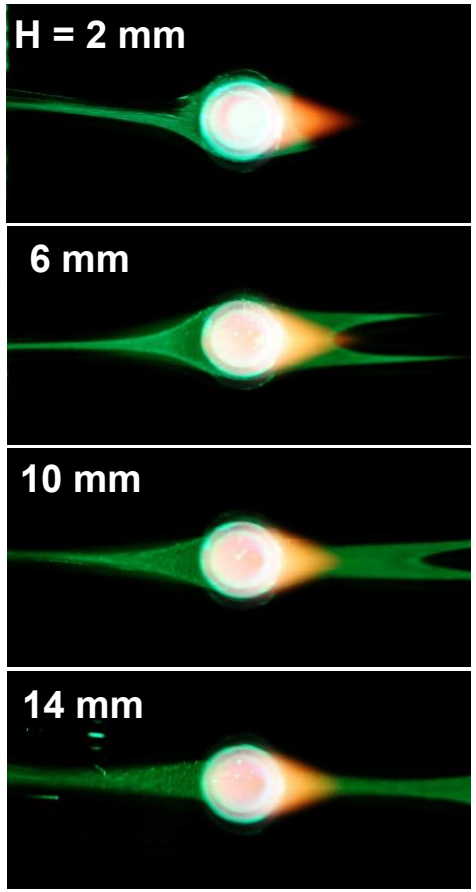


Min Suk Cha

# Counterflow nonpremixed flames: *DC fields*

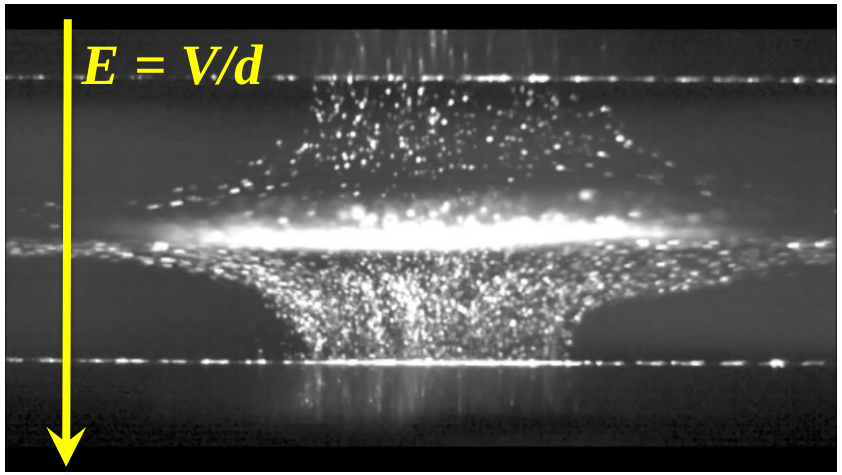


- **Drastic change in flow field**
- **Formation of the dark zone**

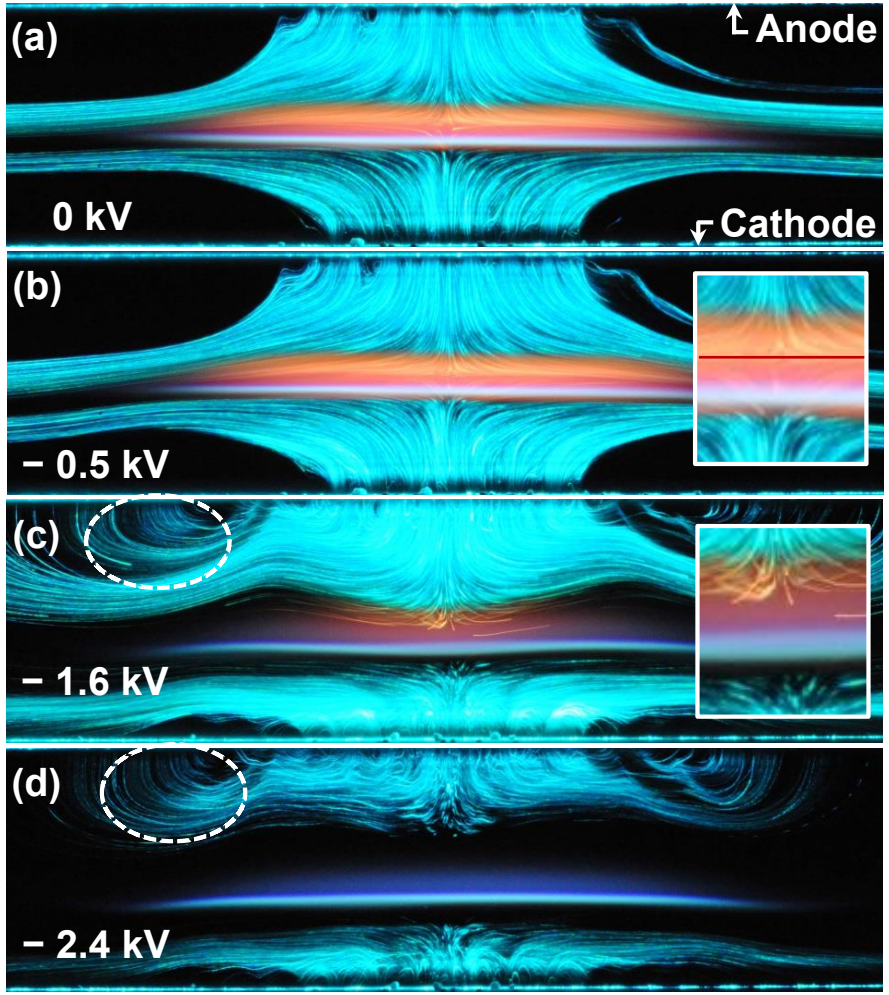


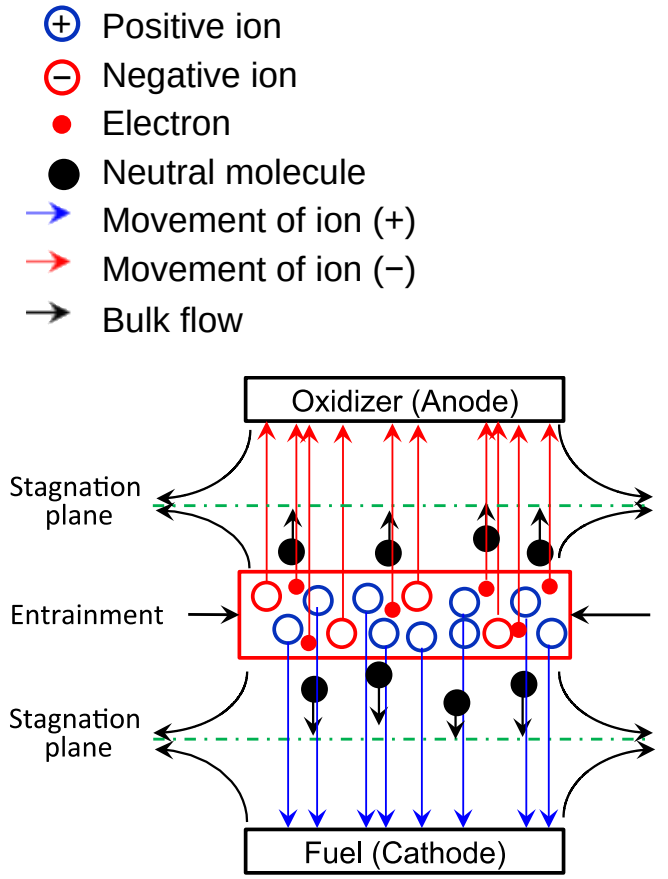


- **Flame acts as a source of flow**
- **Double stagnation planes**

Park and Cha et al., Combust. Flame, 168 (2016)

# Counterflow nonpremixed flames: *AC fields*

**Park and Cha et al.**
**Under preparation**

**No field**

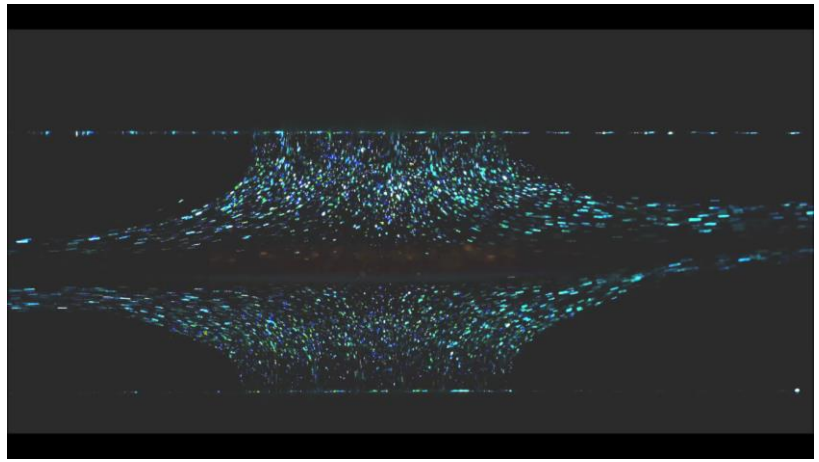

**2 kV, 10 Hz**

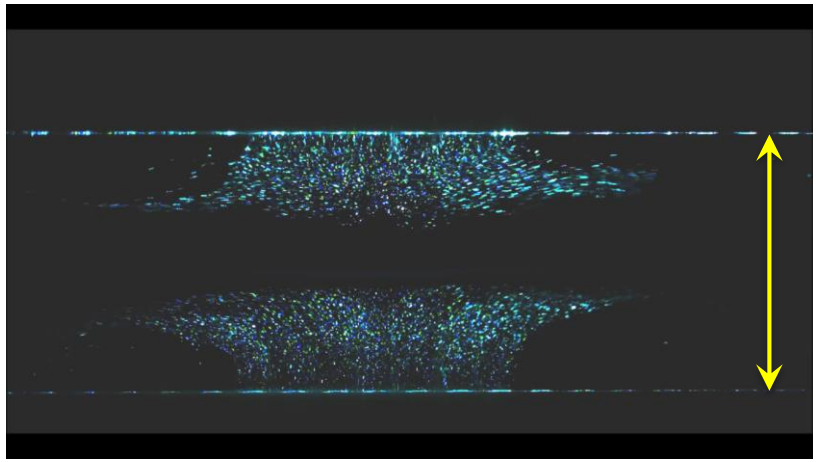

**2 kV, 100 Hz**

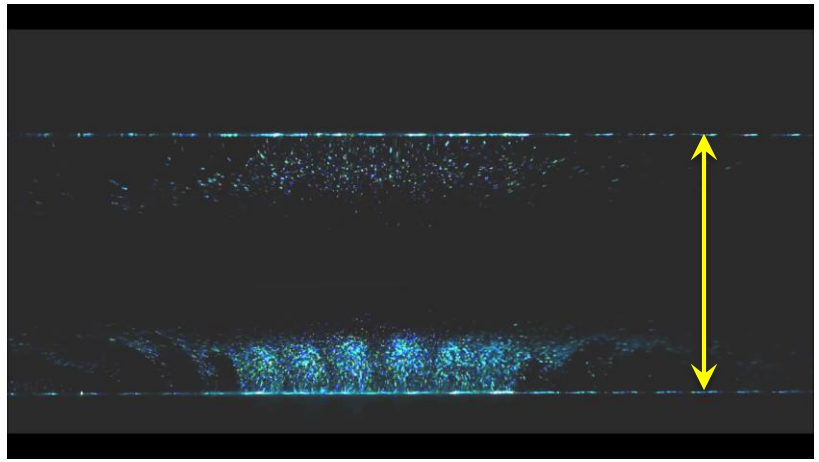

**2 kV, 1000 Hz**

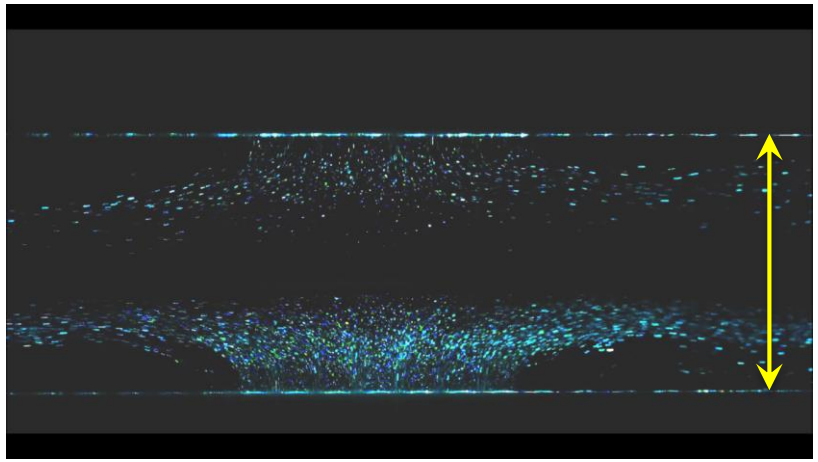

# Propagating edge flames in counterflow: *DC*

## Propagation of nonpremixed edge flames through DC fields

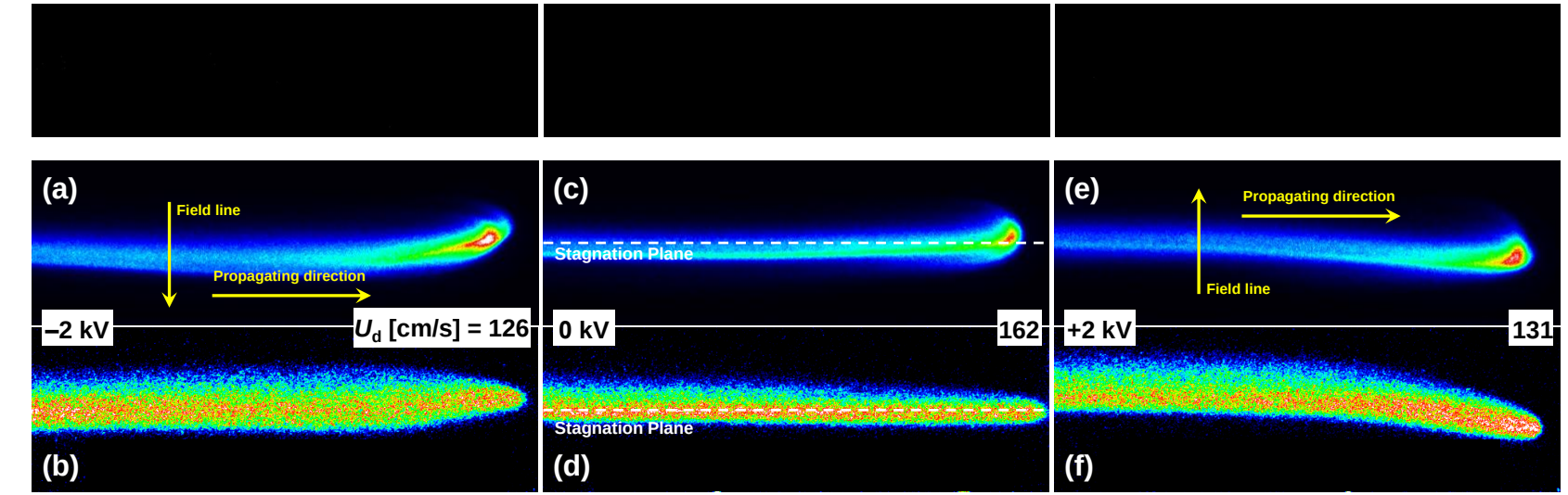


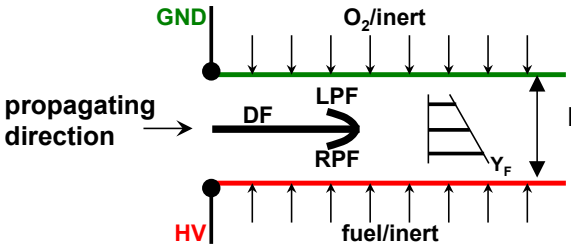


Tran and Cha , Combust. Flame, 173 (2016)

# Propagating edge flames in counterflow: *DC*

$E = V/d$

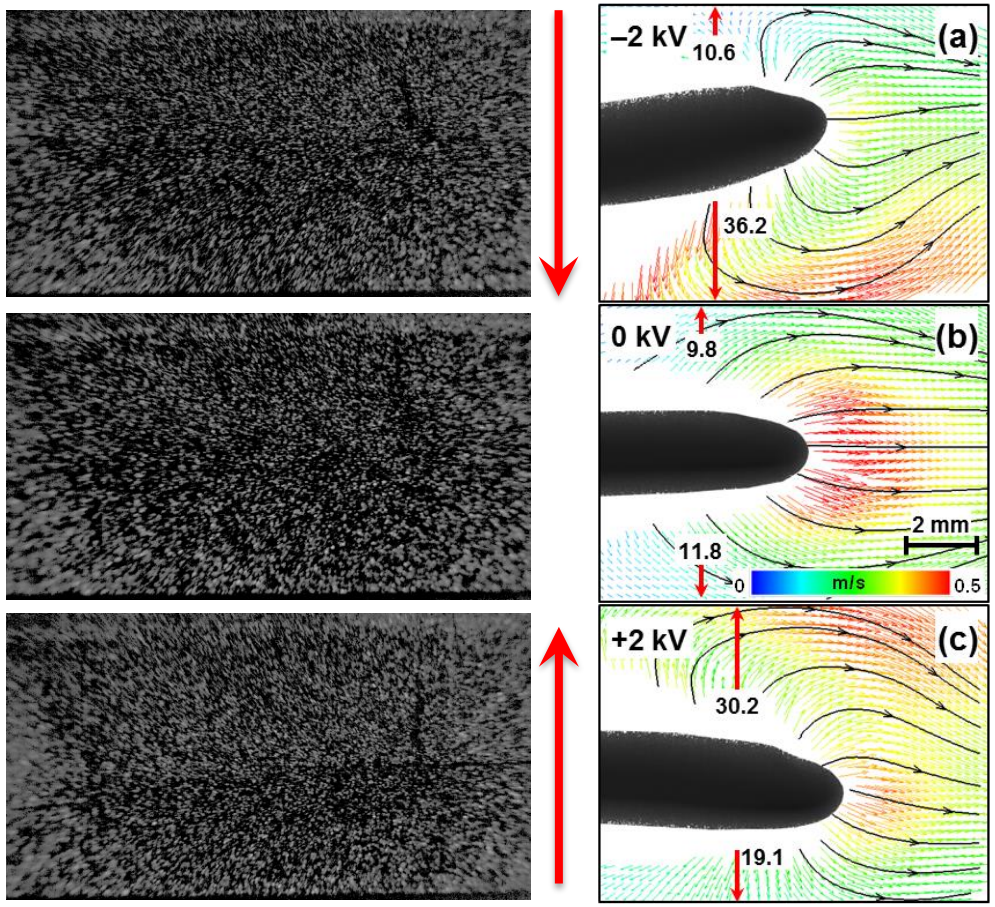


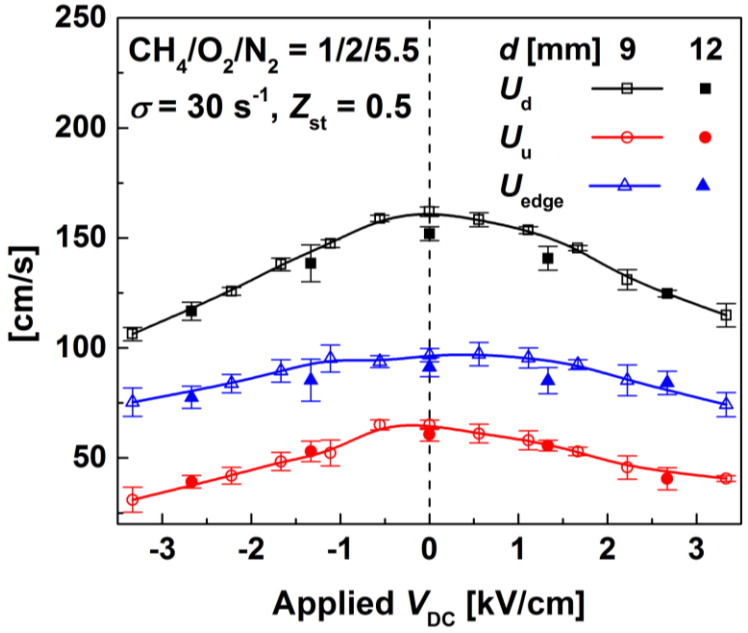


- Ionic wind and secondary flow modification is the most important factor
- Reduced displacement speeds
- Rather unaffected propagation speeds

Combust. Flame 173:114(2016)

# Propagating edge flames in counterflow: *AC*

**Tran and Cha**
**Proc. Combust. Inst., 36 (2017)**

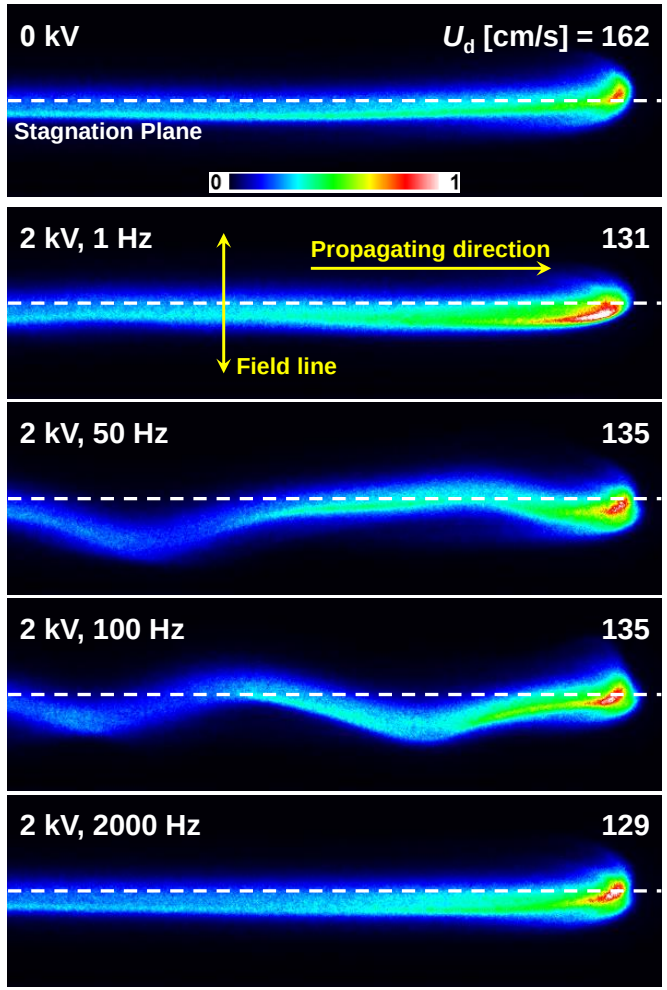


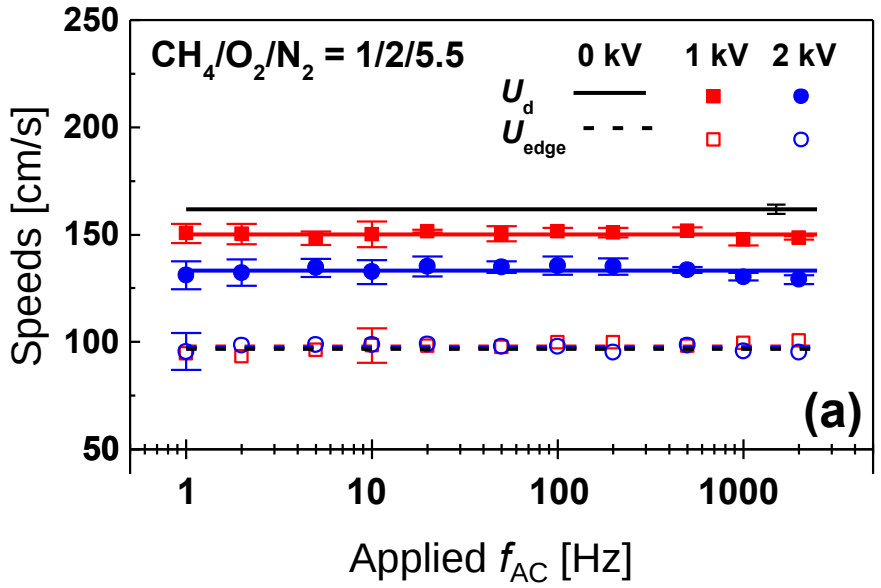


- Wavy motion is closely related with $f_{AC}$.
- Ionic wind and secondary flow modification is the most important factor
- Reduced displacement speeds
- Rather unaffected propagation speeds

Proc. Combust. Inst. 36: (2017)

# DC electric field on flame stability

- Ionic wind
- Corona effect
- Instability
- Electron heating

Fig. 2.29 Image sequence of a propane/air flame with an equivalence ratio of 1.2. The applied dc voltage was slowly increased (left to right), leading to the flame blowing off the burner [65].

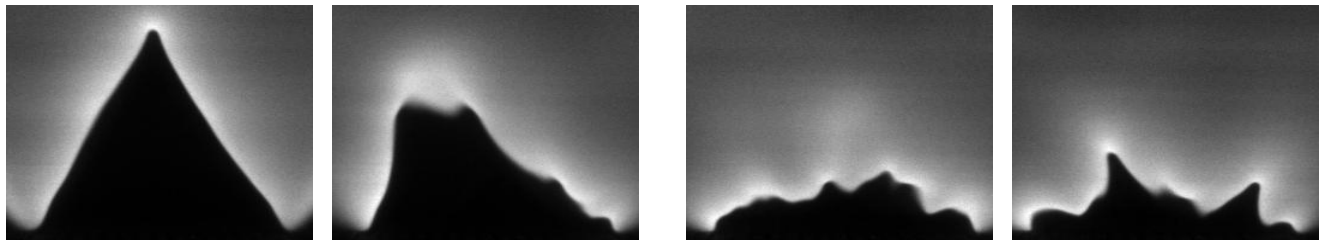

Why?

Instability Growth rate:

$$\sigma = \sqrt{\frac{[n^i q^e E - (\rho_u - \rho_b)g]}{\rho_u + \rho_b} k}$$

Fuel: Methane
Φ = 1.0
Air Flow = 30 slm
Fuel Flow = 3.2 slm
Flow velocity ≈ 1.0 m/s
0 V - 2000 V (DC)

Wisman, D., Ryan, M., Carter, C. and Ganguly, B., 2008. In *46th AIAA Aerospace Sciences Meeting and Exhibit* (p. 1400).

Princeton University

# Reduction of emission via DBD electric field and discharge on a diffusion flame

- E-field makes a flame shorter through ionic wind effect
- As soon as a discharge lights up
  - No yellow luminosity
    - Reduction of soot particles
  - Onset of PAHs is suppressed by DBD

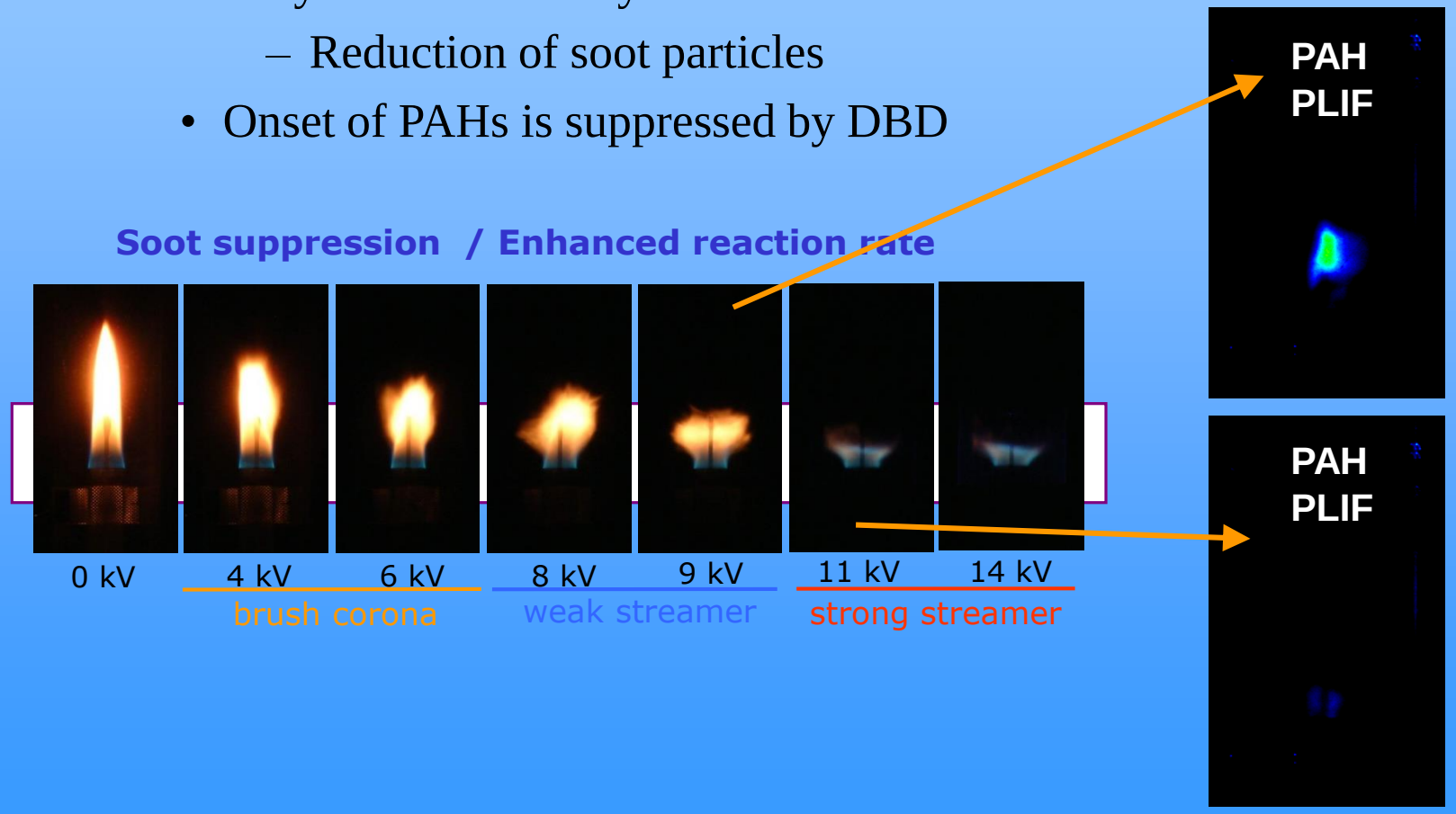


Cha et al., Combust. Flame 141:438, 2005)

*Combustion lab.*

# Effect on microwave electric field on flame speed enhancement

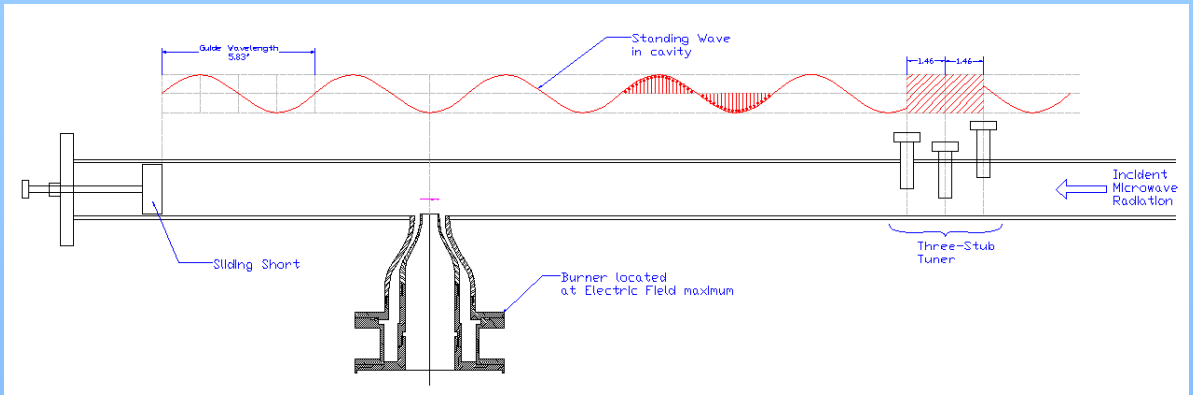


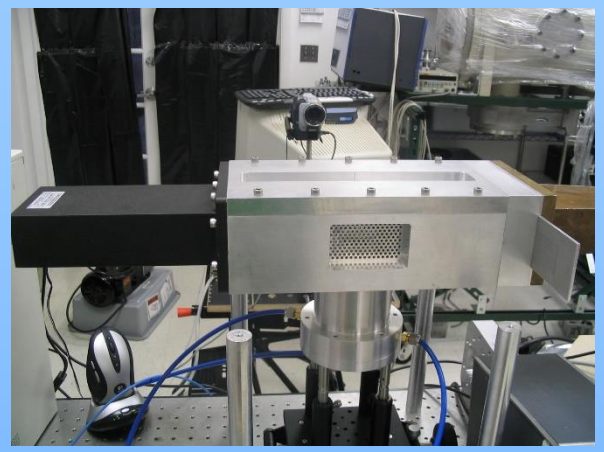

- Microwave frequency is 2.45 GHz
- Three stub tuner to tune the cavity
- Actual Q (5-1000)

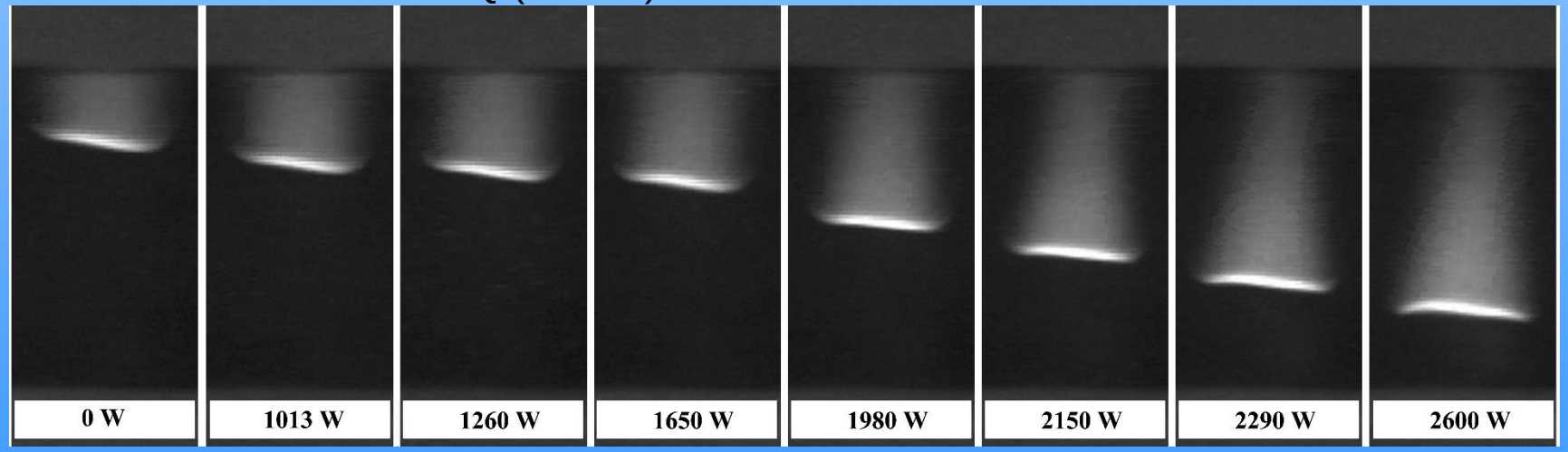


Mass flow rate = 5744 st. $cm^3$/min

Exit velocity = 54 cm/s, Equivalence ratio = 0.70

Zaidi, S., Stockman, E., Qin, X., Zhao, Z., Macheret, S., Ju, Y., Miles, R., Sullivan, D. and Kline, J., 2006, In *44th AIAA Aerospace Sciences Meeting and Exhibit* (p. 1217).

Princeton University

Princeton University

# Estimated vs Experimental Results for Laminar Flame Speed Enhancement

Air/Methane flame

| Equivalence Ratio | Microwave power | Cavity | % increase (flame speed) | Observation |
|---|---|---|---|---|
| 0.77 | 2.6 kW | Low Q cavity | 68% | Estimated – Indirect method |
| 0.77 | 403 W | High Q cavity | 21% | Estimated – Indirect method |
| 0.78 | 1.2 kW | High Q cavity | 34.5% | PIV – direct method |
| 0.74 | 1.2 kW | High Q cavity | 28.28% | PIV-direct method |

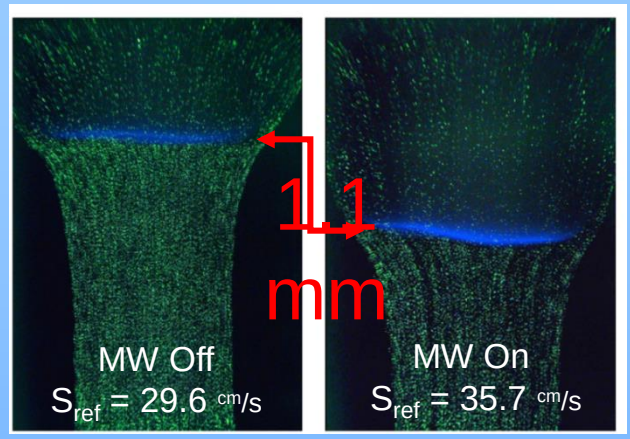


In flames, microwave field mainly heats the electrons and raises flame temperature

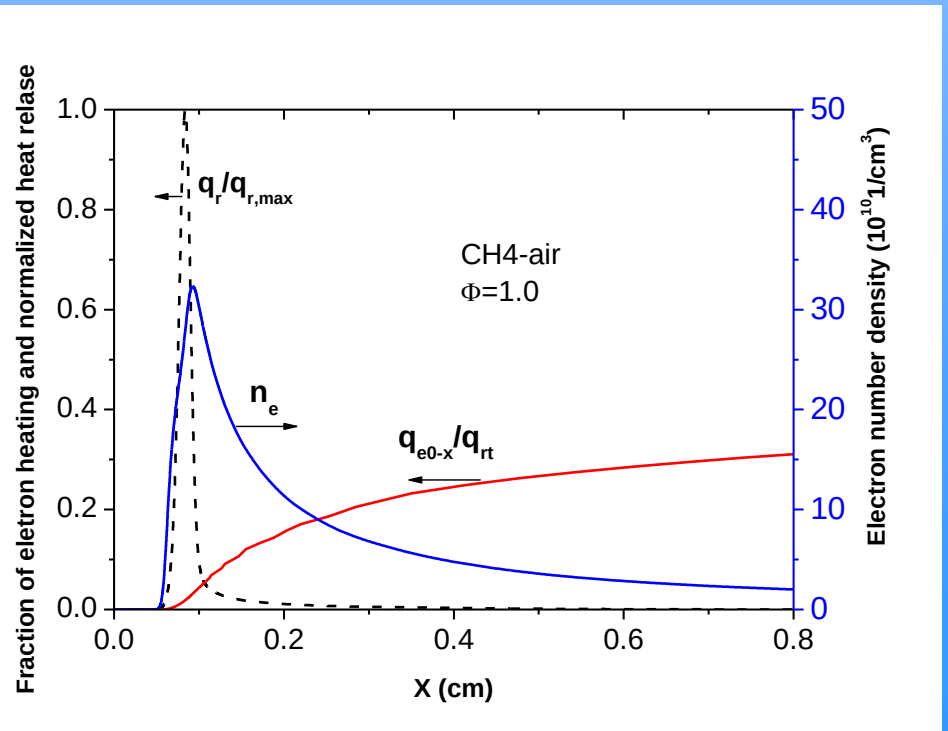

# Planar FRS Measurements

## 30 W Pulsed Microwave Enhancement
## 30 kW-peak, 1 μs, 1000 Hz Pulses

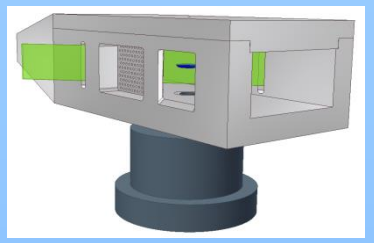

$CH_4$/air, $\phi$ = 0.76

Flame Shifted Coordinates

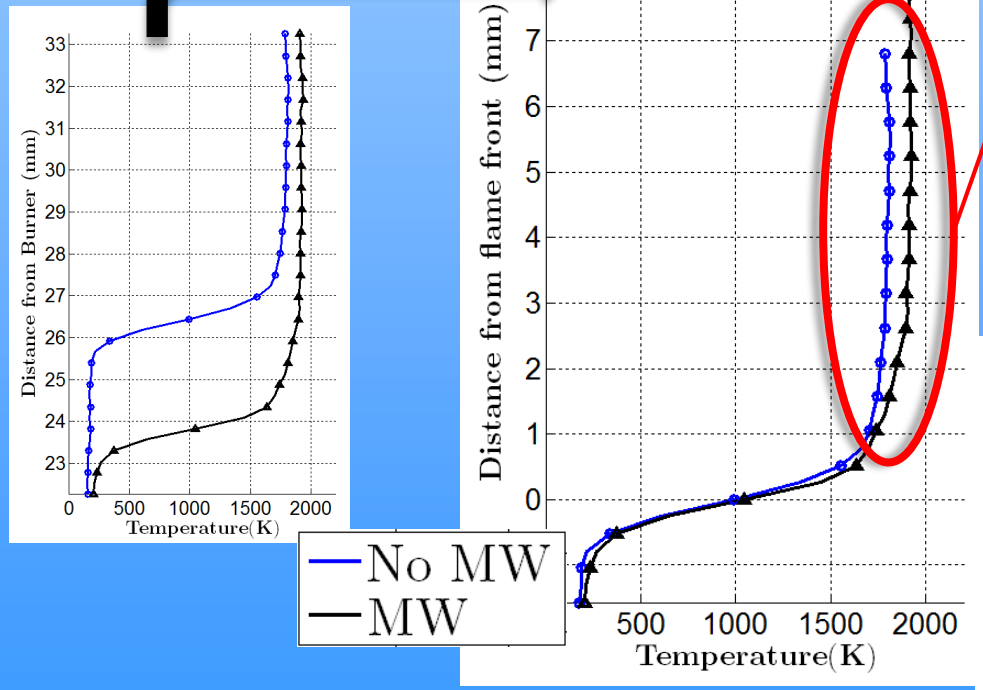


- Observed Flame Speed Effect
  - Increase of 0.25 L/D units → ~6% flame speed enhancement
- **80 K** in post flame temperature (CW saw ~150 K)
- Energy deposited within a few mm of reaction zone

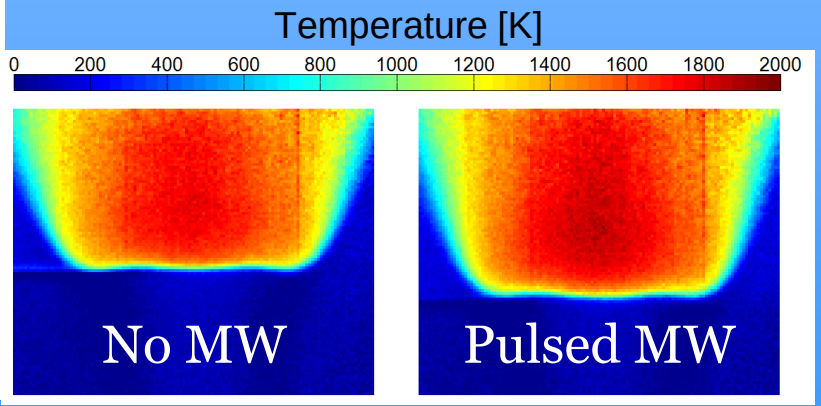


80 K → 12 W energy deposition → 50% magnetron coupling efficiency

Stockman, E.S., Zaidi, S.H., Miles, R.B., Carter, C.D. and Ryan, M.D., 2009. *Combustion and Flame*, *156*(7), pp.1453-1461.

Princeton University

# Combustion enhancement by a gliding arc (Joule heating and kinetic effect)

Princeton University

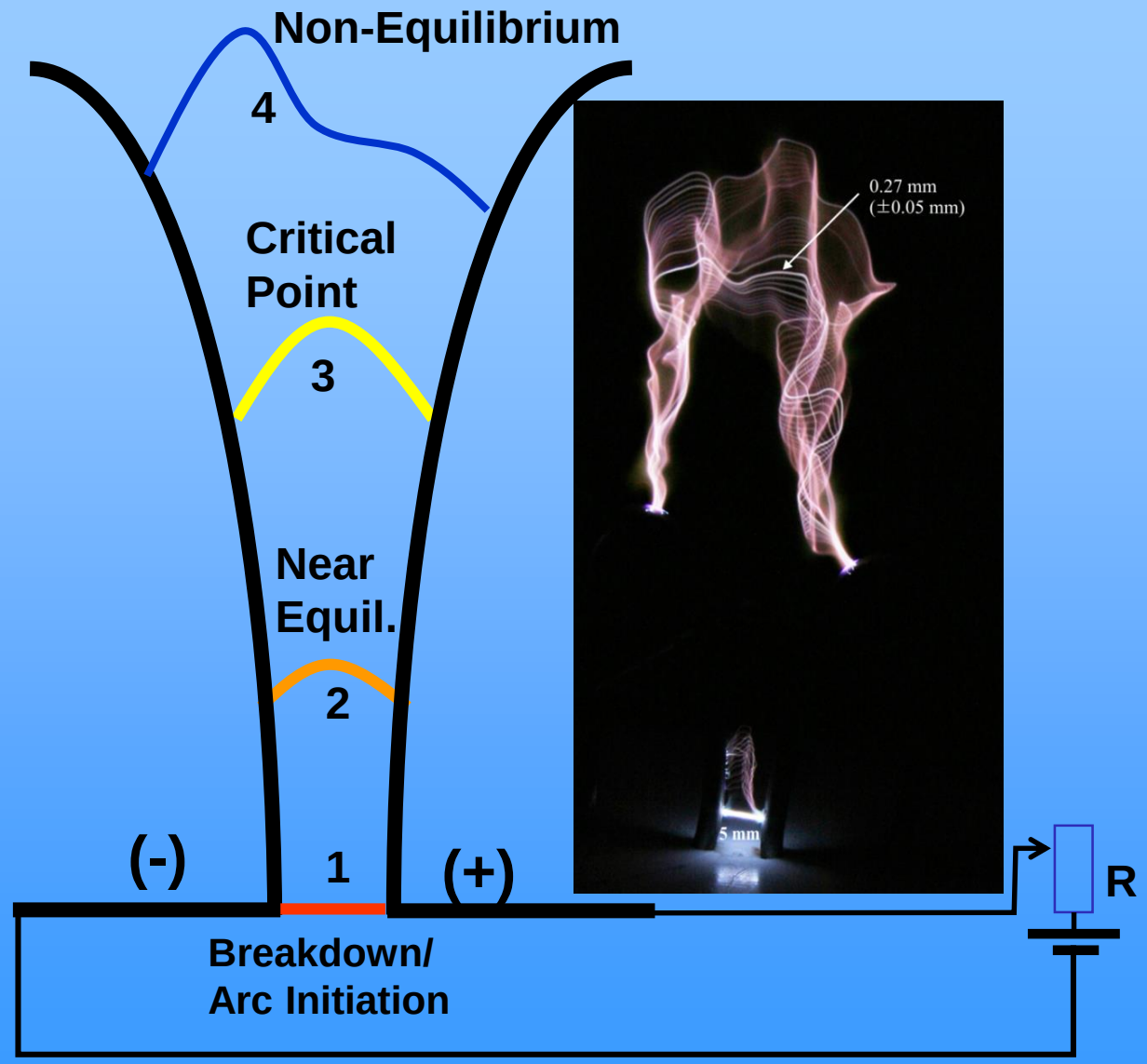


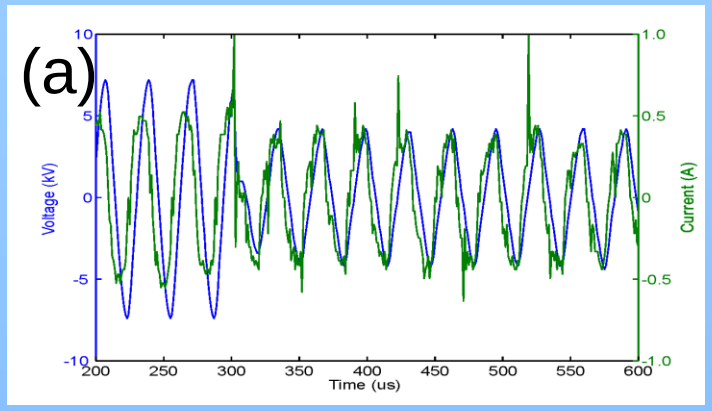


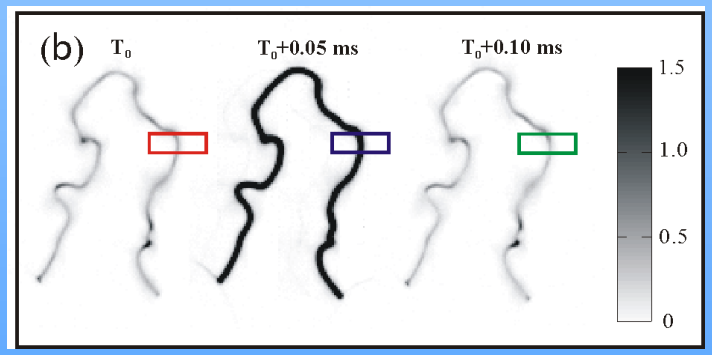


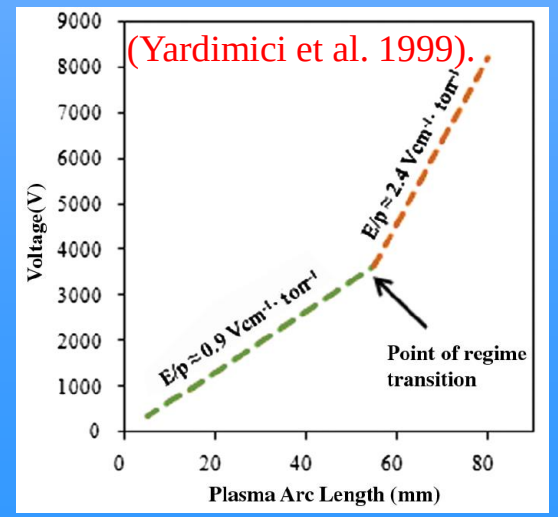

Princeton University

# Short cut event and OH measurements in a gliding arc (air)

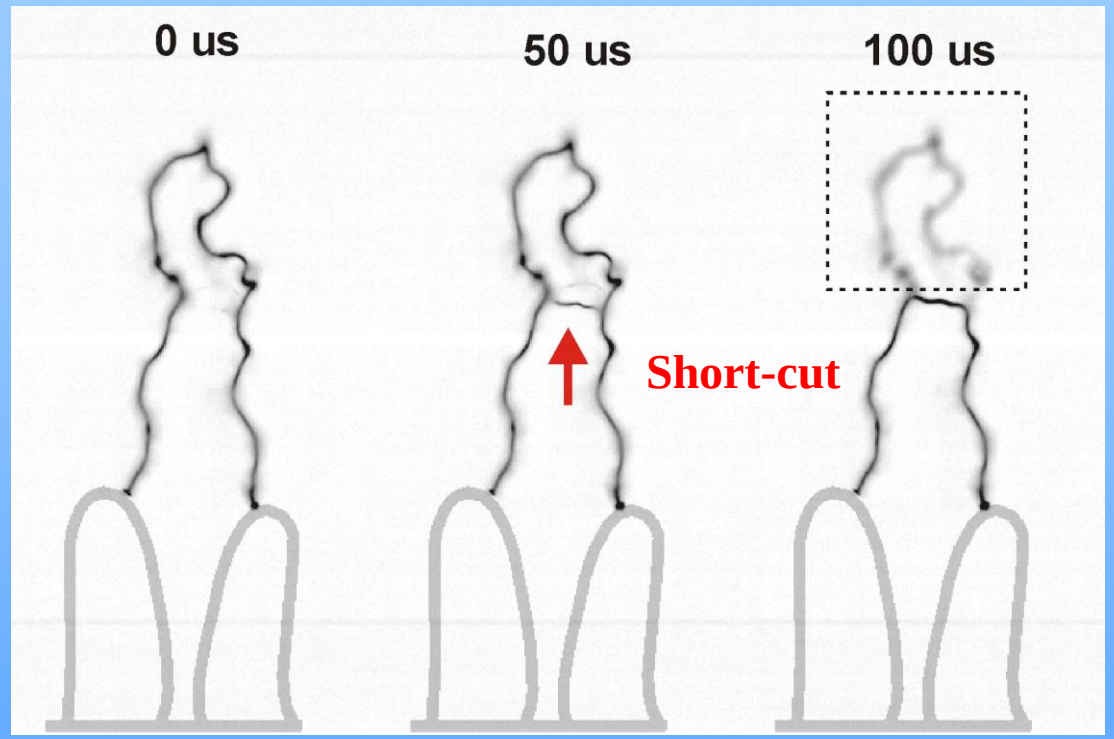


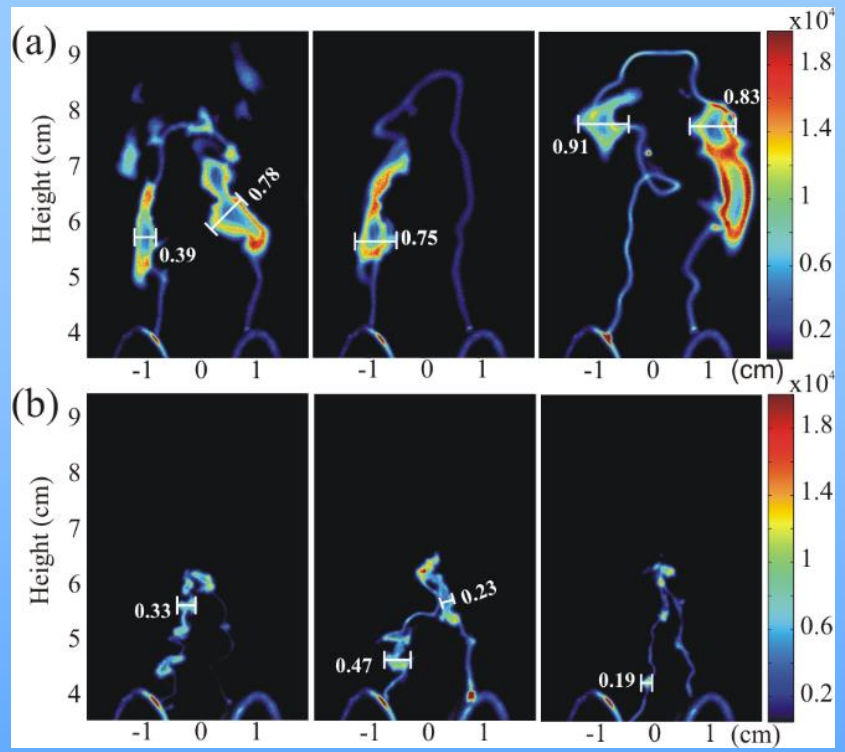


**Left: A short-cut event recorded at 20 kHz framing rate using an exposure time of 13.9 µs. The short-cut current path is indicated by the arrow in the frame of t = 50 µs. Right: Three typical single-shot OH PLIF images of a gliding arc using an exposure time of 2 µs, at two flow rates (a) 17.5 SLM, (b) 42 SLM. The typical thickness of the OH distribution is labelled in the images with unit of centimeters (Courtesy from Dr. Z.S. Li at Lund University)**

The combination of thermal heating and radical production (high electron density and high electron energy) of a non-thermal gliding arc can enhance ignition and flame stabilization in both thermal and kinetic ways.


1. Sun, Z.W., Zhu, J.J., Li, Z.S., Aldén, M., Leipold, F., Salewski, M., Kusano, Y., Optics Express. 2013, 21 (5) 6028-6044.

2. Zhu, J., Sun, Z., Li, Z., Ehn, A., Aldén, M., Salewski, M., Leipold, F., Kusano, Y., Dynamics, Journal of Physics D: Applied Physics. 2014, 47 (29) 295203.

# Summary: Electric field effect on flames

**1. Ionic wind**

- Low frequency electric field generates ionic wind flowing to both electrodes from a flame due to positive and negative charge carriers.
- Ionic wind can reduce soot/NOx formation due to the change of mixing and flame temperature.
- Ionic wind may induce flame instability due to the force field.
- Ionic wind also modifies flame speed and reduces flame temperature due to increased heat losses from the flame zone.

**2. Joule heating**

- Electric field generates Joule heating in the flame zone and at the downstream of the flame.
- The electron Joule heating can enhance flame speed via the increase of flame temperature.
- Microwave Joule heating in flames is not energy efficient because much of the energy absorbed by in the burned gas.

**3. Radical production by strong electric field**

- When the electric field is above the breakdown threshold, a gliding arc or corona can produce radicals to enhance ignition via kinetic pathway.
- A gliding arc has high temperature and high electronic energy and density, which lead to both thermal and non-thermal enhancement effects on flames.

**It is necessary to understand the kinetic effect of non-thermal plasma at high E/N on combustion**

# Lecture 5 Chemistry and Kinetic Studies of Plasma-Assisted Combustion

Yiguang Ju

- Important chain-initiation and branching reactions in combustion
- Plasma chemistry and timescales
- Impact of plasma chemistry on combustion
- Diagnostics of plasma properties and chemistry in PAC

# 1. Important combustion reactions

## 1. Chain initiation and propagation reactions

| | | |
|---|---|---|
| $RH + O_2 \rightarrow R + HO_2$ | High Temperature (>1100 K) | slow |
| $RH + HO_2 \rightarrow R + H_2O_2$ | High pressure/low temperature (>550 K) | slow |
| $R + HO_2 \rightarrow RO + OH$ | High pressure/low temperature (>550 K) | slow |

## 2. important branching reactions at different temperatures

| | | |
|---|---|---|
| $H + O_2 \rightarrow O + OH$ | High Temperature (>1100 K) | Fast |
| $H_2O_2 \rightarrow 2OH$ | Intermediate temperature (800-1100 K) | Slow |
| $R \rightarrow RO_2 \rightarrow QOOH \rightarrow O_2QOOH \rightarrow R'' + 2OH$ | Low temperature (300-800K) | Slower |

## Plasma assisted combustion:

$e + O_2 \rightarrow e + 2O$ ⇒

$O + RH \rightarrow R + OH$

$R \rightarrow R'' + 2OH$

---

$O + RH \rightarrow R'' + 3OH$ Faster

$e + O_2 \rightarrow e + O_2(a^1\Delta_g)$ ⇒ $H + O_2(a^1\Delta_g) \rightarrow OH + O$ Faster

**Plasma provides new reaction pathways to accelerate chain reaction processes**

# Interaction of plasma chemistry with reaction kinetics of large alkanes w/wo in plasma assisted combustion

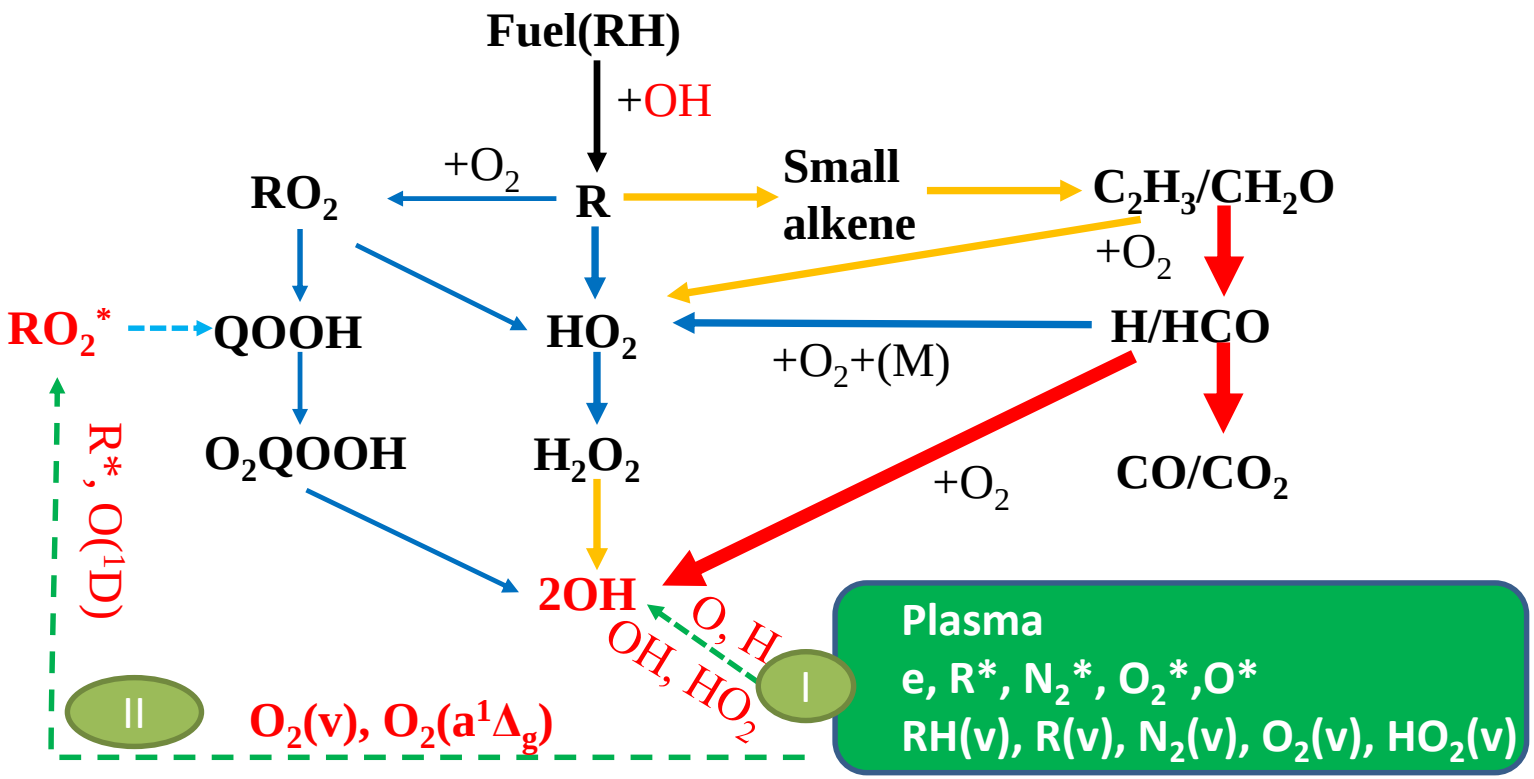


A schematic of the key reaction pathways for high pressure fuel oxidation of at different temperatures (blue arrow: Below 700K; yellow arrow: 700-1050 K; red: above 1050K). Green: plasma activated pathway

## Reaction rate

### Transition state theory

$$A + B \overset{k1}{\leftrightarrow} AB^* \overset{k2}{\rightarrow} C + D$$

$$k(T) = \frac{k_B T}{h} \frac{q_{AB}^{**}}{q_A^* q_B^*} \exp\left(-\frac{E^* - E_{A-B}}{k_B T}\right)$$

How does plasma affect elementary rate constant?

e.g. at 800 K

$O_2(a^1\Delta_g) + H = OH + O$ **Fast**
$O_2 + H = OH + O$ **Slow**

$CH_3 + O_2(v) \rightarrow CH_2O + OH$ **Fast**
$CH_3 + O_2 \rightarrow CH_2O + OH$ **Slow**

# 2. Plasma chemistry and timescales of kinetic processes

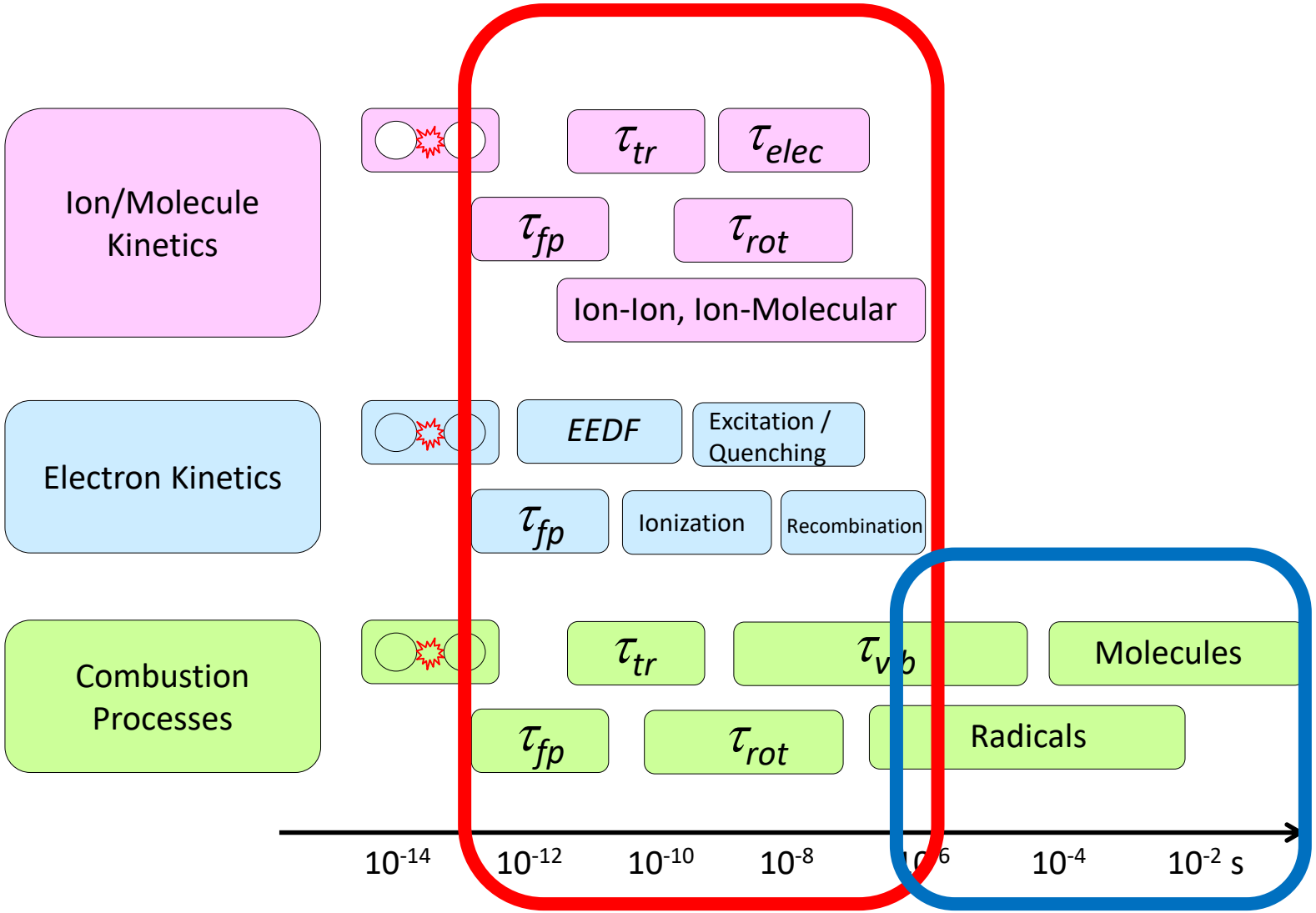


Courtesy of Andrey Starikovskiy

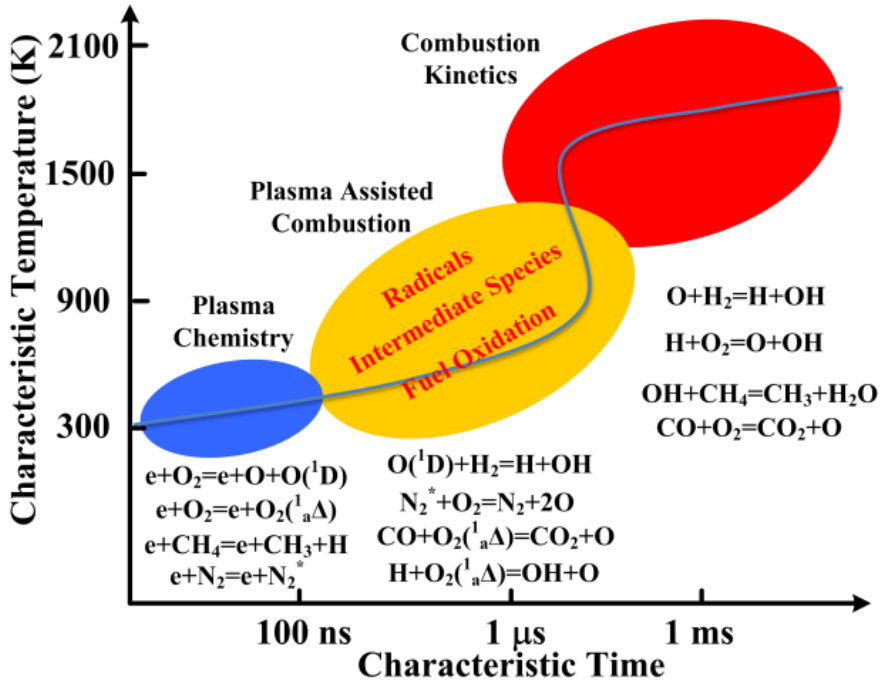


Fig. 1.5 Schematic of timescales and key kinetic pathways at different stages of plasma assisted ignition and combustion.

Ju and Sun, PECS, 2015

# Potential Energy Curves of $O_2$

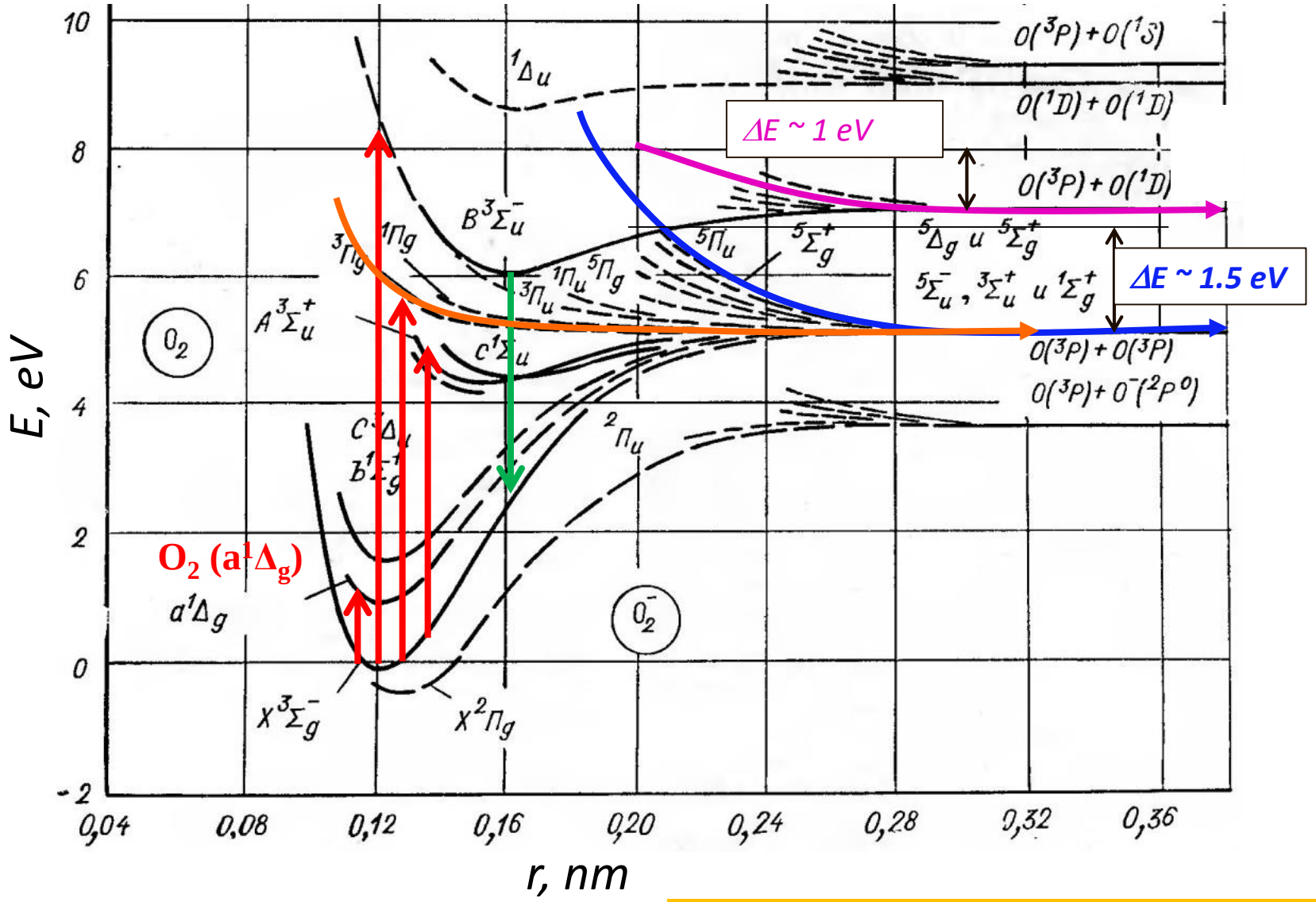


$O_2(B^3\Sigma_u^-)$, 8.4 eV
$\sigma_{max}$ = 1.0 $A^2$ (9.4 eV)

$O_2(^3\Pi_g)$, 5.6 eV
$\sigma_{max}$ = 0.16 $A^2$ (12 eV)

$O_2(A^3\Sigma_u^+)$, 4.5 eV
$\sigma_{max}$ = 0.18 $A^2$ (6.6 eV)

$O_2$ ($b^1\Sigma_g^+$) at 1.6 eV

$O_2$ ($a^1\Delta_g$) at 0.98 eV

**Electron impact reaction is a function of electron energy distribution (E/N)**

# Electron impact reaction cross sections-$O_2$

PRINCETON
Mechanical and Aerospace Engineering

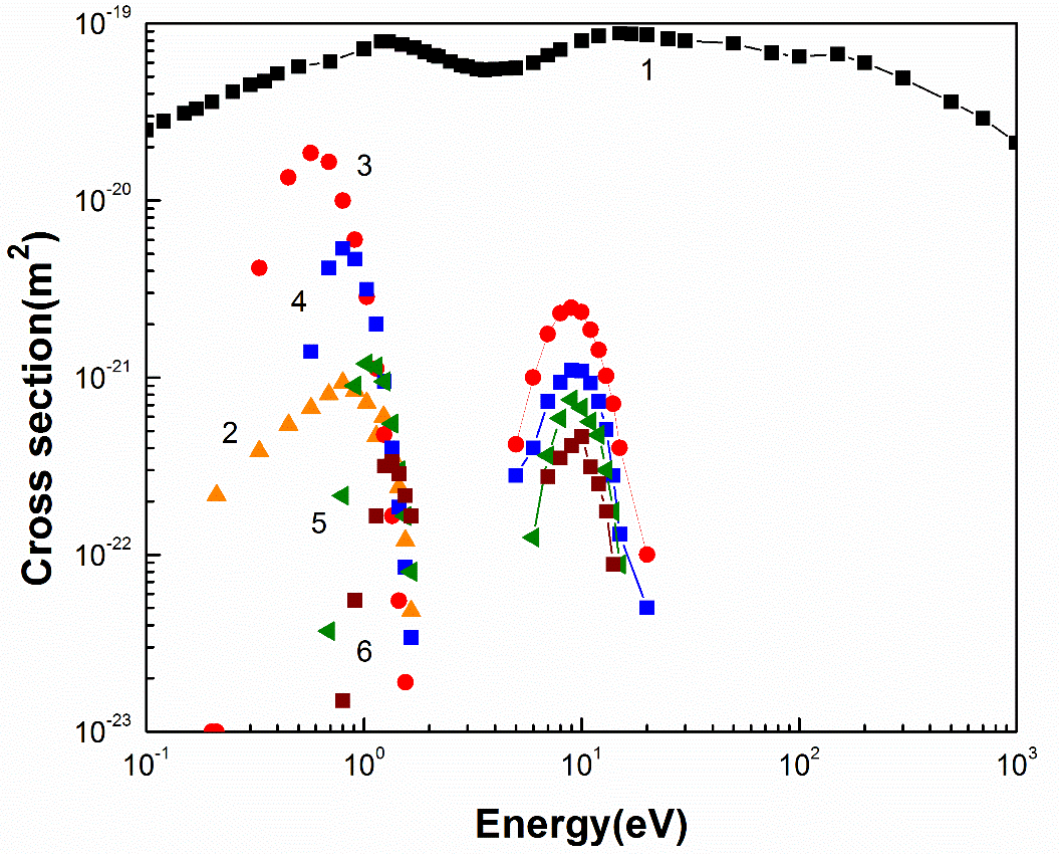


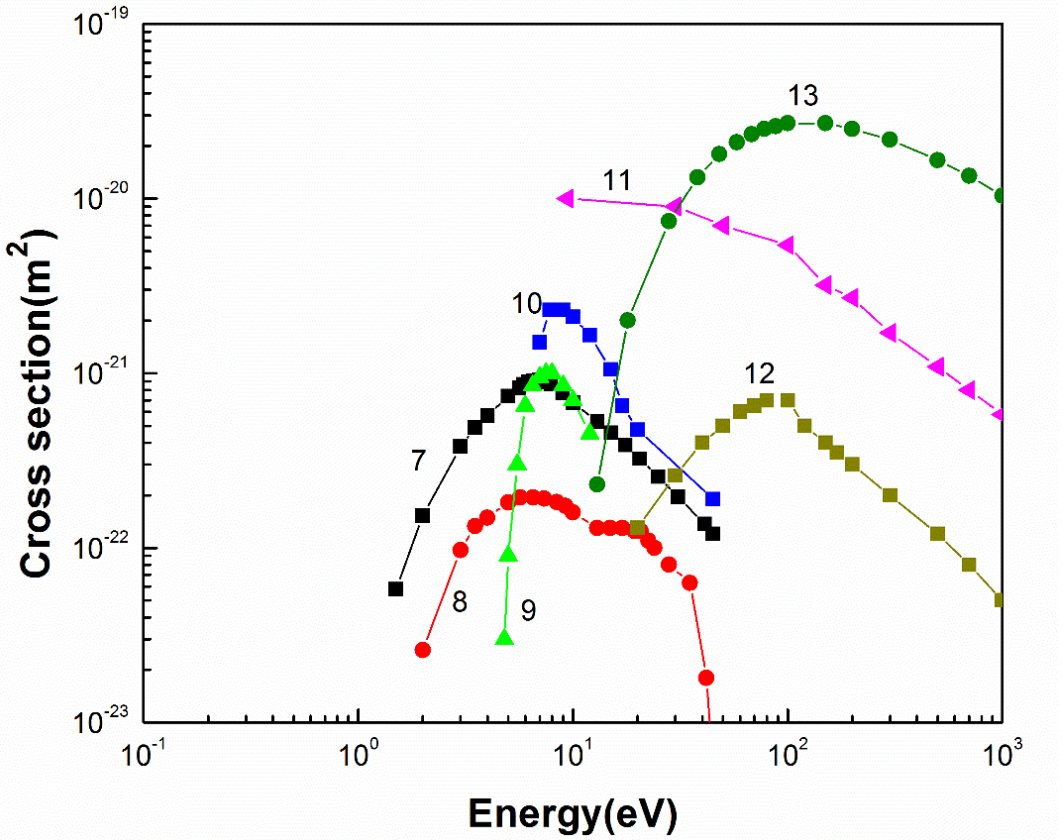


1. effective
2. rotational excitation
3-6. $O_2$(v1) - $O_2$ (v4)

7. $O_2$(a1) 8. $O_2$(b1) 9. $O_2(A^3\Sigma_u^+)$, 4.5 eV
10. O+O 11. O+O(1D) 12. O+O(1S)
13. $O_2^+$

# Potential Energy Curves of N2

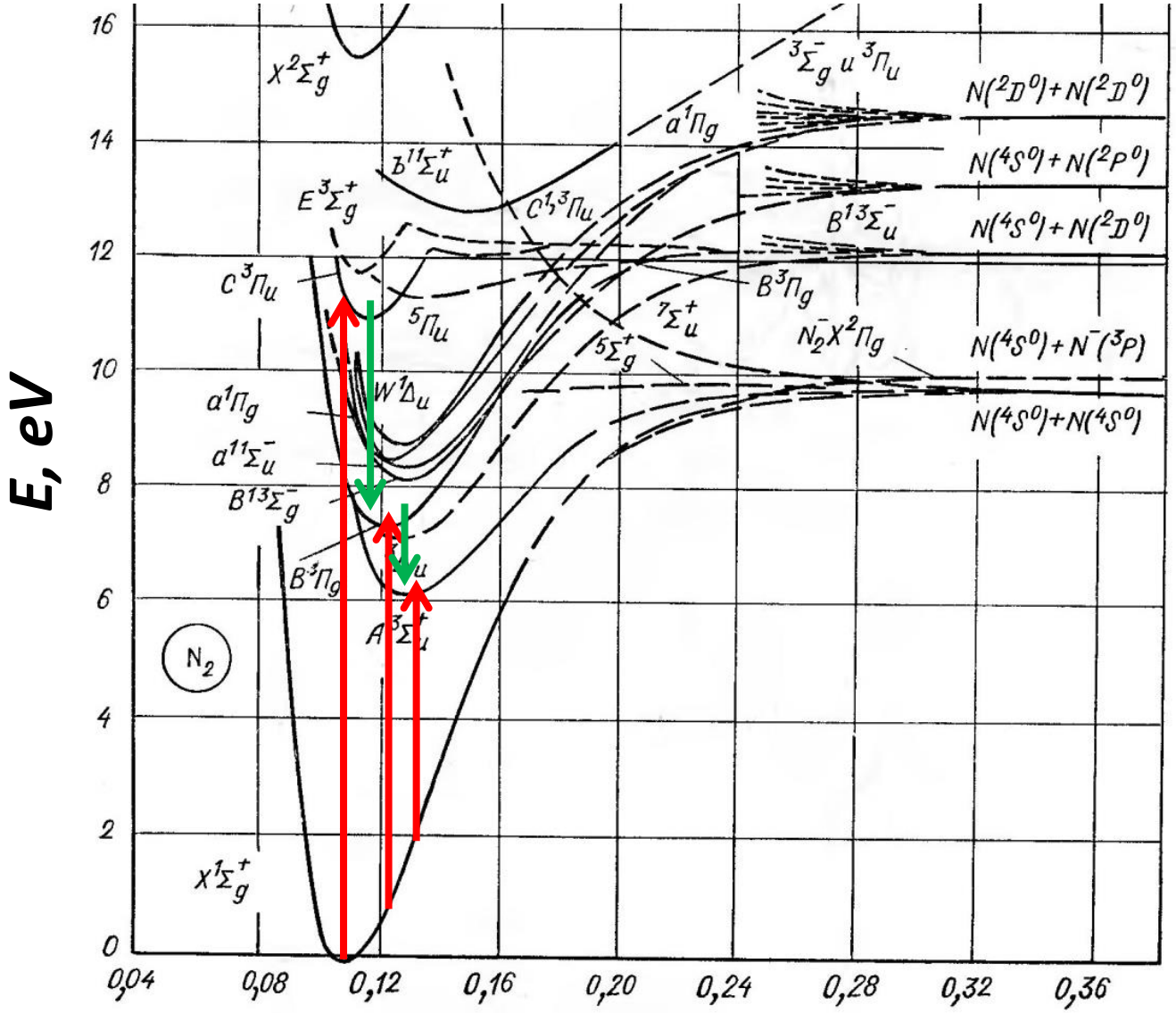


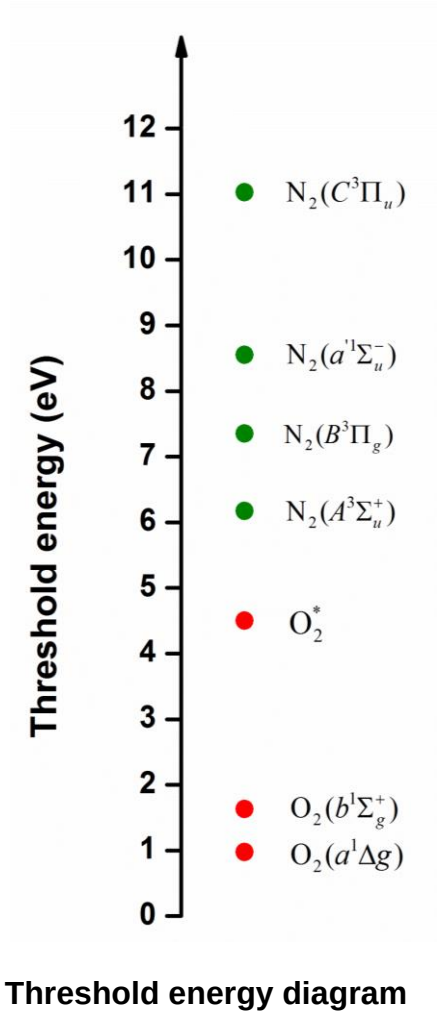


Threshold energy diagram

$N_2(A^3\Sigma_u^+)$, 6.2 eV
$\sigma_{max}$ = 0.08 $A^2$ (10 eV)

$N_2(B^3\Pi_g)$, 7.35 eV
$\sigma_{max}$ = 0.20 $A^2$ (12 eV)

$N_2(C^3\Pi_u)$, 11.03 eV
$\sigma_{max}$ = 0.98 $A^2$ (14 eV)

**Electron impact reaction is a function of electron energy distribution**

# Energy Transfer of non-equilibrium excitation in Plasma Discharge

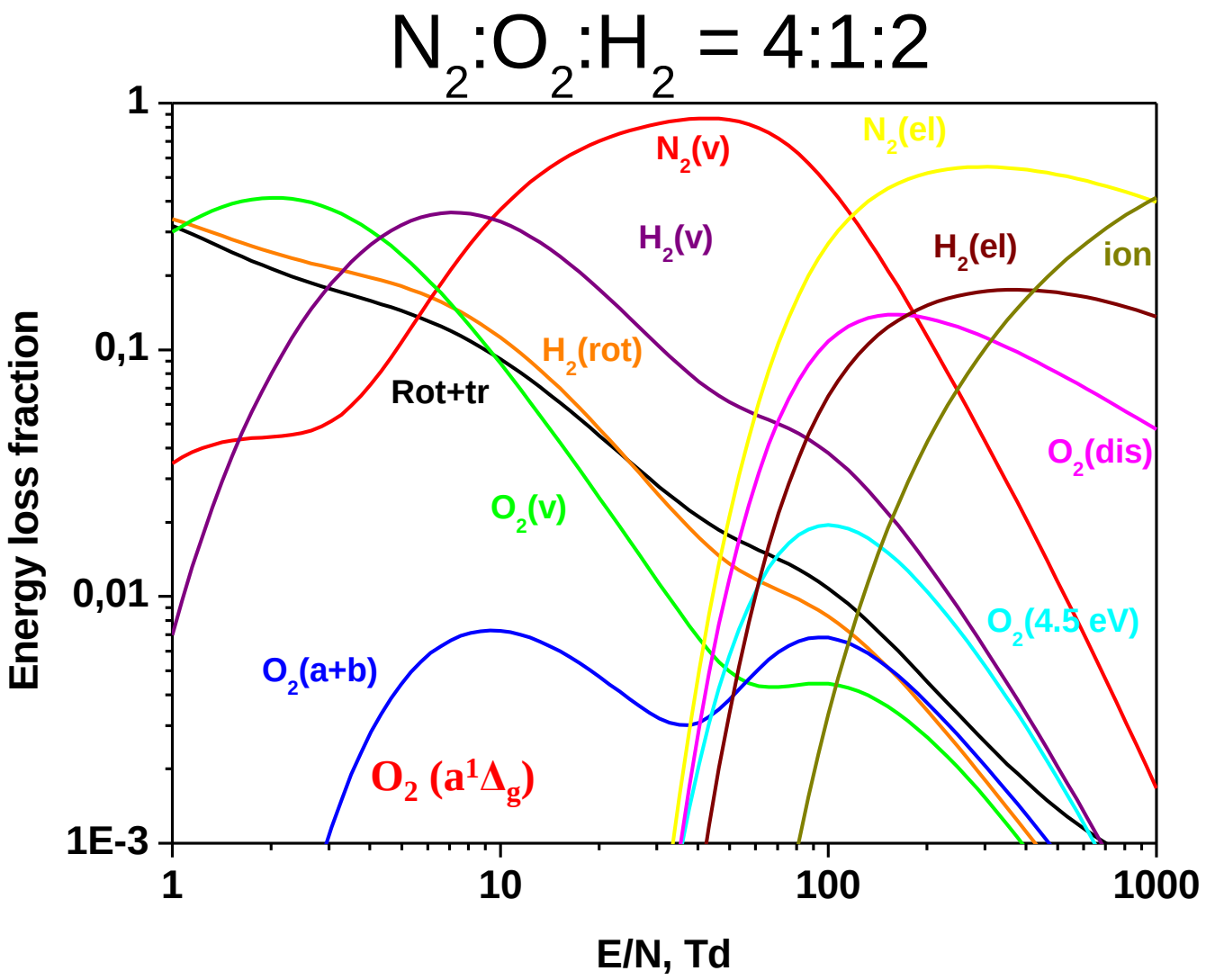

# Influence of Electronic and Vibrational Excitation on Combustion Kinetics

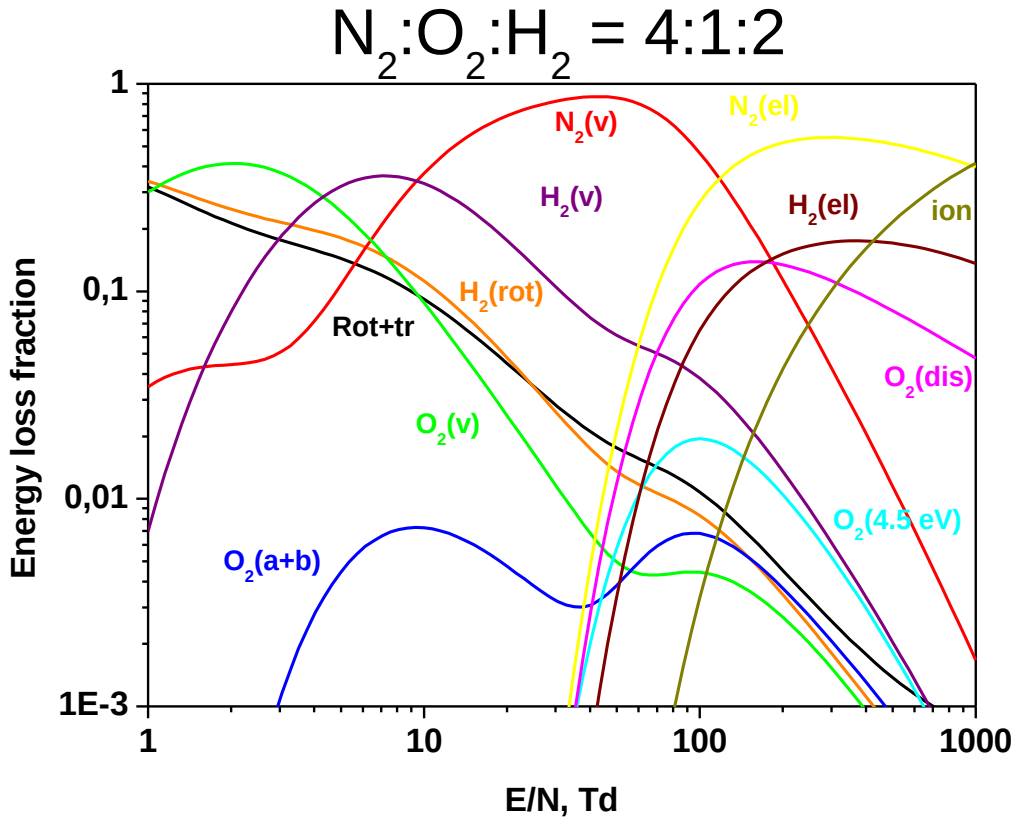


$N_2 + e = N_2(C^3) + e$

$N_2(C^3) + O_2 = N_2 + O + O$

$O_2 + e = O + O + e$

$N_2 + e = N_2(v) + e$

$N_2(v) + HO_2 = N_2 + HO_2(v)$

$HO_2(v) = O_2 + H$

# Influence of Vibrational Excitation on Low-Temperature Kinetics: $H_2O_2$ Decomposition

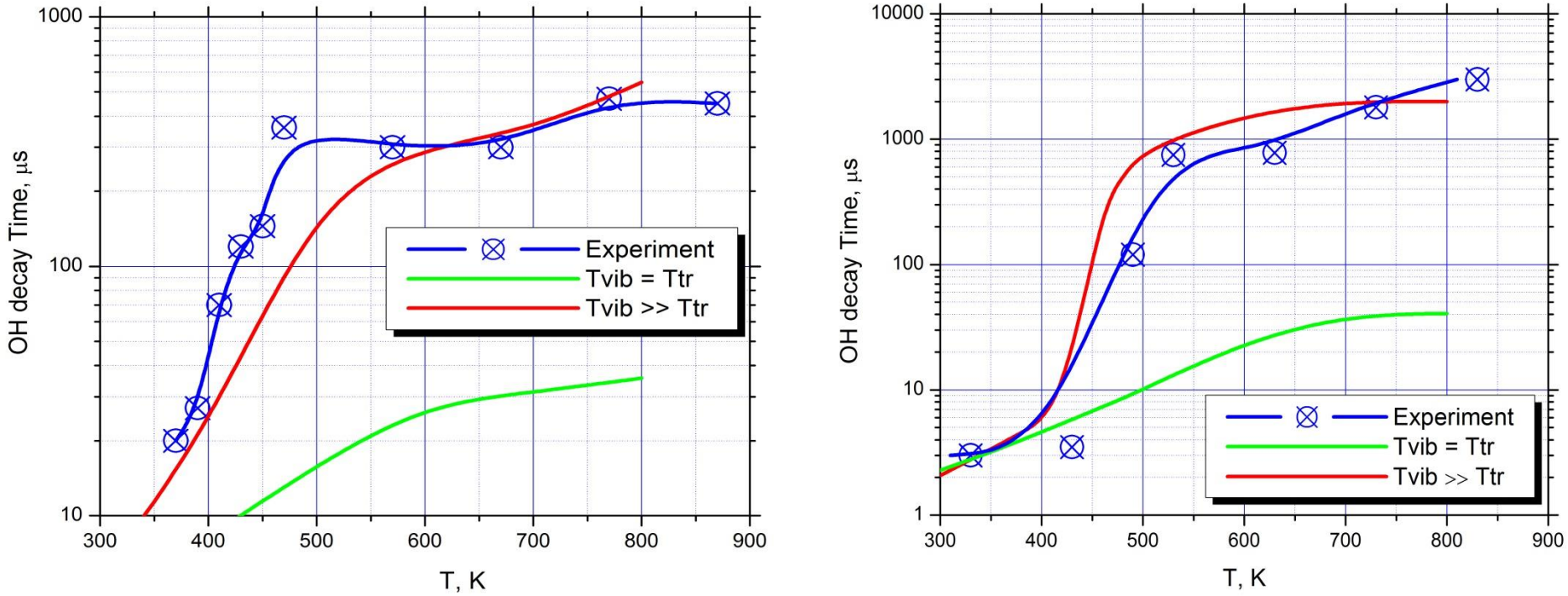


Measured and calculated OH decay time. P = 1 atm.
a) 3%$H_2$ + air; b) 0.3%$C_4H_{10}$ + air.

PRINCETON University

# Effect of "Hot" Atoms on Active Species Production in High-Voltage Pulsed Discharges

**Nonequilibrium distributions of neutral species are formed in different physical situations. In laboratory experiments and in the terrestrial atmosphere, there are numerous collisional processes in which translationally energetic (superthermal) atoms with energies much above thermal energies are produced.**

Potential energy curves and hot atoms formation

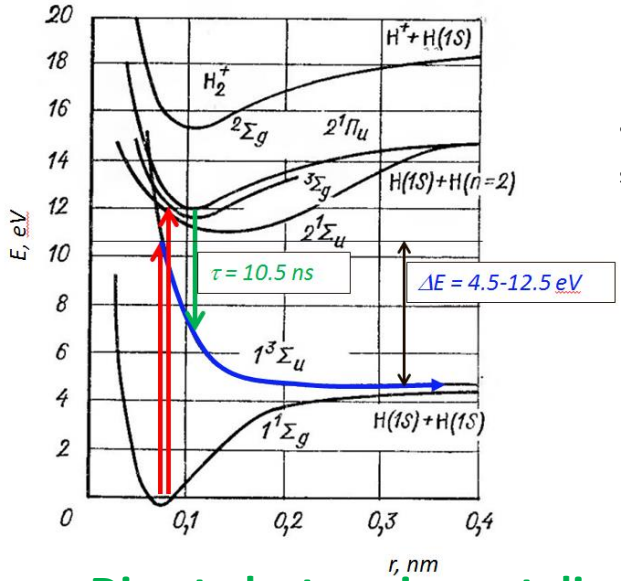


Momentum transfer cross section for the H-$H_2$ scattering

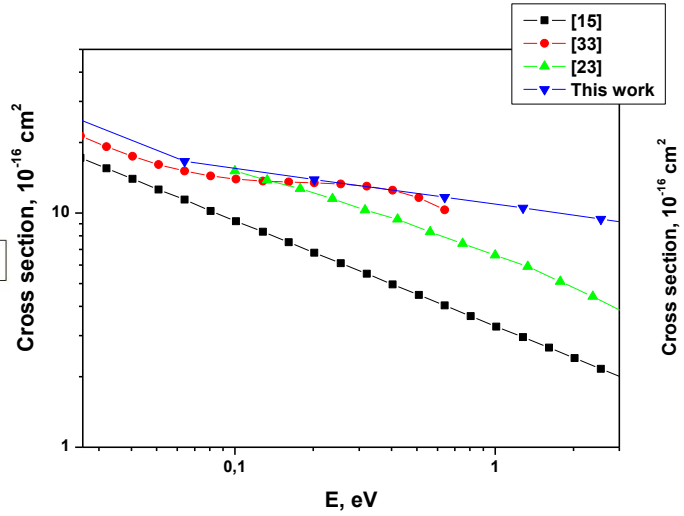


Cross sections for scattering of H atoms with $H_2$, $O_2$, $CH_4$ and $N_2$

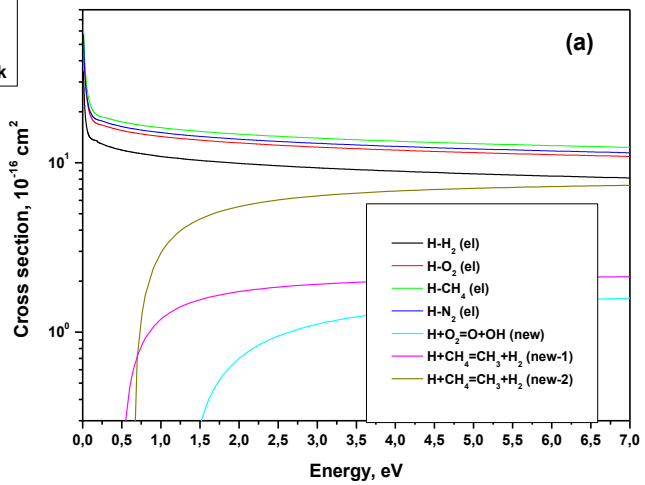


## Direct electron-impact dissociation

$e + O_2 \rightarrow e + O_2^*$ $\quad O_2^* \rightarrow 2O(^3P,^1D) + 1.3$ eV

$e + H_2 \rightarrow e + H_2^*$ $\quad H_2^* \rightarrow 2H(^1S) + 4.5$ eV

$e + CH_4 \rightarrow e + CH_4^*$ $\quad CH_4^* \rightarrow CH_3 + H + 3.5$ eV


Mechanical and Aerospace Engineering
Applied Physics Group

PRINCETON University

# Effect of "Hot" Atoms on Active Species Production in High-Voltage Pulsed Discharges

## Average energy of H atoms in various gaseous mixtures

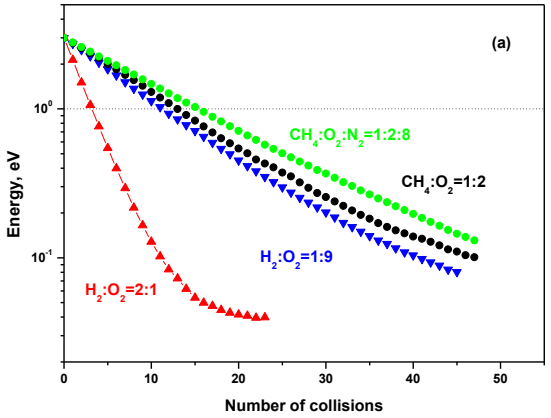


## Species produced during energy degradation of one "hot" H atom

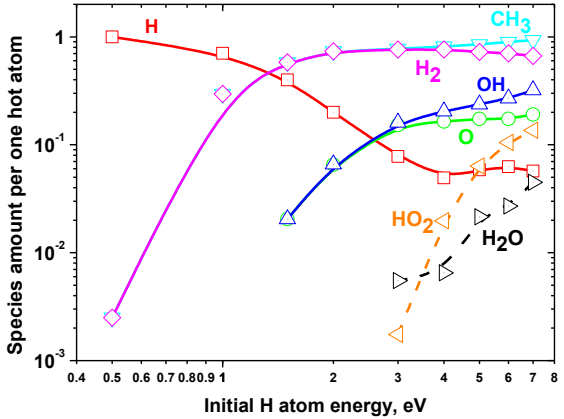


## Plasma-assisted oxidation in H2-O2 mixture

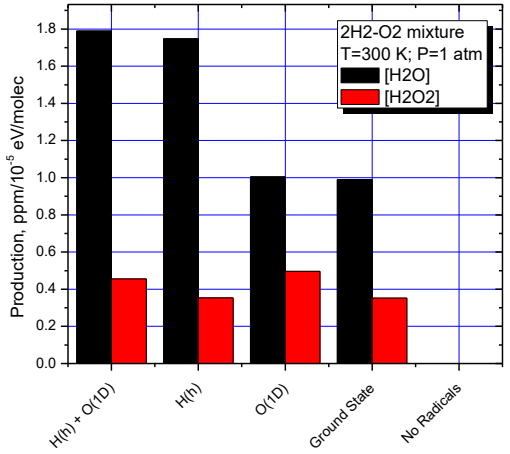


## Plasma-assisted oxidation in CH4-O2 mixture

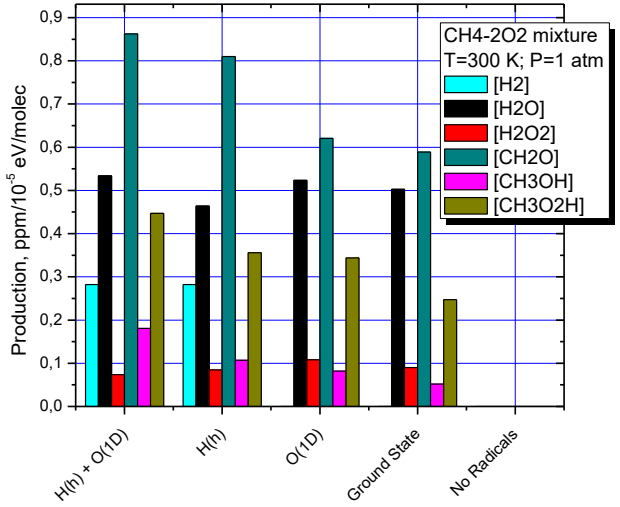


- **Analysis of the effect of formation of "hot" atoms with excessive translational energy shows the important role of these processes in formation of active radicals.**
- **The density of radicals produced in discharge plasma can be several times higher than that produced in the absence of high-energy atoms.**
- **The effect plays a fundamental role in the formation of the initial distribution of active species in combustible mixtures and can greatly influence the kinetics of ignition and oxidation at low gas temperatures.**


Mechanical and Aerospace Engineering
Applied Physics Group

# Gas heating at high E/N

**Fast Gas Heating**

- Electron-ion recombination: $e + O_2^+ \rightarrow O + O^* + \Delta E$
- Ion-ion recombination: $O_2^- + O_2^+ + M \rightarrow 2O_2 + M + \Delta E$
- Collisional energy transfer Electronically-excited species: $N_2(A,B,C,a) + O_2 \rightarrow 2O + \Delta E$
- Hot atom and molecule: $O_2^* \rightarrow 2O(^3P,^1D) + \Delta E$

**Slow Gas Heating**

- Vibrational energy relaxation: $N_2(v) + M = N_2(v-1) + M + \Delta E$

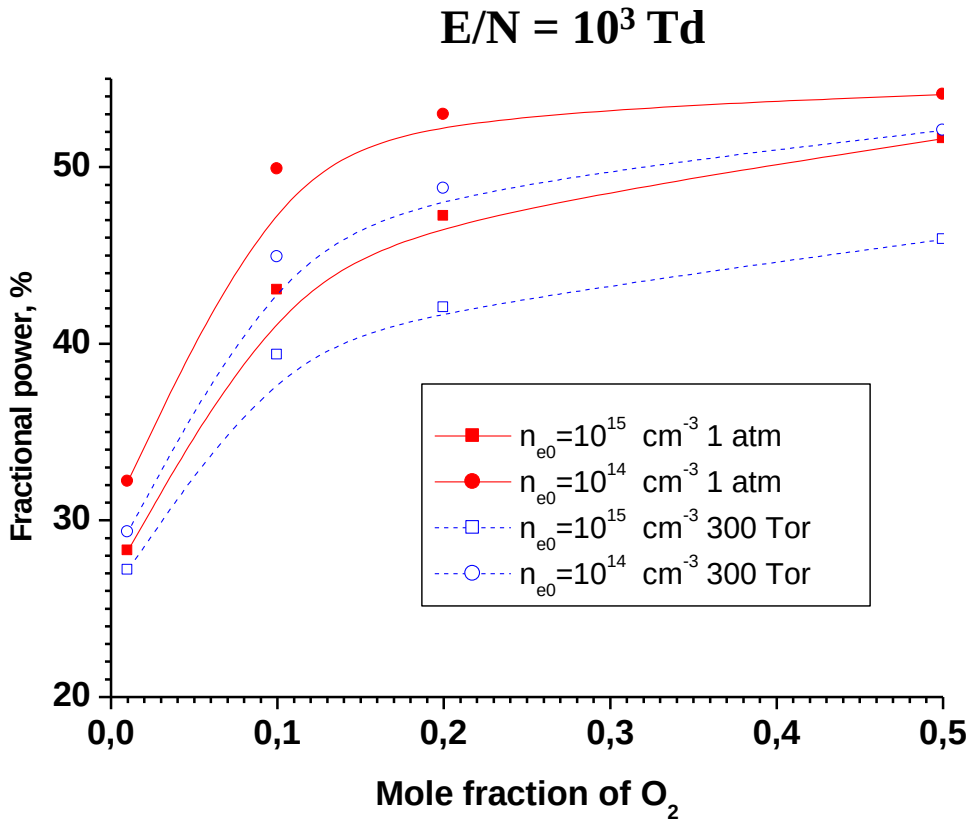


Fractional Electron Power Transferred Into Heat in $N_2$:$O_2$ Mixtures

High oxygen, faster gas heating!

# Princeton Plasma Combustion Kinetics

## *Major Pathways*

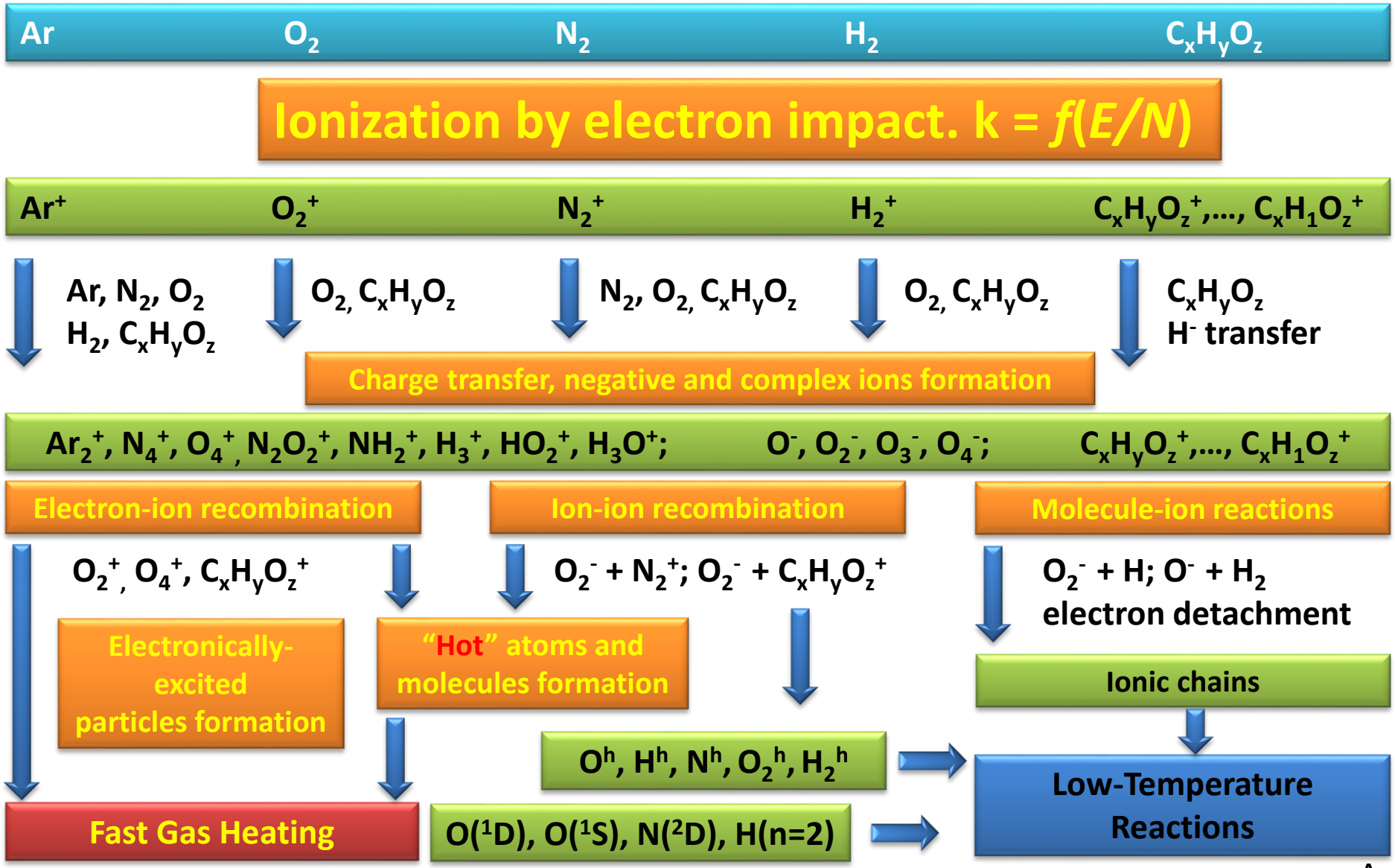


Andrey Starikovskiy

# Princeton Plasma Combustion Kinetics

## *Major Pathways*

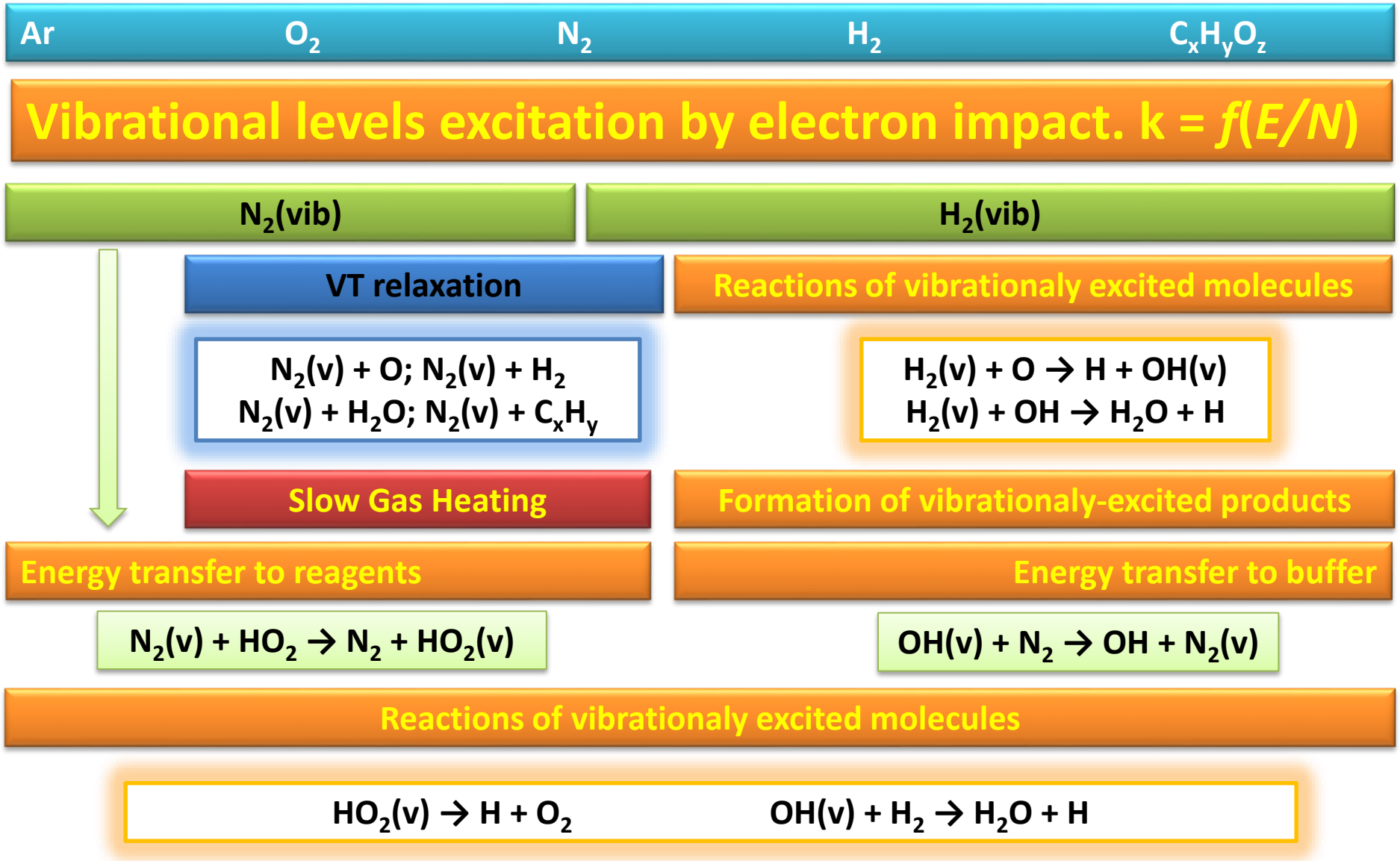
Ar
$O_2$
$N_2$
$H_2$
$C_xH_yO_z$
Vibrational levels excitation by electron impact. k = *f*(*E*/*N*)
$N_2$(vib)
$H_2$(vib)
VT relaxation
Reactions of vibrationaly excited molecules
$N_2(v) + O$; $N_2(v) + H_2$
$N_2(v) + H_2O$; $N_2(v) + C_xH_y$
$H_2(v) + O \rightarrow H + OH(v)$
$H_2(v) + OH \rightarrow H_2O + H$
Slow Gas Heating
Formation of vibrationaly-excited products
Energy transfer to reagents
Energy transfer to buffer
$N_2(v) + HO_2 \rightarrow N_2 + HO_2(v)$
$OH(v) + N_2 \rightarrow OH + N_2(v)$
Reactions of vibrationaly excited molecules
$HO_2(v) \rightarrow H + O_2$
$OH(v) + H_2 \rightarrow H_2O + H$

# Typical plasma reactions for radical production and heating

**Electron impact ionization/dissociation/excitation**

| | | | |
|---|---|---|---|
| >10 eV | $e + O_2 = O^+ + O + 2e$ | (R1a) | Radical production |
| ~10 eV | $e + O_2 = O + O(^1D)$ | (R1b) | Non-equilibrium excitation |
| ~1 eV | $e + O_2 = O_2(^1\Delta_g) + e$ | (R1c) | |
| 0.2-2 eV | $e + O_2 = O_2(v) + e$ | (R1d) | |

**Electron ion recombination, attachment, charge transfer**

| | | |
|---|---|---|
| $e + O_2^+ = O + O(^1D)$ | (R2a) | Recombination/fast heating |
| $O_2^+ + O_2^- = 2O_2$ | (R2b) | Recombination/fast heating |
| $e + O_2 + M = O_2^- + M$ | (R2c) | Attachment |
| $H_2O + N_2^+ = H_2O^+ + N_2$ | (R2d) | Charge Transfer |

**Dissociation and energy transfer by ions and excited species**

| | | |
|---|---|---|
| $N_2(A,B,C) + O_2 = O + O(^1D) + N_2$ | (R3a) | |
| $O(^1D) + H_2 = OH + H$ | (R3b) | |
| $H + O_2(^1\Delta_g) = O + OH$ | (R3c) | |
| $N^+ + O_2 = O^+ + NO$ | (R3d) | |
| $CH_3 + HO_2(v) = CH_2O + OH$ | (R3e) | Slow heating |
| $N_2(v=5) + N_2 = N_2(v=3) + N_2$ | (R3f) | |
| $N_2(v) + HO_2 \rightarrow N_2 + HO_2(v)$ | (R3g) | |

# What are the major species produced by plasma?

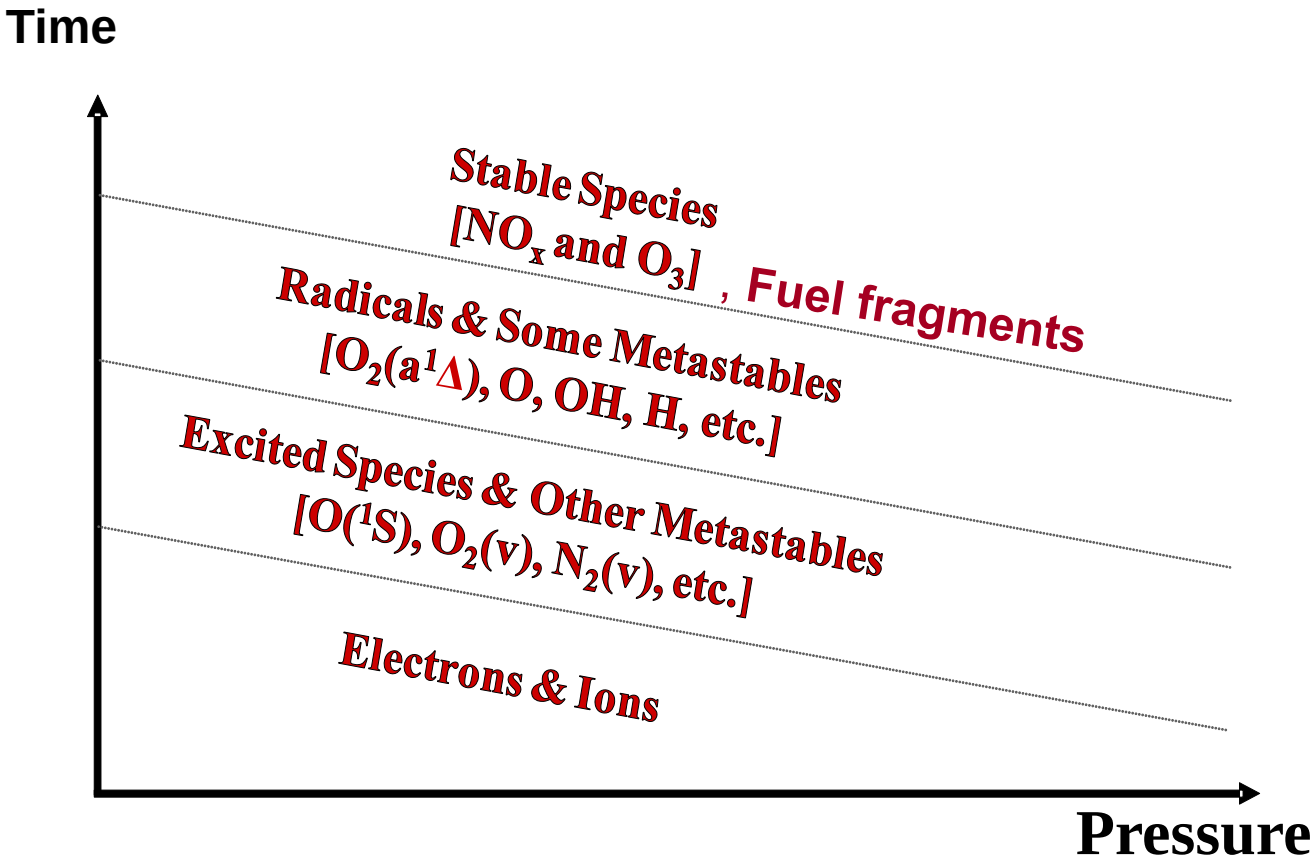


- Long lifetime species? NO, $O_3$, $O_2(a^1\Delta_g)$
- Short lifetime plasma generated species? O, $N_2$ (A,B,C)*

# 3. Impact of plasma chemistry on combustion

**Question: When will electron impact dissociation process become important in combustion?**

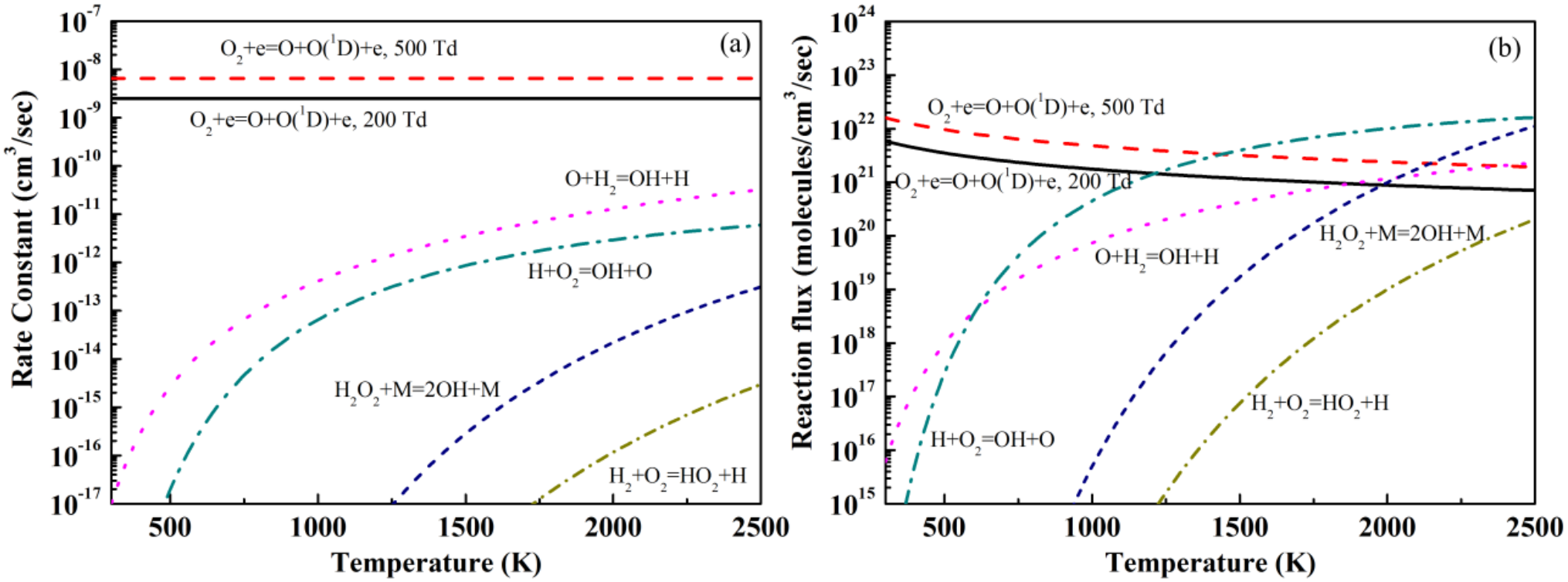


Fig. 3.5: Rate constants (a) and reaction flux (b) for reactions for dissociation by electron impact at electric field values equal to 200 Td and 500 Td and chain branching reactions.

Ju and Sun, PECS, 2015.

# Comparison of the reaction rates of electron impact and excited species for radical production

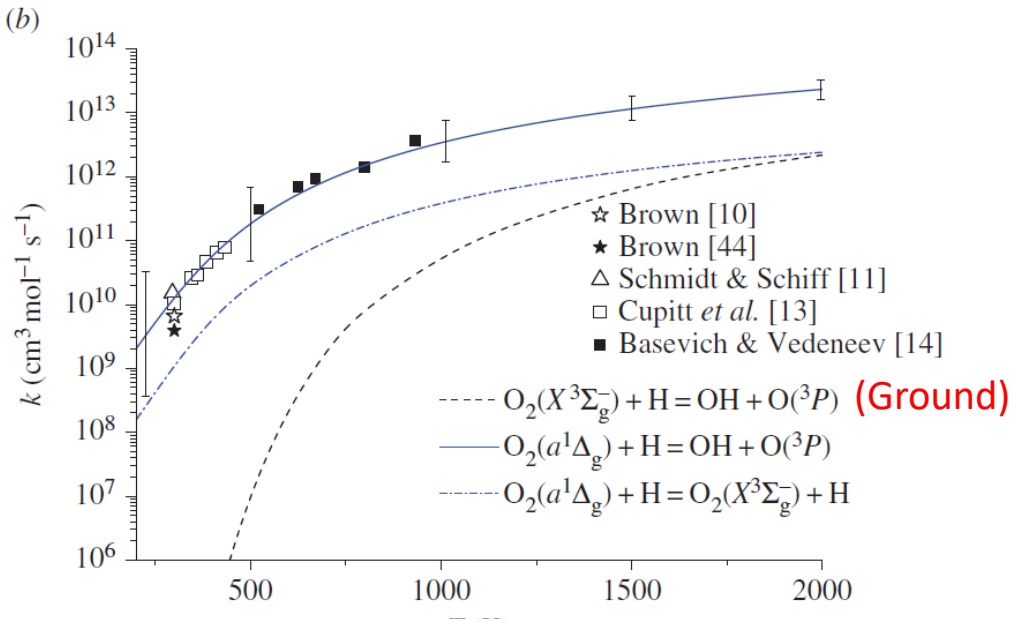
(b)
$k$ (cm$^3$ mol$^{-1}$ s$^{-1}$)
☆ Brown [10]
★ Brown [44]
△ Schmidt & Schiff [11]
□ Cupitt *et al.* [13]
■ Basevich & Vedeneev [14]
$O_2(X^3\Sigma_g^-) + H = OH + O(^3P)$
$O_2(a^1\Delta_g) + H = OH + O(^3P)$
$O_2(a^1\Delta_g) + H = O_2(X^3\Sigma_g^-) + H$
$T$ (K)

(Ground)

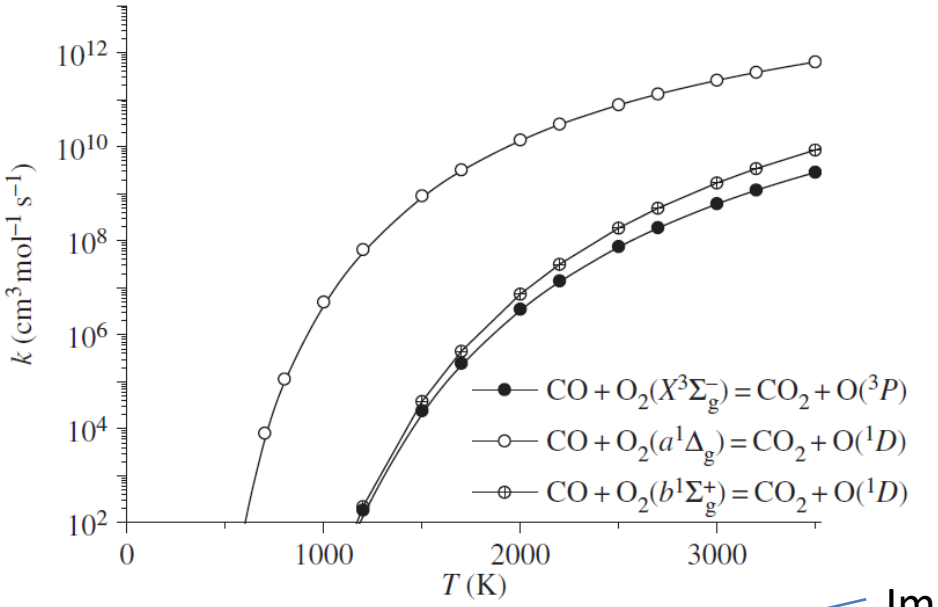


(Ground)

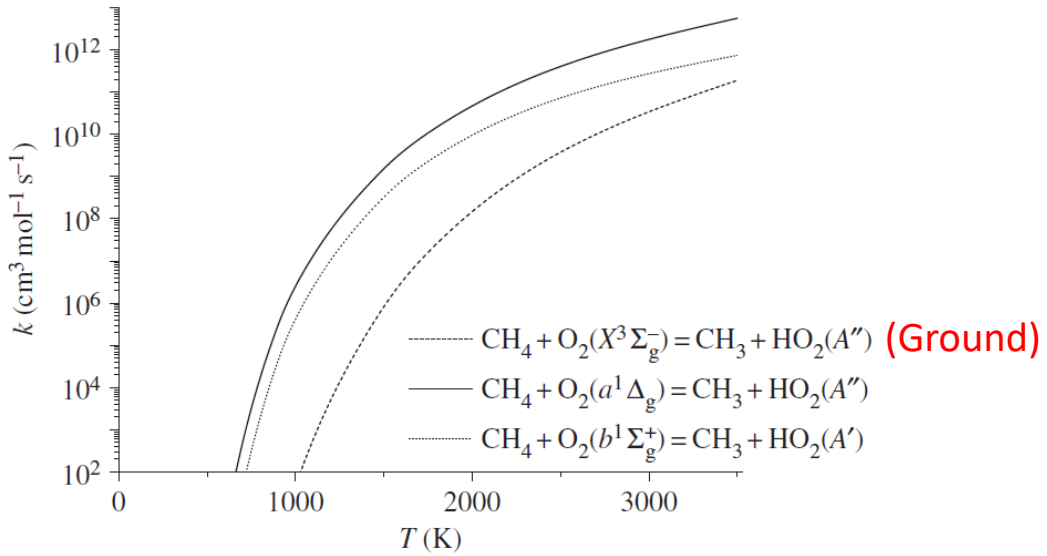


(Ground)

Important radical production channels

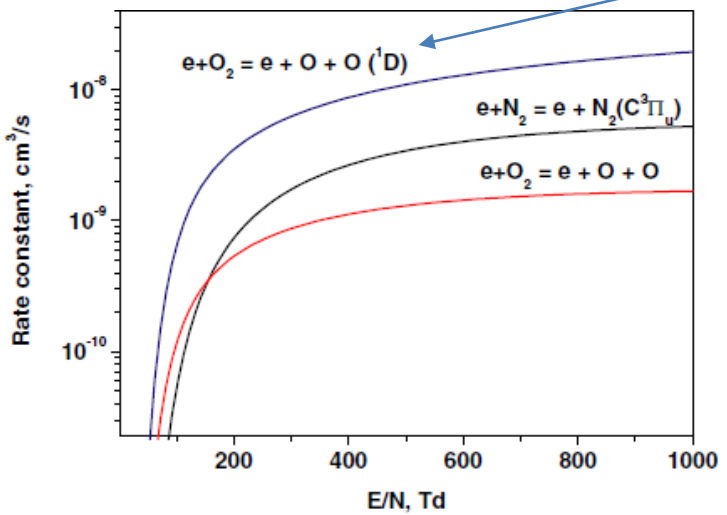


**S M Starikovskaia,** J. Phys. D: Appl. Phys. **47** (2014) 353001

A. M. Starik, B. I. Loukhovitski, A. S. Sharipov and N. S. Titova, *2016, Phil. Trans. R. Soc. A* **373**: 20140341

# PAC: how does plasma change the branching reactions in combustion?

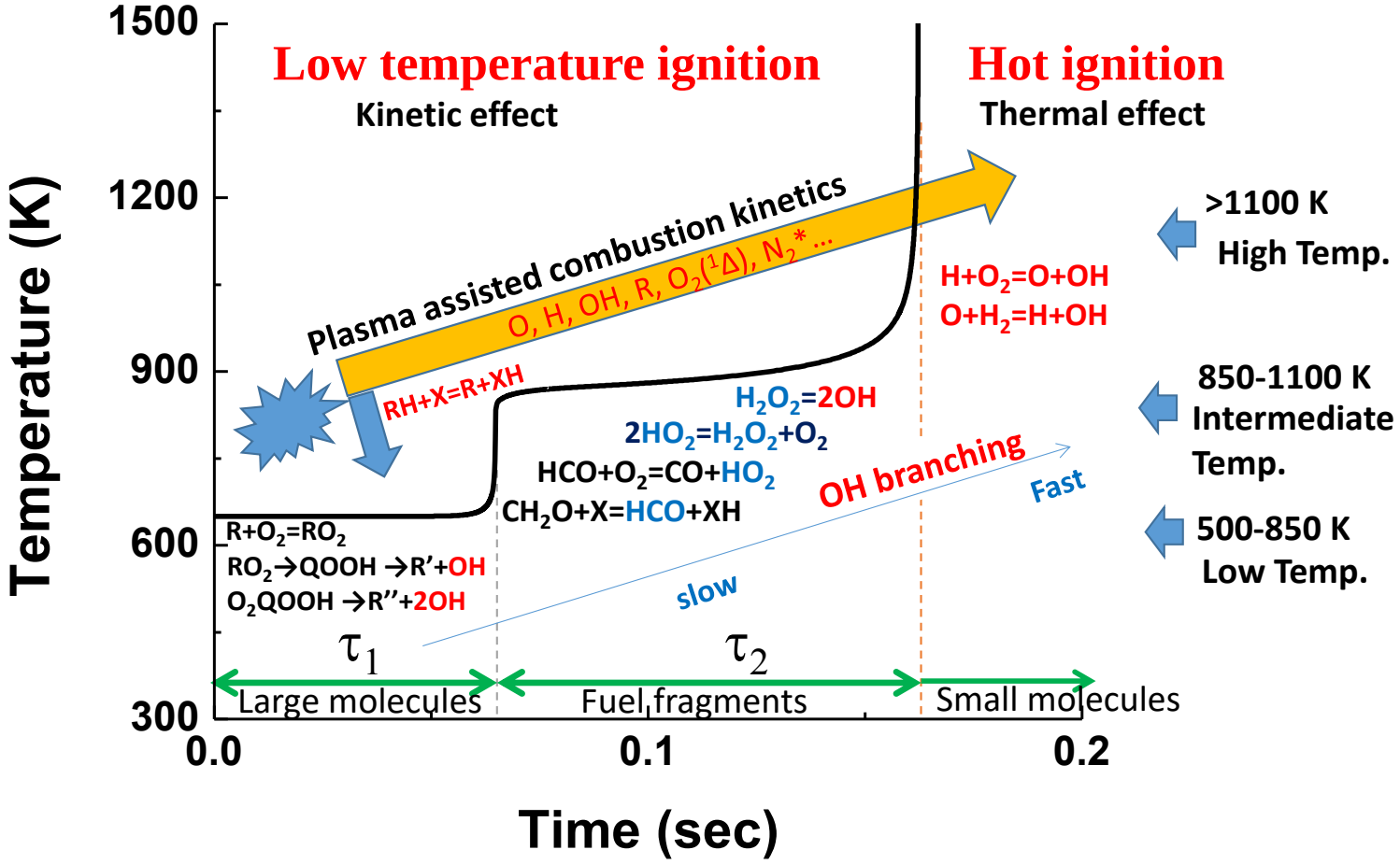


Schematic of kinetic and thermal enhancement pathways of plasma assisted combustion for liquid fuels at high, intermediate, and low temperature, respectively

Y. Ju and W. Sun, Prog. Energy Combust. Sci., 2015

# Plasma activated *Cool Flames* :A new way to burn with plasma

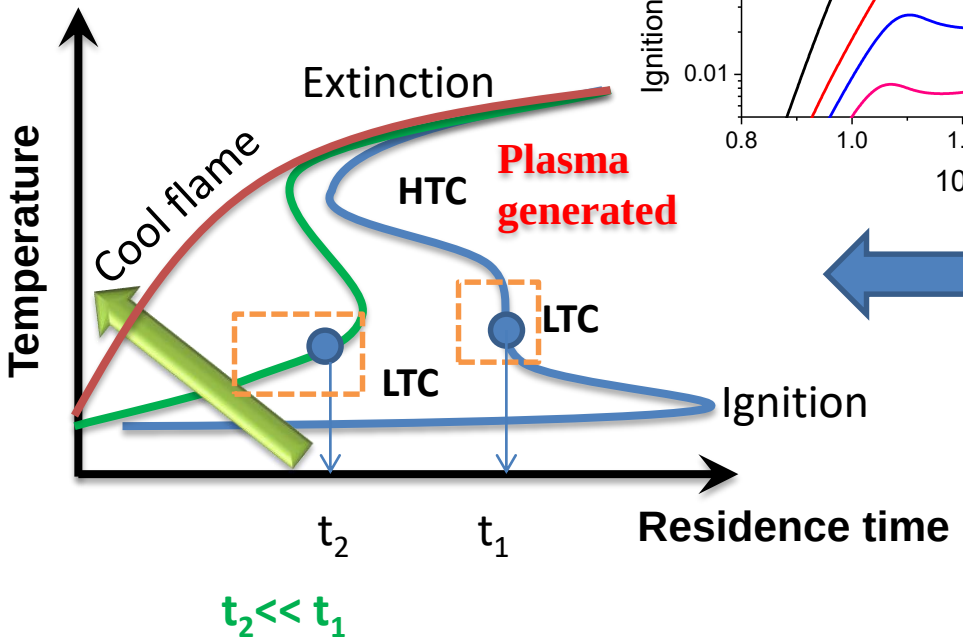


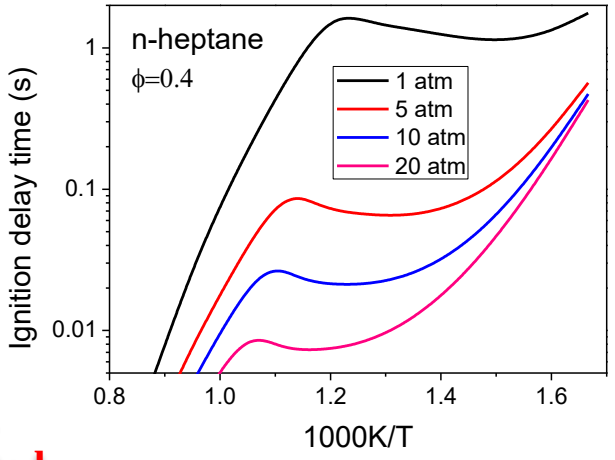


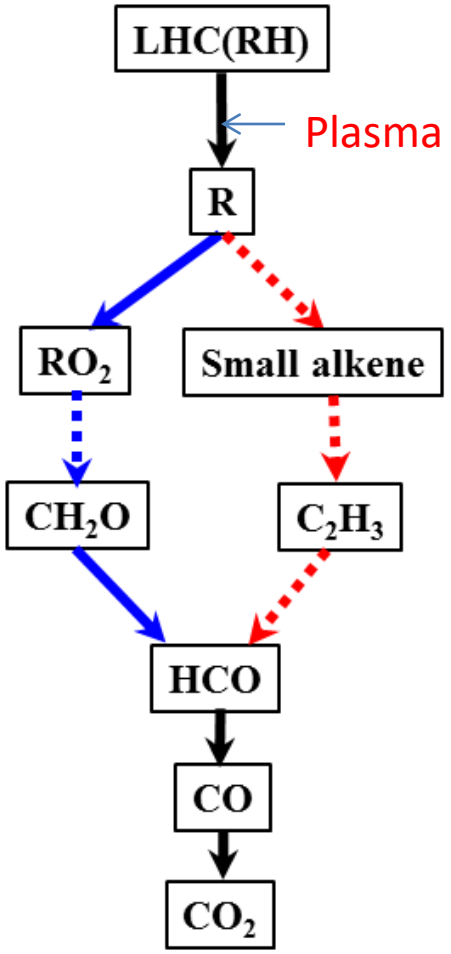


Plasma activated LTC at much shorter time, lower pressure….

We can create cool flames even at 1 atm or below?

# Observation of plasma activated self-sustaining *Cool Flames*

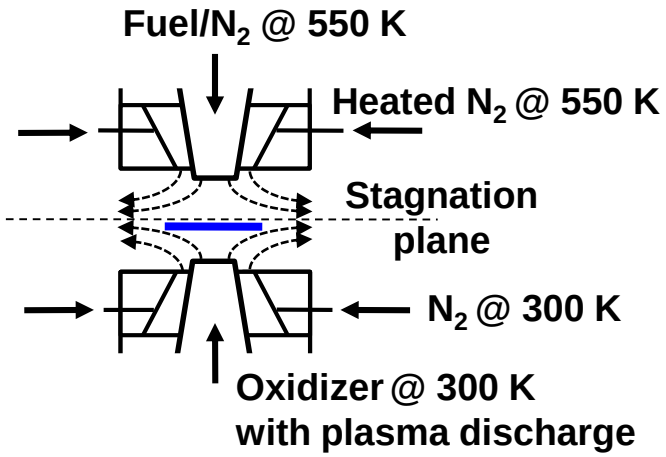


Fig. 1 Schematic of experimental setup

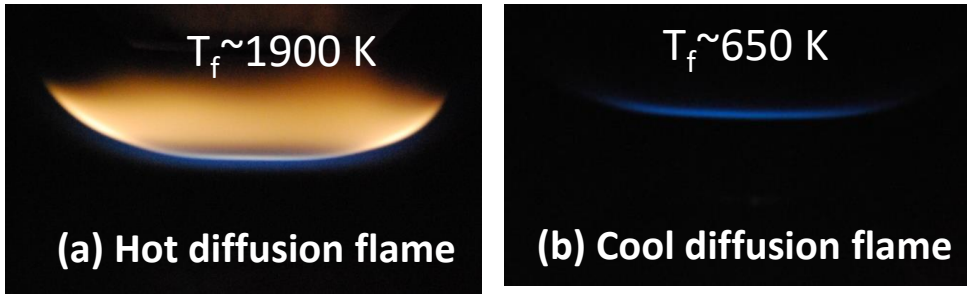


Fig. 2 Hot and cool n-heptane diffusion flames at the same condition

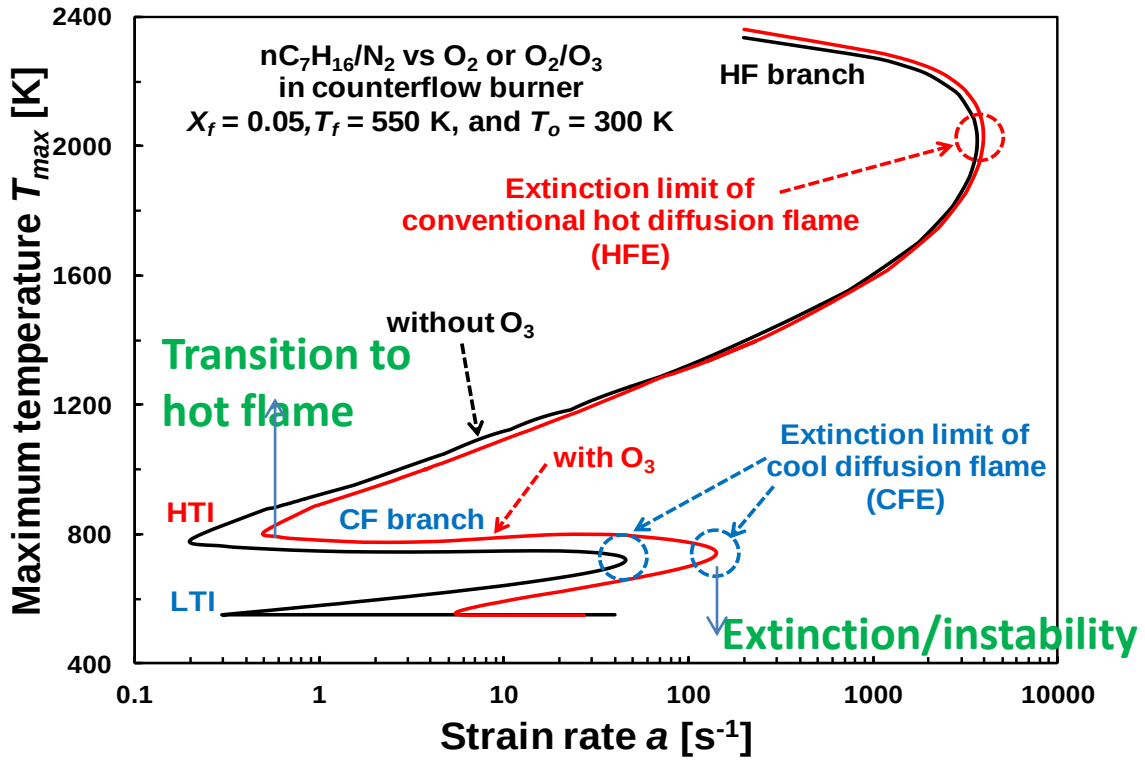



Won, S.H., Jiang, B., Diévart, P., Sohn, C.H. and Ju, Y., 2015. *Proceedings of the Combustion Institute*, *35*(1), pp.881-888.

# Plasma assisted Self-Sustaining Premixed/partially premixed Cool Flames

- Cool diffusion flames
  - n-Heptane/$O_2$/$O_3$
  - Won et al., *Proc. Combust. Inst.* 2015

- Cool premixed flames
  - DME/$O_2$/$O_3$
  - Reuter et al., *Combust. Flame* 2016

- Cool partially premixed flames
  - DME/$O_2$/$O_3$
  - Reuter et al., *Proc. Combust. Inst.* 2017 (hopefully)

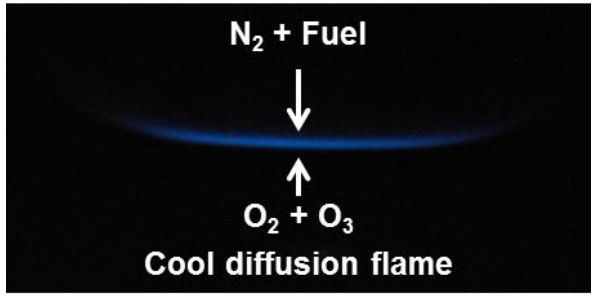


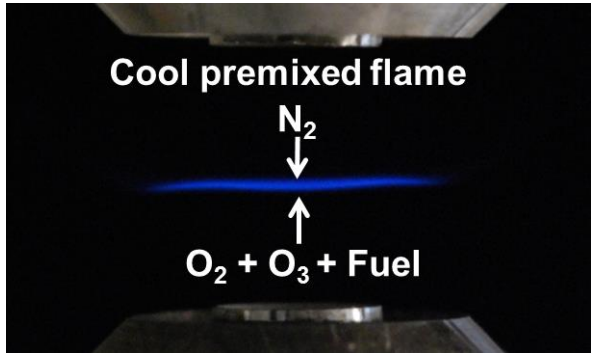


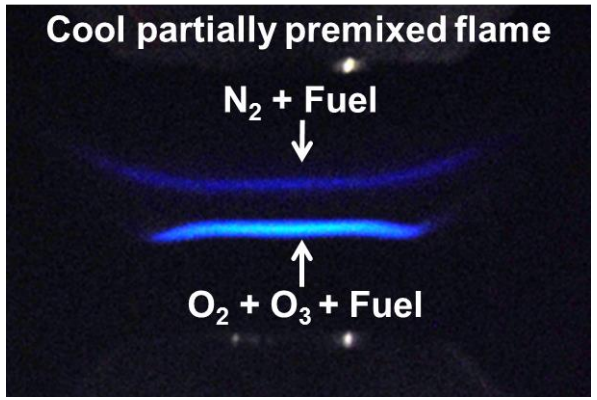


S. H. Won et al., *Proc. Combust. Inst.* 35 (2015) 881-888
C. B. Reuter et al., *Combust. Flame* (2016), in press

# 4. Diagnostics of plasma physics and chemistry in PAC

1. Measurements of plasma properties and kinetic processes

2. Plasma assisted ignition and combustion with active species production

3. Kinetic studies of plasma assisted combustion

# 1. Measurements of Plasma Properties: electron density and temperature Thomson scattering

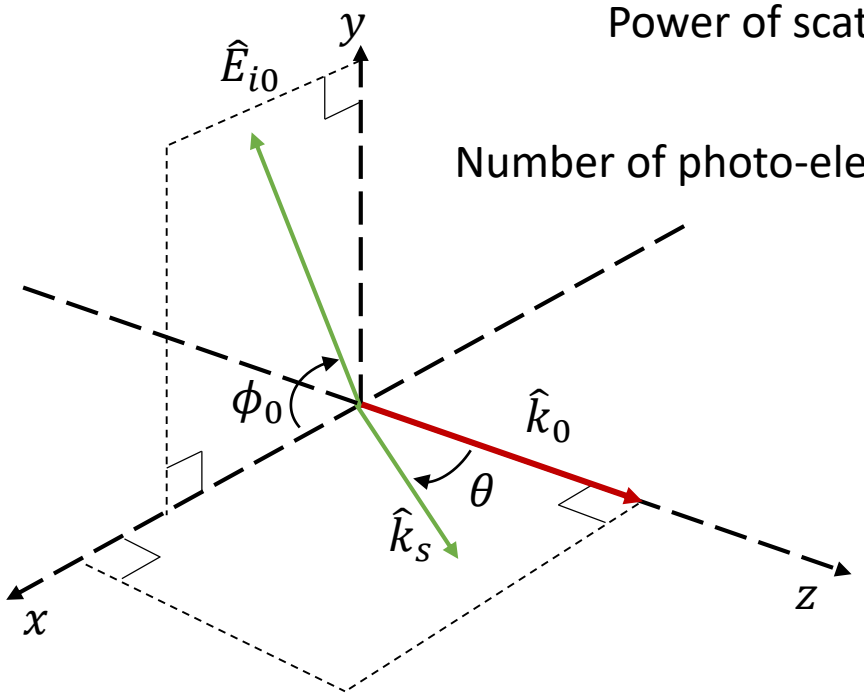


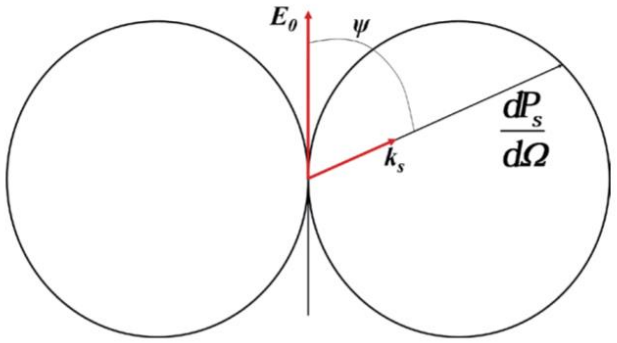


Power of scattering: $P_s \propto 1 - \sin^2\theta \cos^2\phi_0$

Number of photo-electrons: $N_s = \frac{E_L}{h\nu_0} \Delta L \, n_e \frac{d\sigma_e}{d\Omega} \eta$

$$n_e = \frac{\frac{A_e}{A_{N_2}} \left(\frac{d\sigma_{N_2}}{d\Omega}\right)_{532nm}}{\frac{d\sigma_e}{d\Omega}} n_{N_2} f_{J=6}$$

$$\Delta\lambda_{1/e} = \frac{2\lambda_0}{c} \sin\left(\frac{\theta}{2}\right) \left(\frac{2k_B T_e}{m_e}\right)^{\frac{1}{2}}$$

$$T_e = \frac{c^2 m_e}{8k_B \sin^2(\theta/2)} \left(\frac{\Delta\lambda_{1/e}}{\lambda_0}\right)^2$$

$k_0$: Laser beam direction, $k_s$: Scattering signal wave vector

$\hat{E}_{i0}$: Polarized electric field, scattering is rotationally symmetric about $\hat{E}_{i0}$.

x-z plane: the plane of observation

θ: the scattering angle relative to the laser beam.

$\phi_0$: angle between observation plane and the polarization angle.

$A_e$ and $A_{N_2}$: integrated intensities of the Thomson and Raman spectra

$\frac{d\sigma_e}{d\Omega}$ and $\frac{d\sigma_{N_2}}{d\Omega}$ the Thomson and $N_2$ Raman scattering cross sections

$f_{J=6}$: the fraction of $N_2$ molecules in the J = 6 rotational state

$\Delta\lambda_{1/e}$: the half 1/e width of the Gaussian broadening profile

$E_L$: laser energy, η: optical efficiency, ΔL: length of observed scattering segment.


- H. Van der Meiden, "Thomson scattering on low and high temperature plasmas", Ph.D, Technische Universiteit Eindhoven, 2011.
- A. Roettgen, "Vibrational Energy Distribution, Electron Density and Electron Temperature Behavior in Nanosecond Pulse Discharge Plasmas by Raman and Thomson Scattering", Ph.D, The Ohio State University, 2015.

# Thomson Scattering Experimental Setup and Calibration

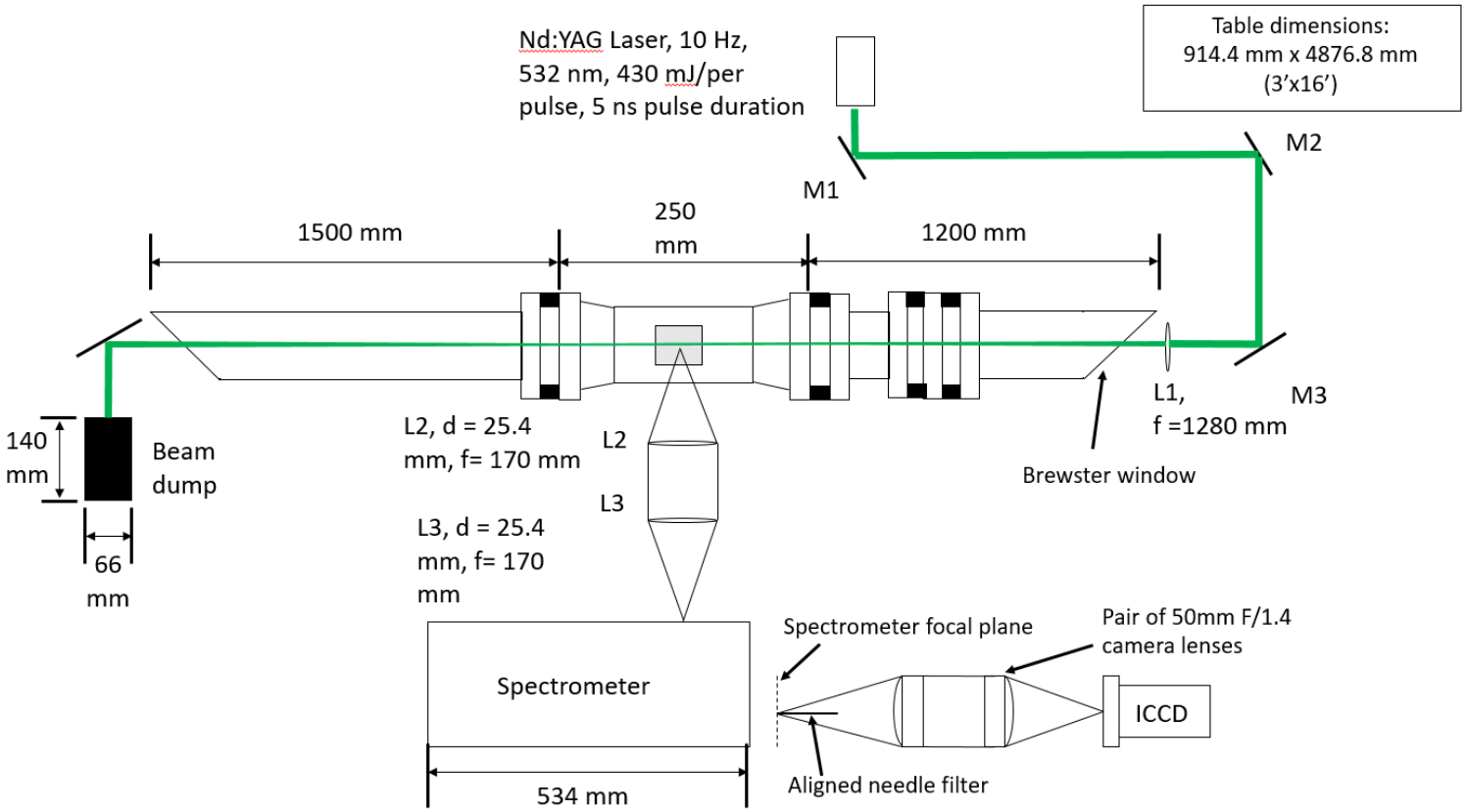


Timothy Chen, Princeton, 2017

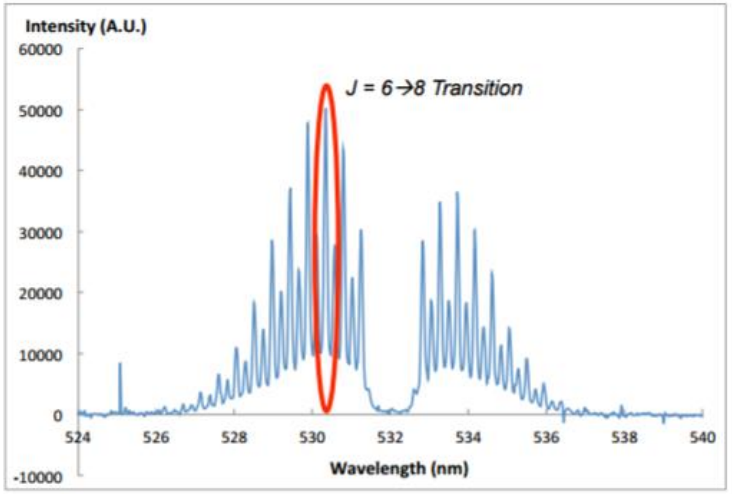


Roettgen (2015): use Rotational Raman Scattering for calibration using the J = 6 → 8 transition of $N_2$ at P = 100 Torr

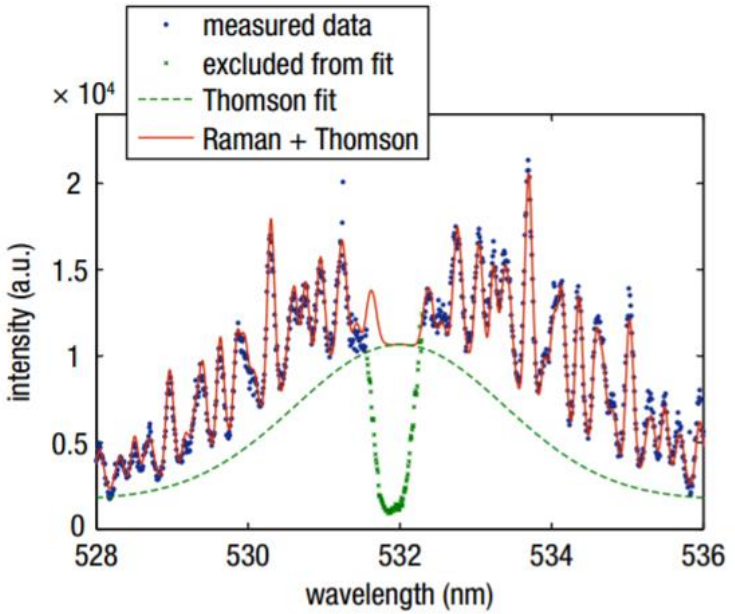


Decoupling Raman and Thomson Signals

A. van Gessel, E. Carbone, P. Bruggeman and J. van der Mullen, *Plasma Sources Science and Technology*, vol. 21, no. 1, p. 015003, 2012.

# Filtered Thomson Scattering: $n_e$ , $T_e$, and EEDF inference

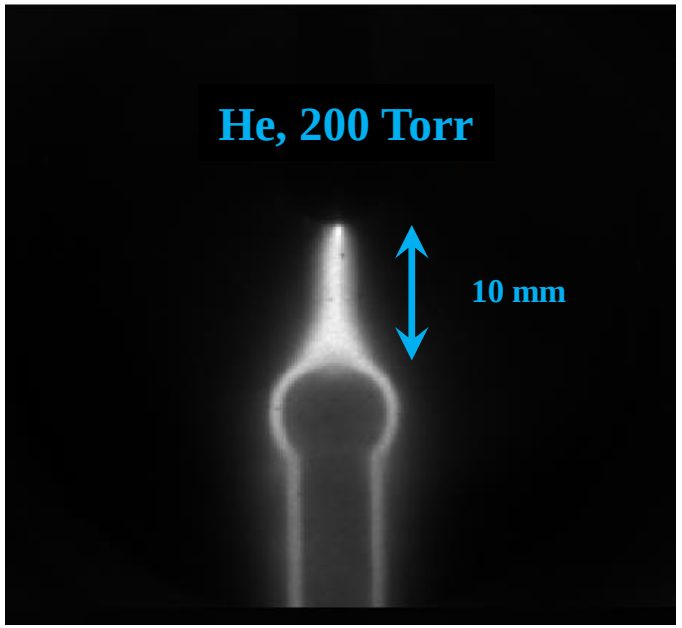


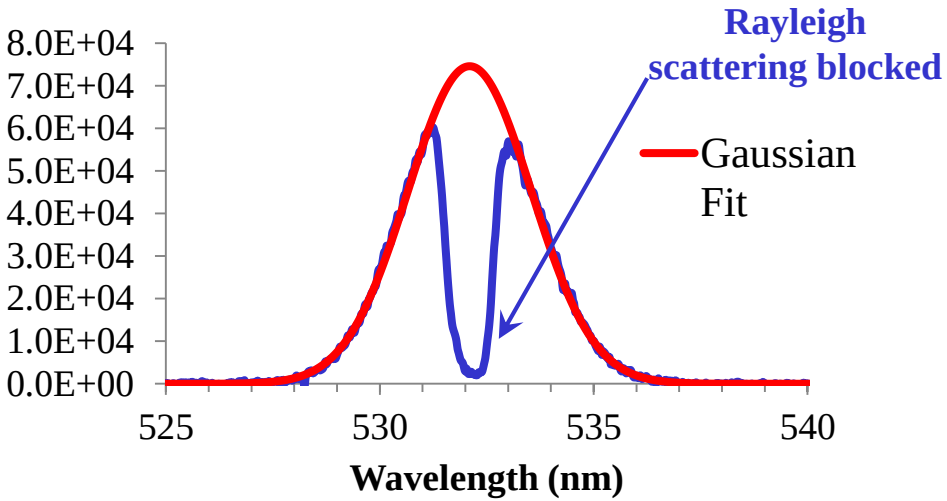


$N_2$ Raman scattering

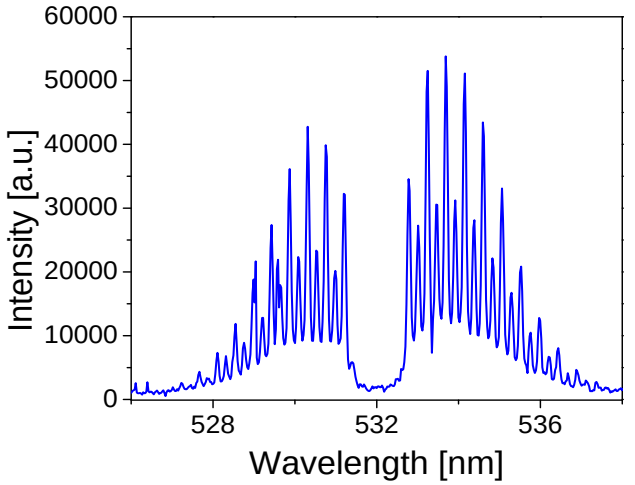


- Electron density: area under Thomson scattering spectrum
- Electron temperature: spectral linewidth
- Gaussian scattering lineshape: Maxwellian EEDF
- Raman scattering rotational transitions in $N_2$ used for absolute calibration

Courtesy of Prof. Igor V. Adamovich

# Thomson Scattering Spectra

## Ns pulse discharge in $H_2$-He and $O_2$-He, P=100 Torr

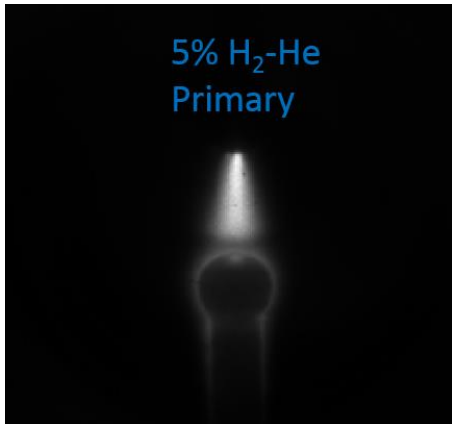


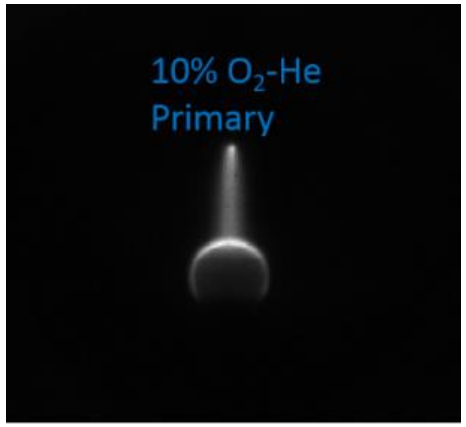


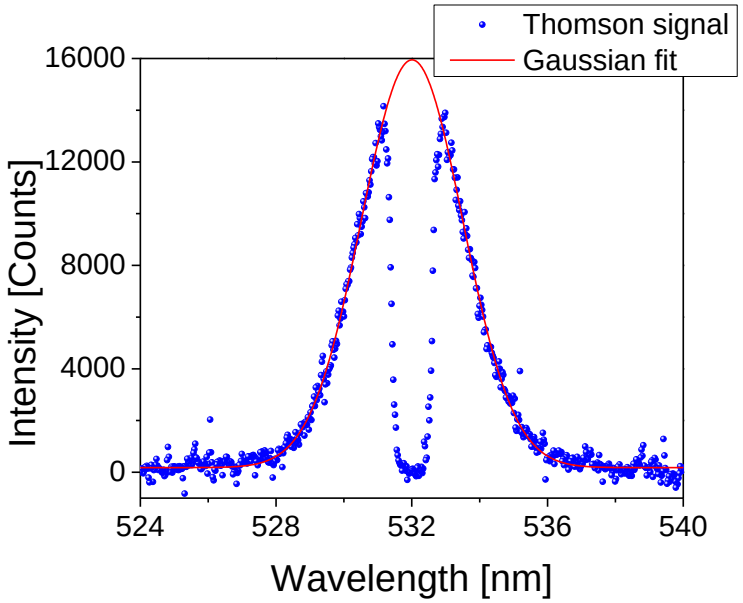


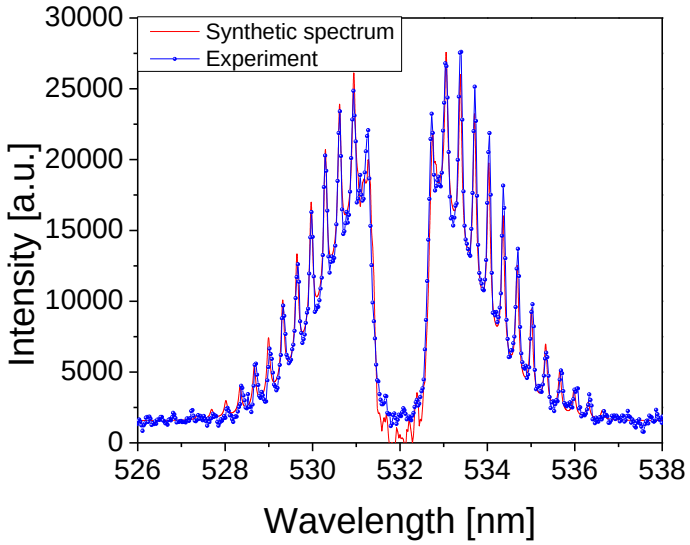


**5% $H_2$-He,**

**$n_e = 1.5 \cdot 10^{14}$ cm$^{-3}$, $T_e = 2.0$ eV**

**10% $O_2$-He**

**$n_e = 1.7 \cdot 10^{13}$ cm$^{-3}$, $T_e = 1.6$ eV, T=350**

# Electron Density and Electron Temperature

## Ns pulse discharge in $O_2$-He

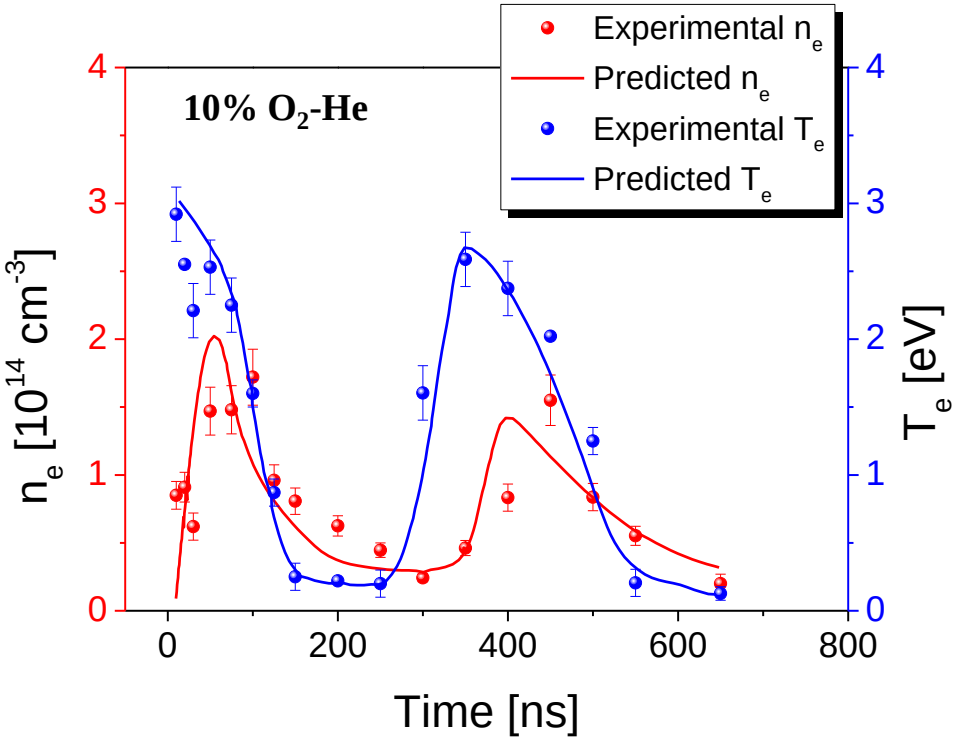


- "Double maxima" in $n_e$, $T_e$ : two discharge pulses ≈ 400 ns apart
- Electron temperature in the afterglow $T_e$ ≈ 0.3 eV (controlled by superelastic collisions)
- Modeling predictions in good agreement with data
- Measurements in air are more challenging (strong interference from $N_2$, $O_2$ Raman scattering)

# Measurements of electron number density

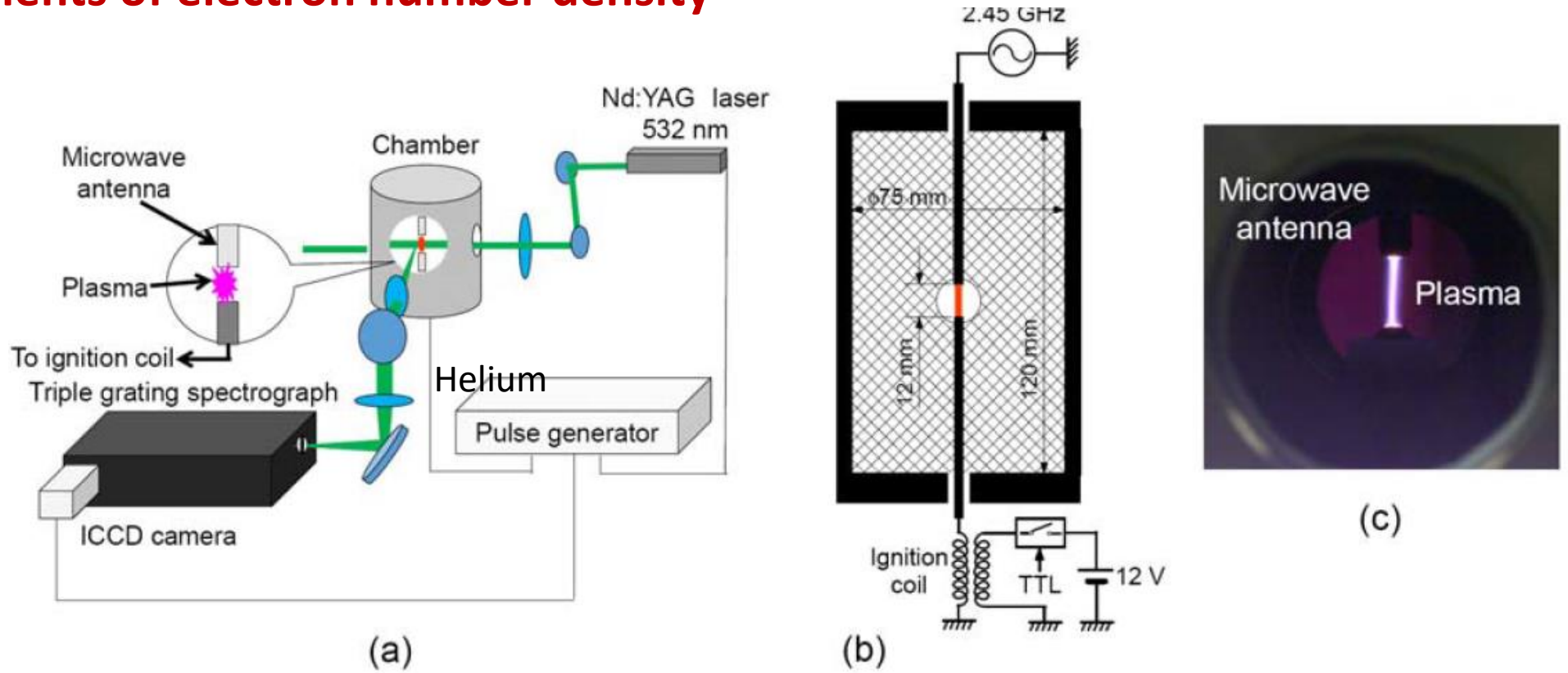


**Fig. 1** Experimental apparatus: (a) schematic of the entire experimental system including the plasma source and the system of laser Thomson scattering, (b) details of the plasma source, and (c) picture of the microwave helium discharge.

K. Sasaki et al., Contrib. Plasma Phys. 55, No. 8, 563 – 569 (2015)

**Thomson scattering profile (Broadening):**

$$\Delta\nu_D' = \frac{2\nu_0}{c}\sqrt{\frac{2\ln(2)k_B T_e}{m_e}}\sin\left(\frac{\theta}{2}\right)$$

$$n_e = \frac{A_e}{A_{He,J}}\frac{\left(\frac{d\sigma}{d\Omega}\right)_{532nm}}{\left(\frac{d\sigma_2}{d\Omega}\right)} n_{He} f_J$$

$\theta$: the scattering angle relative to the laser beam.

$A_e$ : integrated Thomson scattering signal intensity

$A_{He,J}$ : integrated He J level Raman transition intensity

$f_J$ : relative J level population fraction in distribution function

# Measured electron energy distribution, temperature, and number density

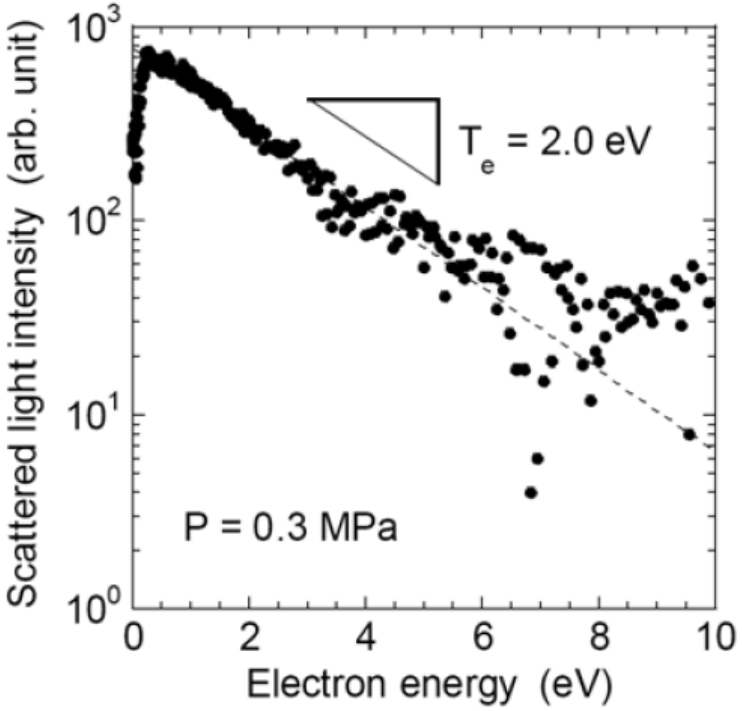


Fig.1Typical electron energy distribution function measured by laser Thomson scattering in a microwave helium plasma at a pressure
of 0.3 MPa.

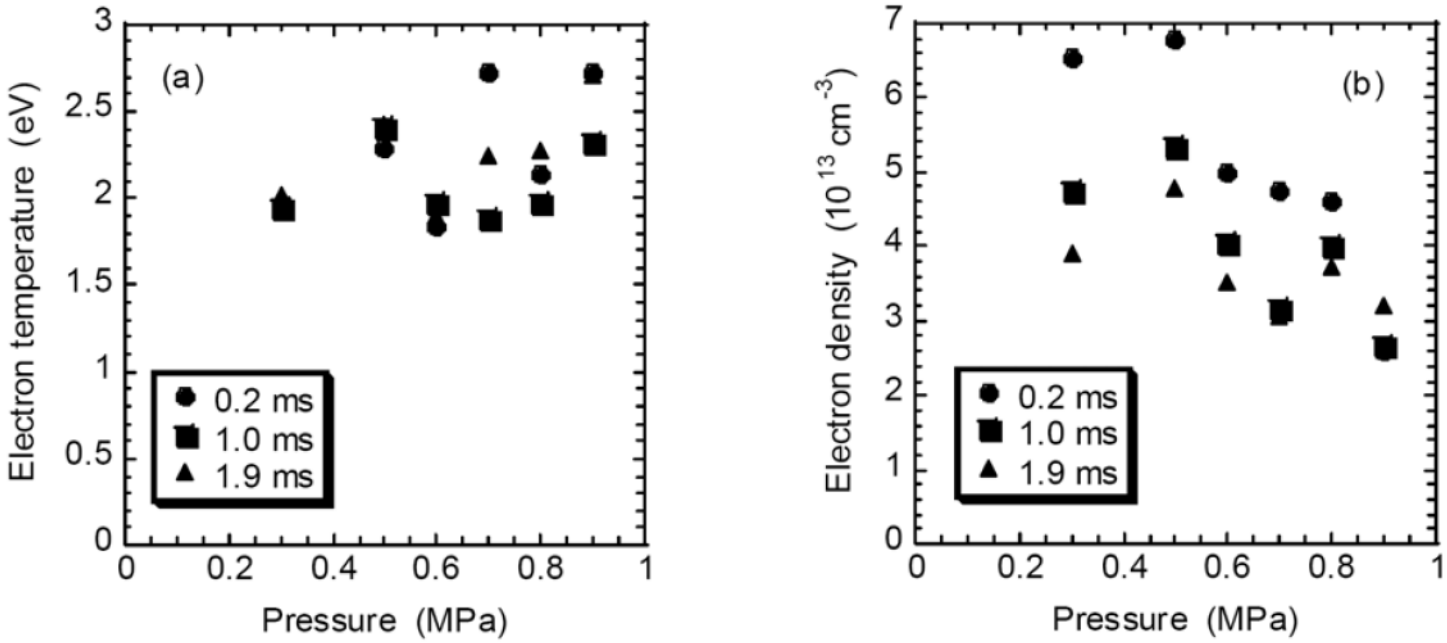


Fig.2 Pressure dependences of (a) the electron density and (b) the electron temperature. Values observed at three delay times after the initiation of the microwave power are plotted.

- Thomson scattering is its weak scattering signal intensity owing to the low number density of free electrons in the plasma.
- Strong interference from Rayleigh scattering as well as plasma emission

K. Sasaki et al., Contrib. Plasma Phys. 55, No. 8, 563 – 569 (2015)

# Femtosecond Localized E-Field Measurement (FLEM)

Mechanical and Aerospace Engineering
Applied Physics Group

- In a centrosymmetric medium, second harmonic generation is impossible
- Applying an electric field destroys that symmetry allowing for E-Field measurements
- Benefits of FLEM Method:
  - Signal scales as $E^2$
  - Works well at higher pressure
  - Time resolution determined by pump beam duration
  - Non-resonant method works in any species and gas mixtures
  - Spatial resolution determined by beam focusing parameter

- Described as a third order nonlinear process:
  - $I^{(2\,\omega)} \propto N^2 (E_{Ext})^2 (I_{Pump})^2$
    - $I^{(2\,\omega)}$ : Second Harmonic Intensity
    - N: Number Density
    - $E_{ext}$: Applied Field to be Measured
    - $I_{Pump}$: Pump Beam Intensity

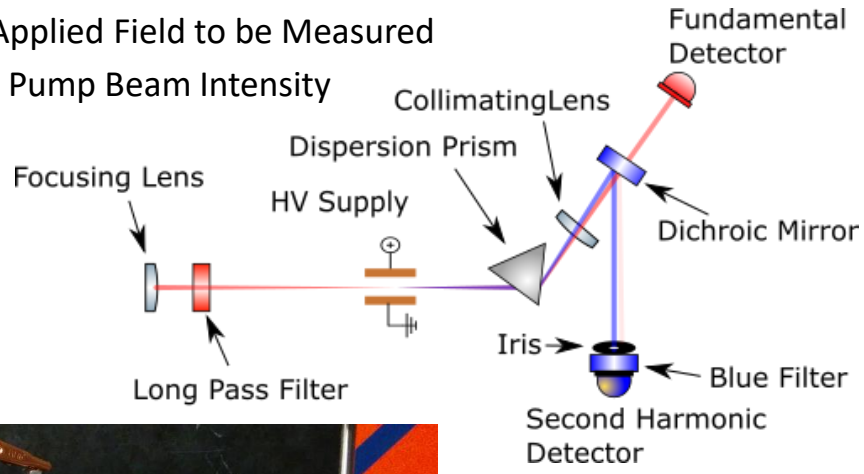


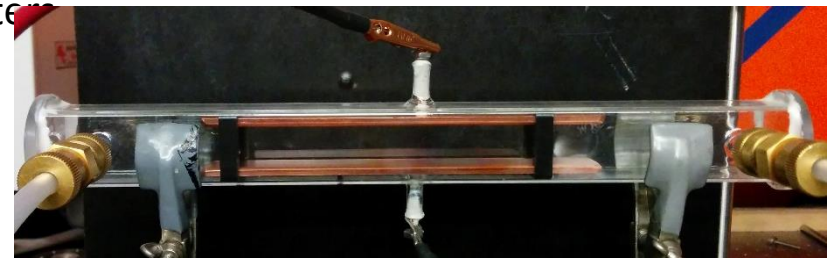

Courtesy of Prof. Richard Miles, Princeton

# Femtosecond Localized E-Field Measurement (FLEM)

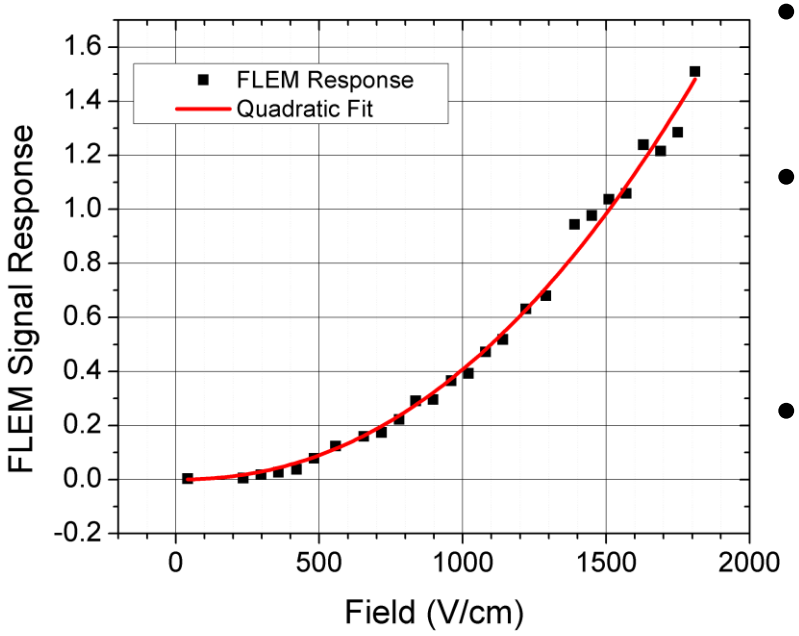


- Sub-breakdown electric field applied
- SHG response, pump intensity, current and voltage monitored
- Quadratic dependence verified
  - We have measured down to 100V/cm in room air

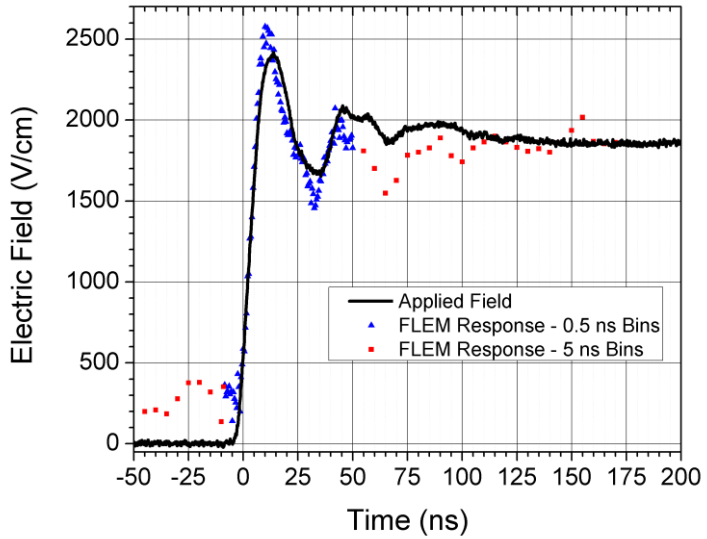


- **Fs laser pulse acts as a δ function compared with ns high voltage pulses**
- **Temporal resolution determined by oscilloscope rather than a physical limit**

Courtesy of Prof. Richard Miles, Princeton

# Electric Field Measurements in 2-D Ns Pulse Discharge in Atmospheric Air

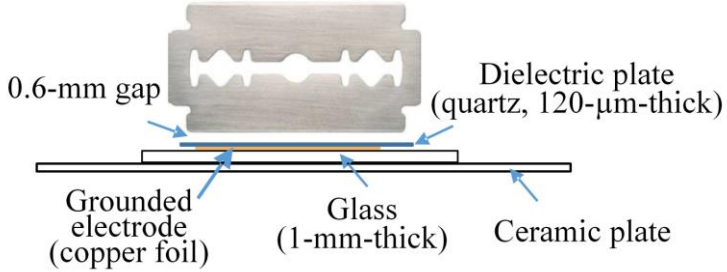


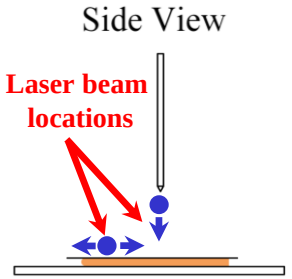


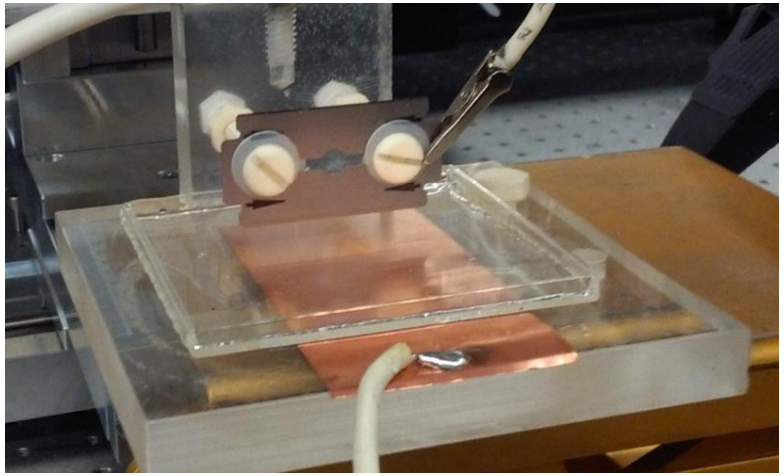

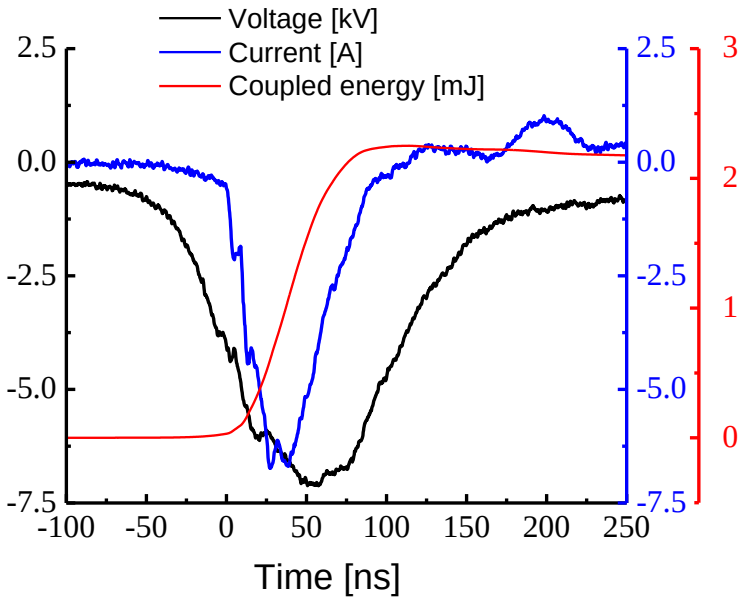


- Ns pulse discharge between a high-voltage electrode and a thin quartz plate
- Discharge gap 0.6 - 1.0 mm, two-dimensional geometry, diffuse plasma
- Time-resolved electric field measured at multiple locations in the discharge gap

# “Curtain Plasma” Images, Negative Polarity Pulse

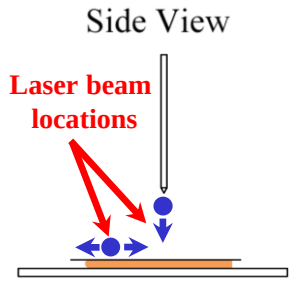


Front view, 100 ns gate

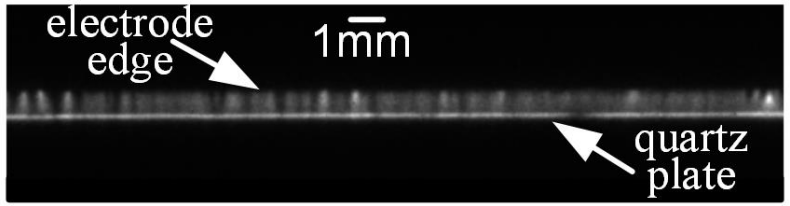


Side view, 2 ns gate

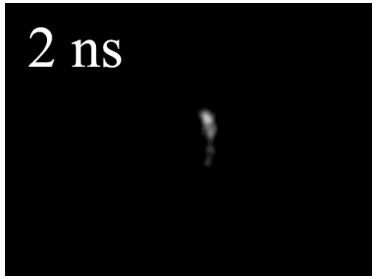


Top view, 2 ns gate

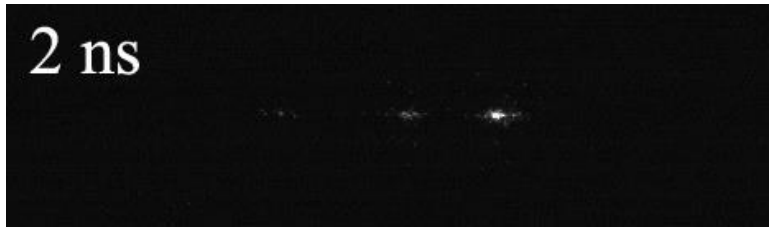


- Surface ionization wave plasma ~ 200 μm thick, wave speed ~ 0.03 mm/ns
- Electric field measured by picosecond four-wave mixing (calibration by electrostatic field)
- Time resolution 2 ns, spatial resolution across laser beam ~ 100 μm
- Objective: electric field mapping in ns pulse discharges in high-pressure fuel-air mixtures

# Electric Field Vector Components in a Surface Ionization Wave Discharge

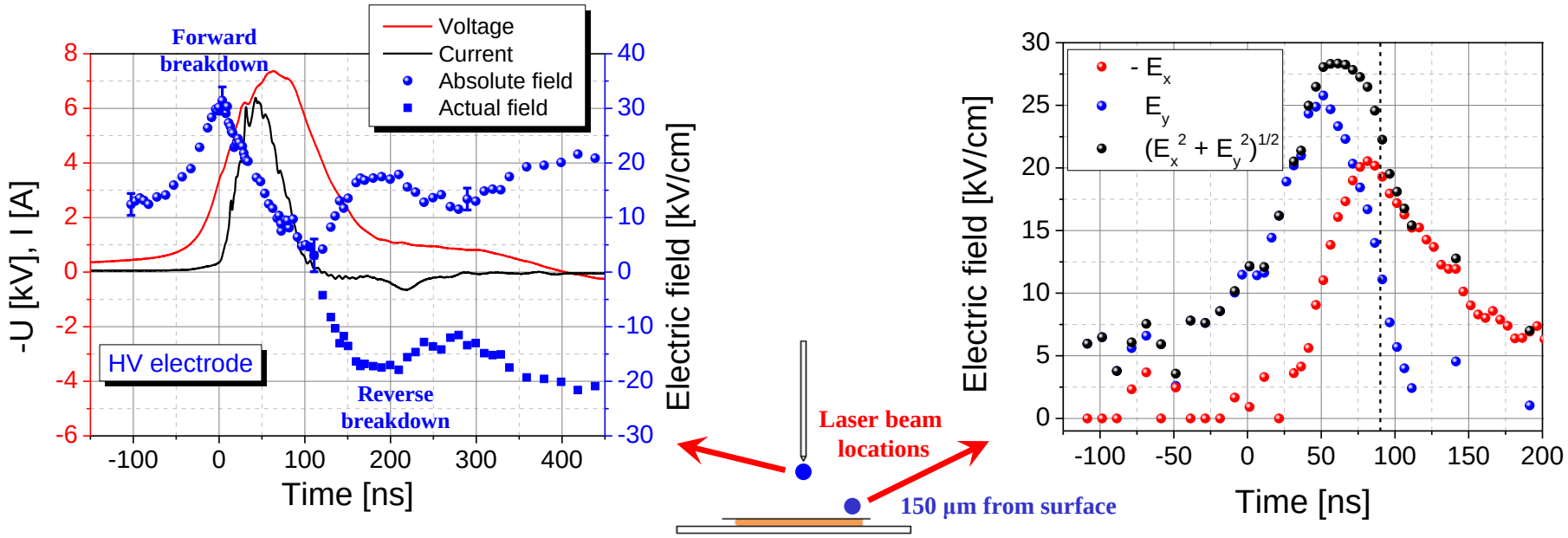


- Initial field offset (at t < 0): charge accumulation on dielectric from previous pulse
- Field follows applied voltage rise, increases until "forward breakdown"
- After breakdown, field reduced due to charge accumulation on dielectric
- Field is reversed after applied voltage starts decreasing
- Away from HV electrode, field peaks later ($E_y$ before $E_x$): surface ionization wave
- Measurements in a hydrogen-air diffusion flame underway

# Plasma property measurements using H2/Ar emission lines

$^3D_1, ^3D_2, ^3D_3,\ \ ^3P_0, ^3P_1, ^3P_2,\ \ ^3S_1,\ \ ^1D_2, ^1P_1, ^1S_0,$

$3s^23p^54p^1$

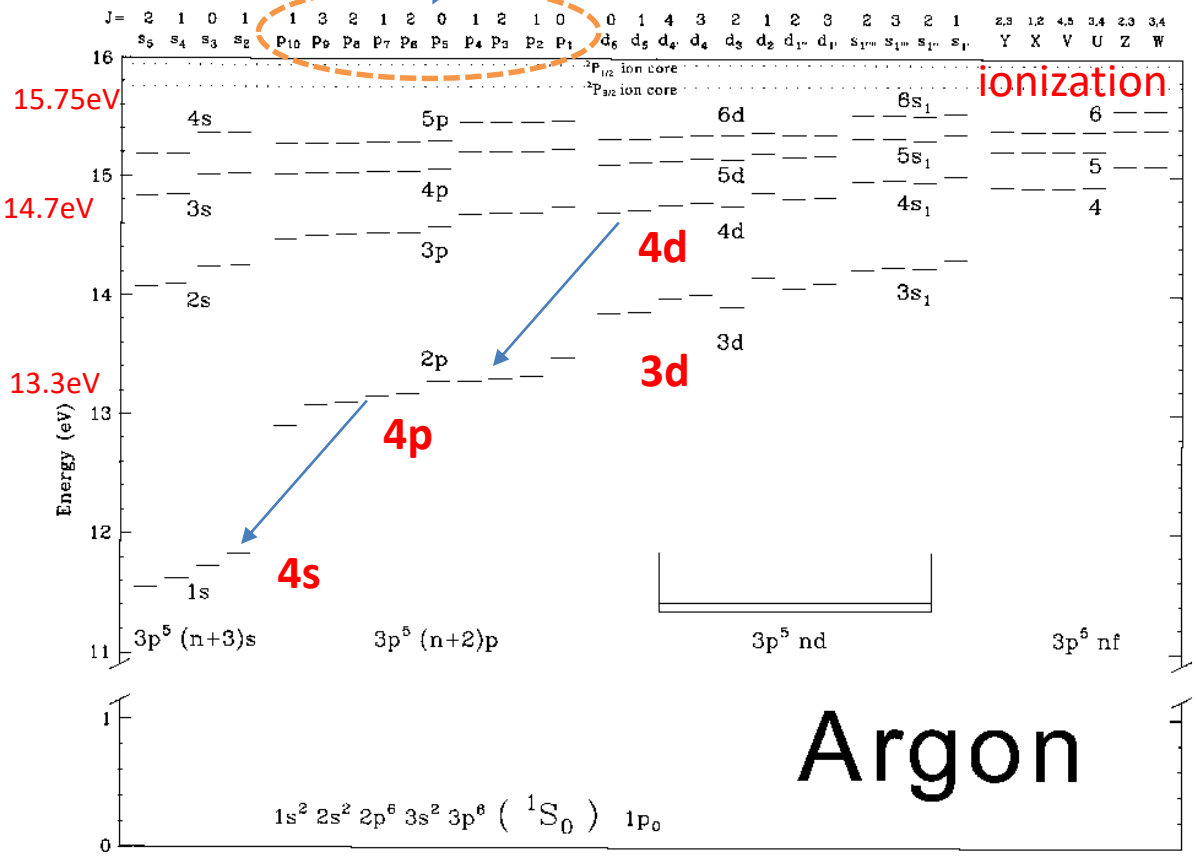


**L-S coupling**

**$3s^23p^6 \leftrightarrow 3s^23p^54S^1$**

$$L = l_1 + l_2 = 1 + 0 = 1$$

$$J = L + S, \ldots |L - S| = 2,1,0$$

$$Term: \ ^3P_0, ^3P_1 \ ^3P_2$$

$$S = S_1 - S_2 = 1/2 - 1/2 = 0$$

$$J = L + S, \ldots |L - S| = 1$$

$$Term: \ ^1P_1$$

**$3s^23p^6 \leftrightarrow 3s^23p^54p^1$**

$$\vec{L} = \vec{l_1} + \vec{l_2} = \vec{1} + \vec{1} = 0,1,2 \text{ (any quantum number)}$$

$$\vec{S} = \vec{s_1} + \vec{s_2} = \frac{\vec{1}}{2} + \frac{\vec{1}}{2} = 0,1$$

$$J = L + S, \ldots |L - S| = \underbrace{2,1,0,}_{S=0} \ \underbrace{1, \ \ 2,1,0, \ \ 3,2,1}_{S=1}$$

$$Term: \ ^1S_0, ^3S_1, \ \ ^1P_1, ^3P_0, ^3P_1, ^3P_2, \ \ ^1D_2, ^3D_1, ^3D_2, ^3D_3$$

# Stark broadening of hydrogen lines and Ar optical emission line-ratio method

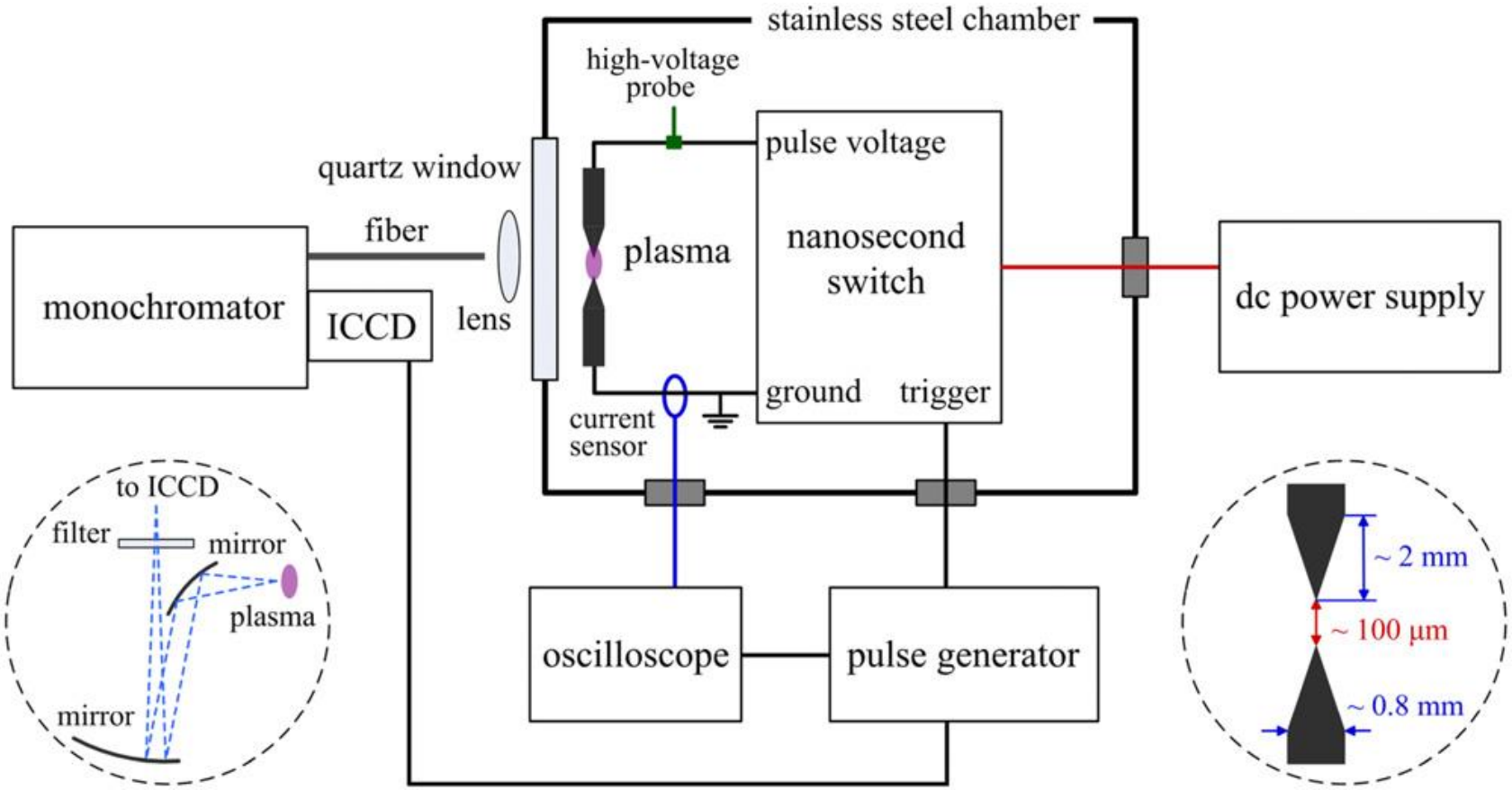


Schematic diagram of the experimental setup. The spatially resolved optical measurement system is shown on the left bottom. On the right bottom is a zoom-in figure showing the stainless steel needle tips and the discharge gap.

Xi-Ming Zhu, James L Walsh, Wen-Cong Chen1 and Yi-Kang Pu, J. Phys. D: Appl. Phys. 45 (2012) 295201 (11pp)

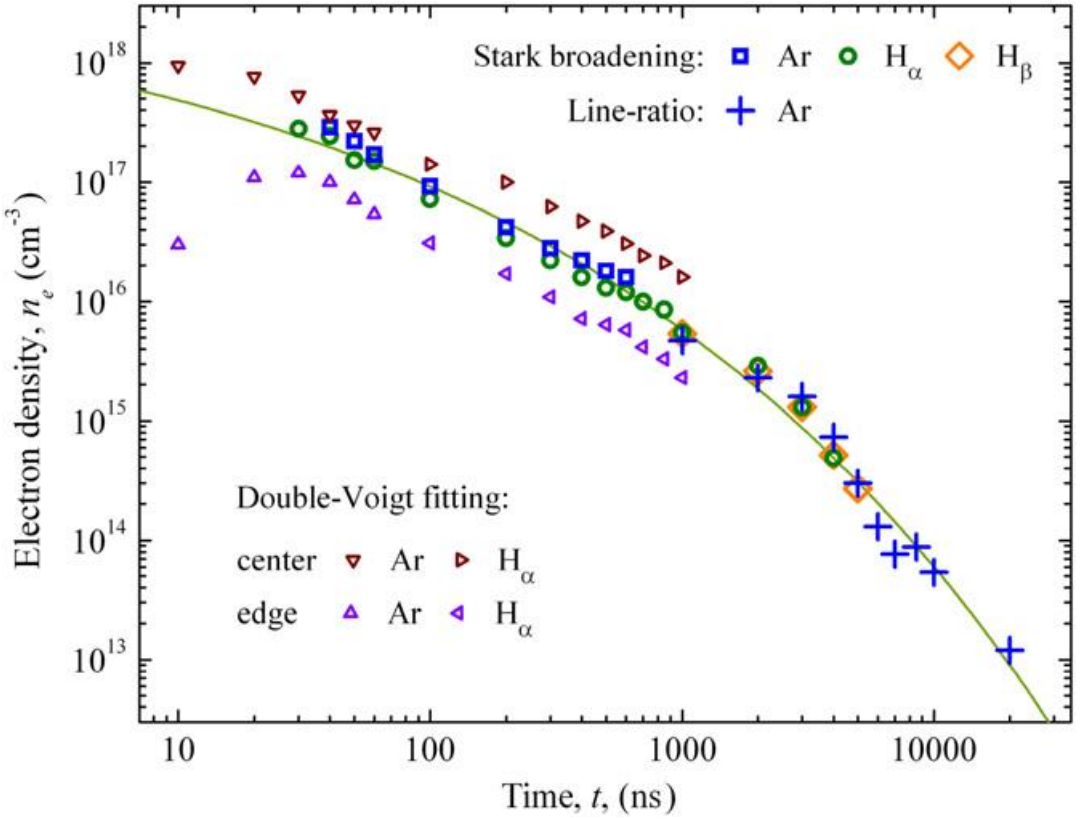


Experimentally measured electron densities in a high-pressure nanosecond pulsed microplasma (Ar/Ne = 700/30 Torr, discharge current lasts for about 100 ns, pulse period 1 ms). In the legend on the right top, 'line ratio' refers to the line-ratio method and 'Stark broadening' refers to the Stark broadening method using Ar 696.5 nm, H*α* and H*β* lines with a single-Voigt fitting procedure. In the legend on the left bottom, 'centre' and 'edge' denote *n*e,centre and *n*e,edge obtained with double-Voigt fitting. The solid line shows a function, *n*e = 6 × 1018 × exp*(−(t/*0.15*)*0.22*)*, where *n*e and *t*are in units of cm−3 and ns, respectively.

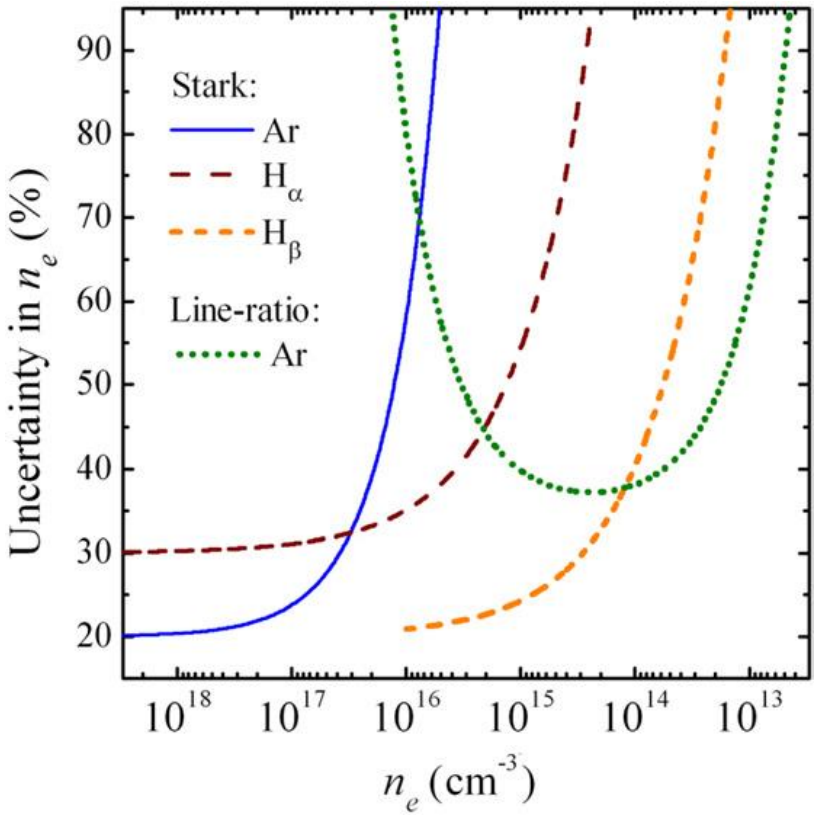


Uncertainties in the *n*e measurement (%) using the Stark roadening method with Ar 696.5 nm line, H*α* line and H*β* line (for *n*e > 1016 cm−3) and that using the line-ratio method.

Xi-Ming Zhu, James L Walsh, Wen-Cong Chen1 and Yi-Kang Pu, J. Phys. D: Appl. Phys. 45 (2012) 295201 (11pp)

# Measurements of temperature, vibrational level populations and fast heating using picosecond CARS

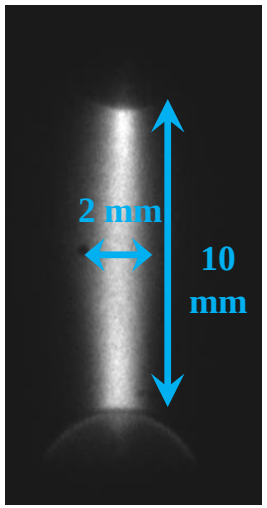


Air, P=100 Torr

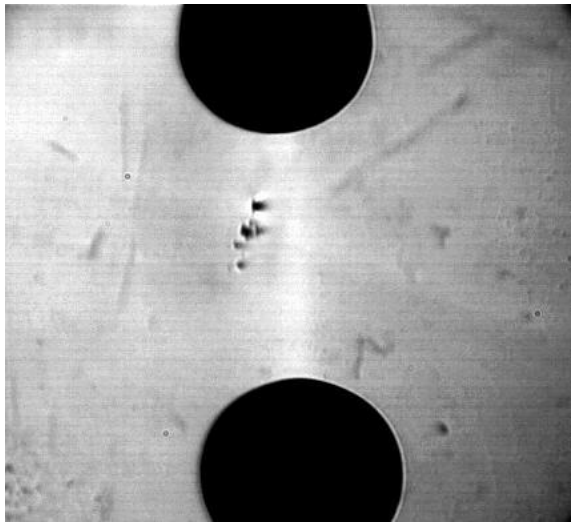

t= 1-10 μs (frames are 1 μs apart)

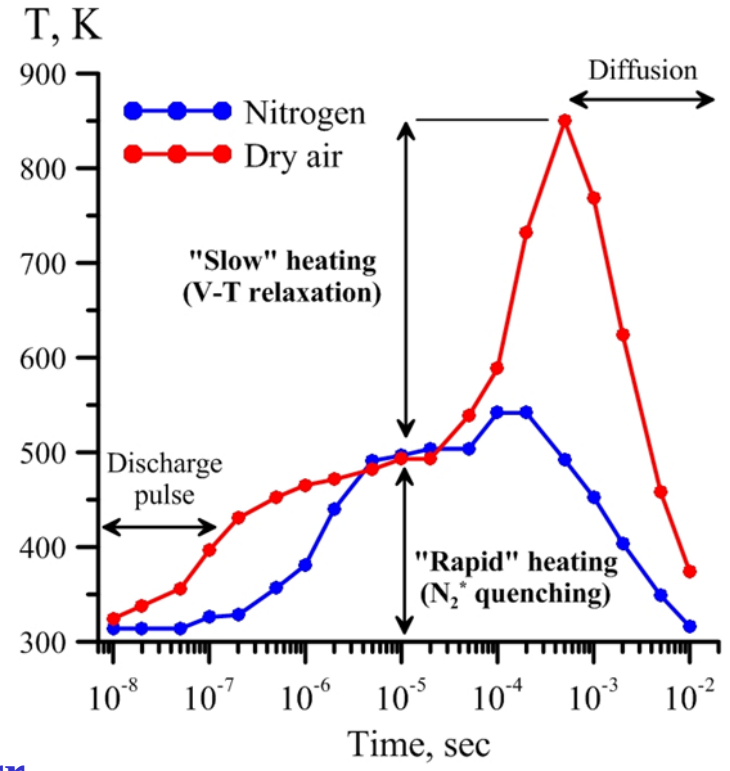


ns pulse discharge and afterglow: Air vs. nitrogen, P=100 Torr

- Compression waves formed by "rapid" heating, on sub-acoustic time scale, $\tau_{acoustic} \sim r / a \sim 2$ μs
- What processes control other features of temperature rise (e.g. "slow" heating")?

# Comparison with modeling predictions in air: vibrational kinetics and temperature rise

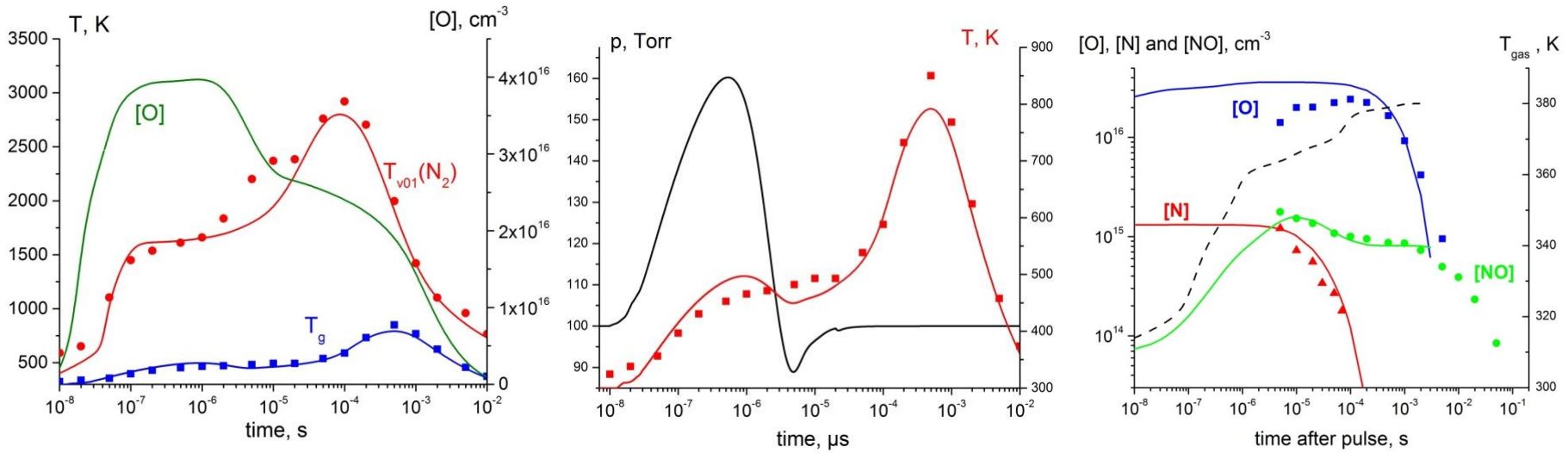


- **Strong vibrational excitation in the discharge, $N_2(v=0\text{-}8)$**
- **$T_v(N_2)$ rise in early afterglow: V-V exchange, $N_2(v) + N_2(v=0) \rightarrow N_2(v\text{-}1) + N_2(v=1)$**
- **$T_v(N_2)$ decay in late afterglow: V-T relaxation, $N_2(v) + O \rightarrow N_2(v\text{-}1) + O$ , radial diffusion**
- **"Rapid" heating: quenching of $N_2$ electronic states, $N_2(C,B,A,a) + O_2 \rightarrow N_2(X) + O + O$**
- **"Slow" heating: V-T relaxation, $N_2(X,v) + O \rightarrow N_2(X,v\text{-}1) + O$**
- **"Rapid" heating: pressure overshoot , compression wave formation**
- **NO formation: dominated by reactions of $N_2$ electronic states, $N_2^* + O \rightarrow NO + N$**

A. Montello, Z. Yin, D. Burnette, I.V. Adamovich, and W.R Lempert, Journal of Physics D: Applied Physics 46 (2013) 464002

# Single-shot measurement rotational and rovibrational energy distributions by Hybrid fs/ps coherent anti-Stokes Raman scattering (CARS) spectroscopy

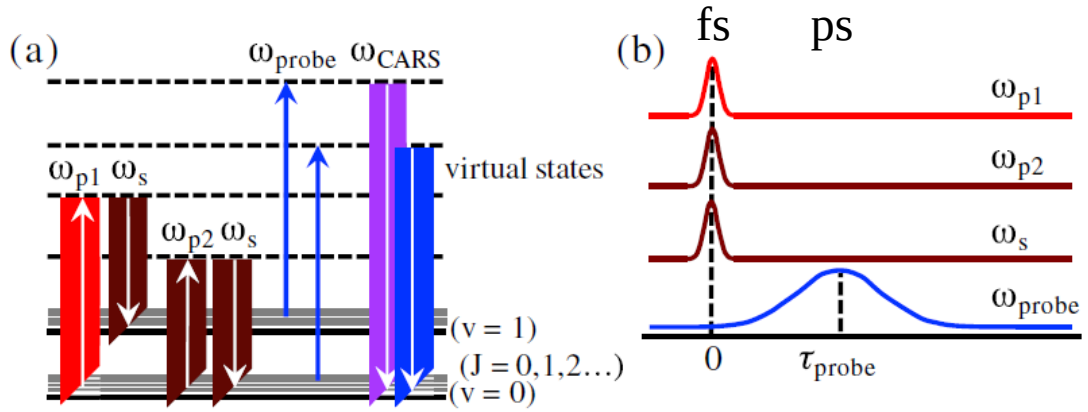


**Fig. 1.** (a) Frequency and (b) timing diagrams for dual-pump fs/ps vibrational/rotational CARS. (Four wave mixing and fs broadband dual pumping

$\omega_{p1}$: Rovibrational Raman transition (Q-branch, Δv=+1, ΔJ =0)
$\omega_{p2}$: pure rotational Raman transition (S-branch, Δv=0, ΔJ =+2)
ωprobe: frequency-narrowed ps probe pulse

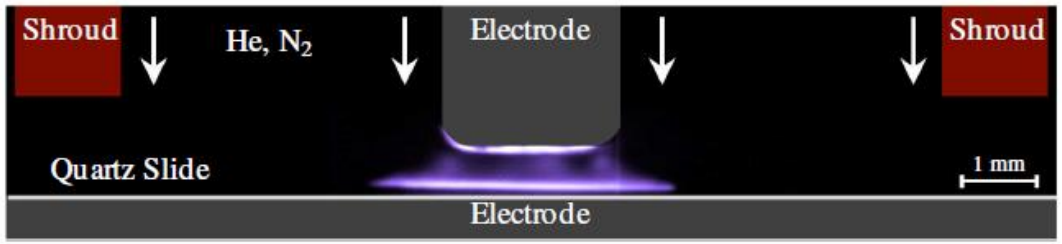


The He/$N_2$ dielectric barrier discharge

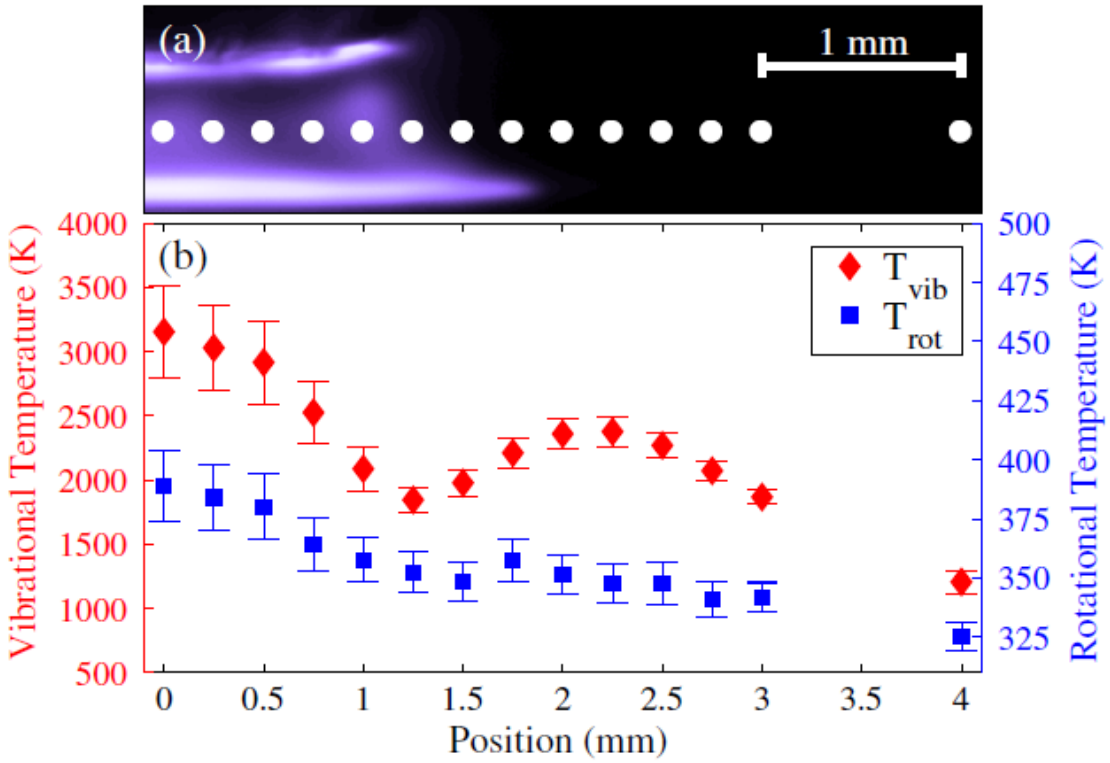


**Fig. 6.** (a) Averaged image of the DBD and CARS measurement locations and (b) corresponding vibrational and rotational temperatures; symbols and bars represent the average and standard deviation of 400 single-shot measurements at each location.


Dedic, C.E., Meyer, T.R. and Michael, J.B., 2017. Single-shot ultrafast coherent anti-Stokes Raman scattering of vibrational/rotational nonequilibrium. *Optica*, *4*(5), pp.563-570.

# Experimental measurements of Plasma chemistry and Kinetic Processes

NRP discharge in
air at 1000 K, 1 atm:

- 10-ns pulse
- 5.7 kV
- 10 kHz
- Gap: 4 mm
- 670 μJ/pulse

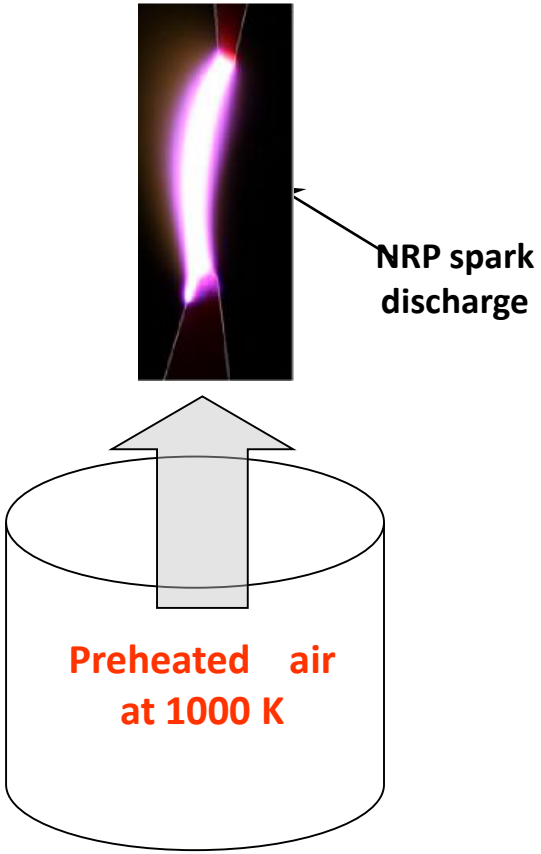


- Measured quantities:
  - O atoms: TALIF with absolute calibration (Xe)
  - $N_2$ (A): CRDS
  - $N_2$ (B) and $N_2$ (C): OES
  - Temperature: OES
  - Electron density: $H_\beta$ Stark broadening

Courtesy of Prof. Christophe Laux

# Measurements of V, I, temperature, densities

Ultrafast heating:
900 K in 20 ns

Ultrafast dissociation of $O_2$

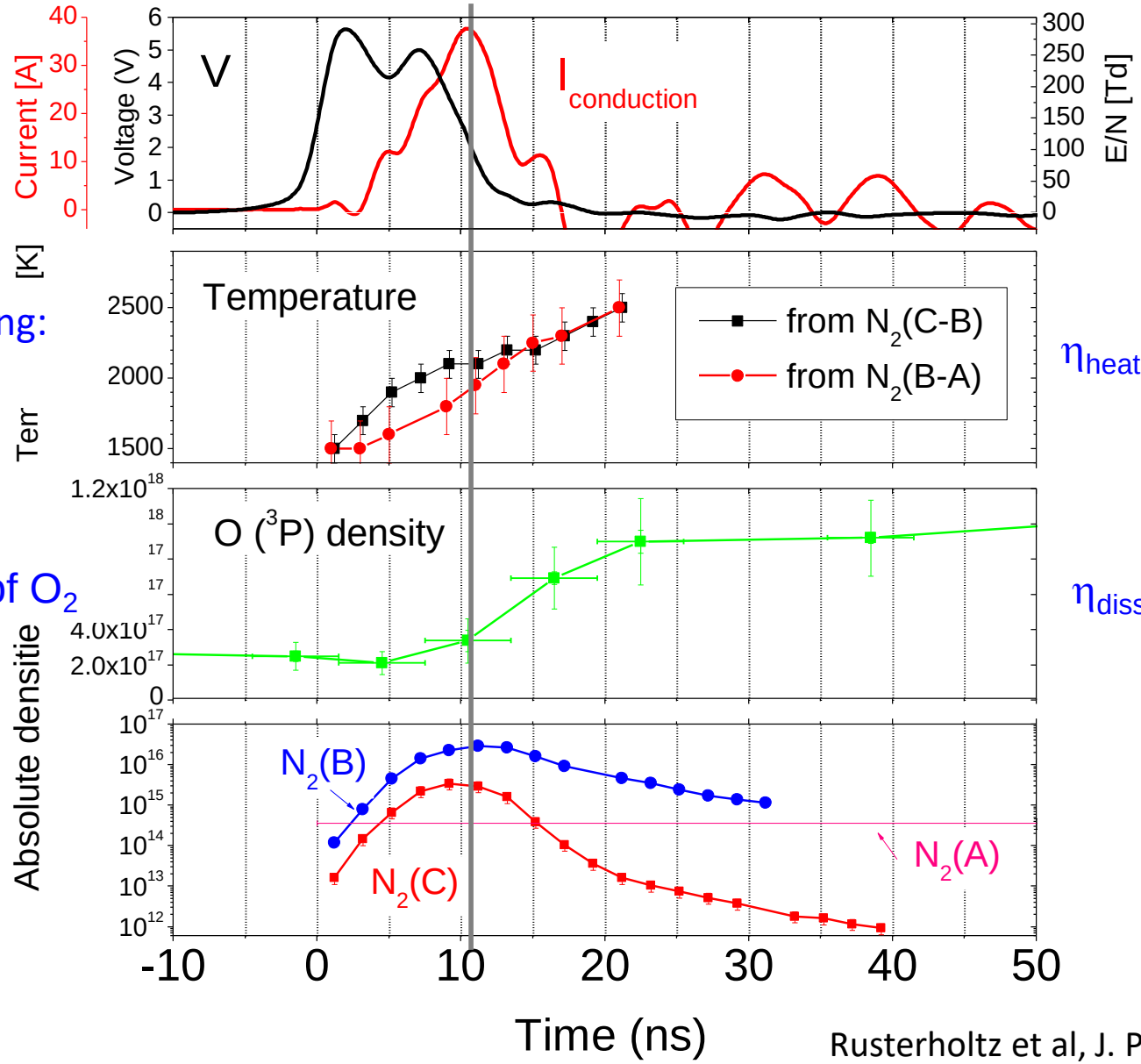


$\eta_{heating}$ =21±5%

$\eta_{diss.}$ = 35±5%

Rusterholtz et al, J. Phys.D, 46, 464010, Dec 2013

# Summary of processes involved in flame stabilization by NRP discharges

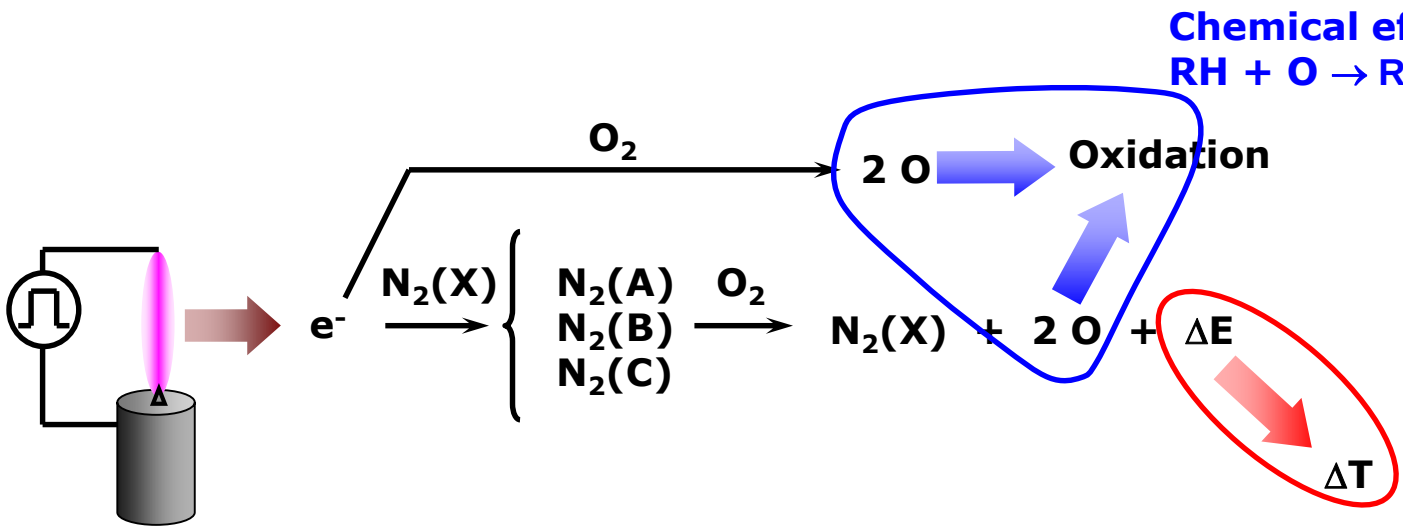


2-step mechanism (Popov, 2001):

$N_2 + e \rightarrow N_2^* + e$ ($N_2^* = N_2$ A, B, C, …)

Thresholds: 6.2, 7.4, 11.0 eV

$N_2^* + O_2 \rightarrow N_2 + O + O + \Delta T$

$\Delta T$ = 1.0, 2.2, 5.9 eV

**5 µs after pulse**
**(Xu et al., APL. 99, 121502, 2011)**

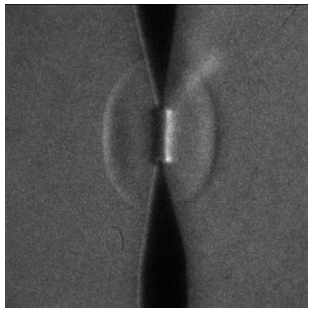

# 2. Measurements of Chemical Processes in Plasma Assisted Ignition and Combustion

**O atom measurements by using TALIF**

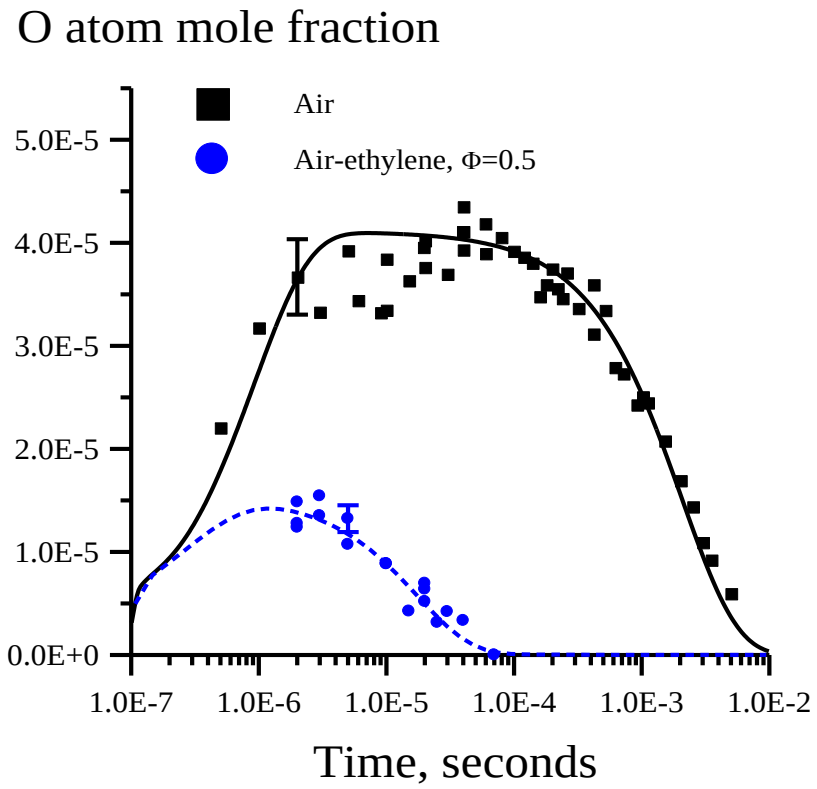


O atom formation in a plasma discharge of air and air-C2H4 mixture in a flow reactor

J. Uddi et al. 2009

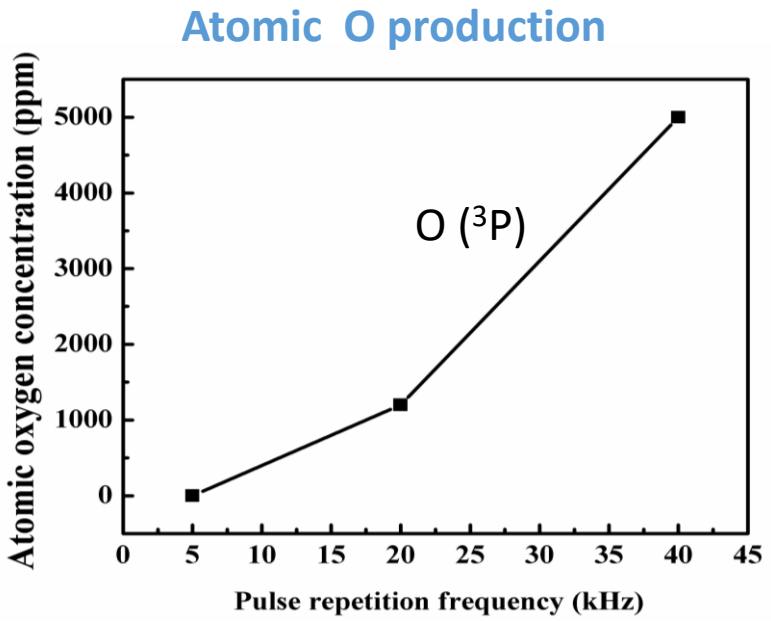


O atom formation in a ns plasma discharge of methane/air counterflow flames

W. Sun et. Al. 2010

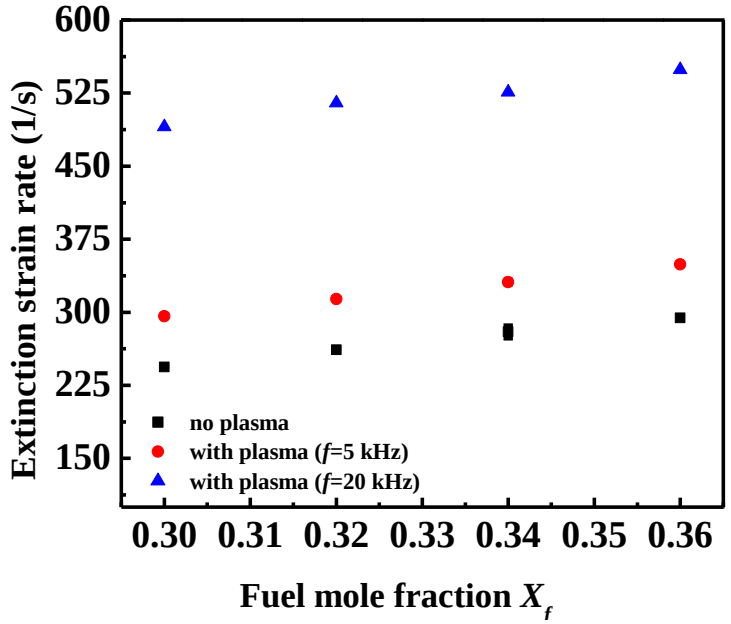


Extension of extinction limit by plasma discharge

# OH measurements in a flow reactor:
## Plasma chemical reactions result in ignition

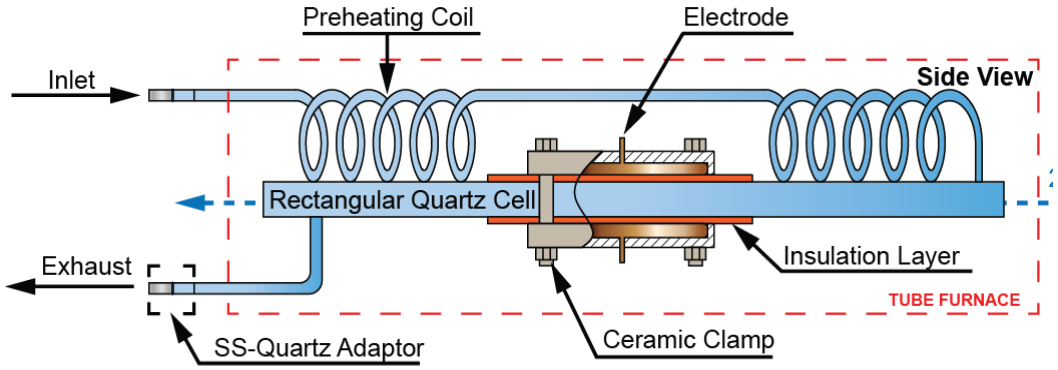


**End View**

| | Pulse #10 | Pulse #100 |
|---|---|---|
| $H_2$ – air, φ=0.3<br>$T_0$=500 K, P=100 torr | | 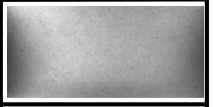 |
| $C_2H_4$ – air, φ=0.3<br>$T_0$=500 K, P=100 torr | 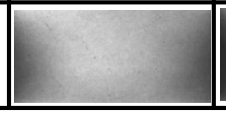 | 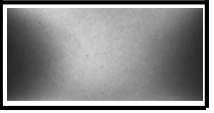 |

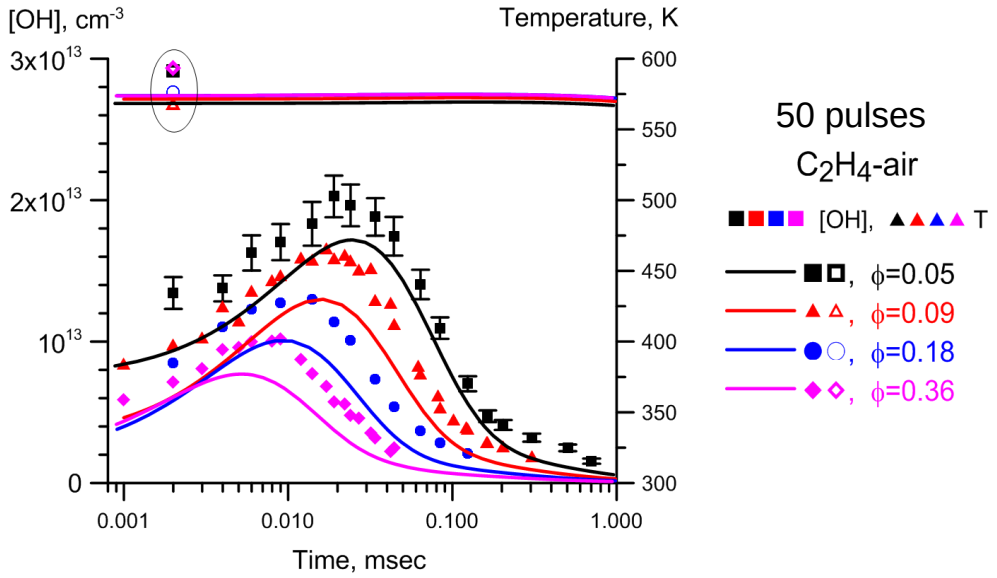


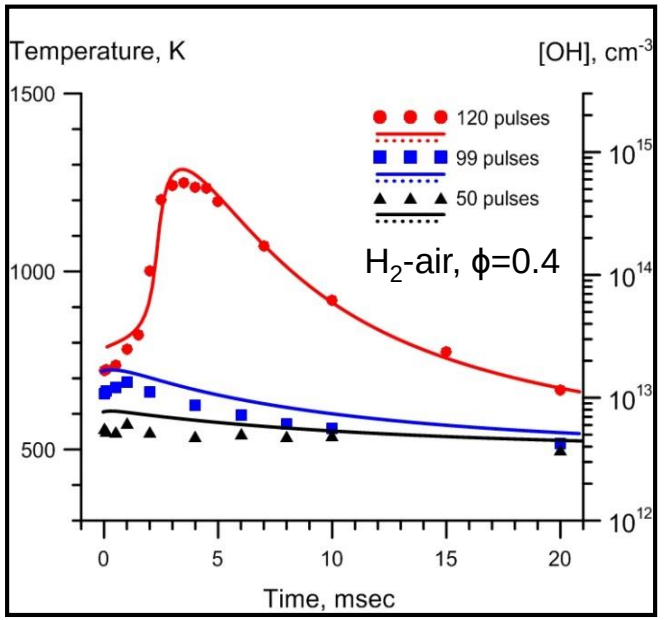


**Short burst: OH transient rise and decay**

**Long burst: plasma assisted ignition, $T_{ignition} \approx 700$ K < $T_{auto\text{-}ignition} \approx 900$ K**

# Plasma Assisted Combustion: Change of ignition and extinction S-curve

## The effect of kinetic enhancement (μs ~ ms, 800-1200 K)

**New "S-curve" by Plasma assisted combustion for small molecule fuel such as $H_2$, $CH_4$**

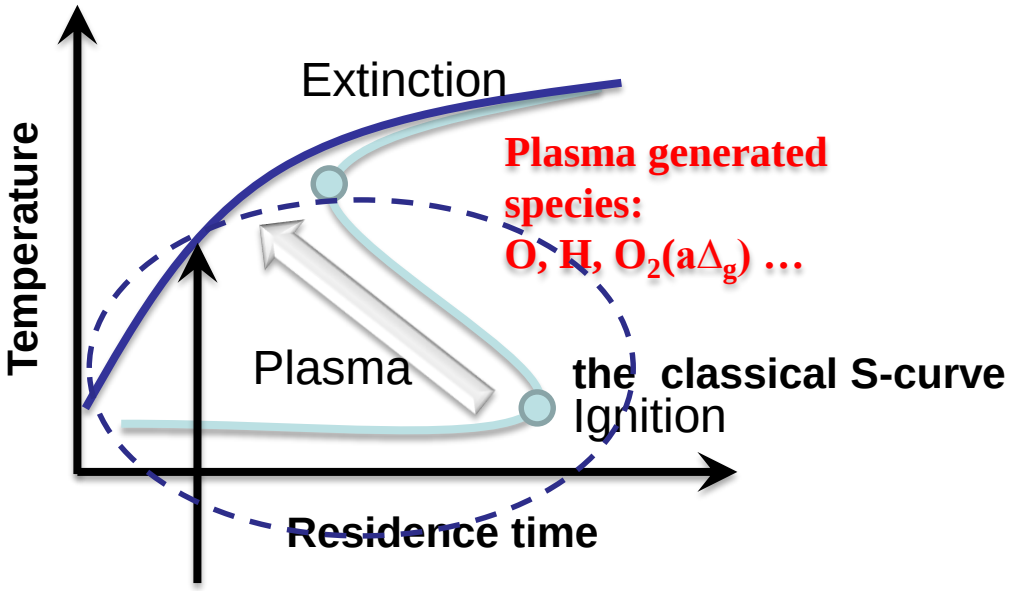


Scramjet, afterburner

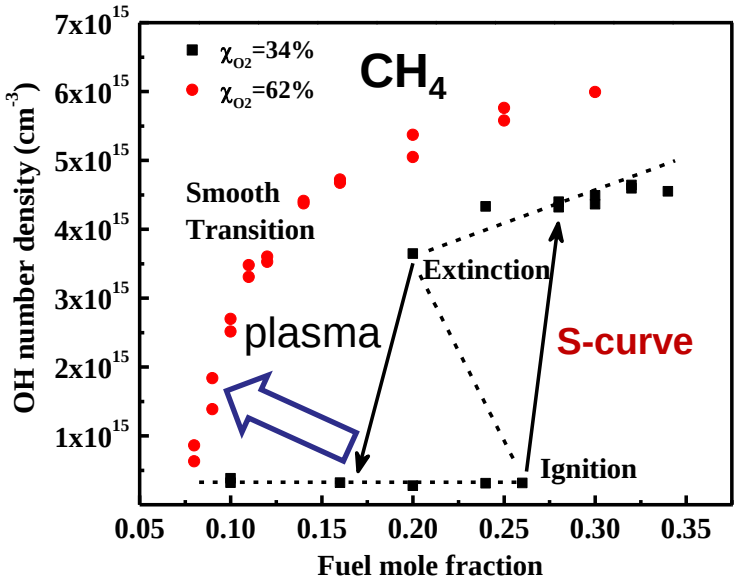


P = 72 Torr, $f$ = 24 kHz, a = 240 1/s

- **Strong kinetic enhancement at intermediate temperature**
- **Less effect at high temperature**

Sun et al. Proc. Comb. Inst. 34, 2010, Combust. Flame 2011, 2012
Ombrello et al. 2008

# Plasma assisted low temperature combustion

## Methane vs. Dimethyl ether (DME)

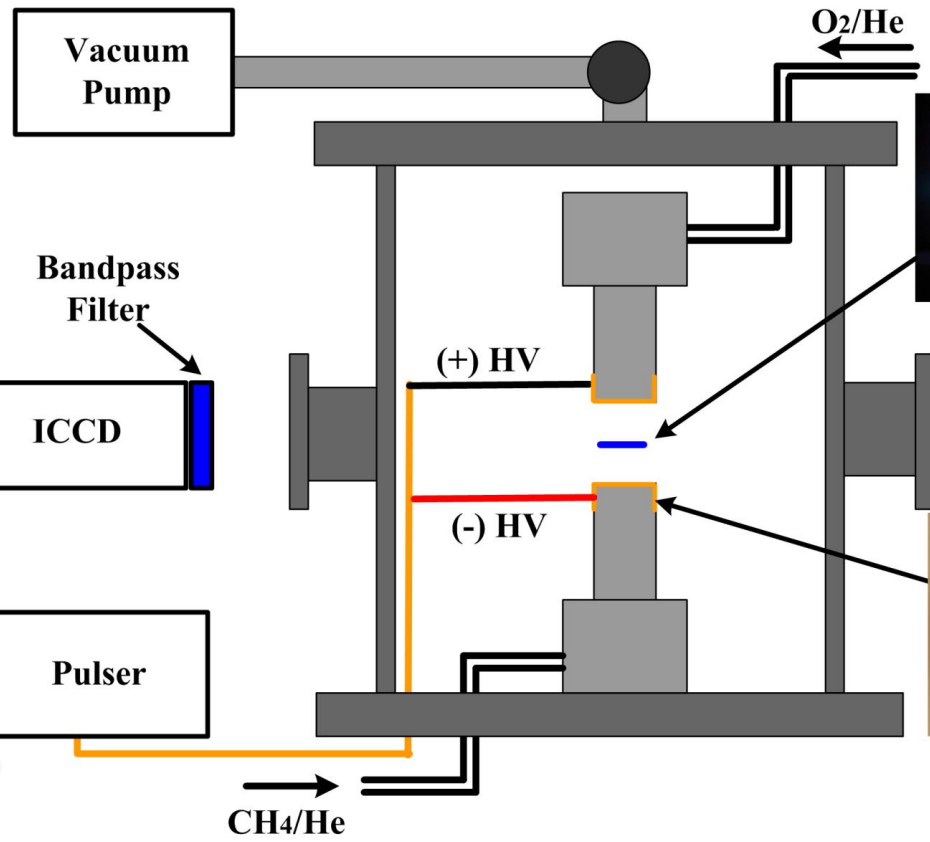


P = 72 Torr
*f* = 24 kHz

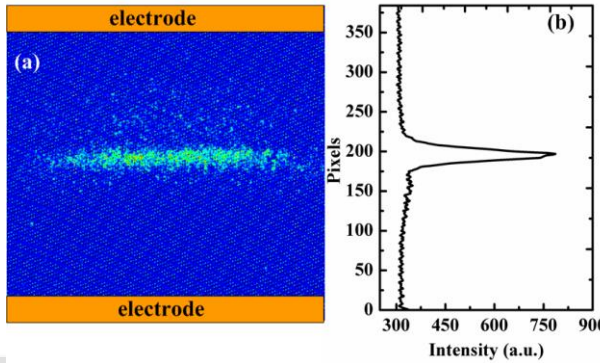


OH* emission ~310 nm
30 μs gate

Laser beam
OH, $CH_2O$ PLIF

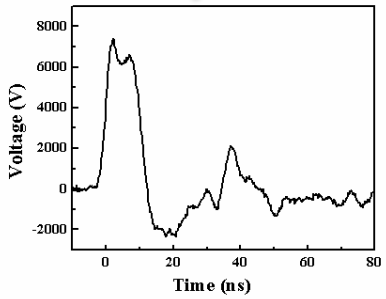


**Peak Voltage = 7.8 KV**

**E = 7500 V/cm, E/N ~ 900 Td**

**Power ~ 17 W (repetitive pulses)**

# OH PLIF measurements in Dimethyl ether (DME) Ignition

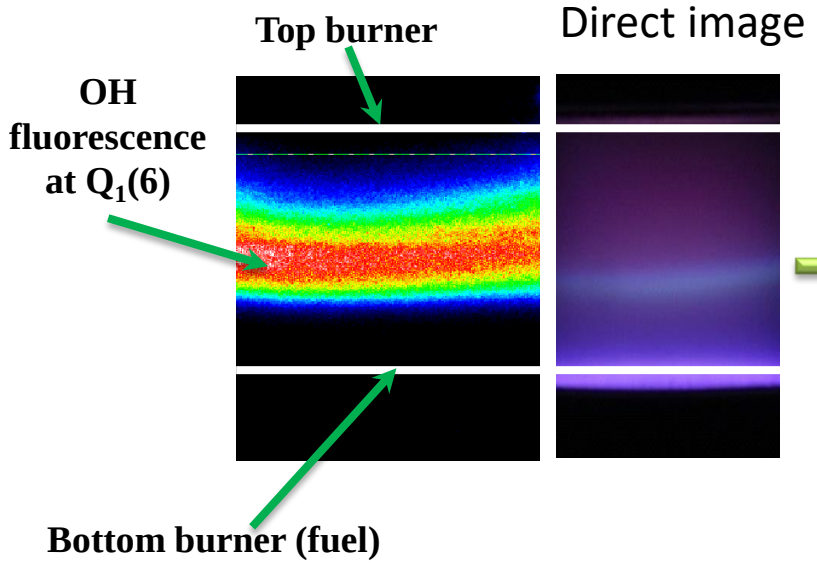


**S-shaped ignition and extinction curves**
**DME vs. CH4**

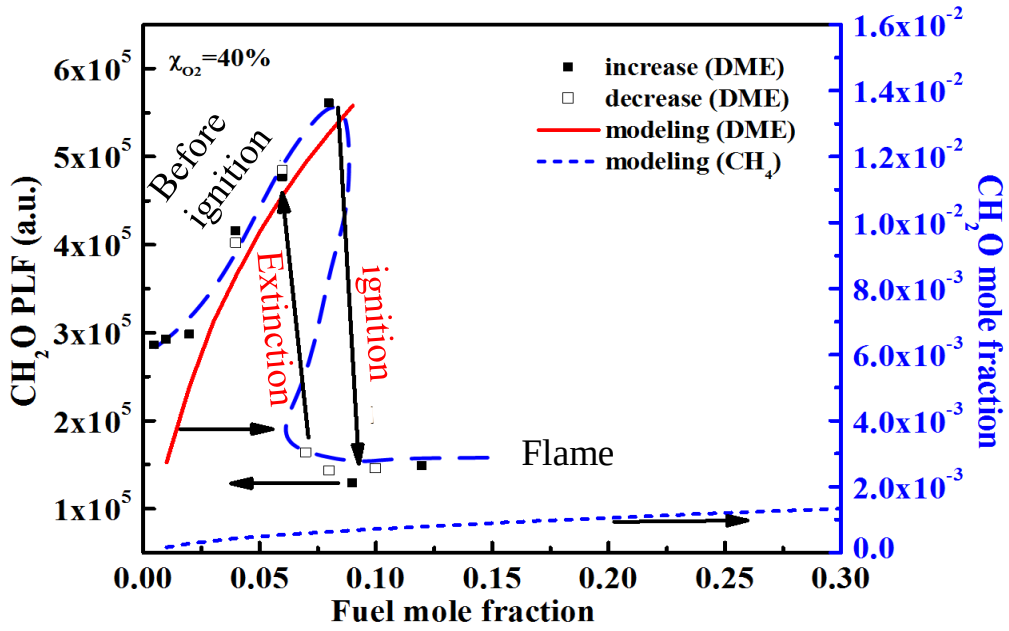


OH density vs. fuel mole fraction $X_O$ = 0.55, P = 72 Torr, $f$ = 24 kHz, for DME (a = 250 1/s) and $CH_4$ (a = 400 1/s,) as the fuel, respectively (solid square symbols: increasing $X_F$, open square symbols: decreasing $X_F$)

**What is the role of plasma before ignition of DME?**

# Plasma activated LTC: change of S-Curve

**P = 72 Torr, a= 250 1/s, *f* = 24 kHz**
**$X_{O_2}$=40%, varying $X_f$**

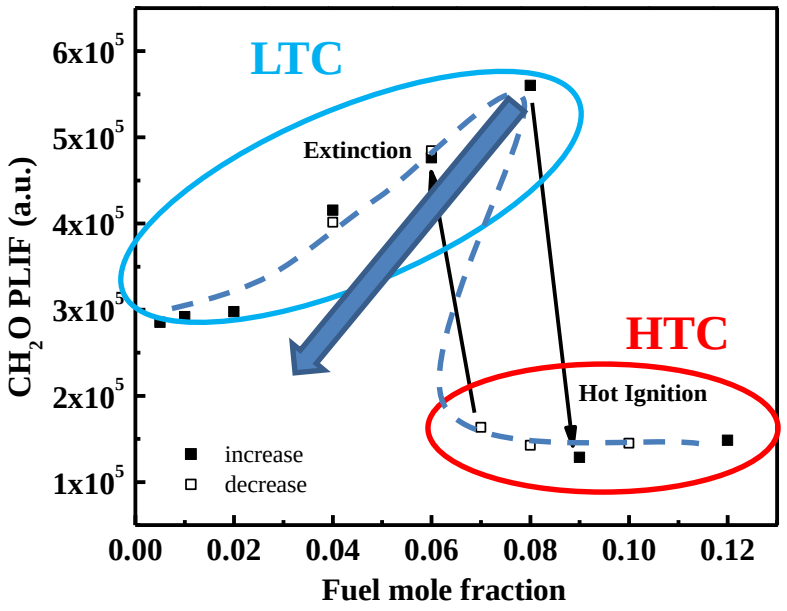


**S-Curve**

**P = 72 Torr, a= 250 1/s, *f* = 34 kHz,**
**$X_{O_2}$=60%, varying $X_f$**

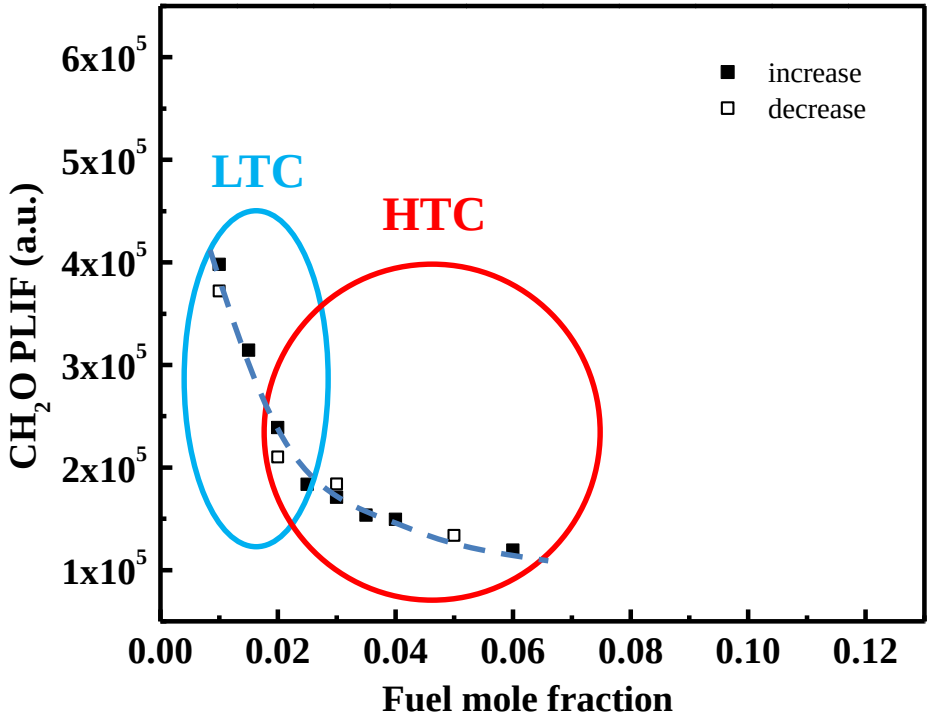


**New ignition/extinction curve without extinction limit**

**Radical production by plasma can activate LTC at much shorter timescale, lower pressure and temperature; and enable new flame regimes**

# Flow reactor studies of plasma assisted low temperature reaction

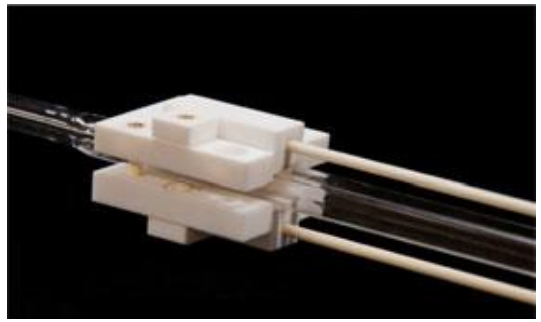

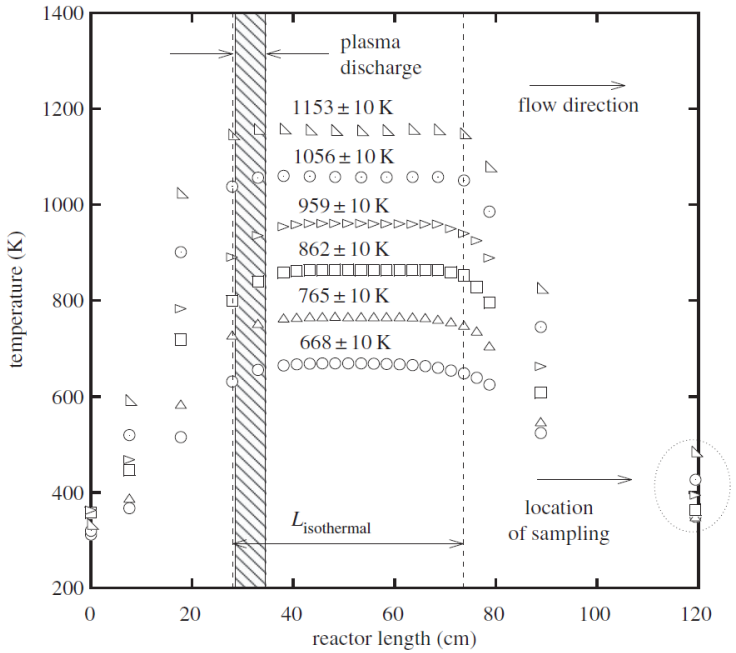


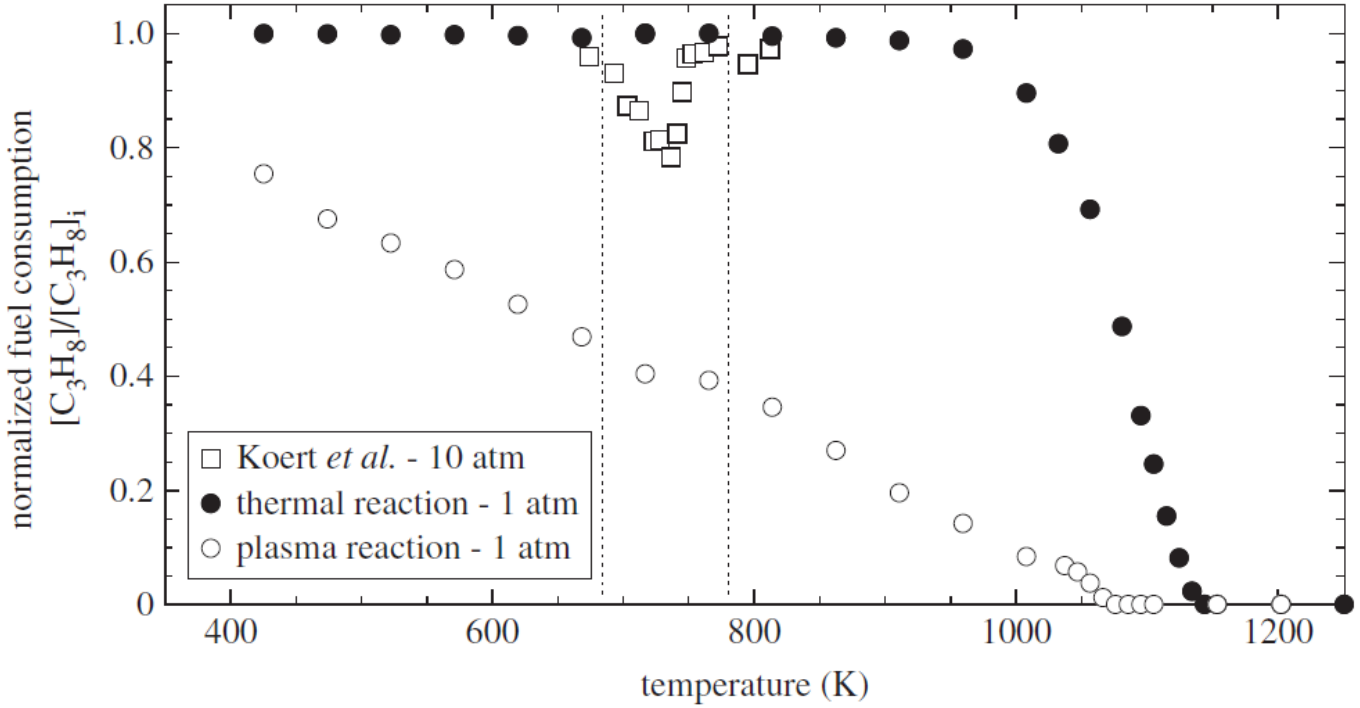


Comparison of thermal (1, 10 atm) and plasma (1 atm) propane fuel consumption as a function of temperature.

Nicholas Tsolas, Jong Guen Lee and Richard A. Yetter, *2015, Phil. Trans. R. Soc. A* **373**: 20140344.

# Plasma activated *Cool Flames* :A new way to burn with plasma

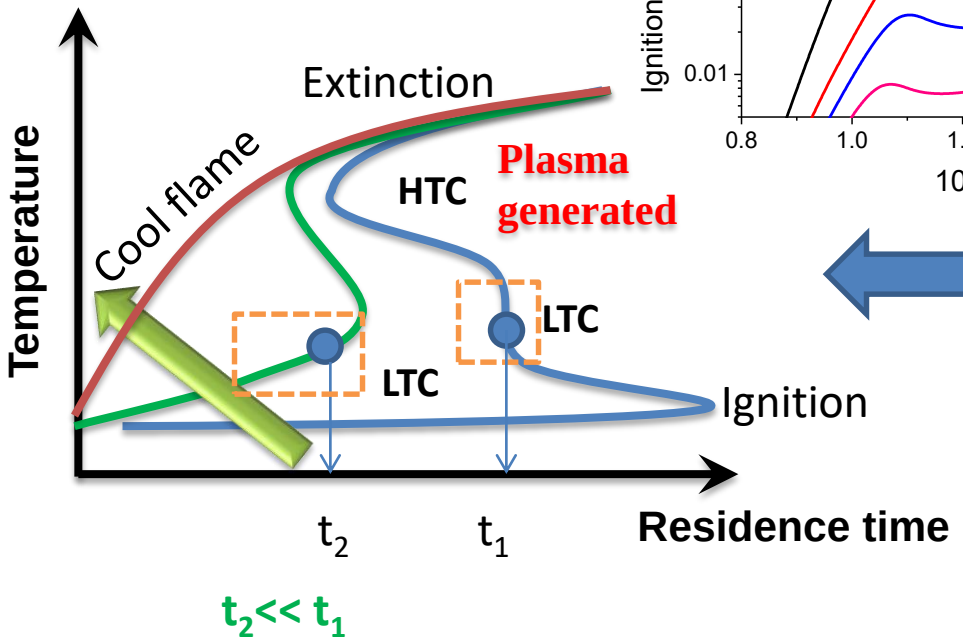


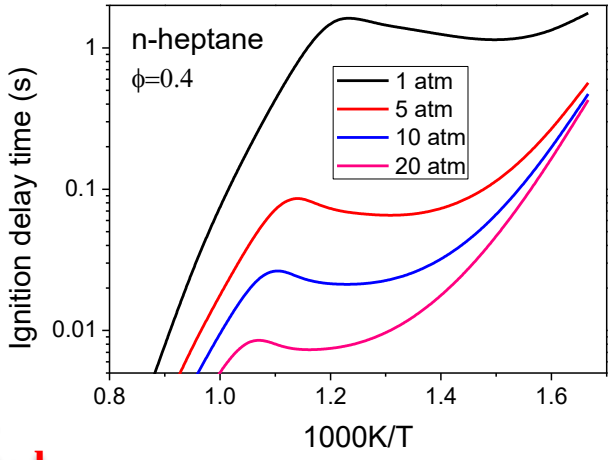


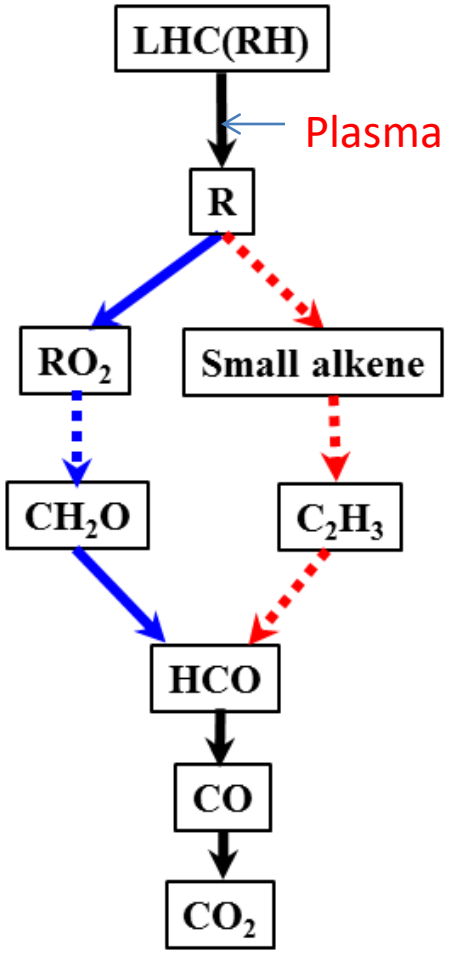


Plasma activated LTC at much shorter time, lower pressure….

We can create cool flames even at 1 atm or below?

# 2. Plasma activated self-sustaining *Cool Diffusion Flames:* A new way to burn

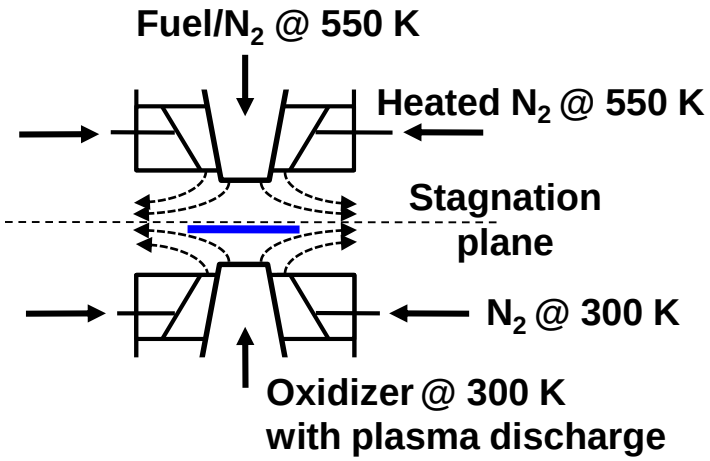


Fig. 1 Schematic of experimental setup

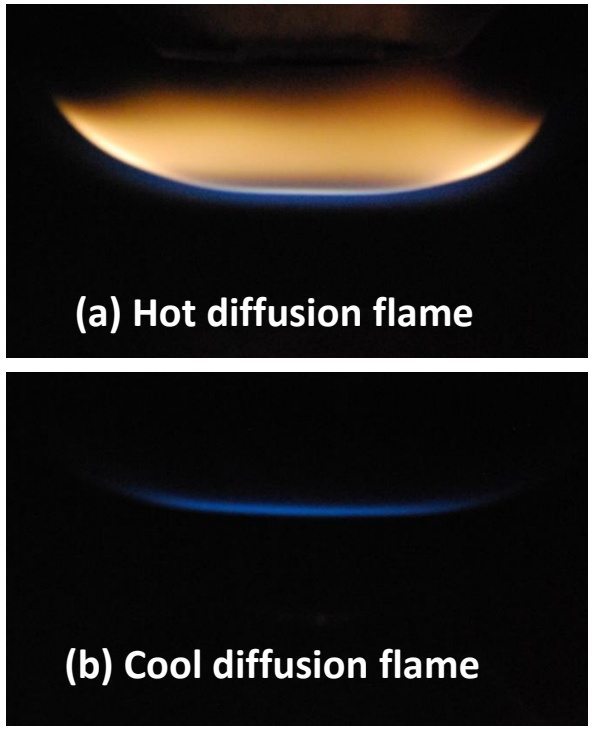


$T_f$~1900 K

$T_f$~650 K

Fig. 2 Hot and cool n-heptane diffusion flames at the same condition

**Won et al., 2014**

# 3. Multispecies diagnostics and kinetic modeling

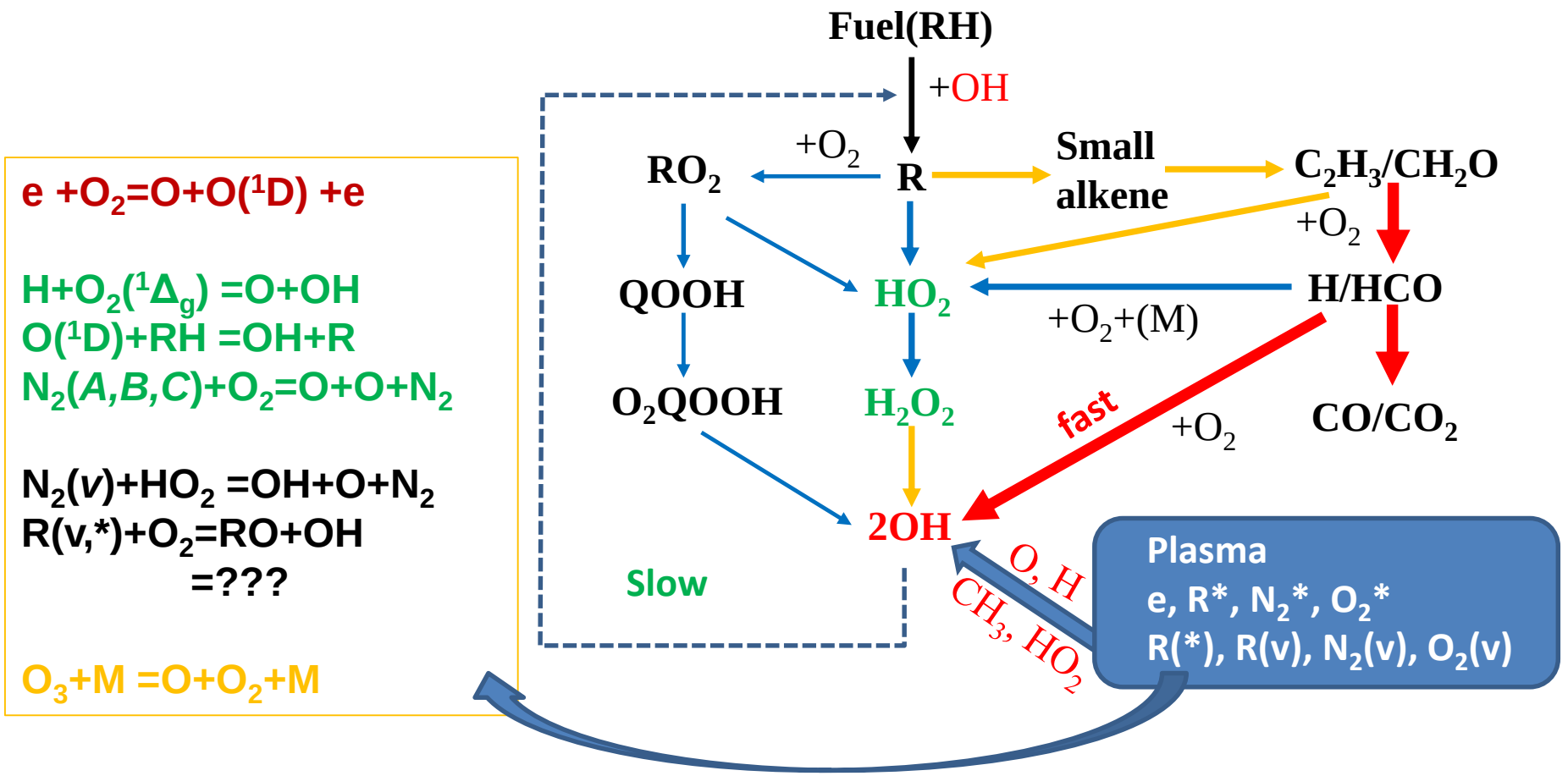


A schematic of the key reaction pathways for high pressure fuel oxidation of at different temperatures
(**blue arrow**: Below 700K; yellow arrow: 700-1050 K;
red arrow: above 1050K).

## Question to aks:

## How does the key plasma reactions affects n-heptane dissociation and oxidation in the first 10 ms with efifferent excitation processes involving Ar and O2?

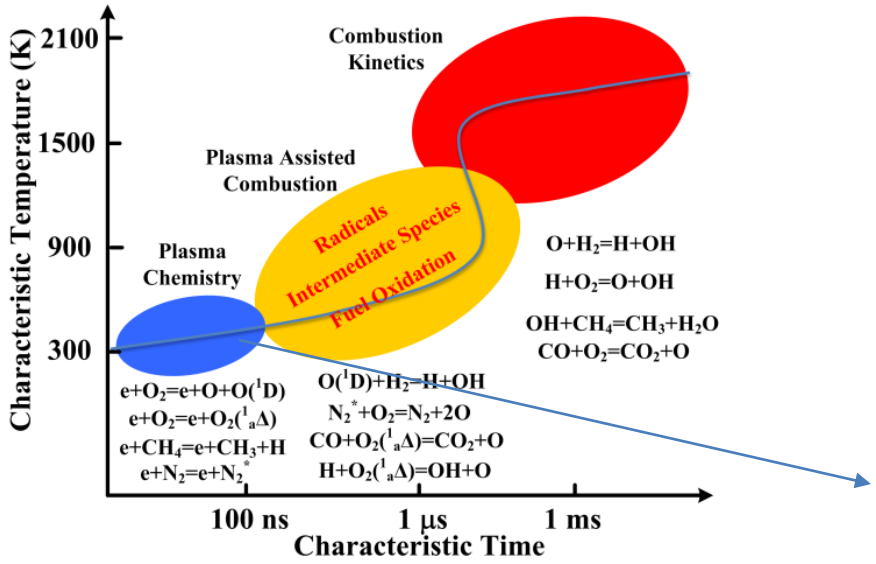


e +Ar =Ar*+e

e +**$O_2$** =O+O($^1$D)

e +**$O_2$** =e + $O_2$(v)

e +**$O_2$** =$O_2^-$

e +C7H16 =H+R

……

Ar* +C7H16 =?

O($^1$D) +C7H16 =?

$O_2$(v) +C7H16 =?

$O_2$(v) +C7H15 =$RO_2$(v)

……

# Plasma chemistry reactor

PRINCETON UNIVERSITY

- Reactor
  - Pressure: 60 Torr
  - Initial Temperature: 300 K
  - Flow speed: 40 cm/s
  - Reactor size: 45 x 14 x 152 $mm^3$
- Nanosecond repetitively pulsed discharge: FID GmbH FPG 30-50MC4
  - Peak Voltage: ~7 kV
  - Pulse Duration: 12 ns FWHM
  - Continuous mode: 0 – 5 kHz
  - Pulse burst mode: 150 pulses, 30 kHz
- Quartz double dielectric barrier: 1.6 mm thickness
- Gap distance: 14 mm

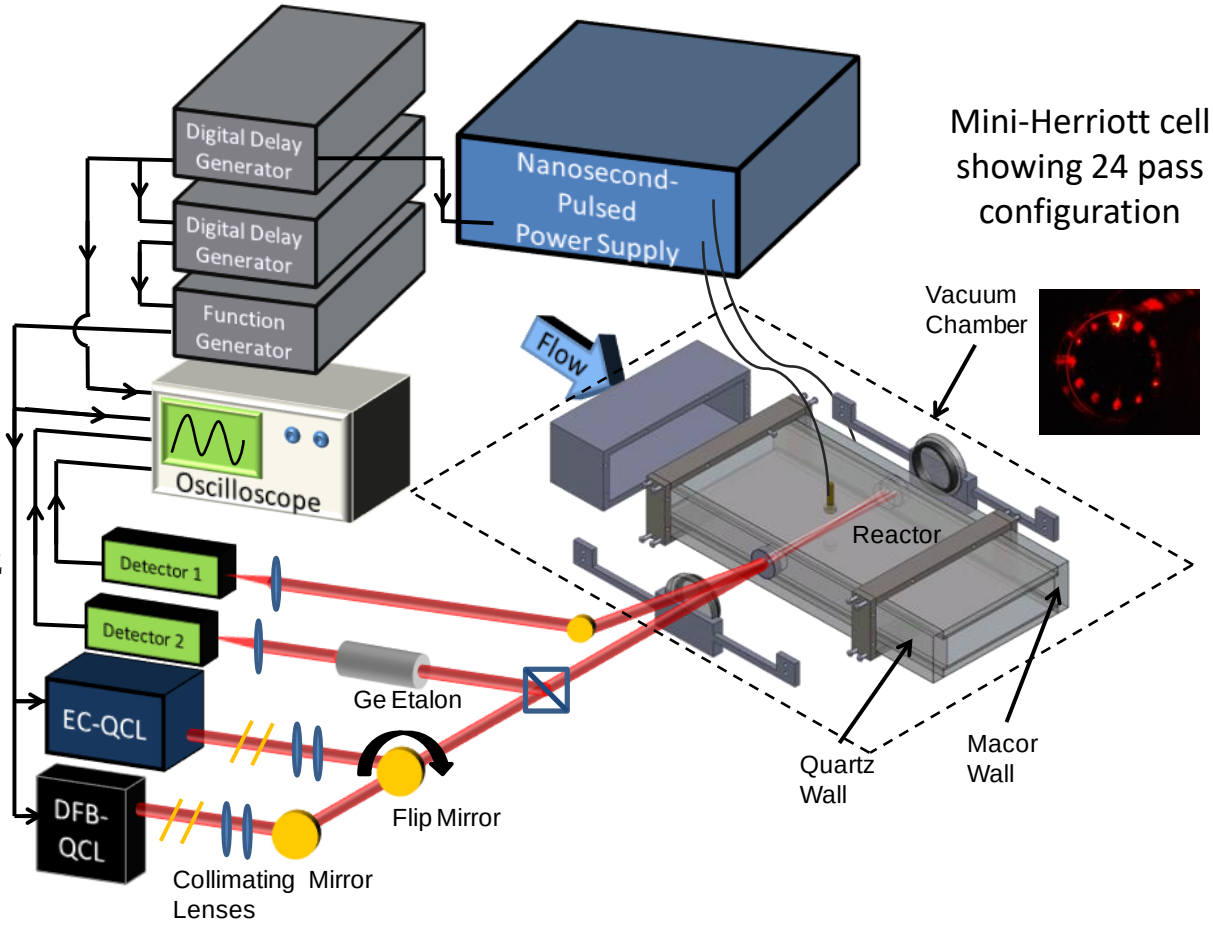


Mini-Herriott cell showing 24 pass configuration

# Experimental Apparatus

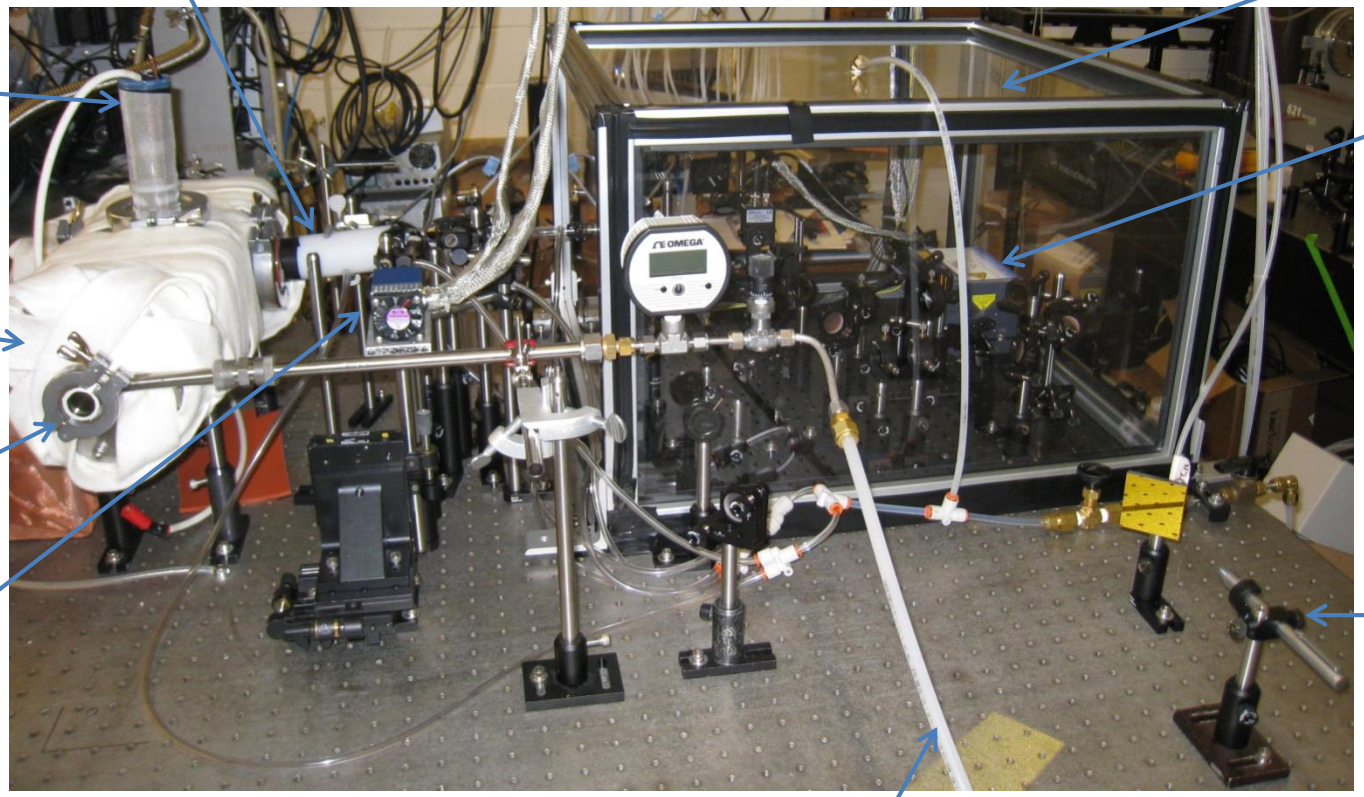

# Direct and ICCD Images of Plasma Discharge in a Reactor

**Stoichiometric mixtures: $C_2H_4/O_2$ with 75% AR, 60 Torr, $V_{max}$= 6 kV**

- Direct Image: 1 kHz, 3.6 mJ/pulse, 2 s exposure time.
- ICCD images: Gate time = 100 ns, Gain = 250

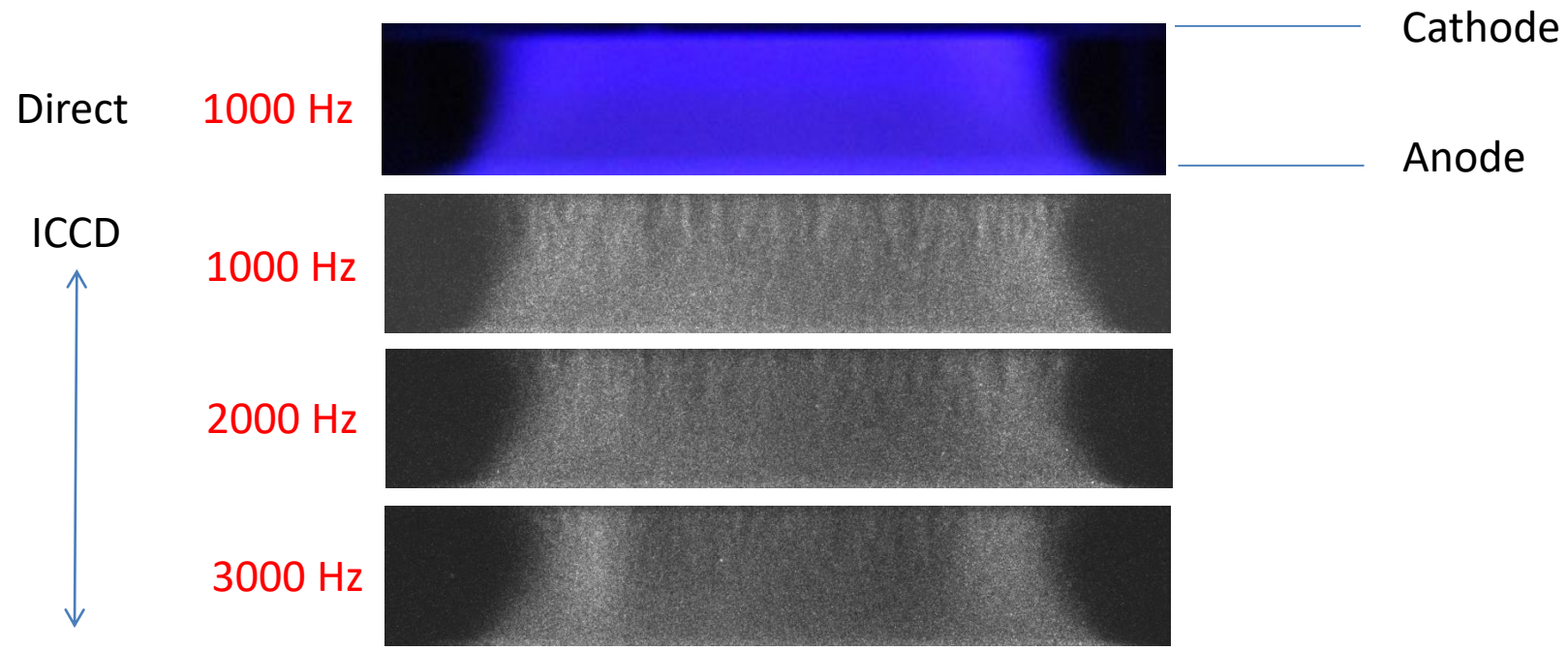

# Experiment/Model Comparison (C2H4)

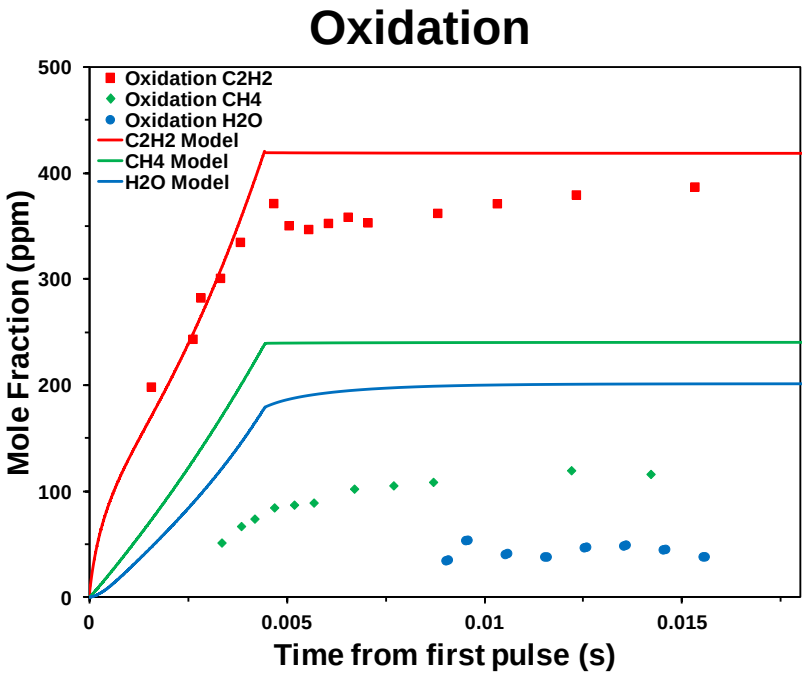


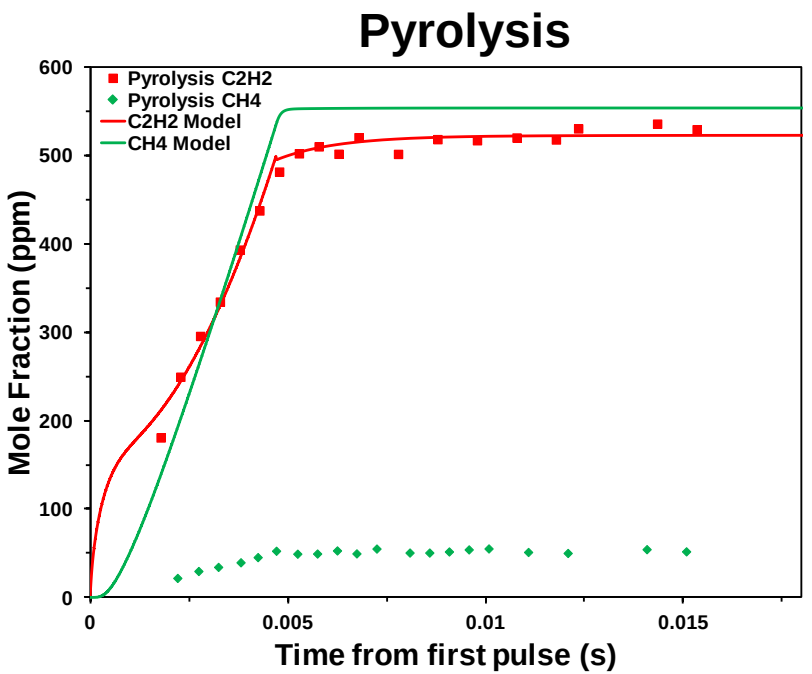


- **Conditions for Oxidiation case:**
  - Stoichiometric $C_2H_4$/O2
  - 25% Reactants, 75% Argon
  - V=40 cm/s
  - P=60 Torr
  - Ti=300 K
  - 150 Pulses, 30 kHz, 10 kV
  - E/n = 37 Td
- Acetylene measurements in the pyrolysis experiment were used to match the E/n ratio of model calculations

- **Conditions for pyrolysis case:**
  - 0.9375 Ar/0.0625 C2H4
  - V=40 cm/s
  - P=60 Torr
  - Ti=300 K
  - 150 Pulses, 30 kHz, 10 kV
  - E/n = 37 Td
- Methane is greatly over-predicted by the model

# Continuous Plasma - Oxidation

PRINCETON UNIVERSITY

- GC and *in situ* IR-LAS measurements
  - Continuous plasma
  - Stoichiometric, 25% Reactant
- Excellent agreement between GC and IR-LAS
- Major Species
  - $CH_2O$
  - $CO$
  - $C_2H_2$
  - $CH_3OH$, $C_2H_4O$
  - $CH_4$

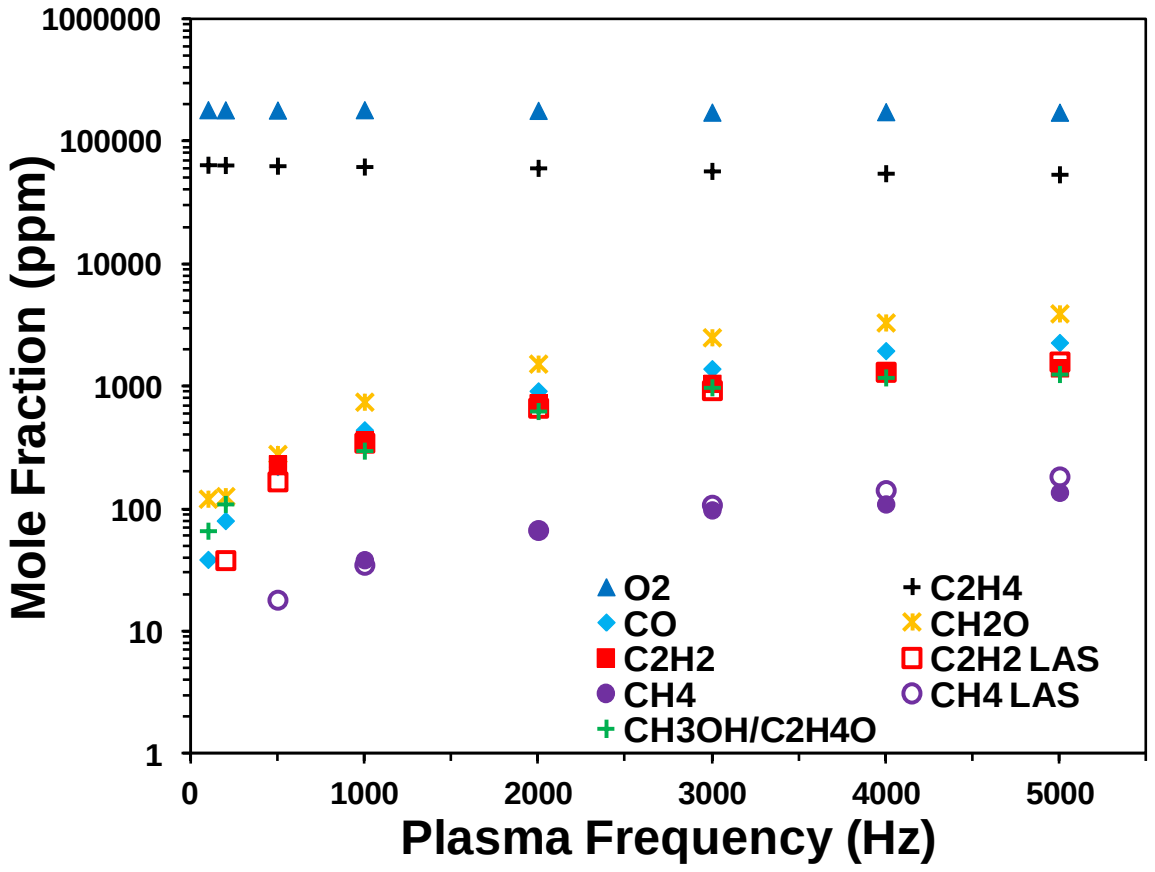


***Plasma activated low temperature fuel oxidation is an important process***

Lefkowitz et al. 2014

# Validation of plasma combustion chemistry of C2H4 oxidation

## $C_2H_4/O_2/Ar$: 6.25/18.75/75

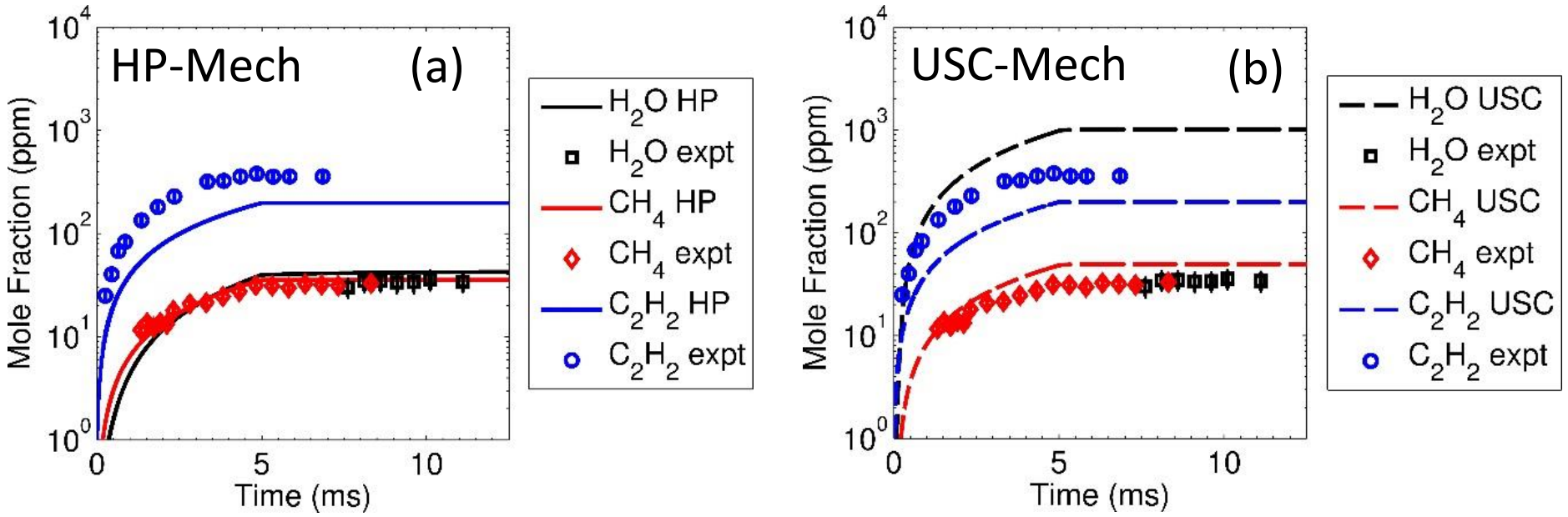


Fig. 16 Measurements and predictions of $C_2H_2$, $CH_4$, and $H_2O$ concentrations after 150 pulses at 30 kHz repetition rate for a mixture of $C_2H_4/O_2/Ar$: 6.25/18.75/75 by using (a) HP-Mech and (b) USC-Mech II.

# Ethylene Oxidation Pathways

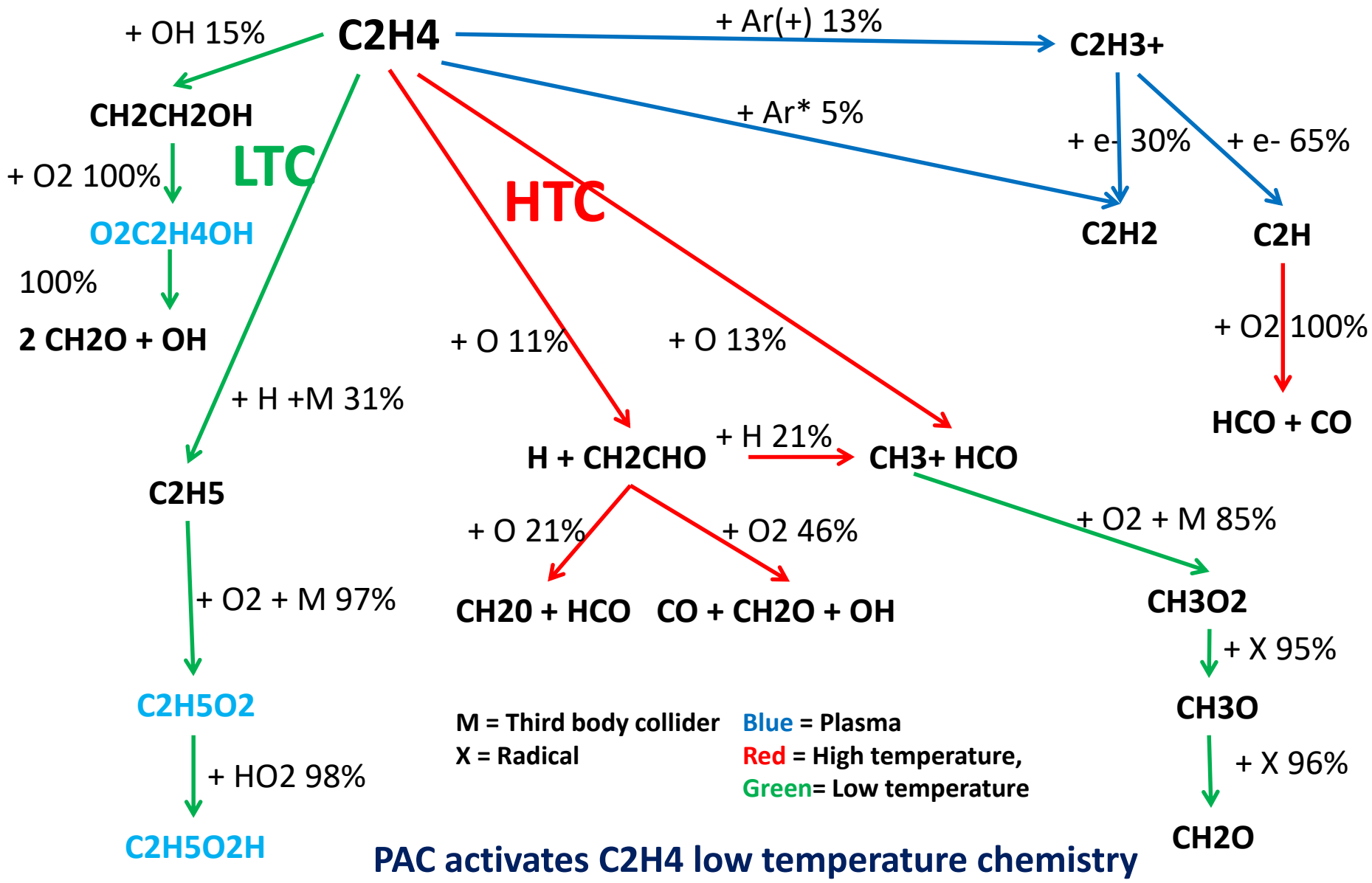

# Challenges: Plasma activated $CH_4/O_2$/He oxidation at 400 K

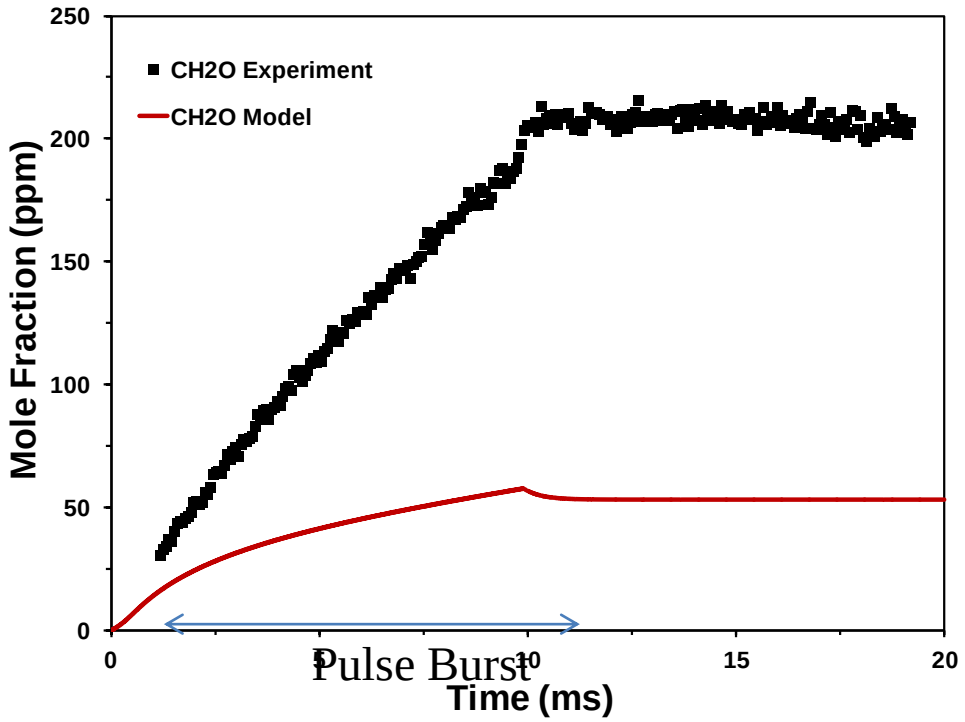


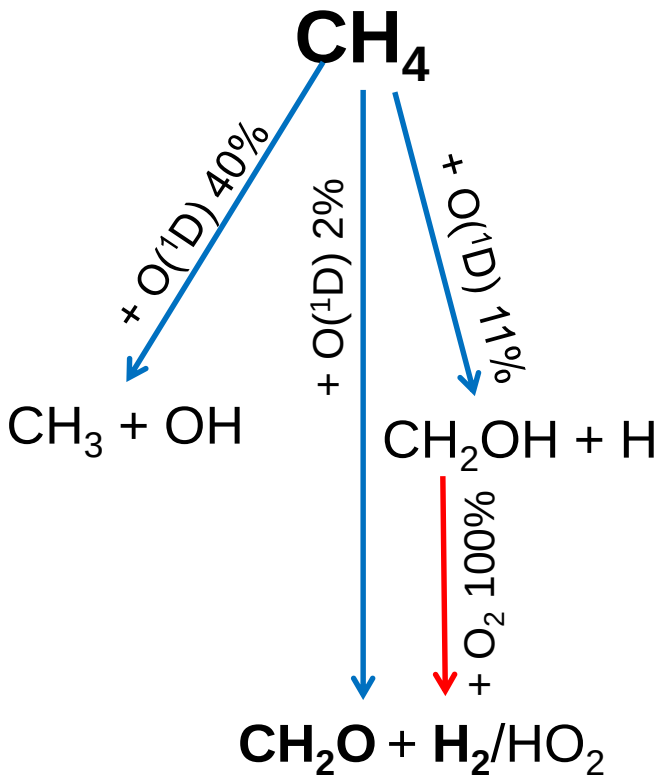


- 300 pulse burst, 8.75 kV peaks voltage, 30 kHz pulse repetition frequency
- Stoichiometric mixture, 75% diluent, 60 Torr, 300 K initial temperature

Lefkowitz, J.K., Guo, P., Rousso, A. and Ju, Y., 2015. *Phil. Trans. R. Soc. A*, *373*(2048), p.20140333.

# Challenges: Time dependent Formaldehyde Measurement

- $CH_2O$ production slightly greater for stoichiometric case
  - Similar linear trend as in n-heptane consumption
    - Lack of further $CH_2O$ production after pulse burst: indicates that only plasma produced species are responsible for fuel oxidation
- **Mode significantly under-predicts measurement by a factor of 40.**
- **Missing pathways for low temperature CH2O formation**

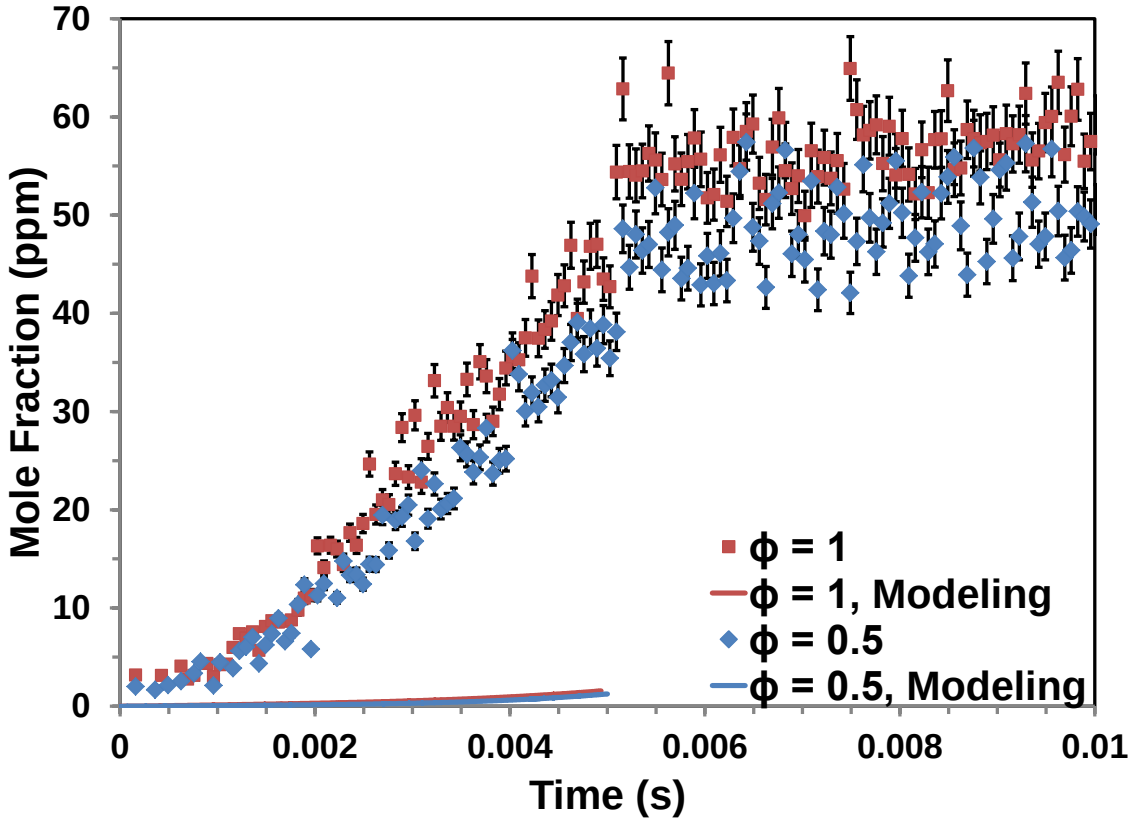


Rousso, Aric, Suo Yang, Joseph Lefkowitz, Wenting Sun, and Yiguang Ju.
" *Proceedings of the Combustion Institute, Vo.36,* 2017, Pages 4105–4112

PRINCETON UNIVERSITY

# Cross-sections database available for electron-molecule collisions

Table 1. Cross-sections database for electron-molecules collisions.

| Atmospheric | Saturated | Unsaturated | Oxygenated | Isomers |
|---|---|---|---|---|
| N2 | CH4 | C2H2 | CO | iso-butane |
| O2 | C2H6 | C2H4 | CH3OH | iso-propane |
| CO2 | C3H8 | C3H6 | C2H5OH | neo-pentane |
| H2O | C4H10 | | CH3OCH3 (DME) | |
| O3 | C5H12 | | | |
| Ar | H2 | | | |
| N2O | | | | |

Andrey Starikovskiy and Nikolay Aleksandrov, AIAA paper-2017-1977

# Non-equilibrium plasma kinetics

## A new reaction pathway of plasma assisted low temperature combustion via excited $RO_2^*(v)$

Vibrational and electronically excited O2(v) collides with fuel radical (R) forming highly energized RO2* in which the vibrational energies are quickly redistributed due to strong coupling between different vibration states. These RO2*, comparing to those formed by ground state oxygen with R, carry much higher internal energies that enable them overcome the barrier TS1, TS2, and TS3 much easier to produce the bimolecular product HO2+Alkene and OH+Ether. Therefore, the ignition processes/species profiles of the mixture can be significantly different from the ground state system.

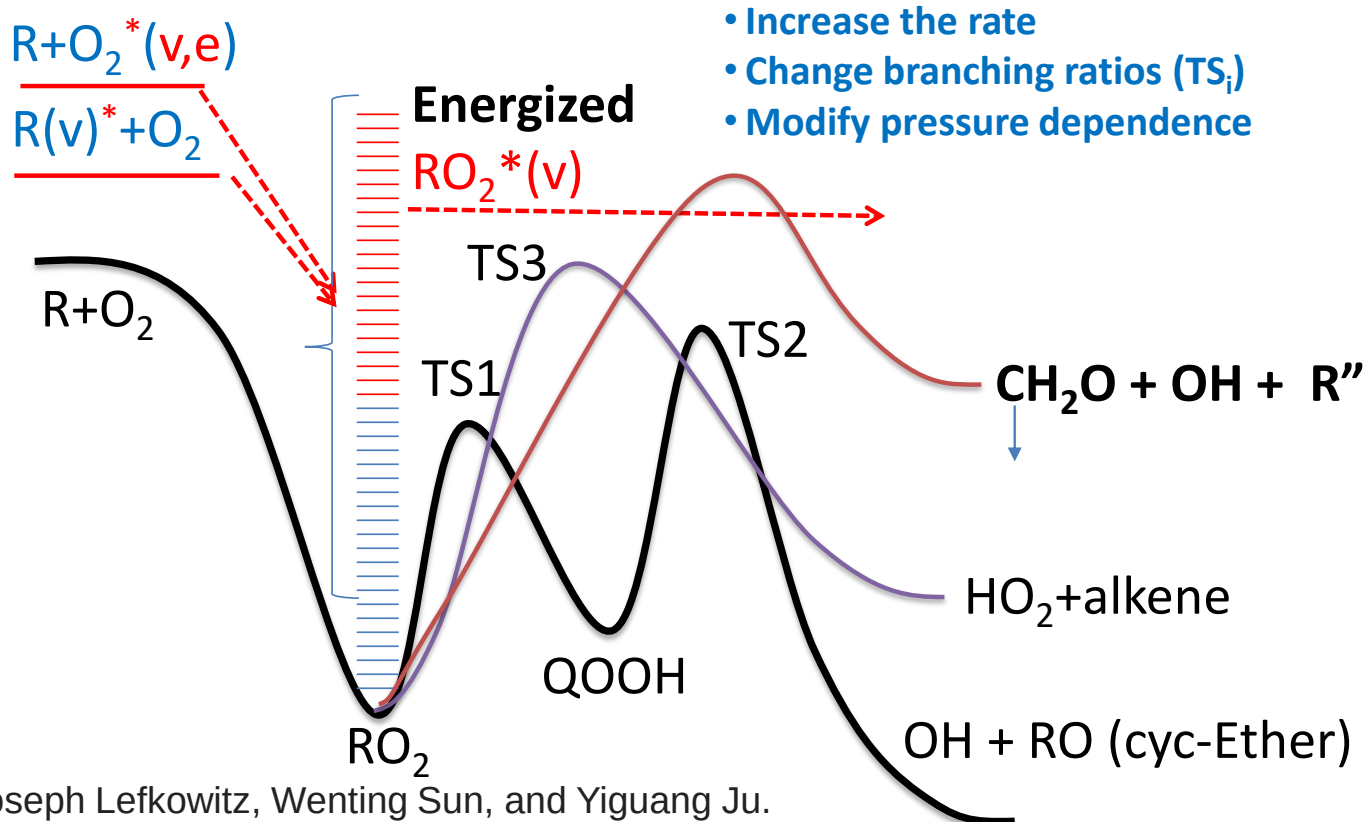


Rousso, Aric, Suo Yang, Joseph Lefkowitz, Wenting Sun, and Yiguang Ju.
" *Proceedings of the Combustion Institute, Vo.36*, 2017, Pages 4105–4112

# O(1D) reaction kinetics:

## Photolysis reactor for elementary kinetic study

**$O(1D)/O_3/O_2/CH_3OH$/Ar mixture**

time dependent measurements of OH, $HO_2$, $CH_2O$,…

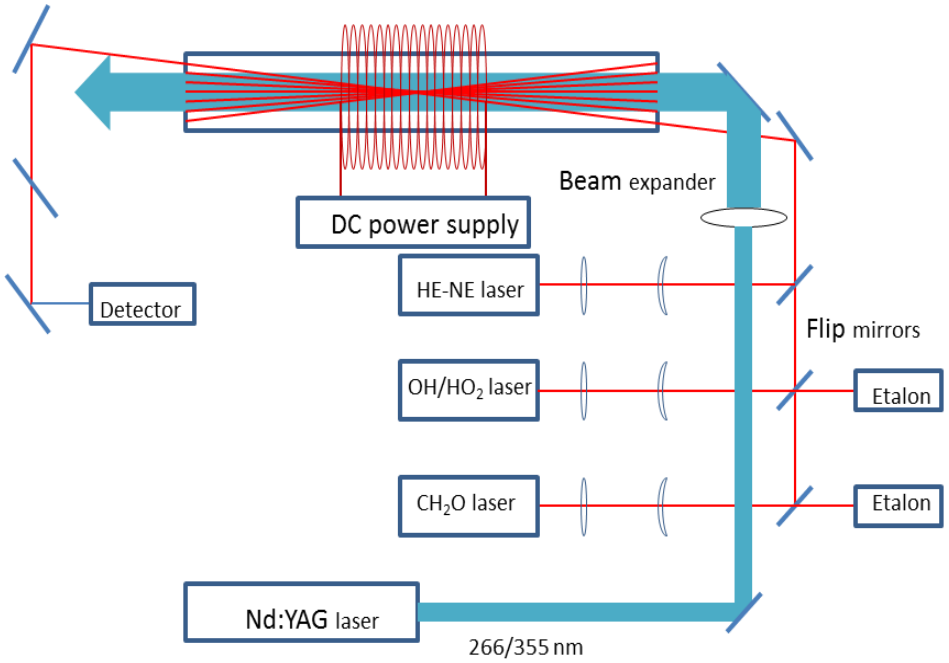


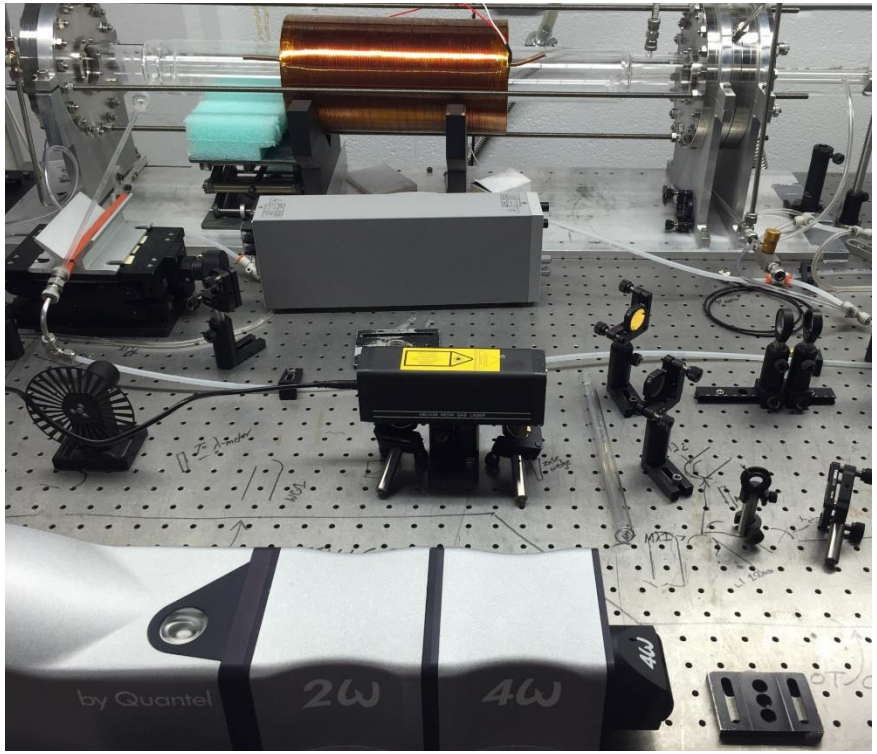


$H_2O$:1338.55 $cm^{-1}$
$CH_2O$:1726.8 $cm^{-1}$
OH: 3568 $cm^{-1}$
HO2: 1397 $cm^{-1}$

913 mm long, 40 mm diameter, multi-pass (21) Herriott cell, a19.17 meter optical path length

Ju, Y., Lefkowitz, J.K., Reuter, C.B., Won, S.H., Yang, X., Yang, S., Sun, W., Jiang, Z. and Chen, Q., 2016. *Plasma Chemistry and Plasma Processing*, *36*(1), pp.85-105.

# Experimental results and model validation: updated model

| | | | |
|---|---|---|---|
| $O(^1D)+CH_3OH \rightarrow CH_2OH+OH$ | $k_{new}=1.5x10^{14}$ | (R27) | |
| $O(^1D)+CH_3OH \rightarrow HOCHOH+H$ | $k_{new}=0.5x10^{14}$ | (R28) | (in mole-cm$^3$-s) |
| $O(^1D)+CH_3OH \rightarrow CH_2O+H_2O$ | $k_{new}=1.0x10^{14}$ | (R29) | |

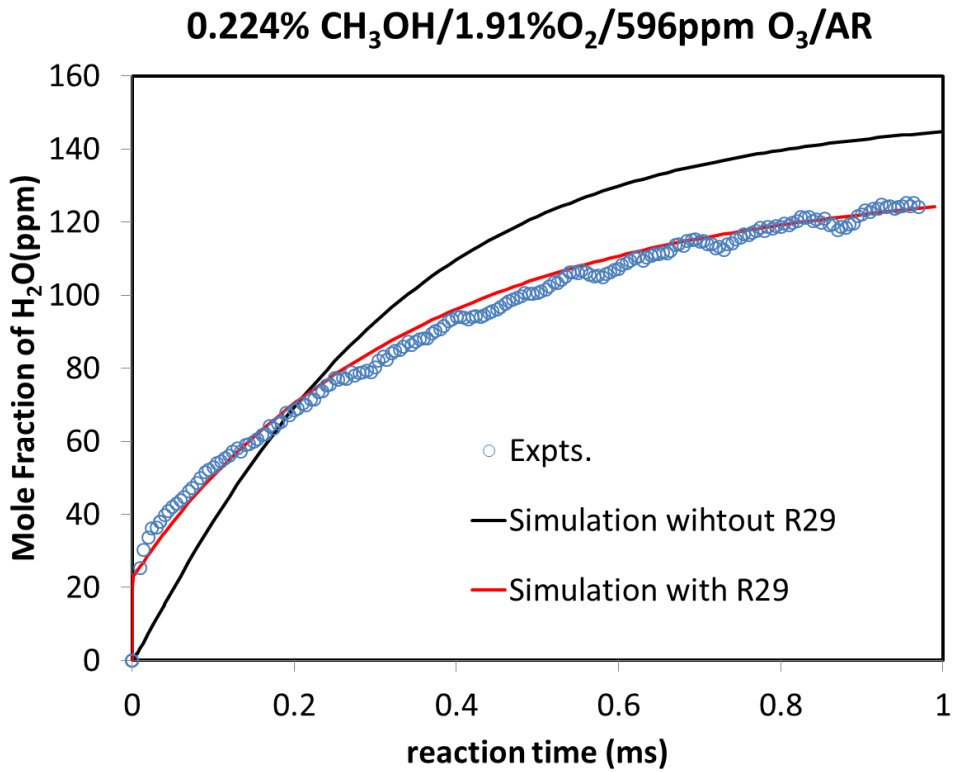


Time-resolved mole fraction of $H_2O$ in the 266 nm laser photolysis of 0.224% $CH_3OH$ 1.91% $O_2$ and 596 ppm $O_3$ in Ar mixture with the variation of $CH_3OH$ flow rate compared to model simulations for 1.0 ml/hour flow of $CH_3OH$. ○: Experimental measurement; — : simulation using the original model. — : simulation with updated reaction rates [38].

Ju, Y., Lefkowitz, J.K., Reuter, C.B., Won, S.H., Yang, X., Yang, S., Sun, W., Jiang, Z. and Chen, Q., 2016. *Plasma Chemistry and Plasma Processing*, *36*(1), pp.85-105.

# Potential energy surface (PES) of $O(^1D)+CH_3OH$

**using M062X/cc-pvtz level**

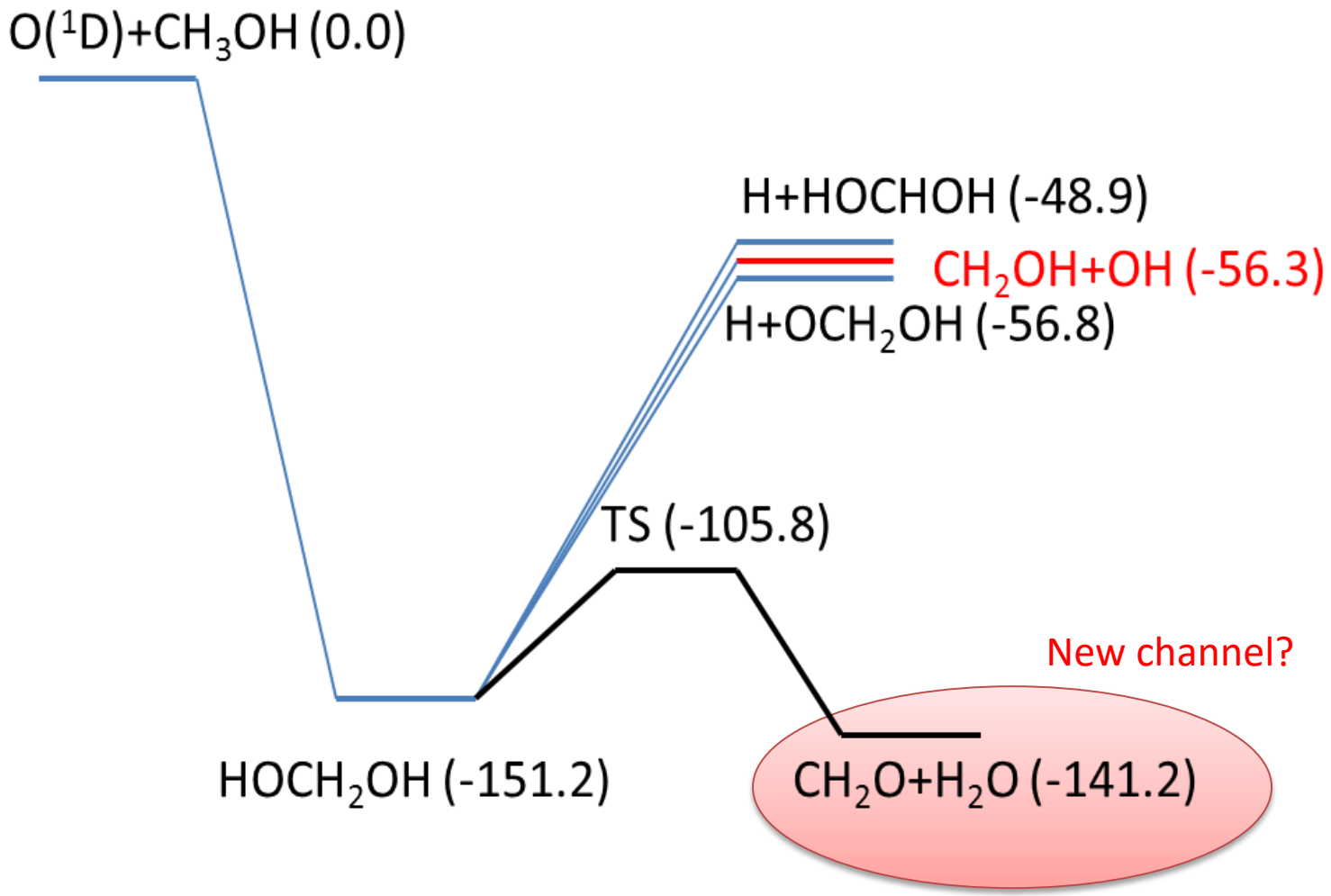


Ju, Y., Lefkowitz, J.K., Reuter, C.B., Won, S.H., Yang, X., Yang, S., Sun, W., Jiang, Z. and Chen, Q., 2016. *Plasma Chemistry and Plasma Processing*, *36*(1), pp.85-105.

# $HO_2$/OH using mid-IR Faraday Rotational Spectroscopy

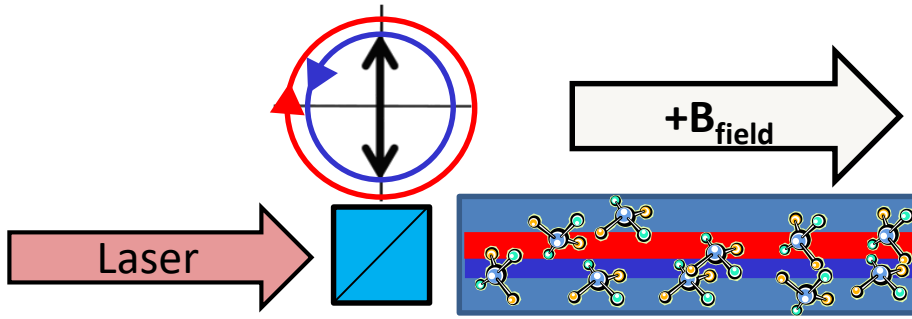


$$V_{RMS}(\tilde{\nu}) = \left(GP_0 \sin 2\theta\right)\Theta_{RMS}$$

$$\Delta n(\tilde{\nu}) = n_{RHCP}(\tilde{\nu}) - n_{LHCP}(\tilde{\nu})$$

Lock-In Amplifier

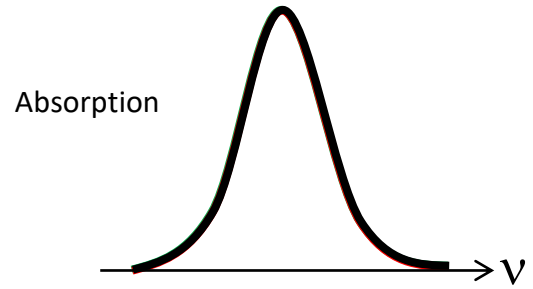


## $HO_2$ energy levels Zeeman splitting

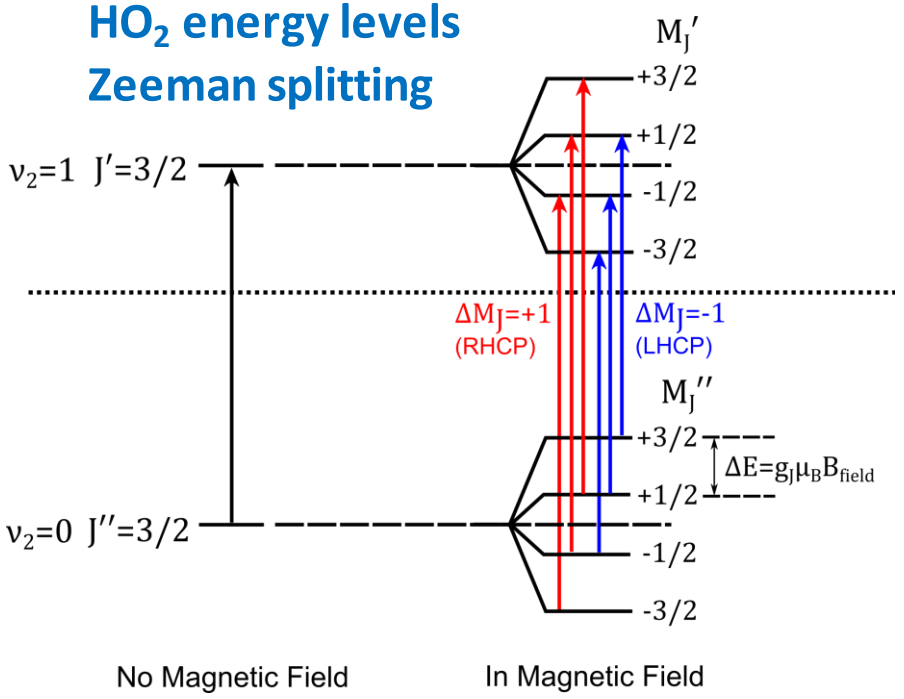

# Experimental results: $HO_2$/OH measurements

Signal

**Sensitivity**

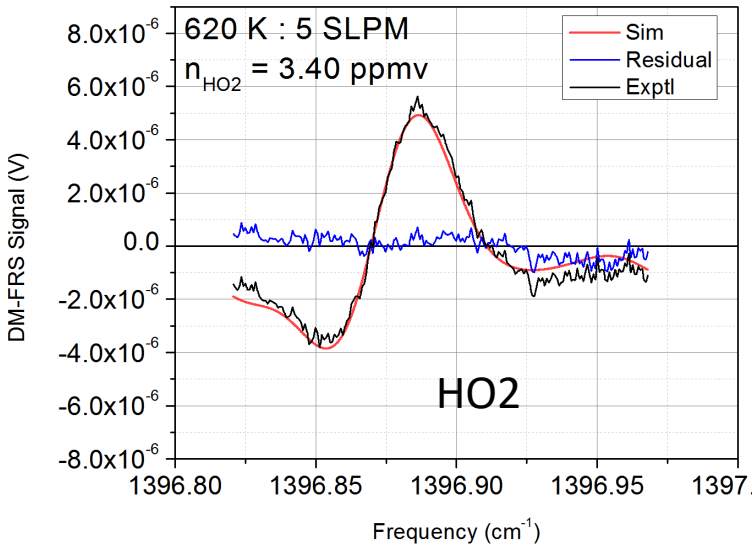


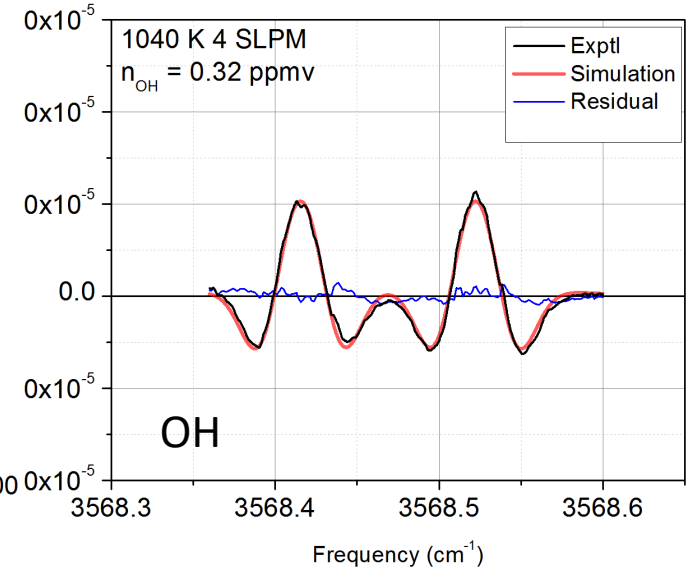


$\sigma$ detection limit $\approx$ 1 ppmv $/\sqrt{Hz}$ 3$\sigma$ detection limit = 20 ppbv $/\sqrt{Hz}$

DME flow reactor model validation

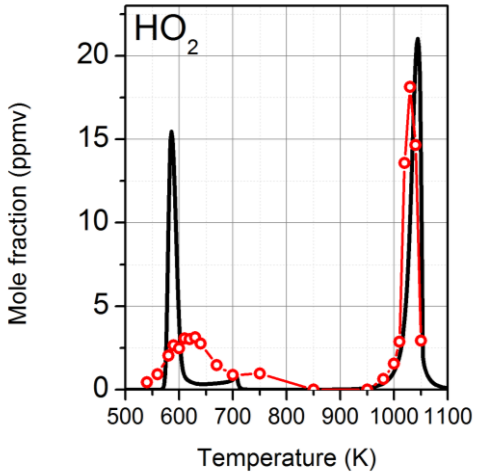


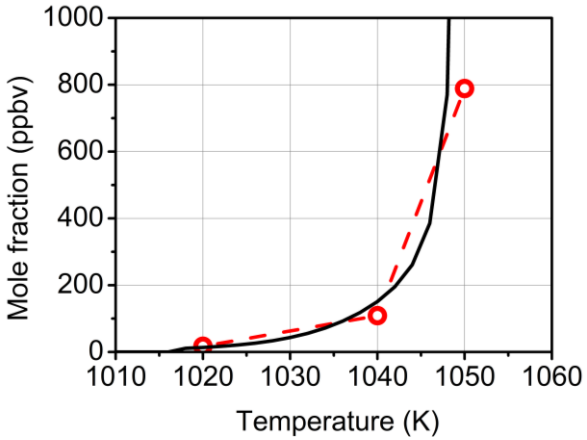


**Implicatio**

**RO2→QOOH→O2QOOH uncertainty**

**HCO+O2=HO2+CO reaction uncertainty and HCO formation pathway?**

Bremfield et al., 2013, JPC letters, 2013; Kurimoto et al. 2014

# Summary

- **Time-resolved, spatially-resolved, in-situ laser diagnostics of electric field, electron density, and electron temperature, excited and radical species greatly enhanced the understanding of plasma kinetic and chemical process in PAC.**
- **Production of O and $O(^1D)$, $O_2$(singlet), $N_2$(*), and $N_2$(v) by the plasma is the major processes in kinetically enhancement of combustion.**
- **Fast and slow heating in PAC is important, but the energy transfer processes are very complicated.**
- **Plasma activated low temperature combustion pathways and enable cool flame formation, but existing mechanisms have large uncertainties, especially for large hydrocarbons.**
- **Electron impact reaction cross-sections of large alkanes and reaction rates involving $O(^1D)$ and non-equilibrium excitations are poorly known.**
- **The effect of vibrational species excitation on PAC is still poorly known.**

# Lecture 5 Chemistry and Kinetic Studies of Plasma-Assisted Combustion

Yiguang Ju

- Important chain-initiation and branching reactions in combustion
- Plasma chemistry and timescales
- Impact of plasma chemistry on combustion
- Diagnostics of plasma properties and chemistry in PAC

# 1. Important combustion reactions

## 1. Chain initiation and propagation reactions

| | | |
|---|---|---|
| $RH + O_2 \rightarrow R + HO_2$ | High Temperature (>1100 K) | slow |
| $RH + HO_2 \rightarrow R + H_2O_2$ | High pressure/low temperature (>550 K) | slow |
| $R + HO_2 \rightarrow RO + OH$ | High pressure/low temperature (>550 K) | slow |

## 2. important branching reactions at different temperatures

| | | |
|---|---|---|
| $H + O_2 \rightarrow O + OH$ | High Temperature (>1100 K) | Fast |
| $H_2O_2 \rightarrow 2OH$ | Intermediate temperature (800-1100 K) | Slow |
| $R \rightarrow RO_2 \rightarrow QOOH \rightarrow O_2QOOH \rightarrow R'' + 2OH$ | Low temperature (300-800K) | Slower |

## Plasma assisted combustion:

$e + O_2 \rightarrow e + 2O$ ⇒

$O + RH \rightarrow R + OH$

$R \rightarrow R'' + 2OH$

---

$O + RH \rightarrow R'' + 3OH$ Faster

$e + O_2 \rightarrow e + O_2(a^1\Delta_g)$ ⇒ $H + O_2(a^1\Delta_g) \rightarrow OH + O$ Faster

**Plasma provides new reaction pathways to accelerate chain reaction processes**

# Interaction of plasma chemistry with reaction kinetics of large alkanes w/wo in plasma assisted combustion

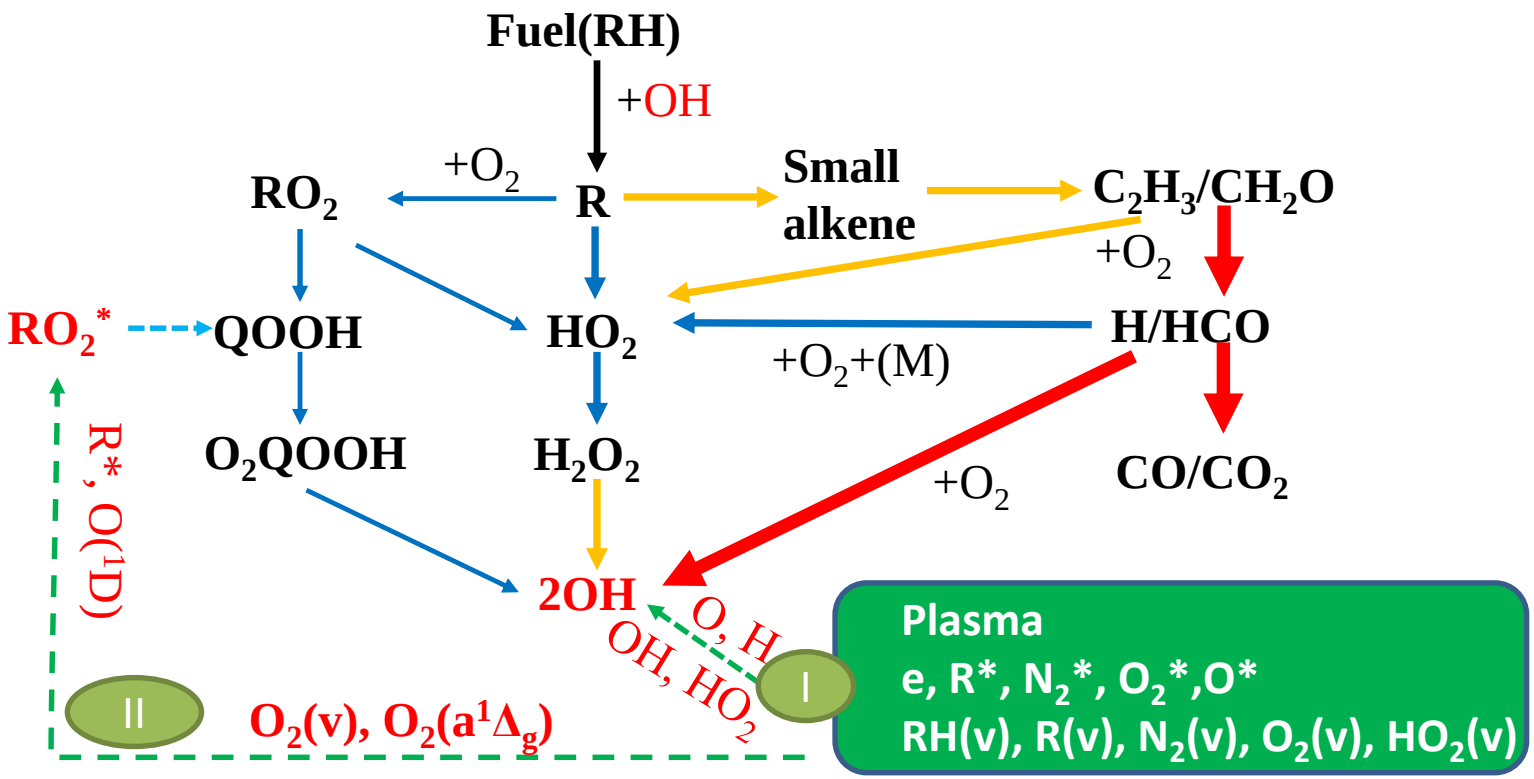


A schematic of the key reaction pathways for high pressure fuel oxidation of at different temperatures (blue arrow: Below 700K; yellow arrow: 700-1050 K; red: above 1050K). Green: plasma activated pathway

## Reaction rate

### Transition state theory

$$A + B \overset{k1}{\leftrightarrow} AB^* \overset{k2}{\rightarrow} C + D$$

$$k(T) = \frac{k_B T}{h} \frac{q_{AB}^{**}}{q_A^* q_B^*} \exp\left(-\frac{E^* - E_{A-B}}{k_B T}\right)$$

How does plasma affect elementary rate constant?

e.g. at 800 K

$O_2(a^1\Delta_g) + H = OH + O$ **Fast**
$O_2 + H = OH + O$ **Slow**

$CH_3 + O_2(v) \rightarrow CH_2O + OH$ **Fast**
$CH_3 + O_2 \rightarrow CH_2O + OH$ **Slow**

# 2. Plasma chemistry and timescales of kinetic processes

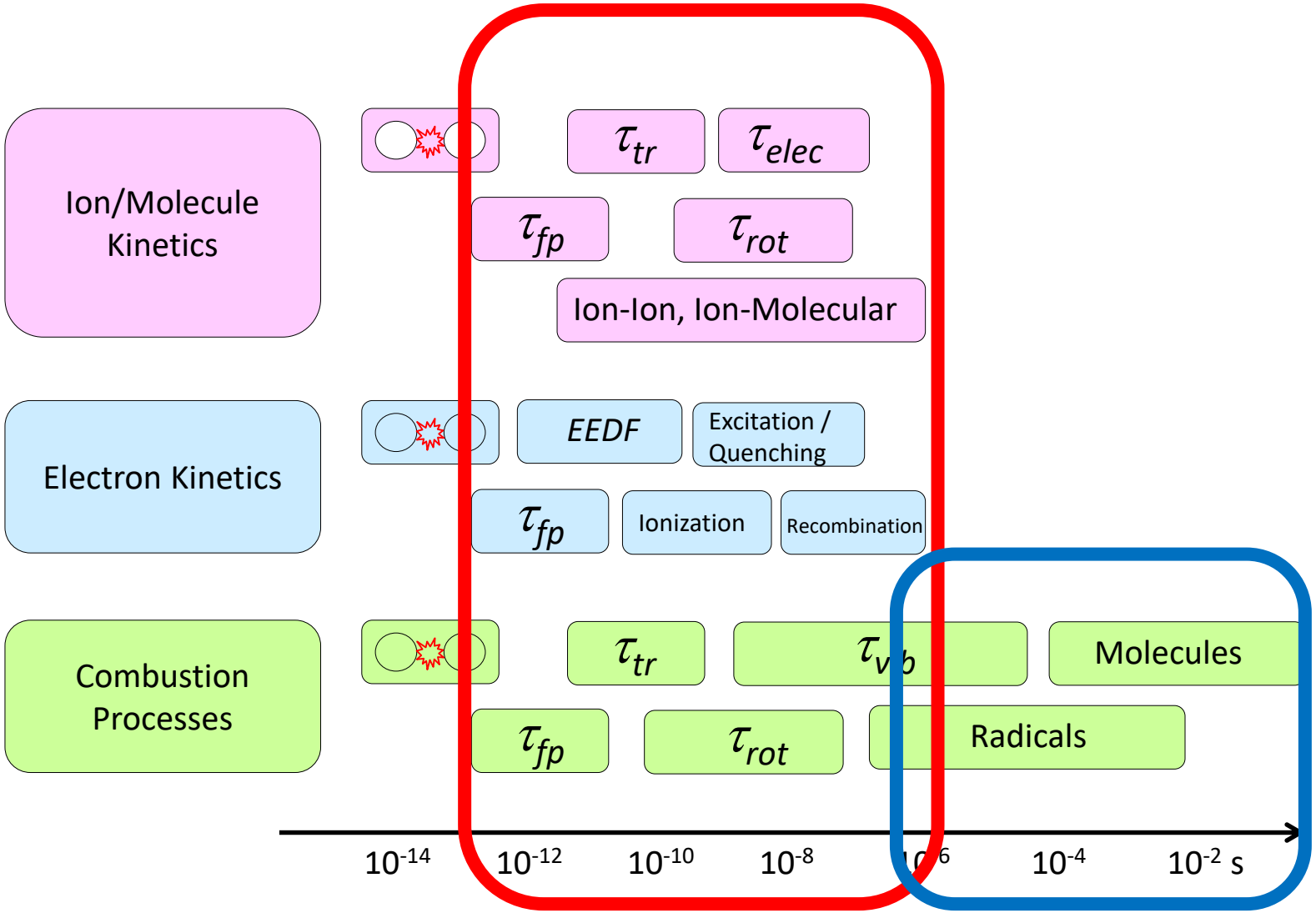


Courtesy of Andrey Starikovskiy

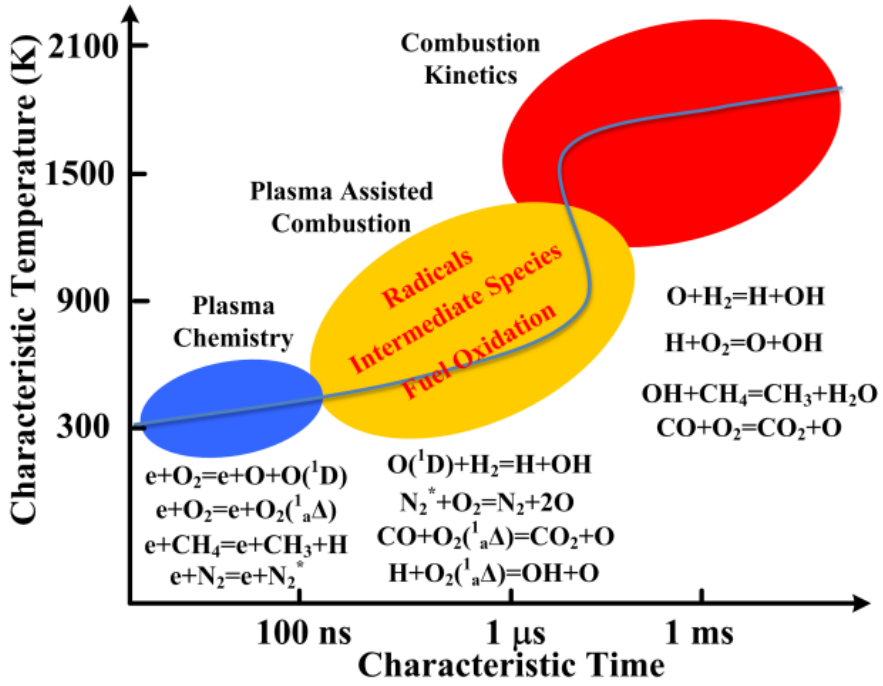


Fig. 1.5 Schematic of timescales and key kinetic pathways at different stages of plasma assisted ignition and combustion.

Ju and Sun, PECS, 2015

# Potential Energy Curves of $O_2$

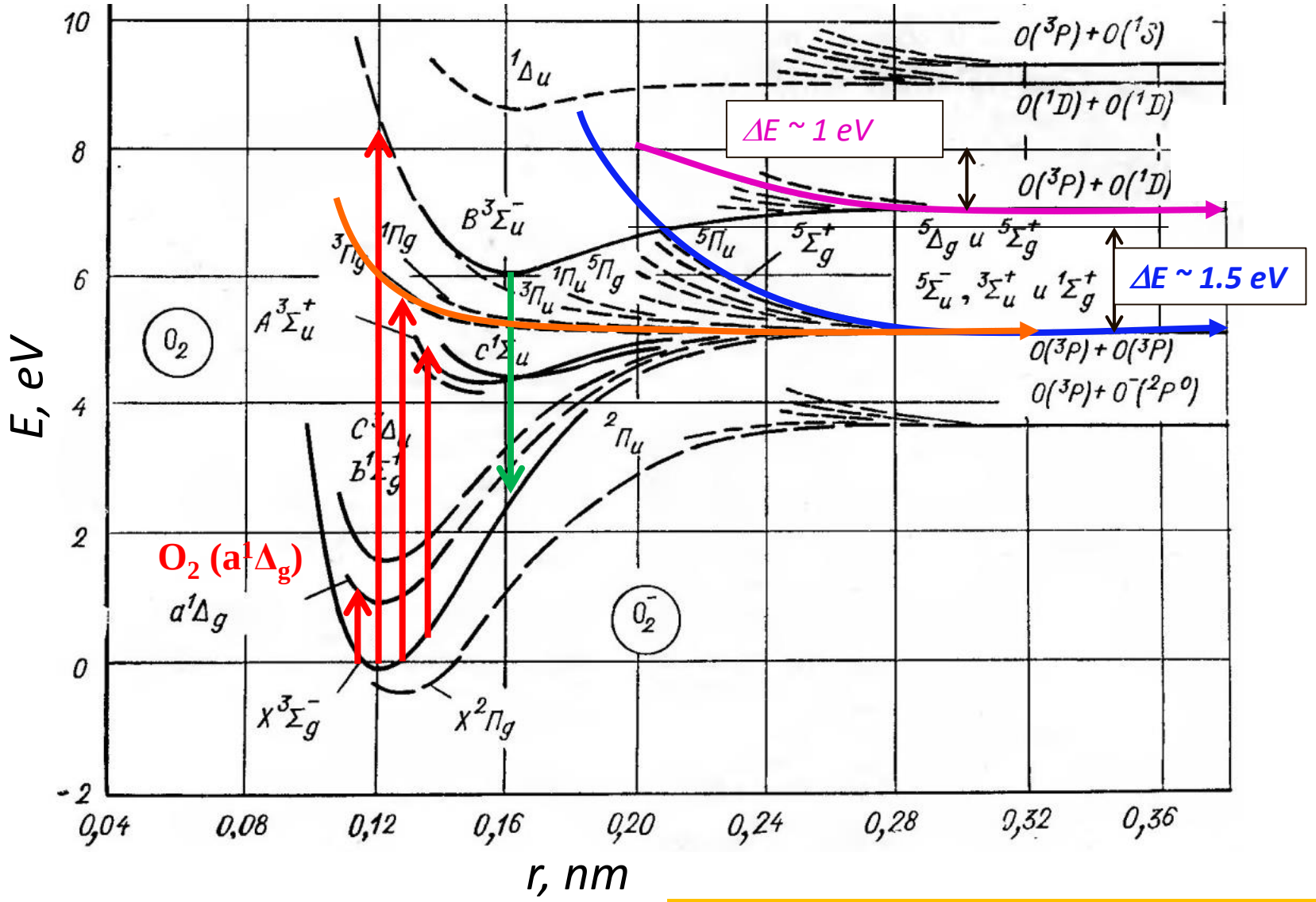


$O_2(B^3\Sigma_u^-)$, 8.4 eV
$\sigma_{max}$ = 1.0 $A^2$ (9.4 eV)

$O_2(^3\Pi_g)$, 5.6 eV
$\sigma_{max}$ = 0.16 $A^2$ (12 eV)

$O_2(A^3\Sigma_u^+)$, 4.5 eV
$\sigma_{max}$ = 0.18 $A^2$ (6.6 eV)

$O_2$ ($b^1\Sigma_g^+$) at 1.6 eV

$O_2$ ($a^1\Delta_g$) at 0.98 eV

**Electron impact reaction is a function of electron energy distribution (E/N)**

# Electron impact reaction cross sections-$O_2$

PRINCETON
Mechanical and Aerospace Engineering

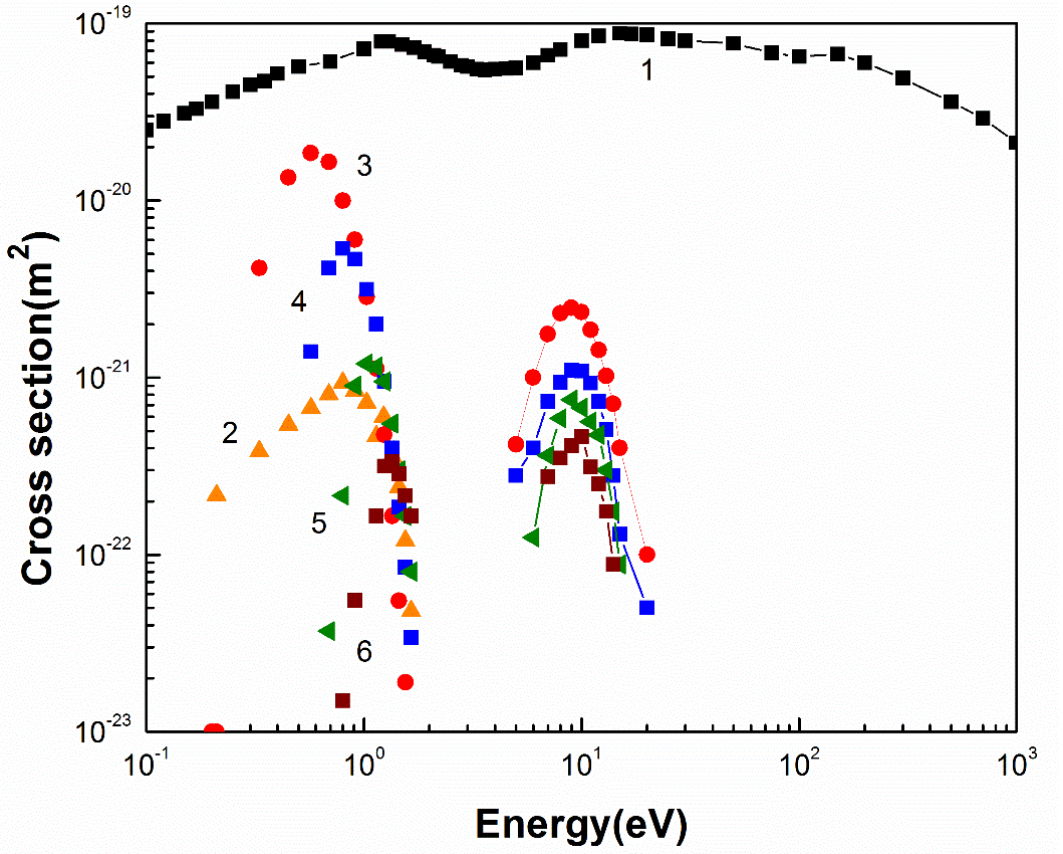


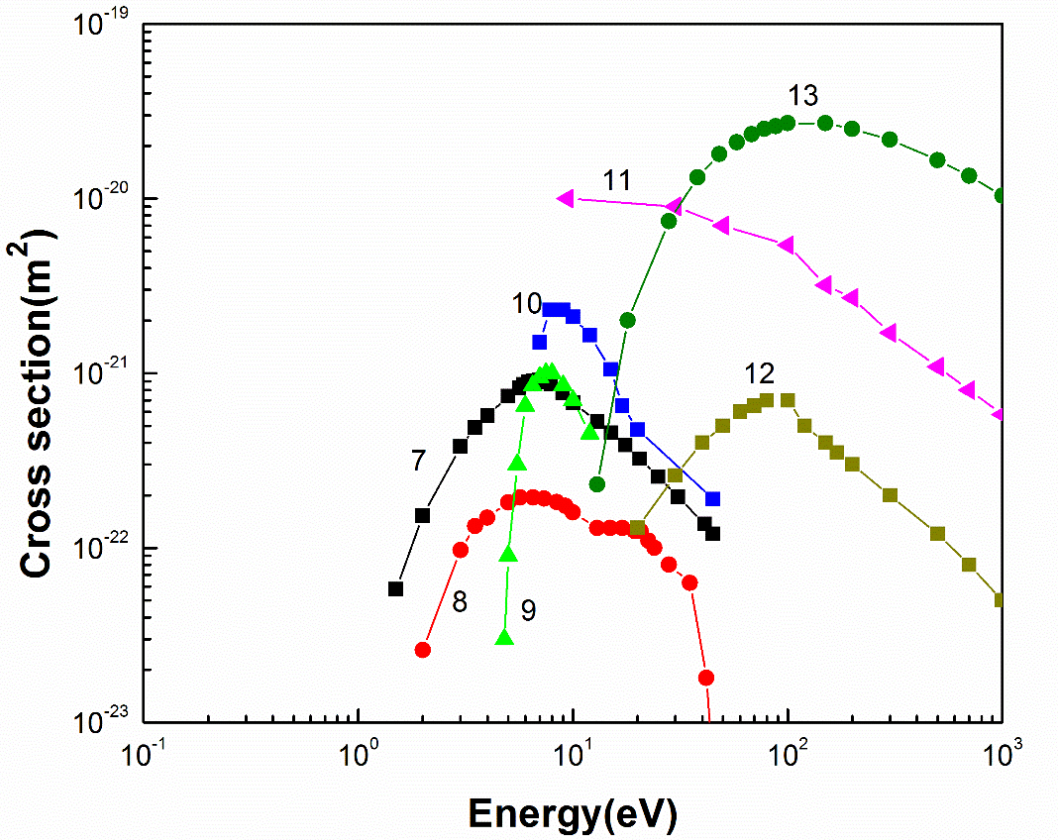


1. effective
2. rotational excitation
3-6. $O_2$(v1) - $O_2$ (v4)

7. $O_2$(a1) 8. $O_2$(b1) 9. $O_2(A^3\Sigma_u^+)$, 4.5 eV
10. O+O 11. O+O(1D) 12. O+O(1S)
13. $O_2^+$

# Potential Energy Curves of N2

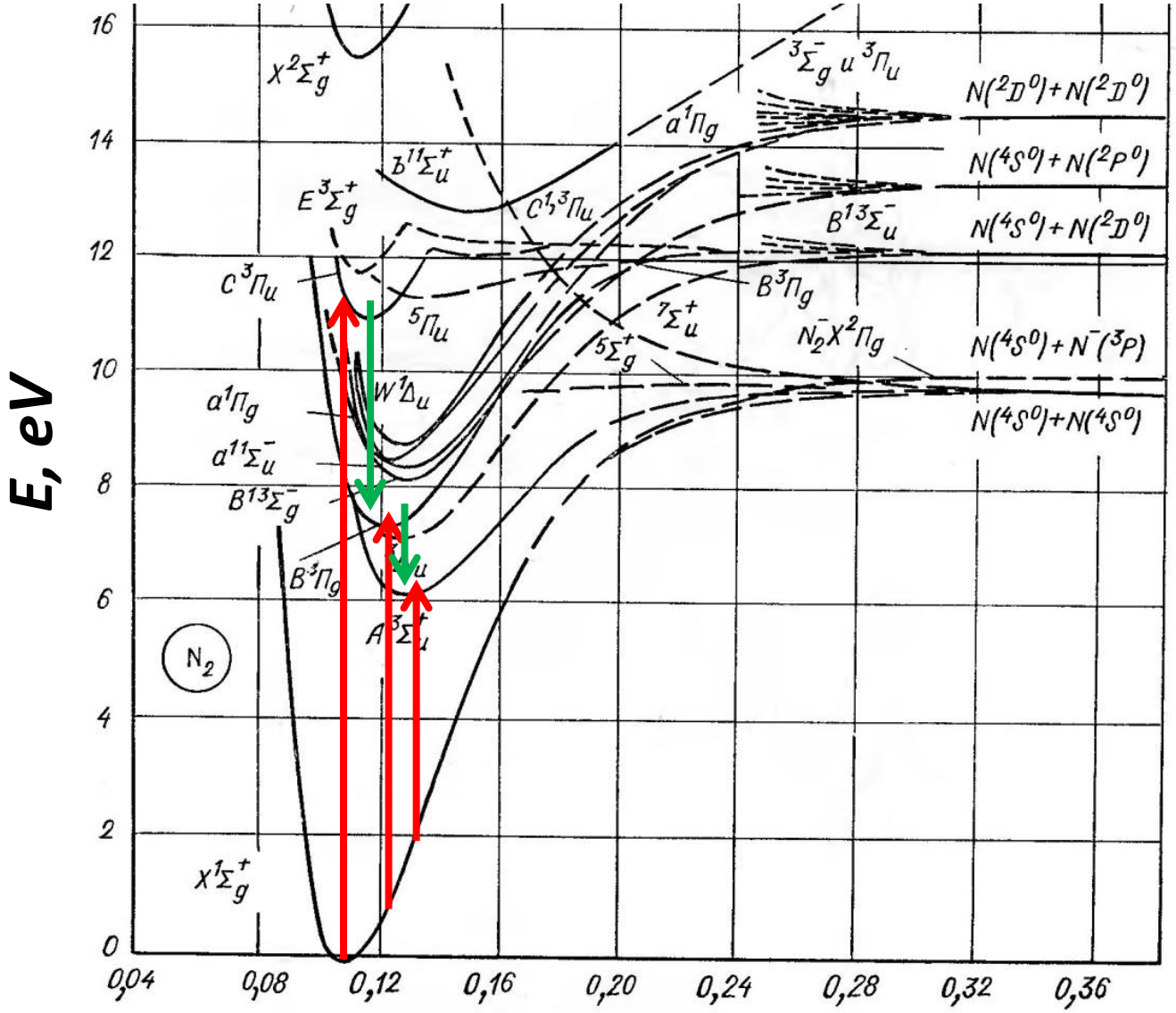


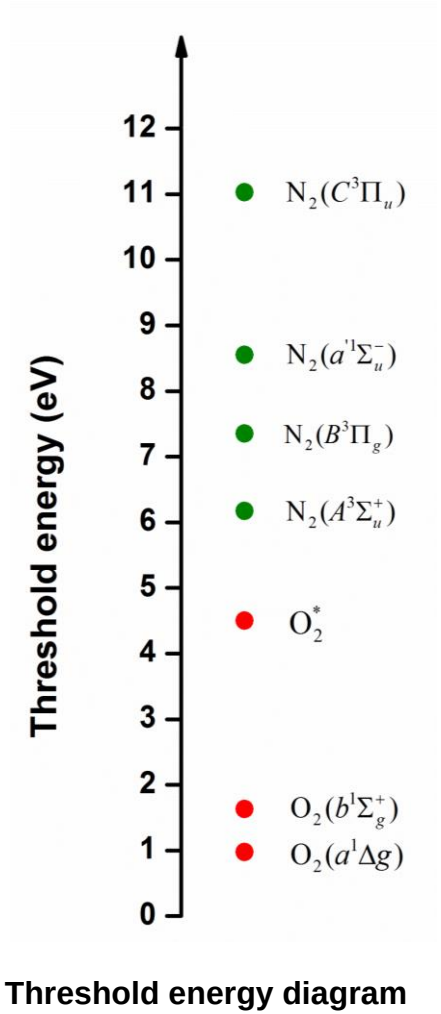


Threshold energy diagram

$N_2(A^3\Sigma_u^+)$, 6.2 eV
$\sigma_{max}$ = 0.08 $A^2$ (10 eV)

$N_2(B^3\Pi_g)$, 7.35 eV
$\sigma_{max}$ = 0.20 $A^2$ (12 eV)

$N_2(C^3\Pi_u)$, 11.03 eV
$\sigma_{max}$ = 0.98 $A^2$ (14 eV)

**Electron impact reaction is a function of electron energy distribution**

# Energy Transfer of non-equilibrium excitation in Plasma Discharge

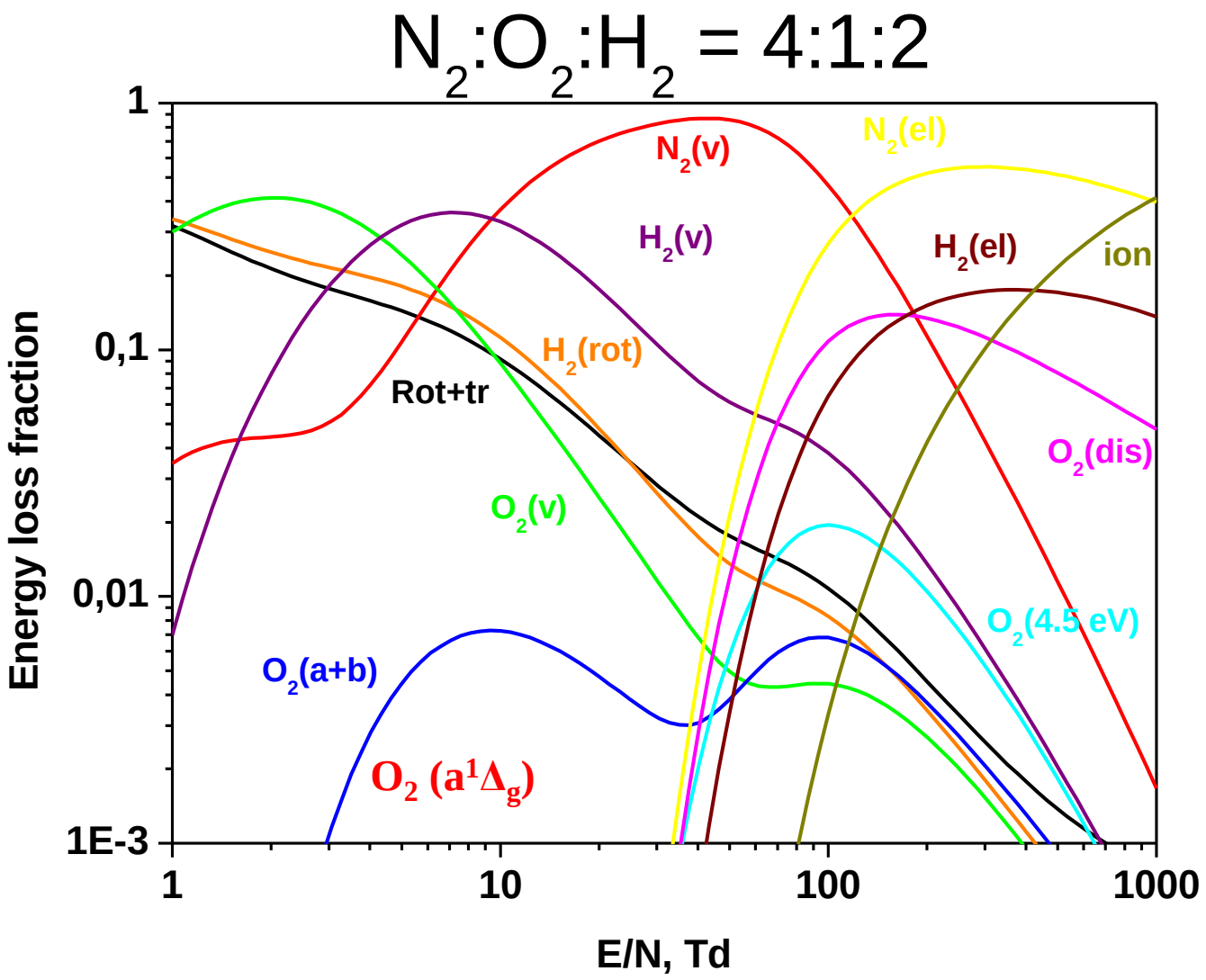

# Influence of Electronic and Vibrational Excitation on Combustion Kinetics

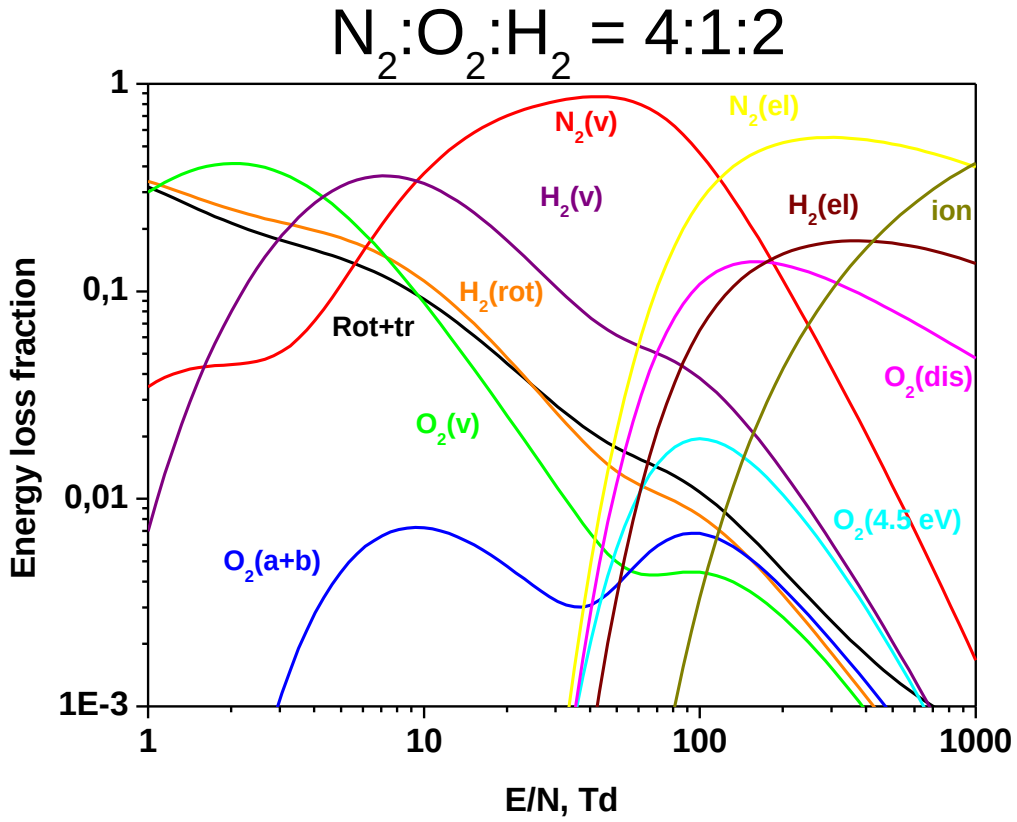


$N_2 + e = N_2(C^3) + e$

$N_2(C^3) + O_2 = N_2 + O + O$

$O_2 + e = O + O + e$

$N_2 + e = N_2(v) + e$

$N_2(v) + HO_2 = N_2 + HO_2(v)$

$HO_2(v) = O_2 + H$

# Influence of Vibrational Excitation on Low-Temperature Kinetics: $H_2O_2$ Decomposition

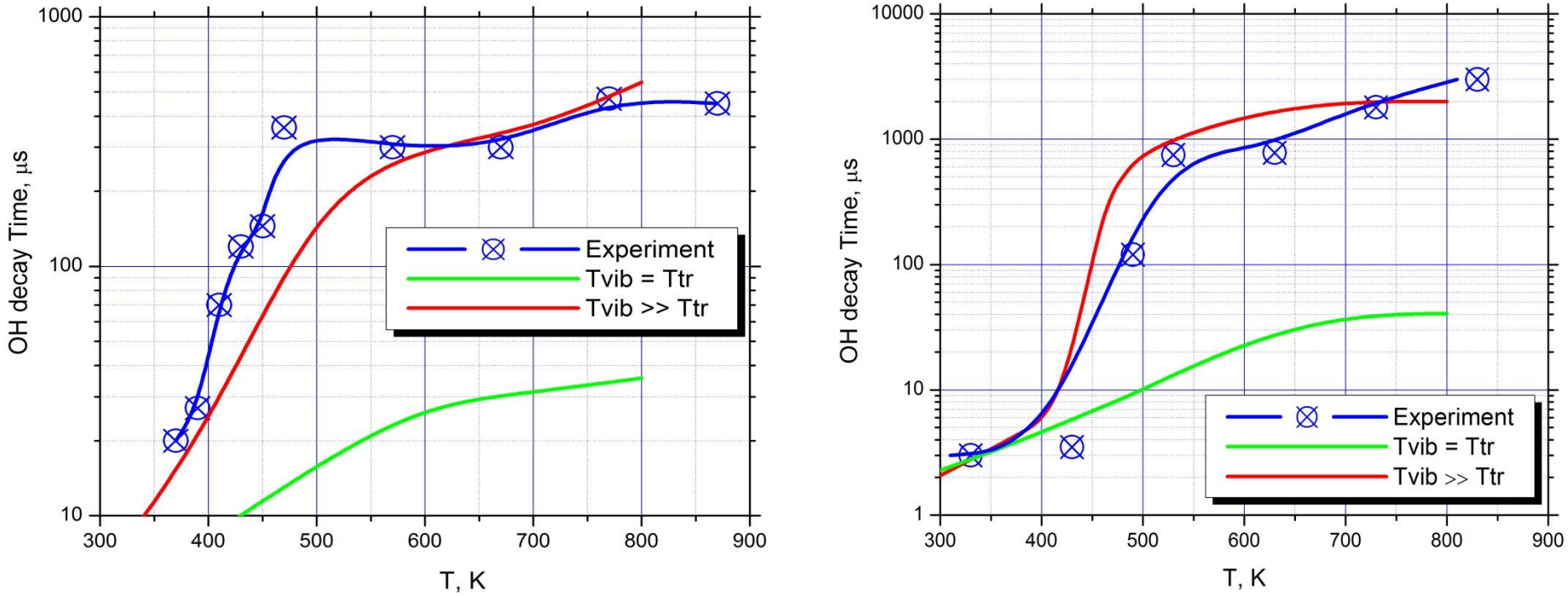


Measured and calculated OH decay time. P = 1 atm.
a) 3%$H_2$ + air; b) 0.3%$C_4H_{10}$ + air.

PRINCETON University

# Effect of "Hot" Atoms on Active Species Production in High-Voltage Pulsed Discharges

**Nonequilibrium distributions of neutral species are formed in different physical situations. In laboratory experiments and in the terrestrial atmosphere, there are numerous collisional processes in which translationally energetic (superthermal) atoms with energies much above thermal energies are produced.**

Potential energy curves and hot atoms formation

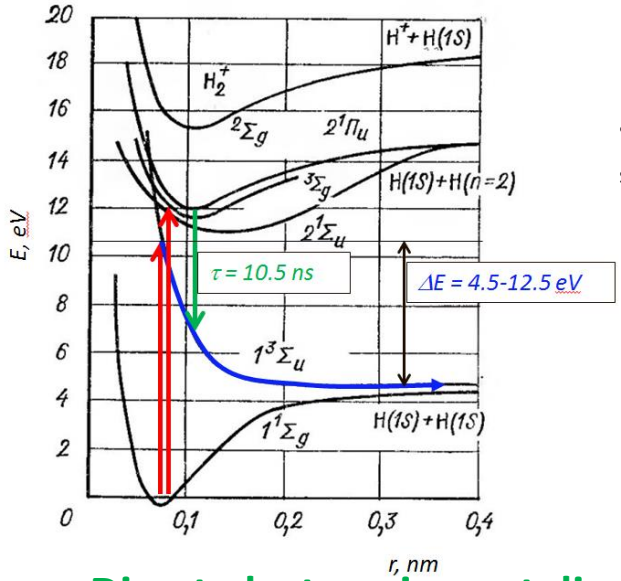


Momentum transfer cross section for the H-$H_2$ scattering

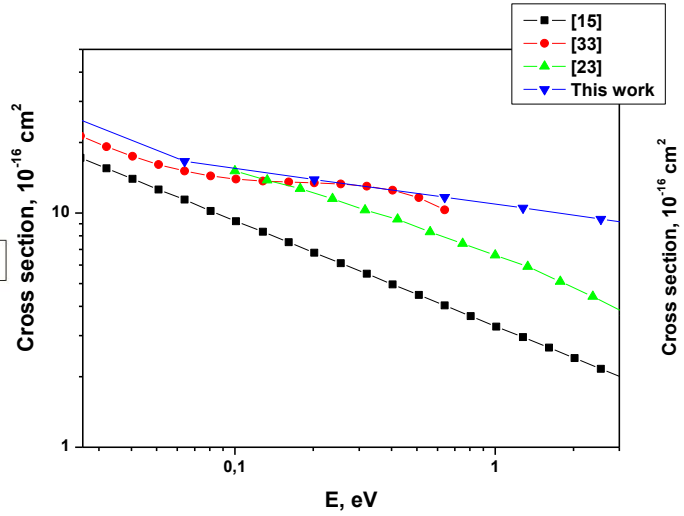


Cross sections for scattering of H atoms with $H_2$, $O_2$, $CH_4$ and $N_2$

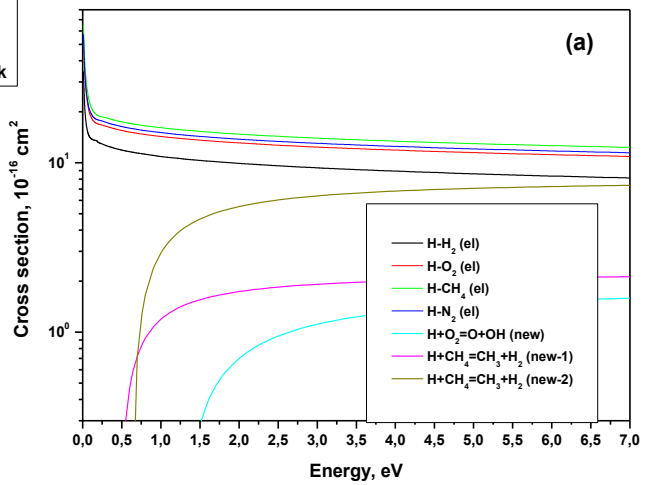


## Direct electron-impact dissociation

$e + O_2 \rightarrow e + O_2^*$ $\quad O_2^* \rightarrow 2O(^3P,^1D) + 1.3$ eV

$e + H_2 \rightarrow e + H_2^*$ $\quad H_2^* \rightarrow 2H(^1S) + 4.5$ eV

$e + CH_4 \rightarrow e + CH_4^*$ $\quad CH_4^* \rightarrow CH_3 + H + 3.5$ eV


Mechanical and Aerospace Engineering
Applied Physics Group

PRINCETON University

# Effect of "Hot" Atoms on Active Species Production in High-Voltage Pulsed Discharges

## Average energy of H atoms in various gaseous mixtures

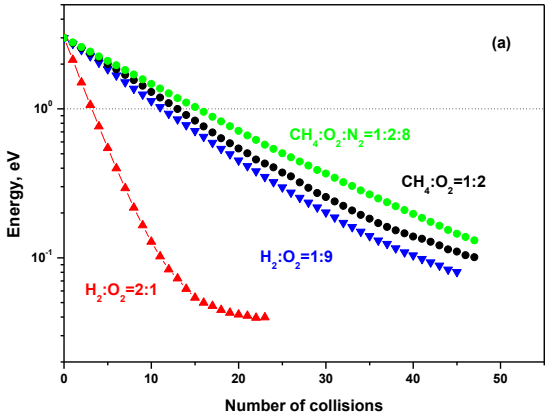


## Species produced during energy degradation of one "hot" H atom

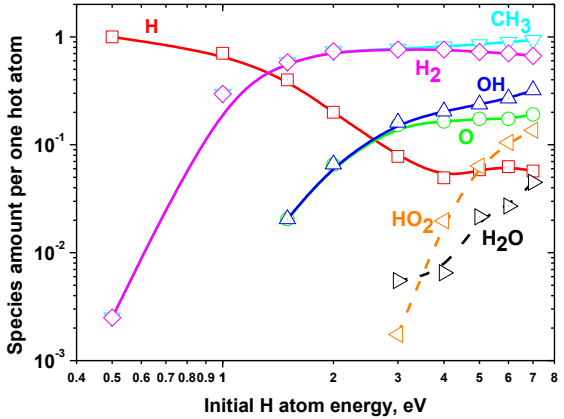


## Plasma-assisted oxidation in H2-O2 mixture

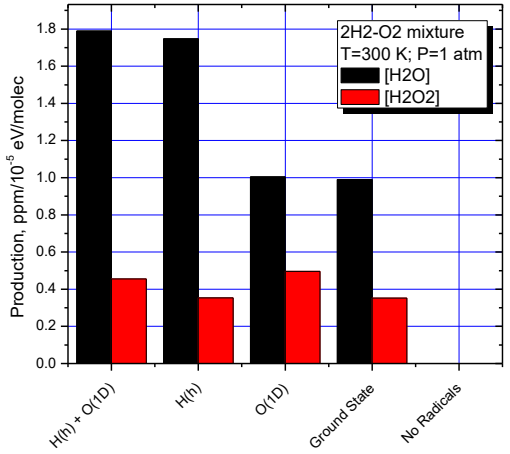


## Plasma-assisted oxidation in CH4-O2 mixture

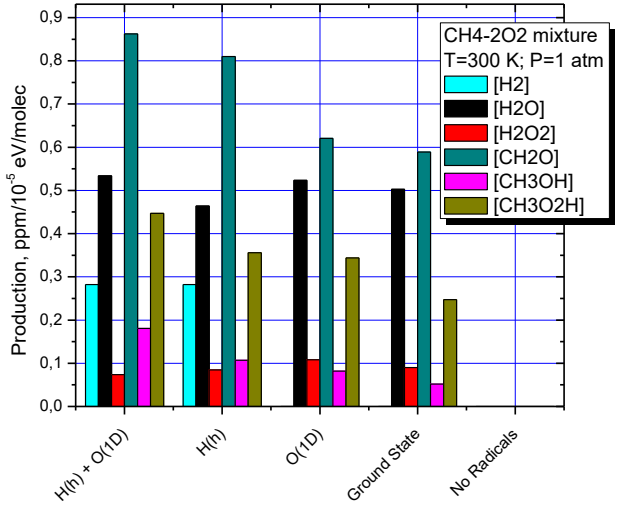


- **Analysis of the effect of formation of "hot" atoms with excessive translational energy shows the important role of these processes in formation of active radicals.**
- **The density of radicals produced in discharge plasma can be several times higher than that produced in the absence of high-energy atoms.**
- **The effect plays a fundamental role in the formation of the initial distribution of active species in combustible mixtures and can greatly influence the kinetics of ignition and oxidation at low gas temperatures.**


Mechanical and Aerospace Engineering
Applied Physics Group

# Gas heating at high E/N

**Fast Gas Heating**

- Electron-ion recombination: $e + O_2^+ \rightarrow O + O^* + \Delta E$
- Ion-ion recombination: $O_2^- + O_2^+ + M \rightarrow 2O_2 + M + \Delta E$
- Collisional energy transfer Electronically-excited species: $N_2(A,B,C,a) + O_2 \rightarrow 2O + \Delta E$
- Hot atom and molecule: $O_2^* \rightarrow 2O(^3P,^1D) + \Delta E$

**Slow Gas Heating**

- Vibrational energy relaxation: $N_2(v) + M = N_2(v-1) + M + \Delta E$

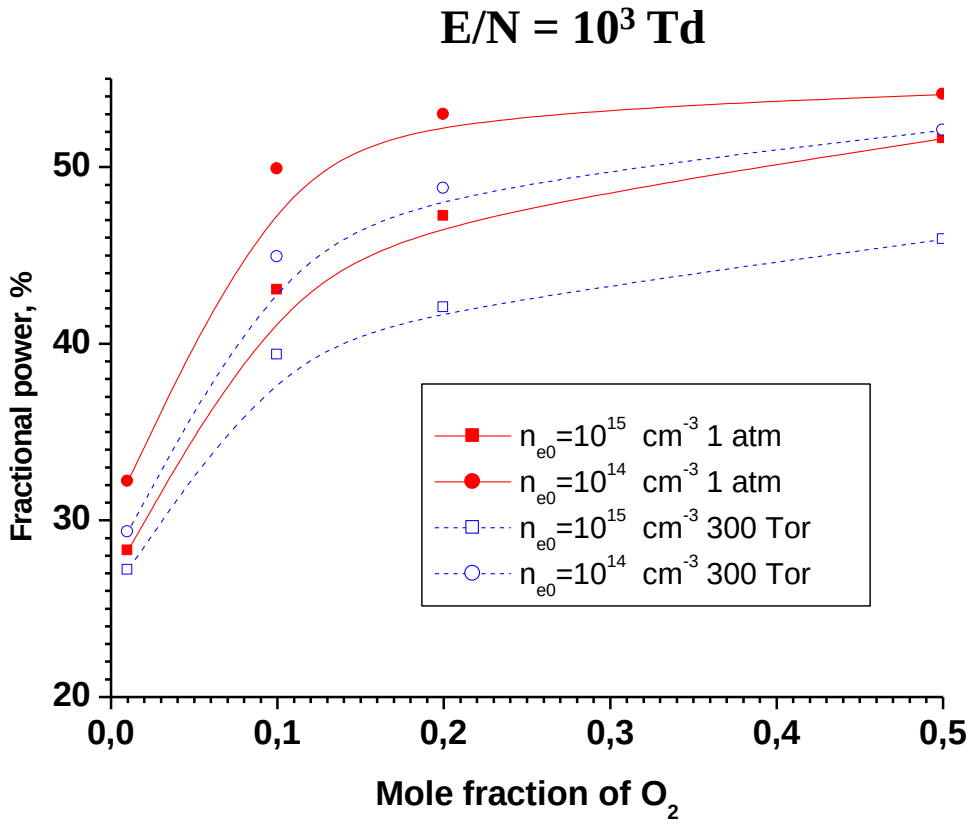


Fractional Electron Power Transferred Into Heat in $N_2$:$O_2$ Mixtures

High oxygen, faster gas heating!

# Princeton Plasma Combustion Kinetics

## *Major Pathways*

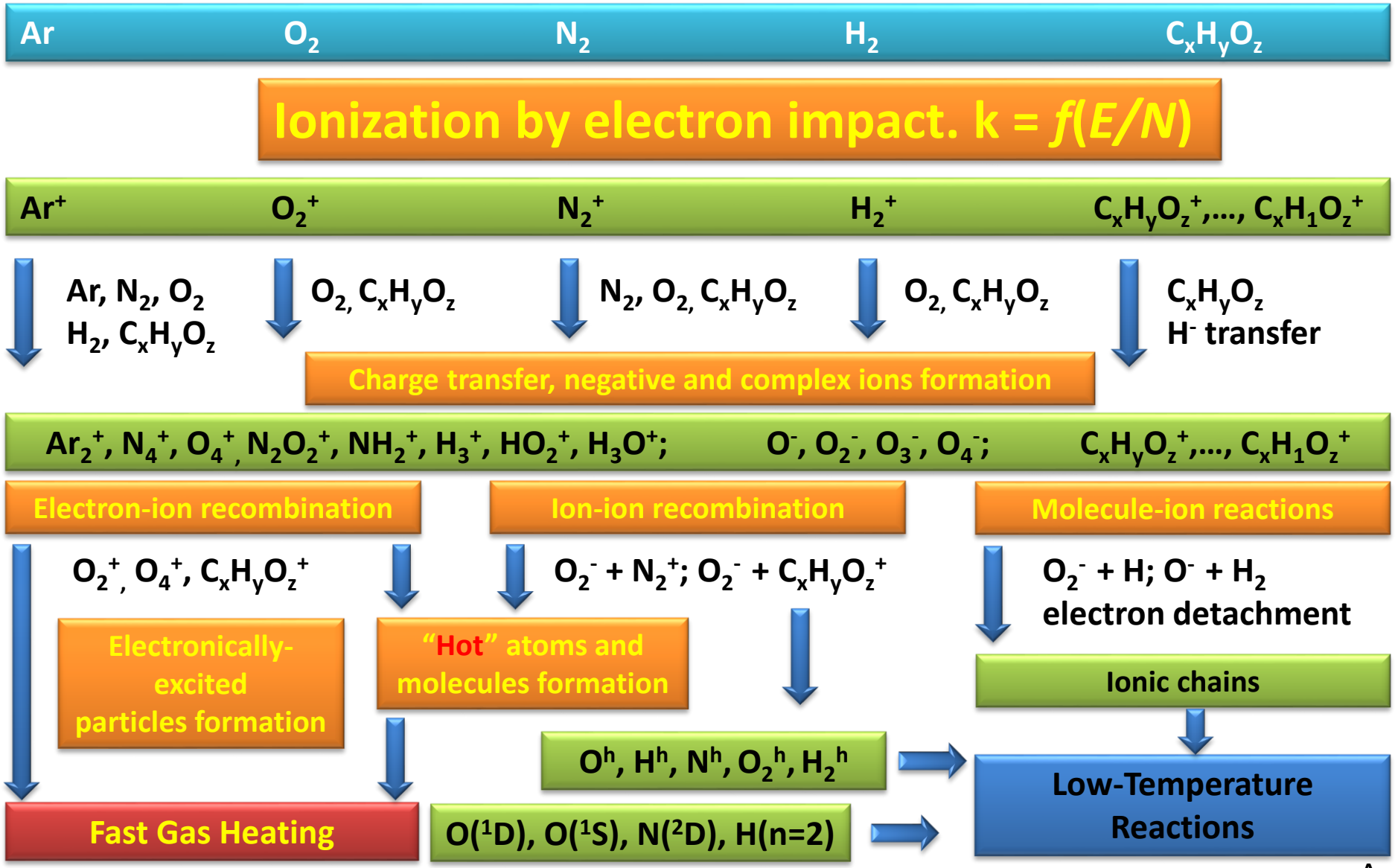


Andrey Starikovskiy

# Princeton Plasma Combustion Kinetics

## *Major Pathways*

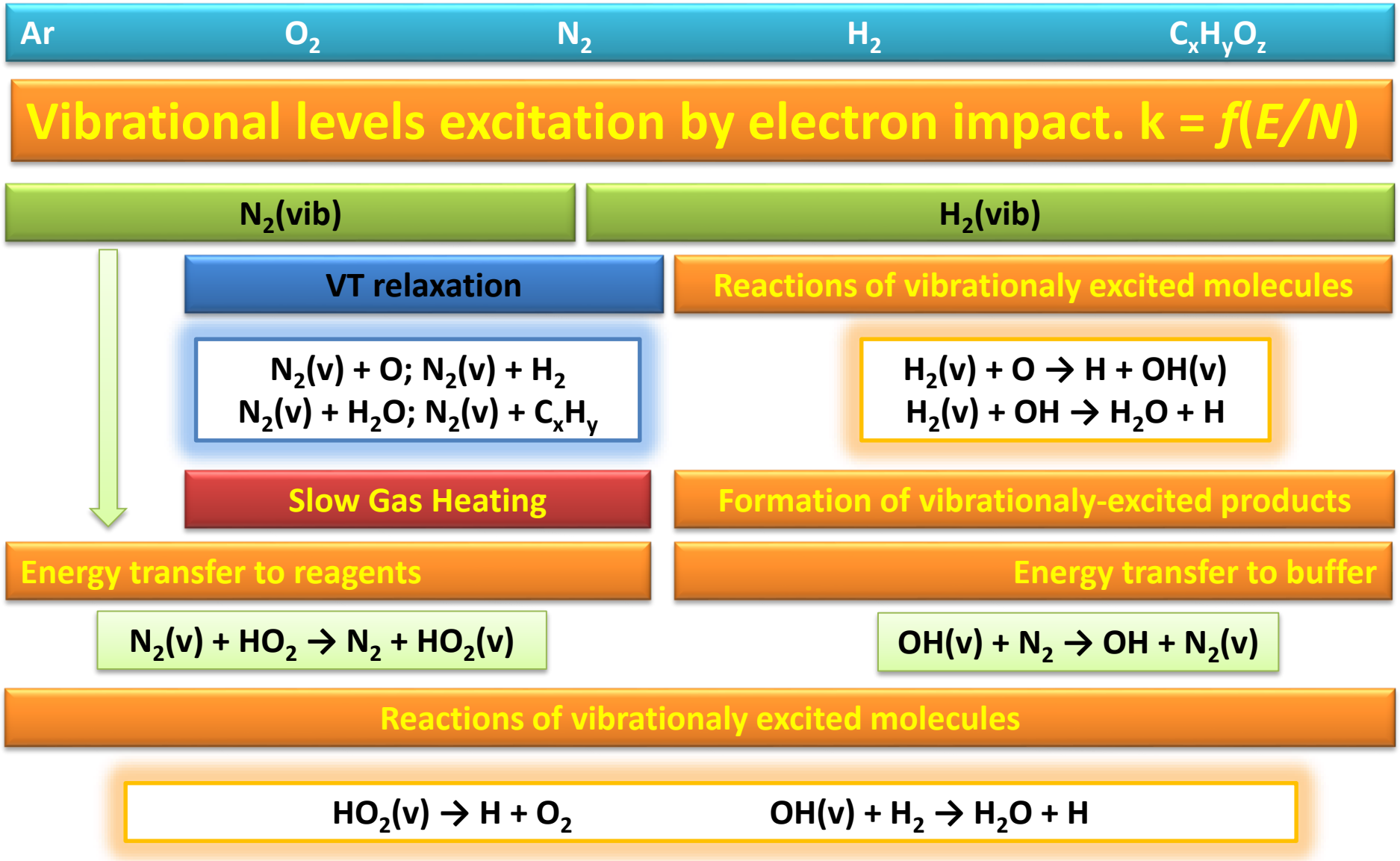
Ar
$O_2$
$N_2$
$H_2$
$C_xH_yO_z$
Vibrational levels excitation by electron impact. k = *f*(*E*/*N*)
$N_2$(vib)
$H_2$(vib)
VT relaxation
Reactions of vibrationaly excited molecules
$N_2(v) + O$; $N_2(v) + H_2$
$N_2(v) + H_2O$; $N_2(v) + C_xH_y$
$H_2(v) + O \rightarrow H + OH(v)$
$H_2(v) + OH \rightarrow H_2O + H$
Slow Gas Heating
Formation of vibrationaly-excited products
Energy transfer to reagents
Energy transfer to buffer
$N_2(v) + HO_2 \rightarrow N_2 + HO_2(v)$
$OH(v) + N_2 \rightarrow OH + N_2(v)$
Reactions of vibrationaly excited molecules
$HO_2(v) \rightarrow H + O_2$
$OH(v) + H_2 \rightarrow H_2O + H$

# Typical plasma reactions for radical production and heating

**Electron impact ionization/dissociation/excitation**

| | | | |
|---|---|---|---|
| >10 eV | $e + O_2 = O^+ + O + 2e$ | (R1a) | Radical production |
| ~10 eV | $e + O_2 = O + O(^1D)$ | (R1b) | Non-equilibrium excitation |
| ~1 eV | $e + O_2 = O_2(^1\Delta_g) + e$ | (R1c) | |
| 0.2-2 eV | $e + O_2 = O_2(v) + e$ | (R1d) | |

**Electron ion recombination, attachment, charge transfer**

| | | |
|---|---|---|
| $e + O_2^+ = O + O(^1D)$ | (R2a) | Recombination/fast heating |
| $O_2^+ + O_2^- = 2O_2$ | (R2b) | Recombination/fast heating |
| $e + O_2 + M = O_2^- + M$ | (R2c) | Attachment |
| $H_2O + N_2^+ = H_2O^+ + N_2$ | (R2d) | Charge Transfer |

**Dissociation and energy transfer by ions and excited species**

| | | |
|---|---|---|
| $N_2(A,B,C) + O_2 = O + O(^1D) + N_2$ | (R3a) | |
| $O(^1D) + H_2 = OH + H$ | (R3b) | |
| $H + O_2(^1\Delta_g) = O + OH$ | (R3c) | |
| $N^+ + O_2 = O^+ + NO$ | (R3d) | |
| $CH_3 + HO_2(v) = CH_2O + OH$ | (R3e) | Slow heating |
| $N_2(v=5) + N_2 = N_2(v=3) + N_2$ | (R3f) | |
| $N_2(v) + HO_2 \rightarrow N_2 + HO_2(v)$ | (R3g) | |

# What are the major species produced by plasma?

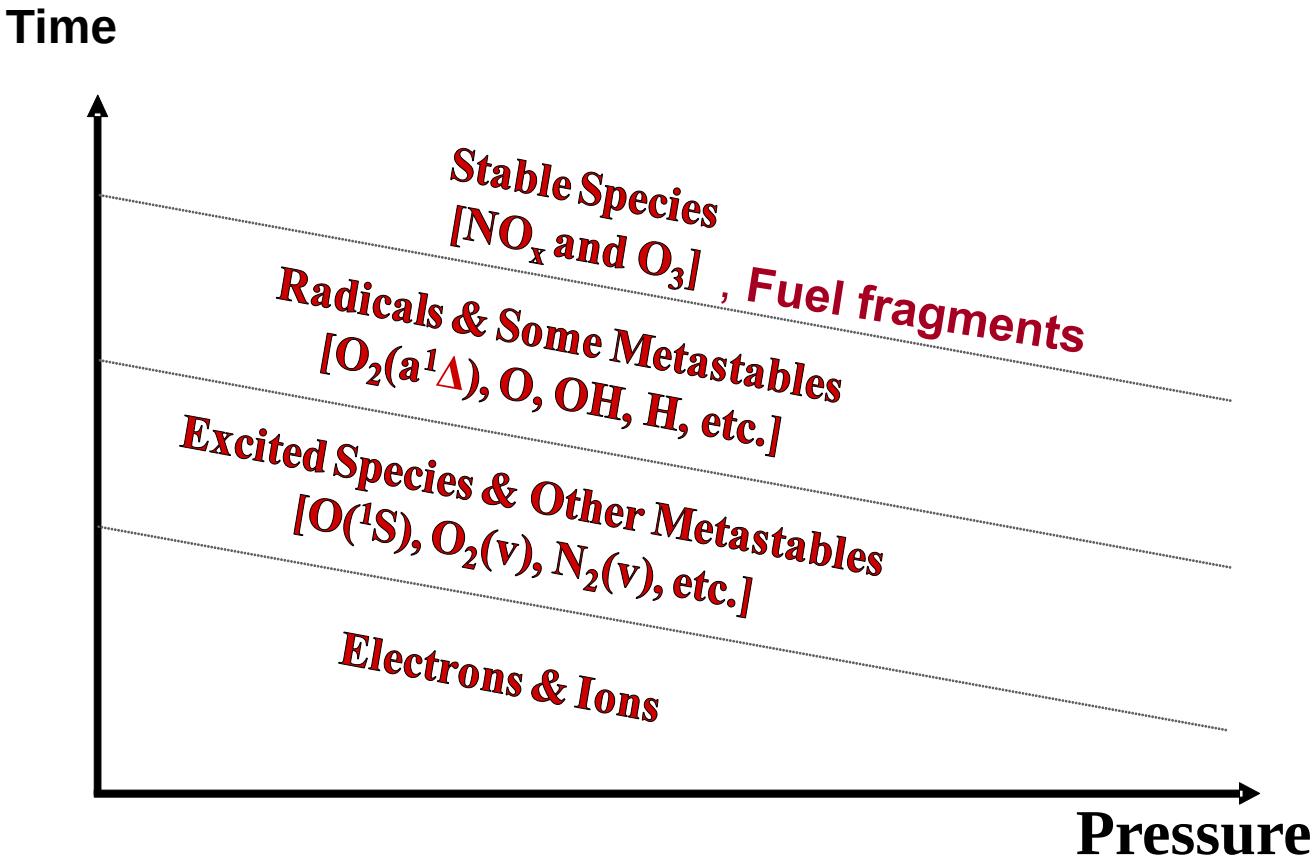


- Long lifetime species? NO, $O_3$, $O_2(a^1\Delta_g)$
- Short lifetime plasma generated species? O, $N_2$ (A,B,C)*

# 3. Impact of plasma chemistry on combustion

**Question: When will electron impact dissociation process become important in combustion?**

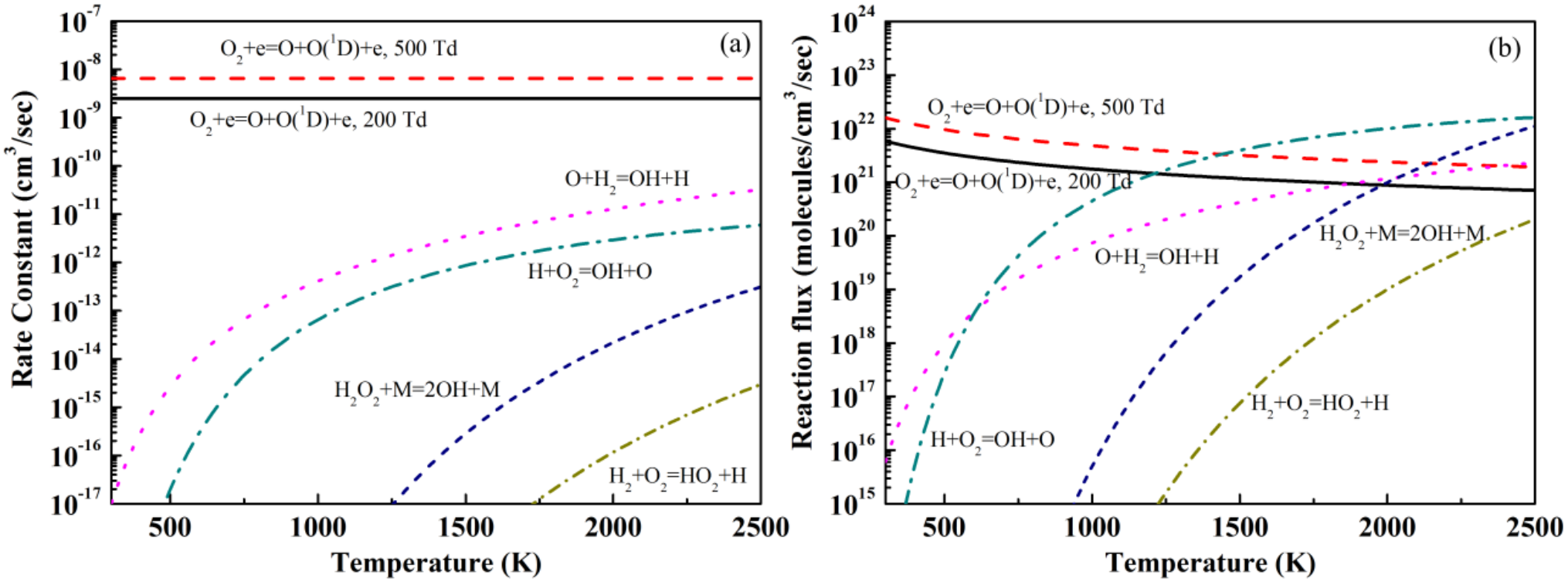


Fig. 3.5: Rate constants (a) and reaction flux (b) for reactions for dissociation by electron impact at electric field values equal to 200 Td and 500 Td and chain branching reactions.

Ju and Sun, PECS, 2015.

# Comparison of the reaction rates of electron impact and excited species for radical production

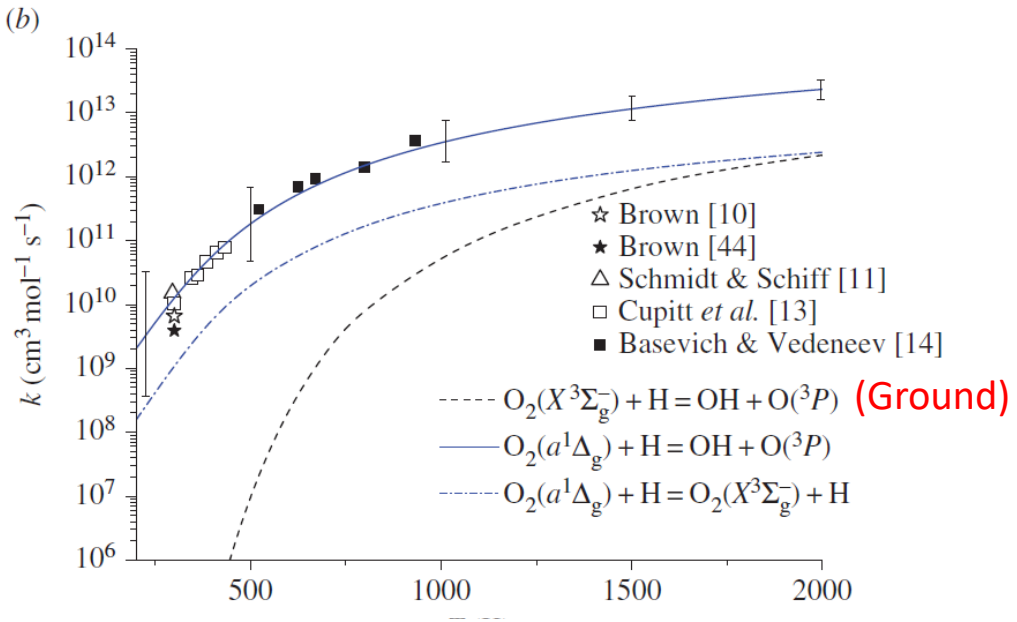
(b)
$k$ (cm$^3$ mol$^{-1}$ s$^{-1}$)
☆ Brown [10]
★ Brown [44]
△ Schmidt & Schiff [11]
□ Cupitt *et al.* [13]
■ Basevich & Vedeneev [14]
$O_2(X^3\Sigma_g^-) + H = OH + O(^3P)$
$O_2(a^1\Delta_g) + H = OH + O(^3P)$
$O_2(a^1\Delta_g) + H = O_2(X^3\Sigma_g^-) + H$
$T$ (K)

(Ground)

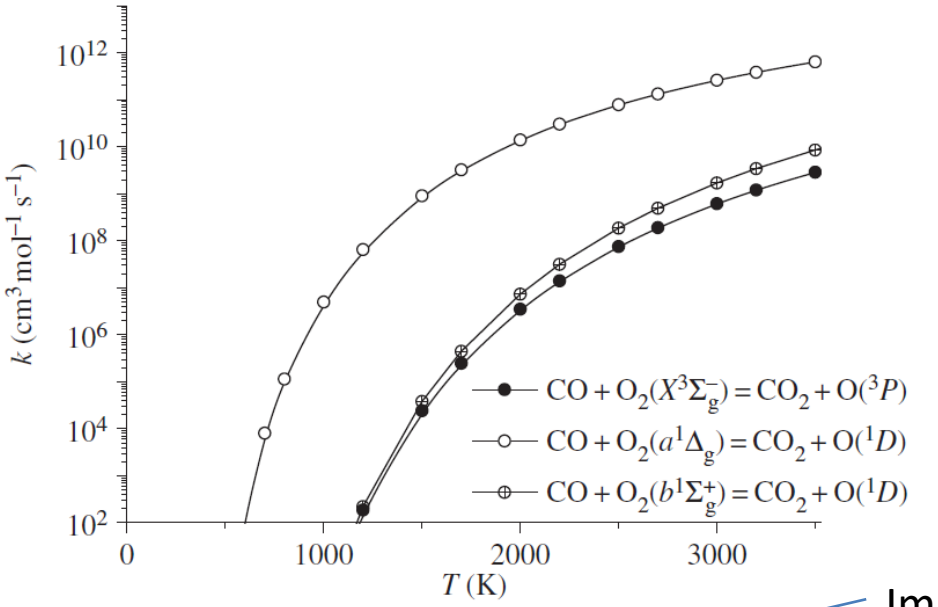


(Ground)

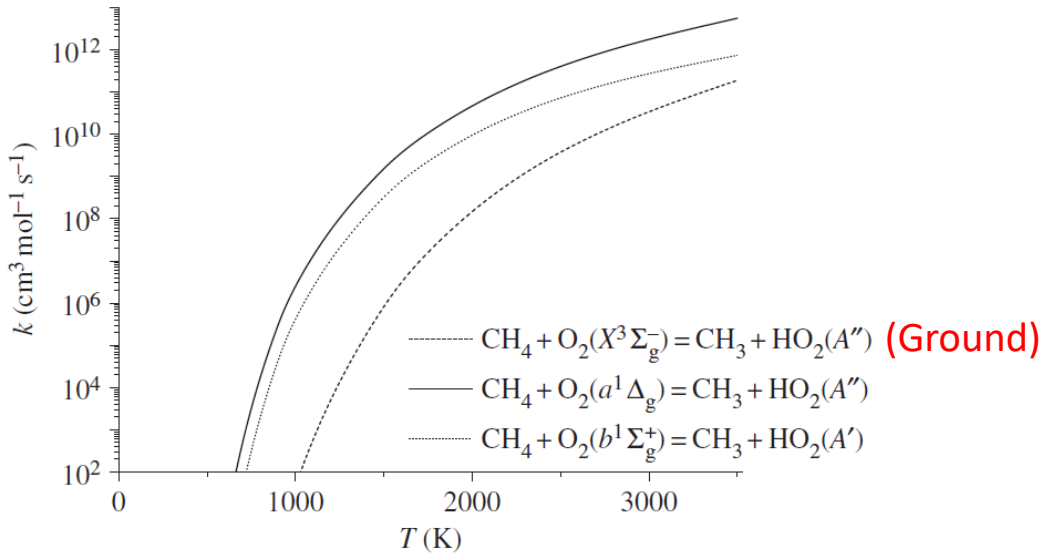


(Ground)

Important radical production channels

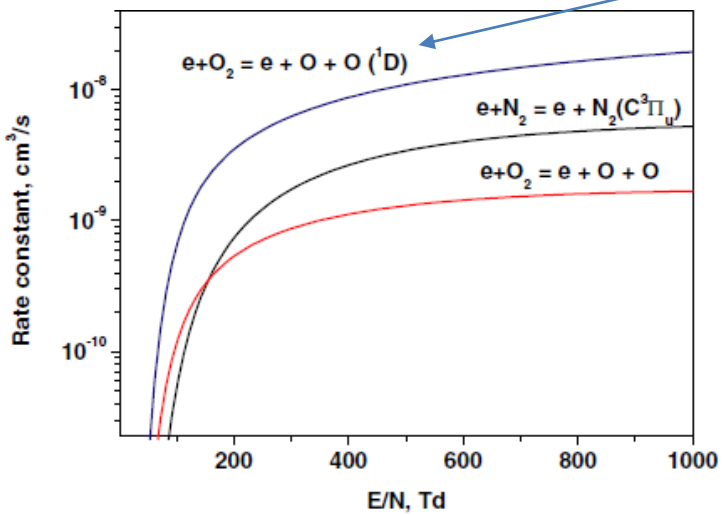


**S M Starikovskaia,** J. Phys. D: Appl. Phys. **47** (2014) 353001

A. M. Starik, B. I. Loukhovitski, A. S. Sharipov and N. S. Titova, *2016, Phil. Trans. R. Soc. A* **373**: 20140341

# PAC: how does plasma change the branching reactions in combustion?

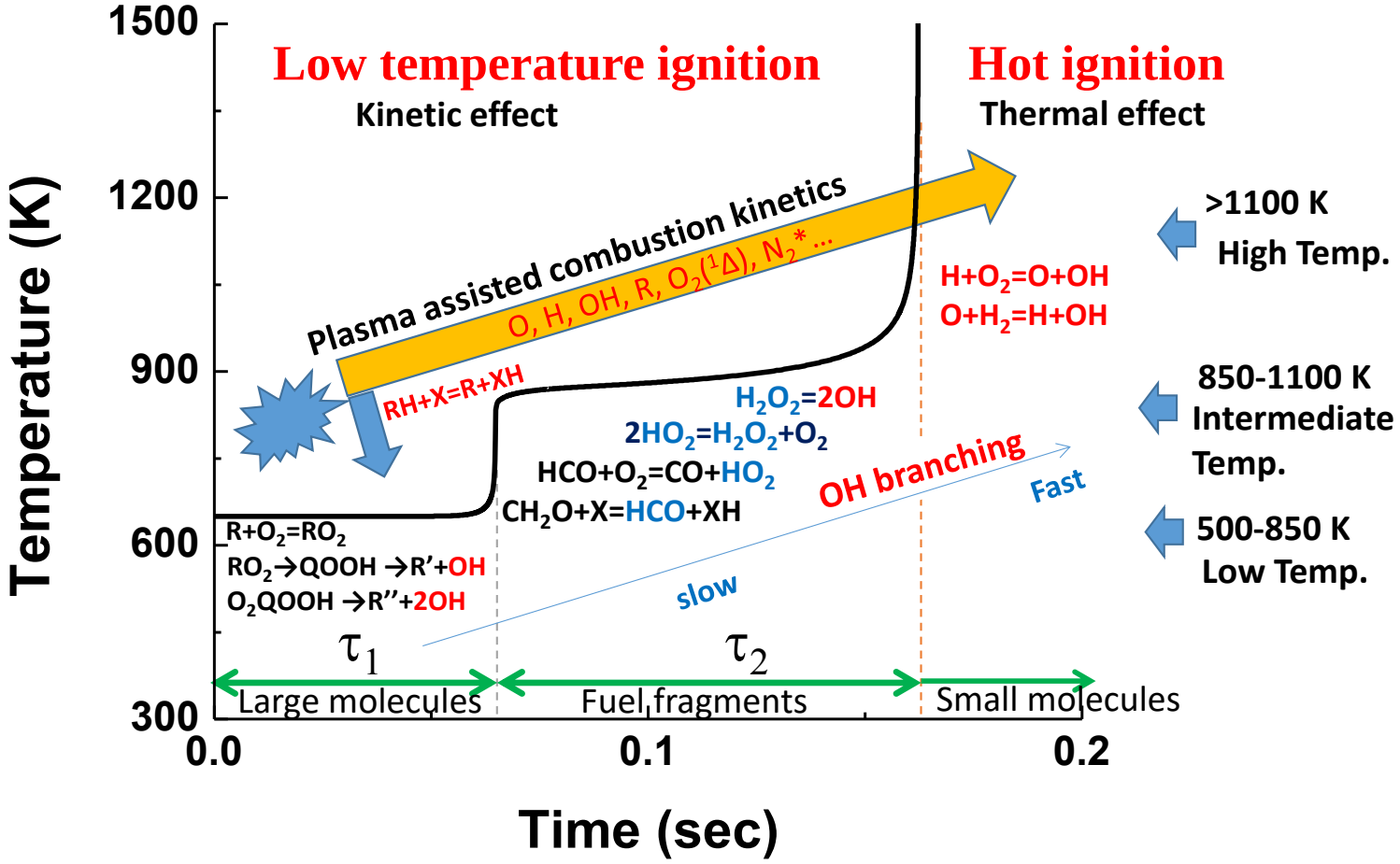


Schematic of kinetic and thermal enhancement pathways of plasma assisted combustion for liquid fuels at high, intermediate, and low temperature, respectively

Y. Ju and W. Sun, Prog. Energy Combust. Sci., 2015

# Plasma activated *Cool Flames* :A new way to burn with plasma

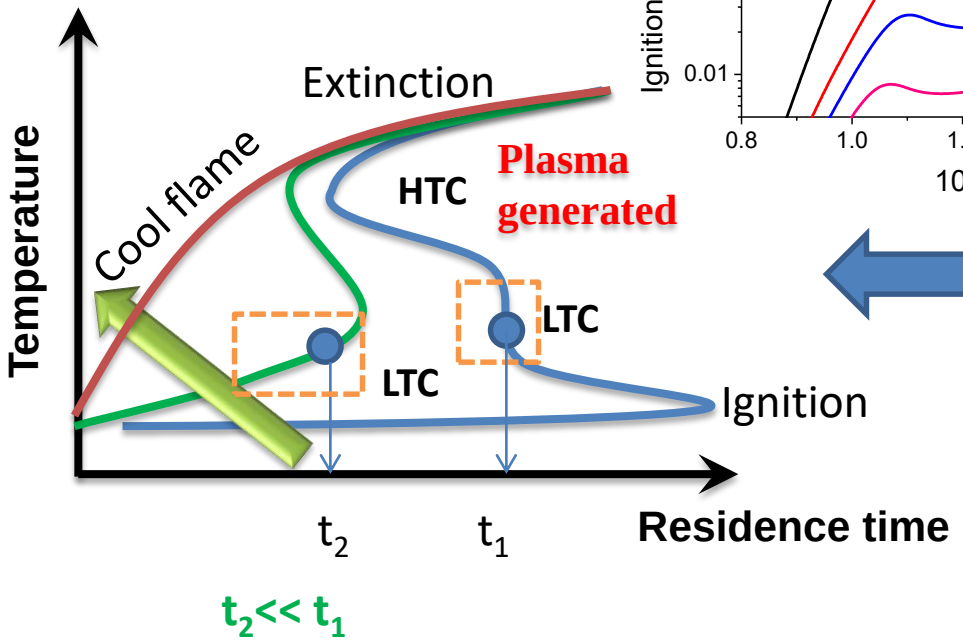


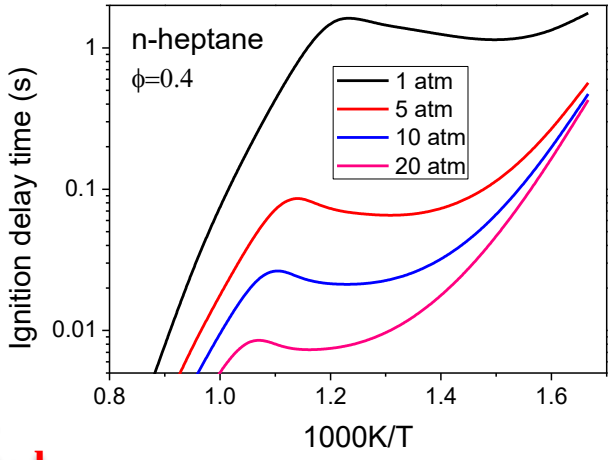


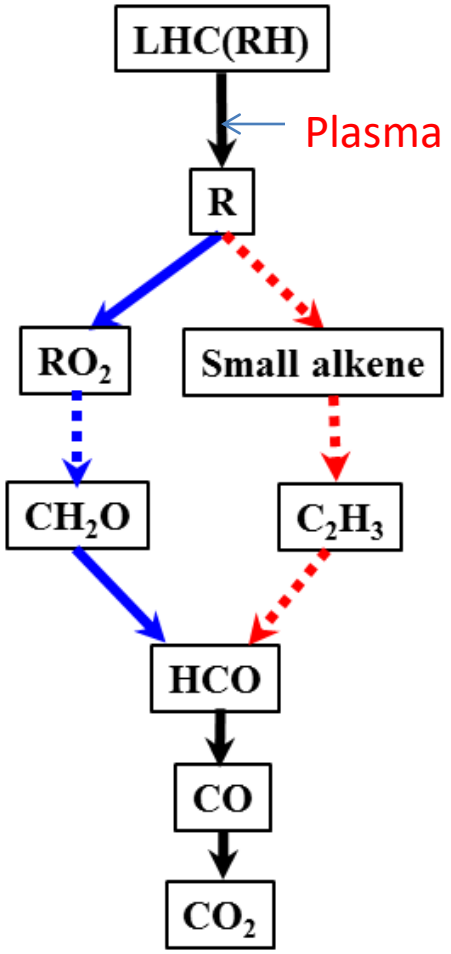


Plasma activated LTC at much shorter time, lower pressure….

We can create cool flames even at 1 atm or below?

# Observation of plasma activated self-sustaining *Cool Flames*

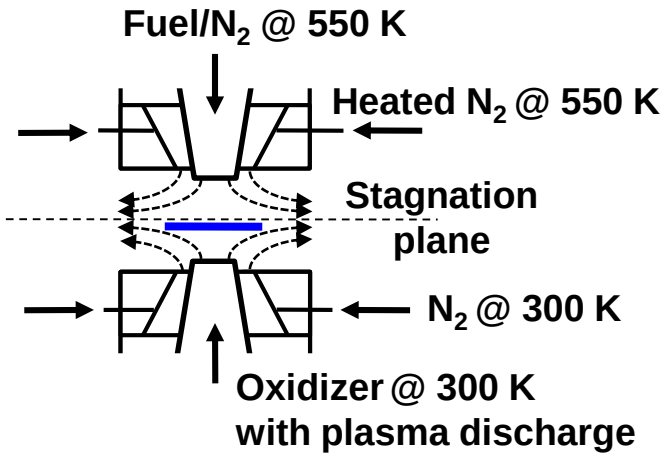


Fig. 1 Schematic of experimental setup

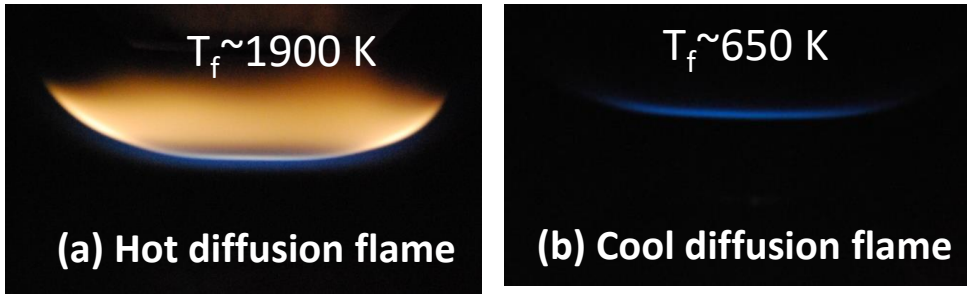


Fig. 2 Hot and cool n-heptane diffusion flames at the same condition

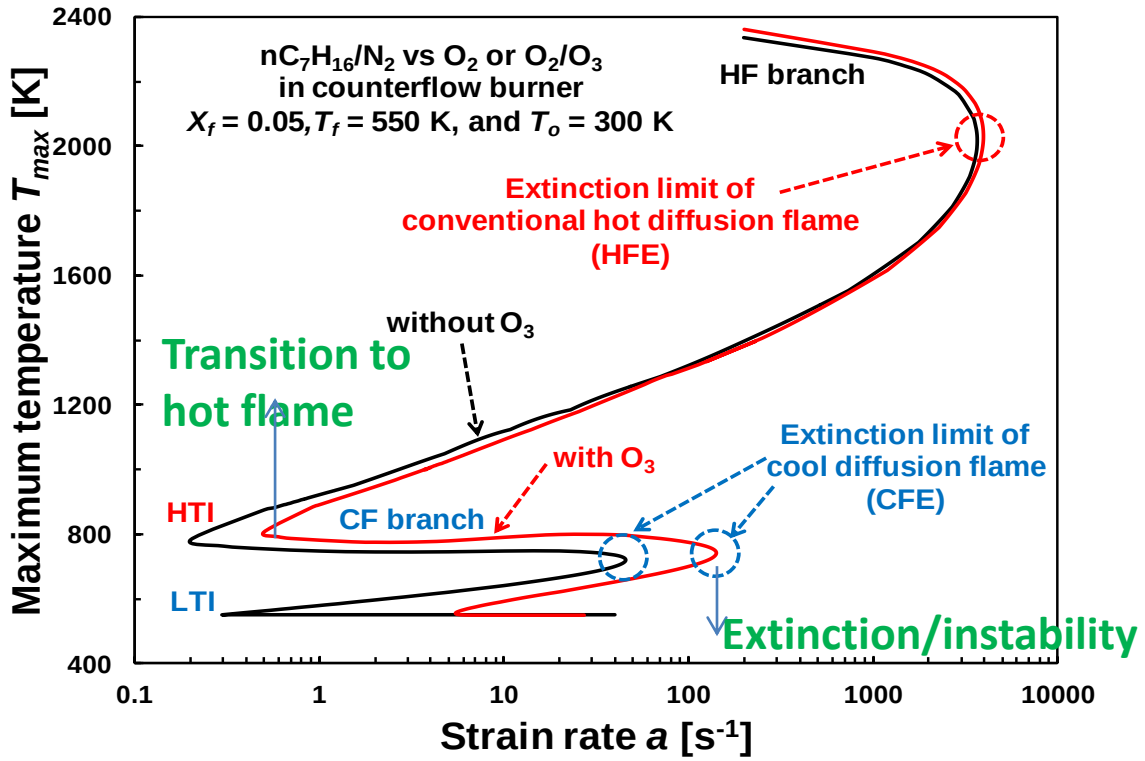



Won, S.H., Jiang, B., Diévart, P., Sohn, C.H. and Ju, Y., 2015. *Proceedings of the Combustion Institute*, *35*(1), pp.881-888.

# Plasma assisted Self-Sustaining Premixed/partially premixed Cool Flames

- Cool diffusion flames
  - n-Heptane/$O_2$/$O_3$
  - Won et al., *Proc. Combust. Inst.* 2015

- Cool premixed flames
  - DME/$O_2$/$O_3$
  - Reuter et al., *Combust. Flame* 2016

- Cool partially premixed flames
  - DME/$O_2$/$O_3$
  - Reuter et al., *Proc. Combust. Inst.* 2017 (hopefully)

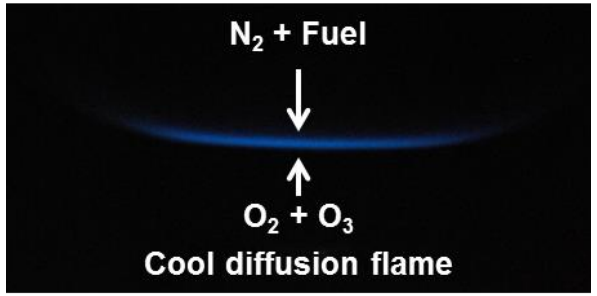


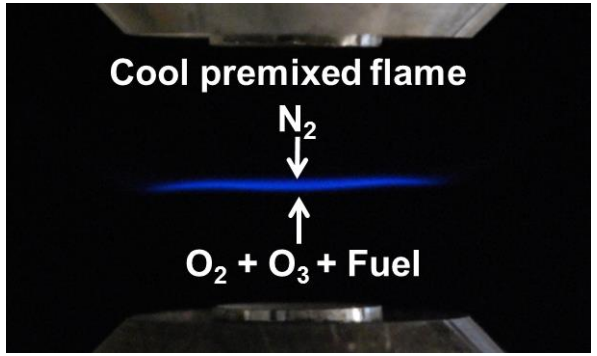


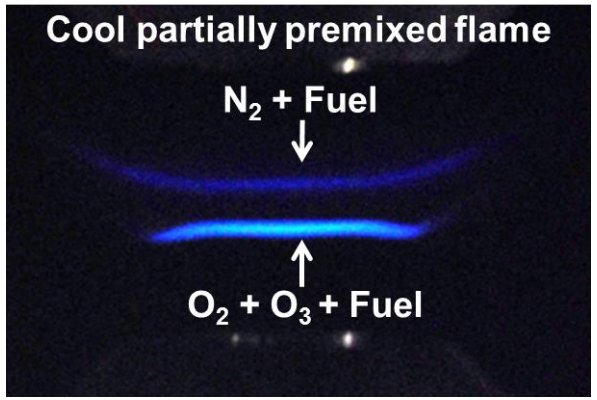


S. H. Won et al., *Proc. Combust. Inst.* 35 (2015) 881-888
C. B. Reuter et al., *Combust. Flame* (2016), in press

# 4. Diagnostics of plasma physics and chemistry in PAC

1. Measurements of plasma properties and kinetic processes

2. Plasma assisted ignition and combustion with active species production

3. Kinetic studies of plasma assisted combustion

# 1. Measurements of Plasma Properties: electron density and temperature Thomson scattering

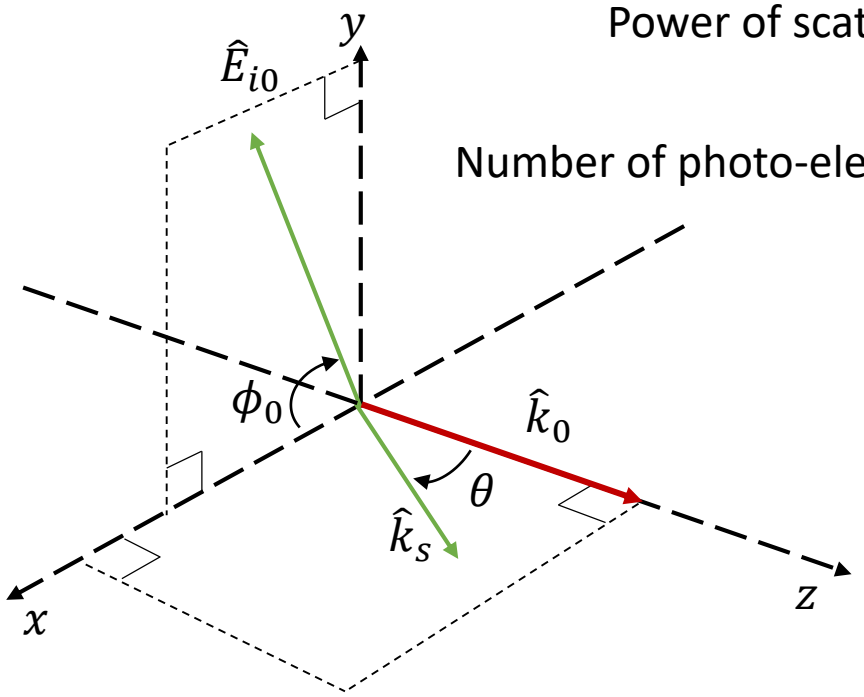


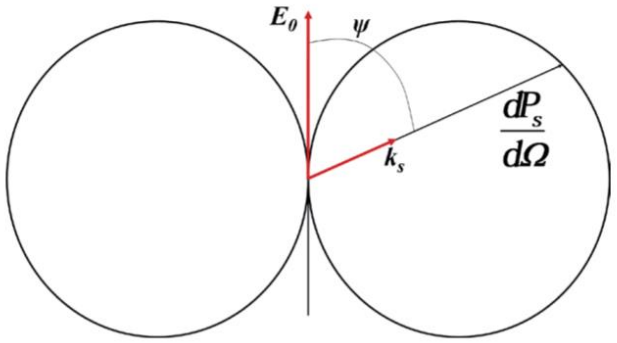


Power of scattering: $P_s \propto 1 - \sin^2\theta \cos^2\phi_0$

Number of photo-electrons: $N_s = \frac{E_L}{h\nu_0} \Delta L \, n_e \frac{d\sigma_e}{d\Omega} \eta$

$$n_e = \frac{\frac{A_e}{A_{N_2}} \left(\frac{d\sigma_{N_2}}{d\Omega}\right)_{532nm}}{\frac{d\sigma_e}{d\Omega}} n_{N_2} f_{J=6}$$

$$\Delta\lambda_{1/e} = \frac{2\lambda_0}{c} \sin\left(\frac{\theta}{2}\right) \left(\frac{2k_B T_e}{m_e}\right)^{\frac{1}{2}}$$

$$T_e = \frac{c^2 m_e}{8k_B \sin^2(\theta/2)} \left(\frac{\Delta\lambda_{1/e}}{\lambda_0}\right)^2$$

$k_0$: Laser beam direction, $k_s$: Scattering signal wave vector

$\hat{E}_{i0}$: Polarized electric field, scattering is rotationally symmetric about $\hat{E}_{i0}$.

x-z plane: the plane of observation

θ: the scattering angle relative to the laser beam.

$\phi_0$: angle between observation plane and the polarization angle.

$A_e$ and $A_{N_2}$: integrated intensities of the Thomson and Raman spectra

$\frac{d\sigma_e}{d\Omega}$ and $\frac{d\sigma_{N_2}}{d\Omega}$ the Thomson and $N_2$ Raman scattering cross sections

$f_{J=6}$: the fraction of $N_2$ molecules in the J = 6 rotational state

$\Delta\lambda_{1/e}$: the half 1/e width of the Gaussian broadening profile

$E_L$: laser energy, η: optical efficiency, ΔL: length of observed scattering segment.


- H. Van der Meiden, "Thomson scattering on low and high temperature plasmas", Ph.D, Technische Universiteit Eindhoven, 2011.
- A. Roettgen, "Vibrational Energy Distribution, Electron Density and Electron Temperature Behavior in Nanosecond Pulse Discharge Plasmas by Raman and Thomson Scattering", Ph.D, The Ohio State University, 2015.

# Thomson Scattering Experimental Setup and Calibration

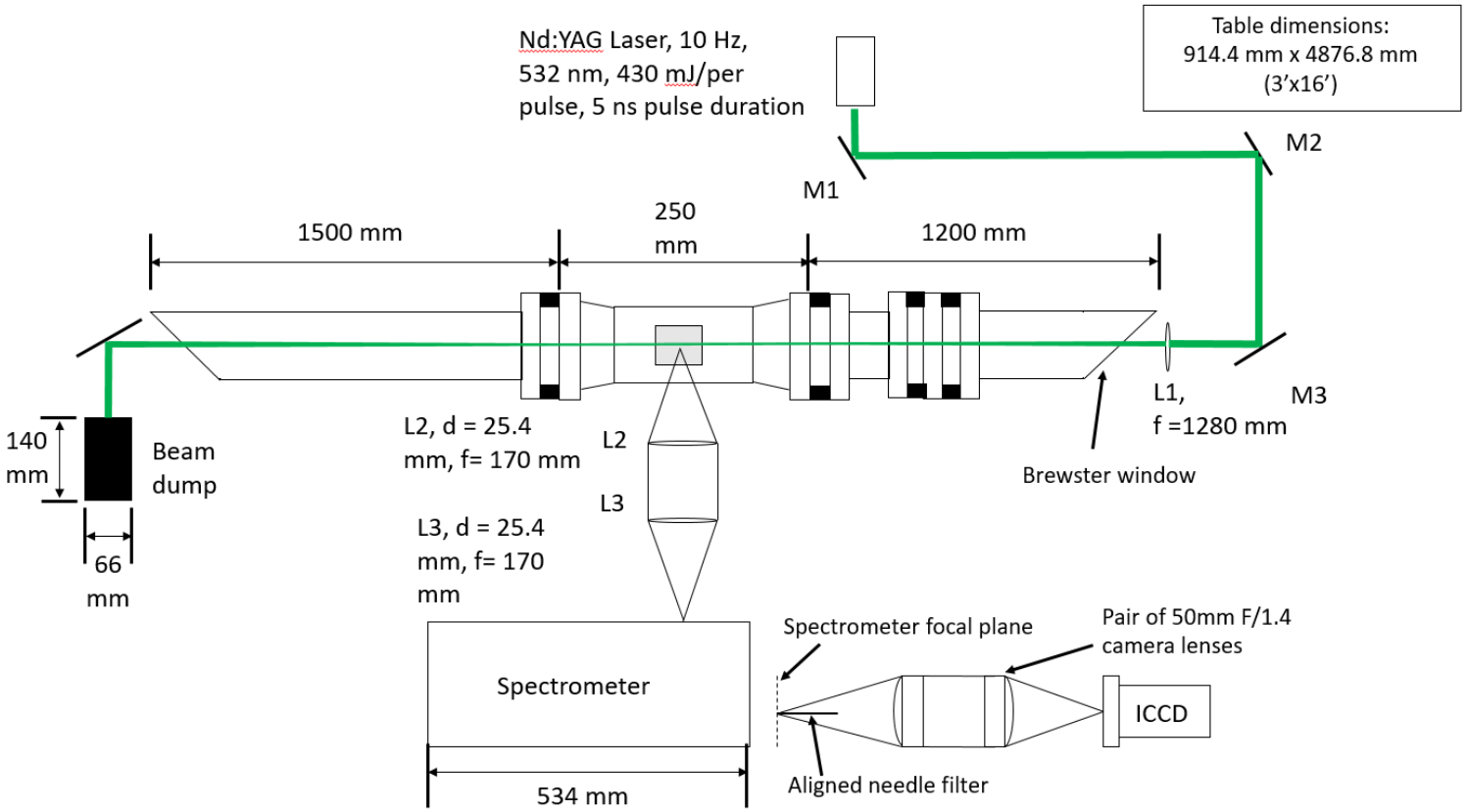


Timothy Chen, Princeton, 2017

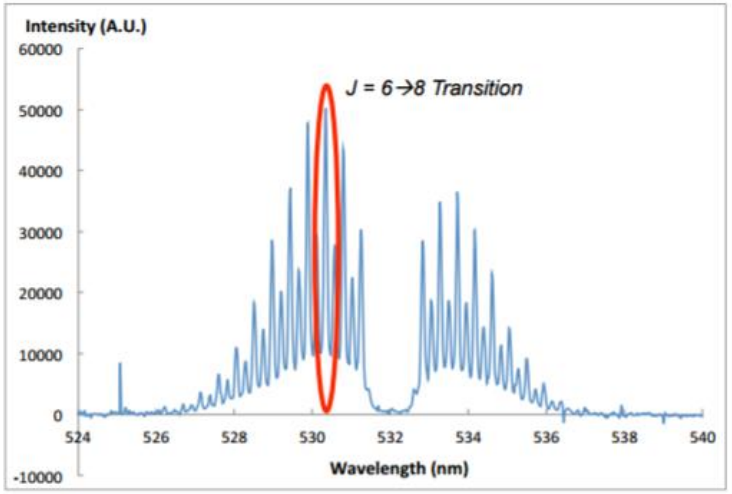


Roettgen (2015): use Rotational Raman Scattering for calibration using the J = 6 → 8 transition of $N_2$ at P = 100 Torr

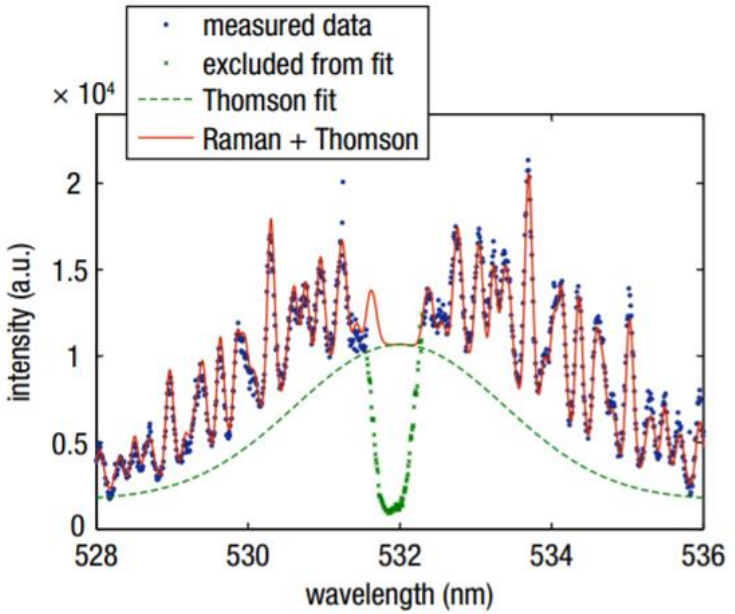


Decoupling Raman and Thomson Signals

A. van Gessel, E. Carbone, P. Bruggeman and J. van der Mullen, *Plasma Sources Science and Technology*, vol. 21, no. 1, p. 015003, 2012.

# Filtered Thomson Scattering: $n_e$ , $T_e$, and EEDF inference

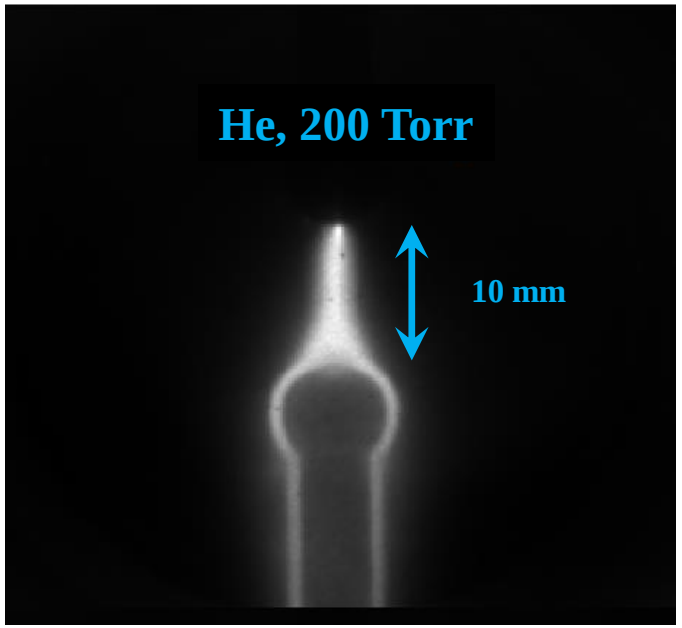


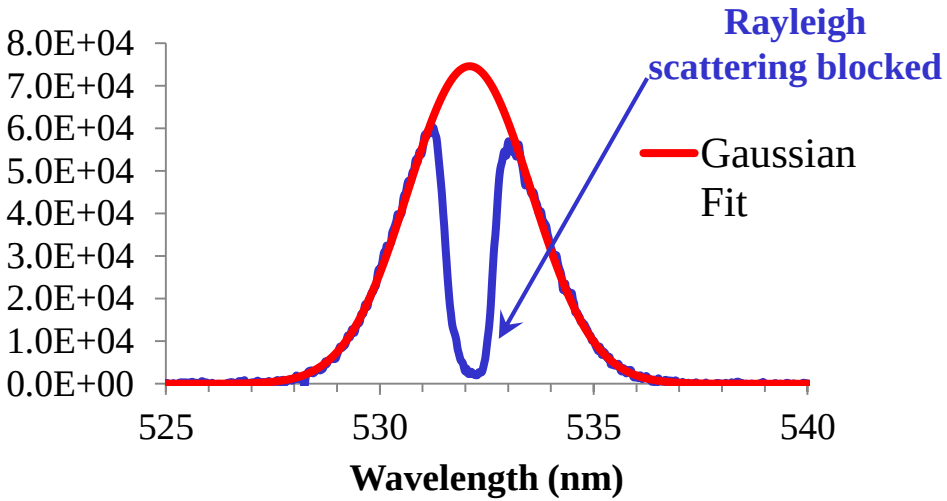


$N_2$ Raman scattering

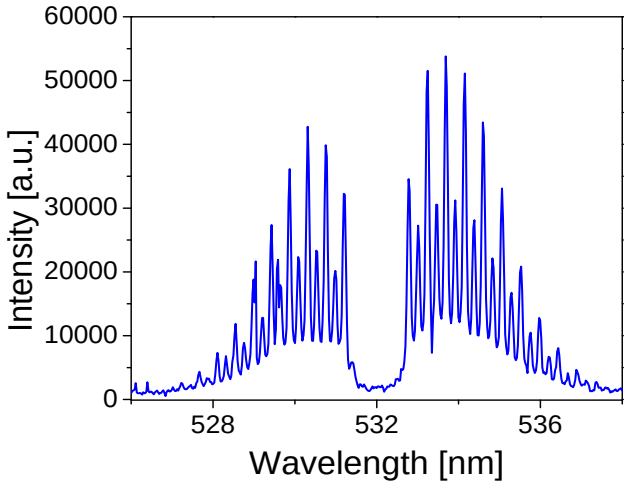


- Electron density: area under Thomson scattering spectrum
- Electron temperature: spectral linewidth
- Gaussian scattering lineshape: Maxwellian EEDF
- Raman scattering rotational transitions in $N_2$ used for absolute calibration

Courtesy of Prof. Igor V. Adamovich

# Thomson Scattering Spectra

## Ns pulse discharge in $H_2$-He and $O_2$-He, P=100 Torr

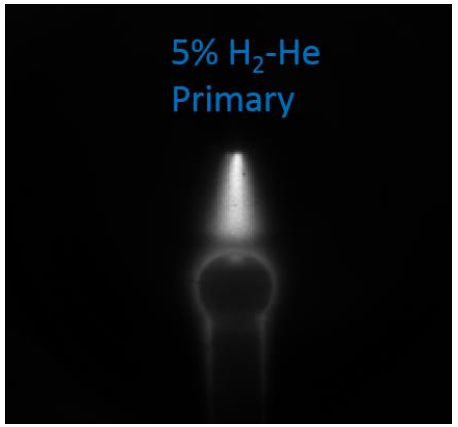


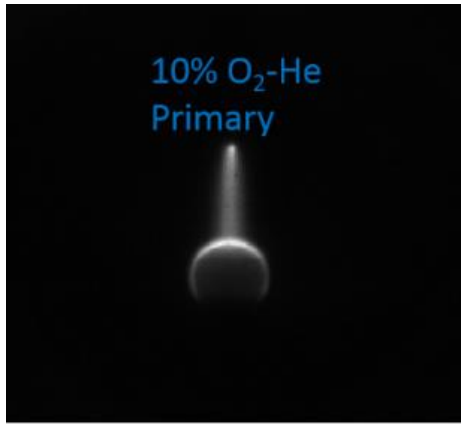


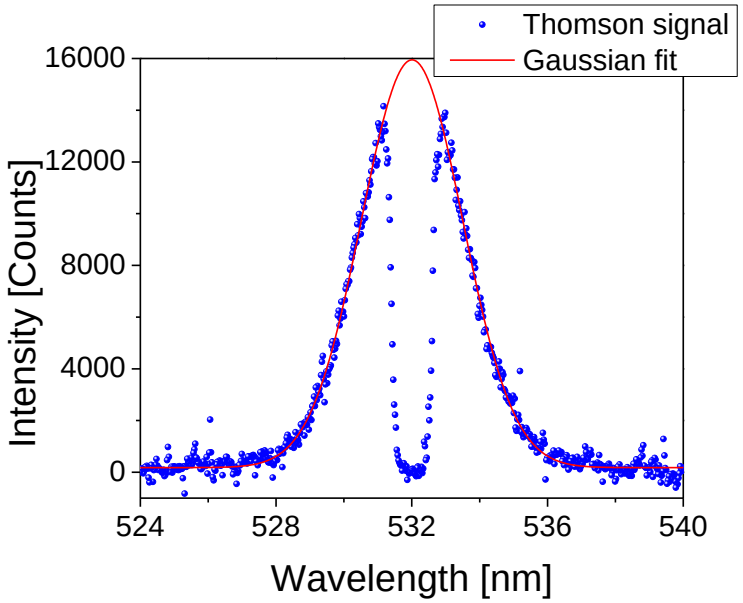


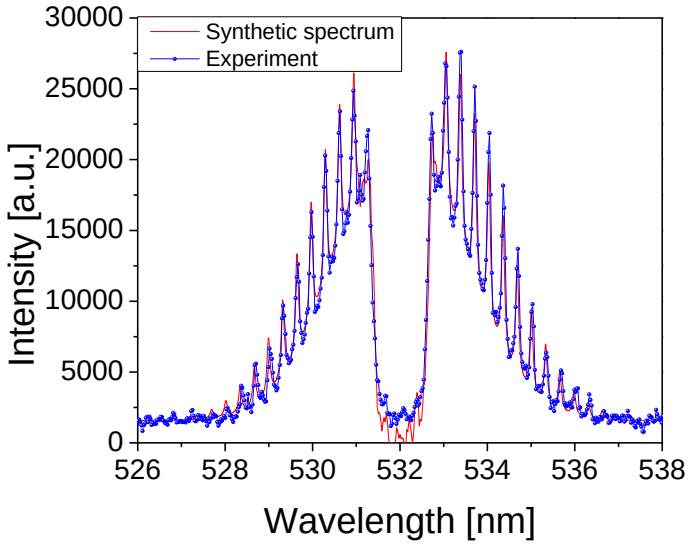


**5% $H_2$-He,**

**$n_e = 1.5 \cdot 10^{14}$ cm$^{-3}$, $T_e = 2.0$ eV**

**10% $O_2$-He**

**$n_e = 1.7 \cdot 10^{13}$ cm$^{-3}$, $T_e = 1.6$ eV, T=350**

# Electron Density and Electron Temperature

## Ns pulse discharge in $O_2$-He

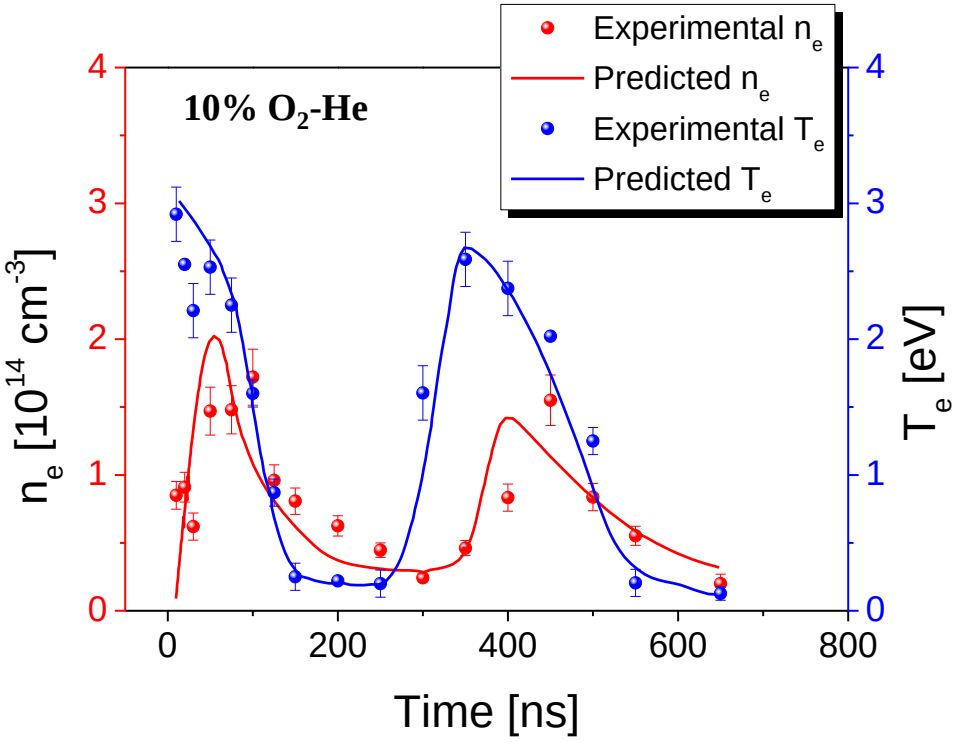


- "Double maxima" in $n_e$, $T_e$ : two discharge pulses ≈ 400 ns apart
- Electron temperature in the afterglow $T_e$ ≈ 0.3 eV (controlled by superelastic collisions)
- Modeling predictions in good agreement with data
- Measurements in air are more challenging (strong interference from $N_2$, $O_2$ Raman scattering)

# Measurements of electron number density

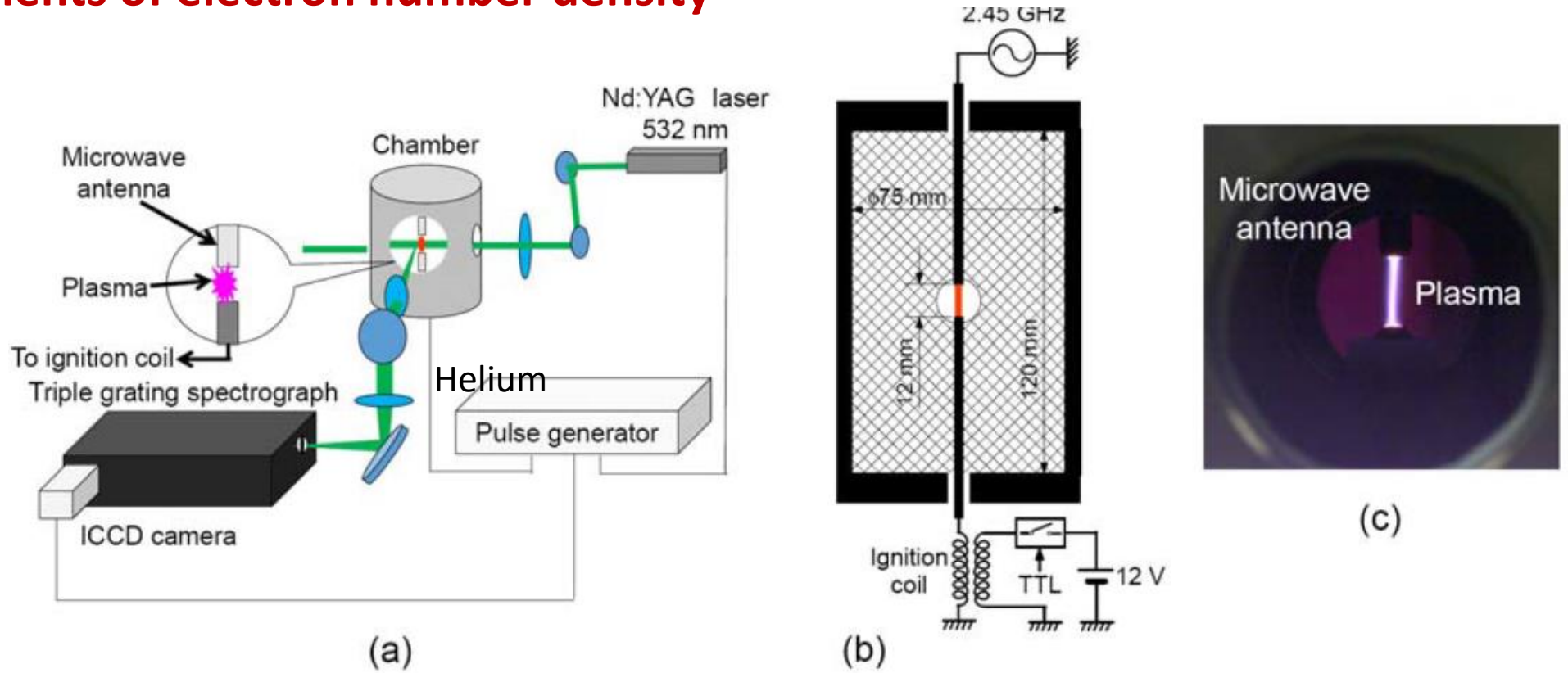


**Fig. 1** Experimental apparatus: (a) schematic of the entire experimental system including the plasma source and the system of laser Thomson scattering, (b) details of the plasma source, and (c) picture of the microwave helium discharge.

K. Sasaki et al., Contrib. Plasma Phys. 55, No. 8, 563 – 569 (2015)

**Thomson scattering profile (Broadening):**

$$\Delta\nu_D' = \frac{2\nu_0}{c}\sqrt{\frac{2\ln(2)k_B T_e}{m_e}}\sin\left(\frac{\theta}{2}\right)$$

$$n_e = \frac{A_e}{A_{He,J}}\frac{\left(\frac{d\sigma}{d\Omega}\right)_{532nm}}{\left(\frac{d\sigma_2}{d\Omega}\right)} n_{He} f_J$$

$\theta$: the scattering angle relative to the laser beam.

$A_e$ : integrated Thomson scattering signal intensity

$A_{He,J}$ : integrated He J level Raman transition intensity

$f_J$ : relative J level population fraction in distribution function

# Measured electron energy distribution, temperature, and number density

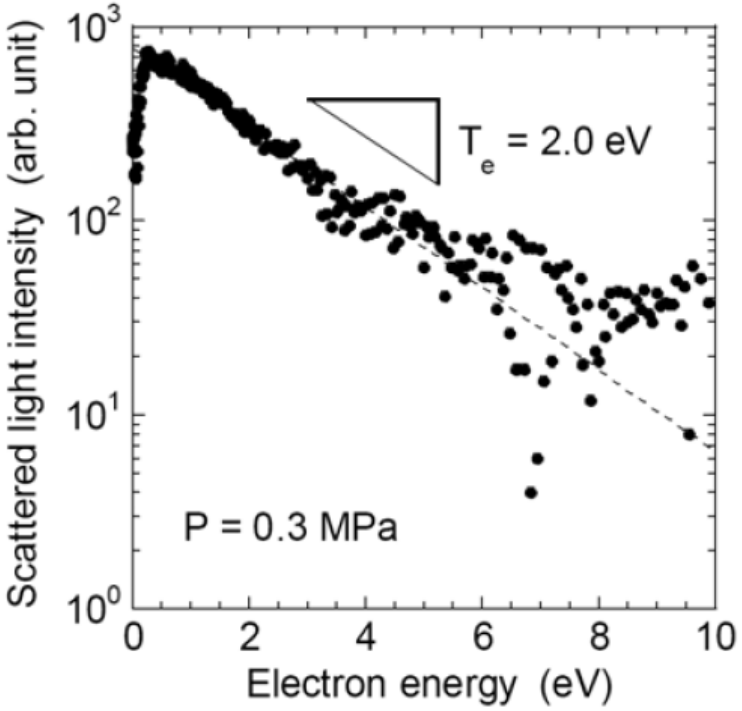


Fig.1Typical electron energy distribution function measured by laser Thomson scattering in a microwave helium plasma at a pressure
of 0.3 MPa.

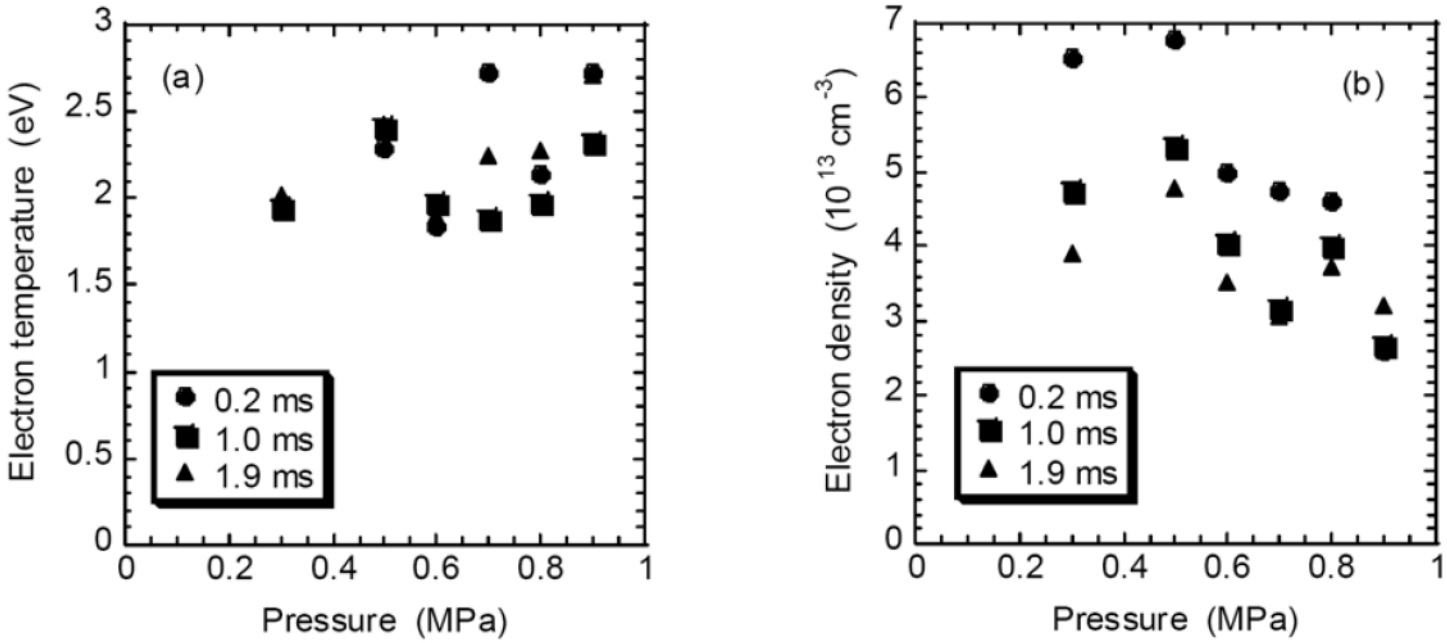


Fig.2 Pressure dependences of (a) the electron density and (b) the electron temperature. Values observed at three delay times after the initiation of the microwave power are plotted.

- Thomson scattering is its weak scattering signal intensity owing to the low number density of free electrons in the plasma.
- Strong interference from Rayleigh scattering as well as plasma emission

K. Sasaki et al., Contrib. Plasma Phys. 55, No. 8, 563 – 569 (2015)

# Femtosecond Localized E-Field Measurement (FLEM)

Mechanical and Aerospace Engineering
Applied Physics Group

- In a centrosymmetric medium, second harmonic generation is impossible
- Applying an electric field destroys that symmetry allowing for E-Field measurements
- Benefits of FLEM Method:
  - Signal scales as $E^2$
  - Works well at higher pressure
  - Time resolution determined by pump beam duration
  - Non-resonant method works in any species and gas mixtures
  - Spatial resolution determined by beam focusing parameter

- Described as a third order nonlinear process:
  - $I^{(2\,\omega)} \propto N^2 (E_{Ext})^2 (I_{Pump})^2$
    - $I^{(2\,\omega)}$ : Second Harmonic Intensity
    - N: Number Density
    - $E_{ext}$: Applied Field to be Measured
    - $I_{Pump}$: Pump Beam Intensity

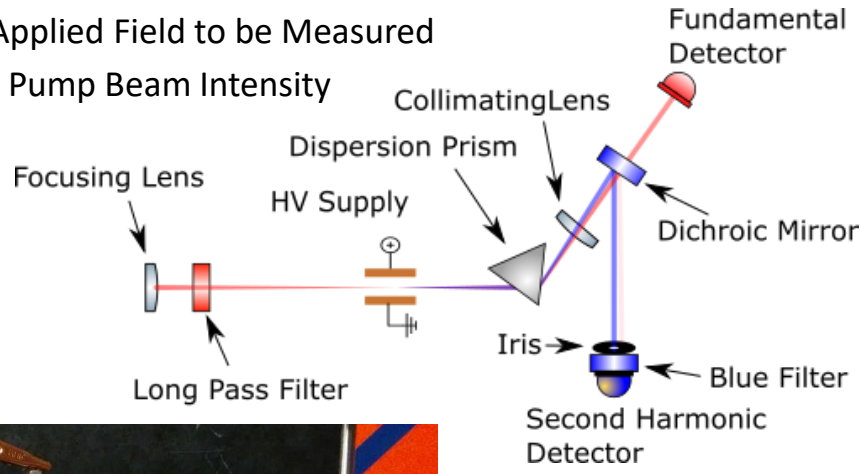


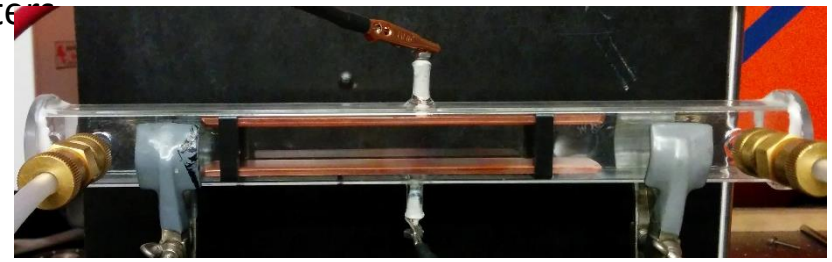

Courtesy of Prof. Richard Miles, Princeton

# Femtosecond Localized E-Field Measurement (FLEM)

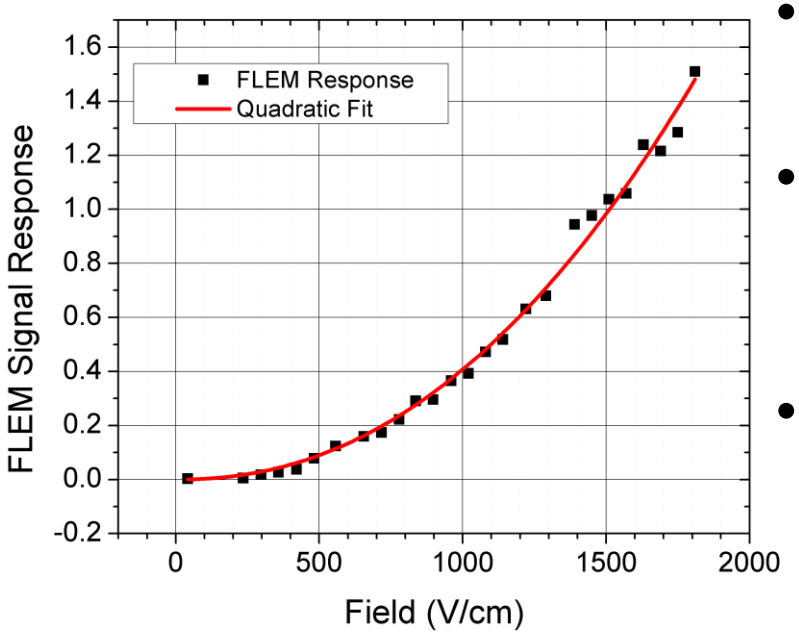


- Sub-breakdown electric field applied
- SHG response, pump intensity, current and voltage monitored
- Quadratic dependence verified
  - We have measured down to 100V/cm in room air

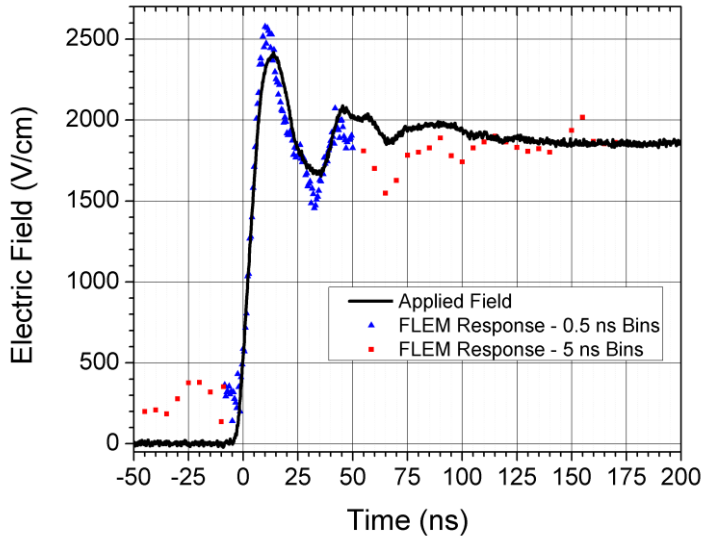


- **Fs laser pulse acts as a δ function compared with ns high voltage pulses**
- **Temporal resolution determined by oscilloscope rather than a physical limit**

Courtesy of Prof. Richard Miles, Princeton

# Electric Field Measurements in 2-D Ns Pulse Discharge in Atmospheric Air

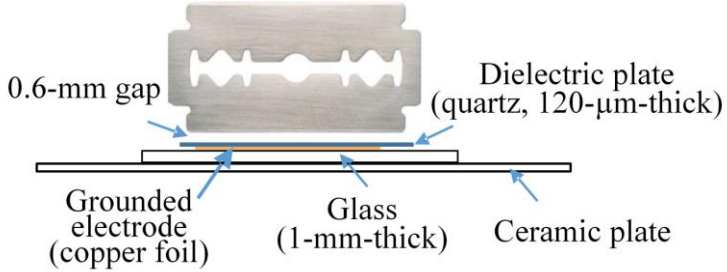


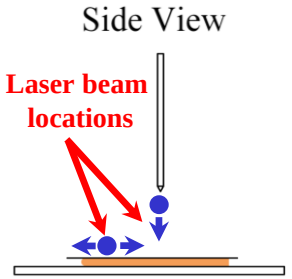


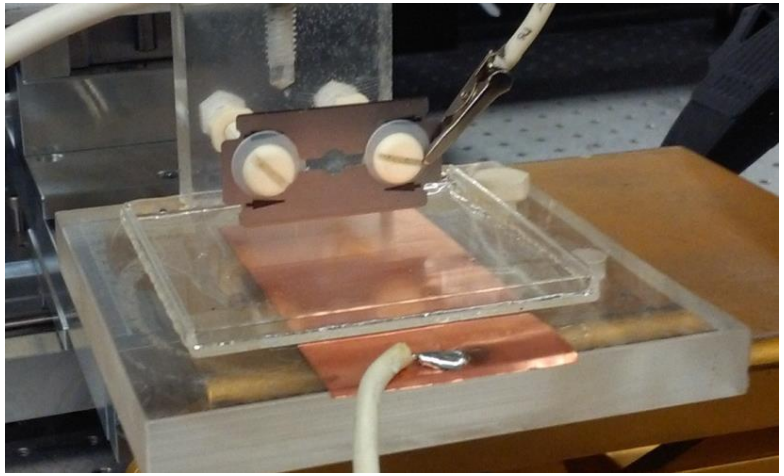

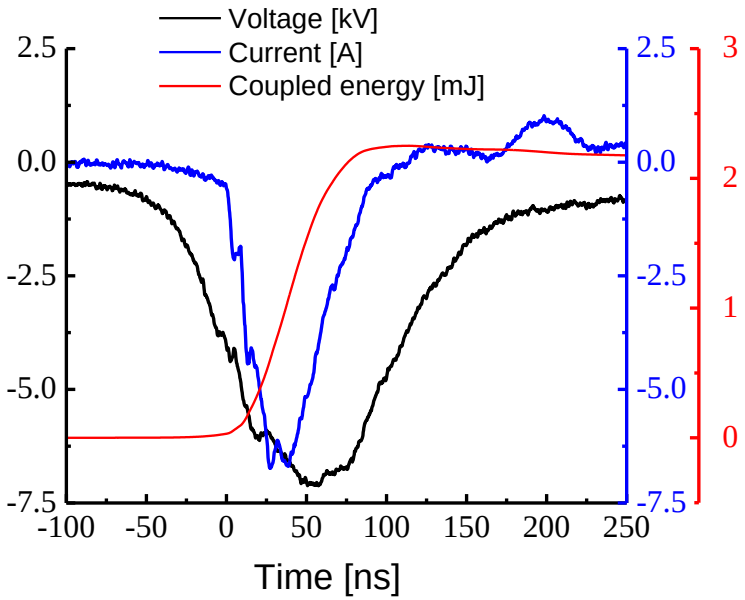


- Ns pulse discharge between a high-voltage electrode and a thin quartz plate
- Discharge gap 0.6 - 1.0 mm, two-dimensional geometry, diffuse plasma
- Time-resolved electric field measured at multiple locations in the discharge gap

# “Curtain Plasma” Images, Negative Polarity Pulse

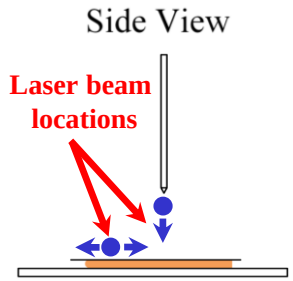


Front view, 100 ns gate

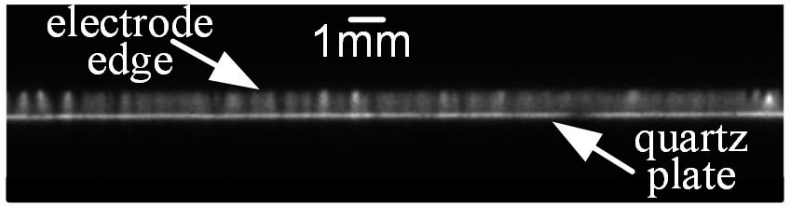


Side view, 2 ns gate

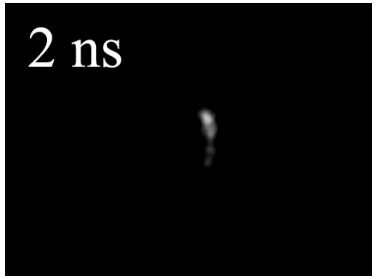


Top view, 2 ns gate

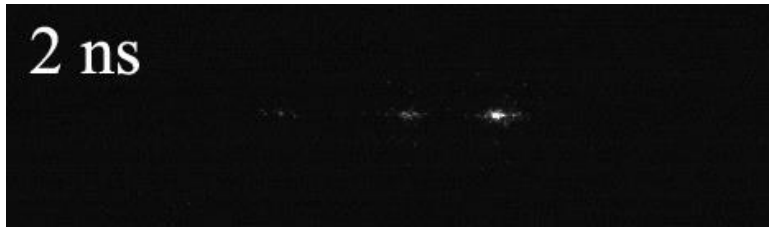


- Surface ionization wave plasma ~ 200 μm thick, wave speed ~ 0.03 mm/ns
- Electric field measured by picosecond four-wave mixing (calibration by electrostatic field)
- Time resolution 2 ns, spatial resolution across laser beam ~ 100 μm
- Objective: electric field mapping in ns pulse discharges in high-pressure fuel-air mixtures

# Electric Field Vector Components in a Surface Ionization Wave Discharge

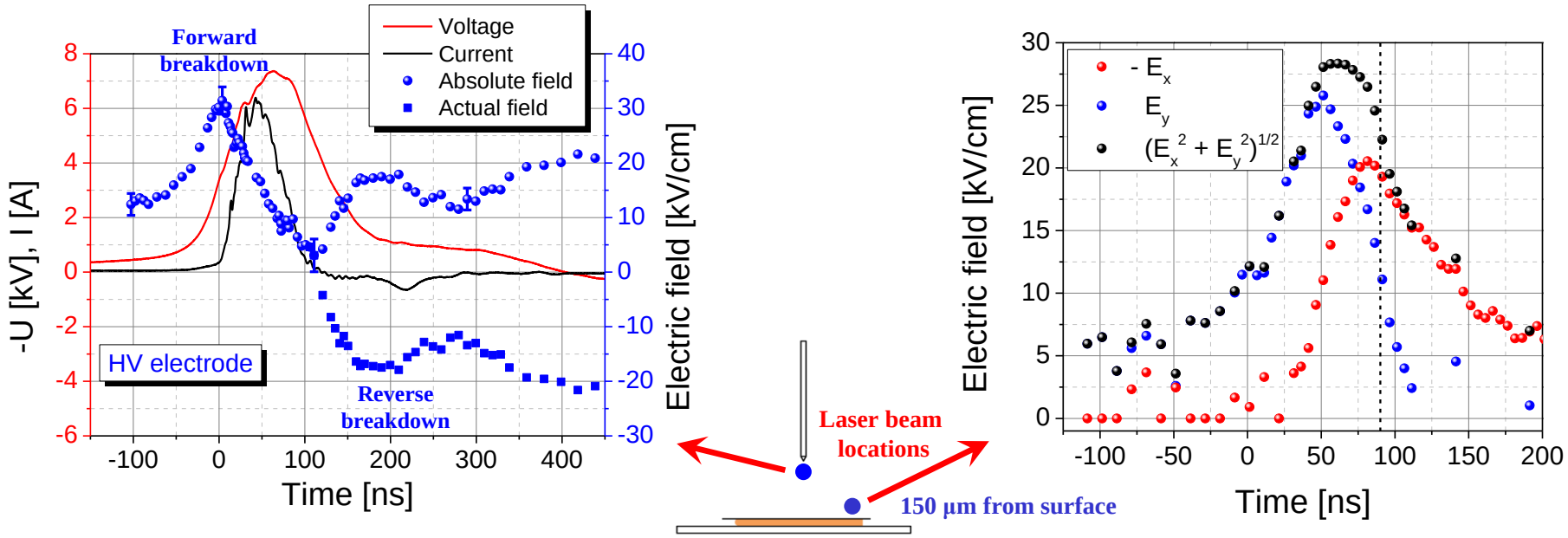


- Initial field offset (at t < 0): charge accumulation on dielectric from previous pulse
- Field follows applied voltage rise, increases until "forward breakdown"
- After breakdown, field reduced due to charge accumulation on dielectric
- Field is reversed after applied voltage starts decreasing
- Away from HV electrode, field peaks later ($E_y$ before $E_x$): surface ionization wave
- Measurements in a hydrogen-air diffusion flame underway

# Plasma property measurements using H2/Ar emission lines

$^3D_1, ^3D_2, ^3D_3,\ \ ^3P_0, ^3P_1, ^3P_2,\ \ ^3S_1,\ \ ^1D_2, ^1P_1, ^1S_0,$

$3s^23p^54p^1$

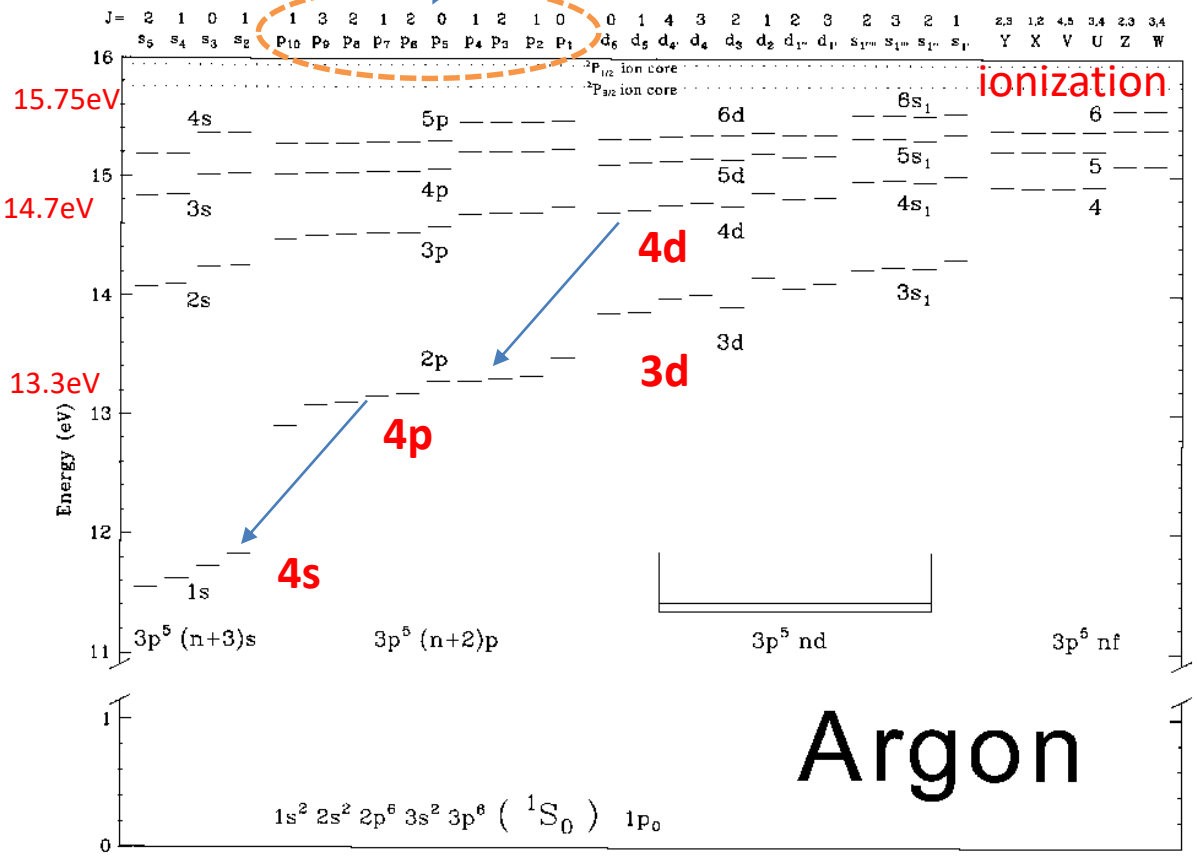


**L-S coupling**

**$3s^23p^6 \leftrightarrow 3s^23p^54S^1$**

$$L = l_1 + l_2 = 1 + 0 = 1$$

$$J = L + S, \ldots |L - S| = 2,1,0$$

$$Term: \ ^3P_0, ^3P_1 \ ^3P_2$$

$$S = S_1 - S_2 = 1/2 - 1/2 = 0$$

$$J = L + S, \ldots |L - S| = 1$$

$$Term: \ ^1P_1$$

**$3s^23p^6 \leftrightarrow 3s^23p^54p^1$**

$$\vec{L} = \vec{l_1} + \vec{l_2} = \vec{1} + \vec{1} = 0,1,2 \text{ (any quantum number)}$$

$$\vec{S} = \vec{s_1} + \vec{s_2} = \frac{\vec{1}}{2} + \frac{\vec{1}}{2} = 0,1$$

$$J = L + S, \ldots |L - S| = \underbrace{2,1,0,}_{S=0} \ \underbrace{1, \ \ 2,1,0, \ \ 3,2,1}_{S=1}$$

$$Term: \ ^1S_0, ^3S_1, \ \ ^1P_1, ^3P_0, ^3P_1, ^3P_2, \ \ ^1D_2, ^3D_1, ^3D_2, ^3D_3$$

# Stark broadening of hydrogen lines and Ar optical emission line-ratio method

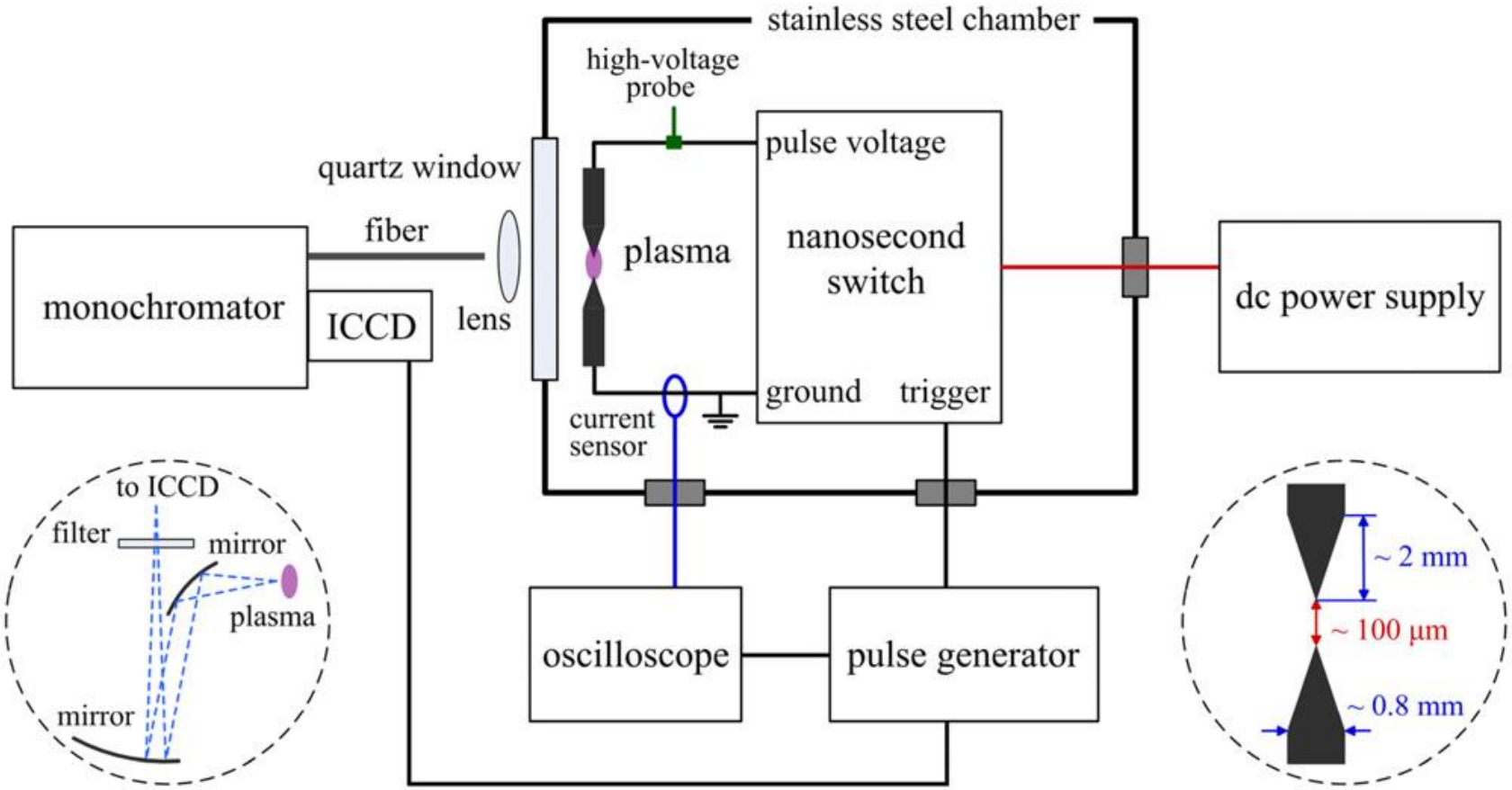


Schematic diagram of the experimental setup. The spatially resolved optical measurement system is shown on the left bottom. On the right bottom is a zoom-in figure showing the stainless steel needle tips and the discharge gap.

Xi-Ming Zhu, James L Walsh, Wen-Cong Chen1 and Yi-Kang Pu, J. Phys. D: Appl. Phys. 45 (2012) 295201 (11pp)

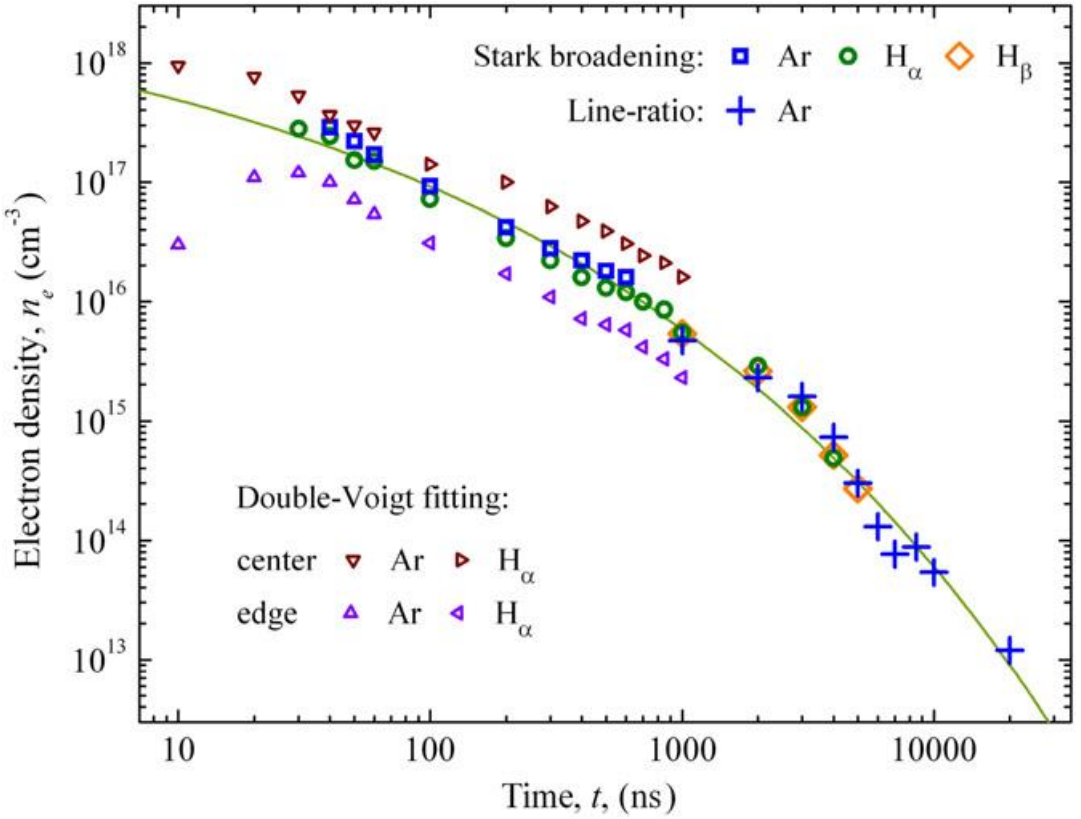


Experimentally measured electron densities in a high-pressure nanosecond pulsed microplasma (Ar/Ne = 700/30 Torr, discharge current lasts for about 100 ns, pulse period 1 ms). In the legend on the right top, 'line ratio' refers to the line-ratio method and 'Stark broadening' refers to the Stark broadening method using Ar 696.5 nm, H*α* and H*β* lines with a single-Voigt fitting procedure. In the legend on the left bottom, 'centre' and 'edge' denote *n*e,centre and *n*e,edge obtained with double-Voigt fitting. The solid line shows a function, *n*e = 6 × 1018 × exp*(−(t/*0.15*)*0.22*)*, where *n*e and *t*are in units of cm−3 and ns, respectively.

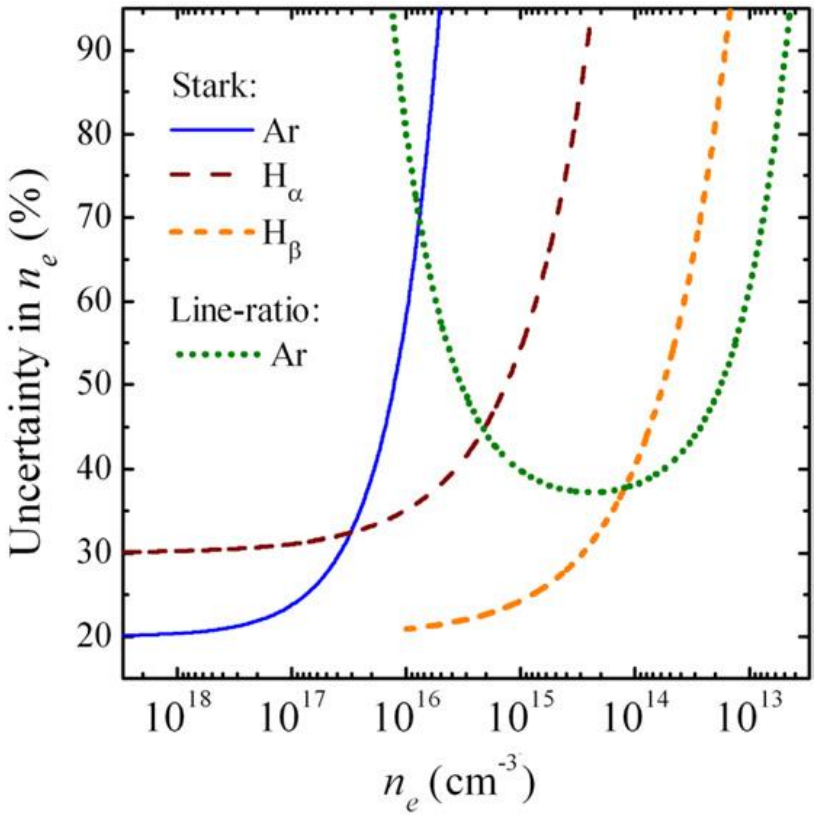


Uncertainties in the *n*e measurement (%) using the Stark roadening method with Ar 696.5 nm line, H*α* line and H*β* line (for *n*e > 1016 cm−3) and that using the line-ratio method.

Xi-Ming Zhu, James L Walsh, Wen-Cong Chen1 and Yi-Kang Pu, J. Phys. D: Appl. Phys. 45 (2012) 295201 (11pp)

# Measurements of temperature, vibrational level populations and fast heating using picosecond CARS

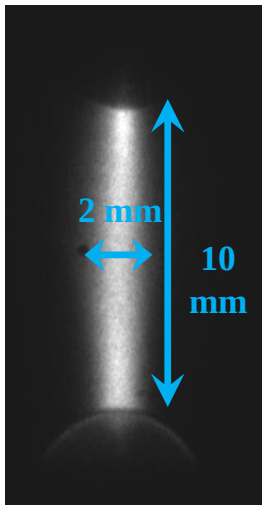


Air, P=100 Torr

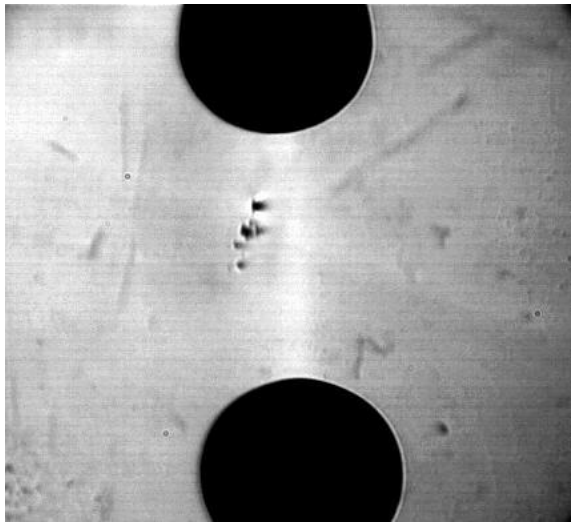

t= 1-10 μs (frames are 1 μs apart)

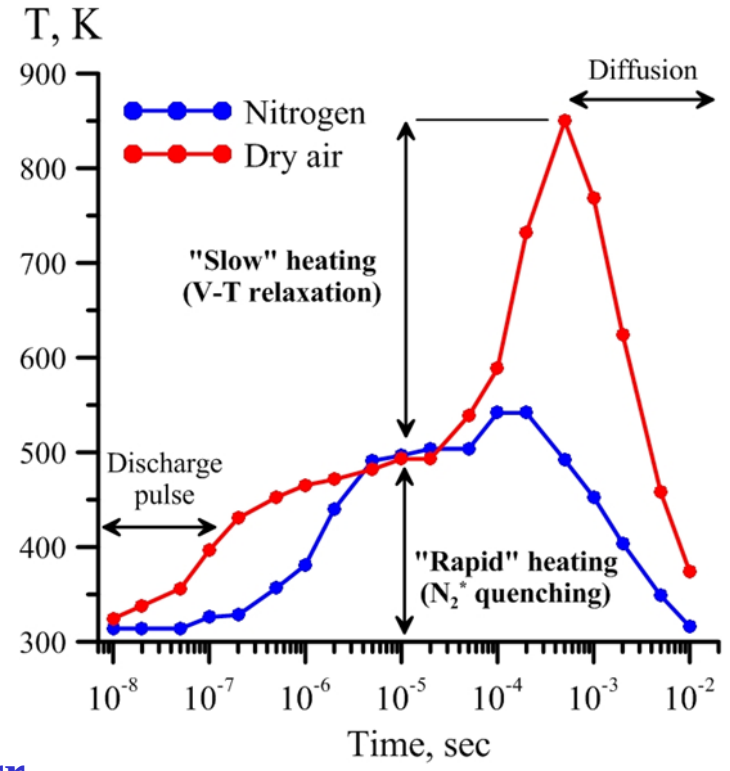


ns pulse discharge and afterglow: Air vs. nitrogen, P=100 Torr

- Compression waves formed by "rapid" heating, on sub-acoustic time scale, $\tau_{acoustic} \sim r / a \sim 2$ μs
- What processes control other features of temperature rise (e.g. "slow" heating")?

# Comparison with modeling predictions in air: vibrational kinetics and temperature rise

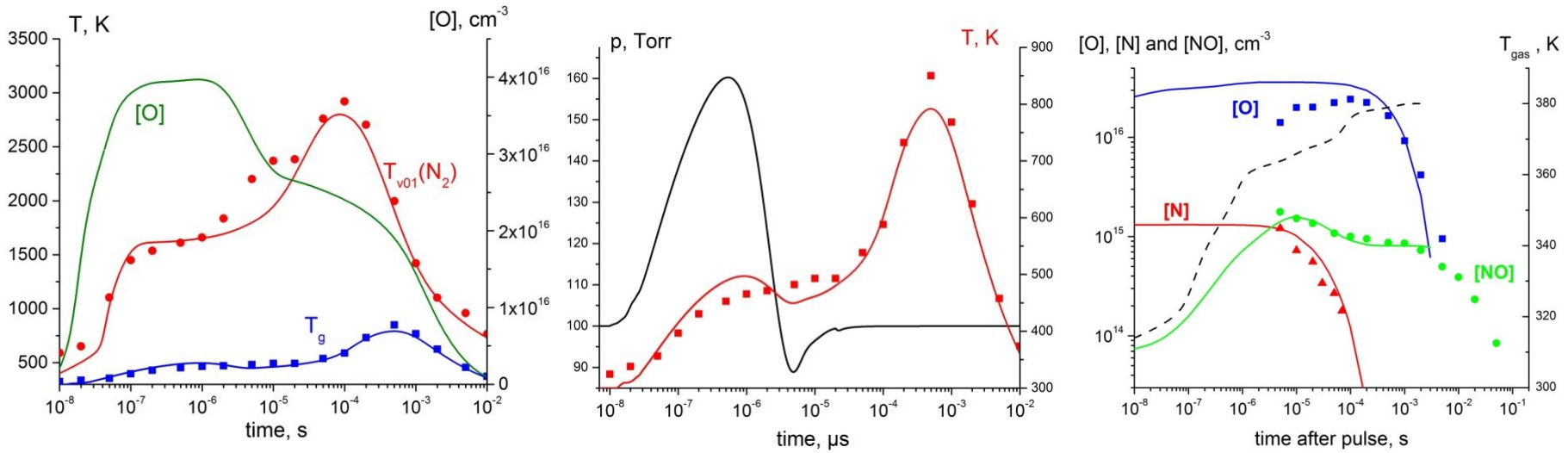


- **Strong vibrational excitation in the discharge, $N_2(v=0\text{-}8)$**
- **$T_v(N_2)$ rise in early afterglow: V-V exchange, $N_2(v) + N_2(v=0) \rightarrow N_2(v\text{-}1) + N_2(v=1)$**
- **$T_v(N_2)$ decay in late afterglow: V-T relaxation, $N_2(v) + O \rightarrow N_2(v\text{-}1) + O$ , radial diffusion**
- **"Rapid" heating: quenching of $N_2$ electronic states, $N_2(C,B,A,a) + O_2 \rightarrow N_2(X) + O + O$**
- **"Slow" heating: V-T relaxation, $N_2(X,v) + O \rightarrow N_2(X,v\text{-}1) + O$**
- **"Rapid" heating: pressure overshoot , compression wave formation**
- **NO formation: dominated by reactions of $N_2$ electronic states, $N_2^* + O \rightarrow NO + N$**

A. Montello, Z. Yin, D. Burnette, I.V. Adamovich, and W.R Lempert, Journal of Physics D: Applied Physics 46 (2013) 464002

# Single-shot measurement rotational and rovibrational energy distributions by Hybrid fs/ps coherent anti-Stokes Raman scattering (CARS) spectroscopy

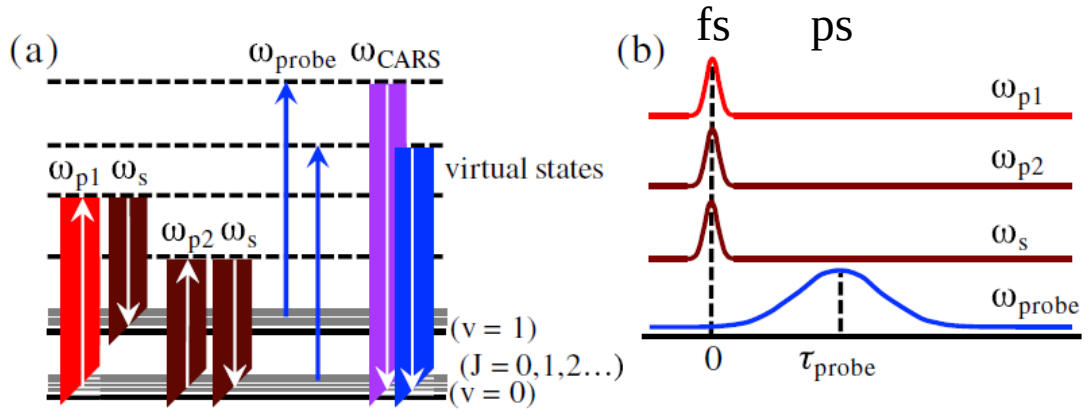


**Fig. 1.** (a) Frequency and (b) timing diagrams for dual-pump fs/ps vibrational/rotational CARS. (Four wave mixing and fs broadband dual pumping

$\omega_{p1}$: Rovibrational Raman transition (Q-branch, Δv=+1, ΔJ =0)
$\omega_{p2}$: pure rotational Raman transition (S-branch, Δv=0, ΔJ =+2)
ωprobe: frequency-narrowed ps probe pulse

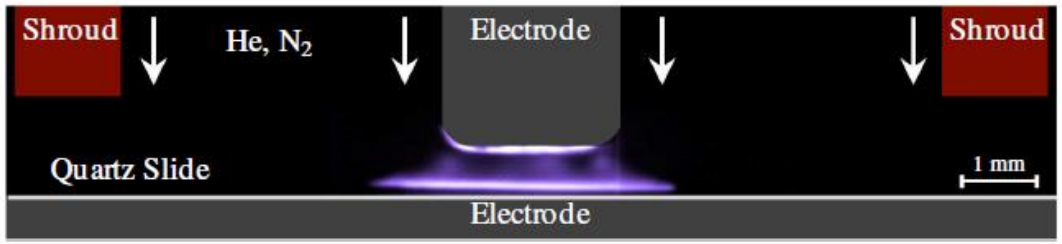


The He/$N_2$ dielectric barrier discharge

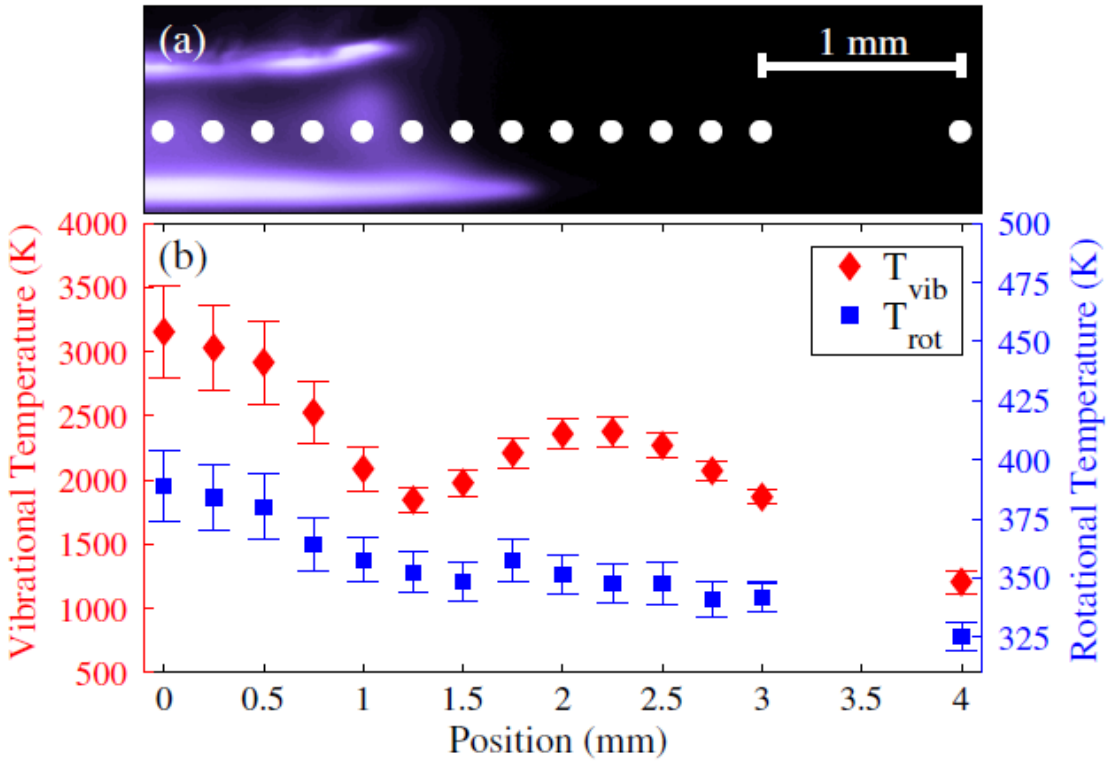


**Fig. 6.** (a) Averaged image of the DBD and CARS measurement locations and (b) corresponding vibrational and rotational temperatures; symbols and bars represent the average and standard deviation of 400 single-shot measurements at each location.


Dedic, C.E., Meyer, T.R. and Michael, J.B., 2017. Single-shot ultrafast coherent anti-Stokes Raman scattering of vibrational/rotational nonequilibrium. *Optica*, *4*(5), pp.563-570.

# Experimental measurements of Plasma chemistry and Kinetic Processes

NRP discharge in
air at 1000 K, 1 atm:

- 10-ns pulse
- 5.7 kV
- 10 kHz
- Gap: 4 mm
- 670 μJ/pulse

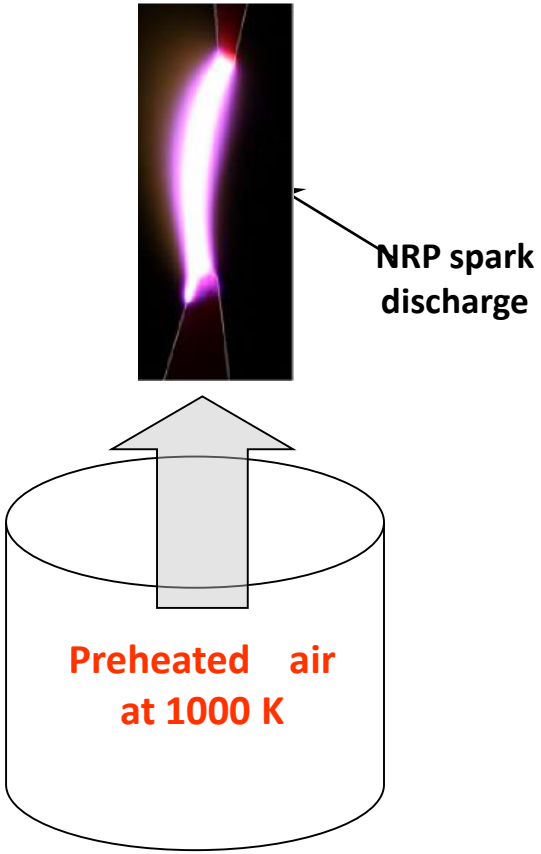


- Measured quantities:
  - O atoms: TALIF with absolute calibration (Xe)
  - $N_2$ (A): CRDS
  - $N_2$ (B) and $N_2$ (C): OES
  - Temperature: OES
  - Electron density: $H_\beta$ Stark broadening

Courtesy of Prof. Christophe Laux

# Measurements of V, I, temperature, densities

Ultrafast heating:
900 K in 20 ns

Ultrafast dissociation of $O_2$

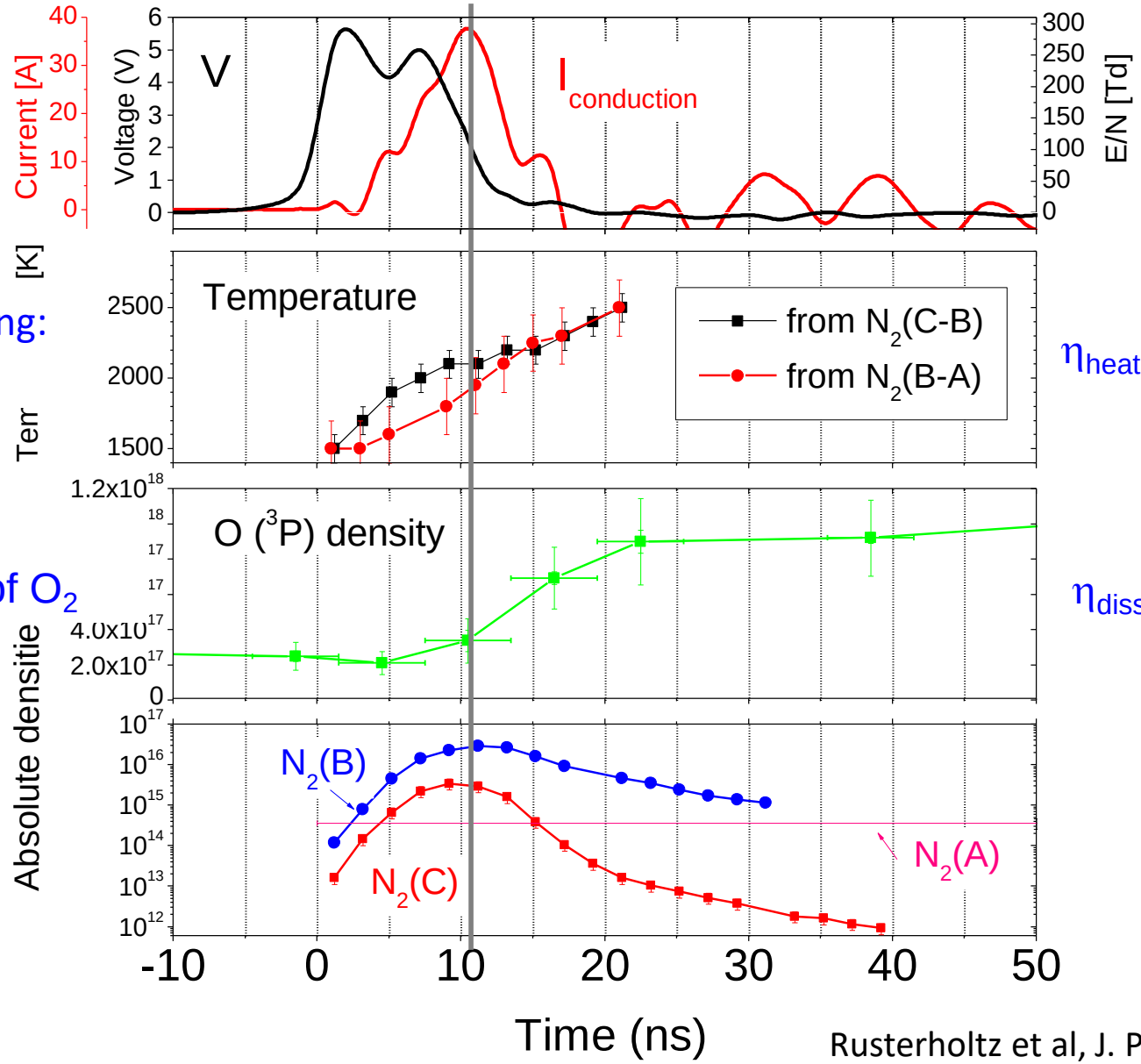


$\eta_{heating}$ =21±5%

$\eta_{diss.}$ = 35±5%

Rusterholtz et al, J. Phys.D, 46, 464010, Dec 2013

# Summary of processes involved in flame stabilization by NRP discharges

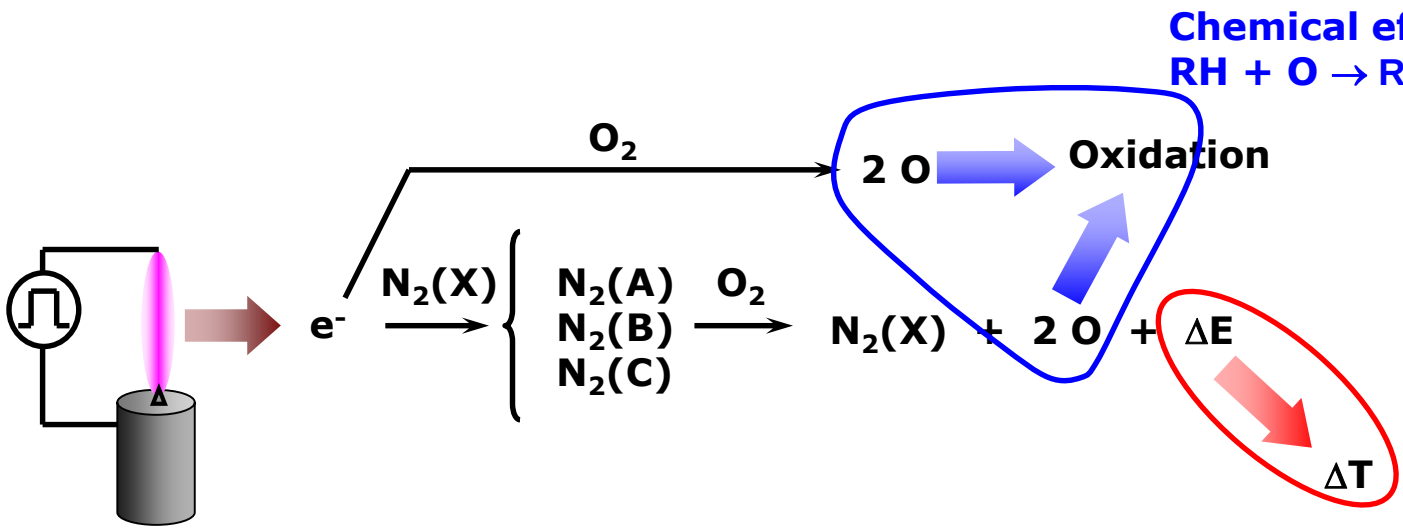


2-step mechanism (Popov, 2001):

$N_2 + e \rightarrow N_2^* + e$ ($N_2^* = N_2$ A, B, C, …)

Thresholds: 6.2, 7.4, 11.0 eV

$N_2^* + O_2 \rightarrow N_2 + O + O + \Delta T$

$\Delta T$ = 1.0, 2.2, 5.9 eV

**5 µs after pulse**
**(Xu et al., APL. 99, 121502, 2011)**

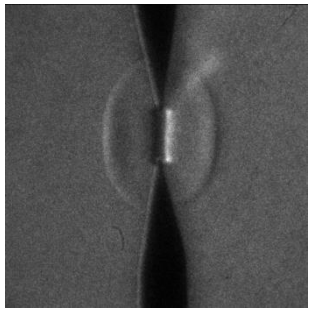

# 2. Measurements of Chemical Processes in Plasma Assisted Ignition and Combustion

**O atom measurements by using TALIF**

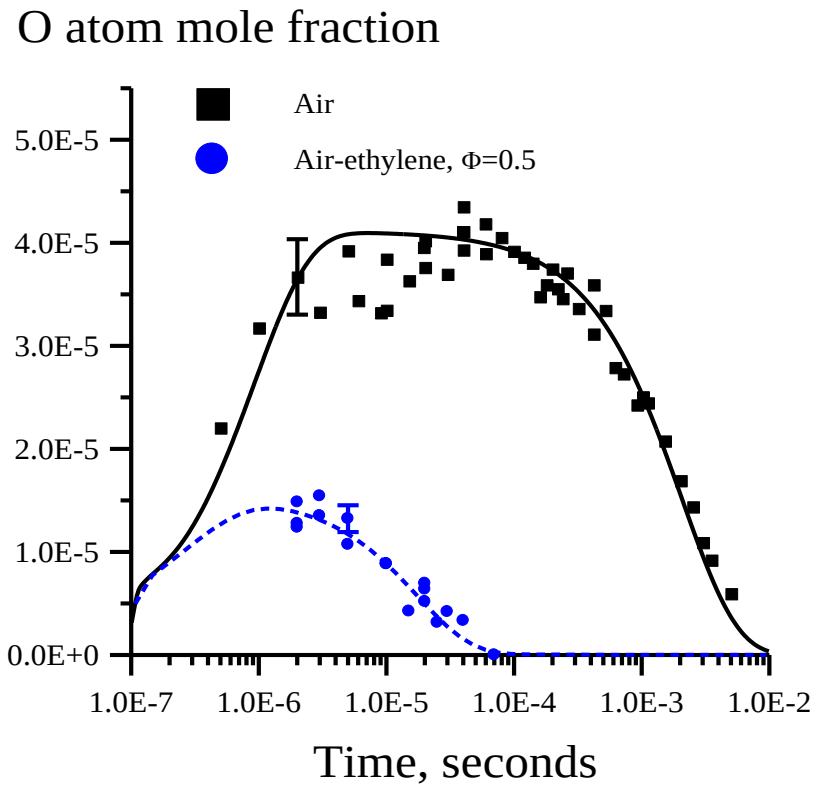


O atom formation in a plasma discharge of air and air-C2H4 mixture in a flow reactor

J. Uddi et al. 2009

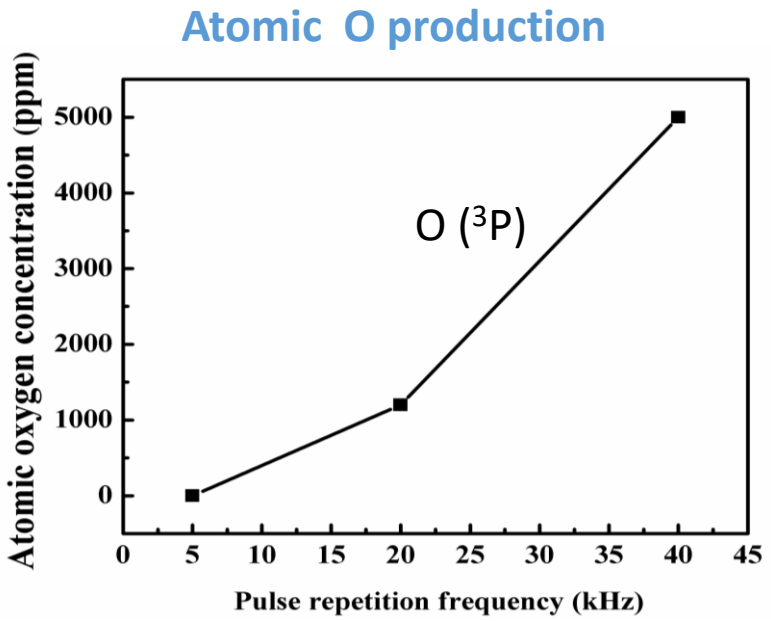


O atom formation in a ns plasma discharge of methane/air counterflow flames

W. Sun et. Al. 2010

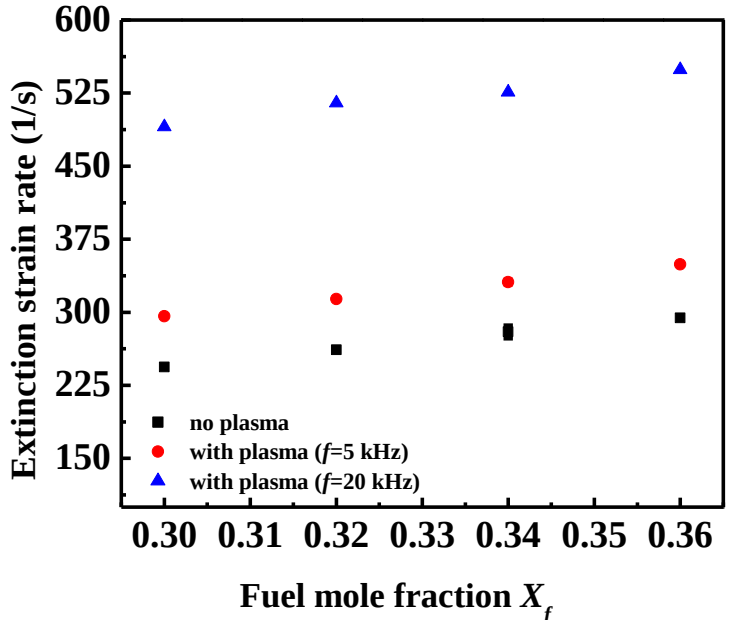


Extension of extinction limit by plasma discharge

# OH measurements in a flow reactor:
## Plasma chemical reactions result in ignition

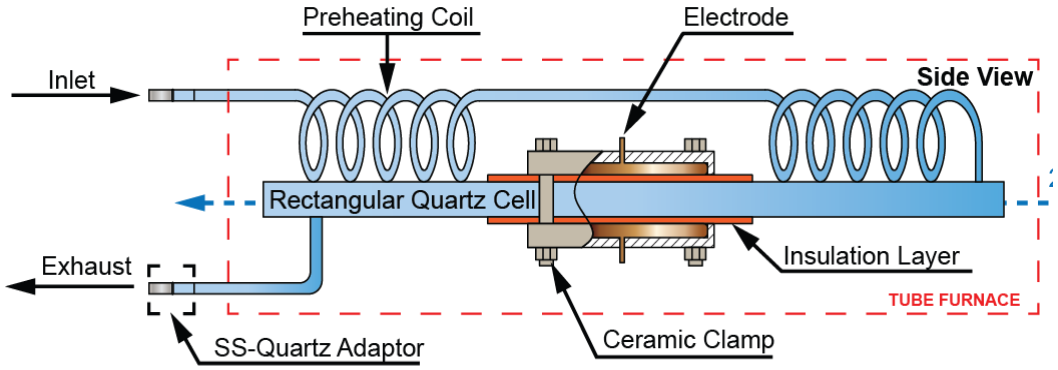


**End View**

| | Pulse #10 | Pulse #100 |
|---|---|---|
| $H_2$ – air, φ=0.3<br>$T_0$=500 K, P=100 torr | | 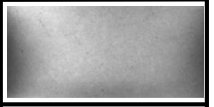 |
| $C_2H_4$ – air, φ=0.3<br>$T_0$=500 K, P=100 torr | 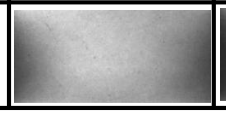 | 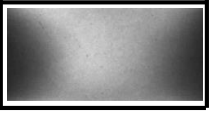 |

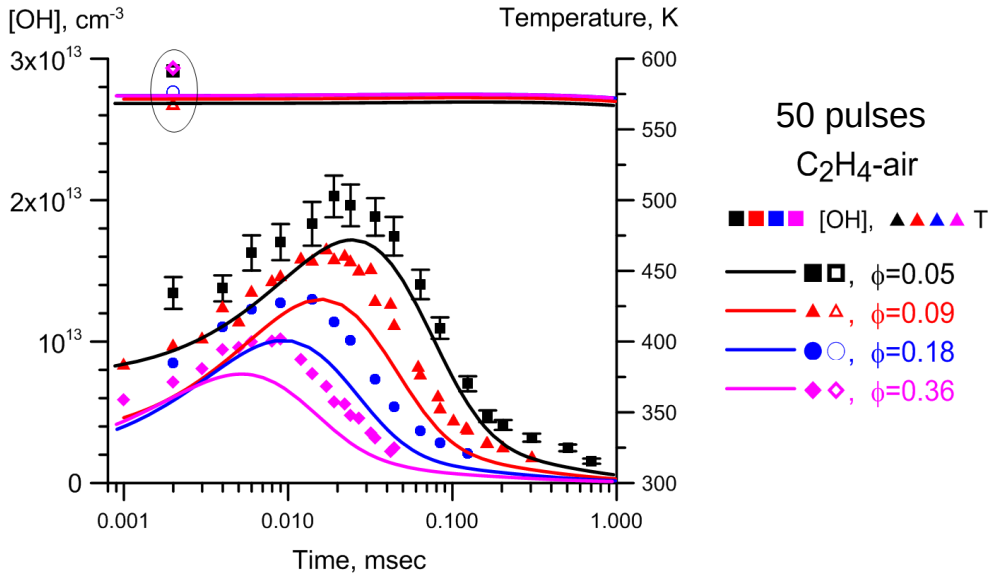


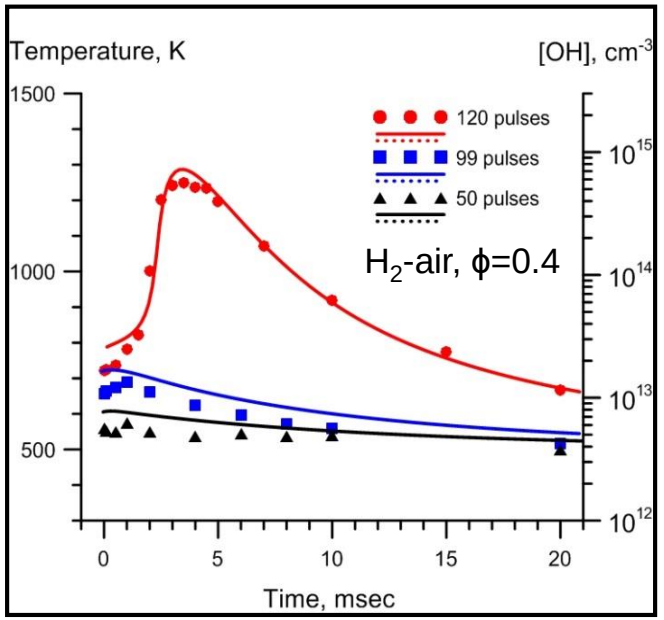


**Short burst: OH transient rise and decay**

**Long burst: plasma assisted ignition, $T_{ignition} \approx 700$ K < $T_{auto\text{-}ignition} \approx 900$ K**

# Plasma Assisted Combustion: Change of ignition and extinction S-curve

## The effect of kinetic enhancement (μs ~ ms, 800-1200 K)

**New "S-curve" by Plasma assisted combustion for small molecule fuel such as $H_2$, $CH_4$**

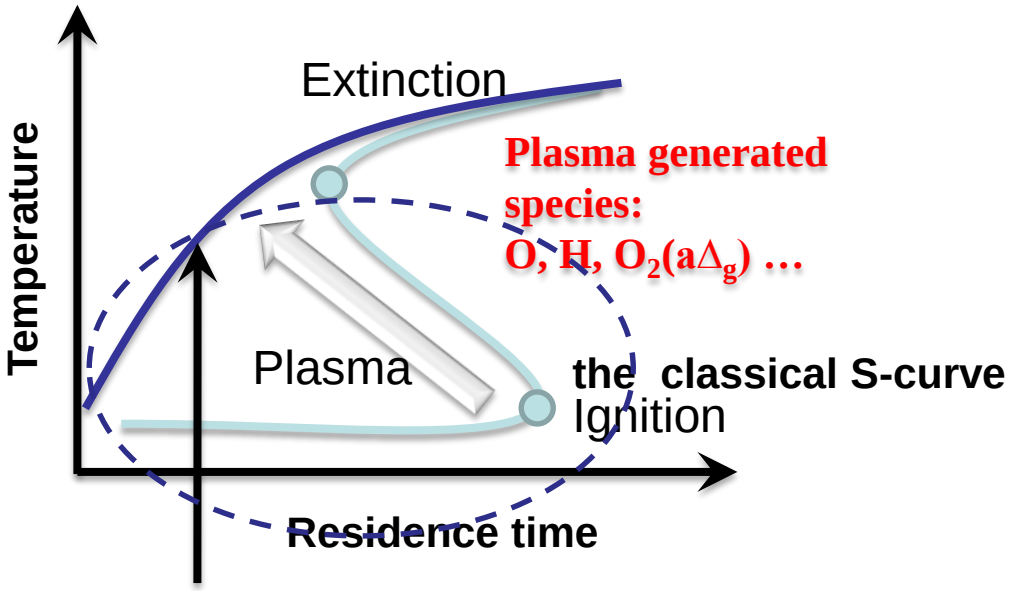


Scramjet, afterburner

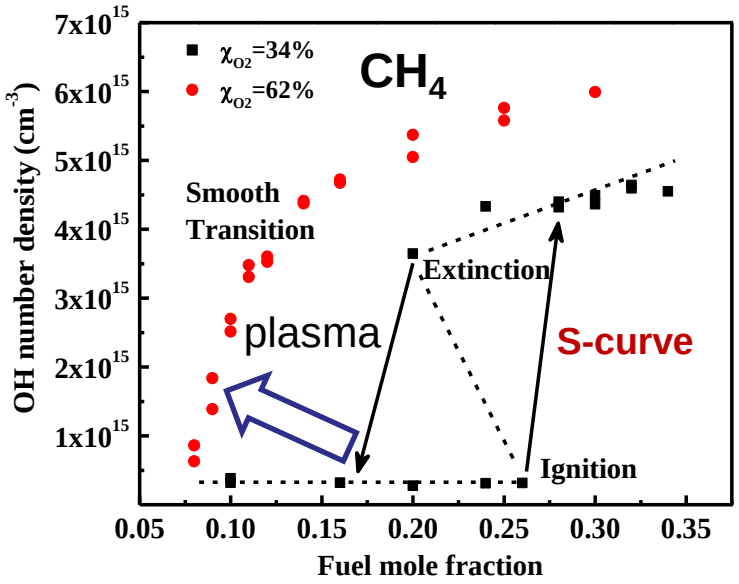


P = 72 Torr, $f$ = 24 kHz, a = 240 1/s

- **Strong kinetic enhancement at intermediate temperature**
- **Less effect at high temperature**

Sun et al. Proc. Comb. Inst. 34, 2010, Combust. Flame 2011, 2012
Ombrello et al. 2008

# Plasma assisted low temperature combustion

## Methane vs. Dimethyl ether (DME)

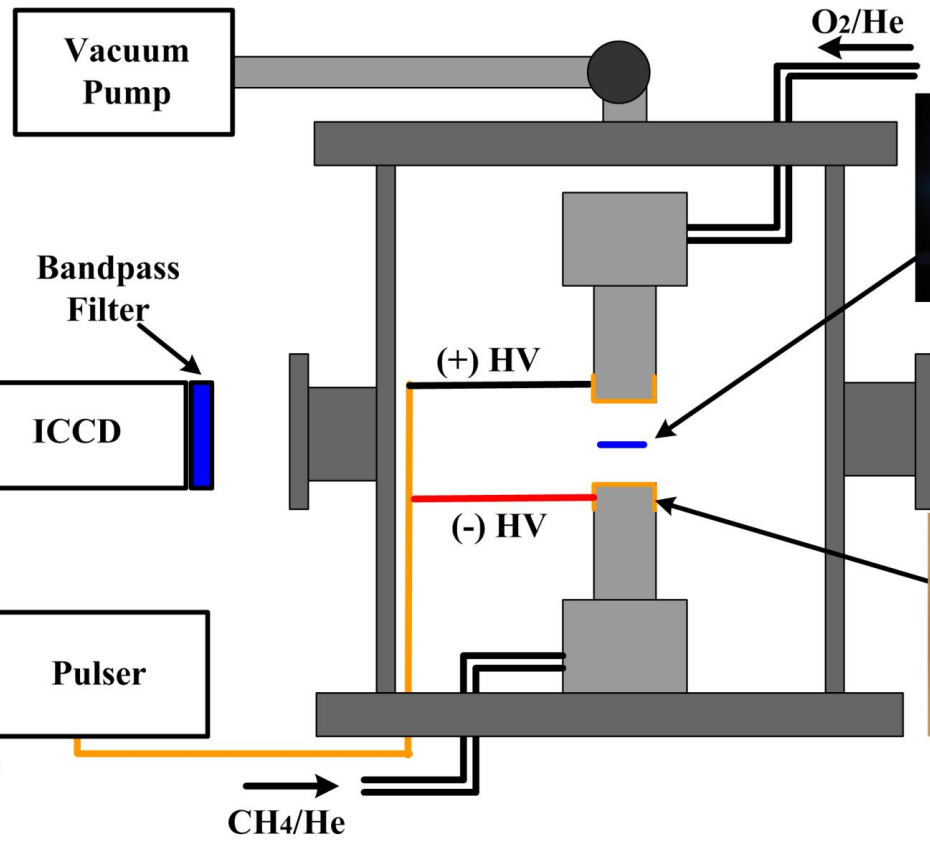


P = 72 Torr
*f* = 24 kHz

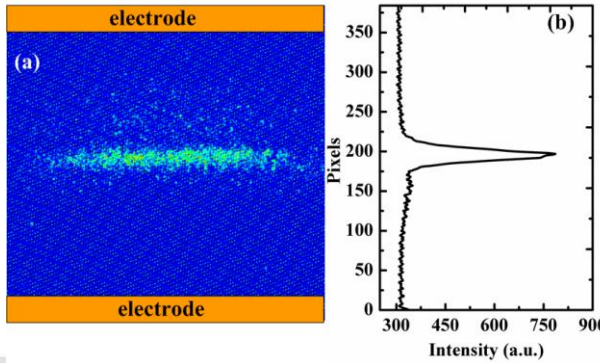


OH* emission ~310 nm
30 μs gate

Laser beam
OH, $CH_2O$ PLIF

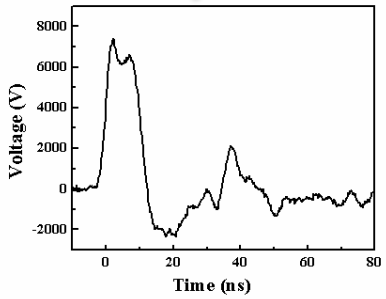


**Peak Voltage = 7.8 KV**

**E = 7500 V/cm, E/N ~ 900 Td**

**Power ~ 17 W (repetitive pulses)**

# OH PLIF measurements in Dimethyl ether (DME) Ignition

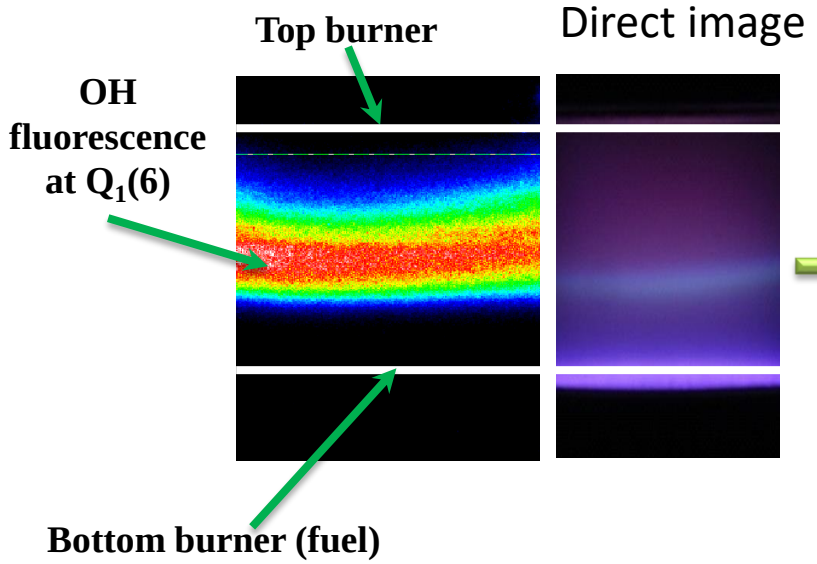


**S-shaped ignition and extinction curves**
**DME vs. CH4**

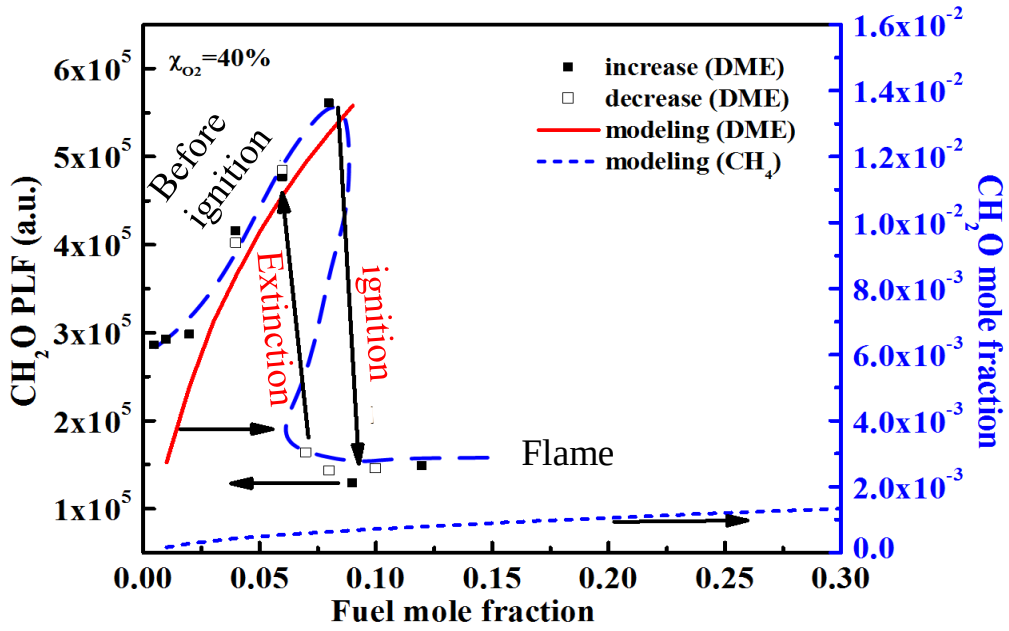


OH density vs. fuel mole fraction $X_O$ = 0.55, P = 72 Torr, $f$ = 24 kHz, for DME (a = 250 1/s) and $CH_4$ (a = 400 1/s,) as the fuel, respectively (solid square symbols: increasing $X_F$, open square symbols: decreasing $X_F$)

**What is the role of plasma before ignition of DME?**

# Plasma activated LTC: change of S-Curve

**P = 72 Torr, a= 250 1/s, *f* = 24 kHz**
**$X_{O_2}$=40%, varying $X_f$**

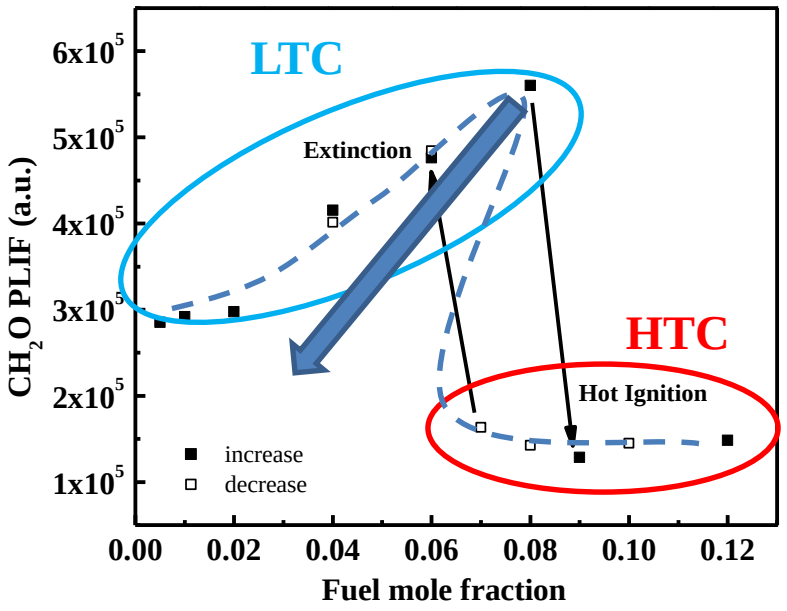


**S-Curve**

**P = 72 Torr, a= 250 1/s, *f* = 34 kHz,**
**$X_{O_2}$=60%, varying $X_f$**

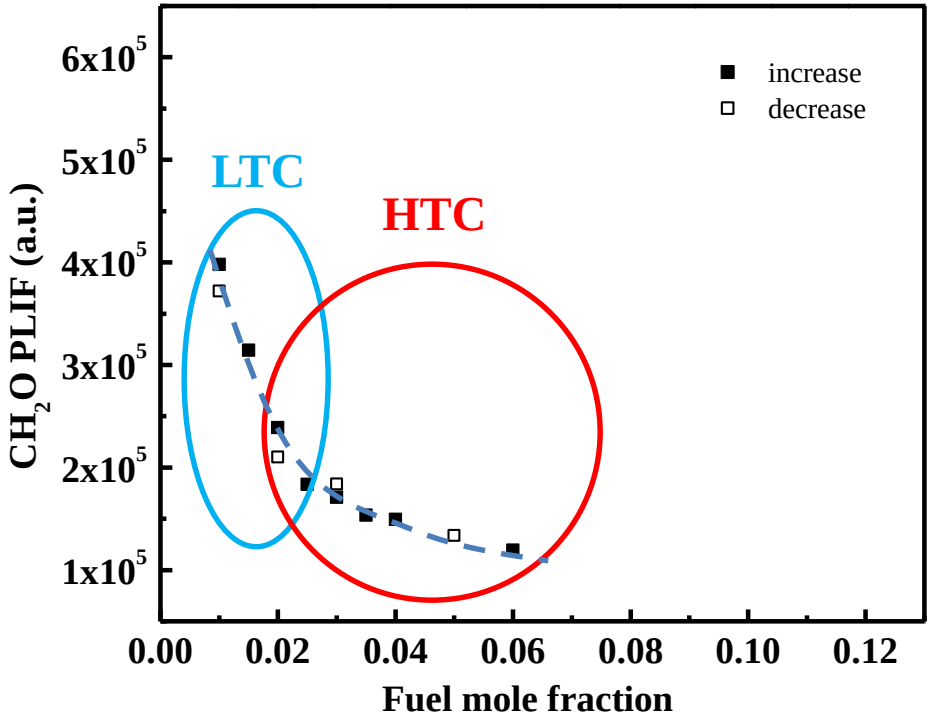


**New ignition/extinction curve without extinction limit**

**Radical production by plasma can activate LTC at much shorter timescale, lower pressure and temperature; and enable new flame regimes**

# Flow reactor studies of plasma assisted low temperature reaction

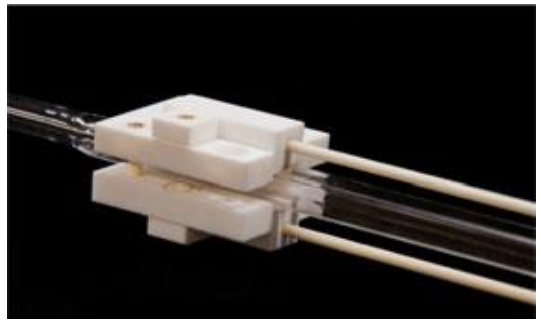

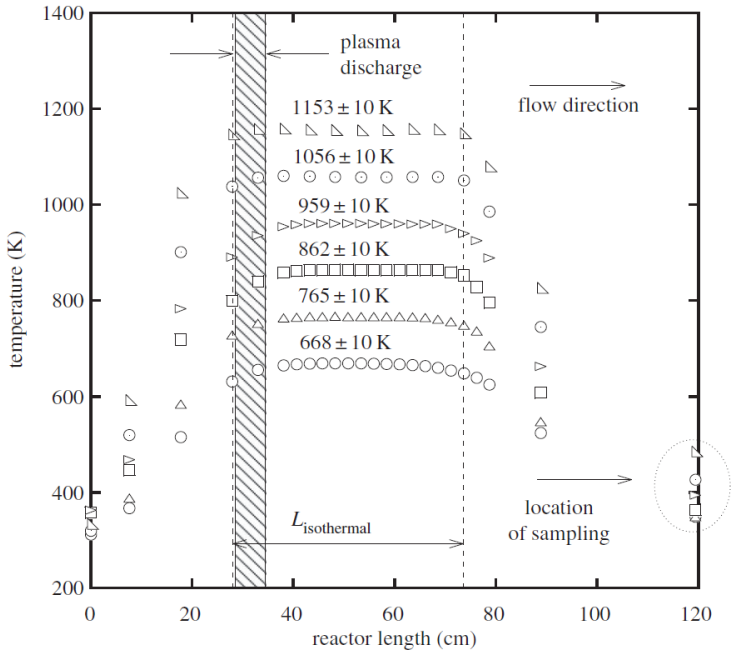


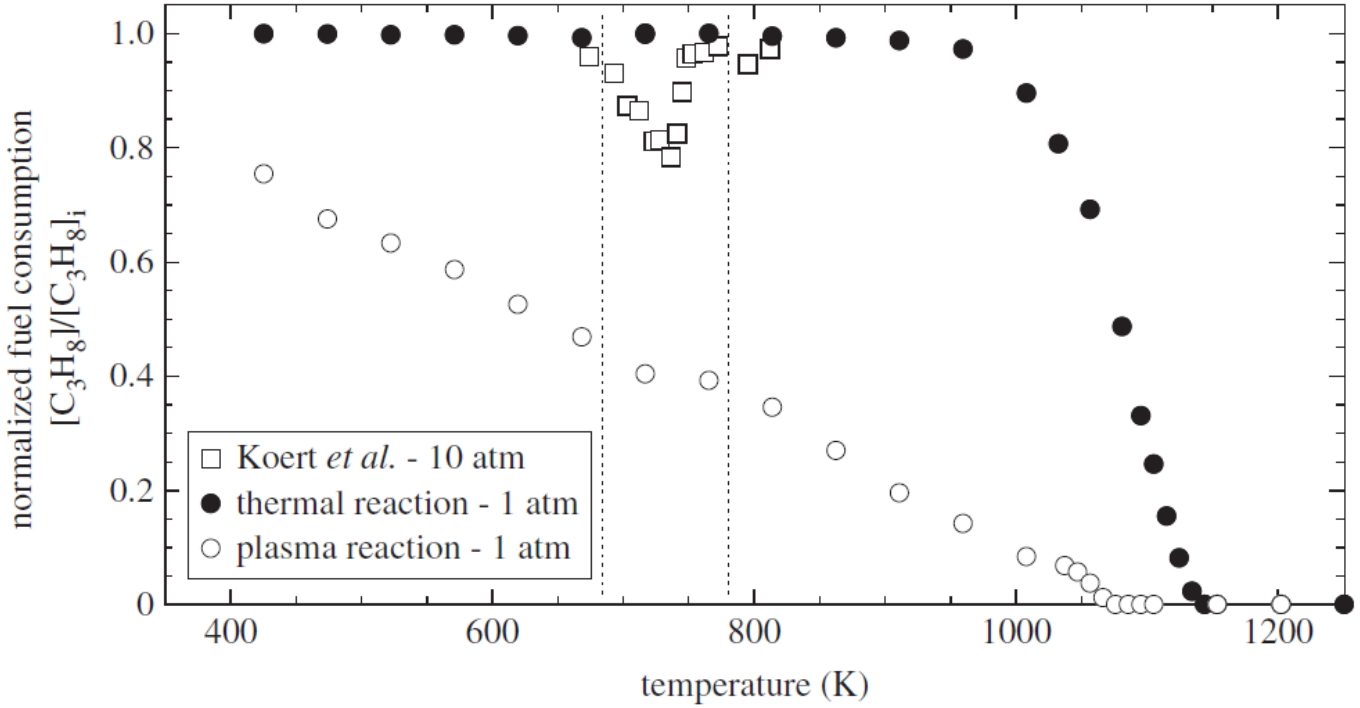


Comparison of thermal (1, 10 atm) and plasma (1 atm) propane fuel consumption as a function of temperature.

Nicholas Tsolas, Jong Guen Lee and Richard A. Yetter, *2015, Phil. Trans. R. Soc. A* **373**: 20140344.

# Plasma activated *Cool Flames* :A new way to burn with plasma

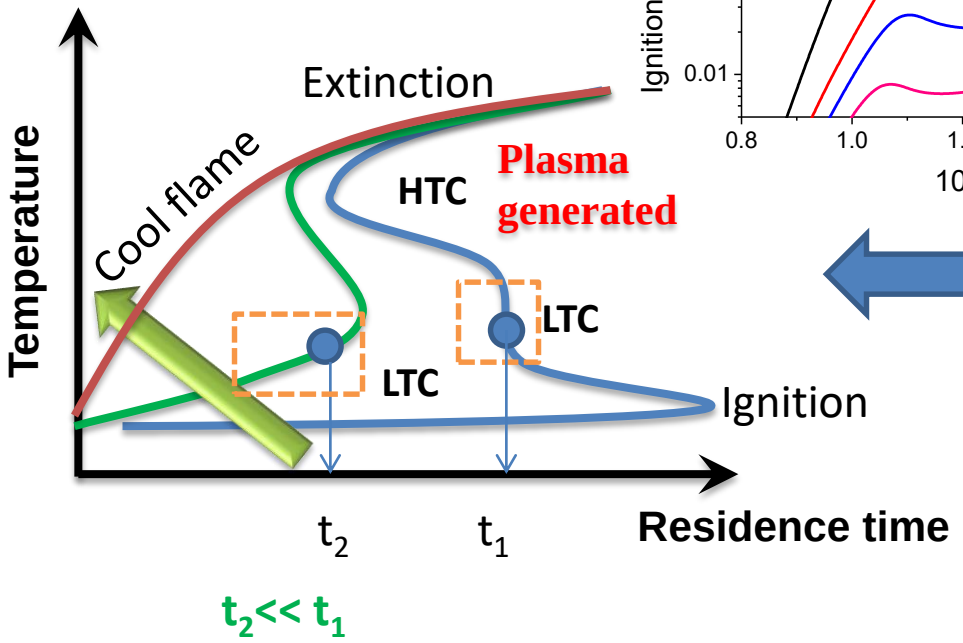


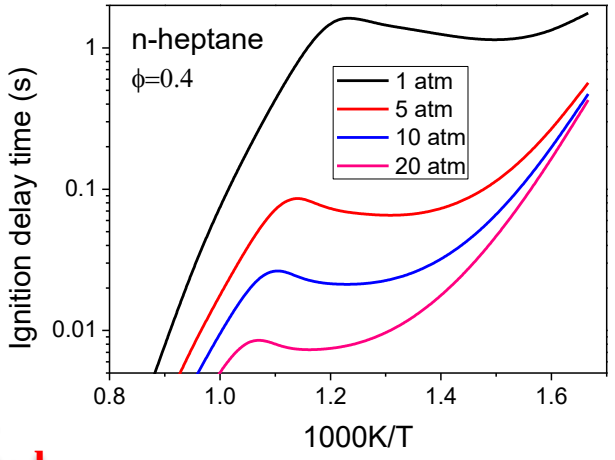


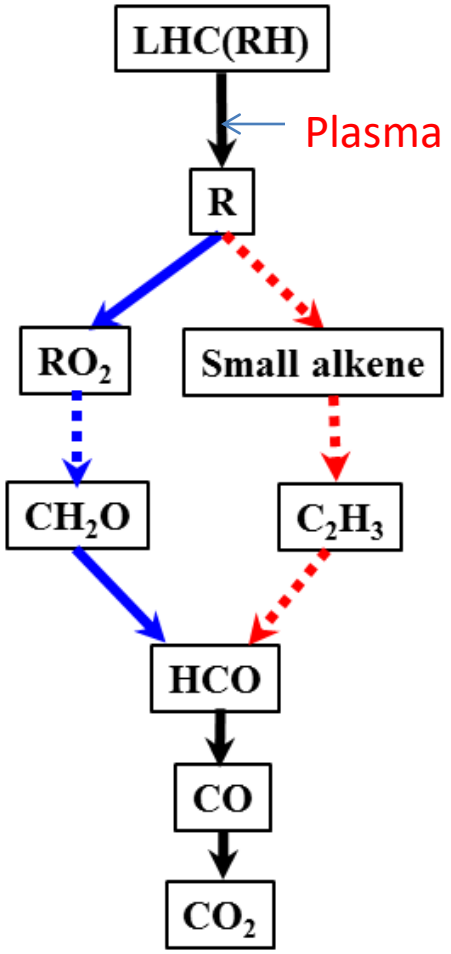


Plasma activated LTC at much shorter time, lower pressure….

We can create cool flames even at 1 atm or below?

# 2. Plasma activated self-sustaining *Cool Diffusion Flames:* A new way to burn

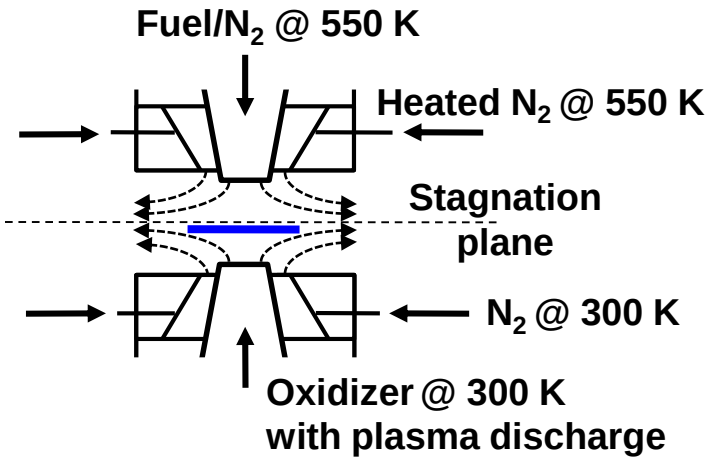


Fig. 1 Schematic of experimental setup

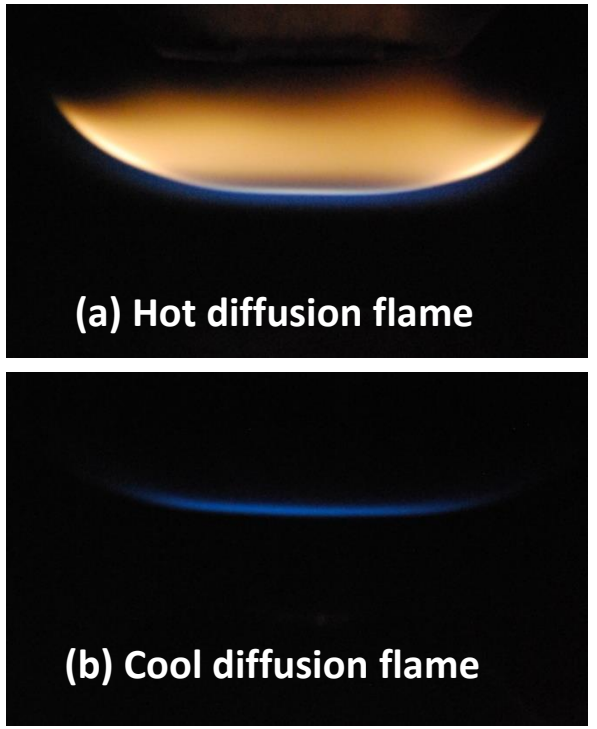


$T_f$~1900 K

$T_f$~650 K

Fig. 2 Hot and cool n-heptane diffusion flames at the same condition

**Won et al., 2014**

# 3. Multispecies diagnostics and kinetic modeling

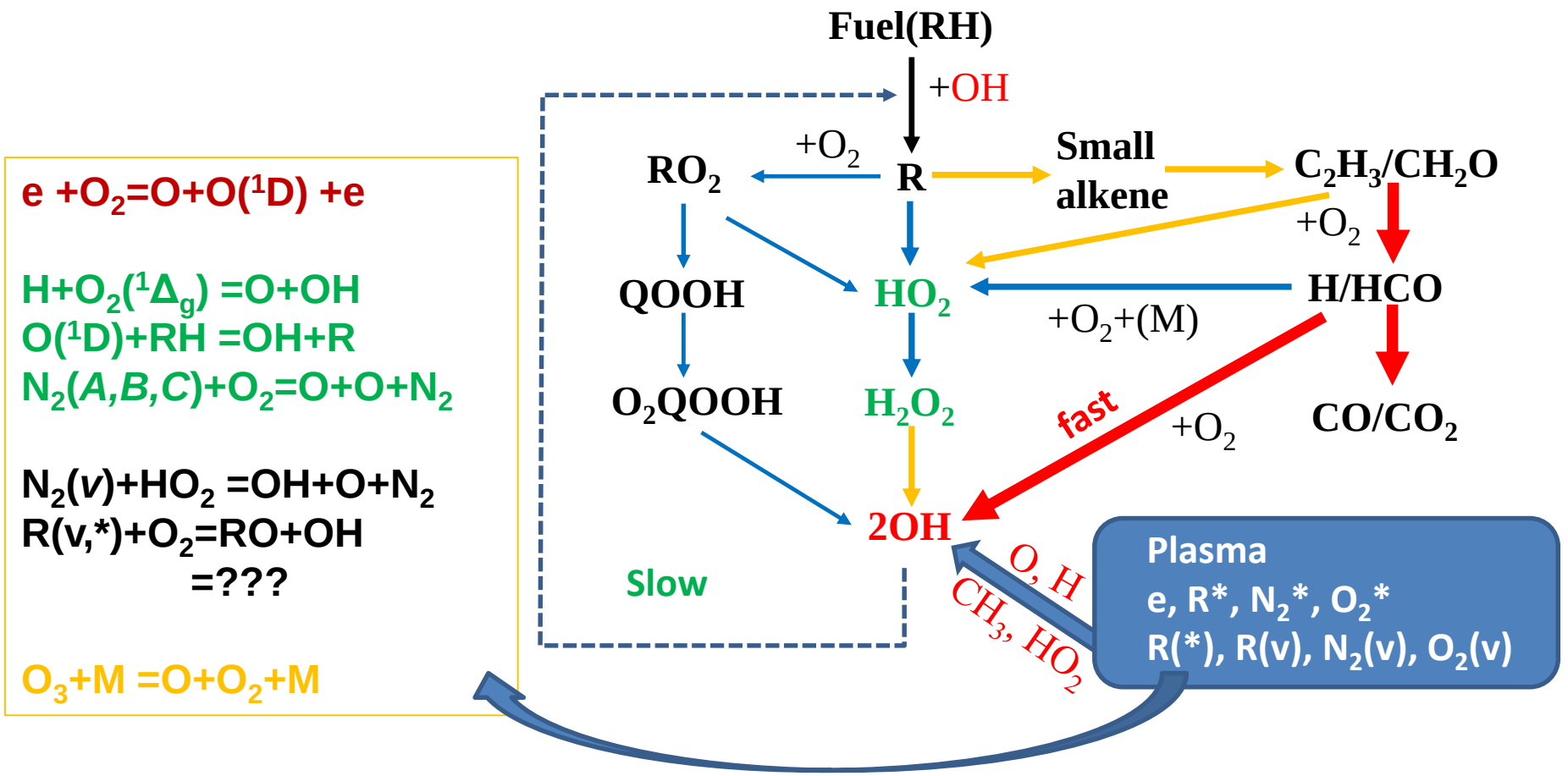


A schematic of the key reaction pathways for high pressure fuel oxidation of at different temperatures
(**blue arrow**: Below 700K; yellow arrow: 700-1050 K;
red arrow: above 1050K).

## Question to aks:

## How does the key plasma reactions affects n-heptane dissociation and oxidation in the first 10 ms with efifferent excitation processes involving Ar and O2?

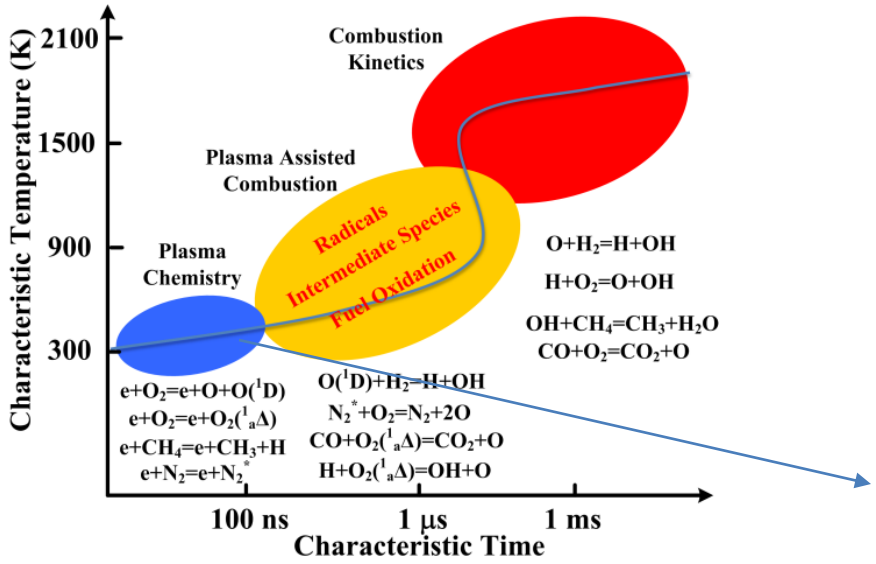


e +Ar =Ar*+e

e +**$O_2$** =O+O($^1$D)

e +**$O_2$** =e + $O_2$(v)

e +**$O_2$** =$O_2^-$

e +C7H16 =H+R

……

Ar* +C7H16 =?

O($^1$D) +C7H16 =?

$O_2$(v) +C7H16 =?

$O_2$(v) +C7H15 =$RO_2$(v)

……

# Plasma chemistry reactor

PRINCETON UNIVERSITY

- Reactor
  - Pressure: 60 Torr
  - Initial Temperature: 300 K
  - Flow speed: 40 cm/s
  - Reactor size: 45 x 14 x 152 $mm^3$
- Nanosecond repetitively pulsed discharge: FID GmbH FPG 30-50MC4
  - Peak Voltage: ~7 kV
  - Pulse Duration: 12 ns FWHM
  - Continuous mode: 0 – 5 kHz
  - Pulse burst mode: 150 pulses, 30 kHz
- Quartz double dielectric barrier: 1.6 mm thickness
- Gap distance: 14 mm

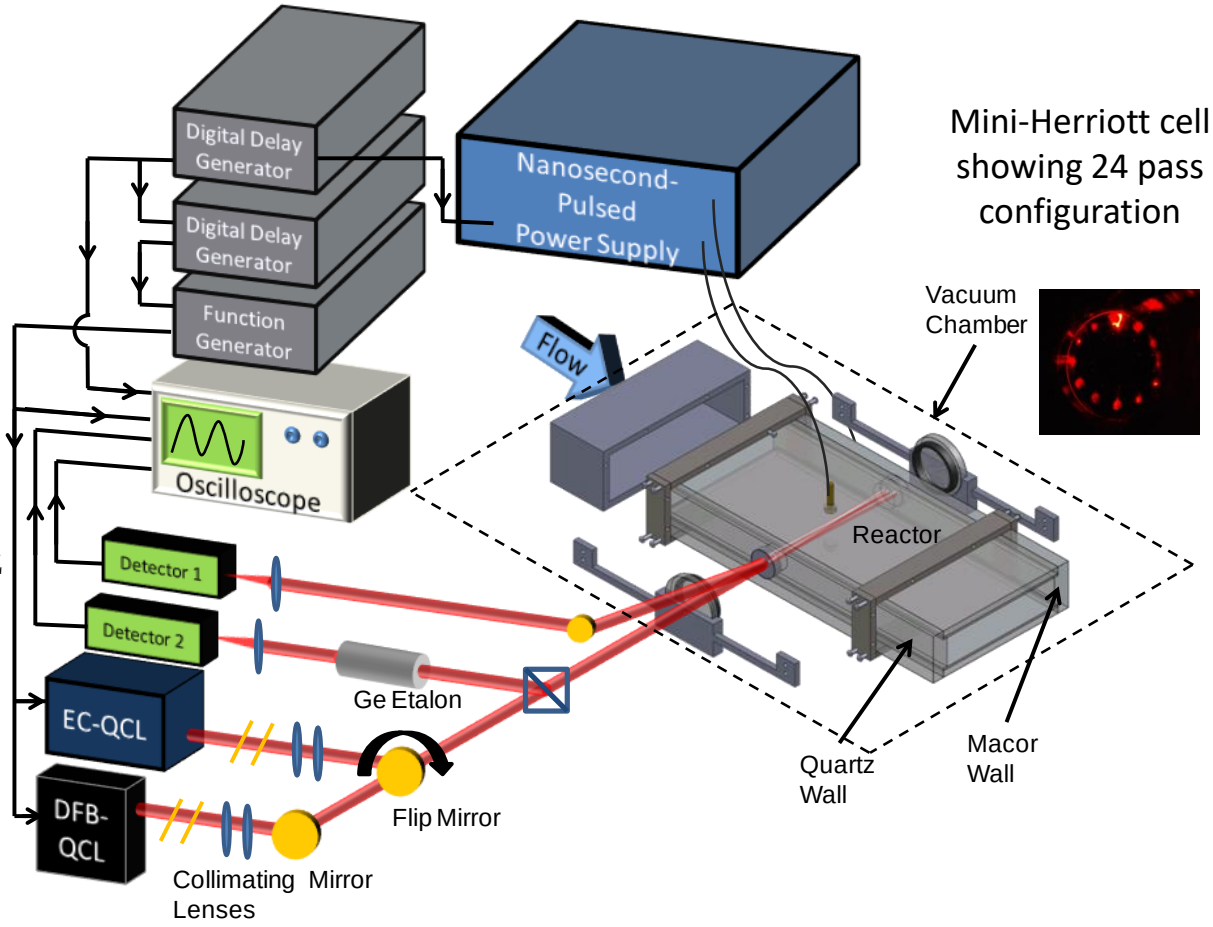


Mini-Herriott cell showing 24 pass configuration

# Experimental Apparatus

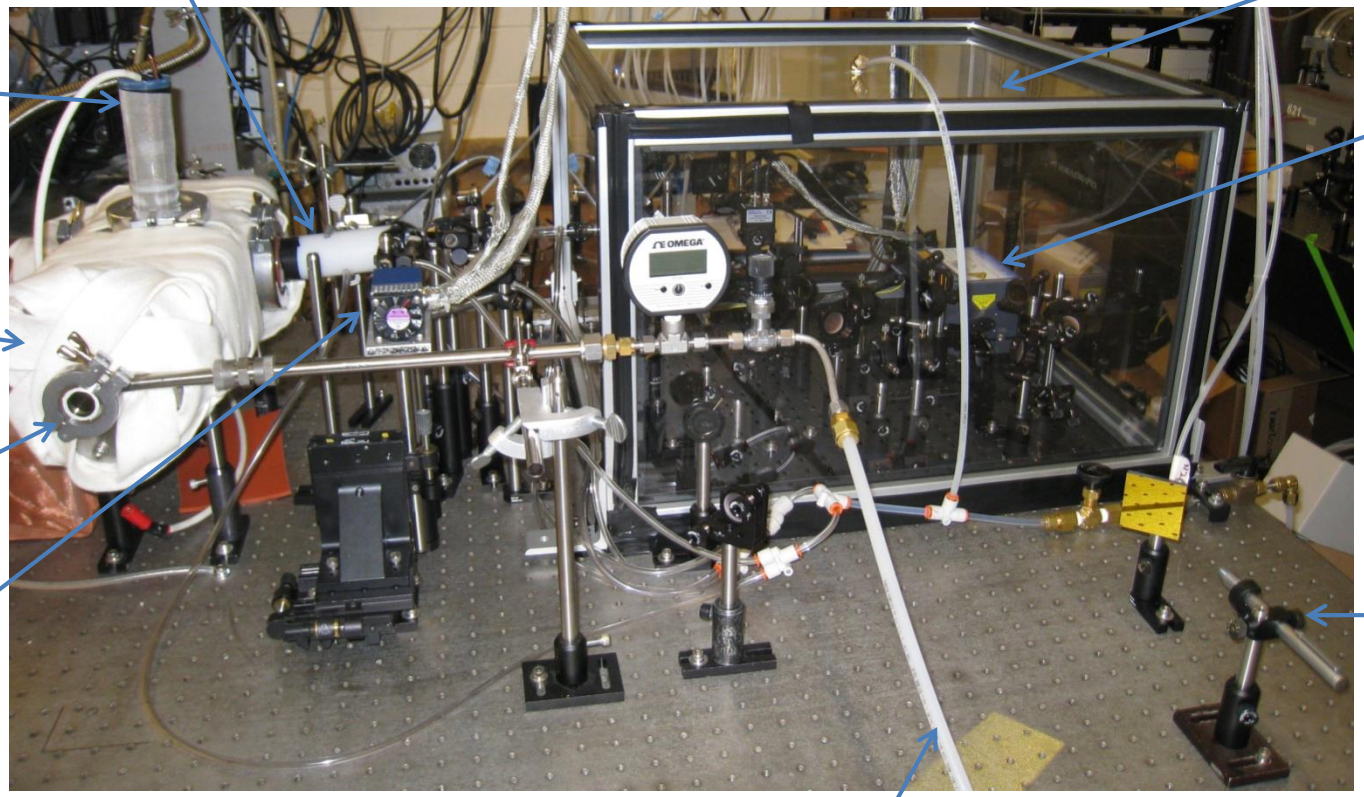

# Direct and ICCD Images of Plasma Discharge in a Reactor

**Stoichiometric mixtures: $C_2H_4/O_2$ with 75% AR, 60 Torr, $V_{max}$= 6 kV**

- Direct Image: 1 kHz, 3.6 mJ/pulse, 2 s exposure time.
- ICCD images: Gate time = 100 ns, Gain = 250

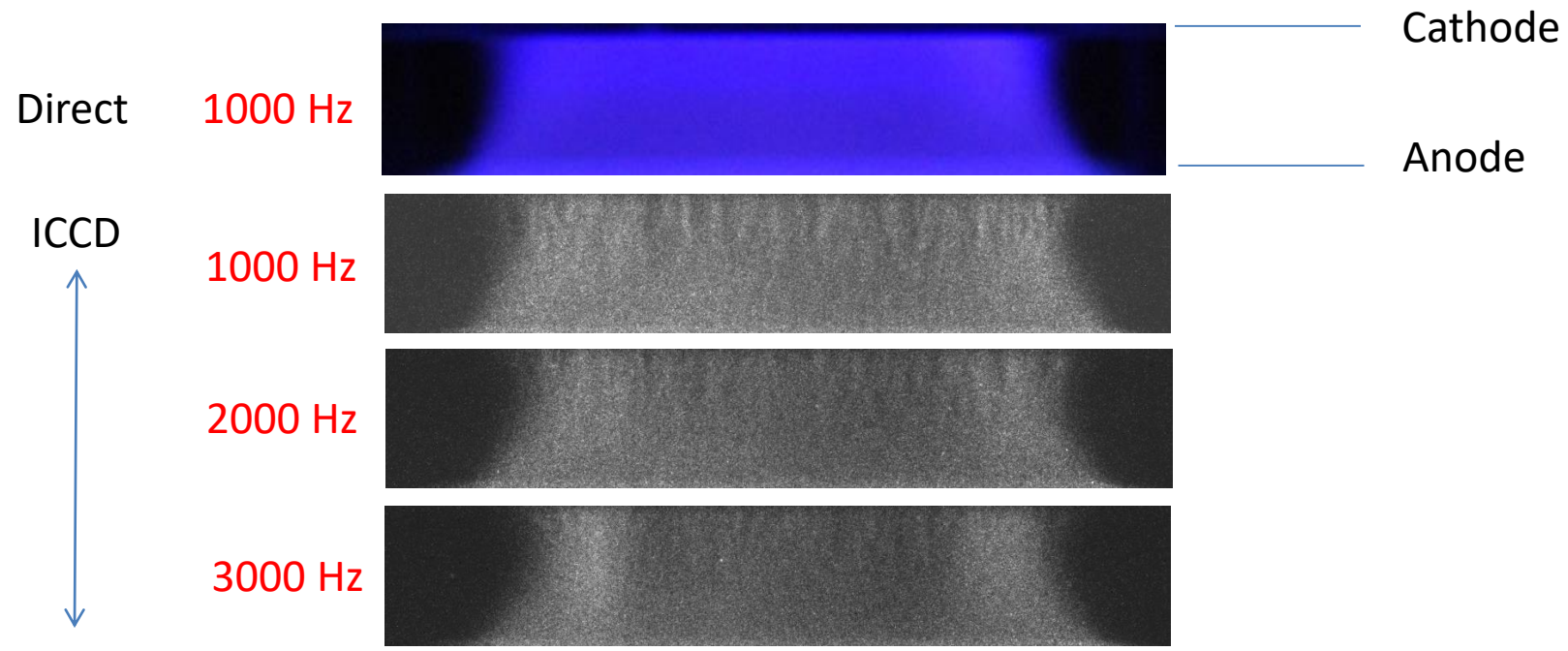

# Experiment/Model Comparison (C2H4)

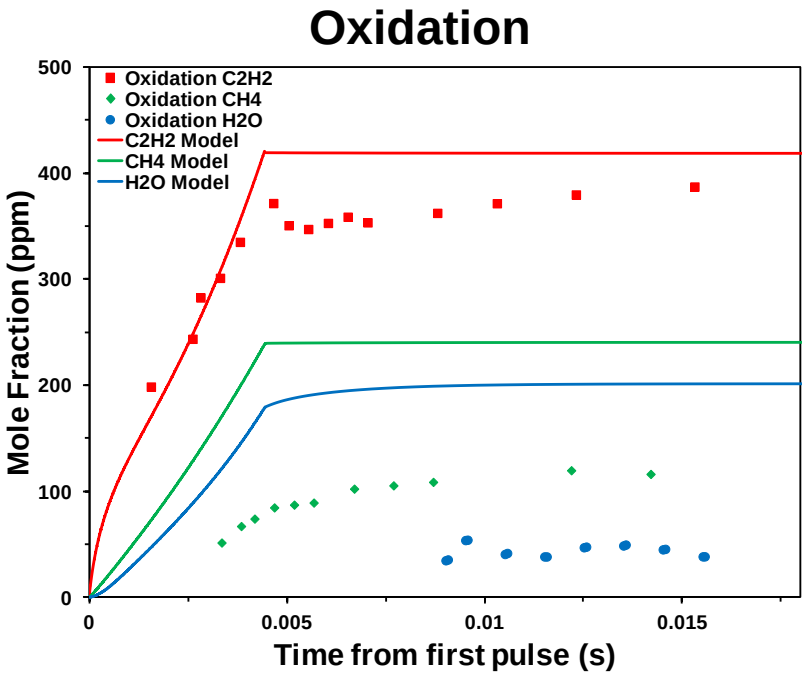


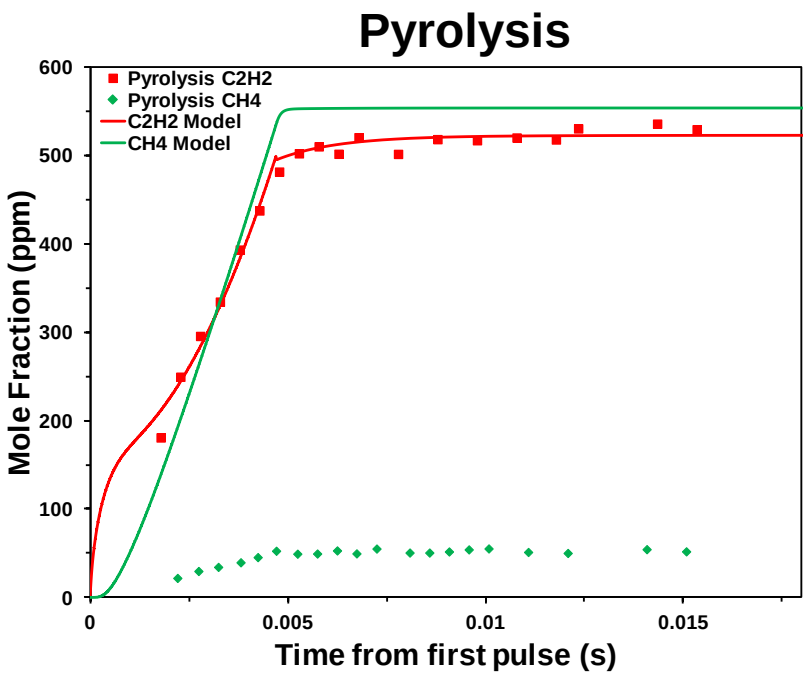


- **Conditions for Oxidiation case:**
  - Stoichiometric $C_2H_4$/O2
  - 25% Reactants, 75% Argon
  - V=40 cm/s
  - P=60 Torr
  - Ti=300 K
  - 150 Pulses, 30 kHz, 10 kV
  - E/n = 37 Td
- Acetylene measurements in the pyrolysis experiment were used to match the E/n ratio of model calculations

- **Conditions for pyrolysis case:**
  - 0.9375 Ar/0.0625 C2H4
  - V=40 cm/s
  - P=60 Torr
  - Ti=300 K
  - 150 Pulses, 30 kHz, 10 kV
  - E/n = 37 Td
- Methane is greatly over-predicted by the model

# Continuous Plasma - Oxidation

PRINCETON UNIVERSITY

- GC and *in situ* IR-LAS measurements
  - Continuous plasma
  - Stoichiometric, 25% Reactant
- Excellent agreement between GC and IR-LAS
- Major Species
  - $CH_2O$
  - $CO$
  - $C_2H_2$
  - $CH_3OH$, $C_2H_4O$
  - $CH_4$

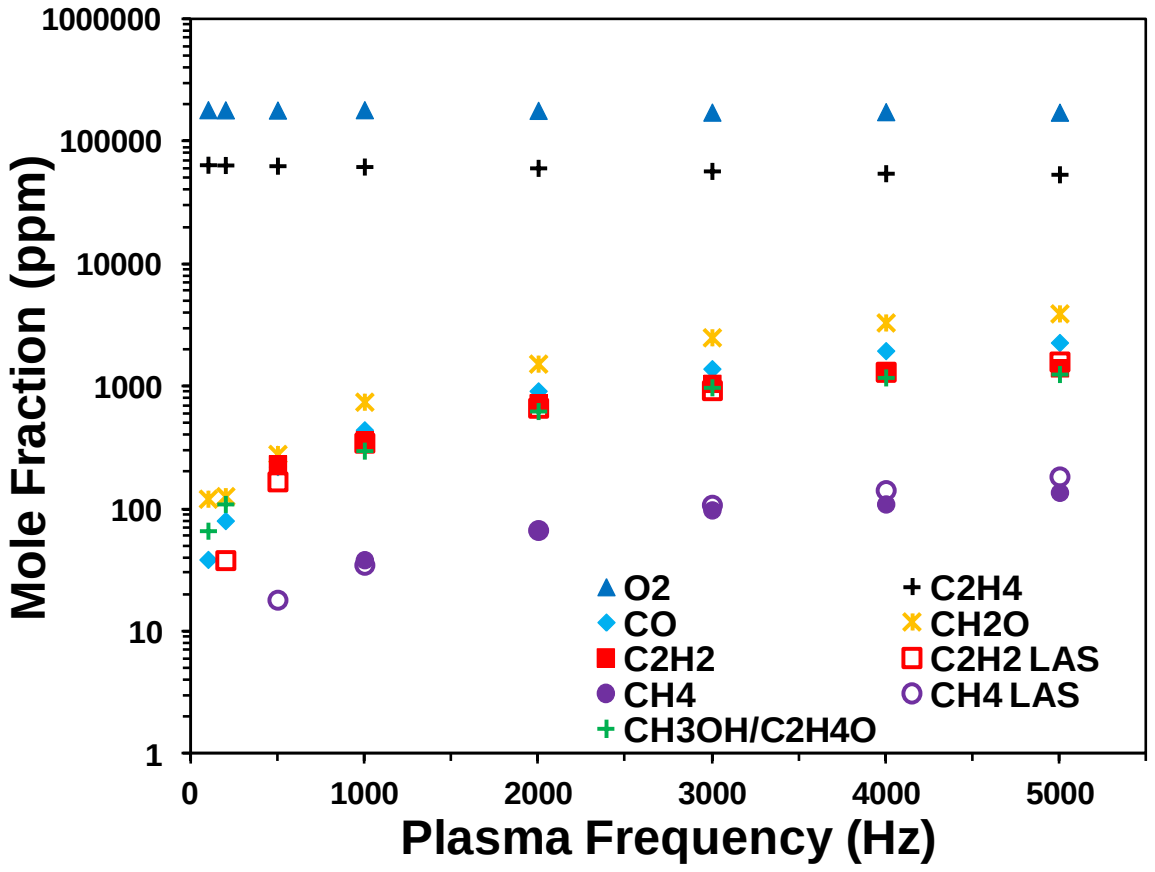


***Plasma activated low temperature fuel oxidation is an important process***

Lefkowitz et al. 2014

# Validation of plasma combustion chemistry of C2H4 oxidation

## $C_2H_4/O_2/Ar$: 6.25/18.75/75

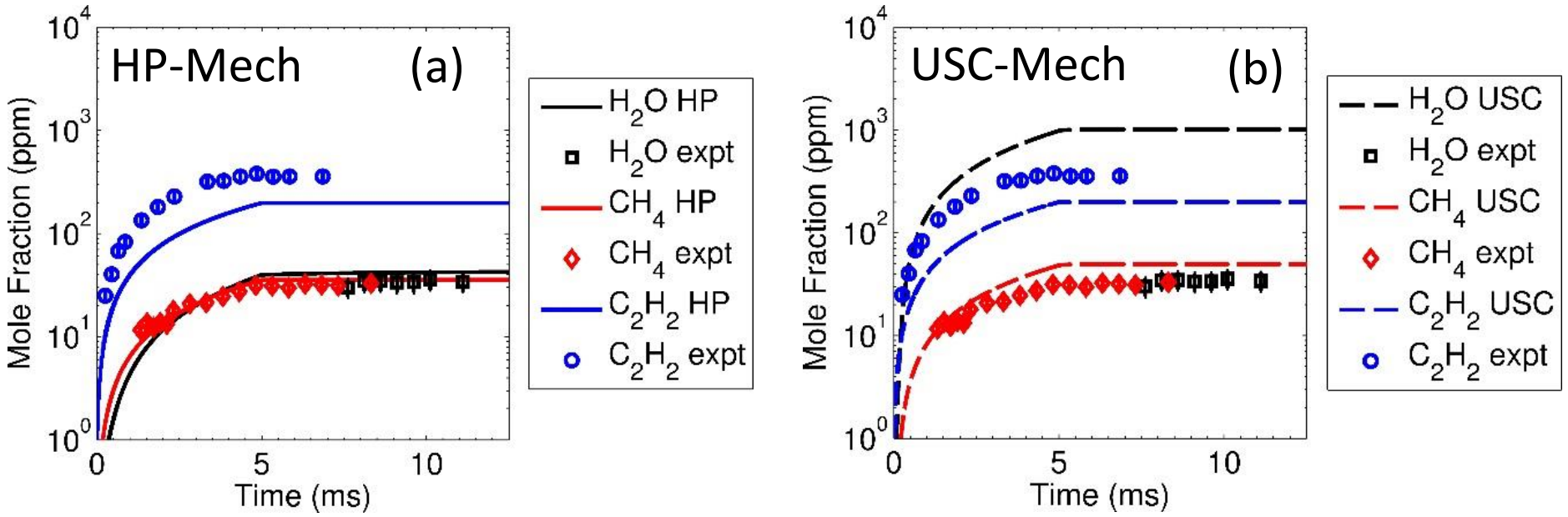


Fig. 16 Measurements and predictions of $C_2H_2$, $CH_4$, and $H_2O$ concentrations after 150 pulses at 30 kHz repetition rate for a mixture of $C_2H_4/O_2/Ar$: 6.25/18.75/75 by using (a) HP-Mech and (b) USC-Mech II.

# Ethylene Oxidation Pathways

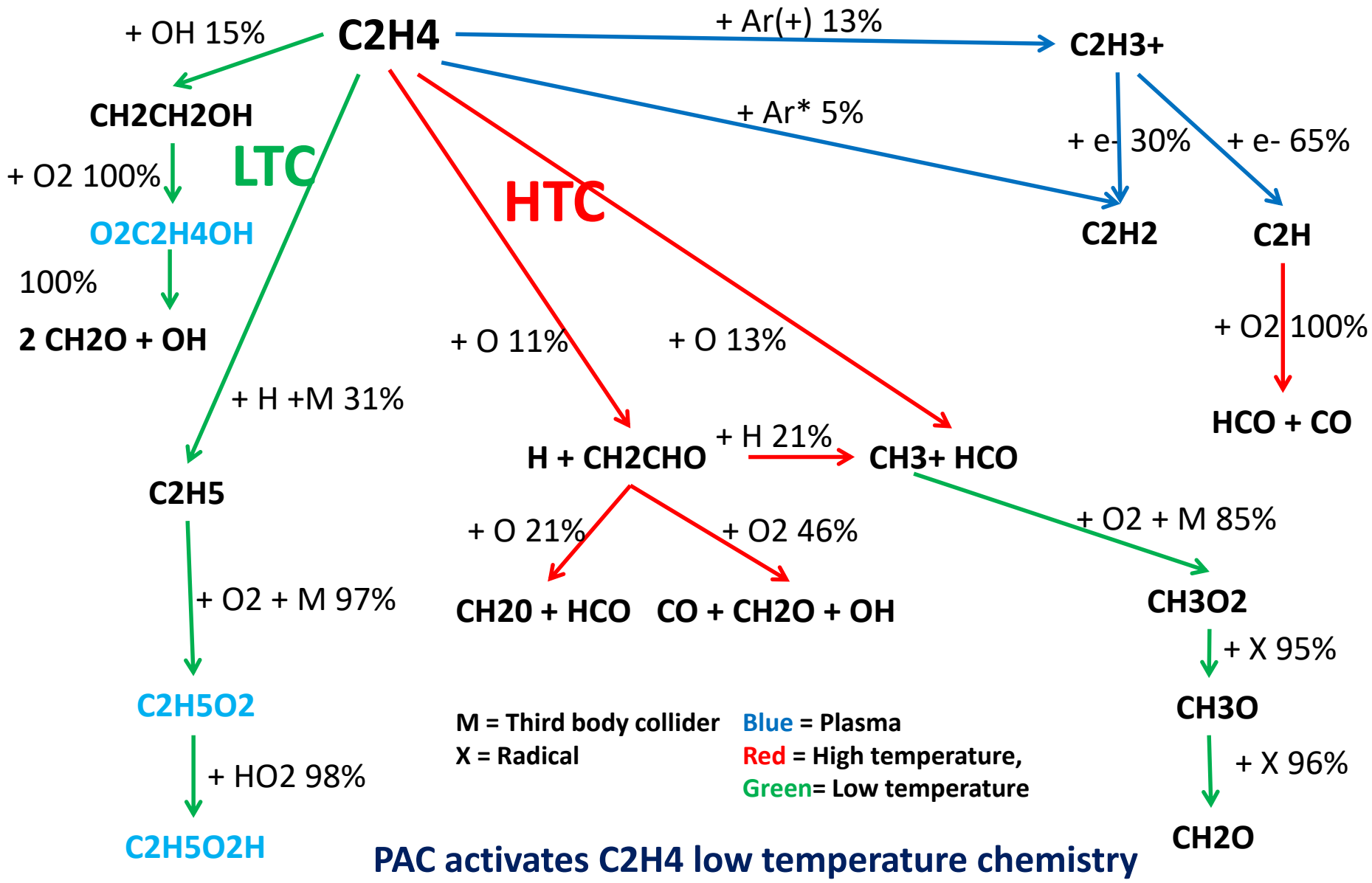

# Challenges: Plasma activated $CH_4/O_2$/He oxidation at 400 K

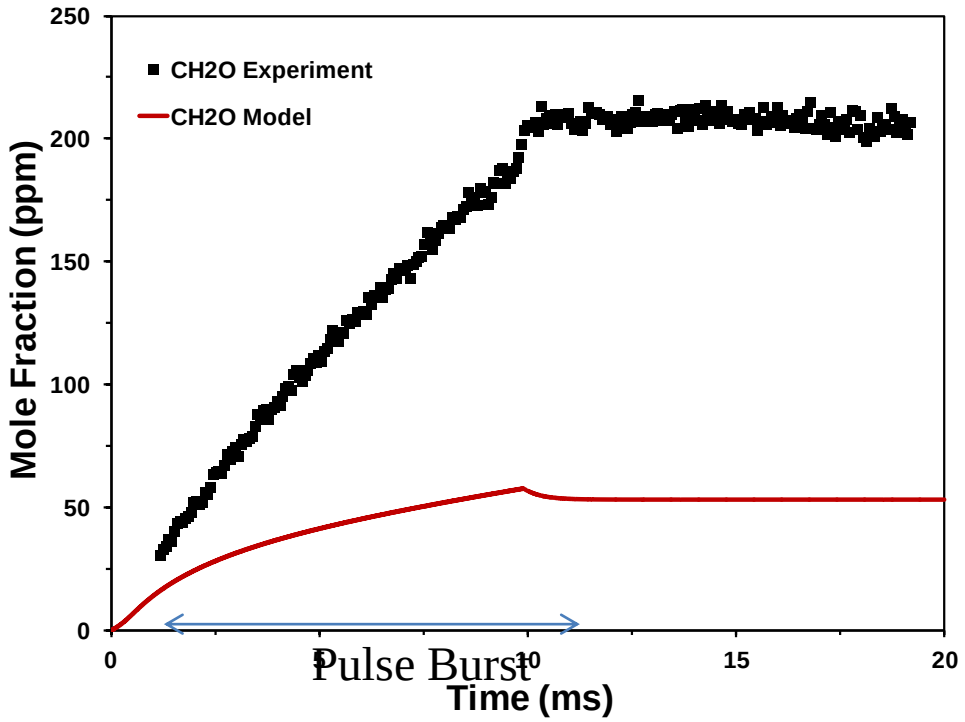


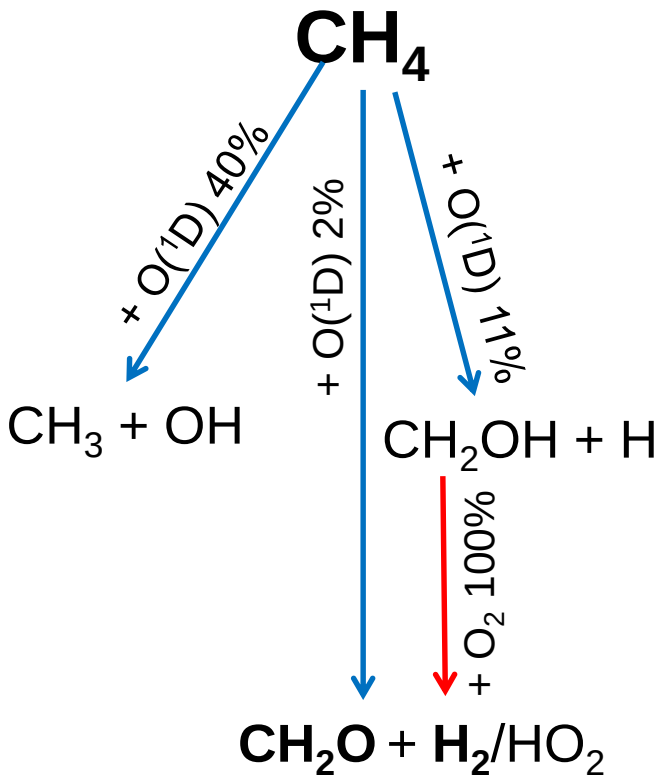


- 300 pulse burst, 8.75 kV peaks voltage, 30 kHz pulse repetition frequency
- Stoichiometric mixture, 75% diluent, 60 Torr, 300 K initial temperature

Lefkowitz, J.K., Guo, P., Rousso, A. and Ju, Y., 2015. *Phil. Trans. R. Soc. A*, *373*(2048), p.20140333.

# Challenges: Time dependent Formaldehyde Measurement

- $CH_2O$ production slightly greater for stoichiometric case
  - Similar linear trend as in n-heptane consumption
    - Lack of further $CH_2O$ production after pulse burst: indicates that only plasma produced species are responsible for fuel oxidation
- **Mode significantly under-predicts measurement by a factor of 40.**
- **Missing pathways for low temperature CH2O formation**

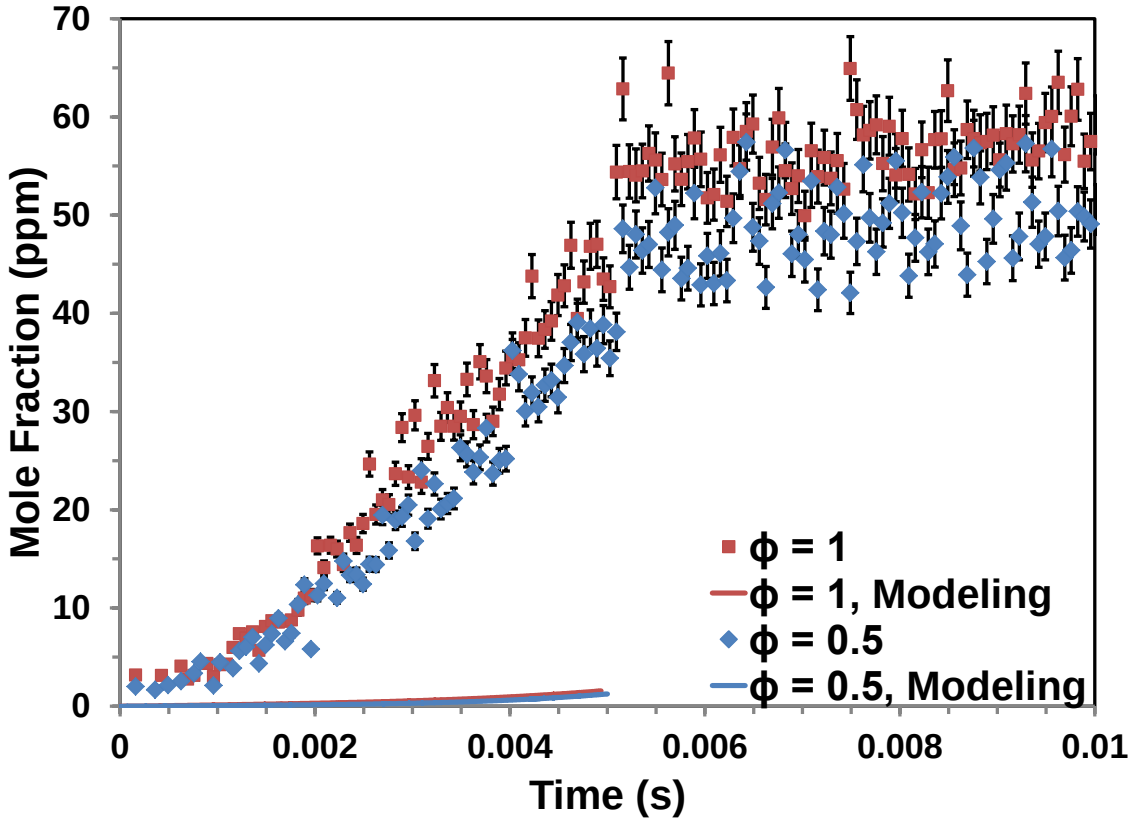


Rousso, Aric, Suo Yang, Joseph Lefkowitz, Wenting Sun, and Yiguang Ju.
" *Proceedings of the Combustion Institute, Vo.36,* 2017, Pages 4105–4112

PRINCETON UNIVERSITY

# Cross-sections database available for electron-molecule collisions

Table 1. Cross-sections database for electron-molecules collisions.

| Atmospheric | Saturated | Unsaturated | Oxygenated | Isomers |
|---|---|---|---|---|
| N2 | CH4 | C2H2 | CO | iso-butane |
| O2 | C2H6 | C2H4 | CH3OH | iso-propane |
| CO2 | C3H8 | C3H6 | C2H5OH | neo-pentane |
| H2O | C4H10 | | CH3OCH3 (DME) | |
| O3 | C5H12 | | | |
| Ar | H2 | | | |
| N2O | | | | |

Andrey Starikovskiy and Nikolay Aleksandrov, AIAA paper-2017-1977

# Non-equilibrium plasma kinetics

## A new reaction pathway of plasma assisted low temperature combustion via excited $RO_2^*(v)$

Vibrational and electronically excited O2(v) collides with fuel radical (R) forming highly energized RO2* in which the vibrational energies are quickly redistributed due to strong coupling between different vibration states. These RO2*, comparing to those formed by ground state oxygen with R, carry much higher internal energies that enable them overcome the barrier TS1, TS2, and TS3 much easier to produce the bimolecular product HO2+Alkene and OH+Ether. Therefore, the ignition processes/species profiles of the mixture can be significantly different from the ground state system.

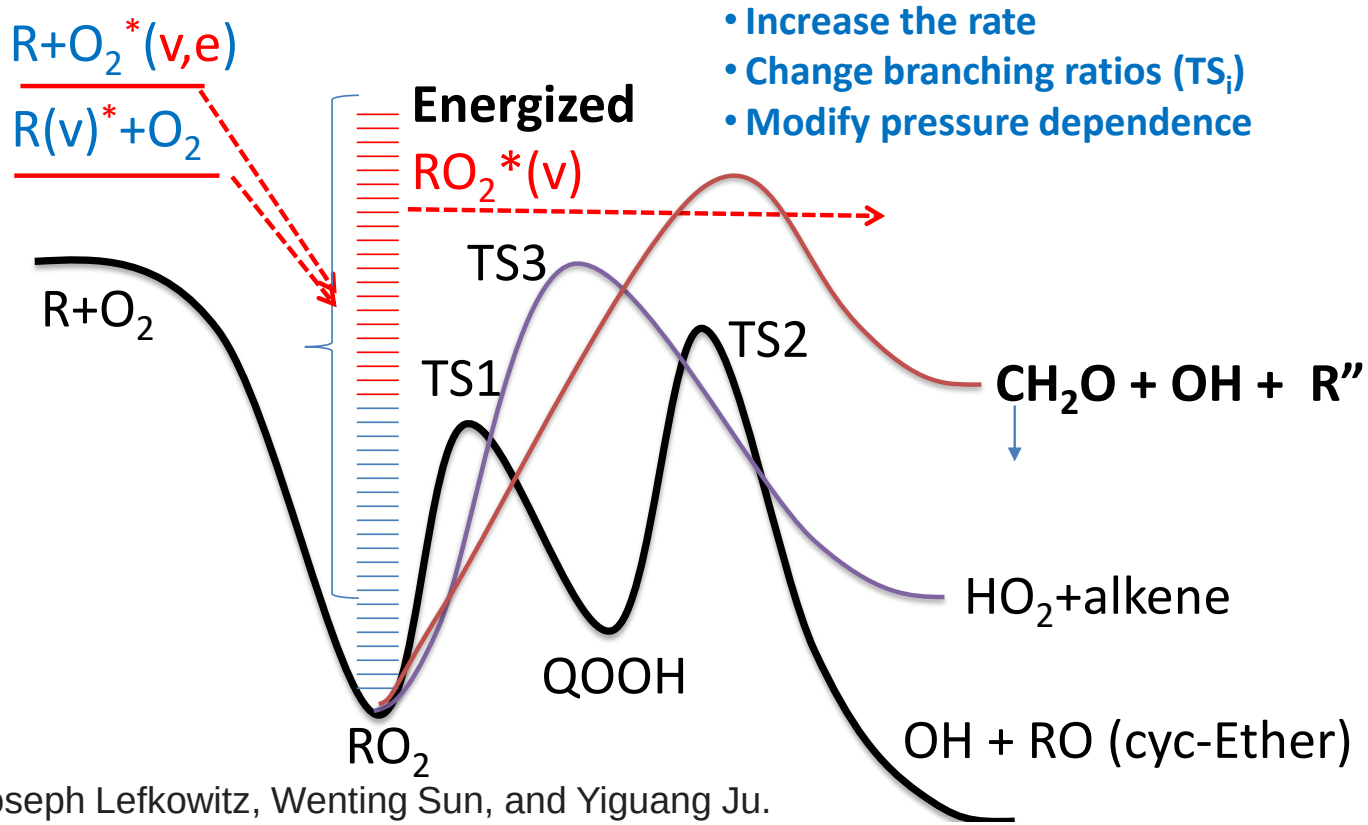


Rousso, Aric, Suo Yang, Joseph Lefkowitz, Wenting Sun, and Yiguang Ju.
" *Proceedings of the Combustion Institute, Vo.36*, 2017, Pages 4105–4112

# O(1D) reaction kinetics:

## Photolysis reactor for elementary kinetic study

**$O(1D)/O_3/O_2/CH_3OH$/Ar mixture**

time dependent measurements of OH, $HO_2$, $CH_2O$,…

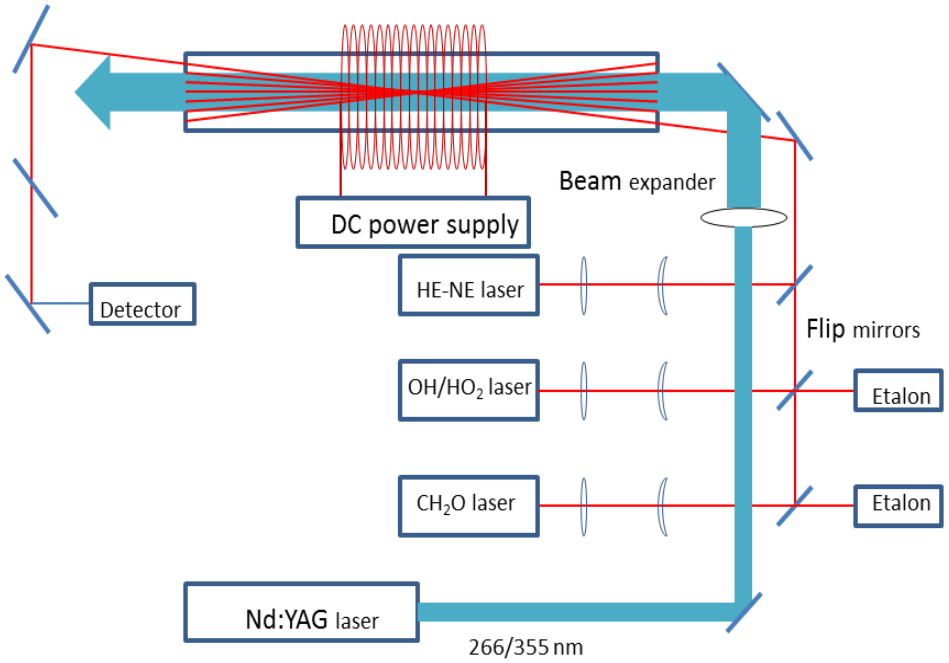


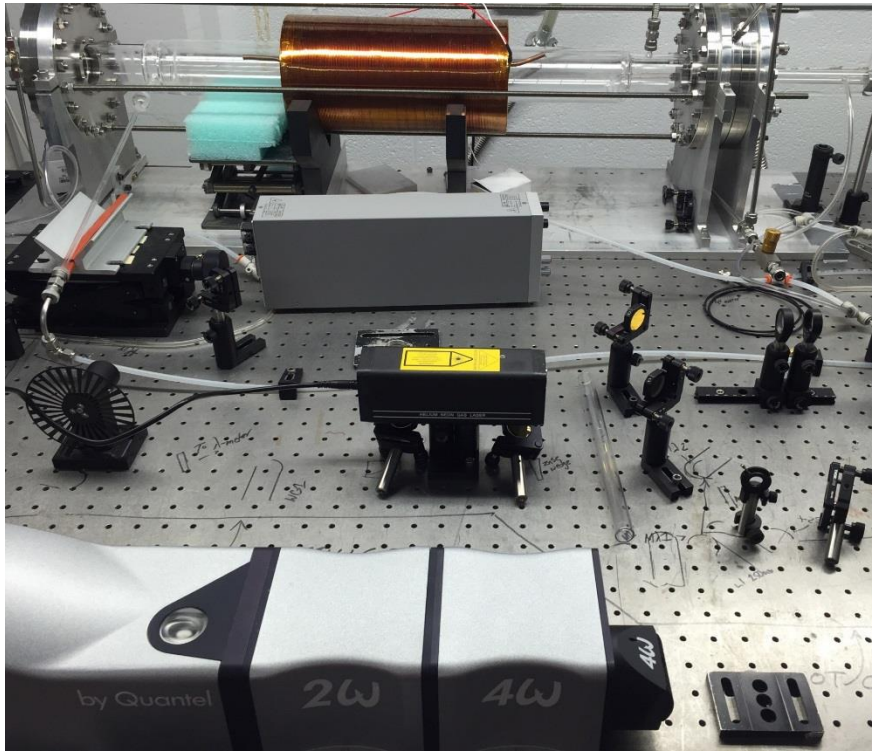


$H_2O$:1338.55 $cm^{-1}$
$CH_2O$:1726.8 $cm^{-1}$
OH: 3568 $cm^{-1}$
HO2: 1397 $cm^{-1}$

913 mm long, 40 mm diameter, multi-pass (21) Herriott cell, a19.17 meter optical path length

Ju, Y., Lefkowitz, J.K., Reuter, C.B., Won, S.H., Yang, X., Yang, S., Sun, W., Jiang, Z. and Chen, Q., 2016. *Plasma Chemistry and Plasma Processing*, *36*(1), pp.85-105.

# Experimental results and model validation: updated model

| | | | |
|---|---|---|---|
| $O(^1D)+CH_3OH \rightarrow CH_2OH+OH$ | $k_{new}=1.5x10^{14}$ | (R27) | |
| $O(^1D)+CH_3OH \rightarrow HOCHOH+H$ | $k_{new}=0.5x10^{14}$ | (R28) | (in mole-cm$^3$-s) |
| $O(^1D)+CH_3OH \rightarrow CH_2O+H_2O$ | $k_{new}=1.0x10^{14}$ | (R29) | |

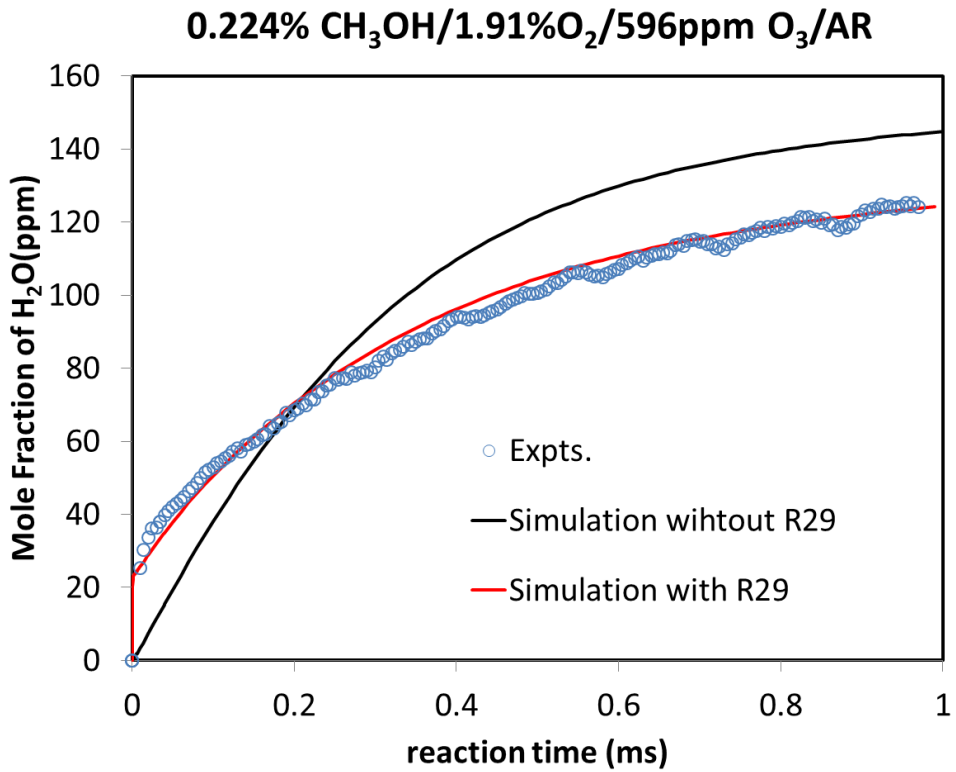


Time-resolved mole fraction of $H_2O$ in the 266 nm laser photolysis of 0.224% $CH_3OH$ 1.91% $O_2$ and 596 ppm $O_3$ in Ar mixture with the variation of $CH_3OH$ flow rate compared to model simulations for 1.0 ml/hour flow of $CH_3OH$. ○: Experimental measurement; — : simulation using the original model. — : simulation with updated reaction rates [38].

Ju, Y., Lefkowitz, J.K., Reuter, C.B., Won, S.H., Yang, X., Yang, S., Sun, W., Jiang, Z. and Chen, Q., 2016. *Plasma Chemistry and Plasma Processing*, *36*(1), pp.85-105.

# Potential energy surface (PES) of $O(^1D)+CH_3OH$

**using M062X/cc-pvtz level**

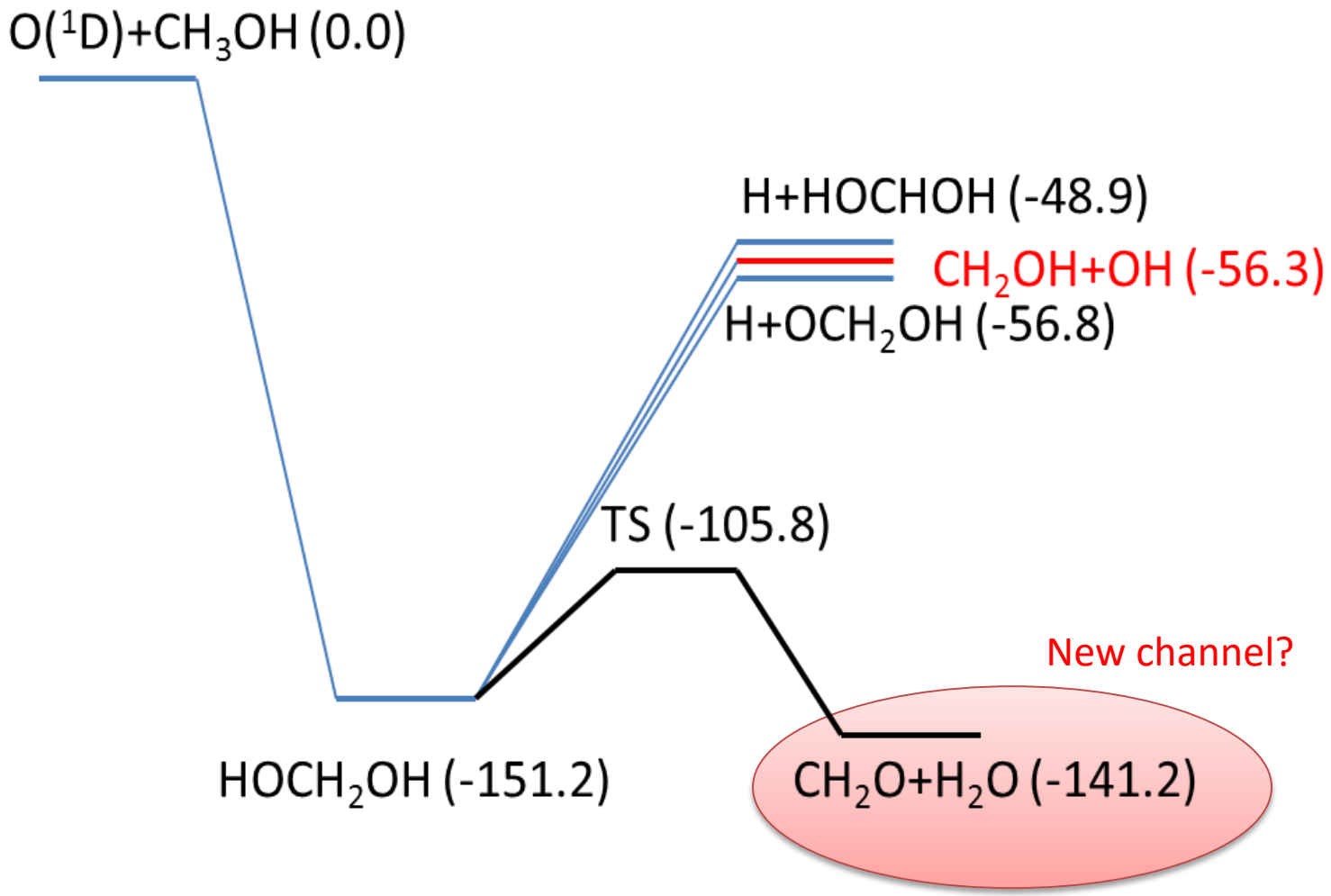


Ju, Y., Lefkowitz, J.K., Reuter, C.B., Won, S.H., Yang, X., Yang, S., Sun, W., Jiang, Z. and Chen, Q., 2016. *Plasma Chemistry and Plasma Processing*, *36*(1), pp.85-105.

# $HO_2$/OH using mid-IR Faraday Rotational Spectroscopy

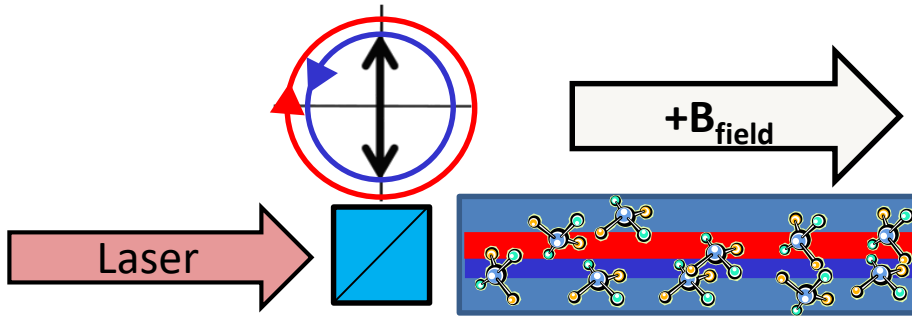


$$V_{RMS}(\tilde{\nu}) = \left(GP_0 \sin 2\theta\right)\Theta_{RMS}$$

$$\Delta n(\tilde{\nu}) = n_{RHCP}(\tilde{\nu}) - n_{LHCP}(\tilde{\nu})$$

Lock-In Amplifier

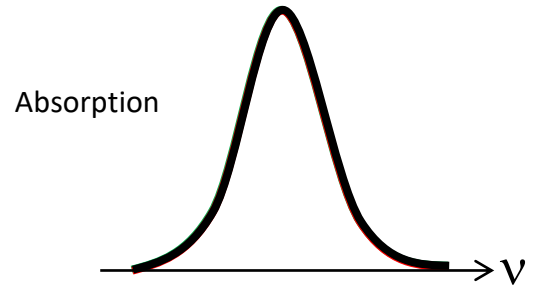


## $HO_2$ energy levels Zeeman splitting

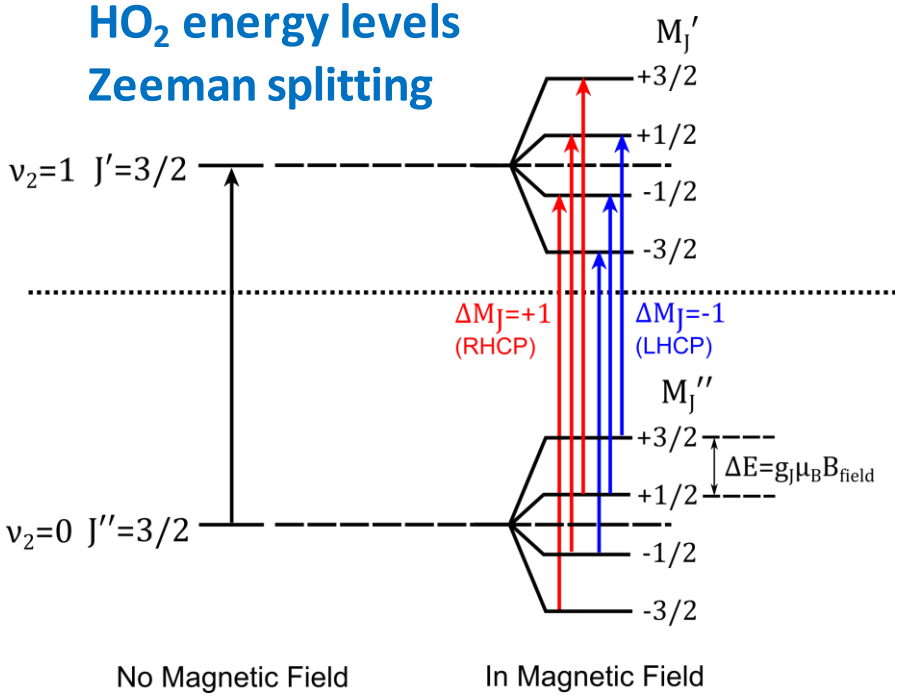

# Experimental results: $HO_2$/OH measurements

Signal

**Sensitivity**

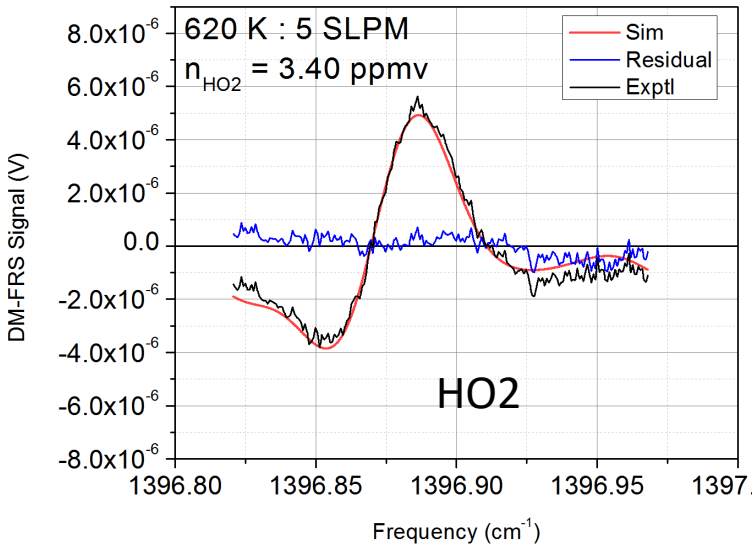


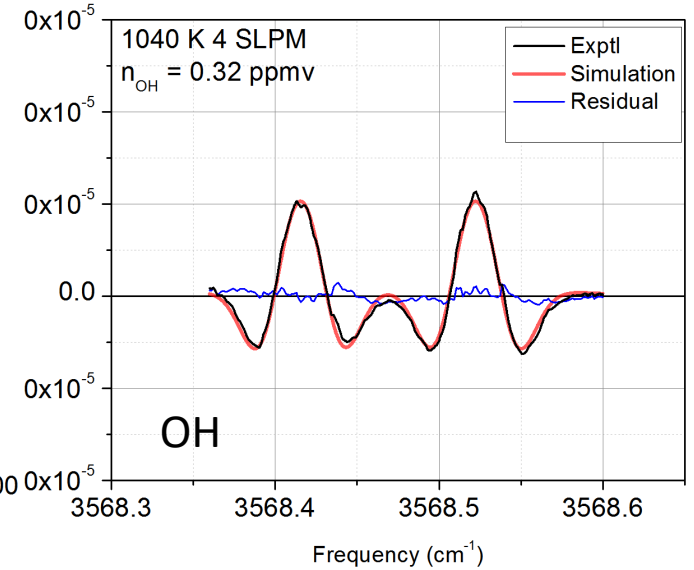


$\sigma$ detection limit $\approx$ 1 ppmv $/\sqrt{Hz}$ 3$\sigma$ detection limit = 20 ppbv $/\sqrt{Hz}$

DME flow reactor model validation

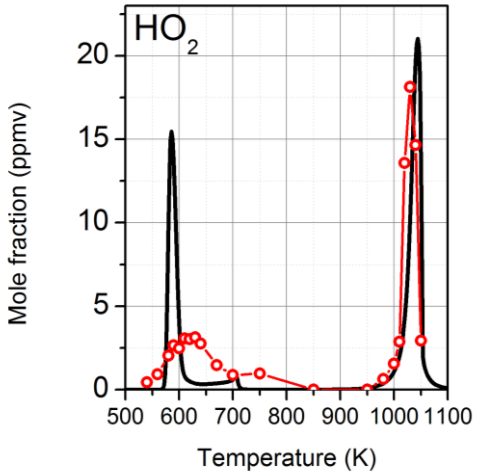


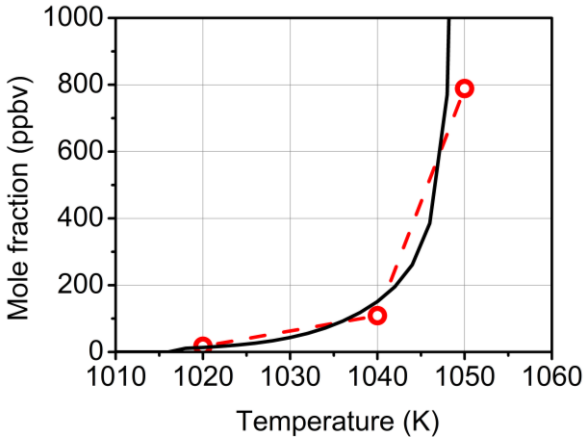


**Implicatio**

**RO2→QOOH→O2QOOH uncertainty**

**HCO+O2=HO2+CO reaction uncertainty and HCO formation pathway?**

Bremfield et al., 2013, JPC letters, 2013; Kurimoto et al. 2014

# Summary

- **Time-resolved, spatially-resolved, in-situ laser diagnostics of electric field, electron density, and electron temperature, excited and radical species greatly enhanced the understanding of plasma kinetic and chemical process in PAC.**
- **Production of O and $O(^1D)$, $O_2$(singlet), $N_2$(*), and $N_2$(v) by the plasma is the major processes in kinetically enhancement of combustion.**
- **Fast and slow heating in PAC is important, but the energy transfer processes are very complicated.**
- **Plasma activated low temperature combustion pathways and enable cool flame formation, but existing mechanisms have large uncertainties, especially for large hydrocarbons.**
- **Electron impact reaction cross-sections of large alkanes and reaction rates involving $O(^1D)$ and non-equilibrium excitations are poorly known.**
- **The effect of vibrational species excitation on PAC is still poorly known.**

# Lecture 6 Plasma Kinetic Modeling

Yiguang Ju

Contribution of Xingqian Mao

# 6.1 Electron impact reactions

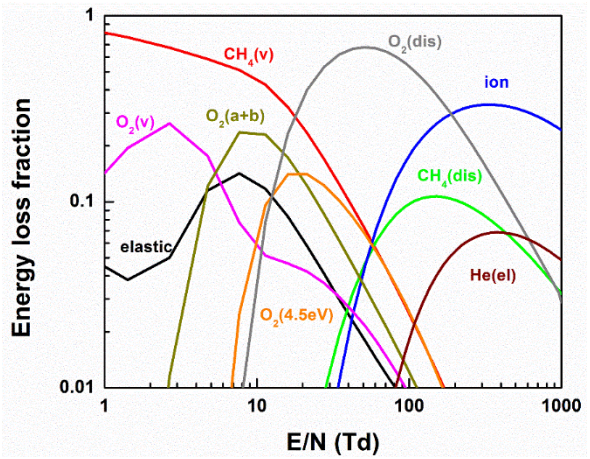


$CH_4$:$O_2$:He=1:2:9

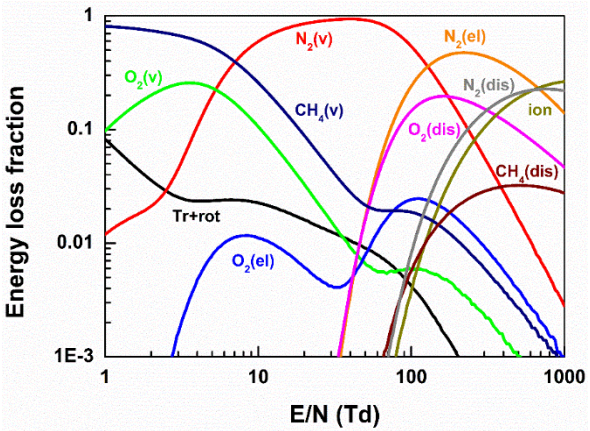


$CH_4$:$O_2$:$N_2$=1:2:3.76

**Energy loss fraction:** Fraction for net energy loss per unit time in each individual collision process k.

**Energy loss coefficients(eV m³/s)**

For elastic collisions: $K_k = \frac{2m_e}{M_k}\gamma\int_0^\infty[\sigma_k(\varepsilon^2 f_0 + \frac{k_B T}{e}\frac{\partial f_0}{\partial \varepsilon})]d\varepsilon$

For inelastic collisions: $K_k = U_k k_k \qquad \gamma = (2e/m_e)^{1/2}$

- **E/N (electric field / molecule number density)**:

Electron impact reactions depend on the electron energy distribution function (or electron temperature) and the electron collisional cross-section areas of a molecule. The electron energy is controlled by the electric field strength, E/N.

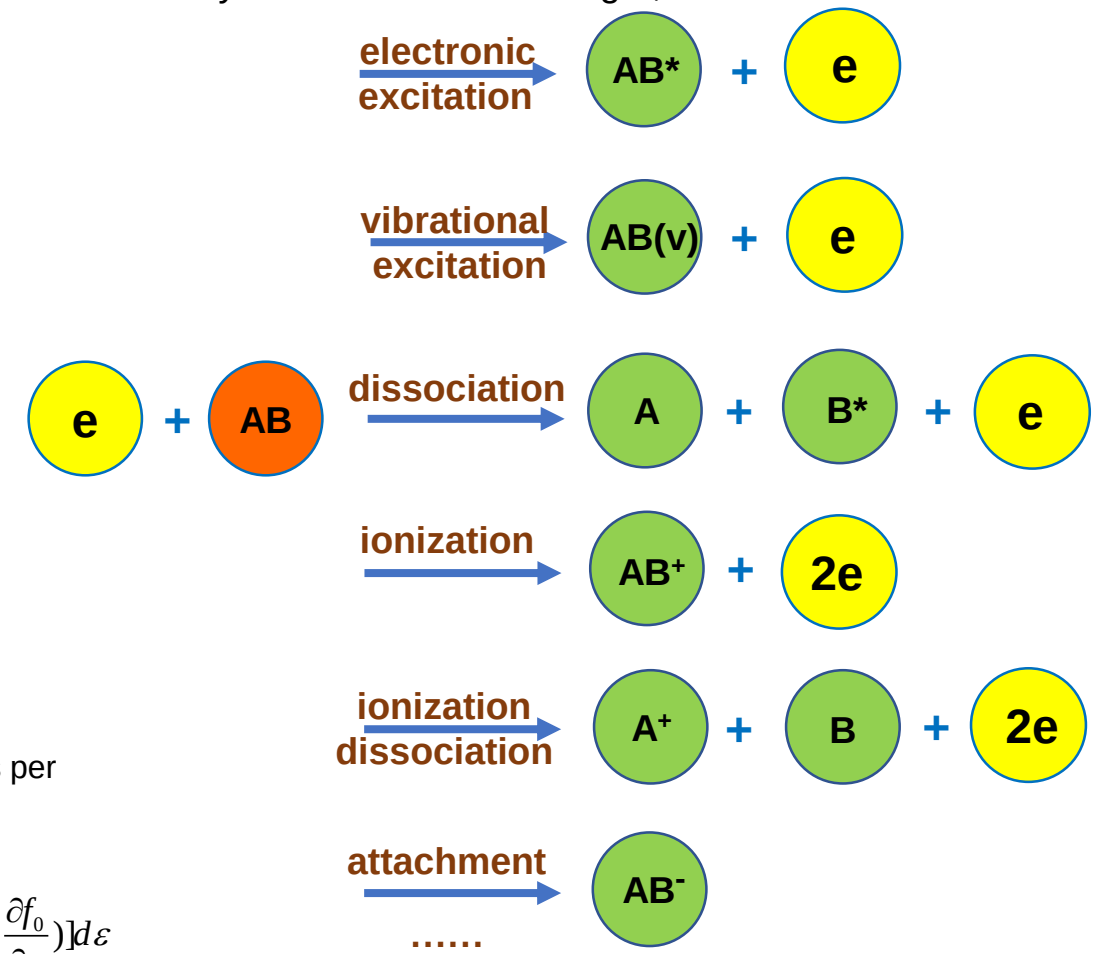


$M_k$: particle mass of target particles of collision process k.
$U_k$: threshold energy of inelastic collision process k.

# Cross-sections database available for electron-molecule collisions

Table 1. Cross-sections database for electron-molecules collisions.

| Atmospheric | Saturated | Unsaturated | Oxygenated | Isomers |
|---|---|---|---|---|
| N2 | CH4 | C2H2 | CO | iso-butane |
| O2 | C2H6 | C2H4 | CH3OH | iso-propane |
| CO2 | C3H8 | C3H6 | C2H5OH | neo-pentane |
| H2O | C4H10 | | CH3OCH3 (DME) | |
| O3 | C5H12 | | | |
| Ar | H2 | | | |
| N2O | | | | |

Andrey Starikovskiy and Nikolay Aleksandrov, AIAA paper-2017-1977

# Electron impact electronic excitation reactions

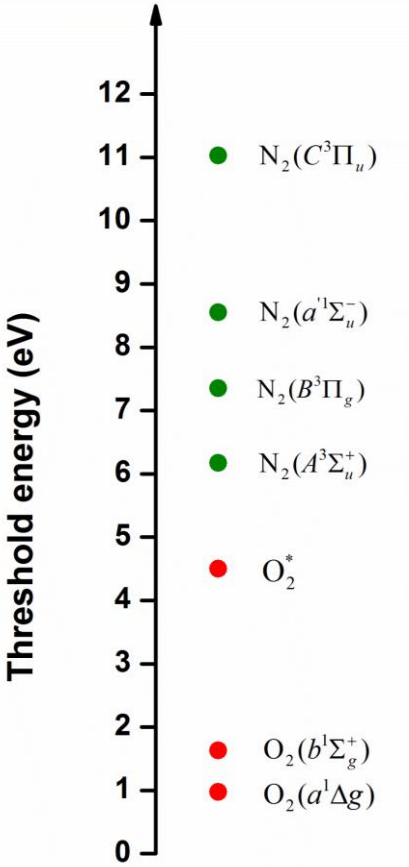


**Threshold energy diagram**

$e + N_2 \rightarrow e + N_2(A, B, a', C)$

$e + O_2 \rightarrow e + O_2(a^1\Delta_g), O_2(b^1\Sigma_g^+), O_2^*$

**Reaction rate coefficients** for each individual collision process k ($m^3/s$)

$$k_k = \gamma \int_0^\infty \varepsilon \sigma_k f_0 d\varepsilon$$

$\varepsilon$: electron energy.

$f_0$: isotropic part of electron distribution function, corresponding to zeroth-order term of spherical harmonics expansion in velocity space.

$\sigma_k$: cross section areas of electron-neutral collision process k.

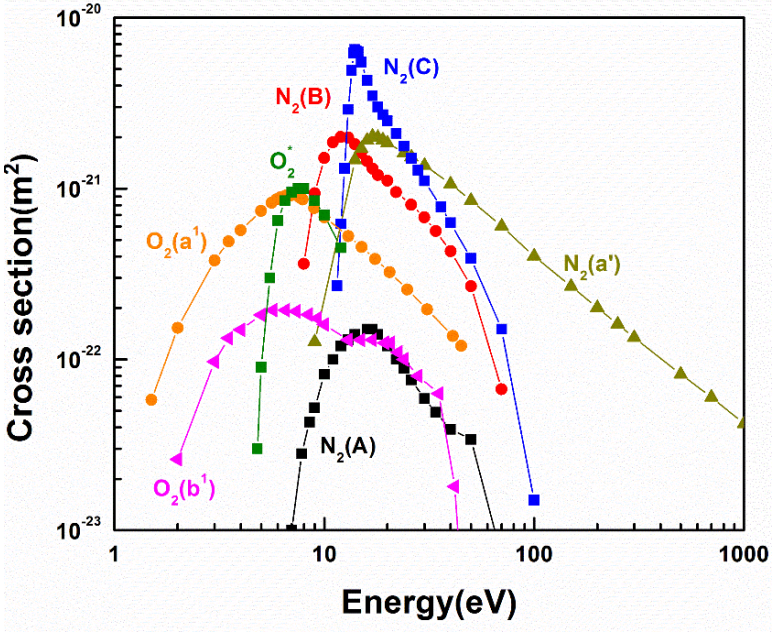


**Impact on combustion**

$N_2(A,B,a',C) + O_2 \rightarrow N_2 + 2O$

$H + O_2(a^1\Delta_g) \rightarrow OH + O$

$H + O_2 = OH + O$

- Cross section area data comes from Lxcat database. (www.lxcat.net)

# Electron impact dissociation reactions

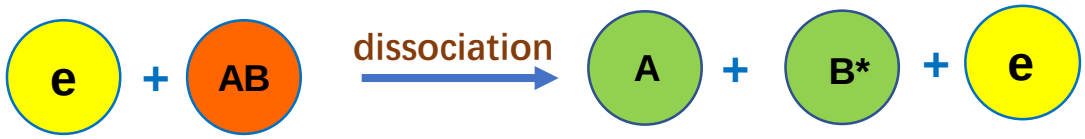


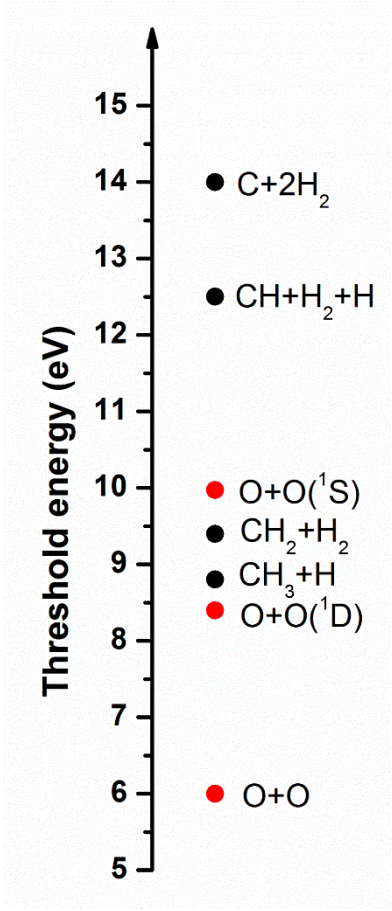


Threshold energy diagram

$e + O_2 \rightarrow e + O + O$

$e + O + O(^1D)$

$e + O + O(^1S)$

$e + CH_4 \rightarrow e + CH_3 + H$

$e + CH_2 + H_2$

$e + CH + H_2 + H$

$e + C + 2H_2$

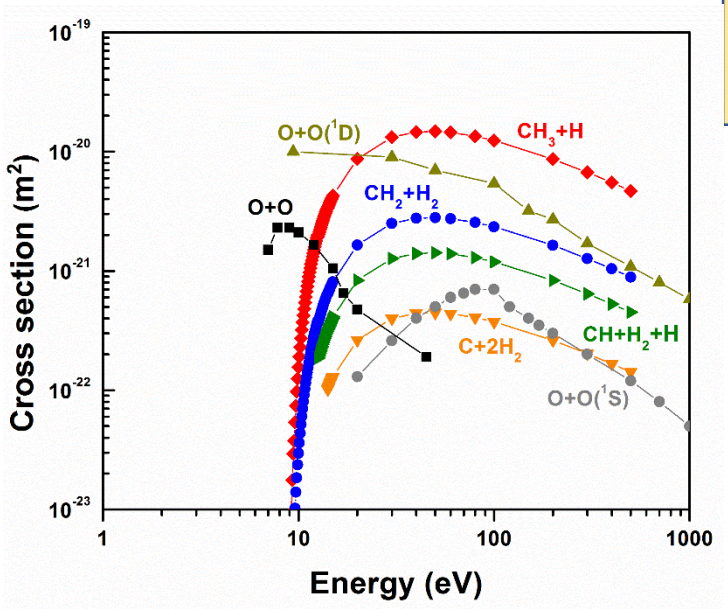


## Impact on combustion

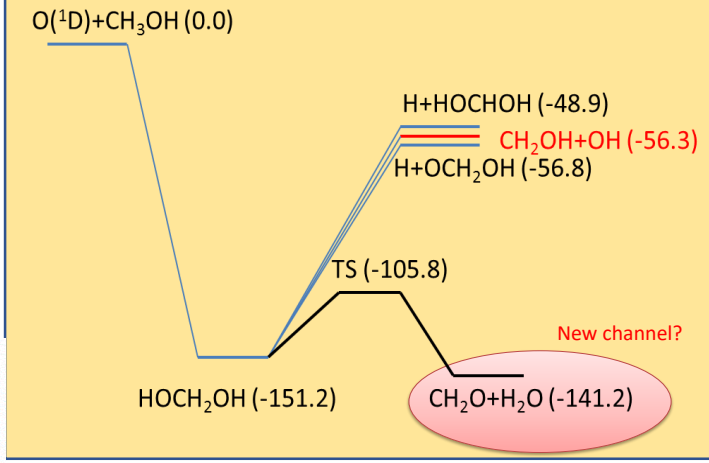

# Electron impact ionization reactions

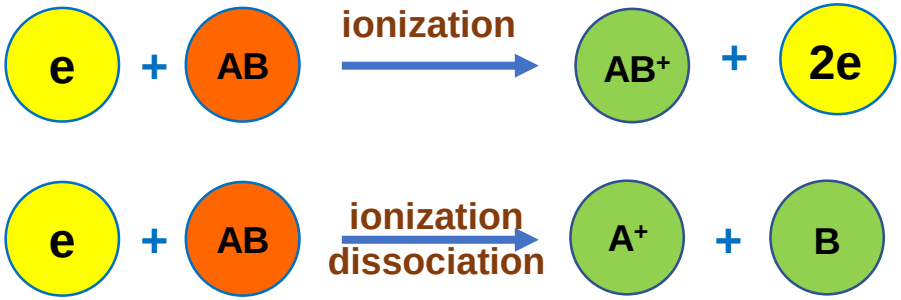


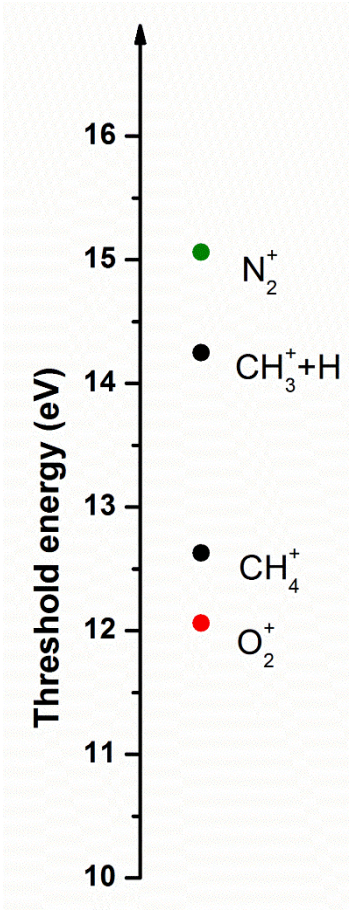


Threshold energy diagram

$e + O_2 \rightarrow 2e + O_2^+$

$e + N_2 \rightarrow 2e + N_2^+$

$e + CH_4 \rightarrow 2e + CH_4^+$

$2e + CH_3^+ + H$

**Electron and ion production**

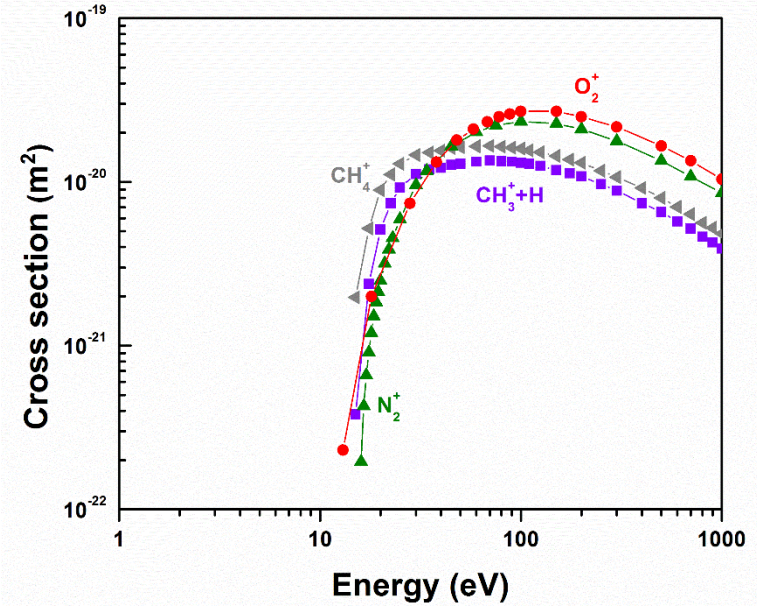


## Impact on combustion: radical production and gas heating

dissociation

$N_2^+ + CH_4 \rightarrow N_2 + H + CH_3^+$

recombination

$e + O_2^+ \rightarrow O + O$

# Electron attachment reactions

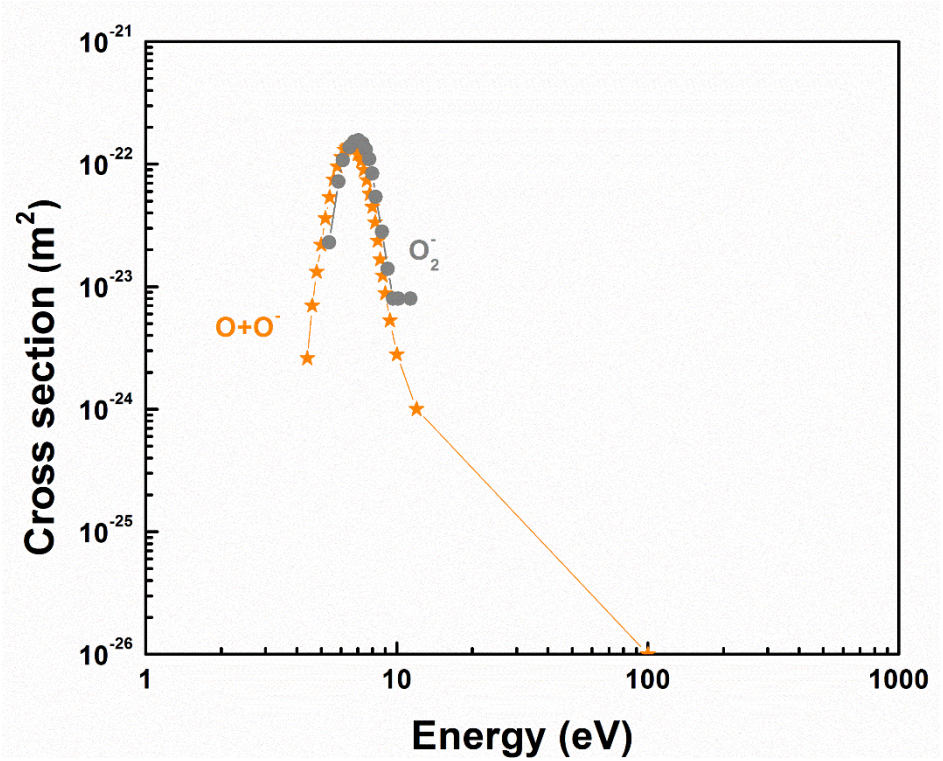


$e + O_2 \rightarrow O_2^-$

$e + O_2 \rightarrow O + O^-$

**Impact on combustion**

$O_2^- + H \rightarrow OH^- + O$

$O_2 + H = OH + O$

~5 orders of magnitude faster at 1000K

# Electron impact vibrational excitation reactions

$e + N_2 \rightarrow e + N_2(v)$ $\quad e + O_2 \rightarrow e + O_2(v)$

$e + CH_4 \rightarrow e + CH_4(v)$ $\quad e + CO_2 \rightarrow e + CO_2(v)$

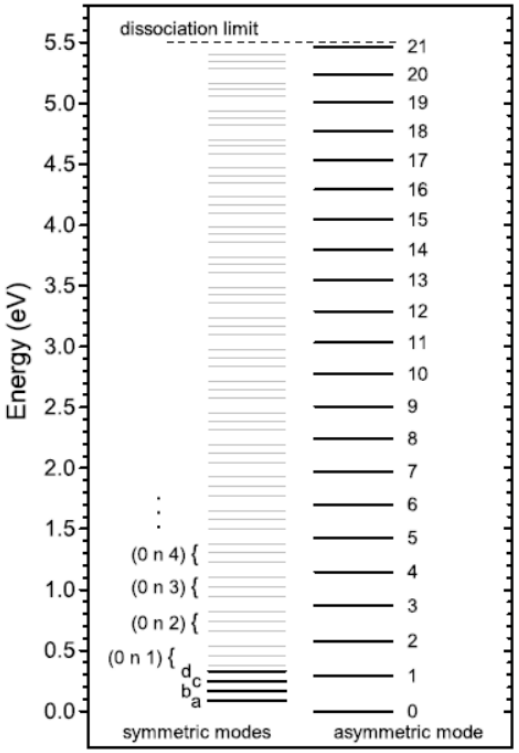


**Vibrational modes of $CH_4$**

| | Mode | Energy(eV) |
|---|---|---|
| v1 | Symmetric stretching | 0.362 |
| v2 | Twisting | 0.190 |
| v3 | Asymmetric stretching | 0.374 |
| v4 | Scissoring | 0.162 |

**Vibrational modes of $O_2$**

| | Energy(eV) |
|---|---|
| v1 | 0.19 |
| v2 | 0.38 |
| v3 | 0.57 |
| v4 | 0.75 |

**Vibrational modes of $N_2$**

| | Energy(eV) |
|---|---|
| v1 | 0.29 |
| v2 | 0.59 |
| … | … |
| v8 | 2.35 |

**Vibrational modes of $CO_2$**

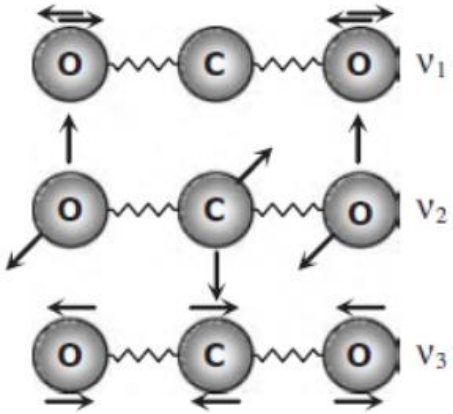


$\nu_1$:symmetric valence vibrations;
$\nu_2$: double degenerate symmetric deformation vibrations;
$\nu_3$:asymmetric valence vibrations.


1. Mi-Young Song, et al. J. Phys. Chem. Ref. Data, 44 (2015).
2. Tomas Kozak and Annemie Bogaerts. Plasma Sources Sci. Technol., 23 (2014).
3. Alexander Fridman. Plasma Chemistry, (2008).

# Reactions involving vibrationally excited species

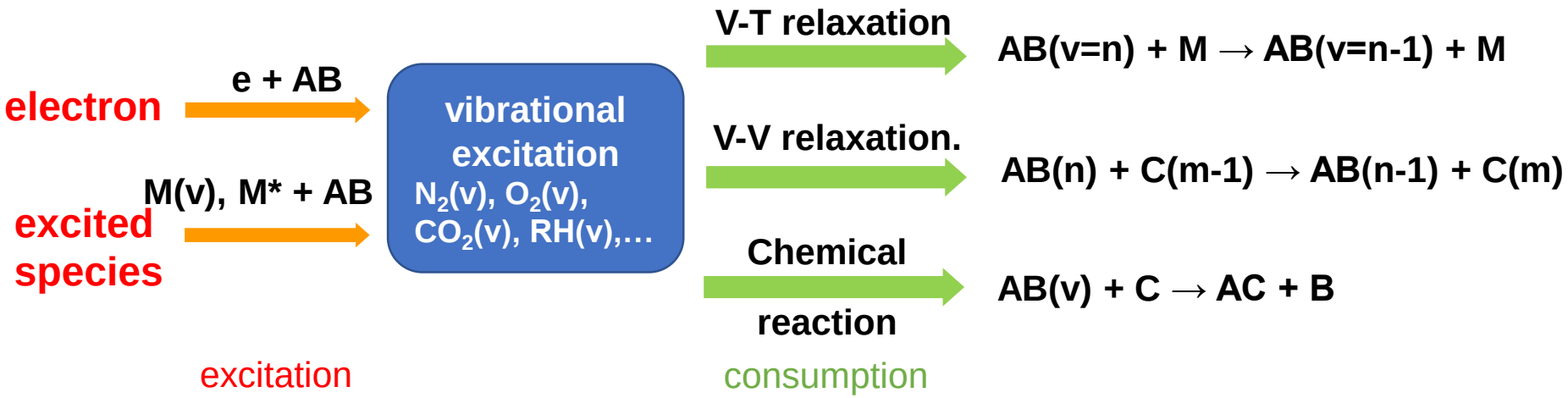


- VT relaxation: Energy transfer between vibrational and translational degrees of freedoms.
- VV relaxation: Energy transfer between vibrational states of different molecules.
- Vibrationally excited reaction: A reaction between a vibrational excited molecule with a neutral molecule. It will increase the reaction rate, add new reaction pathways, and modify heat release rate.

# Reaction rate of vibrationally excited molecules: Fridman-Macheret α-Model

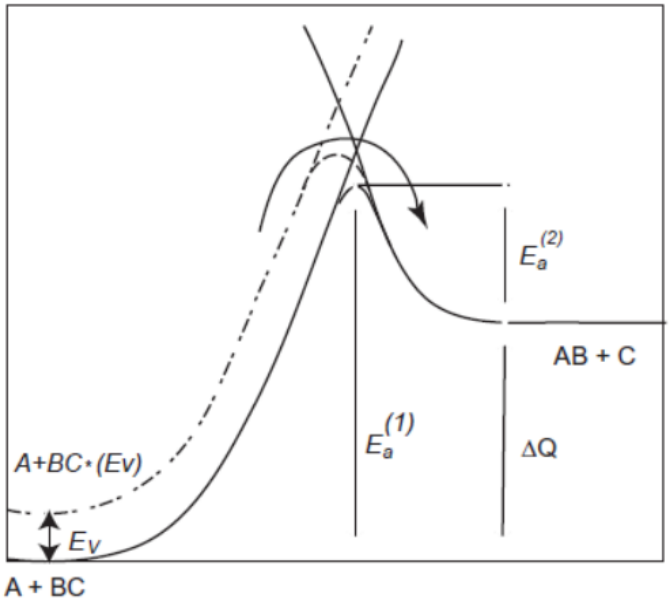


An effective decrease of activation energy

$$\Delta E_a = E_v \frac{F_{A+BC}}{F_{A+BC} + F_{AB+C}}$$

$$\frac{F_{A+BC}}{F_{AB+C}} = \frac{\gamma_1 E_a^{(1)}}{\gamma_2 E_a^{(2)}}$$

$$\alpha = \frac{\gamma_1 E_a^{(1)}}{\gamma_1 E_a^{(1)} + \gamma_2 E_a^{(2)}} = \frac{E_a^{(1)}}{E_a^{(1)} + (\gamma_1/\gamma_2) E_a^{(2)}} \qquad \gamma_1/\gamma_2 \approx 1$$

$$\alpha = \frac{E_a^{(1)}}{E_a^{(1)} + E_a^{(2)}}$$

$F_{A+BC}$ $F_{AB+C}$: are characteristic slopes of the terms A+BC and AB+C.
$\gamma$: reverse radii of corresponding exchange forces.
1: forward reaction direction.
2: reverse reaction direction.

A + BC → AB + C

A + BC*(Ev) → AB + C

$$k(E_v) = AT^n \exp(-\frac{E_a - \alpha E_v}{T})$$

If Ea>0, the overall activation energy decreases

- The efficiency α of vibrational energy is the highest for strongly endothermic reactions with activation energies closest to the reaction enthalpy (close to 100%).
- The efficiency of vibrational energy is the lowest for exothermic reactions without activation energies (close to 0).

Alexander Fridman. Plasma Chemistry, (2008).

# Vibrational-translational (V-T) relaxation for diatomic molecules

$AB(v=n) + M \rightarrow AB(v=n-1) + M$

$AB(v=1) + M \rightarrow AB + M$

- V-T relaxation rate constants of diatomic molecules

$$k_{10}(cm^3/s) = AT^n \exp\left(-\frac{B}{T^{1/3}} + \frac{C}{T^m}\right) \times \left[1 - D \times \exp\left(-\frac{E_{10}}{T}\right)\right]^{-1}$$

The probability of the vibrational transition n in one collision

$$P_{nm} = P_{mn} \exp\left(-\frac{E_m - E_n}{k_B T}\right)$$

$$k_{nm} = k_{mn} \exp\left(-\frac{E_m - E_n}{k_B T}\right)$$

Single-quantum transitions with probabilities

$$P_{n+1,n} = (n+1)P_{10}$$

$$k_{n+1,n} = (n+1)k_{10}$$

Values of parameters for rate coefficients of the processes of $N_2(v1) + M \rightarrow N_2 + M$

| M | n | m | A | B | C | D |
|---|---|---|---|---|---|---|
| $N_2$ | 1 | 1 | $7.8\times10^{-12}$ | 218 | 690 | 1 |
| $H_2$ | 1 | 2/3 | $4.9\times10^{-12}$ | 167.1 | 394 | 1 |
| $H_2O$ | 1 | 0 | $2.5\times10^{-15}$ | 21.18 | 0 | 0 |
| $CO_2$ | 1 | 1 | $1.1\times10^{-12}$ | 218 | 690 | 1 |

Values of parameters for rate coefficients of the processes of $O_2(v1) + M \rightarrow O_2 + M$

| M | n | m | A | B | C | D |
|---|---|---|---|---|---|---|
| $O_2$ | 1 | 0 | $1.35\times10^{-12}$ | 137.9 | 0 | 1 |
| $H_2$ | 1 | 0 | $2.69\times10^{-12}$ | 91.5 | 0 | 1 |
| He | 1 | 0 | $4.54\times10^{-15}$ | 60.85 | 0 | 1 |
| Ar | 1 | 2 | $3.14\times10^{-12}$ | 173.1 | $6.2\times10^{5}$ | 1 |

M. Capitelli, et al. Plasms Kinetics in Atmospheric Gases, (2000).

# V-T relaxation and V-V relaxation for non-diatomic molecules

- V-T relaxation rate constants calculation by Schwartz, Slawsky, and Herzfeld (SSH theory)

$$k_{n,n-1} = k_{1,0} Z_n \frac{F(\gamma_n)}{F(\gamma_1)}$$

$$Z_n = n\frac{1-x_e}{1-nx_e}$$

$$F(\gamma) = \frac{1}{2}\left[3-\exp(-\frac{2}{3}\gamma)\right]\exp(-\frac{2}{3}\gamma)$$

$$\gamma_n = \frac{0.32\Delta E}{\alpha}(\frac{\mu}{T_g})^{1/2}$$

$$\Delta E = E_n - E_{n-1}$$

$$\alpha = 17.5 / r_0$$

$Z_n$: scaling factor.
$x_e$ : the anharmonicity of the energy levels.
$\gamma_n$ : a parameter which is a measure of adiabaticity of the reaction.
$\alpha$ : a parameter of the exponential repulsive potential between the colliding species.
$\mu$ : reduced mass of the collision species.
$r_0$ : the radius parameter of the Lennard-Jones Potential. 3.94 Å for $CO_2$.

- V-V exchange rate constants

AB(n) + CD(m-1) → AB(n-1) + CD(m)

$$k_{n,n-1}^{m-1,m} = k_{1,0}^{0,1} Z_n Z_m \frac{F(\gamma_{nm})}{F(\gamma_{11})}$$

Vibrational energy transfer reactions of $CO_2$

| Reaction | $x_e(10^{-3})$ | |
|---|---|---|
| $CO_2(v_a) + M \rightarrow CO_2 + M$ | 0.0 | a |
| $CO_2(v_1) + M \rightarrow CO_2(v_a) + M$ | 3.7 | b |
| $CO_2(v_1) + M \rightarrow CO_2(v_b) + M$ | 1.0 | b |
| $CO_2(v_1) + M \rightarrow CO_2(v_c) + M$ | -15.6 | b |
| $CO_2(v_1) + CO_2 \rightarrow CO_2(v_b) + CO_2(v_a)$ | 2.8 | |
| $CO_2(v_1) + CO_2 \rightarrow CO_2(v_a) + CO_2(v_b)$ | 17.6 | |
| $CO_2(v_1) + CO \rightarrow CO_2 + CO(v_1)$ | 5.25;6.13 | |

a. Multiply by 1.0, 0.7 and 0.7 for M=$CO_2$, CO and O2
b. Multiply by 1.0, 0.3 and 0.4 for M=$CO_2$, CO and O2


1. M. Capitelli, et al. Plasms Kinetics in Atmospheric Gases, (2000).
2. Tomas Kozak and Annemie Bogaerts. Plasma Sources Sci. Technol., 23 (2014).
3. Alexander Fridman. Plasma Chemistry, (2008).
4. M. Capitelli. Nonequilibrium Vibrational Kinetics,(1986).

# 6.2 Simulation of plasma assisted combustion

## Challenges:

- Multi-physics problems: photons, electrons, electronic and vibrational excitations
- Electromagnetic field, acoustic waves, shockwaves, ignition and combustion waves
- Multi-length scale: Sheath (Debye length), diffusion & reaction zones, mixing layer, far field effects
- Multi-timescale: from plasma, reactive flow, to combustion (ps-ms)
- Multi-species and stiffness of reactions
- Multi-dimension and far non-equilibrium (not Maxwellian distribution)
- ...

## Kinetic description of plasma

– distribution function
– kinetic equation
– collisional energy transfer

## Multi-fluid description of plasma

– Fluid conservation equations
– Input of transport coefficients and rate coefficients, e.g. fitted as functions of E/N
– Different energy modes (electrons, vibration, neutral temperature)
– Coupling between neutral and charged particles

# Plasma Modeling: A Hybrid ZDPlasKin-CHEMKIN Model (0D)

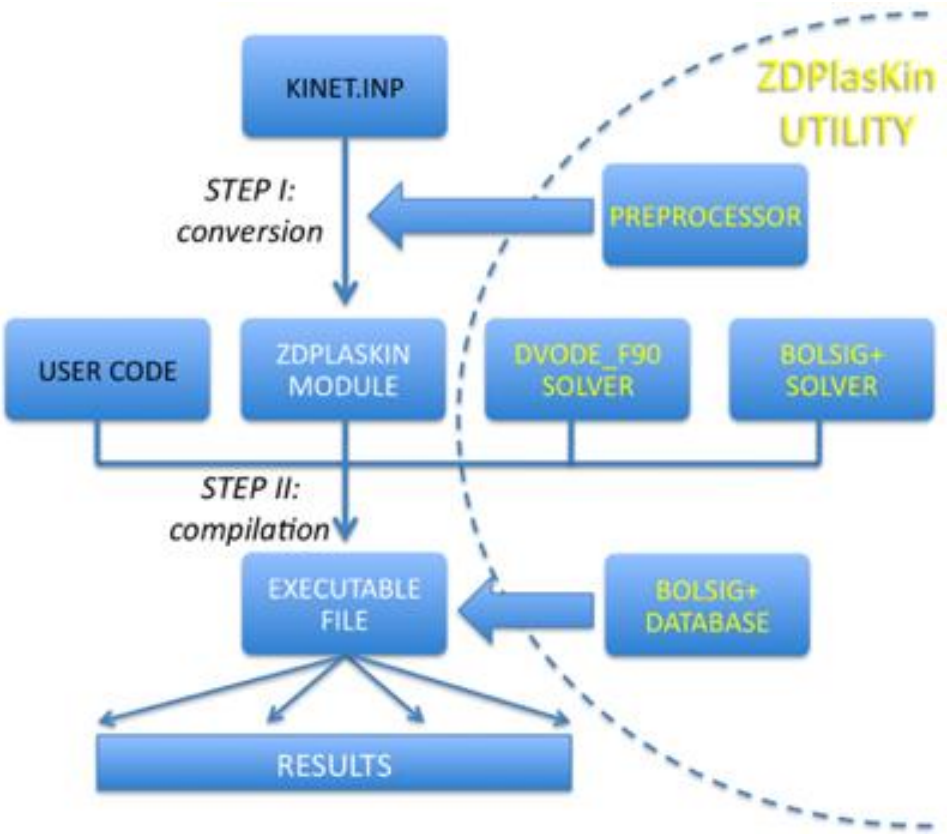


- **ZDPlasKin[1]**: A zero-dimensional Plasma Kinetics solver which is a Fortran 90 module designed to follow the time evolution of the species densities and gas temperature in a non-thermal plasma with an arbitrarily complex chemistry.


[1].S. Pancheshnyi, B. Eismann, G.J.M. Hagelaar, L.C. Pitchford, Computer code ZDPlasKin, http://www.zdplaskin.laplace.univ-tlse.fr (University of Toulouse, LAPLACE, CNRS-UPS-INP, Toulouse, France, 2008).
[2]. G.J.M. Hagelaar, et al. Plasma Sources Sci. Technol., 14 (2005).


- **BOLSIG+**: incorporated in ZDPlasKin[1], a computer program for the numerical solution of the Boltzmann equation for electrons in weakly ionized gases in uniform electric field.

Boltzmann equation for electron energy distribution function (EEDF) in a plasma is:

$$\frac{\partial f}{\partial t} + \upsilon \cdot \nabla f - \frac{e}{m} E \cdot \nabla_{\upsilon} f = C[f]$$

$f$ : electron distribution in six-dimensional phase space.
$\upsilon$ : velocity coordinates.
$\nabla_V$: the velocity-gradient operator.
$C$ : the rate of change in $f$ due to collisons.

Assume: a steady state problem and the electric field and the collision probabilities are spatially uniform, on the scale of the collisional mean free path (elastic collision), using the two-term approximation expansion in spherical coordinates

$$f(v, \cos\theta, z, t) = f_0(v, z, t) + f_1(v, z, t)\cos\theta$$

isotropic part (temporal dependence)

anisotropic part (spatial dependence)

$v$ : the magnitude of the velocity.
$\theta$ : the angle between the velocity and the field direction.
$z$ : the position along this direction.

**BOLSIG+** solver: https://www.bolsig.laplace.univ-tlse.fr

# Plasma Modeling: A Hybrid ZDPlasKin-CHEMKIN Model

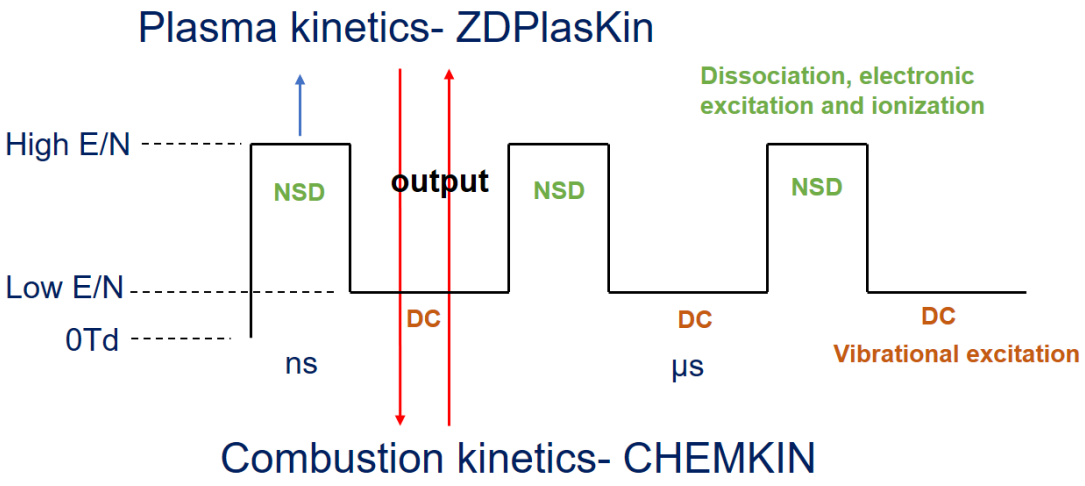


- A combined ns-plasma and DC discharge to control electronic and vibrational excitation and selective reactivity in plasma.

➢ Time evolutions of the species and temperature of plasma reactions using ZDPlasKin

$$\frac{\mathrm{d}N_i}{\mathrm{d}t} = \sum_{j=1}^{j_{\max}} Q_{ij}(t)$$

Deposited energy: $P_{\mathrm{ext}} = P_{\mathrm{gas}} + P_{\mathrm{elec}} + P_{\mathrm{chem}}$

Translational degree of freedom of electrons: $P_{\mathrm{elec}} = \frac{3}{2}\mathrm{k_B}\frac{\mathrm{d}(N_{\mathrm{e}}T_{\mathrm{e}})}{\mathrm{d}t}$

Translational degree of freedom of the gas: $P_{\mathrm{gas}} = \frac{1}{\gamma - 1}\mathrm{k_B}\frac{d(NT)}{dt}$

Internal degree of freedom of the gas: $P_{\mathrm{chem}} = \sum_i \varepsilon_i \frac{\mathrm{d}N_i}{\mathrm{d}t}$

➢ Time evolutions of the species and temperature in combustion using CHEMKIN

$$\rho\frac{\mathrm{d}Y_i}{\mathrm{d}t} = \omega_i W_i$$

$$\rho C_p \frac{\mathrm{d}T}{\mathrm{d}t} = -\sum_{i=1}^{i\max} e_i \omega_i W_i$$

➢ Coupling of ZDPlasKin and CHEMKIN

$$\frac{\rho_i^{n+1} - \rho_i^n}{\Delta t} = \omega_i^{\mathrm{combustion}} + \omega_i^{\mathrm{plasma}} \qquad \frac{T_{n+1} - T_n}{\Delta t} = \Delta T_{\mathrm{combustion}} + \Delta T_{\mathrm{plasma}}$$

$$\frac{\rho_i^{*} - \rho_i^n}{\Delta t} = \omega_i^{\mathrm{combustion}} \qquad \frac{T^{*} - T_n}{\Delta t} = \Delta T_{\mathrm{combustion}}$$

$$\frac{\rho_i^{n+1} - \rho_i^{*}}{\Delta t} = \omega_i^{\mathrm{plasma}} \qquad \frac{T_{n+1} - T^{*}}{\Delta t} = \Delta T_{\mathrm{plasma}}$$

$\rho_i^*$ and $T^*$ are the intermediated density and temperature between the calculation of CHEMKIN and ZDPlasKin.


1. A.E. Lutz, et al. SEKIN, (1998).
2. P.N. Brown, et al. J Sci. Stat. Comput., 10 (1989).
3. J.K. Lefkowitz, Y. Ju, et al. Phil. Trans. Soc. A, (2015).

# 0-Dimensional model approximation

- Plane to plane
- Homogenous
- Square wave of the E/N

## Kinetics model

- Species 100

- Reactions
  Plasma kinetics: 541(ZDPlasKin)
  HP-mech: 595 (C1-C2) (CHEMKIN)

## Modelling conditions

- Pressure 60torr
- Temperature 373K
- Frequency 30kHz
- Pulse number 300
- NSD 180Td
- DC 1Td, 5Td, 10Td, 20Td
- Mixture 8.333% CH4, 16.667% O2, 75% He

http://engine.princeton.edu/mechanism/HP-Mech.html

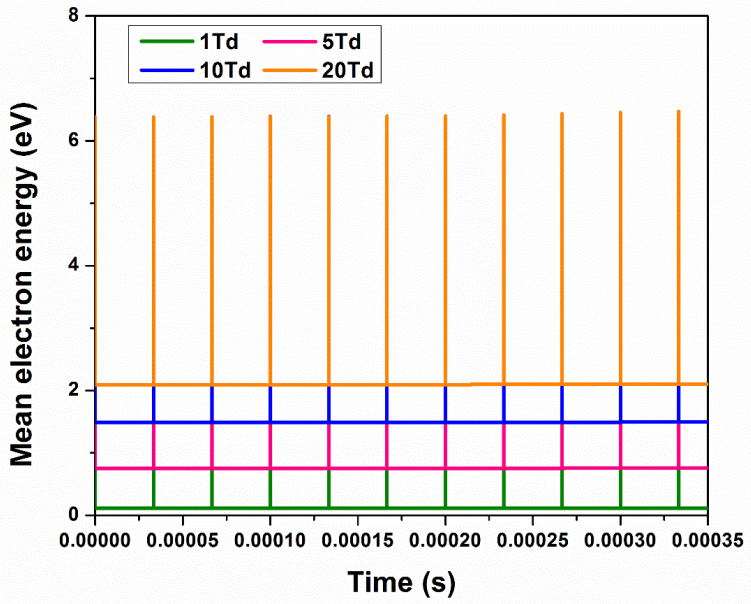


Mean electron energy

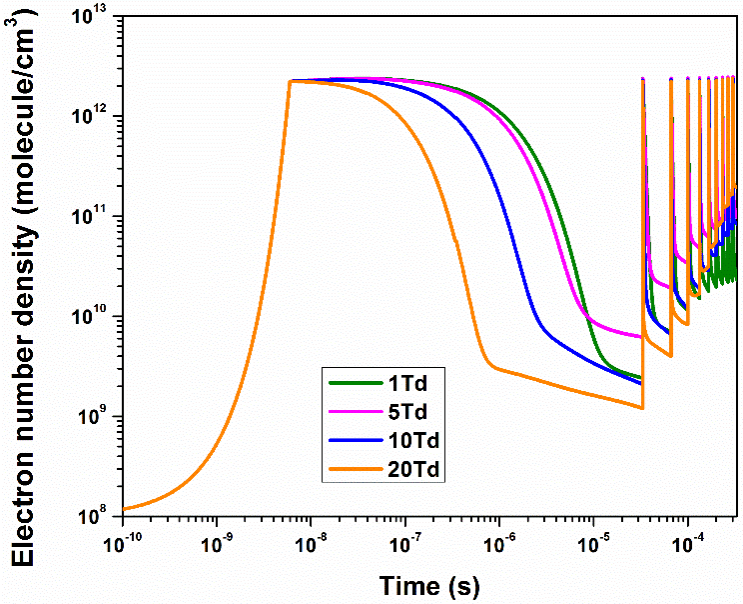


Electron number density

# Time evolution of the vibrationally excited species

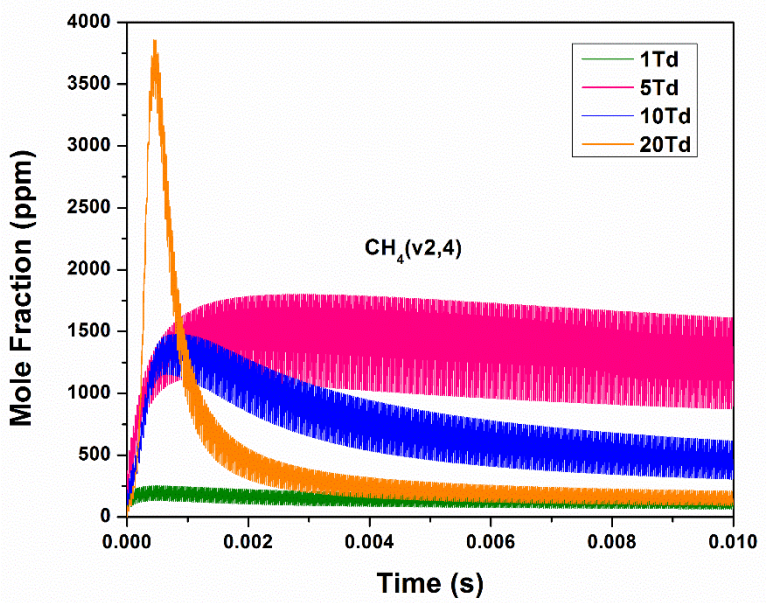


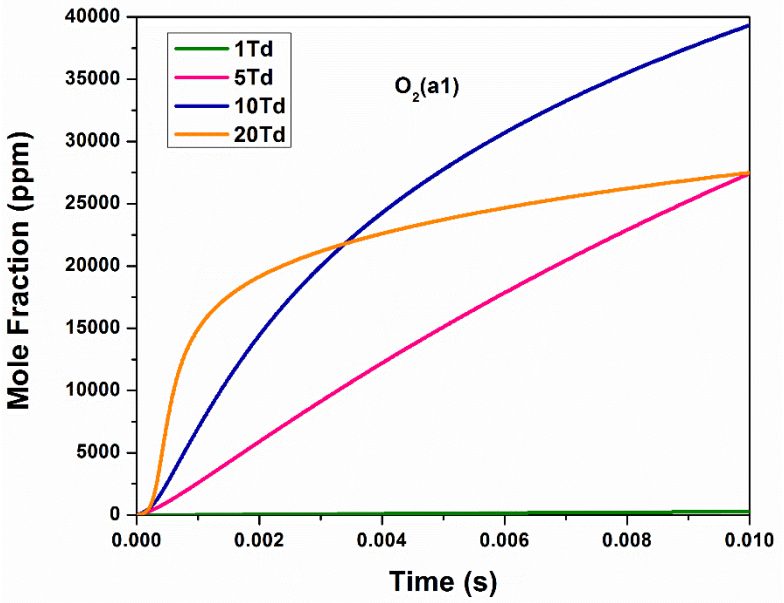


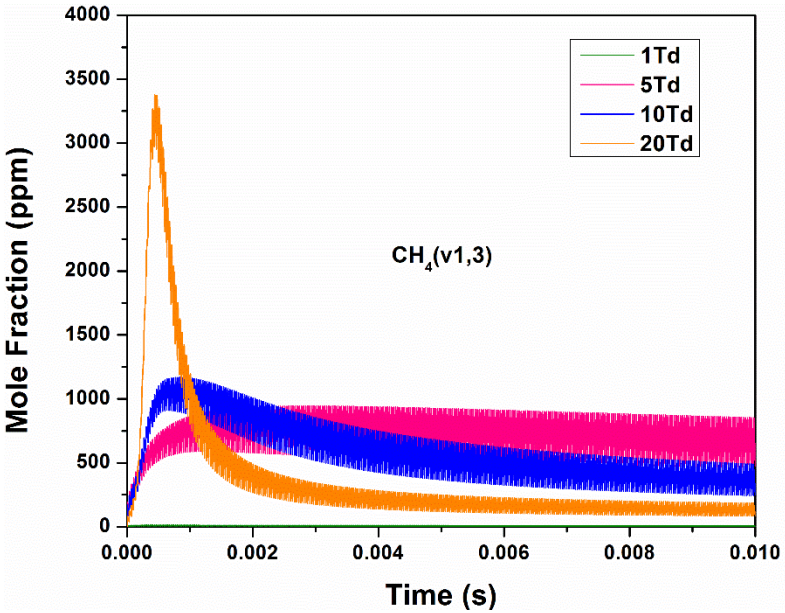


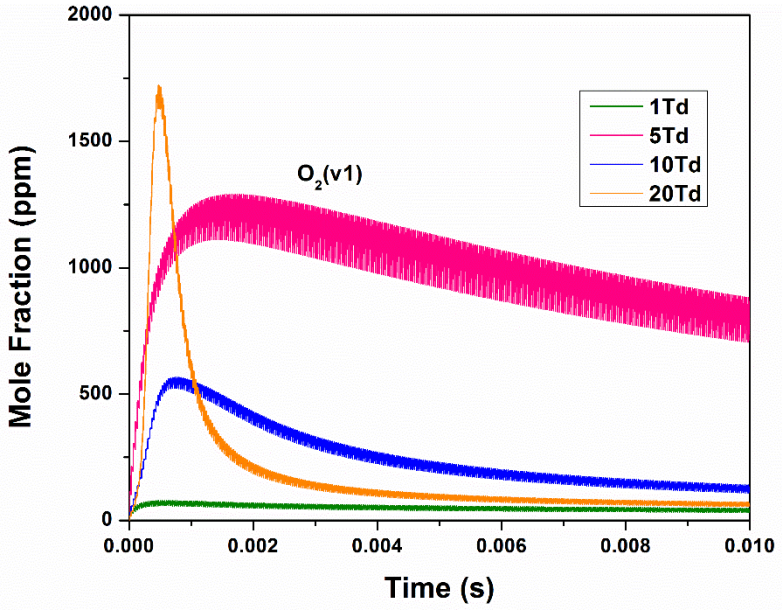

# Reaction rates in the first 20 pulses at 20Td

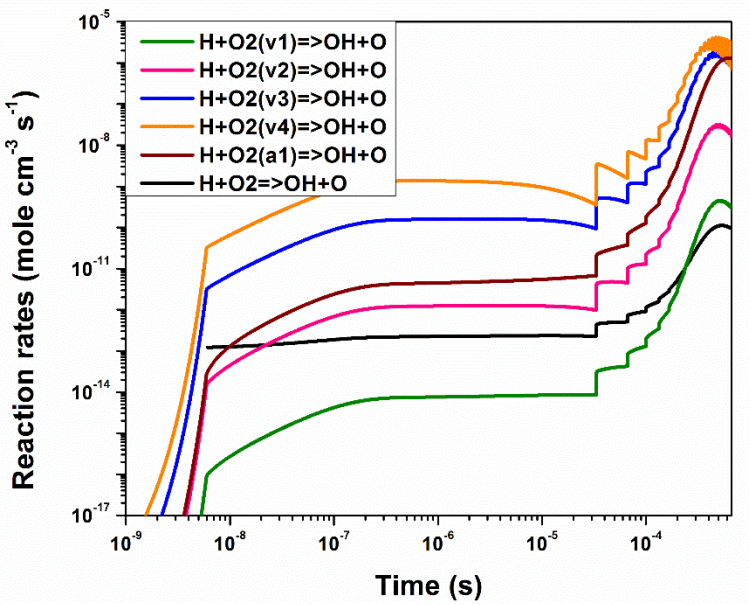


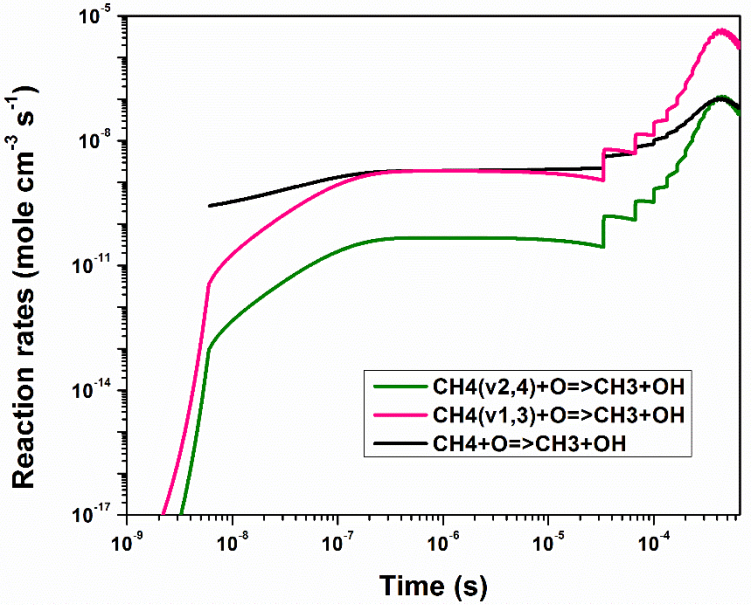


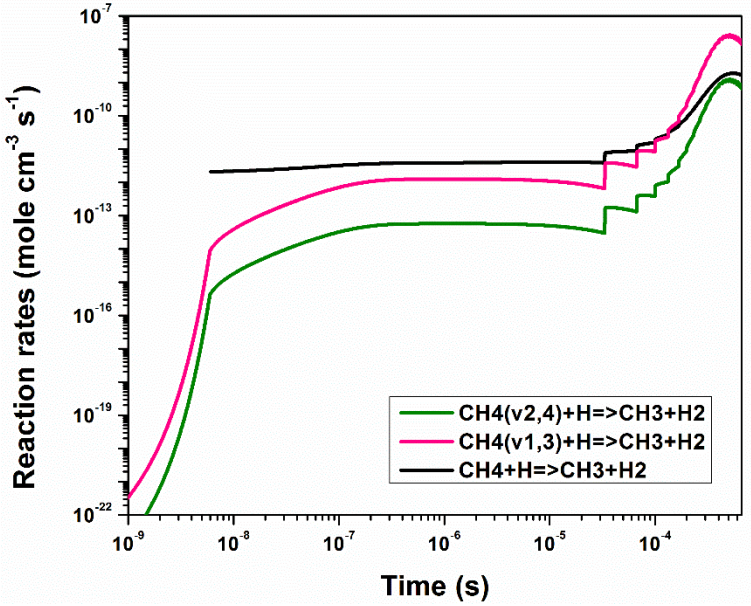


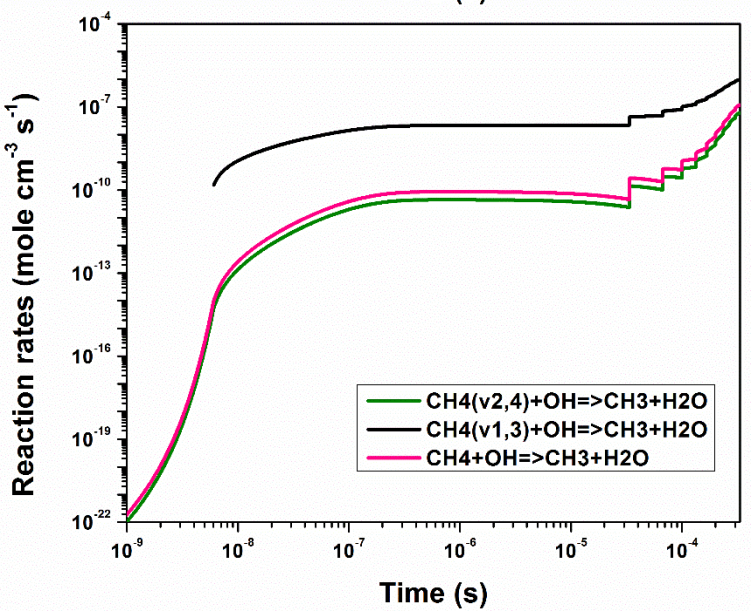

# 1D Plasma Modeling

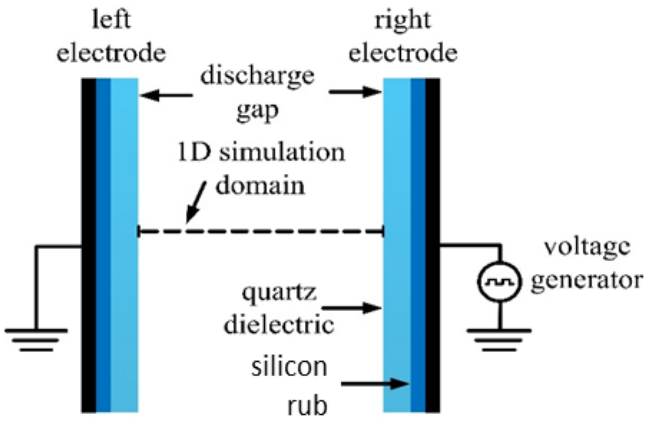


- Kinetic model of Nagaraja *et al. (2015)*
  - $\nabla \cdot (\epsilon \nabla \phi) = -e(n_+ - n_- - n_e)$
  - $\frac{\partial n_\epsilon}{\partial t} + \nabla \cdot \boldsymbol{J}_\epsilon = \dot{Q}_\epsilon$
  - $\frac{\partial n_k}{\partial t} + \nabla \cdot \boldsymbol{J}_k = \dot{\omega}_k$
  - $\frac{\partial \rho}{\partial t} + \frac{\partial \rho u_i}{\partial x_i} = 0$
  - $\frac{\partial \rho u_i}{\partial t} + \frac{\partial (\rho u_i u_j)}{\partial x_j} = -\frac{\partial p}{\partial x_i} + \frac{\partial \tau_{ij}}{\partial x_j} + F_i^{EHD}$
  - $\frac{\partial \rho E}{\partial t} + \frac{\partial [(\rho E + p) u_i]}{\partial x_i} = -\frac{\partial q_i}{\partial x_i} + \frac{\partial (u_i \tau_{ij})}{\partial x_j} + \dot{Q}^{JH}$
- Transport coefficients of electron and rate coefficients of electron impact reactions: BOLSIG

$\phi$: potential (voltage)

$u_i$: *Velocity*

$n_k$: *number density of kth species*

$E$: *Total energy*

$n_\epsilon$: electron energy density, $n_e$*$E_e$

## Multi-scale modeling

- Adaptive time-stepping: small ($10^{-13}$ - $10^{-12}$ s) during each discharge pulse; larger ($10^{-10}$ s) in the gap between 2 consecutive pulses.

Nagaraja, S., Yang, V. and Adamovich, I., 2013.. *Journal of Physics D: Applied Physics*, *46*(15), p.155205.

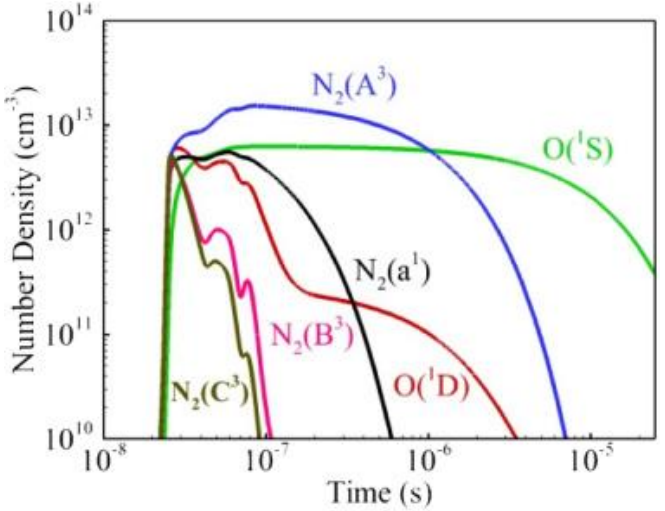


Fig. Time evolution of short lived electronically excited species after a single nanosecond pulse in air at 60 Torr and 300 K

# Multi-timescale modeling method

## Multi-timescale (MTS) Method

$$\tau_i = -\left[\frac{\partial}{\partial Y_i}\left(\frac{dY_i}{dt}\right)\right]^{-1} \qquad Y_k = K_k e^{-\frac{t}{\tau_k}}$$

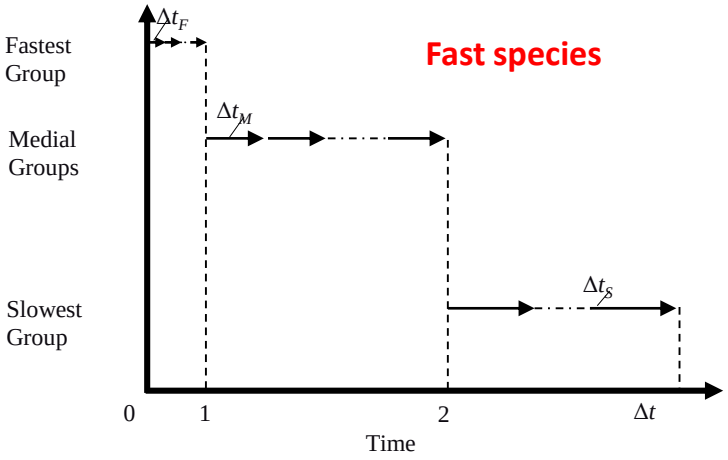


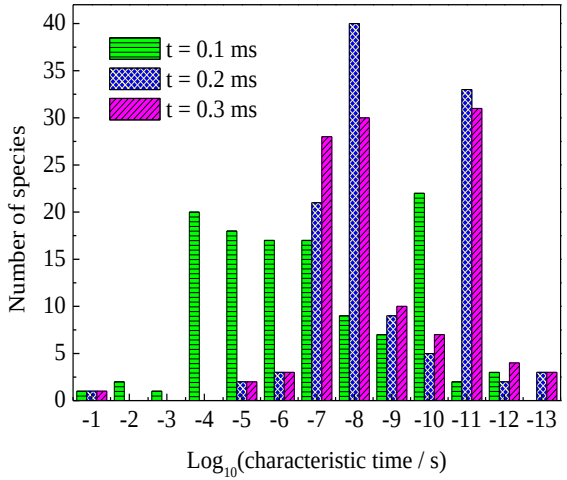


**Diagram of multi time scale scheme**

**$\Delta t_F$ is the time step of the fastest group, $\Delta t_M$ is the time step of the medial group, and $\Delta t_S$ is the time step of the slowest group**

Gou, Sun, Chen and Ju., Combust. Flame, 2010, 2013

# Hybrid Multi-Time Scale (HMTS) Method

- HMTS method:

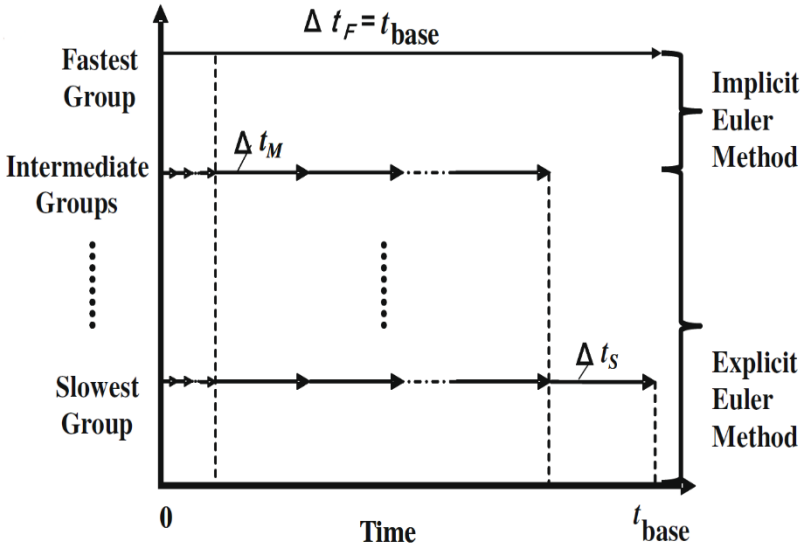


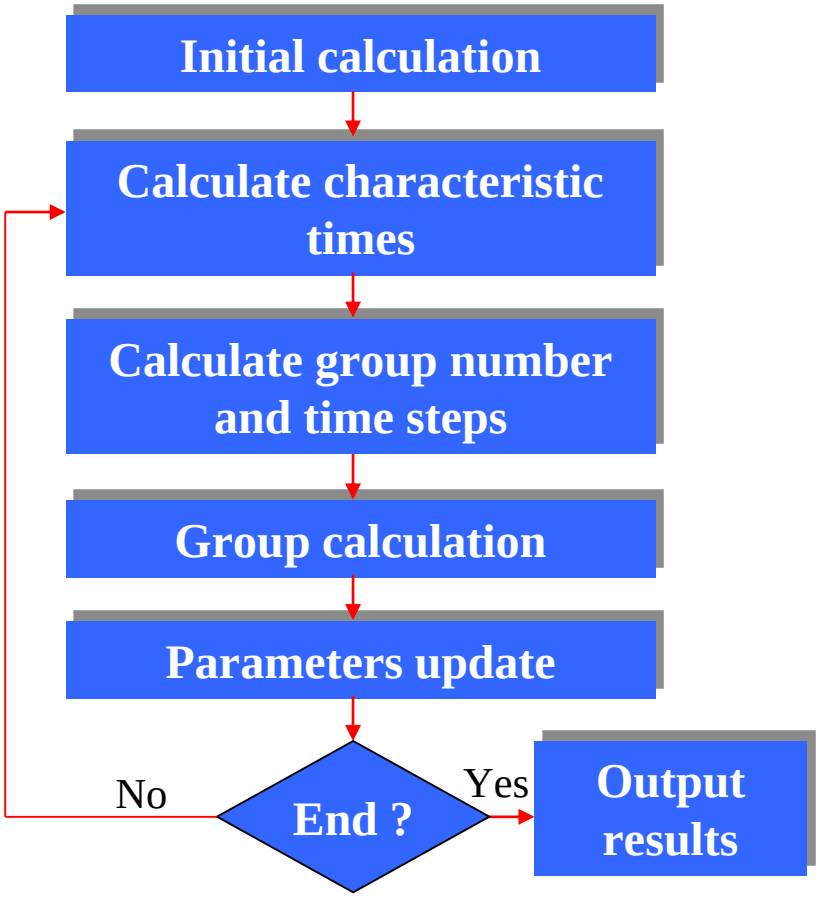


*X.L. Gou, W.T. Sun, Z. Chen, Y.G. Ju, Combust. Flame 157 (6) (2010) 1111–1121.*

# HTMS Validation: Homogeneous ignition

Ignition in homogeneous mixture

**n-decane/Air** **121 species (M. Chaos, IJCK,2007)**

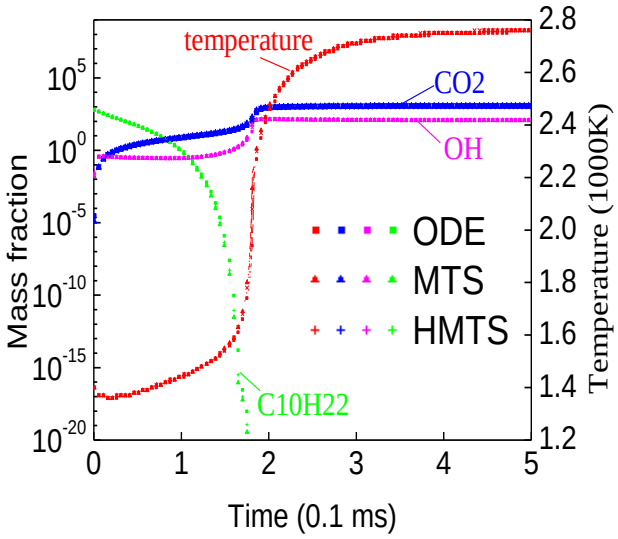


**Temperature and species profiles**

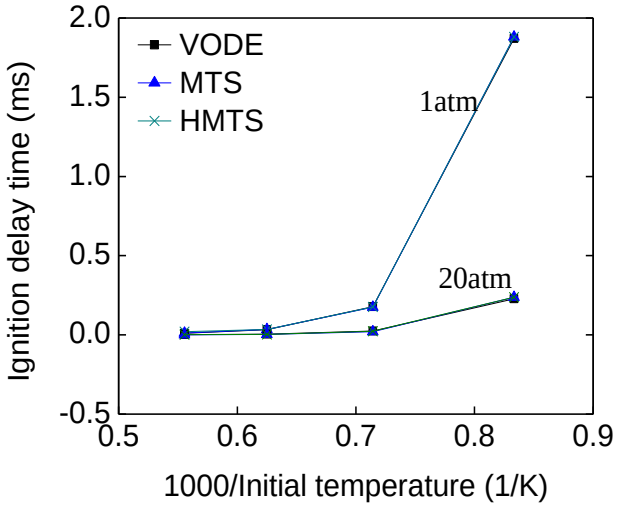


**Ignition delay time for n-decane-air**

# Comparison of computation efficiency: same mechanism with HMTS, HMTS/DAC vs. VODE, VODE/DAC

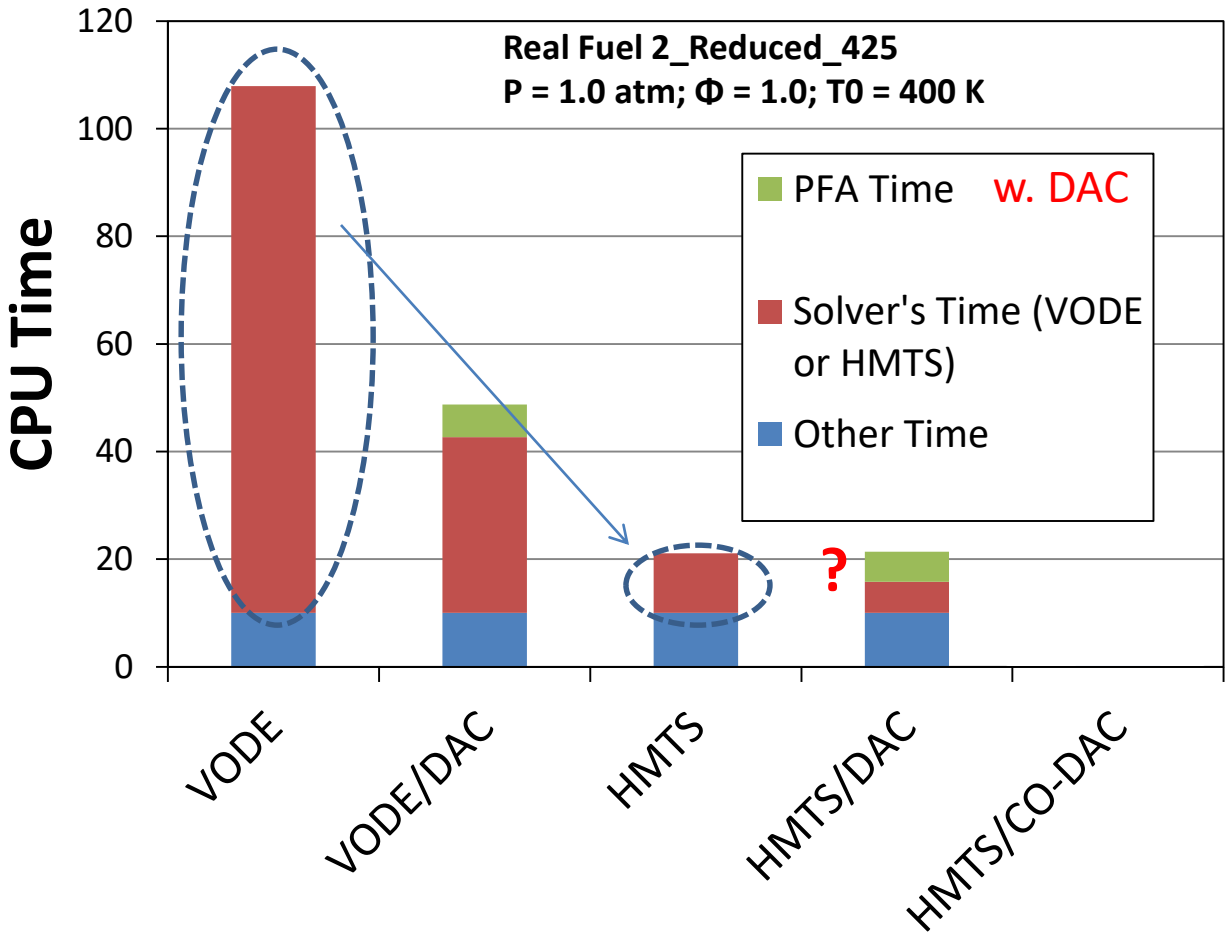


**1D unsteady Flame propagation**

# Methodology

## Correlated DAC (CO-DAC) method

- Correlated groups

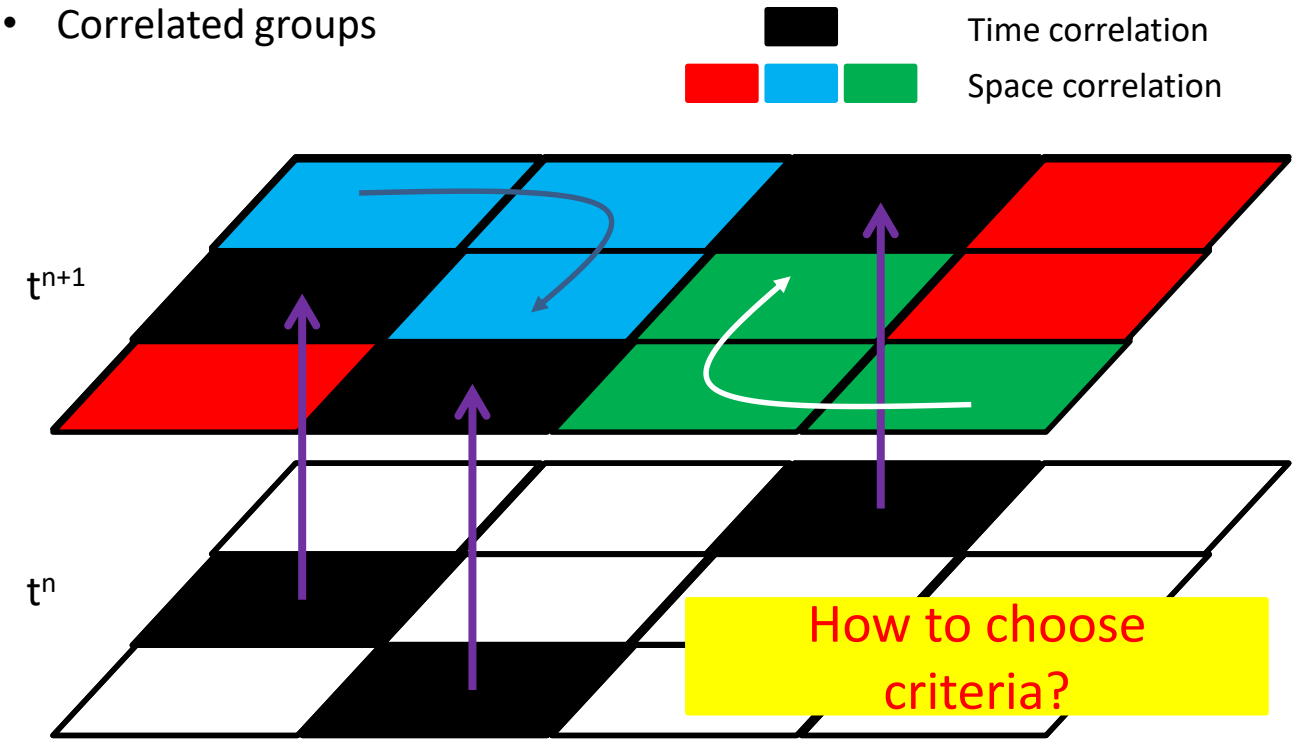


Sun, W., Gou, X., El-Asrag, H.A., Chen, Z. and Ju, Y., 2015. Multi-timescale and correlated dynamic adaptive chemistry modeling of ignition and flame propagation using a real jet fuel surrogate model. *Combustion and Flame*, *162*(4), pp.1530-1539.

# Spherically Propagating Flame

- Computation time

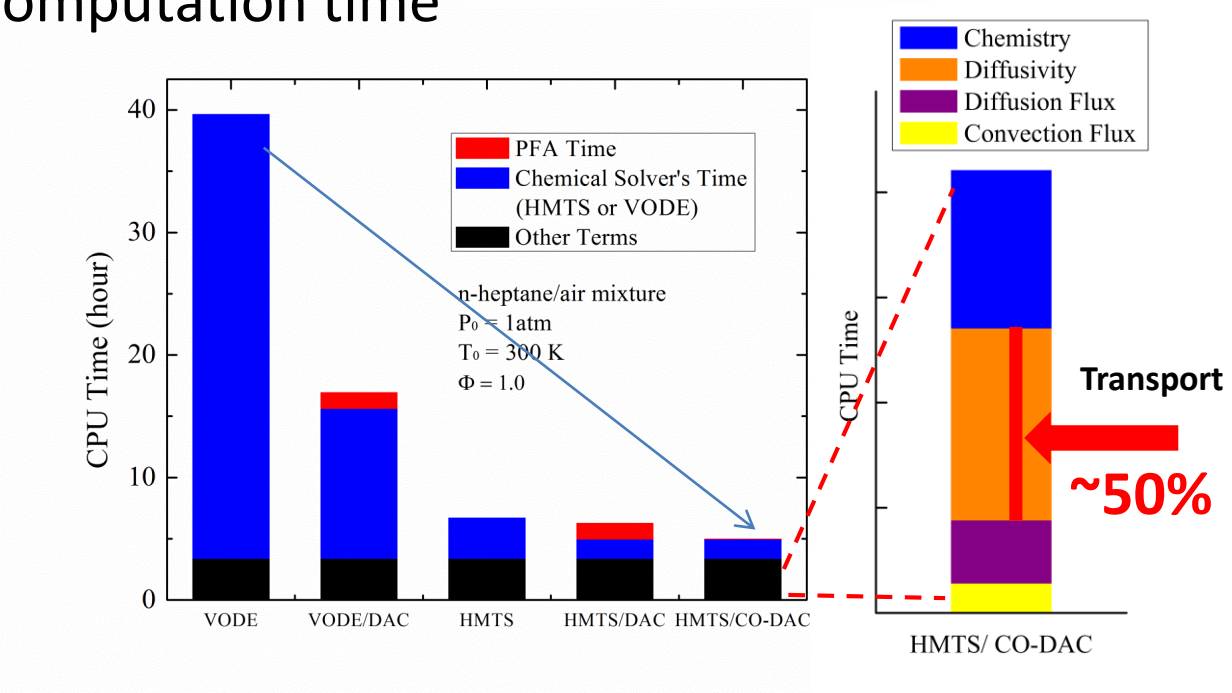


Sun, W., Gou, X., El-Asrag, H.A., Chen, Z. and Ju, Y., 2015. Multi-timescale and correlated dynamic adaptive chemistry modeling of ignition and flame propagation using a real jet fuel surrogate model. *Combustion and Flame*, *162*(4), pp.1530-1539.

# Spherically Propagating Flame

- Temperature and Radicals Profile

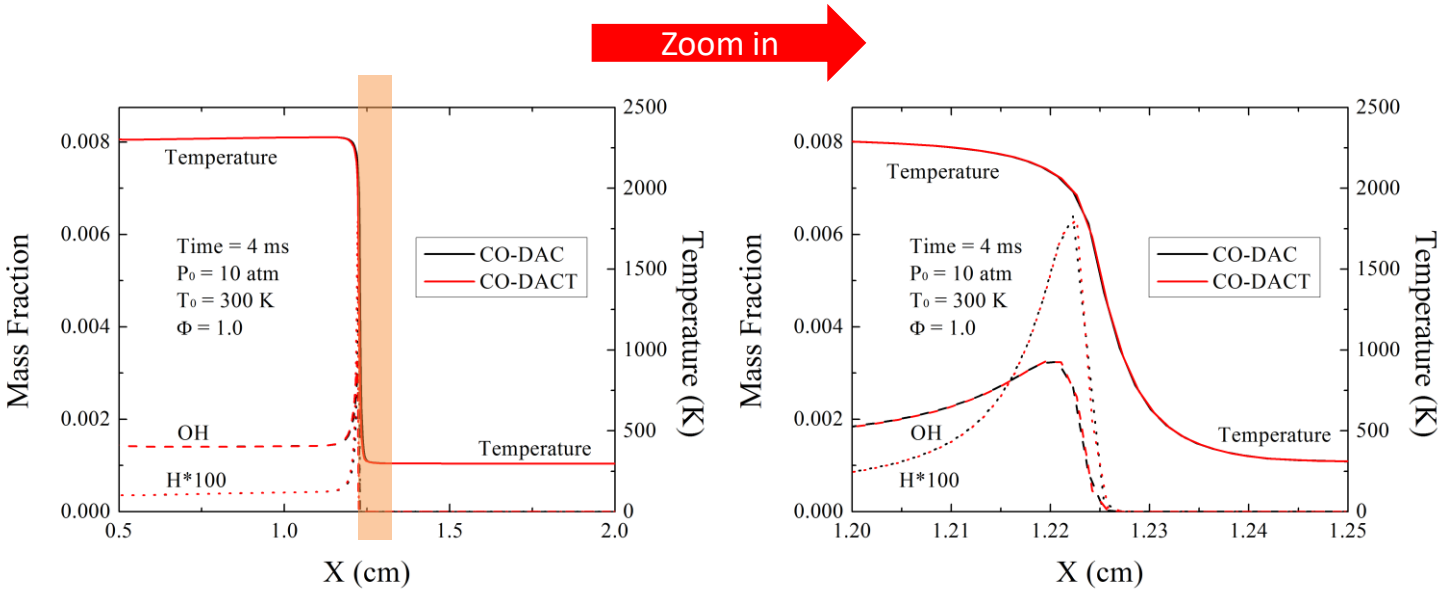


Shifted 0.3%

# Correlated Dynamic Adaptive Chemistry and Transport (CO-DACT) Method

- CO-DACT

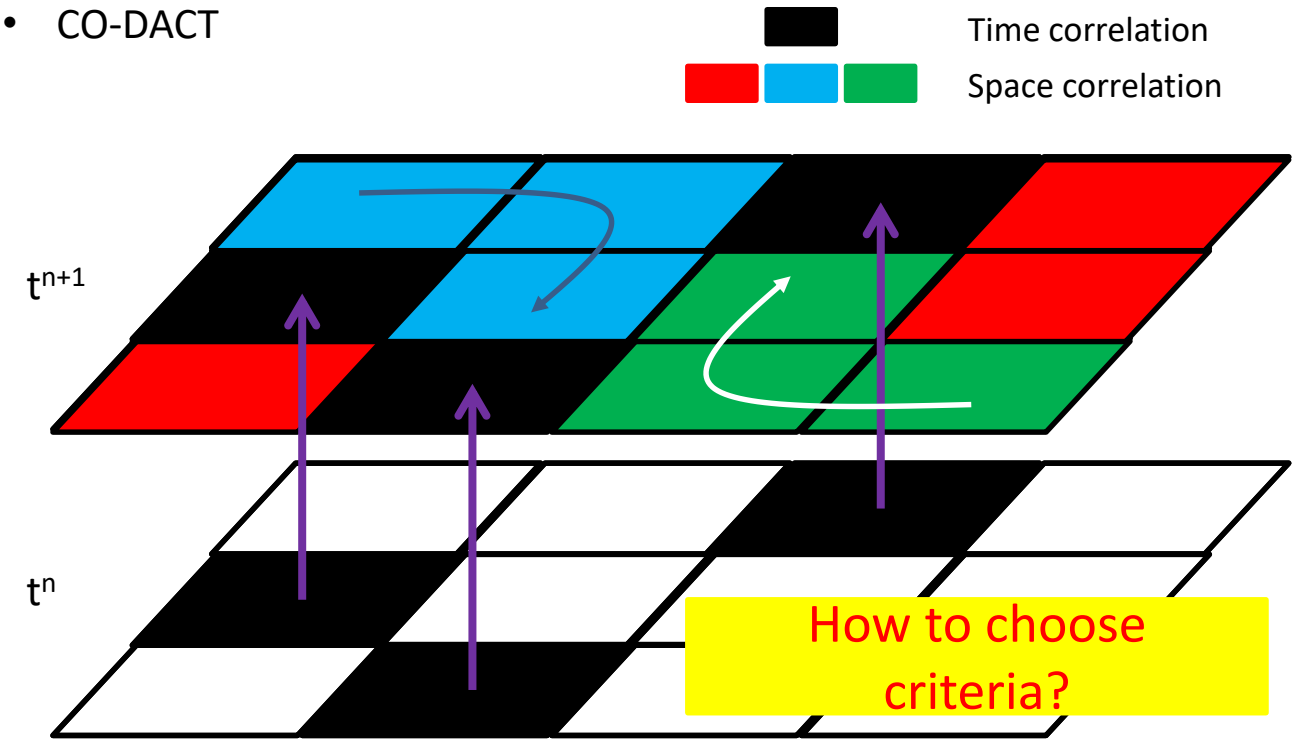


Sun, W., and Ju, Y., 2016. A Multi-timescale and Correlated Dynamic Adaptive Chemistry and Transport (CO-DACT) Method for Computationally Efficient Modeling of Jet Fuel Combustion with Detailed Chemistry and Transport. *Combustion and Flame*, *submitted.*

# Phase Parameters & Similarity Criteria

- How to choose criteria?
  - $\eta_k$, $\lambda_k$ and $D_{jk}$ ⇒ T
  - $\eta$, $\lambda$ and $D_{mk}$ ⇒ $X_i$

  ⇒ $(T, N_2, O_2, Fuel, H_2O, H_2, CO_2, CO, CH_2O)^T$
- Major species: of $N_2$, $O_2$, Fuel, $H_2O$, $H_2$, $CO_2$, CO, CH2O, C2H4
  - In most combustion systems, the summation of these major reactants and productions account for at least 95% of the molar fraction in total.
  - $CH_2O$ is dominating in low temperature region.
- Criteria:

$$d = \left\| \begin{matrix} \Delta T/T^0 \\ \Delta X_{N_2}/X^0_{N_2} \\ \Delta X_{O_2}/X^0_{O_2} \\ \Delta X_{Fuel}/X^0_{Fuel} \\ \Delta X_{H_2O}/X^0_{H_2O} \\ \Delta X_{H_2}/X^0_{H_2} \\ \Delta X_{CO_2}/X^0_{CO_2} \\ \Delta X_{CO}/X^0_{CO} \\ \Delta X_{CH_2O}/X^0_{CH_2O} \end{matrix} \right\|_\infty \le \varepsilon$$

Error in transport ~ $O(\varepsilon)$

If extrapolated, Error ~ $O(\varepsilon^2)$

$$\eta = \sum_{k=1}^{K} \frac{X_k \eta_k}{\sum_{j=1}^{K} X_j \Phi_{kj}}$$

$$\lambda = \frac{1}{2}\left( \sum_{k=1}^{K} X_k \lambda_k + \frac{1}{\sum_{k=1}^{K} X_k / \lambda_k} \right)$$

$$D_{km} = \frac{\sum_{j \neq k}^{K} X_j W_j}{\overline{W} \sum_{j \neq k}^{K} X_j / \mathcal{D}_{jk}}$$

# Spherically Propagating Flame

- Computation efficiency:

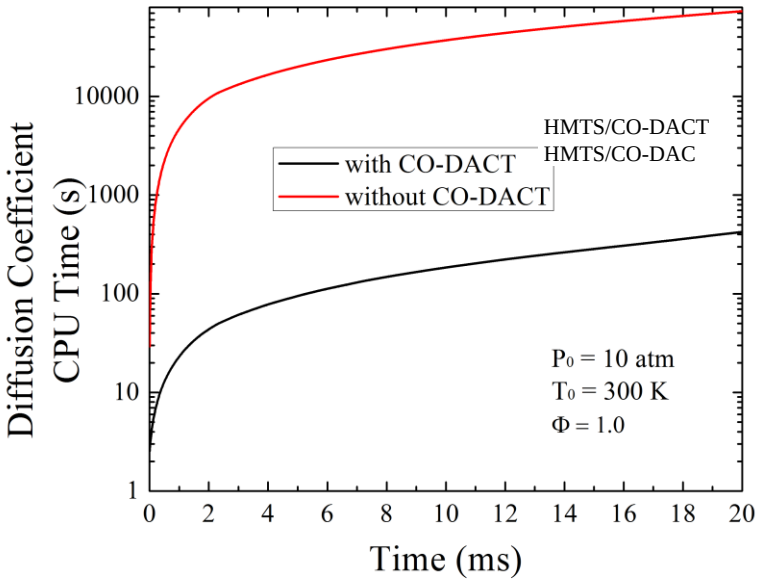


**More than 200 time faster**

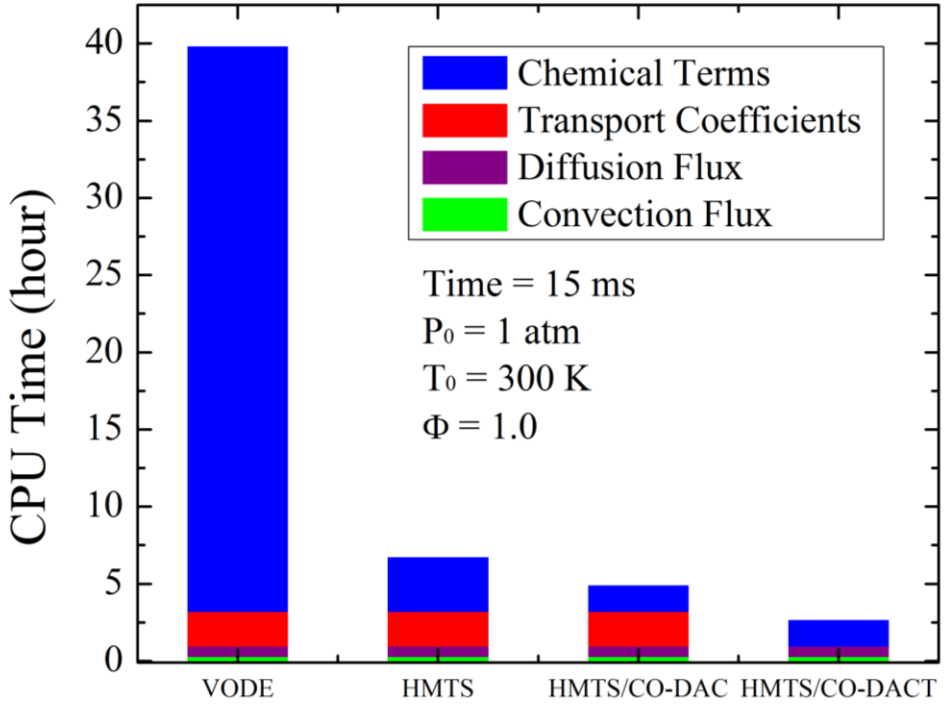


Sun, W., and Ju, Y., 2017. A Multi-timescale and Correlated Dynamic Adaptive Chemistry and Transport (CO-DACT) Method for Computationally Efficient Modeling of Jet Fuel Combustion with Detailed Chemistry and Transport. *Combustion and Flame, 2017.*

# Comparison: CPU Time Dependence on species number

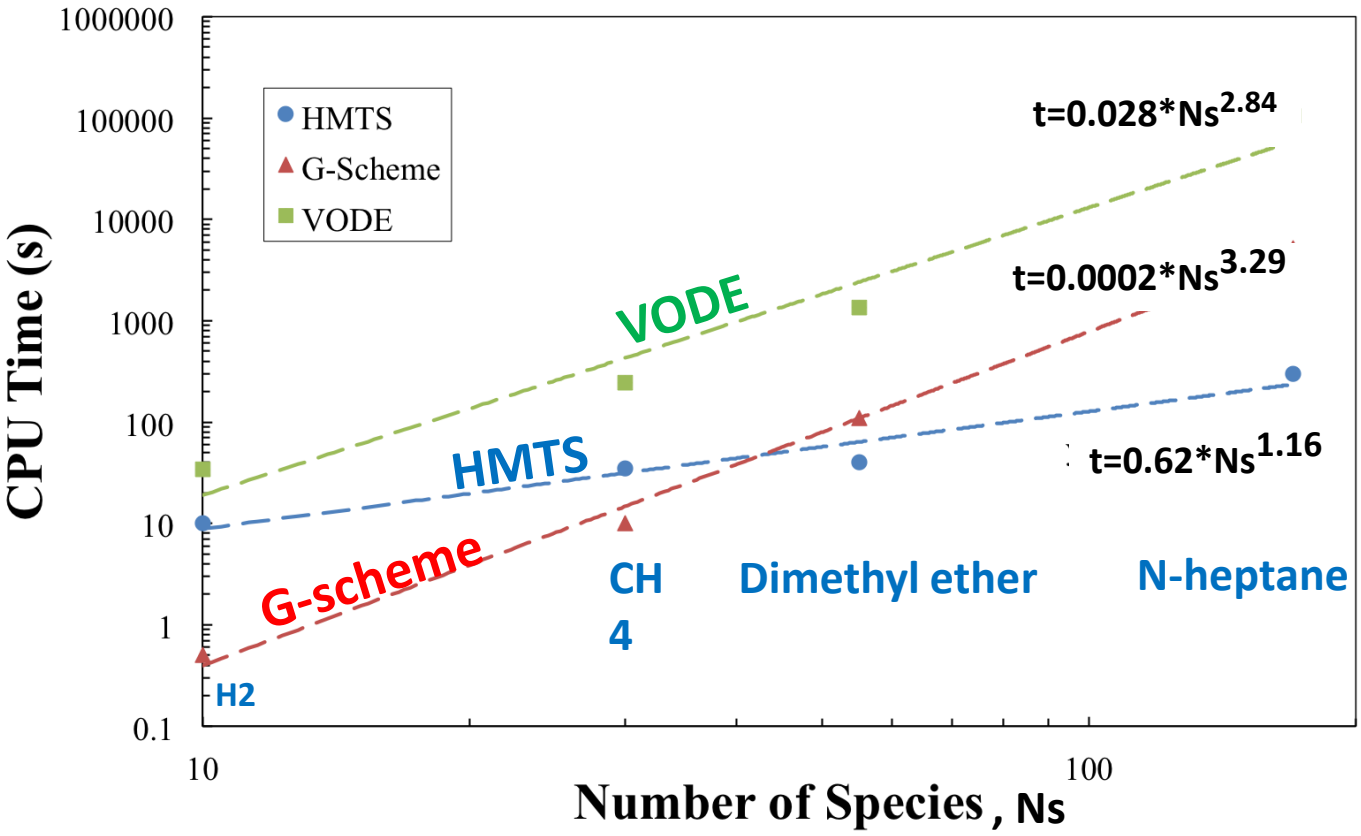


**Opportunity: adaptive HMTS/G-scheme**

# 2D fluid model for plasma assisted combustion

- Classical **2D fluid model** for a nanosecond discharge between two point electrodes separated by 2.5 mm.

Input of transport coefficients and rate coefficients, e.g. fitted as functions of E/N

$$\left.\begin{aligned} &\frac{\partial n_\alpha}{\partial t} + \boldsymbol{\nabla}\cdot\boldsymbol{\Gamma}_\alpha = R_\alpha, \\ &\boldsymbol{\Gamma}_\alpha = \frac{q_\alpha}{|q_\alpha|} n_\alpha \mu_\alpha \boldsymbol{E} - D_\alpha \nabla n_\alpha, \\ &\boldsymbol{\nabla}\cdot(\varepsilon_0 \nabla\varphi) = -\sum_\alpha q_\alpha n_\alpha, \\ &\boldsymbol{E} = -\boldsymbol{\nabla}\varphi, \end{aligned}\right\} \quad (1)$$

- Electron transport parameters and impact rate coefficients pre-calculated as a function of the reduced electric field for $H_2$/air mixtures at 1 atm with $\phi \in \{0, 0.3, 1.5\}$
- **Voltage pulse**: rise and decrease in 2ns; plateau at 5kV of 2.6 to 3.5ns

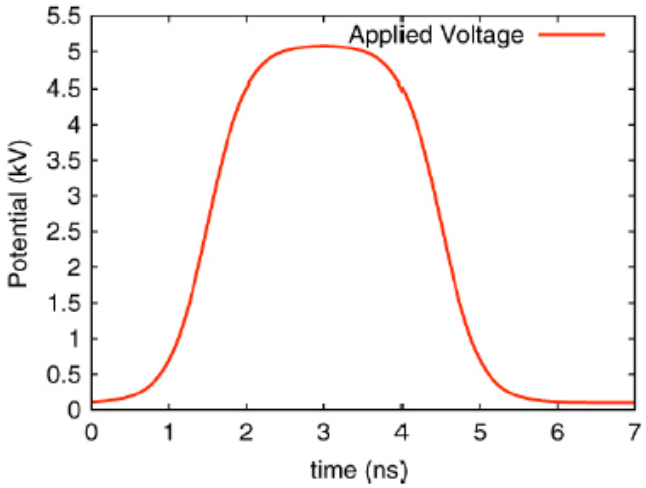


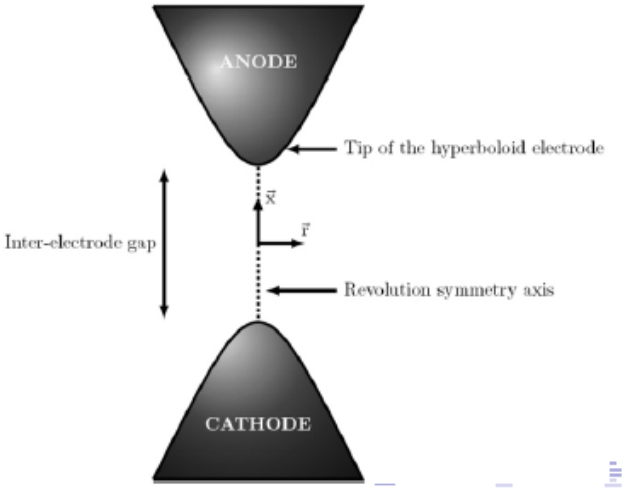

# Discharge dynamics and structure for various $\phi$

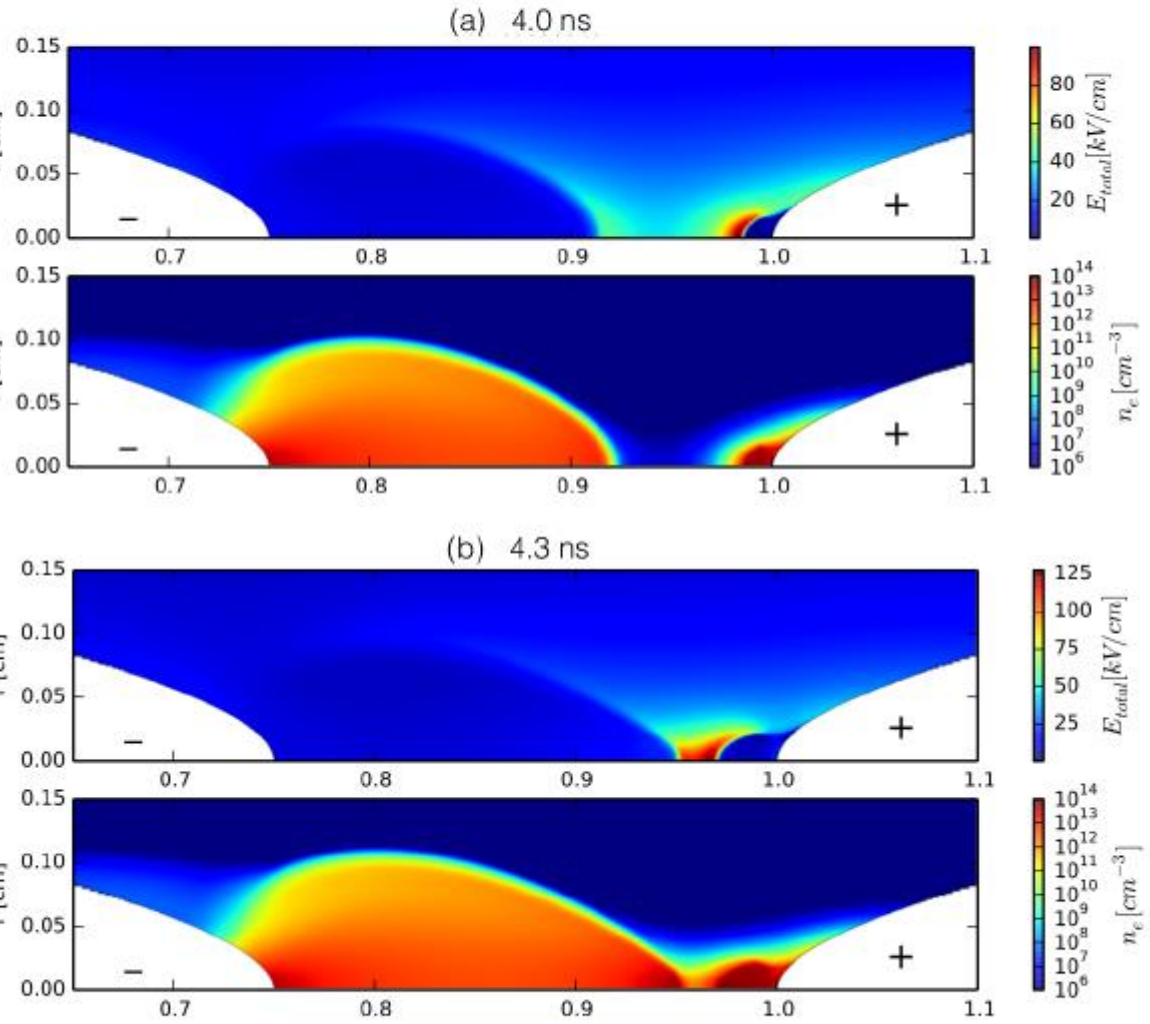


| $\phi$ | Discharge start (−) | Discharge start (+) | connect |
|---|---|---|---|
| 0 | 2.1 ns | 3.5 ns | 4.5 ns |
| 0.3 | 2.0 ns | 3.4 ns | 4.3 ns |
| 1 | 2.0 ns | 3.3 ns | 4.1 ns |
| 1.5 | 2.0 ns | 3.2 ns | 4.0 ns |

- (−) Start after rise time
- (+) Delayed > 1 ns

- With addition of $H_2$: discharge develops slightly faste

Figure for $\phi = 0.3$

# Time histories of species and temperature

For $\phi$ = 0.3, voltage plateau of 3.5 ns.

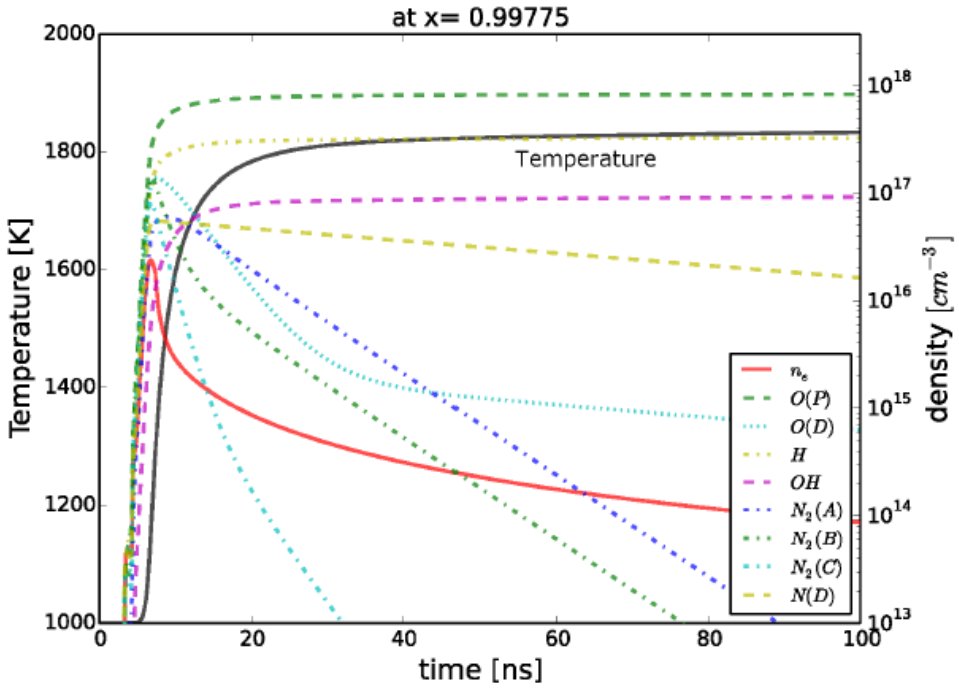


- Rapid decrease of ne at the end of the voltage pulse, then a much slower decrease up to 100 ns
- O(P), H and OH are mainly produced in the post-discharge by dissociative quenching reactions

## Key reactions for gas heating

Temperature rise at t=100.0 ns for $\phi$ = 0.3, plateau of 3.5 ns.

| | | | | |
|---|---|---|---|---|
| $N_2(A) + O_2$ | => | $N_2 + O(P) + O(P)$ | (1.00 eV) | +2 K |
| **$N_2(B) + O_2$** | **=>** | **$N_2 + O(P) + O(P)$** | **(2.35 eV)** | **+281 K** |
| $O(D) + O_2$ | => | $O(P) + O_2(b)$ | (0.34 eV) | + 10 K |
| $O(D) + H_2$ | => | $H + OH$ | (1.89 eV) | +105 K |
| $O(D) + N_2$ | => | $O(P) + N_2$ | (1.37 eV) | +92 K |
| $O_2(b) + H_2$ | => | $O_2(a) + H_2$ | (0.65 eV) | +1 K |
| **$N_2(C) + O_2$** | **=>** | **$O(P) + O(D) + N_2$** | **(4.83 eV)** | **+241 K** |
| **$N_2(C) + H_2$** | **=>** | **$H + H + N_2$** | **(6.55 eV)** | **+196 K** |

**3 reactions are responsible for ~ 80 % of total fast heating.**

# 7. Future research of plasma assisted reactive flow

Yiguang Ju, 2017

## 1. Game changers in PAC applications

- Engines (ICEs: lean burn, Turbine engine: relight, ignition)
- $CO_2$ capture and chemicals : $CO_2$ utilization and methane reforming (plasma catalyst)
- Bio-medicine
- Materials synthesis
- …

## 2. Game changers in plasma control

- High pressure volumetric discharge
- Selective excitation (electronic and vibrational)
- Selective species/radicals production
- Low cost and low electronic noise
- …

## 3. Fundamental Research of PAC

- Plasma properties: Electric field, electron number density, excitation states, non-equilibrium temperatures
- Plasma physics: Energy transfer processes between different excited states
- Plasma chemistry: Low temperature kinetic pathways, non-equilibrium kinetics
- Kinetic process: Key species, reaction rates, and cross-section areas for large fuel molecules
- Multi-dimensional modeling tools